

An alternative synthesis of aromatic carbon-sulfur bonds: thiol addition to *ortho*-quinones

Elizabeth J. Li, Department of Chemistry
McGill University, Montreal

April 2016

A thesis submitted to McGill University in partial fulfillment of the requirements of the degree of Master of Science

© Elizabeth J. Li, 2016

Abstract

Sulfur is an element that is fundamental to all forms of life. It can be found in the naturally occurring glutathione, the vitamin biotin, and the fundamental amino acid cysteine. As a result, the study of sulfur and sulfur-containing compounds has received significant attention. Aromatic carbon-sulfur bonds are fundamentally important as they repeatedly appear as functional moieties in a vast number of biologically active molecules, including heterocycles such as benzothiazepines, benzothiophenes, and aryl sulfones. Despite the privileged nature of aryl C-S bonds, their installation remains challenging. In summarizing classical and modern methods of S-arylation, the limitations of current approaches will be highlighted. These methods are mainly reliant upon traditional metal mediated cross-coupling reactions, generally requiring precious metals, long reaction times and pre-functionalization of the starting material. As a response to these often severe, drawbacks, novel methods for the increased efficiency of S-arylation are required.

Advances by the Lumb group toward an atom economic synthesis of structurally diverse *ortho*-quinones has recently allowed the consideration of *ortho*-quinones as thiol acceptors. This strategy allows for rapid and facile entry to aryl C-S bond containing molecules formed by sulfur addition to *ortho*-quinones, a reaction while well documented in nature (e.g. melanogenesis and detoxification pathways) it has, to this point, remained unharnessed by synthetic chemists.

Due to its prevalence in biological systems, considerable effort has been placed on describing this reactivity. Drawing from this, hypothesized mechanisms and reactivity trends will be discussed within. Herein, a novel and general method for the formation of aryl C-S bonds using sulfur addition to *ortho*-quinones will be described. The optimization of reaction conditions for applications in synthesis, as well as expansion of substrate scope will be discussed. Subtle factors, including steric and electronic effects, governing the reactivity will be detailed. Lastly, initial experiments into the application of sulfur containing catechol products for iron-oxide nanoparticle conjugation will be outlined.

Résumé

Le soufre est un élément fondamental pour toutes les formes de vie. Il peut être trouvé dans le glutathion, d'origine naturelle, dans la vitamine biotine et dans la cystéine, un acide aminé essentiel. Par conséquent, l'étude du soufre et des composés contenant du soufre a reçu une attention considérable. Les liaisons de carbone-soufre aromatiques sont fondamentalement importantes car elles apparaissent plusieurs fois comme des groupements fonctionnels dans un grand nombre de molécules biologiquement actives, y compris des hétérocycles tels que les benzodiazépines, les benzothiophènes et les sulfones d'aryl. En dépit de la nature privilégiée des liaisons d'aryles C-S, leur installation reste difficile. En résumant les méthodes classiques et modernes de l'arylation-S, les limites des approches actuelles seront mises en évidence. Ces méthodes sont principalement dépendantes des réactions traditionnelles de couplage croisé à médiation de métal, ce qui nécessite en général des métaux précieux, de longs temps de réaction et la pré-fonctionnalisation du matériau de départ. En réponse à ces souvent graves inconvénients, de nouvelles méthodes pour une efficacité accrue de l'arylation-S sont nécessaires.

Le progrès réalisé par le groupe Lumb vers une synthèse d'atome économique de quinones ortho structuellement diverses a récemment permis l'examen des quinones ortho comme accepteurs de thiol. Cette stratégie permet l'entrée rapide et facile à des liaisons de molécules contenant de l'aryl C-S formées par l'addition de soufre en quinones ortho, une réaction bien documentée dans la nature (par exemple, la mélanogénèse et des voies de détoxification), qui, jusqu'à ce moment, est toutefois restée inexploitée par les chimistes de synthèse.

En raison de sa prévalence dans les systèmes biologiques un effort considérable a été mis dans la description de cette réactivité. S'inspirant de cela, des mécanismes d'hypothèse et des tendances de réactivité seront discutés ici. Ici, un nouveau procédé général pour la formation de liaisons d'aryle C-S à l'aide de l'addition de soufre aux quinones ortho sera décrit. L'optimisation des conditions de réaction pour des applications dans la synthèse, ainsi que l'expansion de champ substrat seront discutées. Des facteurs subtils, y compris des effets stériques et électroniques, régissant la réactivité seront détaillés. Enfin, les premières expériences dans l'application des produits de catéchol contenant du soufre pour la conjugaison nanoparticule de l'oxyde de fer seront présentées.

Acknowledgements

I am indebted to all who have made contributions to the research in this thesis. First and foremost, I would like to express my deepest gratitude to my thesis supervisor and advisor, Dr. Jean-Philip Lumb. His constant guidance, enthusiasm, and relentless pursuit of excellence have been an unforgettable source of motivation during my undergraduate and graduate career.

I would like to thank my committee members Dr. Jim Gleason and Dr. Youla Tsantrizos, for their insightful comments and unlimited thought-provoking questions. I would also like to thank Dr. Karine Auclair, whose support first allowed me to begin my graduate career. I extend my gratitude to all of the faculty members and staff at McGill for graciously allowing me the use of chemicals, equipment, and facilities in the department. I gratefully acknowledge the McGill CIHR Training in Drug Development Program (DDTP) and McGill University for my funding support.

I would like to thank Dr. Robin Stein, Dr. Fred Morin, Dr. Alexander Wahba, and Dr. Nadim Saade for their technical and spectroscopic assistance. All HRMS data were efficiently produced by Alex and Nadim. In particular, I would especially like to thank Robin, who has been an invaluable source of numerous insightful NMR discussions. I would also like to thank the administrative staff, Chantal Marotte, Alison McCaffrey, Sandra Aersson, and Karen Turner. I would especially like to thank Chantal, without whom I would be surely be credits short and forms lacking.

Amidst the daily reactions and purifications, I feel especially lucky to have somehow found not one, but two constant pillars of support. These are my mentor and friend Kenneth Esguerra, and Adam Elmehriki, without whom all of this truly would not be possible. I would like to thank them for being boundless sources of sage advice and inspiration, and I will never forget the laughs, tears, and serendipitous chaos shared along the way.

To my labmates, Anna, Martin, Matt, Zheng, Ohhyeon, and Wenbo, thank you so much for fostering the engaging and boisterous camaraderie that comes with being a member of the Lumb group, and for being the best company that made many sleepless nights pass all the quicker. To all my extraordinary friends in the department, I feel blessed to have worked among such amazing people- thank you for all the great memories.

Lastly, I would like to extend my deep and heartfelt gratitude to my parents and brother, whose constant unconditional and selfless love has supported me for a lifetime.

Table of Contents

Abstract	2
Resumé	3
Acknowledgements	4
Table of Contents	5
List of Abbreviations	6
List of Figures	8
List of Schemes	9
List of Tables	12
Chapter 1: Previous Methods of Carbon-Sulfur Bond Formation	13
1.1 Introduction	13
1.2 Overview of Chapter 1	13
1.3 Classical Methods of S-Arylation	15
1.3.1 The Ullmann Condensation Reaction	15
1.3.2 The Chan-Lam Coupling	19
1.3.3 The Buchwald-Hartwig, Pd-Mediated S-Arylation	22
1.4: Recent Advances in C-S Bond Formation	25
1.4.1 Transition Metal Catalyzed	25
1.4.1.1 Palladium	26
1.4.1.2 Copper	31
1.4.1.3 Other Transition Metals	35
1.4.2 Nucleophilic Aromatic Substitution (S _N Ar)	40
1.4.3 Electrophilic Sulfur Strategies	44
1.4.4 Trifluoromethylthiolation (SCF ₃) Reactions	46
1.5 Summary of Chapter 1	52
1.6 References	54
Chapter 2: Sulfur Addition to <i>ortho</i>-Quinones in Biological Contexts	62
2.1 Introduction	62
2.2 Melanogenesis	62
2.3 Addition to <i>ortho</i> -quinones in Detoxification Pathways	69
2.4 Studies on Thiol Addition to <i>ortho</i> -Quinones	73
2.5 Plausible Mechanisms	76
2.6 Summary of Chapter 2	77
2.7 References	77
Chapter 3: Experiments	81
3.1 Introduction	81
3.2 Initial Experiments	81
3.3 Expansion of Thiol Substrate Scope	83
3.4 Optimization of Thiol Addition	88
3.5 Assignment of Regioisomers 3.3.6 and 3.4.3 from Spectral Data	93
3.6 Expansion of <i>ortho</i> -quinone Scope and Observed Regioselectivity	99
3.7 Investigations into the Role of MgBr ₂ ·Et ₂ O as Additive	107
3.8 Mechanism of Thiol Addition and Factors Governing Regioselectivity	108
3.9 Application of Method to Access a Library of Catechols for Iron-Oxide Nanoparticle (IONP) Functionalization	111
3.10 Summary	119
3.11 References	120
Appendix: Experimental Procedures and Spectral Data	123
A1 Experimental Procedures and Results	123
A2 Spectral Data	170

List of Abbreviations

°C- Degrees Celcius
Å – Angstrom
μM- micromolar
1,10-phen- 1,10 phenanthroline
1-1 ADEQUATE-*Adequate* Sensitivity Double-Quantum Spectroscopy
1°- primary
2°-secondary
3°-tertiary
¹H- proton
Ac₂O- acetic anhydride
Ar- aryl
AcOH- acetic acid
BHT- 2,6-Bis(1,1-dimethylethyl)-4-methylphenol
Bn- benzyl
Boc- *tert*-Butyloxycarbonyl
Boc-Cys- *N*-(*tert*-Butoxycarbonyl)-L-cysteine methyl ester
CO₂- carbon dioxide
CTQ- cysteine tryptophilquinone
CyPF-tBu- Hartwig's Josiphos ligand
d- doublet
DBU- 1,8-Diazabicycloundec-7-ene
Dippf- 1,1'-bis(diisopropylphosphino)ferrocene
DIPEA- N,N-Diisopropylethylamine
DCE- dichloroethane
DCM- dichloromethane
DMAP- 4-dimethylaminopyridine
DME- dimethoxyethane
DMF- dimethylformamide
DMSO- dimethyl sulfoxide
DNA- deoxyribonucleic acid
DTBP- di-*tert*-butyl peroxide
Et- ethyl
EtOAc- ethyl acetate
EtOH- ethanol
EtSH- ethanethiol
EWG- electron withdrawing group
h- hour(s)
HMBC- heteronuclear multiple bond correlation
HRMS- high resolution mass spectroscopy
HSQC- heteronuclear single quantum correlation
Hz- Hertz
IONP- iron-oxide nanoparticle
i-PrOH- isopropanol
i-PrSH- 2-propanethiol
J- coupling constant
Kcal/mol- kilocalorie per mol
KOH- potassium hydroxide
KO^tBu- potassium *tert*-butoxide
L- ligand

m-multiplet
 M- mol/L
 $M^{-1}sec^{-1}$ - /mol /sec
*m*CPBA- *meta*-chloroperoxybenzoic acid
 Me- methyl
 MeCN- acetonitrile
 MeOH- methanol
 $MgBr_2 \cdot Et_2O$ - magnesium bromide di-ethyl etherate
 Min- minute(s)
 mM- millimolar
 mol- mole (s)
 NaHMDS- sodium bis(trimethylsilyl)amide
 NaOH- sodium hydroxide
 NaOtBu- sodium *tert*-butoxide
*n*Bu₃N- N,N-Dibutyl-1-butanamine
 NHC- *N*-heterocyclic carbene
 NMR- nuclear magnetic resonance
 OAc- acetate
 Oct- octyl
 OH- Hydroxyl Group
 PEG-400- low-molecular-weight grade of polyethylene glycol
 Ph- Phenyl
 PhSH- thiophenol
 pH- decimal logarithm of the reciprocal of the hydrogen ion activity in a solution
 pK_a-acid dissociation constant
 PTS- polyoxyethynyl α -tocopheryl sebacate
p-TsOH- *para*-toluene sulfonic acid
 q- quartet
 QSAR- quantitative structure activity relationship
 s- singlet
 sec- second (s)
 S_NAr- nucleophilic aromatic substitution
 t- triplet
*t*Bu- *tert*-butyl
 TBS- *tert*-butyldimethylsilyl
 TBSCl- *tert*-butyldimethylsilyl chloride
 TEMPO- (2,2,6,6-Tetramethylpiperidin-1-yl)oxyl
 TFA- trifluoroacetic acid
 THF- tetrahydrofuran
 TGA-thermogravimetric analysis
 UV-Vis-Ultraviolet Visible

List of Figures

Figure 1.1.1- Examples of Aromatic Carbon-Sulfur Bond Containing Pharmaceutical Drugs	14
Figure 1.3.1.1- Proposed Catalytic Cycle for the Cu-Catalyzed Ullmann Reaction	16
Figure 3.3.1-Quinones selected for Initial Substrate Scope	84
Figure 3.5.1- ¹ H-NMR Spectrum of 3.3.6 in CDCl ₃	94
Figure 3.5.2- ¹ H-NMR Spectrum of 3.4.3 , in CDCl ₃	94
Figure 3.5.3- Detection of Regioisomers 3.3.6 and 3.4.3 through ¹ H-NMR studies	95
Figure 3.5.4- ¹³ C-NMR Spectrum of 3.3.6 , in CDCl ₃	95
Figure 3.5.5- ¹³ C- NMR Spectrum of 3.4.3 , in CDCl ₃	96
Figure 3.5.6- HSQC Correlations, leading to partial ¹³ C assignment of 3.3.6 and 3.4.3	96
Figure 3.5.7- HMBC Correlations, as seen for 3.3.6 and 3.4.3	97
Figure 3.5.8- ¹³ C- NMR Spectrum Labels of 3.3.6 & 3.4.3	97
Figure 3.5.9- Key Correlation in 1,1'-ADEQUATE NMR Spectrum of 3.3.6 , in CDCl ₃	98
Figure 3.5.10- Key Correlations in 1,1'-ADEQUATE Spectra of 3.4.3 , in CDCl ₃	98
Figure 3.5.11- Correlations shown in the 1,1'-ADEQUATE Spectra for Proton A, 3.3.6 , and Proton C, 3.4.3	98
Figure 3.5.12- Chemical Shift of the Proton Singlet Signal in Sulfur Adducts of Quinones 3.3.1 and 3.3.2	99
Figure 3.6.1- Hypothesized Mechanism of Action of DMAP on Regioselectivity	102
Figure 3.6.2- ortho-Quinone Substrate Scope	106
Figure 3.6.3- Control Experiment to Determine Stability of quinone 3.6.23 in Basic Media, performed by Zheng Huang	106
Figure 3.7.1- Hypothesized Role of MgBr ₂ Et ₂ O as Additive	108
Figure 3.8.1- Proposed Mechanism of Thiol Addition for quinone 3.2.2 , 1,6-Addition	109
Figure 3.8.2- Summary of the regiochemistry observed for quinones	110
Figure 3.9.1- Lumb Group Thiol Addition Provides Access to Catechols Ranging in Electronic Properties	112
Figure 3.9.2- A General Graphic Depiction of the Lumb Group/Blum Group Collaboration for the Development of Functionalized Catechols for IONP Functionalization	113
Figure 3.9.3- Proposed Synthesis of Alkynyl Catechols	114
Figure 3.9.4- Catechols conjugated to IONPs by the Blum Group vs. Our alkynyl catechols	117

List of Schemes

Scheme 1.3.1.1- A General Scheme of The Ullmann-Condensation Reaction for S-Arylation	15
Scheme 1.3.1.2- Palomo's Preparation of Aryl Thioethers	17
Scheme 1.3.1.3- S-Arylation of Aryl Iodides by Venkatamaran <i>et al.</i>	17
Scheme 1.3.1.4- Buchwald's Cu-Mediated Cross Coupling of Aryl Iodides and Thiols	18
Scheme 1.3.1.5- General Scheme for Ullmann-type S-Arylation Conditions	18
Scheme 1.3.2.1- A General Scheme of the Chan-Lam Coupling for Aryl Thioethers	19
Scheme 1.3.2.2- A General Mechanism of the Chan-Lam Coupling of Thiols and Arylboronic Acids with a Stoichiometric Copper(II) Reagent	19
Scheme 1.3.2.3- Guy <i>et al.</i> 's Chan-Lam type Coupling for Aryl Sulfides	20
Scheme 1.3.2.4- Cu-Catalyzed Cross Coupling of Aryl Boronic Acids and N-ThioImides by Liebeskind <i>et al.</i>	21
Scheme 1.3.2.5- A General Summary of Current Chan-Lam-type Reactions for S-Arylation	22
Scheme 1.3.3.1- A General Scheme of Pd-Mediated Cross-Coupling of Aryl Halides and Thiols	22
Scheme 1.3.3.2- General Mechanism for Palladium-Mediated S-Arylations	23
Scheme 1.3.3.3- Buchwald's Pd-Mediated Cross Coupling of Aryl Halides with Thiols	23
Scheme 1.3.3.4- Hartwig's Preparation of Aryl Sulfides via Pd-Mediated Cross-Coupling of Aryl Chlorides and Thiols	24
Scheme 1.3.3.5- A General Summary of Pd-Catalyzed S-Arylation Methods	25
Scheme 1.4.1.1- Wang's Pd-Mediated Synthesis of Aryl Alkyl Thioethers from Aryl chlorides, Alkyl Bromides, and Thiourea	27
Scheme 1.4.1.2- A Pd-Mediated Synthesis of Aryl Alkyl Thioethers using Sodium Thiosulfate as Sulfur Source, by Jiang <i>et al.</i>	28
Scheme 1.4.1.3- A Pd-Mediated Preparation of Arylthioethers with N-Amidoimidazolium Salt Ligands	29
Scheme 1.4.1.4- Nolan's Pd-NHC mediated Preparation of Aryl Thioethers	30
Scheme 1.4.1.5- Pd-Mediated S-Arylation of Arenes with Disulfides by Nishihara <i>et al.</i>	30
Scheme 1.4.1.6- A Ligand-Free Preparation of Aryl Thioethers with a Cu ₂ O Powder Catalyst, by Lee <i>et al.</i>	31
Scheme 1.4.1.7- Chen's Cu-mediated Preparation of Symmetrical Aryl Sulfides with Aryl Halides and Sodium Sulfide, using PEG-400 as solvent	31
Scheme 1.4.1.8- Microwave-assisted Synthesis of Assymetrical Thioethers with Aryl Halides and Sulfonyl Hydrazides as Sulfur Source, by Singh <i>et al.</i>	32
Scheme 1.4.1.9- A Cu-Mediated Synthesis of Assymetrical Thioethers through Sodium Sulfothioates and Arylboronic Acids in a CO ₂ Atmosphere , by Jiang <i>et al.</i>	33
Scheme 1.4.1.10- A Cu-Mediated S-Arylation of Thiols with Boronic Acids, by Feng <i>et al.</i>	34
Scheme 1.4.1.11- Wang's Cu-Mediated Cross-Coupling of Di(pyrimidin-2-yl) Disulfides with Arylboronic Acids	35
Scheme 1.4.1.12- Shi's Ni-Catalyzed C-H Activation of Arenes with the PIP Directing Group	36
Scheme 1.4.1.13- Cu-Mediated C-H Sulfonylation with Sodium Sulfinates	36
Scheme 1.4.1.14- A Bi ^{III} -Mediated Synthesis of Aryl Sulfides in Water, by Chakraborty <i>et al.</i>	37
Scheme 1.4.1.15- Lee <i>et al.</i> 's Rh-Catalyzed Preparation of Aryl Iodides with Thiols	38
Scheme 1.4.1.16- Ozerov <i>et al.</i> 's Rh-Catalyzed Synthesis of Aryl Thioethers	39
Scheme 1.4.1.17- Baba <i>et al.</i> 's Indium Catalyzed Synthesis of Arylthioethers	40
Scheme 1.4.2.1- Frieman's One-Pot Synthesis of 4-sulfonyl benzoic acids	41
Scheme 1.4.2.2- Naemi's Preparation of Aryl Thioethers from Electron-Deficient Nitroarenes	41
Scheme 1.4.2.3- Synthesis of Aryl and Alkyl Sulfides via Reaction of Bunte Salts with Grignard Reagents by Reeves <i>et al.</i>	42
Scheme 1.4.2.4- Synthesis of nitro-Thioethers through S-alkylisothiuronium Salts from	

Thiourea by Lu <i>et al.</i>	43
Scheme 1.4.2.5- Sanford's Triflic Acid Mediated Coupling of Disulfides with Diaryliodonium Salts	44
Scheme 1.4.3.1- Cossy's Sulfenylation of Arenes with Alkyl and Aryl Thio-Succinimides	45
Scheme 1.4.3.2- A Preparation of Aryl Thioethers from Grignard Reagents and Sulfenyl Chlorides arising from N-Chlorosuccinimide	46
Scheme 1.4.3.3- Synthesis of Arylthioethers from Arylzinc Reagents and Sulfenyl Chlorides, by Jarvo <i>et al.</i>	46
Scheme 1.4.4.1- Daugulis' Directed C-H di-trifluoromethylthiolation of Arenes	47
Scheme 1.4.4.2- A Pd-Mediated C-H Trifluoromethylthiolation of Arenes by Shen <i>et al.</i>	48
Scheme 1.4.4.3- Huang's Pd-Mediated <i>ortho</i> -Selective Trifluoromethylthiolation	49
Scheme 1.4.4.4- A Cu-Mediated Trifluoromethylthiolation of Aryl Halides with Directing Groups, by Liu <i>et al.</i>	50
Scheme 1.4.4.5- A Dinuclear Pd ^{II} -Catalyst Mediated Trifluoromethylthiolation by Schoenebeck <i>et al.</i>	51
Scheme 1.5.1- General Summary of Transition Metal Catalyzed S-Arylation in Chapter 1	53
Scheme 1.5.2- General Summary of S _N Ar, Electrophilic Sulfur, and Trifluoromethylthiolation S-Arylation Methods in Chapter 1	54
Scheme 2.1.1-General Scheme of Sulfur Addition to <i>ortho</i> -Quinones	62
Scheme 2.2.1- The First Steps of the Biosynthetic Pathway of Eumelanin in Melanogenesis	63
Scheme 2.2.2- Early Isolation of Trichochromes E 2.2.7 and F 2.2.8 from Enzymatic Oxidation of Dopa 2.2.4 in Presence of Cysteine	64
Scheme 2.2.3- Proposed Incorporation of Cysteine into Pheomelanin Pigments by Protá <i>et al.</i>	64
Scheme 2.2.4- Synthesis of Cysteinyl dopas with Mushroom Tyrosinase by Itoh <i>et al.</i>	65
Scheme 2.2.5- Reactions of Cysteine and Glutathione with Dopachrome 2.2.5 , by Protá <i>et al.</i>	66
Scheme 2.2.6- Calculated Rate Constants for the Thiol Addition of Cysteine to Dopachrome, and for the Redox Exchange between dopachrome and Cysteinyl dopa Products	67
Scheme 2.2.7- Thiol Addition: The Branch Point in Melanogenesis	68
Scheme 2.2.8- A General Scheme for the Process of Redox-Exchange	69
Scheme 2.3.1- A Regiospecific Addition of N-Acetylcysteine to Urushiol Quinones, by Castagnoli <i>et al.</i>	70
Scheme 2.3.2-Sulfur Addition to Catechol Estrogen Quinones by Cavalieri <i>et al.</i>	72
Scheme 2.4.1-Thiol-Additions to 4-Methyl- <i>ortho</i> -Quinone in Acidic, Aprotic, or Basic Media, by Castagnoli <i>et al.</i>	74
Scheme 2.4.2- A Synthesis of a Model Compound of the Organic Co-Factor in the γ -Subunit of QH-AmDH	75
Scheme 2.4.3- Addition of thiophenol to 3-benzyl- <i>ortho</i> -quinone 2.4.11 , by Pettus <i>et al.</i>	75
Scheme 2.5.1- A General Mechanism of 1,6-Addition to <i>ortho</i> -Quinone	76
Scheme 2.5.2- A General Mechanism of the Thiol-Ene Reaction	77
Scheme 3.2.1- Initial Experiment Investigating the Addition of Sulfur Nucleophiles to <i>ortho</i> -Quinones	82
Scheme 3.3.1- Isolation of Multiple Products from Reaction of <i>ortho</i> -quinone 3.3.2 and thiophenol	86
Scheme 3.3.2- Experiments Probing Redox-Exchange with A) 3.2.1 , B) 3.2.3 , C) 3.3.2	87
Scheme 3.4.1- Investigation into effects of DMAP with quinone 3.2.1	93
Scheme 3.7.1-Probing the effects of MgBr ₂ ·Et ₂ O on Redox-Exchange between quinone 3.2.1 and product catechol 3.4.2	107
Scheme 3.7.2- Investigation into MgBr ₂ ·Et ₂ O as Additive with quinone 3.6.1 and catechol 3.7.1	108
Scheme 3.9.1- Synthetic Routes examined for the Synthesis of 4-pentyn-1-thiol 3.9.4	114
Scheme 3.9.2- Synthesis of Alkynyl Bis-Acetates 3.9.5 , 3.9.6 , and 3.9.7	115
Scheme 3.9.3- Synthesis of Catechols 3.9.8 , Sulfoxide 3.9.9 , and Sulfone 3.9.10	116

Scheme 3.9.4- Alternative Targeted Catechol 3.9.16 for IONP functionalization	118
Scheme 3.9.5- Future Synthetic Route to Sulfoxide and Sulfone- Dopamine Derivative Catechols 3.9.20, 3.9.21	119

List of Tables

Table 3.2.1-Initial Experiments with <i>ortho</i> -Quinone 3.2.3	83
Table 3.3.1- Initial Thiol Substrate Scope with <i>ortho</i> -Quinone 3.2.3	84
Table 3.3.2- Initial Thiol Substrate Scope with <i>ortho</i> -Quinone 3.2.1	85
Table 3.3.3- Initial Thiol Substrate Scope with <i>ortho</i> -Quinones 3.3.1 and 3.3.2	85
Table 3.4.1- Optimization of Thiol Addition with <i>ortho</i> -Quinone 3.2.1 & 2-propanethiol	89
Table 3.4.2- Investigation into Protecting Group Additives and Observation of Regioisomers with quinone 3.2.1	92
Table 3.6.1- Reaction Conditions Arising from Investigation of Thiol Addition	99
Table 3.6.2- Evaluating reaction conditions with <i>mono</i> -substituted quinone 3.6.1	100
Table 3.6.3- Evaluating Reaction Conditions with <i>mono</i> -substituted quinone 3.6.9	103
Table 3.6.4- Re-evaluation of sulfur addition to quinone 3.3.2 under Optimized Conditions	104
Table 3.8.1- Exploring Reactivity with Radical Scavengers with quinone 3.6.1	110

1 Existing Methods of Carbon-Sulfur Bond Formation

1.1 Introduction

Sulfur is a reactive element that is ubiquitous in nature and all living organisms. In ancient times, elemental sulfur was referred to as *brimstone* and was mined from volcanic regions in Sicily.¹ Today however, sulfur is produced mostly as a by-product from industrial processes such as oil refinement, where it is extracted from unwanted or toxic waste by-products in the form of hydrogen sulfide.² This hydrogen sulfide is then converted to elemental sulfur through the Claus process.² As a result, there are now large amounts of elemental sulfur stored in Alberta, Canada, arising from the Athabasca Oil Sands.³

As an element, sulfur occupies a position in the third row, group 16 on the periodic table, has an atomic radius of 1.80 Å, and an electronegativity of 2.58⁴. Although it possesses the same number of valence electrons as oxygen, their reactivities differ greatly. Unlike nitrogen and oxygen, sulfur is a unique heteroatom in organic structures as it exemplifies characteristics and properties not observed with analogous nitrogen and oxygen containing compounds. In addition, it possesses the ability to access a variety of oxidation states, most commonly seen as sulfides, sulfates, sulfoxides, and sulfones. A fundamental aspect of sulfur is its tendency to form S-S bonds, more commonly referred to as disulfide linkages. Upon comparison of bond dissociation energies between H-S and C-S bonds vs. the oxygen analogues, the energies of the former are weaker.⁵ However, in the case of disulfide linkages, the bond dissociation energies of S-S linkages are 25-30 kcal/mol higher than the analogous O-O bonds.⁵ This ability to access relatively strong bonds is integral in establishing the structure of proteins.

The ubiquity of sulfur in biology is present primarily as organosulfur compounds, *e.g.* methionine, cysteine, and glutathione. As a result, significant attention has been given to the synthesis and study of sulfur-containing compounds. More specifically, aromatic carbon-sulfur bonds are fundamentally important as functional portions of a vast number of biologically active molecules. Prontosil, a sulfonamide, was the world's first systematically used antibiotic drug, and catapulted the development of hundreds of sulfa drug derivatives.⁶ Other scaffolds include benzothiazepines, benzothiophenes, and aryl sulfones, which are frameworks frequently found in pharmaceuticals that account for over 9 billion USD in sales per year (Figure 1.1.1).⁷ Six of the

top two hundred most profitable pharmaceutical drugs contain aryl C-S bonds. Other applications include the use of sulfur in materials science, where sulfur atoms are critical for modulating the physical, electronic, and surface properties of metal surfaces.⁸ Despite the clear prevalence of aryl-C-S bonds in biology, biochemistry, and the pharmaceutical industry, their synthesis remains challenging. When looking at traditional methods of making C-S bonds, many require pre-functionalization of the starting material, require high temperatures, and generate unwanted by-products. Therefore, increased attention has been given to direct methods of C-S bond formation with improved efficiency.

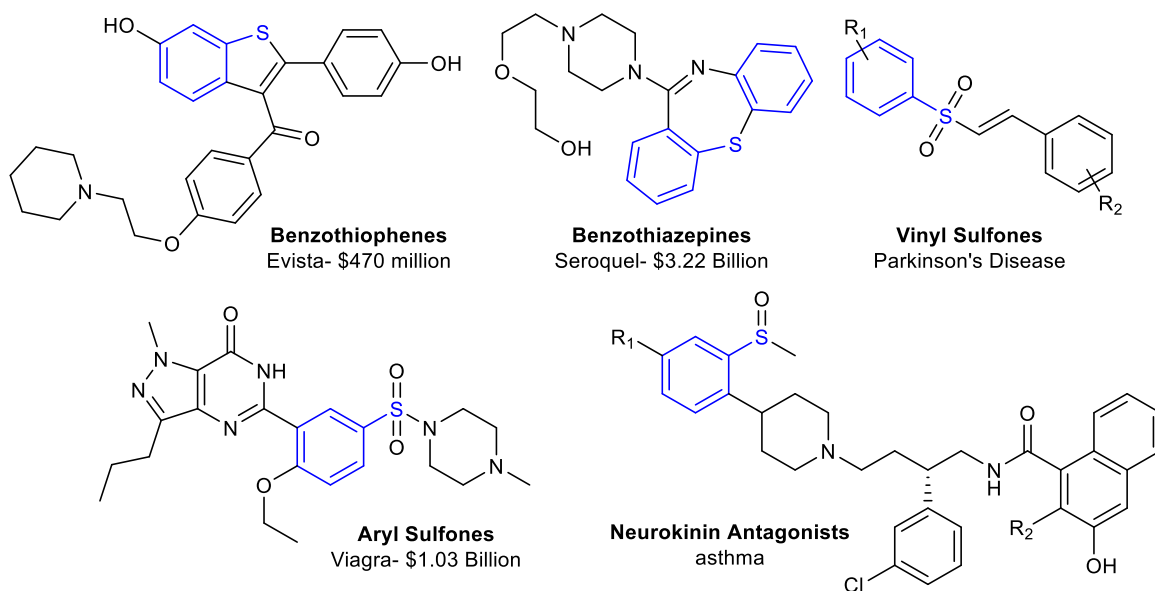


Figure 1.1.1- Examples of Aromatic-Carbon-Sulfur-Bond Containing Pharmaceutical Drugs

In this thesis, general and current methods for S-arylation will be reviewed in Chapter 1. In Chapter 2, the ubiquity of sulfur in nature will be highlighted in the pigmentation process of melanogenesis and detoxification process in biological systems. Sulfur addition to *ortho*-quinones, a common theme in these systems, will be examined. Finally, Chapter 3 will detail our experiments involving the development of an application of sulfur addition to *ortho*-quinones for a facile S-arylation method. Our application of this method to the synthesis of catechol ligands for iron nanoparticle functionalization will also be discussed.

1.2 Overview of Chapter 1

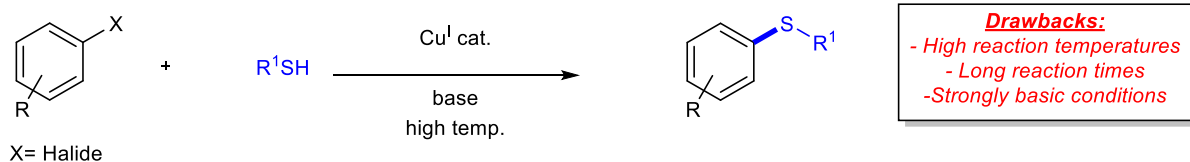
There have been many published methods of S-arylation reactions, and this chapter will provide a brief historical perspective on those which have been most influential. Section 1.3 will

detail classical methods including the Ullmann Reaction, the Chan-Lam Coupling and the Buchwald-Hartwig, Pd-Mediated Cross-Coupling. Finally, Section 1.4 will discuss the principal advances of methodologies published within the past 5 years.

1.3 Classical methods of S-Arylation

1.3.1 The Ullmann Condensation Reaction

The Ullmann Condensation reaction refers to the original work by Ullmann and Goldberg on copper-mediated cross coupling reactions to generate aryl-heteroatom (O, N) bonds, which has been extended to include C-S bond formation.⁹ However, significant limitations include the requirement for high reaction temperatures, long reaction times and the use of stoichiometric metal reagents. A significant challenge with S-arylation is the tendency of thiols to oxidize to di-sulfides, a competitive pathway that remains difficult to suppress.



Scheme 1.3.1.1- A General Scheme of The Ullmann-Condensation Reaction for S-Arylation

Various copper salts and oxides including Cu⁰, Cu^I and Cu^{II} have been reported to catalyze the Ullmann reaction for the formation of C-N and C-O bonds¹⁰, however, it was first hypothesized by Weingarten that a Cu^I species is the common intermediate in all of these reactions¹¹. Numerous studies by Weingarten¹¹, Paine¹², Taillefer¹³, and Chen¹⁴, show that the active catalyst in the reaction is a Cu^I species. Various mechanisms have been proposed for the reaction, however, the generally accepted mechanism is that of an oxidative addition-reductive elimination cycle (Figure 1.3.1.1).¹⁵ The exact order of steps is still unknown, i.e. whether the oxidative addition step takes place first, or transmetallation.¹⁶ The exact oxidation state of Cu is still in debate, and the evidence supporting and refuting these mechanisms is discussed at length in a review by McGowan¹⁷. Recent work by Ribas *et al.* highlights the observation of a macrocyclic aryl-Cu^{III} complex by UV-Vis studies¹⁸, however, it has been noted that the macrocyclic system examined was extremely stable and may not be applicable to typical reaction systems.

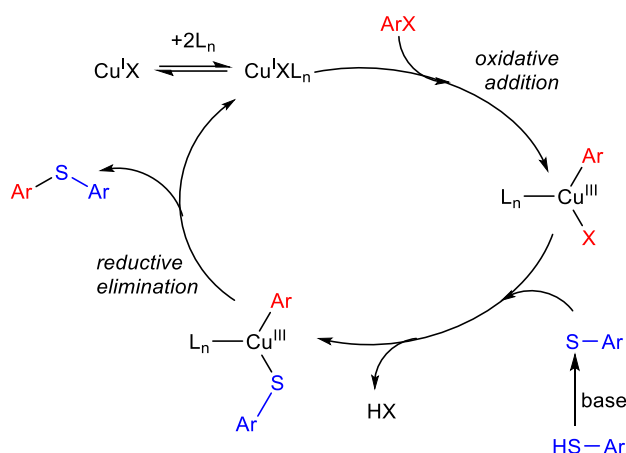
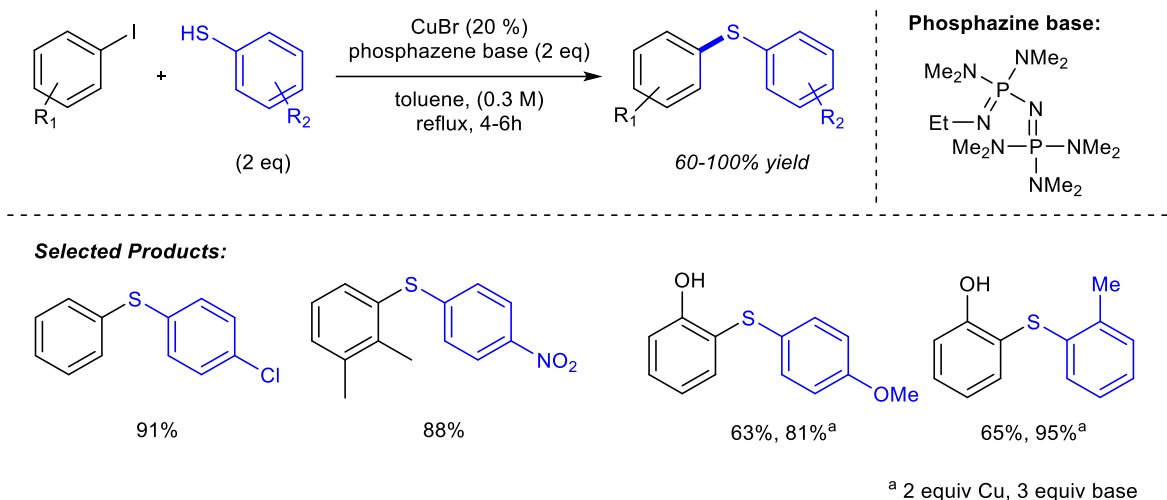


Figure 1.3.1.1- Proposed Catalytic Cycle for the Cu-Catalyzed Ullmann Reaction

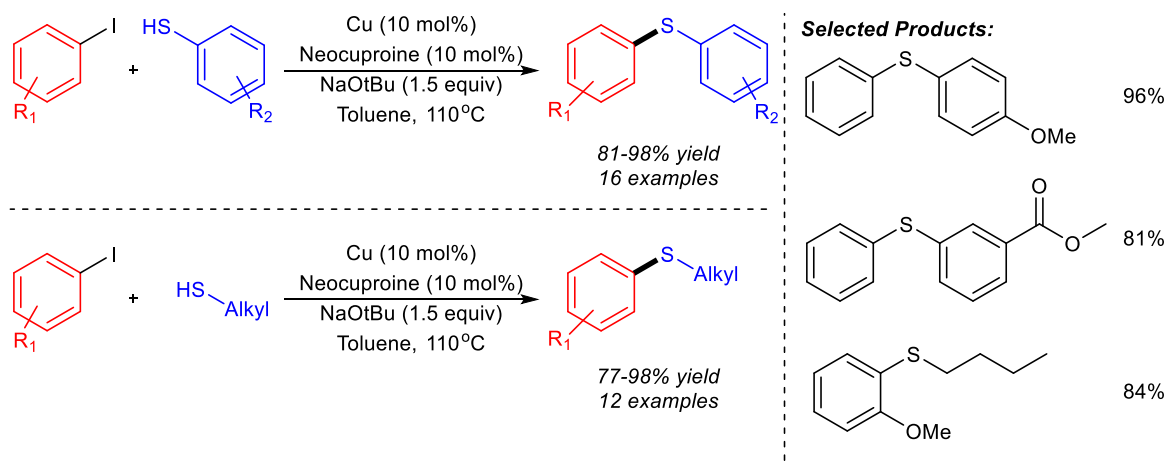
It was hypothesized that the ligands functioned to stabilize the reactive Cu^{I} species, increase solubility, and prevent imidazole from aggregating to the Cu catalyst irreversibly.¹⁹ The use of ligands in the reaction has since allowed for milder conditions, lowering the classical high temperatures of 200°C to around $80\text{--}100^\circ\text{C}$. Bidentate ligands have been found to be the most effective due to their ability to occupy two adjacent coordination sites on copper, allowing for facile reductive elimination between nucleophile and aryl partner.²⁰ Current hypothesized roles of the ligand and mechanistic evidence for C-N and C-O bond formation was examined in detail by McGowan¹⁷.

Although the Ullmann reaction has been heavily explored for arylation reactions with amines, alcohols, and amides, investigations into S-arylations have only begun in the last twenty years. In 2000, Palomo et al. reported a preparation of aryl thioethers from aryl iodides using a CuBr as catalyst and phosphazene bases, in toluene at reflux (Scheme 1.3.1.2)⁹. In addition to playing its role as base to generate the thiolate, the phosphazene base was hypothesized to chelate to copper and act as a ligand. It was noted that DBU was an efficient alternative to the phosphazene ligand but demanded longer reaction times. A total of 17 biaryl sulfides were reported with various electron-rich and electron-poor substituents in good yields, notably, including OH. The reaction was also observed to be chemoselective for aryl iodides as chloride-bearing aryl iodides reacted preferentially with the iodide. Limitations of this method include the high cost of the phosphazene bases, high catalyst loading, and elevated reaction temperatures. Alkyl thiols were not amenable to the reaction.



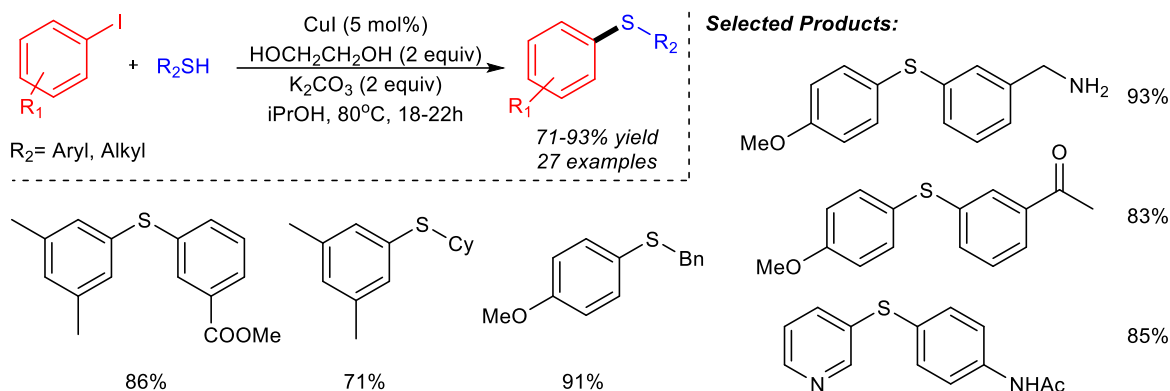
Scheme 1.3.1.2- Palomo's Preparation of Aryl Thioethers

Venkatamaraman *et al.* reported another method of S-arylation from aryl iodides using catalytic amounts of Cu^I and neocuproine as ligand (Scheme 1.3.1.3).²¹ Distinct from the method disclosed by Palomo, these conditions were able to couple both alkyl and aryl thiols. Various aryl and bi-aryl sulfides were produced in good to excellent yields. Both primary and secondary alkyl thiols were also amenable to the reaction. No reaction was observed in the absence of the neocuproine ligand, and a pre-formed catalyst was also effective in catalyzing the reaction.



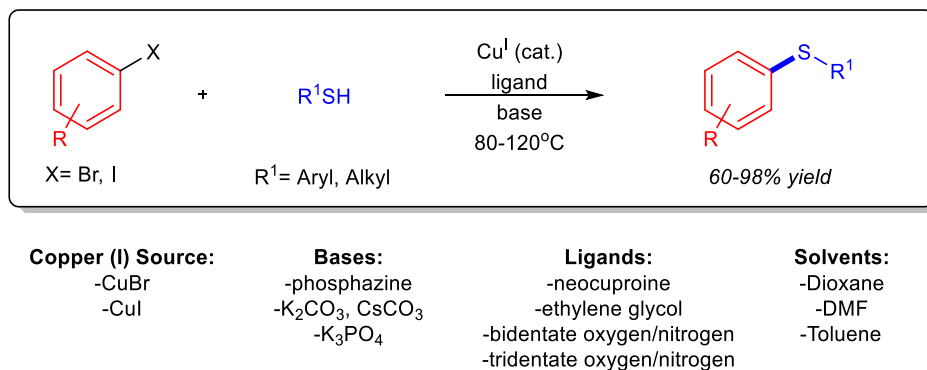
Scheme 1.3.1.3- S-Arylation of Aryl Iodides by Venkatamaraman et al.

Buchwald *et al.* also reported an alternative method shortly after, using Cu^I as catalyst, K₂CO₃ as base, *i*-PrOH as solvent, and two equivalents of ethylene glycol (Scheme 1.3.1.4).²² This method was also able to couple both aryl and alkyl (1°, 2°) thiols. In this reaction, the ethylene glycol was hypothesized to act as ligand to stabilize the copper species during the transformation.



Scheme 1.3.1.4- Buchwald's Cu-Mediated Cross Coupling of Aryl Iodides and Thiols

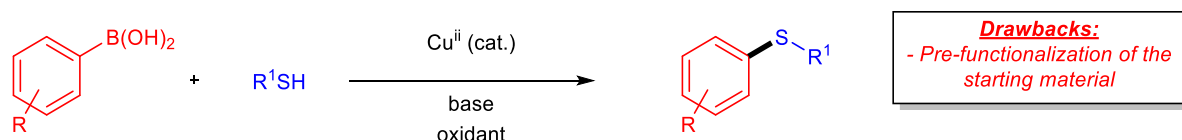
It can be said that significant strides have been made in the field of Ullmann-type S-arylation, with state of the art methods able to couple aryl and alkyl thiols. The use of catalytic systems involving ligands such as neocuproine, ethylene glycol, and bi- and tri-dentate oxygen/nitrogen species have allowed for the use of milder reaction conditions of 80-120°C. Coinciding with the judicious choice of ligands, the scope of bases amenable to this transformation have expanded to include mild bases such as cesium carbonate and tripotassium phosphate. The development of these cheaper, more efficient catalytic systems have now begun to supplant the analogous palladium catalyzed transformations. Many developments on Cu-catalyzed S-arylation reactions have been reported by various research groups and are thoroughly discussed in various reviews by Ley²³, Kunz²⁴, Stambuli²⁵, McGowan¹⁷, Ananikov²⁶, and Anilkumar²⁷, covering literature up to 2015. A general scheme summarizing this transformation is shown in Scheme 1.3.1.5. A notable omission in this summary is the copper catalyzed Chan-Lam type coupling involving the reaction of arylboronic acids, which will be discussed in the section following.



Scheme 1.3.1.5- General Scheme for Ullmann-type S-Arylation Conditions

1.3.2 The Chan-Lam Coupling

Advances in copper mediated heteroatom arylations arose in the seminal work of Chan and Lam in 1998, now known as the Chan-Lam Coupling. The Chan-Lam Coupling refers to the Cu^{II} -mediated coupling of aryl- and alkenyl- boronic acids with heteroatom nucleophiles (O, N, S) (Scheme 1.3.2.1). This reaction provided a significant advantage over previous methods such as the Ullmann reaction due to its ability to be performed under milder conditions (i.e. room temperature) and ambient atmosphere. Additionally, it utilized aryl boronic acids which had become readily available through the Miyaura borylation. However, the majority of advancements on this method since the original report in 1998 have focused primarily on C-N and C-O bond formation, with few utilizing thiols. The aerobic atmosphere that could be employed for O- and N-arylation is not amenable to thiols due to their sensitivity to air oxidation to disulfides, and the conditions developed by Chan and Lam led to competitive thiol oxidation.²⁸ Most reaction conditions reported use stoichiometric amounts of copper, due to the generation of Cu^0 and the absence of an oxidant to complete the catalytic cycle. The current proposed mechanism for the transformation is shown in Scheme 1.3.2.2.²⁹



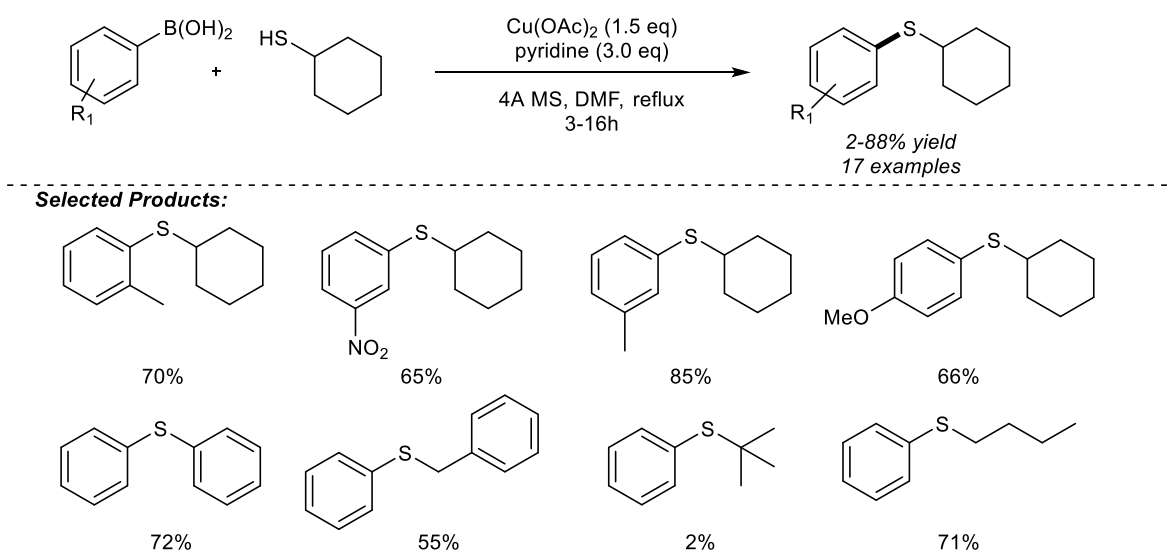
Scheme 1.3.2.1- A General Scheme of the Chan-Lam Coupling for Aryl Thioethers



Scheme 1.3.2.2- A General Mechanism of the Chan-Lam Coupling of Thiols and Arylboronic Acids with a Stoichiometric Copper(II) Reagent

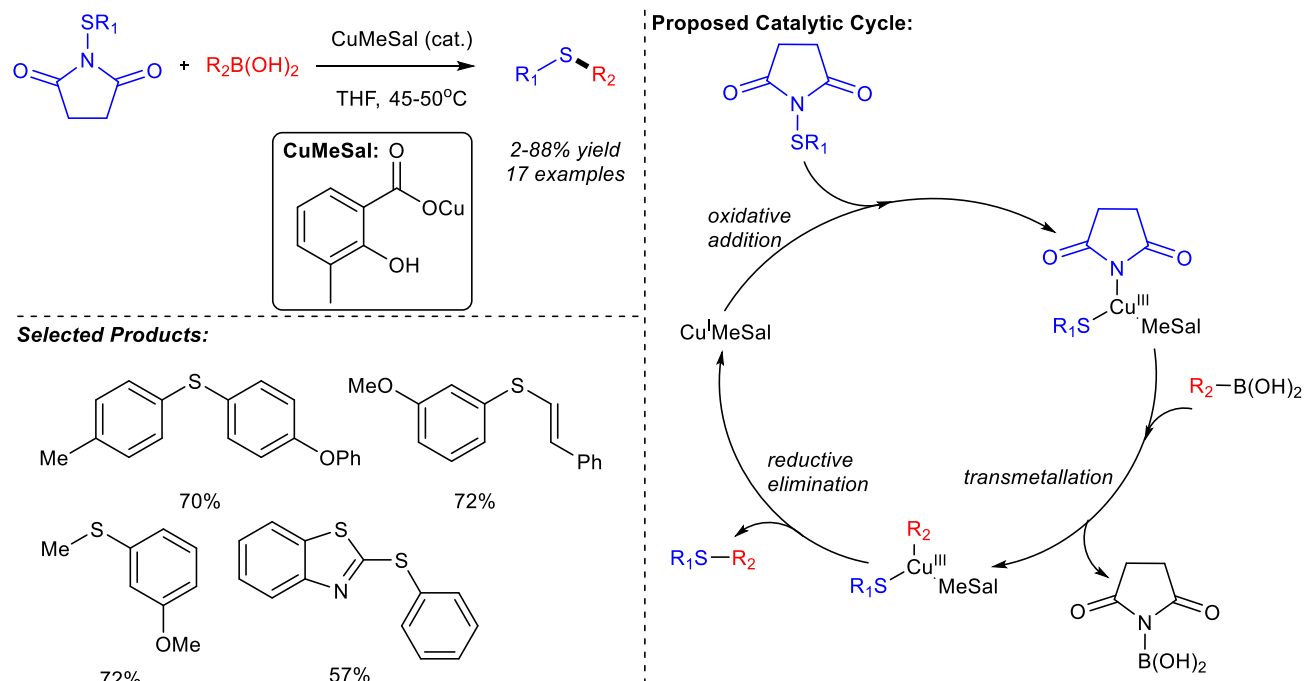
The first description of Chan-Lam type coupling with thiols was reported by Guy *et al.* in 2000 (Scheme 1.3.2.3).²⁸ It involved the use of 2.0-2.2 eq of an arylboronic acid and alkyl thiols with a stoichiometric amount of Cu(OAc)_2 and pyridine at reflux in DMF. The reaction conditions reported were able to tolerate various electronic substituents on the aryl boronic acid, however, it had limitations attributed to steric effects. Some drawbacks also included the incapability to generate tertiary alkyl aryl sulfides (tertiary thiols) and aryl thioesters. The reaction conditions

afforded the desired aryl thioether in low to high yields. It was postulated in a later work by Liebskind *et al.* that it was improbable that the reaction followed the mechanism in Scheme 1.3.2.2, due to the tendency of thiols to oxidize in the presence of Cu^{II} .³⁰ Instead, it was proposed that the reaction proceeded via a Cu^{I} catalyst to couple the arylboronic acid with a dialkyl disulfide, which is generated under the reaction conditions.



Scheme 1.3.2.3- Guy *et al.*'s Chan-Lam type Coupling for Aryl Sulfides

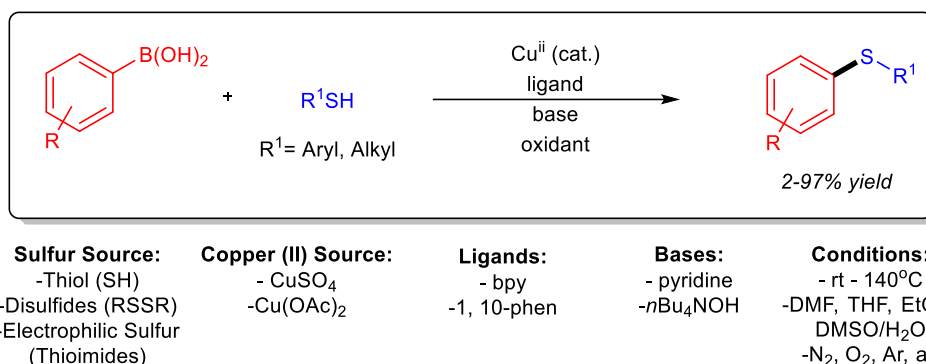
In 2002, Liebeskind *et al.* reported a preparation of thioethers from arylboronic acids and thioimide derivatives using a Cu^{I} catalyst in moderate yields (Scheme 1.3.2.4).³⁰ It was proposed that the reaction proceeded through a $\text{Cu}^{\text{I}}/\text{Cu}^{\text{III}}$ catalytic cycle. Many aryl-substitution products arising from succinimide coupling partners were reported, but only one alkyl-S coupling partner was described. The thioimide coupling partners are generated either from the reaction of the corresponding thiol and N-chlorosuccinimide or the reaction of disulfide with 2 eq of N-bromosuccinimide.



Scheme 1.3.2.4- Cu-Catalyzed Cross Coupling of Aryl Boronic Acids and N-ThioImides by Liebeskind et al.

Further developments of the Chan-Lam coupling to yield mild catalytic conditions were examined by various authors, covering literature up to 2015.^{23, 31} This progression includes the evolution from the initial stoichiometric use of copper (II) to catalytic conditions. However, the coupling of thiols with arylboronic acids still has its limitations. As disulfide formation from thiols does not allow for the open-air conditions amenable to C-O and C-N bond forming transformations, reactions require the use of inert atmospheres. Despite limitations posed by disulfide formation, some progress has been made in the use of disulfides as the sulfur source in such transformations. In these cases, the use of an inert atmosphere is not necessary.³² A general summary of current methods available is found in Scheme 1.3.2.5. These have established the

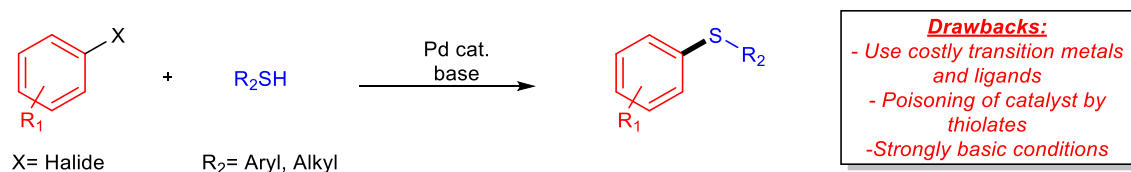
Chan-Lam as a reliable method of S-arylation with broad functional group tolerance in ambient conditions.



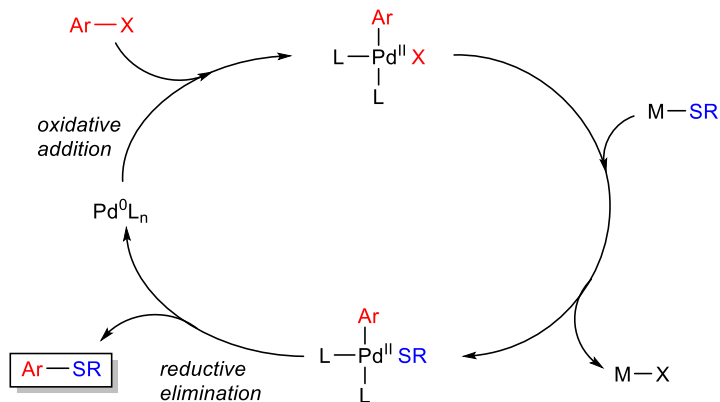
Scheme 1.3.2.5- A General Summary of Current Chan-Lam-type Reactions for S-Arylation

1.3.3 Palladium Mediated S-Arylation Reactions

Since the discovery of palladium-mediated arylation reactions with amines and alcohols, many methods of C-O, and C-N bond formation have been reported. Though Migita made his report of Pd-mediated cross coupling in 1980³³, Pd-catalyzed S-arylation (Scheme 1.3.3.1) has only received significant attention in recent years. Many of these advances employ the use of bidentate phosphine ligands, which have been found to catalyze the reaction most efficiently. The mechanism for most Pd-mediated S-arylations is thought to proceed via the standard mechanism found for palladium-catalyzed heteroatom cross-coupling reactions (Scheme 1.3.3.2).¹⁵

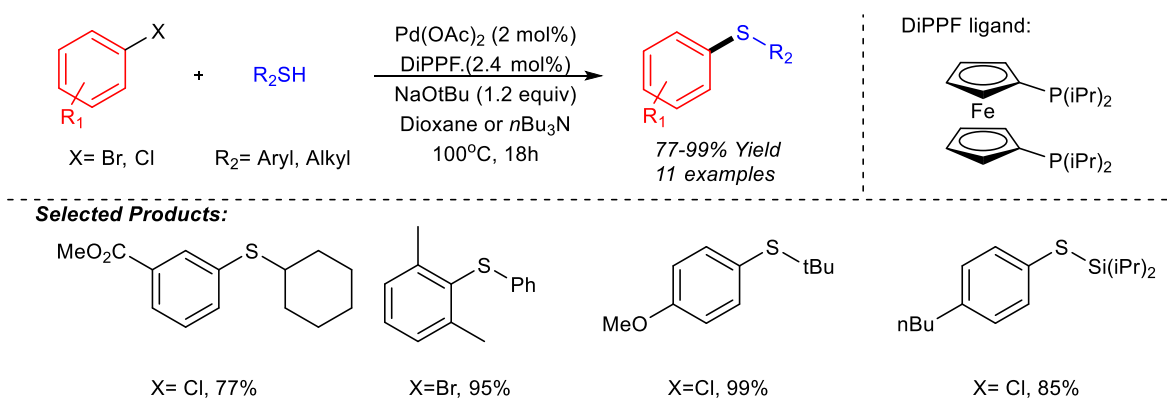


Scheme 1.3.3.1- A General Scheme of Pd-Mediated Cross-Coupling of Aryl Halides and Thiols



Scheme 1.3.3.2- General Mechanism for Palladium-Mediated S-Arylations

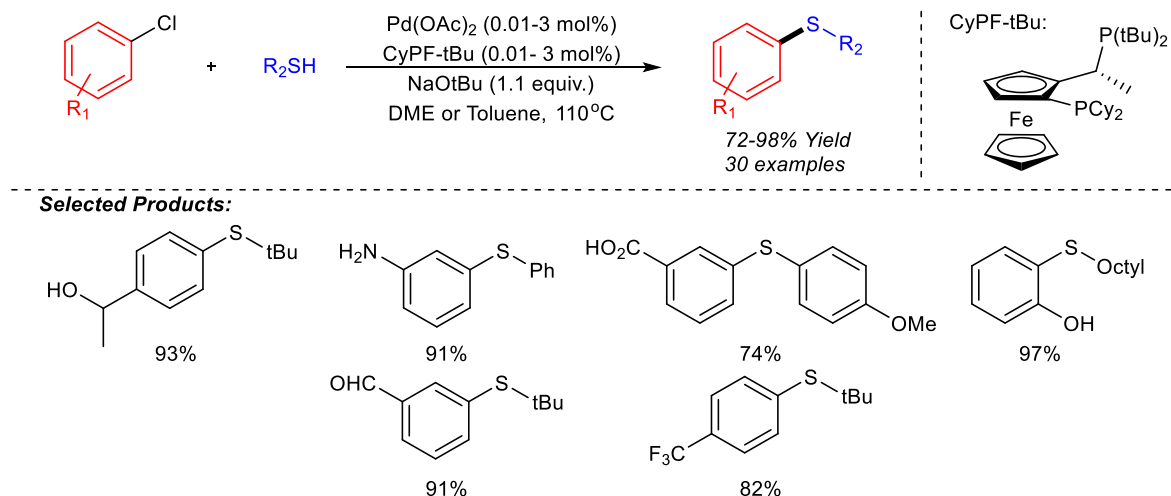
In 2004, Buchwald *et al.* reported a general protocol for the Pd-mediated cross coupling of aryl halides with aliphatic and aromatic thiols (Scheme 1.3.3.3).³⁴ This catalytic system used 1,1'-bis(diisopropylphosphino)ferrocene (dippf) as ligand and NaOtBu as the base. A variety of monodentate- and bidentate- phosphine ligands were evaluated for efficiency, and all large bulky monodentate ligands were found to be unreactive. It was suggested that monodentate ligands were ineffective due to being displaced by the thiolate, rendering Pd-catalyst inactive. It was noted that in order to prevent the common problem of disulfide formation, *n*Bu₃N was used as solvent for the coupling of aryl thiols as opposed to dioxane. All cross-coupled aryl thioether products were reported in good to excellent yields.



Scheme 1.3.3.3- Buchwald's Pd-Mediated Cross Coupling of Aryl Halides with Thiols

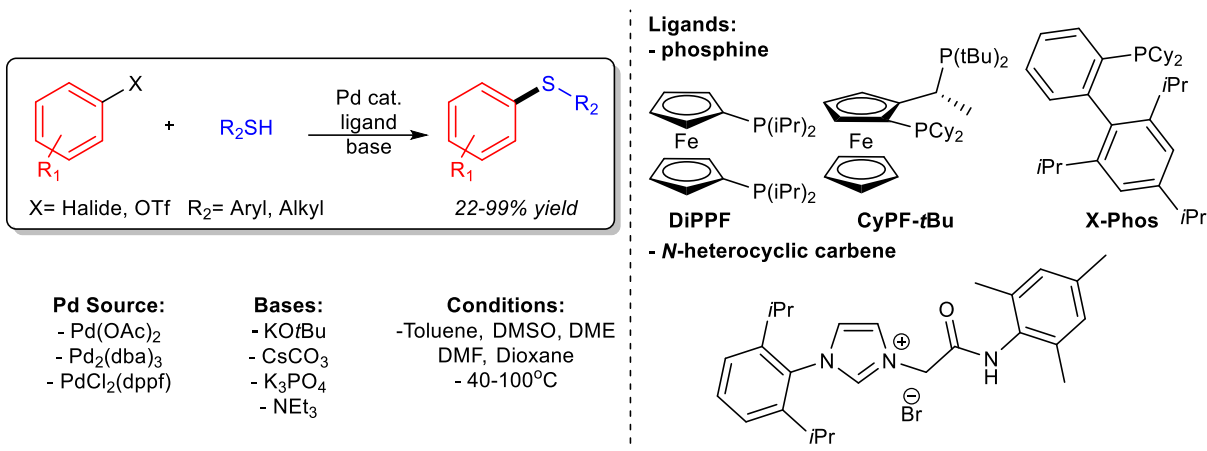
Another Pd-mediated preparation of aryl sulfides was reported in 2006 by Hartwig *et al.*, by coupling aryl chlorides with thiols using Pd(OAc)₂, the bidentate Josiphos ligand (CyPF-tBu), NaOtBu, in DME (Scheme 1.3.3.4).³⁵ Arguably the most prolific system thus far, this catalytic

system was reported to have turnover numbers of 8500 for aryl chlorides and 84000 for aryl iodides, 2 to 3 orders of magnitude greater than those of previously published catalytic systems. This is attributed to the Josiphos ligand, a highly electron-rich alkyl-biphosphine, which strongly coordinates to Pd, creating an extremely stable catalyst for the transformation. Substrate scope was broad, with the ability to tolerate phenols, amides, anilines, and carboxylic acids, in good to excellent yields.



Scheme 1.3.3.4- Hartwig's Preparation of Aryl Sulfides via Pd-Mediated Cross-Coupling of Aryl Chlorides and Thiols

Numerous alternative methods utilizing Pd-catalysis have been published and are evaluated in a variety of reviews, which include C-S bond formation through C-H bond functionalization and decarboxylation.^{23, 25-26, 36} Advancements follow a similar progression as copper-catalyzed cross-coupling, such as the movement from *tert*-butoxide base to cesium carbonate. Phosphine ligands continue to be employed with high efficiency in addition to the introduction of *N*-heterocyclic carbene species ligands, and temperatures remain elevated at 50-120°C. A general summary of the current Pd-mediated S-arylation is presented in Scheme 1.3.3.5. Recent advances in Pd-mediated S-arylations as well as other transition metal mediated processes will be discussed in the next section.



Scheme 1.3.3.5- A General Summary of Pd-Catalyzed S-Arylation Methods

1.4 Recent Advances in C-S Bond Formation

Due to the increasing significance of organosulfur compounds in biological and pharmaceutical industries, greater effort has been devoted toward the development of novel methods for their synthesis. Focus has now turned to developing milder and more efficient conditions for this transformation, as well alternatives to transition metal catalysis. These aryl-C-S bond forming reactions can be organized into four categories and will be discussed as follows. The transformations discussed here will be that of the last five years.

1.4.1. Transition Metal Catalyzed

1.4.1.1. Palladium

1.4.1.2. Copper

1.4.1.3. Other Transition Metals

1.4.2. Nucleophilic Aromatic Substitution (S_NAr)

1.4.3. Electrophilic Sulfur Strategies

1.4.4. Trifluoromethylthiolation (SCF₃) Reactions

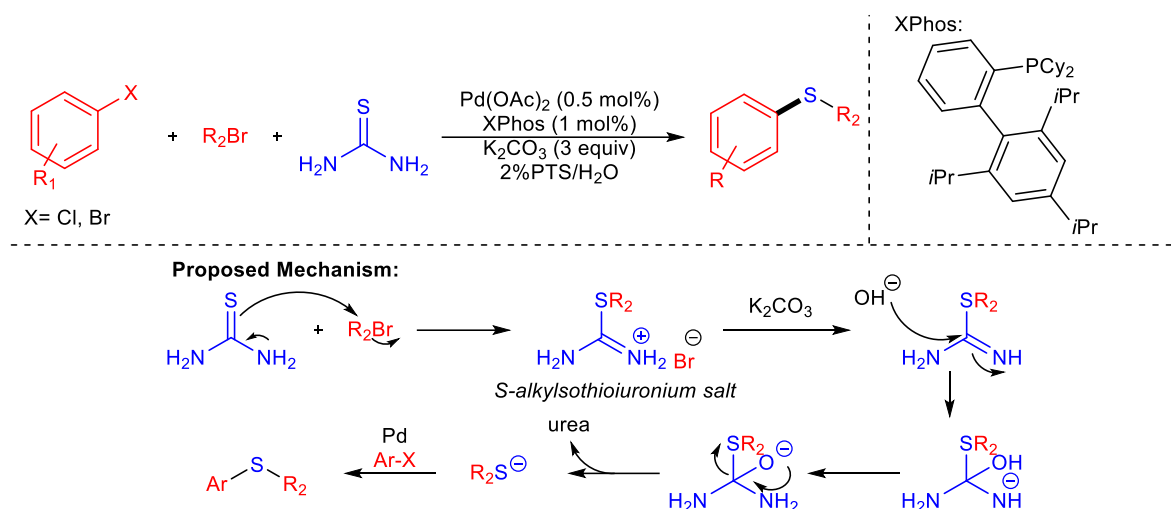
1.4.1 Transition Metal Catalyzed

Transition metal catalysis has been investigated extensively for aryl C-O and C-N bond formation and has proven to be an efficient method to forge desired key aryl C-S linkages. Many methods have been published in recent years, primarily using palladium-, copper-, and nickel-catalysis. While the method developed by Hartwig originally in 2006 is arguably still the most successful, the use of the Josiphos ligand comes at a high cost (hundreds of dollars per gram). In

addition, the coupling of *ortho*-substituted aryl groups with sulfur have all necessitated the use of transition metals palladium or copper. However, pre-existing methods still include the requirement of pre-functionalization of the starting materials, and the requirement of highly basic conditions. Thus, there are constantly novel methods being developed with the aim of using a reduced amount of or less costly transition metals and in milder conditions. Attempts have also been focused on employing alternative sulfur sources to free thiols.

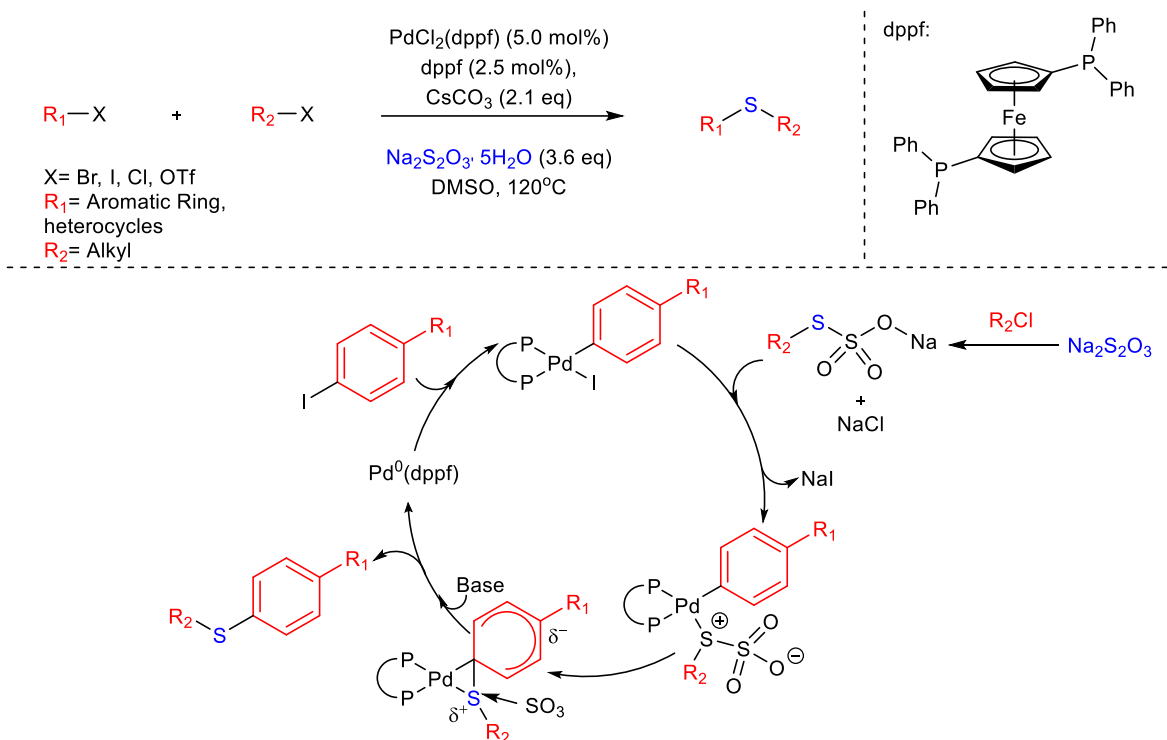
1.4.1.1 Palladium

A distinct disadvantage of using thiols is their smell and volatility. Efforts have been made to use surrogates for free thiols such as thiourea³⁷, potassium ethyl xanthogenate³⁸, and potassium thiocyanate³⁹. In 2012, Wang et al. published a one-pot Pd-catalyzed synthesis of aryl alkyl sulfides using aryl halides, thiourea, and alkyl bromides in water, along with polyoxyethynyl α -tocopheryl sebacate (PTS) as amphiphile (Scheme 1.4.1.1).⁴⁰ Substrate scope was broad both in respect to the aryl chloride and alkyl bromide. The reaction was found to be less efficient for electron-donating groups in the *para*-position of aryl chlorides, including amino, methyl, and methoxy groups, but this was compensated for with longer reaction times and elevated temperatures. A mechanism was proposed in which the thiolate is generated *in situ* through the hydrolysis of the S-alkylthioiuronium salt, the product of the reaction between thiourea and the alkyl bromide (Scheme 1.4.1.1). Following addition of hydroxide, thiolate is released, and enters into the usual Pd-mediated oxidative addition/reductive elimination cycle, as discussed above.



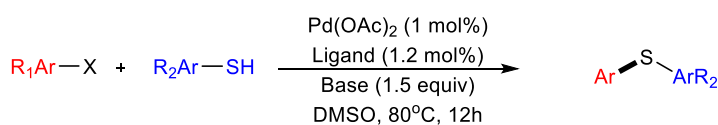
Scheme 1.4.1.1- Wang's Pd-Mediated Synthesis of Aryl Alkyl Thioethers from Aryl chlorides, Alkyl Bromides, and Thiourea

A method using sodium thiosulfate as a the source of sulfur was recently reported by Jiang *et al.* (Scheme 1.4.1.2).⁴¹ Various aryl iodides were evaluated and ones bearing electron withdrawing groups, along with various substitutions proceeded smoothly. However, electron rich substituents could not be tolerated. Various heterocyclic and secondary halides were amenable to the reaction in moderate yields. The proposed mechanism involves oxidative addition of the Pd catalyst to the aryl halide. The alkyl chloride reacts with the thiosulfate to generate an organo-thiosulfate substituted salt, which then undergoes ligand exchange with iodide on the Pd complex. Subsequent reductive elimination and release of SO₃ then furnishes the desired aryl thioether.



Scheme 1.4.1.2- A Pd-Mediated Synthesis of Aryl Alkyl Thioethers using Sodium Thiosulfate as Sulfur Source, by Jiang et al.

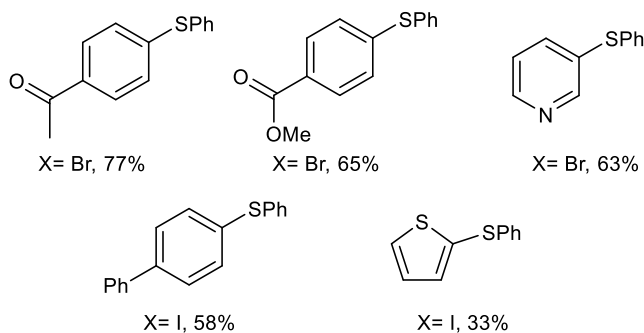
As an alternative to sensitive phosphine ligands, N-heterocyclic carbenes (NHC) have been found to be efficient ligands for Pd-mediated S-arylations.⁴² Seminal work by Lee *et al.* illustrated another Pd-catalyzed S-arylation of thiols and aryl halides employing *N*-amido imidazolium salts as ligands (Scheme 1.4.1.3).⁴³ *N*-amido imidazolium compounds, precursors to *N*-heterocyclic carbenes (NHC), had recently been reported as ligands for Pd-mediated Suzuki-Miyaura coupling reactions of aryl bromides.⁴⁴ Reaction conditions were individually optimized based on reactivity with aryl iodides and bromides. Aryl chlorides were attempted as coupling partners but most attempts were unsuccessful. Substrate scope with aryl bromides could be extended to *para*-substituted electron-withdrawing groups such as nitro or nitrile, and notably, ester and ketone functionalities could also be tolerated, albeit in moderate yields.



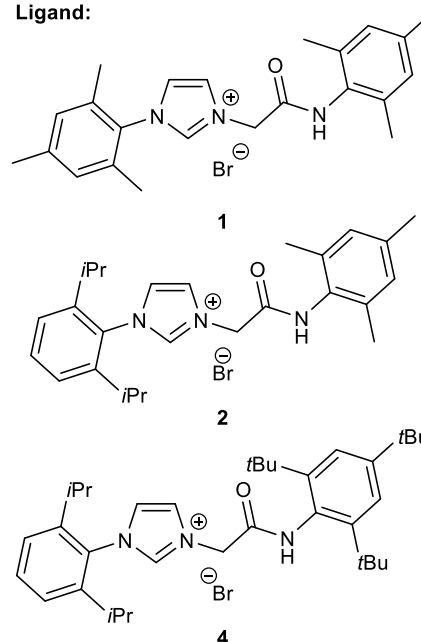
X= Br, Base= NaHMDS, Ligand **2**

X= I, Base= KOtBu, Ligand **1**

Selected Products:

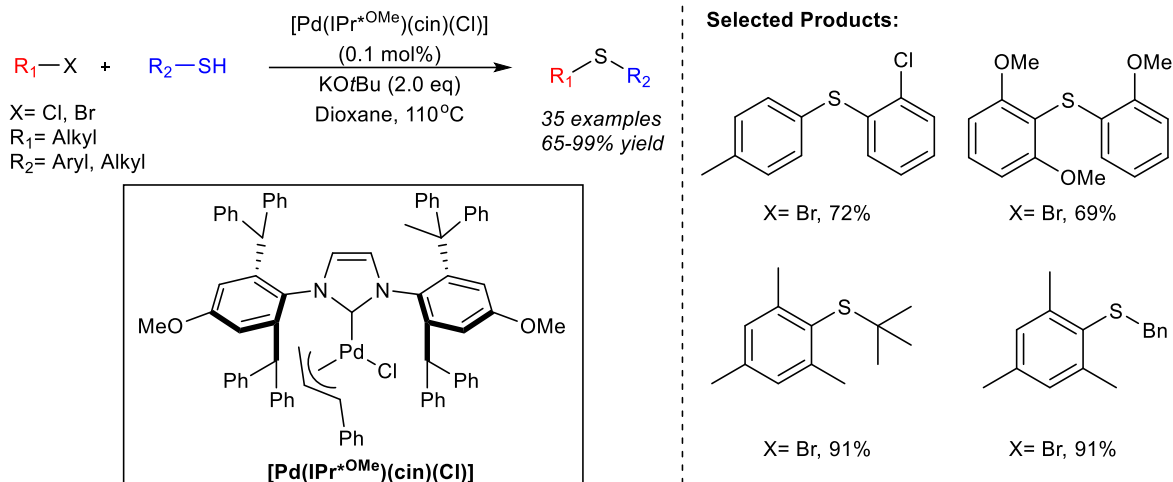


Ligand:



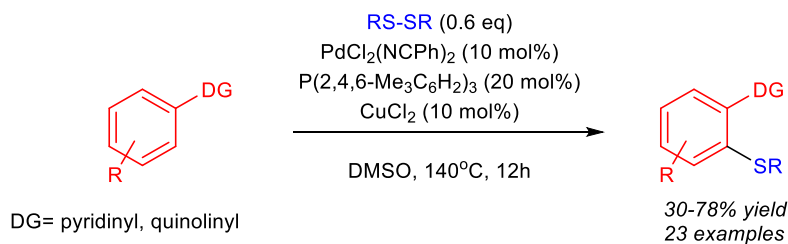
Scheme 1.4.1.3- A Pd-Mediated Preparation of Arylthioethers with N-Amidoimidazolium Salt Ligands

A novel method for the preparation of aryl sulfides from thiols and aryl halides using a Pd-NHC catalyst ($[\text{Pd}(\text{IPr}^{\text{OMe}})(\text{cin})\text{Cl}]$) was disclosed by Nolan et al in 2013 (Scheme 1.4.1.4).⁴⁵ Using KOtBu as base and dioxane as solvent, the reaction demonstrated selectivity for aryl bromides in the presence of chlorides, allowing a handle for further functionalizations. The substrate scope was broad, and furnished products in good to moderate yields. It was noted that the reaction did not proceed in the absence of KOtBu, even when using a sodium thiolate. It was thus proposed that the need for the potassium thiolate in the reaction was due to its low solubility, thereby preventing the deactivation of the Aryl-Pd^{II}Ln-SR complex by keeping the overall concentration of thiolate low. Significant drawbacks include the pre-formation of the active catalyst in a glove-box and high reaction temperatures.



Scheme 1.4.1.4- Nolan's Pd-NHC mediated Preparation of Aryl Thioethers

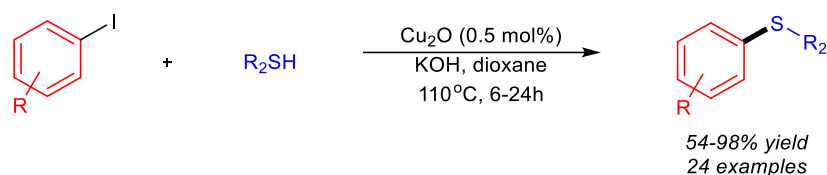
Recently, a Pd and Cu co-catalyzed direct C-H functionalization of arenes with disulfides was reported by Nishihara *et al.* (Scheme 1.4.1.5).⁴⁶ A series of 2-phenyl pyridine derivatives were examined and were found to undergo thiolation at the *ortho*- position with various electron donating and withdrawing substations on the phenyl ring. There was no conclusive mechanism proposed, but from mechanistic studies, it was determined that the proposed mechanism is dissimilar from the traditional Pd⁰/Pd^{II} catalytic cycle. Instead, they propose a Pd^{II}/Pd^{IV} mechanism similar to C-H halogenation⁴⁷ where a dimeric chloro(2-pyridylphenyl)palladium complex participates in the oxidative addition of the disulfide to generate a Pd^{IV} species, and subsequent reductive elimination to generate the aryl-S bond.⁴⁸ It is hypothesized that the remaining equivalent of thiolate is reoxidized to the disulfide in order to re-enter the catalytic cycle. However, their attempts at isolating the Pd^{IV} species were unsuccessful. It is noted that another possible mechanism involves oxidative addition of the disulfide to Cu^I to generate a Cu^{III} species, followed by transmetalation of thiolate to Pd^{II} and reductive elimination to generate the product.



Scheme 1.4.1.5- Pd-Mediated S-Arylation of Arenes with Disulfides by Nishihara *et al.*

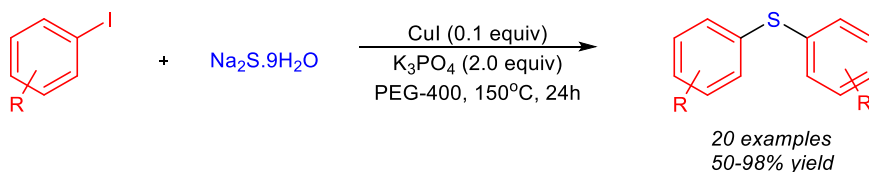
1.4.1.2 Copper

In 2011, Lee *et al.* demonstrated that Cu₂O powder could be used as an efficient copper source for the coupling of aryl iodides with thiols (Scheme 1.4.1.6).⁴⁹ In contrast to other reported methods, this transformation could be carried out with ligand-free conditions, and employed low catalyst loading. Substrates reported include diverse functionalities including esters, unprotected amines, alcohols, as well as heterocycles. In addition, primary and secondary alkyl groups were compatible. No mechanism was proposed by the authors, but may be hypothesized to undergo a catalytic cycle similar to the Ullmann reaction discussed above.



Scheme 1.4.1.6- A Ligand-Free Preparation of Aryl Thioethers with a Cu₂O Powder Catalyst, by Lee *et al.*

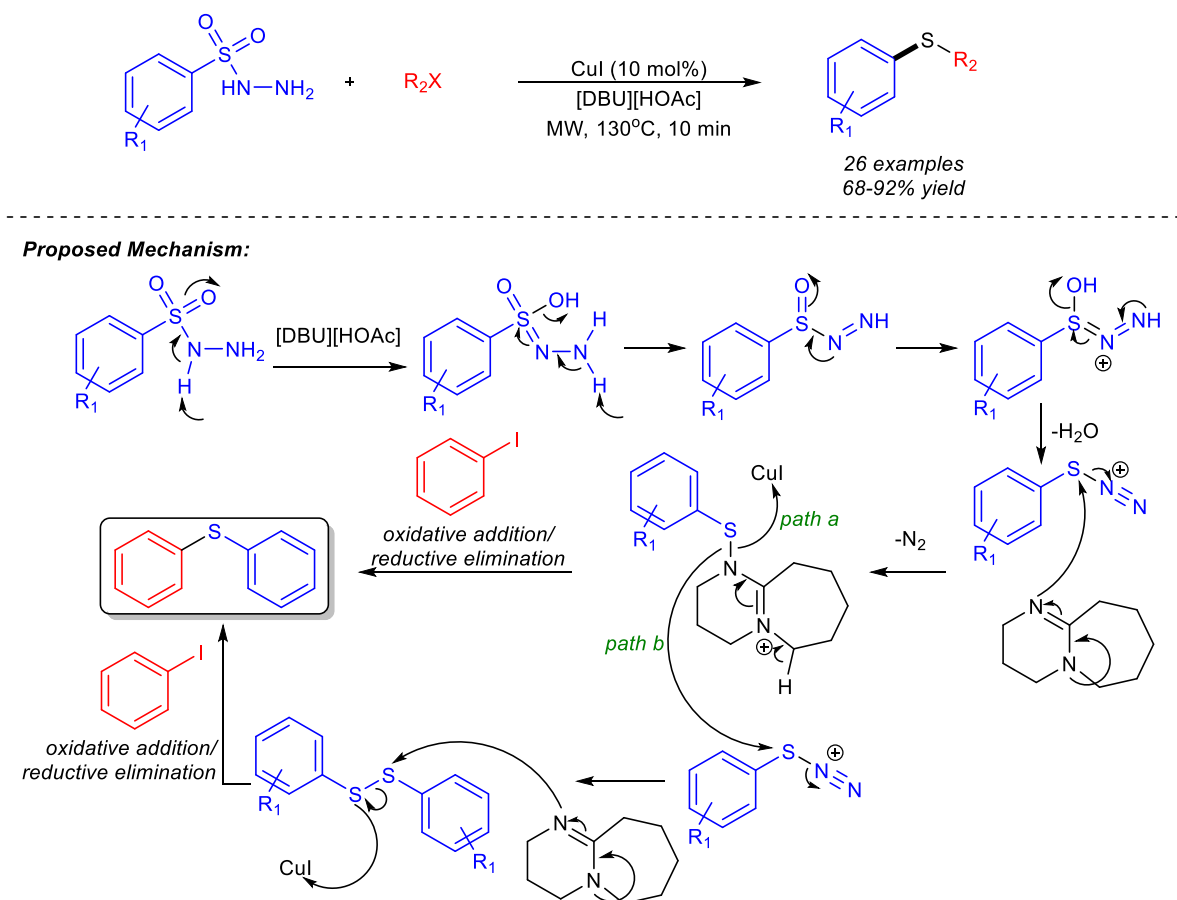
As discussed previously, attempts at finding alternative sulfur sources to free thiols has been of interest recently with Pd-mediated S-arylations. The same is true for Cu-mediated processes.^{37, 39, 50} Chen *et al.* has reported a method of Cu-catalyzed S-arylation with sodium sulfide and aryl halides (Scheme 1.4.1.7).⁵¹ However, unlike most protocols requiring the use of solvents such as DMF or dioxane, this method used PEG-400. The use of PEG-400 has recently come to light as it is non-toxic, environmentally friendly, and inexpensive. High yields were obtained for the symmetrical aryl sulfides reported with the exception of *meta*- and *para*-phenolic aryl halides.



Scheme 1.4.1.7- Chen's Cu-mediated Preparation of Symmetrical Aryl Sulfides with Aryl Halides and Sodium Sulfide, using PEG-400 as solvent

A microwave irradiated Cu-catalyzed synthesis of asymmetric aryl sulfides from aryl halides and sulfonyl hydrazides was then reported by Singh *et al.* (Scheme 1.4.1.8).⁵² A large number of aryl sulfides and alkyl benzyl sulfides were generated, all in moderate to excellent yields. The reaction was amenable to the use of a range of aryl halides, including electron-donating

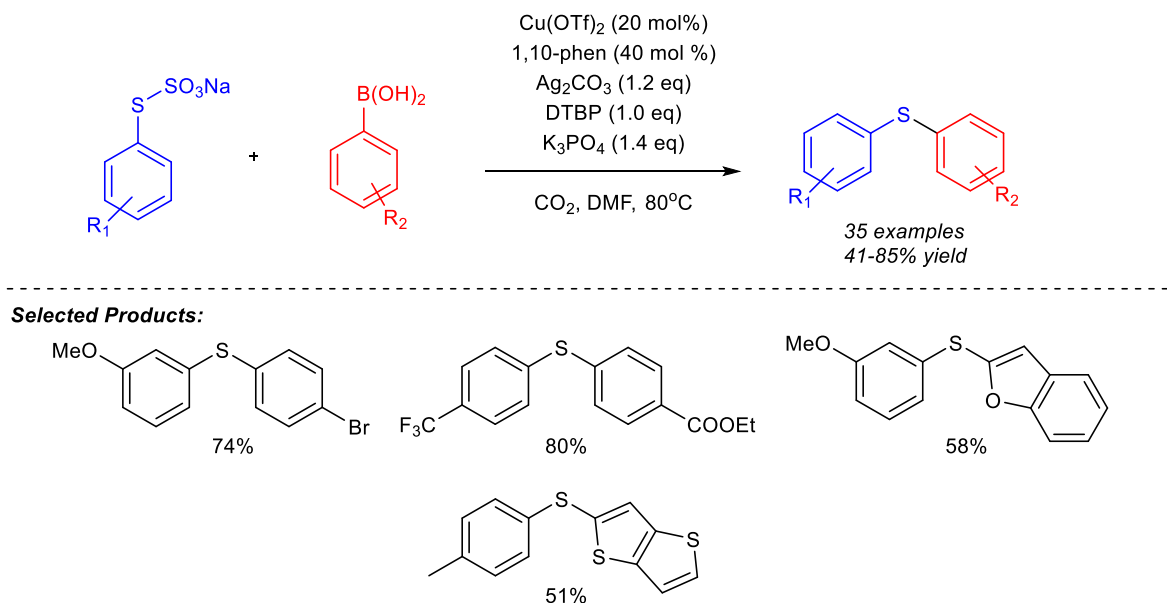
and electron withdrawing groups, as well as various substitution patterns on the sulfonyl hydrazides. Although this method presents an alternative to using free thiols, there still remains the drawback of needing to prepare the sulfur reagent, since only eight sulfonyl hydrazides are available for purchase from Sigma-Aldrich.



Scheme 1.4.1.8- Microwave-assisted Synthesis of Asymmetrical Thioethers with Aryl Halides and Sulfonyl Hydrazides as Sulfur Source, by Singh et al.

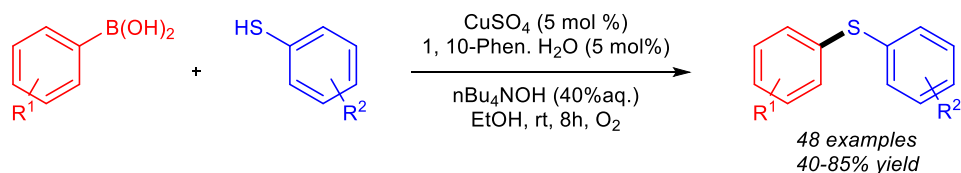
Jiang *et al.* recently reported a Cu-catalyzed oxidative cross-coupling between arylboronic acids and sodium sulfthioates as an alternative sulfur reagent (Scheme 1.4.1.9).⁵³ The reaction was also applied to the cross coupling of heteroaromatic boronic acids. 35 examples were reported, including various *ortho*-, *meta*-, and *para*- electron donating and withdrawing substituents. Various atmospheres were evaluated for the reaction conditions, including N_2 , CO , H_2 , and O_2 , but an atmosphere of CO_2 provided the highest yield of the desired product. Further studies, including TGA analysis, led the authors to hypothesize that that CO_2 suppressed the formation of disulfides in the form of physical absorption. One major drawback to the reaction conditions is that it requires

the discrete synthesis of *both* coupling partners, the prerequisite sulfathioate salt, as well as the arylboronic acid.

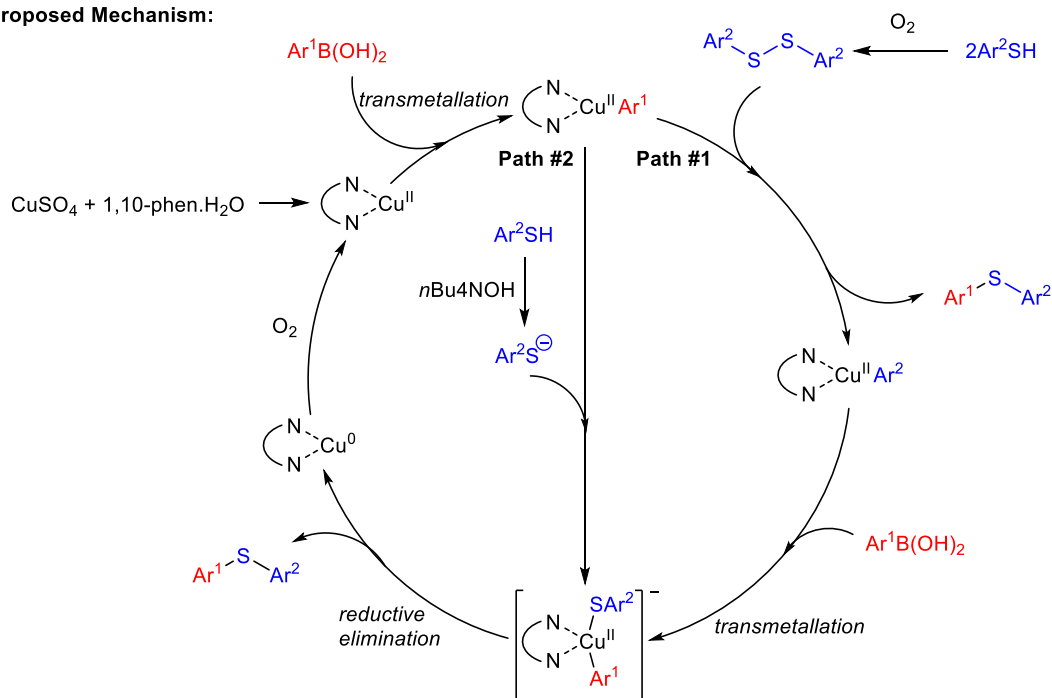


Scheme 1.4.1.9- A Cu-Mediated Synthesis of Asymmetrical Thioethers through Sodium Sulfathioates and Arylboronic Acids in a CO_2 Atmosphere , by Jiang et al.

In 2012, a Cu-catalyzed Chan-Lam type S-arylation of arylboronic acids was reported (Scheme 1.4.1.10).^{32c} Other Cu-catalyzed S-arylations with aryl boronic acids and diaryldisulfides in air or O_2 had been reported previously, but required mixed solvent systems of DMSO and H_2O at elevated temperatures of 100°C . The report in 2012 involved the use of a catalytic amount of CuSO_4 , 1,10-Phen· H_2O as ligand, and an organic base $n\text{Bu}_4\text{NOH}$ under an O_2 atmosphere at room temperature to achieve the desired S-cross coupled products. Electron-rich and -poor thiol substrates could be tolerated in moderate yields. It must be noted that this method is unable to tolerate aliphatic thiols or alkyl boronic acids. Ester and aldehyde bearing aryl boronic acids or aryl thiols were not reported. The authors proposed the following mechanism shown in Scheme 1.4.1.10. Path #2 was proposed as occurring concomitantly with Path #1 after a control experiment with 1,2-diphenyldisulfide and phenylboronic acid under the usual reaction conditions yielded singularly 67% of the desired product (vs. 83% yield observed in scope with thiophenol).



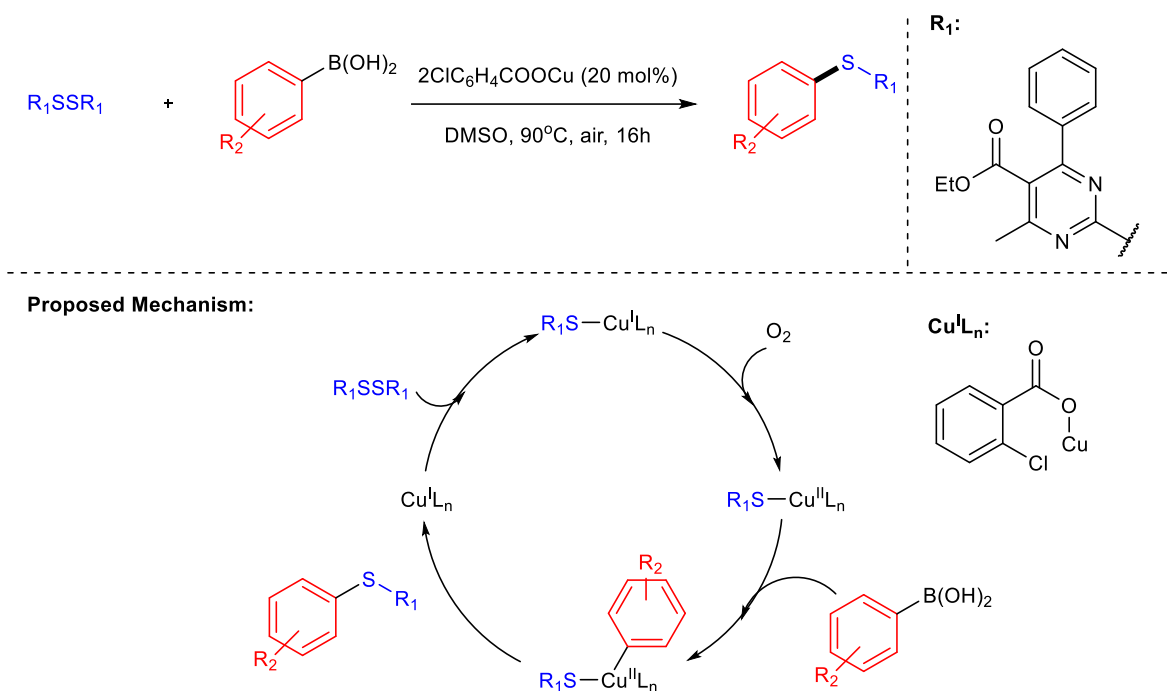
Proposed Mechanism:



Scheme 1.4.1.10- A Cu-Mediated S-Arylation of Thiols with Boronic Acids, by Feng et al.

Seminal work by Wang *et al.* describes a Cu-catalyzed cross-coupling of di(pyrimidin-2-yl) disulfides with aryl boronic acids (Scheme 1.4.1.11).⁵⁴ Various disulfides were reacted with a series of aryl boronic acids, generating a range of thioethers. *Para*-substituted aryl boronic acids were found to be compatible with the reaction, as well as *para*-substituted electron donating and electron withdrawing groups. *Meta*- and *ortho*-substituted boronic acid substrates were not reported, and nitro-, carboxyl-, and formyl- bearing substrates only resulted in trace amounts of

desired products. The proposed mechanism is depicted in Scheme 1.4.1.11, where the 2-chlorobenzoyloxy species acts as a bi-dentate ligand.

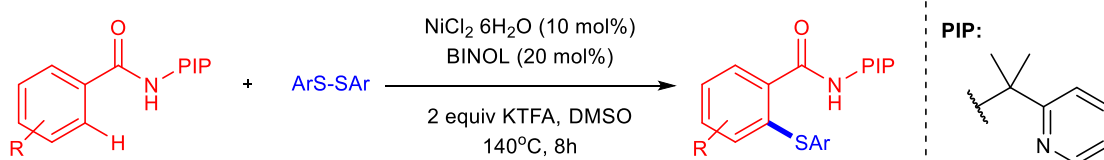


Scheme 1.4.1.11- Wang's Cu-Mediated Cross-Coupling of Di(pyrimidin-2-yl) Disulfides with Arylboronic Acids

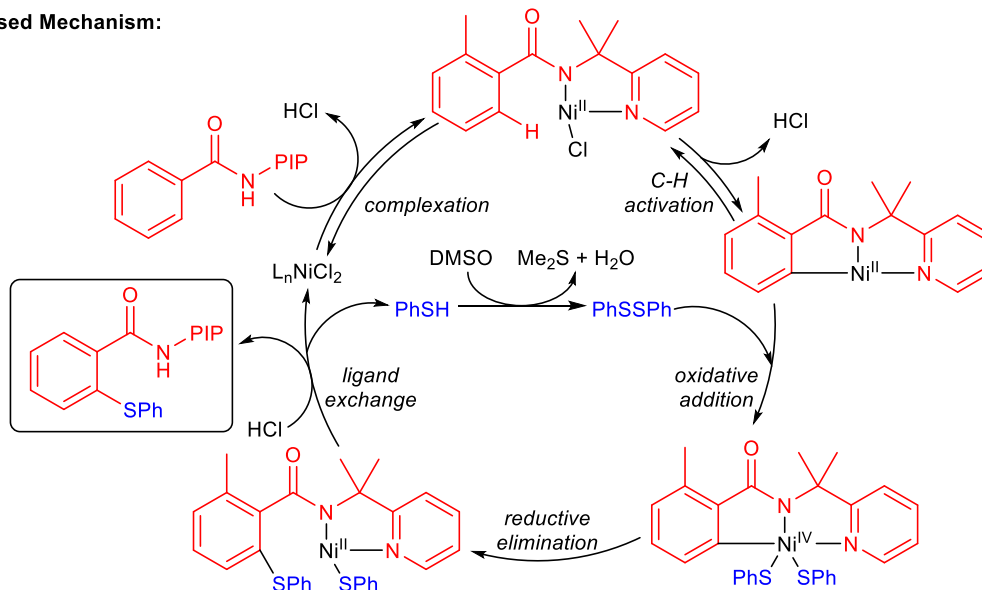
1.4.1.3 Other Transition Metals

In 2015, Shi *et al.* published a nickel-catalyzed thiolation of aryl C-H bonds with disulfides (Scheme 1.4.1.12).⁵⁵ Applying their team's recently developed PIP-directing group, a diverse range of aryl sulfides benzamides were generated. Heterocyclic benzamides such as benzothiophene, thiophene, and furan were also compatible. However, chemoselectivity could not be achieved for simpler unsubstituted aryl rings on the benzamide, where both mono- and di-thiolated products were isolated. Radical scavengers, such as (2,2,6,6-Tetramethylpiperidin-1-yl)oxyl (TEMPO) and 1,4-diphenylethylene were used to probe the reaction mechanism. These reagents were not found to affect the reactivity, leading the authors to conclude that radical intermediates were not involved. Instead, the proposed mechanism is postulated to proceed via the formation of a Ni(II) pincer complex, followed by subsequent oxidative addition of the disulfide and reductive elimination to form the desired C-S bond (Scheme 1.4.1.12). Regeneration of the disulfide from the free thiol is proposed to be mediated by DMSO.⁵⁶ Shortly after, the same research group published a similar Cu-mediated PIP-directed *ortho*-C-H functionalization with sodium sulfinates to generate aryl sulfones (Scheme 1.4.1.13).⁵⁷ Once again, the reaction was

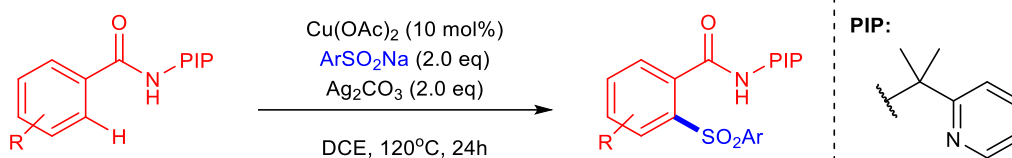
regioselective for the less sterically hindered *ortho*-position. The reaction was proposed to undergo a similar catalytic cycle with a C,N,N-pincer type Cu^{III} intermediate.



Proposed Mechanism:



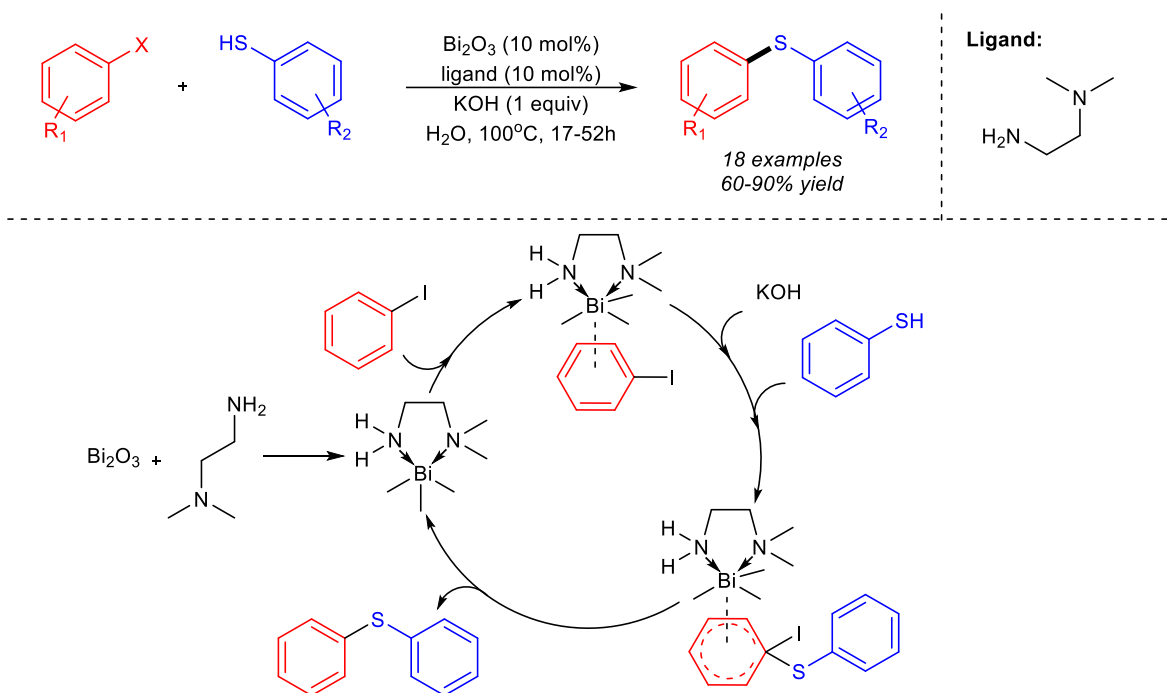
Scheme 1.4.1.12- Shi's Ni-Catalyzed C-H Activation of Arenes with the PIP Directing Group



Scheme 1.4.1.13- Cu-Mediated C-H Sulfonylation with Sodium Sulfonates

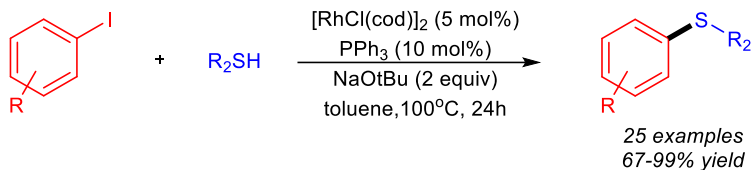
Recently, bismuth compounds have emerged as alternative catalyst for organic reactions due to its low toxicity and environmental impact. As such, a Bi^{III}-catalyzed synthesis of aryl sulfides in water was published by Chakraborty *et al.* (Scheme 1.4.1.14).⁵⁸ The reaction was found to be most efficient with substituents at either the *ortho*- and *para*- positions. Bromides and iodides were compatible with the cross-coupling, with the reaction was shown to be chemoselective for the iodide. The proposed mechanism (Scheme 1.4.1.14) for the reaction involves first the coordination of Bi₂O₃ with the ligand to form the catalytic complex, which is followed by

coordination of the aryl halide to this complex. Subsequently, the thiolate attacks this complex, followed by elimination to generate the aryl-sulfide product.

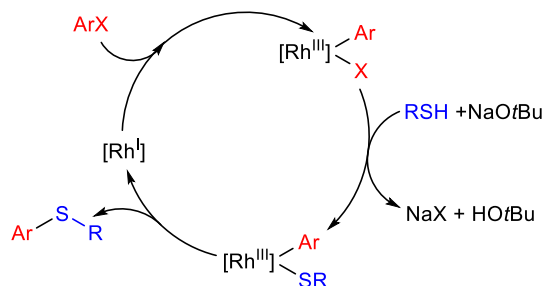


Scheme 1.4.1.14- A Bi^{III}-Mediated Synthesis of Aryl Sulfides in Water, by Chakraborty *et al.*

Rhodium has also been regarded as an effective metal for heteroatom-bond forming reactions, including C-C⁵⁹, C-N⁶⁰, and C-O⁶¹. However, there are few protocols that forge C-S bonds.⁶² In 2012, Lee *et al.* reported a Rh-catalyzed cross-coupling of aryl iodides with thiols (Scheme 1.4.1.15).⁶³ A total of 25 examples were published, with electron donating and withdrawing groups at the *para*-position of the aryl iodide. Primary and secondary aliphatic thiols were also compatible with the reaction. There were no mechanistic studies performed in this study in addition to no proposed mechanism, but the reaction is likely to undergo the general Rh^I/Rh^{III} cycle as shown in Scheme 1.4.1.15.

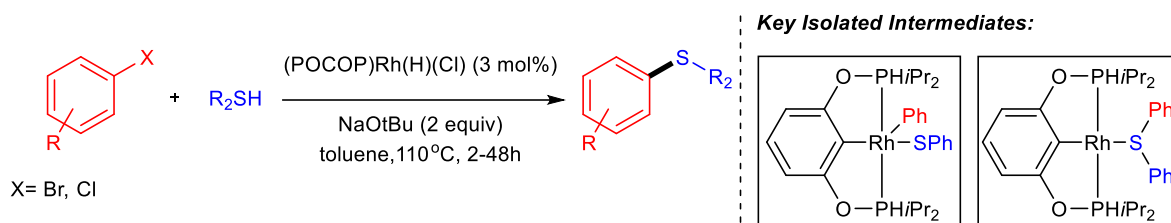


General Rh^I/Rh^{III} Catalytic Cycle for Coupling of Aryl Halides with Thiols:

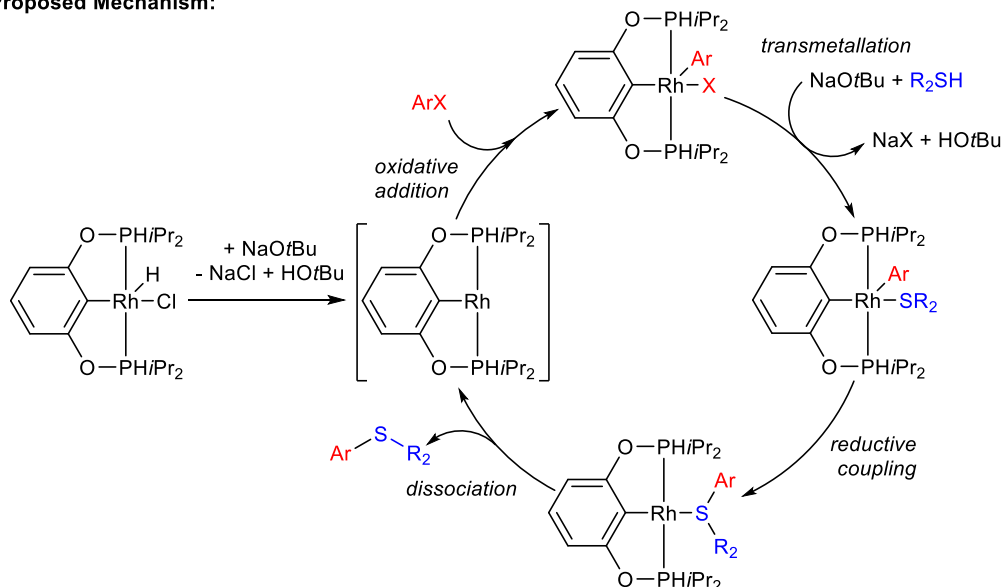


Scheme 1.4.1.15- Lee *et al.*'s Rh-Catalyzed Preparation of Aryl Iodides with Thiols

Recently, Ozerov *et al.* published a defined Rh-catalyzed cross-coupling of aryl chlorides and bromides with thiols using a POCOP pincer ligand (Scheme 1.4.1.16).⁶⁴ Various aryl sulfides were synthesized with *para*- substituents, *ortho*- substituents were tolerated but only on the thiol coupling partner. The authors highlighted certain trends that complement trends in the reactivity of this system that are also found with Pd-catalysis. Aryl bromide substrates were found to be more reactive than aryl chloride substrates, and electron-poor aryl halides also reacted quicker. Primary and secondary thiols were found to be more reactive than aryl thiols. Lastly, increasing the steric bulk on the substituents inhibited the reaction, but the thiol and aryl halide coupling partners affect the catalysis to a different degree. Mechanistic intermediates of the transformation were isolated and characterized by single crystal X-ray diffractometry, and from this a mechanism was proposed, shown in Scheme 1.4.1.16.

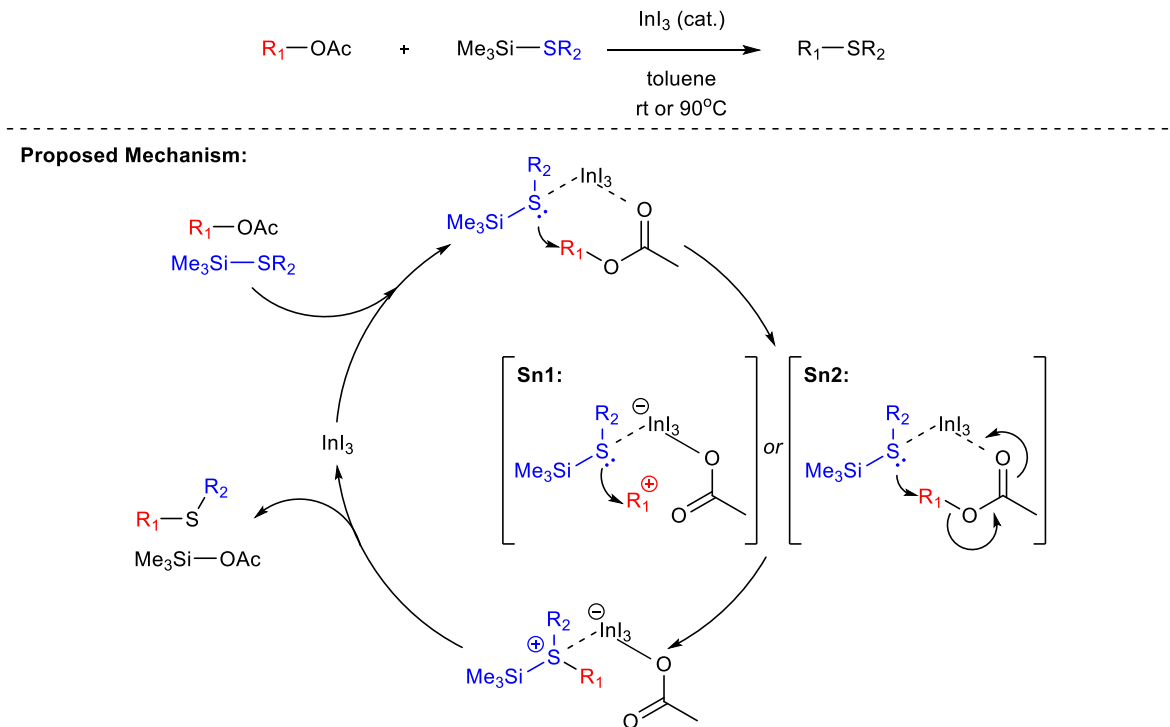


Proposed Mechanism:



Scheme 1.4.1.16- Ozerov et al.'s Rh-Catalyzed Synthesis of Aryl Thioethers

An indium triiodide catalyzed coupling of alkyl acetates with thiosilanes was reported by the research group of Baba.⁶⁵ Notable substrates include benzylic acetates containing both electron withdrawing and donating substitutions, in addition to significantly sterically hindered substrates such as adamantyl groups. The mechanism for this transformation is suggested to be dependent on the alkyl acetate substrate, and has two pathways: 1) It may undergo a $\text{S}_{\text{N}}1$ mechanism, via a carbocation intermediate, in the case of 2° and 3° alkyl, benzylic, propargylic, allylic substrates, or 2) through an $\text{S}_{\text{N}}2$ pathway for 1° alkyl and α -acetoxy substrates (Scheme 1.4.1.17).

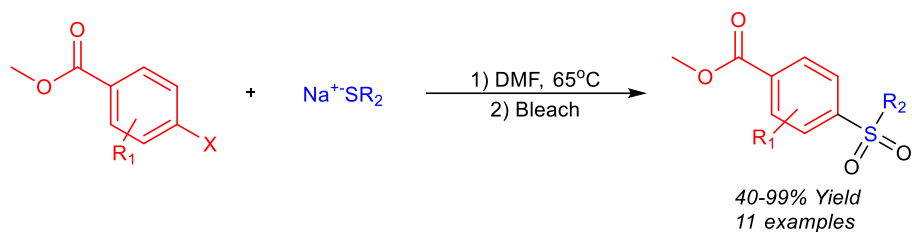


In general, transition metal catalysis is a thoroughly developed avenue in forging desired aryl C-S linkages. Existing systems make use of primarily palladium and copper catalysis, but as shown above, these are not limited to such but also include metals such as nickel, rhodium, indium and bismuth. Sulfur sources have begun to expand from simple free thiols to disulfides, thioureas, thiosulfates, sulfothioates, and hydrazides. However, it remains that current protocols still necessitate the use of elevated temperatures and harsh bases. In addition, the use of aryl halides and arylboronic acids demands the requirement of pre-functionalization of starting material. Therefore, in order to improve atom- and step-economy, other methods must also be considered and developed for the area of S-arylation.

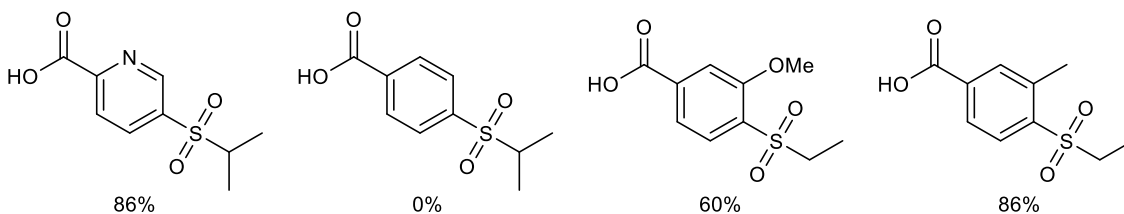
1.4.2 Nucleophilic Aromatic Substitution, $\text{S}_{\text{N}}\text{Ar}$ Mechanisms:

$\text{S}_{\text{N}}\text{Ar}$ strategies are appealing due to their mild conditions, low environmental impact, and no requirement for extraneous ligands or transition metal catalysis. A number of S-arylations proceeding through a $\text{S}_{\text{N}}\text{Ar}$ pathway have been developed.⁶⁶ A one-pot synthesis of 4-sulfonyl benzoic acids through $\text{S}_{\text{N}}\text{Ar}$ was disclosed by Frieman (Scheme 1.4.2.1).⁶⁷ Sodium thiolates were reacted with various 4-methyl ester substituted aryl halides in DMF at 65°C to generate 4-substituted sulfone benzoic acids after an oxidative bleach workup. Aldehyde and methoxy

functionalities could be tolerated but *ortho*-substituents (with respect to the methyl ester) were not, highlighting a significant limitation.

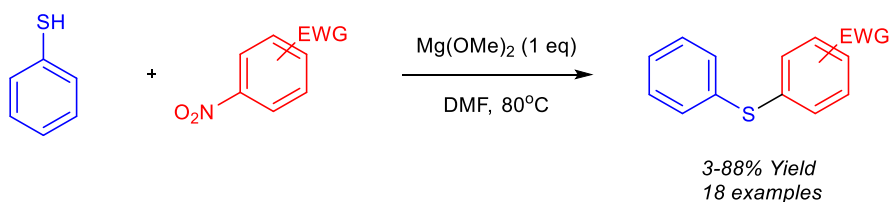


Selected Products:

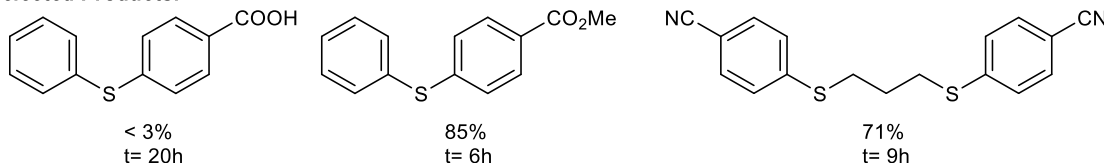


Scheme 1.4.2.1- Frieman's One-Pot Synthesis of 4-sulfonyl benzoic acids

A synthesis of aryl thioethers through displacement of nitrite in electron-deficient nitroarenes was reported by Naeimi *et al.* (Scheme 1.4.2.1).⁶⁸ It had been previously disclosed that displacement of a nitro group by thiolates occurs easily at room temperature.⁶⁹ Electron-withdrawing substituted nitroarenes were tolerated, including formyl, ketone, nitro, and cyano groups. However, unactivated substrates such as nitrobenzene and 3-nitrobenzaldehyde did not yield any product. Interestingly, the use of 1,3-propanedithiol yielded the disubstituted diphenyl product in good yields.



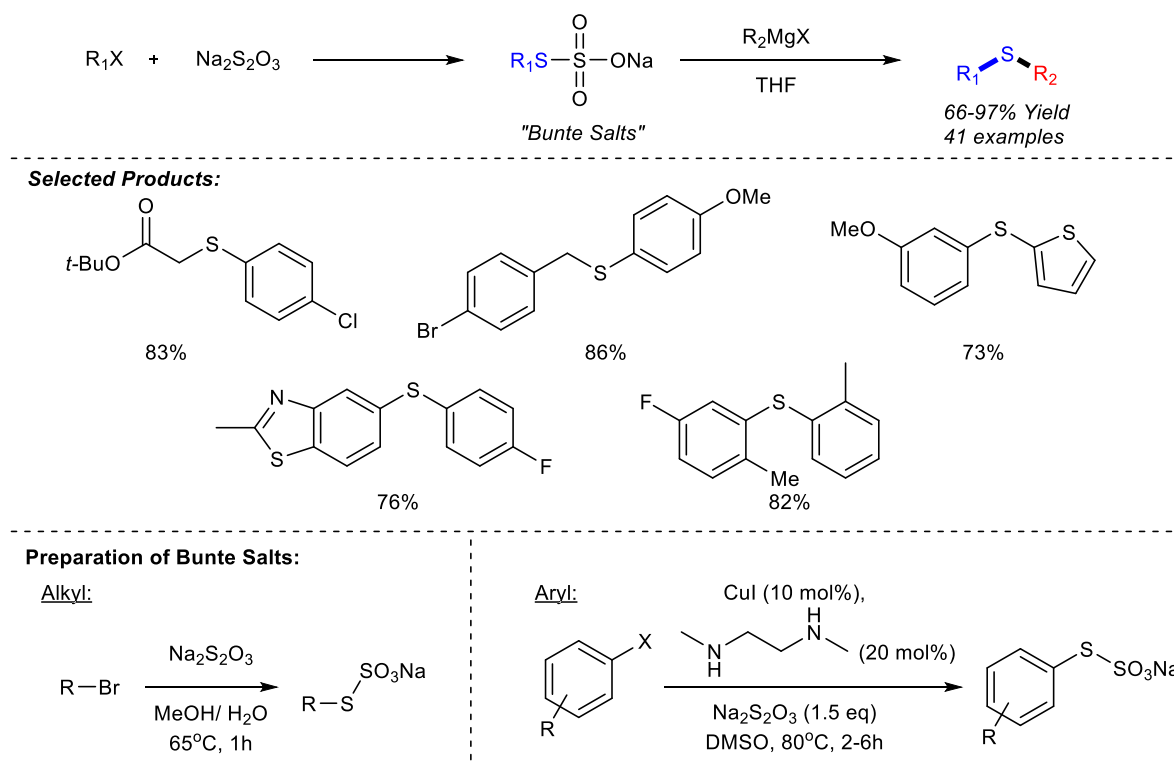
Selected Products:



Scheme 1.4.2.2- Naemi's Preparation of Aryl Thioethers from Electron-Deficient Nitroarenes

As in the case with transition metal catalysis, efforts have been directed to finding alternative sulfur sources in S-arylations. A noteworthy route to aryl sulfides via reaction of

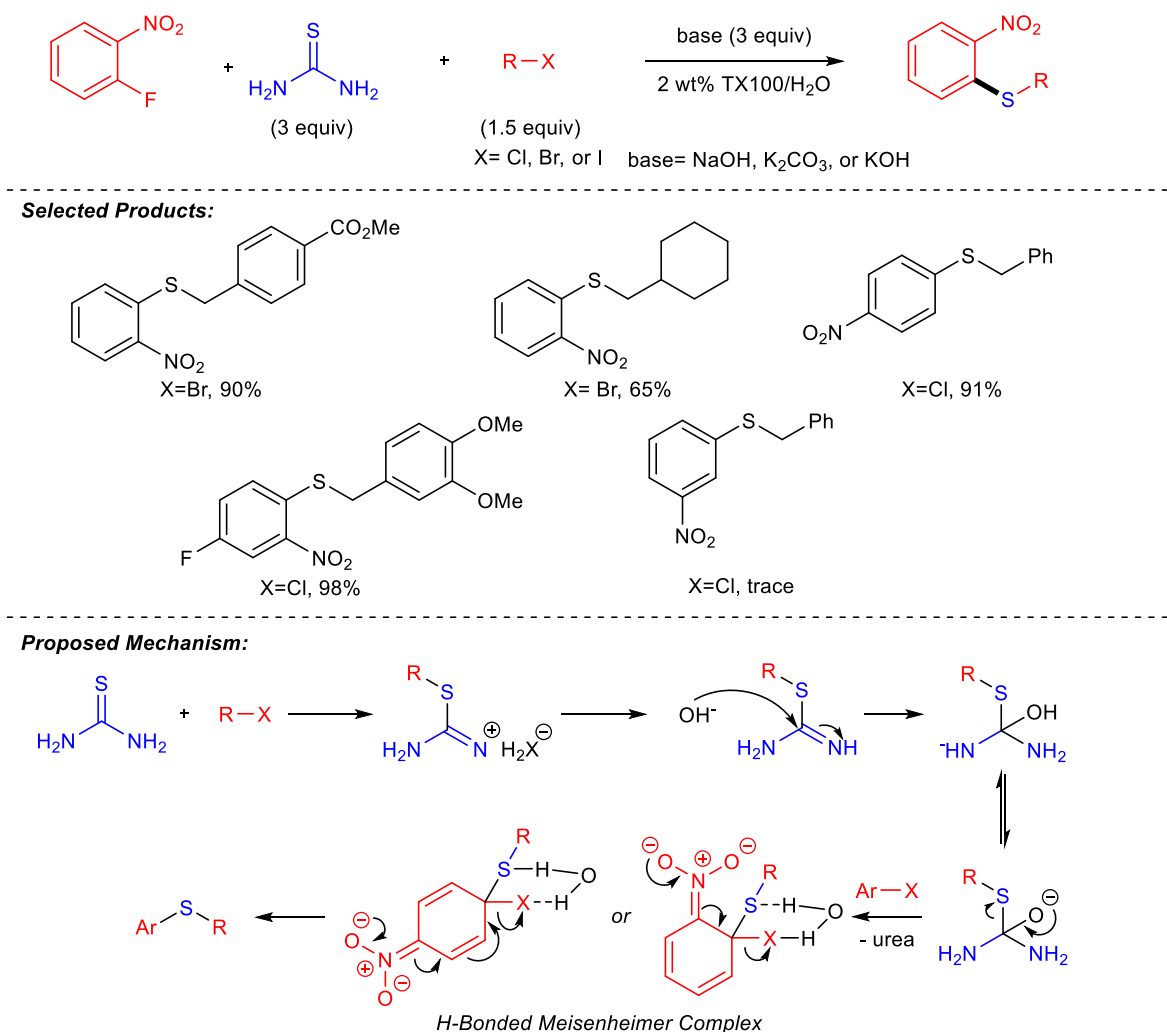
Grignard reagents with “Bunte Salts” was described by Reeves *et al.* in 2014 (Scheme 1.4.2.3).⁷⁰ Alkyl bunte salts were prepared by reaction of an alkyl halide with sodium thiosulfate, however, preparation of the aryl bunte salts required a different method. Various alkyl, aryl, heteroaryl, vinyl and alkynyl Grignard reagents were reported to be effective, along with a diverse number of bunte salts including benzylic, primary, secondary, allylic, propargylic and vinylic. In the case of aryl bunte salts, electron donating and withdrawing substituents in *ortho*-, *meta*- or *para*-positions were tolerated. The desired aryl sulfides were produced in good to excellent yields, however, drawbacks include the lack of atom economy in the reaction and the requirement for purchasing or synthesizing pre-functionalized organic halides. In addition, only substrates that are stable to Grignard reagents are tolerated.



Scheme 1.4.2.3- Synthesis of Aryl and Alkyl Sulfides via Reaction of Bunte Salts with Grignard Reagents by Reeves et al.

In 2014, a one-pot synthesis of nitroaryl thioethers was reported by Lu *et al.* (Scheme 1.4.2.4).⁷¹ Various sulfides were produced through an *in situ* generation of *S*-alkylisothiuronium salts from thiourea, nitro aryl halides, and organic halides in a Triton X-100 aqueous micelle solution. With respect to the organic halide, benzyl halides reacted readily, as well as vinyl and alkyl substrates. The authors proposed an addition-elimination mechanism (Scheme 1.4.2.4). It

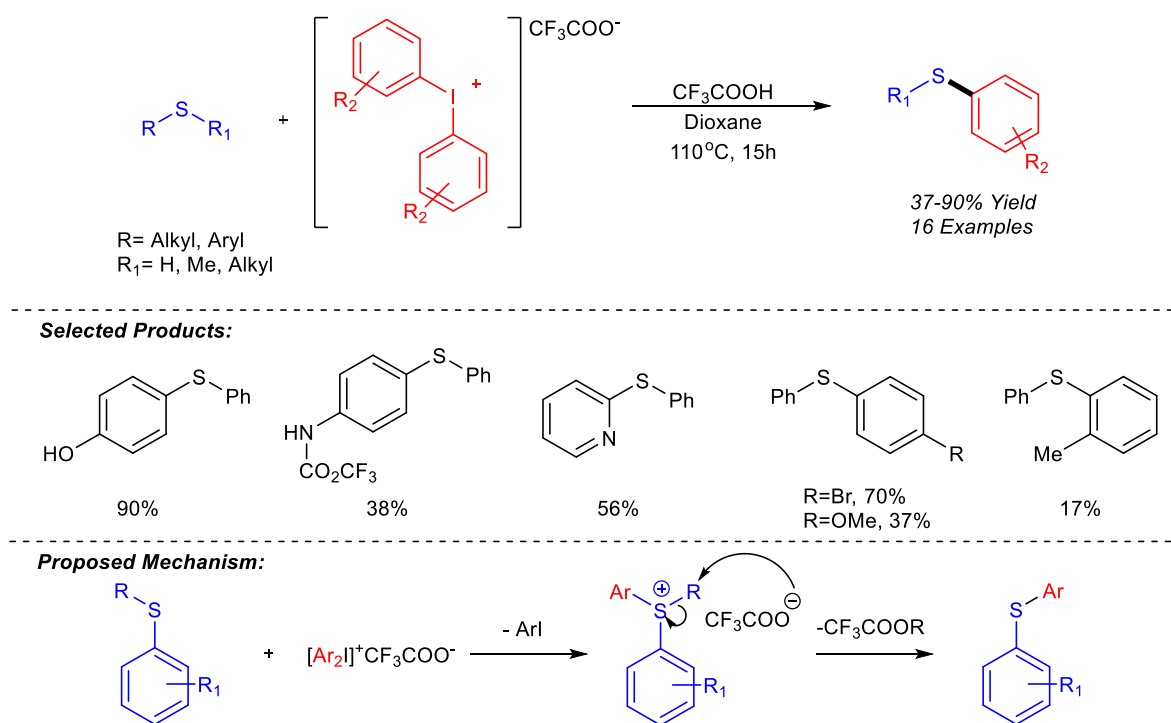
was found that the electronics of the reaction, and its ability to form a hydrogen-bonded Meisenheimer complex, affected the scope greatly. Thus, 3-nitrobenzene halides, which are unable to form this complex, were not amenable to the reaction and only traces of the desired product were isolated after extended reaction times.⁷² The role of the Triton X-100 micelles was hypothesized to aid the reaction by allowing the base to be in contact with the substrates due to their large interfacial area. Additionally, the micelles were hydrophobic enough to exclude fluoride ion and urea, which consistently drove the reaction forward.



Scheme 1.4.2.4- Synthesis of nitro-Thioethers through S-alkylisothiuronium Salts from Thiourea by Lu et al.

The vast majority of methods discussed thus far for the generation of aryl sulfides has required the use of transition metal catalysts or strongly basic conditions. In contrast, in 2014, Sanford *et al.*⁷³ reported a preparation of aryl sulfides with diaryliodonium salts from thiols or

thioanisoles, through a triflic acid-mediated coupling (Scheme 1.4.2.5). Diaryliodonium salts were prepared from a reaction of aryl iodides and arylboronic acids according to a previously reported method by Olofsson⁷⁴, and subsequent anion exchange. The mechanism was proposed to proceed via a sulfonium salt intermediate, which then undergoes nucleophilic substitution (Scheme 1.4.2.5). Various aryl sulfides were generated in low to good yields. Electron rich and poor thioanisoles could be tolerated, in addition to primary and secondary alkyl thiols, however, tertiary alkyl thiols were not reported. Notable substrates include pyridine and quinoline-substituted thiols, which are typically incompatible with transition metal catalysis.

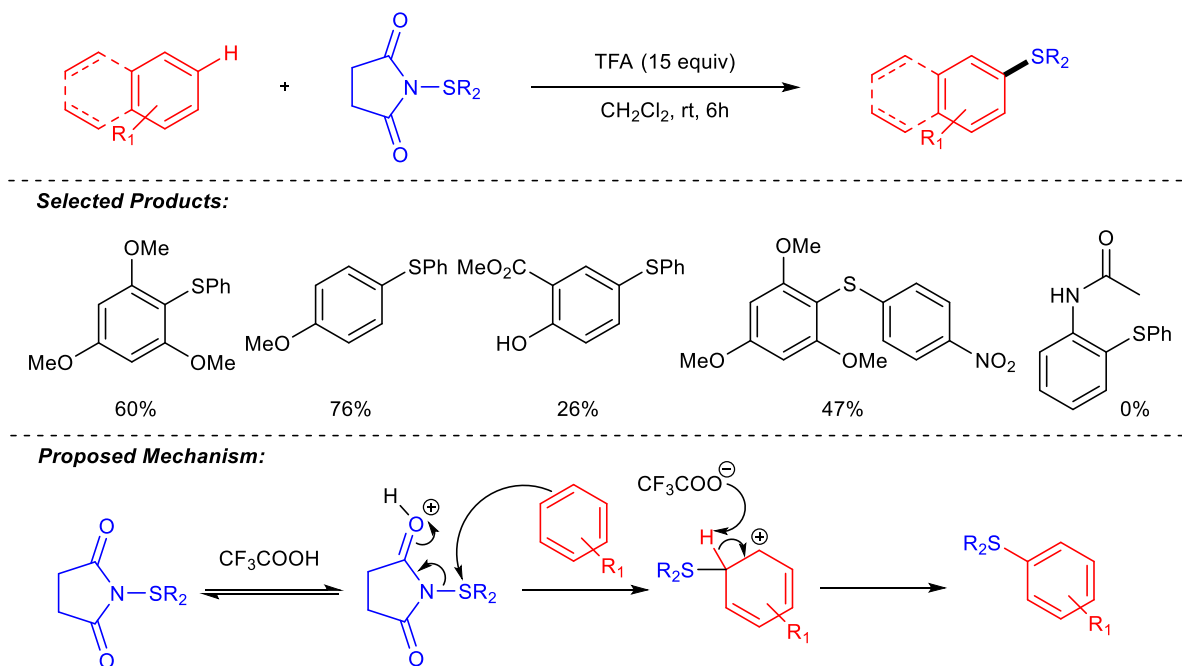


Scheme 1.4.2.5- Sanford's Triflic Acid Mediated Coupling of Disulfides with Diaryliodonium Salts

1.4.3 Electrophilic Sulfur Strategies

Strategies involving electrophilic sulfur species have begun to emerge as viable approaches for S-arylation. Cossy *et al.* recently reported a C-H sulfenylation of arenes using alkylthio- and arylthio- succinimides in the presence of TFA at room temperature (Scheme 1.4.3.1).⁷⁵ Various arenes were reacted with the optimized conditions and were found to be regioselective according to Holleman's rules governing electrophilic aromatic substitution (In general, electron-donating substituents direct substitution in the order of *para* > *ortho* > *meta*, where electron-withdrawing substituents direct substitution in order of *meta* > *ortho* > *para*).^{76,77} The reaction was not

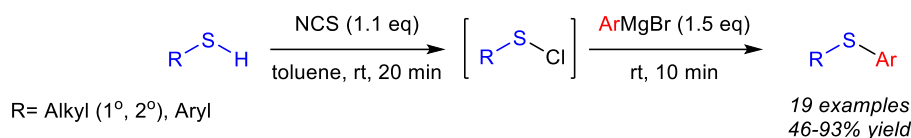
compatible with acetanilide arenes or nitro aryl succinimides. Based on the scope and the reactivity, a mechanism was proposed and is shown in Scheme 1.4.3.1. Although moderate to high yields were achieved for most substrates, the scope is limited to electron-rich arenes due to the inherent mechanism of the reaction.



Scheme 1.4.3.1- Cossy's Sulfonylation of Arenes with Alkyl and Aryl Thio-Succinimides

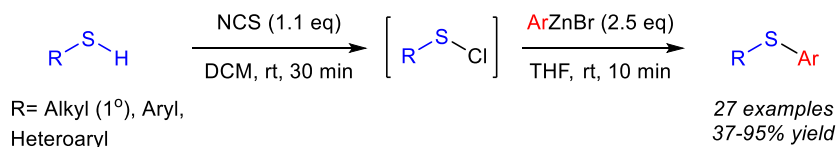
Another approach to generating aryl sulfides has been the use of sulfonyl chlorides as a sulfur source. The generation of the sulfonyl chloride from sulfuryl chloride or chlorine typically results in low yields and has limited scope. Conversely, the formation of sulfonyl chlorides from N-chlorosuccinimide has been reported.⁷⁸ This milder method allowed for a broader substrate scope, including thermally unstable alkyl sulfonyl chlorides.

Lee *et al.* published a synthesis in 2012 of aryl sulfides through N-chlorosuccinimide activation of thiols (Scheme 1.4.3.2).⁷⁹ Here, they performed an *in situ* generation of the electrophilic sulfonyl chloride, which was then reacted with a Grignard reagent to generate the desired aryl sulfide. Various alkyl (1°, 2°) and aryl substrates were generated in moderate to excellent yields, including one example bearing an ester functionality. However, *ortho*-bearing aryl thiols Grignard reagents were not reported.



Scheme 1.4.3.2- A Preparation of Aryl Thioethers from Grignard Reagents and Sulfenyl Chlorides arising from N-Chlorosuccinimide

In 2014, a similar synthesis was reported by Jarvo *et al.* using another organometallic nucleophile (Scheme 1.4.3.3). Here, they generated diaryl and heteroaryl sulfides from sulfenyl chlorides and arylzinc reagents, as opposed to Grignard reagents.⁸⁰ Due to the use of arylzinc reagents, *para*-ketone-functionalities could also be tolerated, unlike the previously discussed method employing Grignard reagents. A broad range of heterocyclic functionalized thiols including benzothiazoles, benzoxazoles, tetrazole, pyrimidine, oxadiazole, and imidazoles were also amenable to the reaction.



Scheme 1.4.3.3- Synthesis of Arylthioethers from Arylzinc Reagents and Sulfenyl Chlorides, by Jarvo et al.

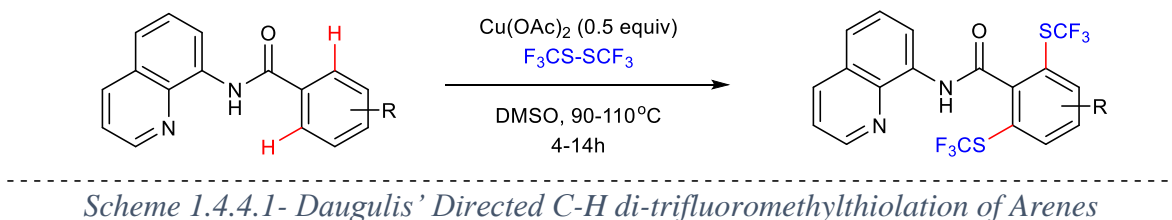
As demonstrated, S-arylation umpolung strategies involving an electrophilic sulfur have allowed for much milder approaches. The examples highlighted above have shown general functional group tolerance in moderate to high yields. Reaction times required at ambient temperatures are well below the usual 8-16h reaction lengths seen in transition metal catalysis. A key notable advantage is the absence of the requirement for designer ligands and harsh bases. Given this potential, it is expected that developments in this area of S-arylation will continue to be explored, as well as approaches to alternative sulfur sources.

1.4.4 Development of Trifluoromethylthiolation (SCF₃) Reactions

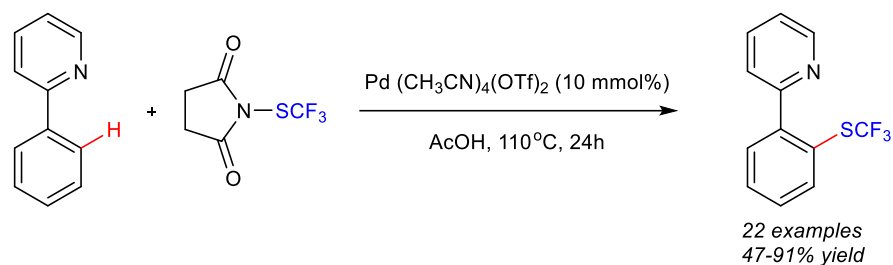
Due to their medicinal and pharmaceutical potential, the synthesis of SCF₃-containing compounds has been of great interest. It is a functional group that is targeted often due to its high lipophilicity (Hansch parameter= 1.44⁸¹), metabolic stability, and imparts to compounds the ability to easily cross lipid membranes. Early efforts to install SCF₃ groups included halogen-fluorine exchange reactions of halogenated methyl thioethers⁸² and trifluoromethylation of sulfur compounds such as thiols, disulfides, and thiocyanates.⁸³ Initial developments included radical

transformations^{83a, 84}, electrophilic processes^{83a, 85}, and nucleophilic SCF₃ installations^{83a, 84b, 86}. These are detailed more thoroughly in recent reviews by Billard⁸⁷ and Toste⁸⁸. There have also been a few examples of trifluoromethylthiolation of aryl halides^{86c, 89}. However, recent efforts have been led toward direct C-H trifluoromethylthiolation techniques.

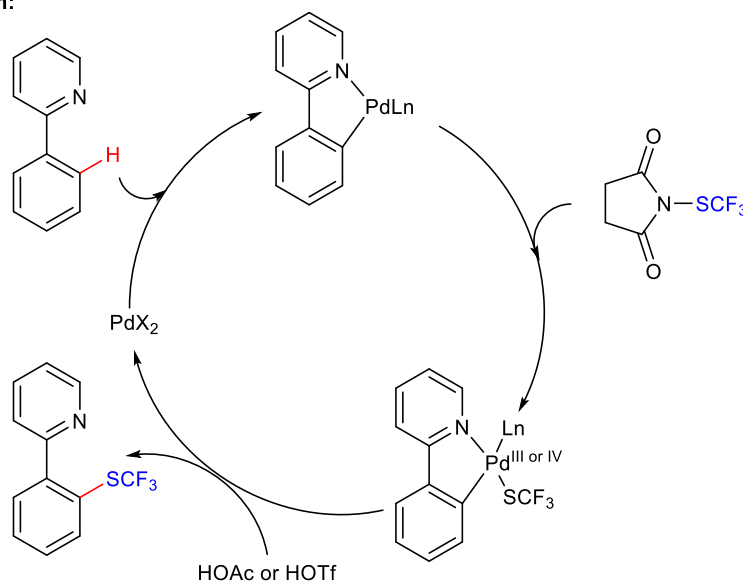
The first method for direct C-H di-trifluoromethylthiolation of arenes was reported by Daugulis *et al.*⁹⁰, using a sub-stoichiometric amount of Cu (Scheme 1.4.4.1). However, the reaction could not be controlled to yield the mono-trifluoromethylthiolation, and also utilized the toxic reagent CF₃SSCF₃. There were no studies done to probe the mechanism of the reaction, but the authors alluded to it proceeding via a Cu^{III}-intermediate. They note that sulfides are able to stabilize Cu^{III}⁹¹, and in some cases are able to oxidize Cu^I to Cu^{III}⁹². In addition, they point out that Stahl has recently demonstrated that nucleophiles react with aryl-Cu^{III} complexes to yield the C-heteroatom coupled products.⁹³



Recently, Shen *et al.* reported the first Pd-catalyzed mono-trifluoromethylthiolation of aryl C-H bonds (Scheme 1.4.4.2).⁹⁴ A range of SCF₃-substrates were generated in good to moderate yields, and no di-trifluoromethylthiolated products were observed. The reaction was found to be regioselective for the less sterically hindered position on the arene *ortho*- to the directing group. Various substitution patterns on the arene were tolerated for methyl and alkoxy functional groups, in addition to naphthalenes and benzothiophenes. Mechanistic studies were conducted and it was determined that the C-H activation was not the rate-limiting step of the reaction. It was suggested that it was possible for the mechanism to proceed through a Pd^{IV}-complex. Upon these studies, a mechanism was proposed for the reaction (Scheme 1.4.4.2). Still, the authors were unable to provide evidence of the oxidative-addition product in the catalytic cycle, and thus suggest that an alternative mechanism of Pd-C bond cleavage/C-SCF₃ formation can proceed by electrophilic substitution.

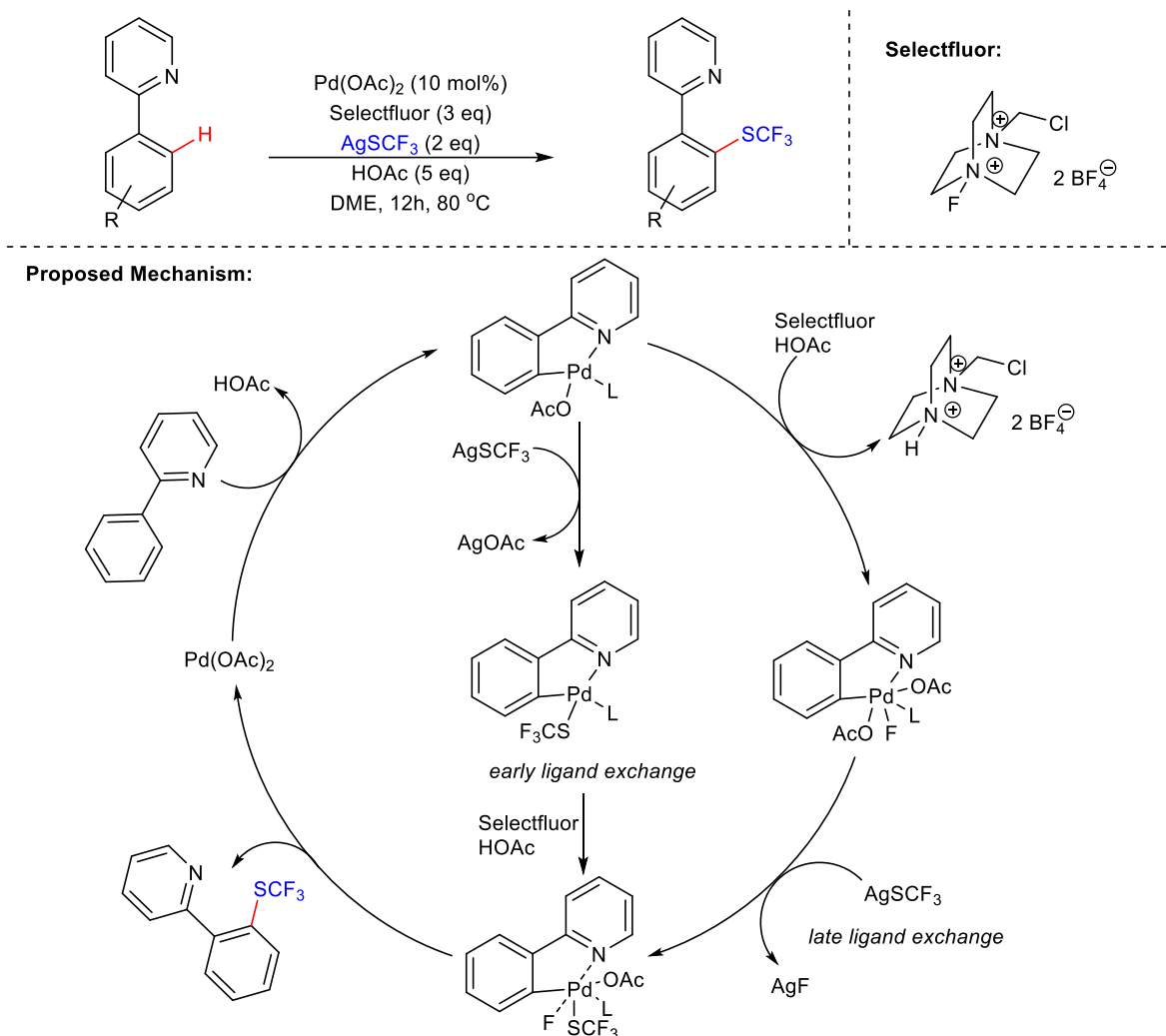


Proposed Mechanism:

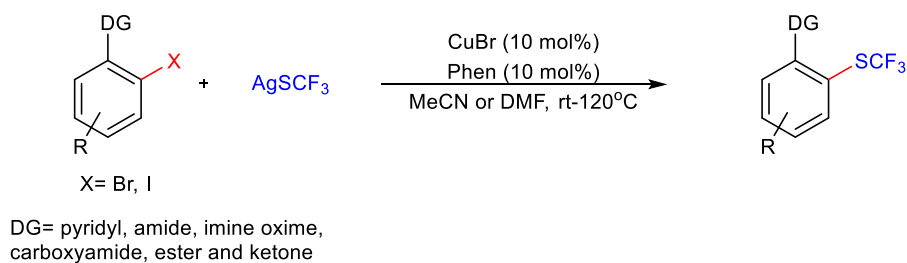


Scheme 1.4.4.2- A Pd-Mediated C-H Trifluoromethylthiolation of Arenes by Shen *et al.*

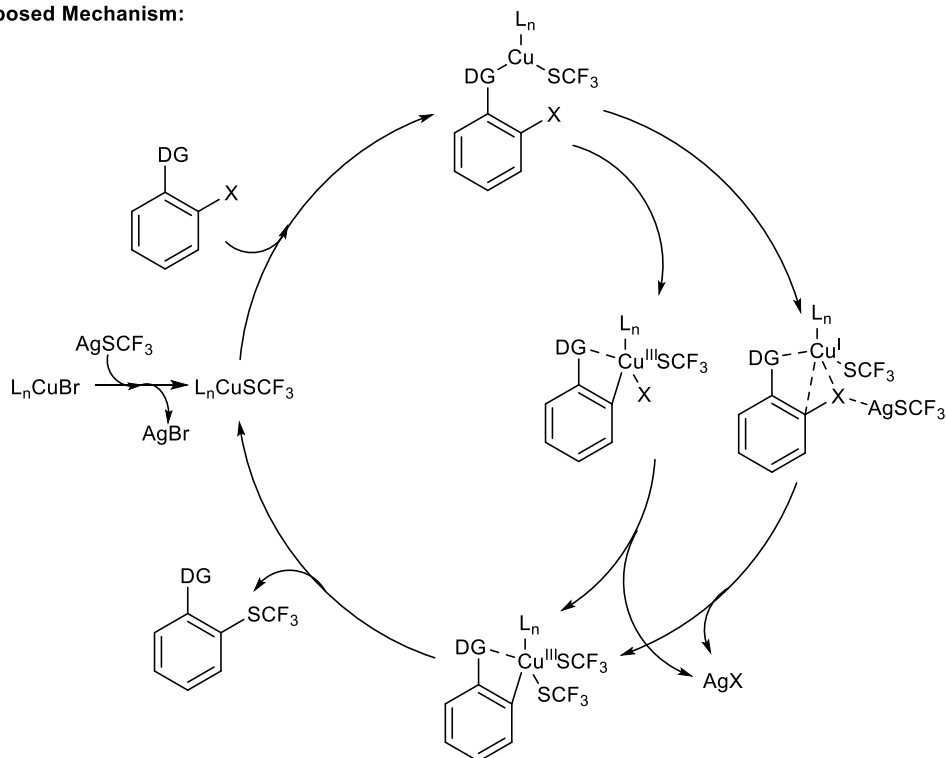
Huang *et al.* recently reported a Pd-catalyzed *mono*-trifluoromethylthiolation of arenes using an anionic SCF_3 species (Scheme 1.4.4.3).⁹⁵ In this method they employ a ligand exchange strategy using Selectfluor and AgSCF_3 . A broad substrate scope on the arenes could be tolerated, and the reaction conditions were found to be *ortho*-selective. Most pyridine directing groups were found to react well, as well as pyrimidine and benzoquinoline. Control experiments were performed to find that the Ag^+ cation plays an important role to mediate SCF_3 exchange with fluoride. From these studies, the authors proposed a mechanism involving a Pd(II)/Pd(IV) cycle.



There has also been recent attention given to the utility of inexpensive metal catalysts such as copper for the introduction of SCF₃ groups. A number of methods have been reported, but require the use of a stoichiometric amount of a copper salt.⁹⁶ Liu *et al.* recently disclosed a Cu-catalyzed directed trifluoromethylthiolation of aryl bromides using phenanthroline as a ligand and AgSCF₃ as a source of SCF₃ (Scheme 1.4.4.4).⁹⁷ The substrate scope of the arene was broad, and was able to tolerate a variety of electron-withdrawing and –donating substituents. It was found that imine directing groups were also amenable to the reaction, and reaction with various heteroaromatic bromides (bromopyridine and bromothiophene) furnished the desired SCF₃-coupled products. Aryl iodides also yielded the desired coupled products when the solvent was switched to DMF. No mechanistic studies were performed but a mechanism was proposed, with two possible routes (Scheme 1.4.4.4).

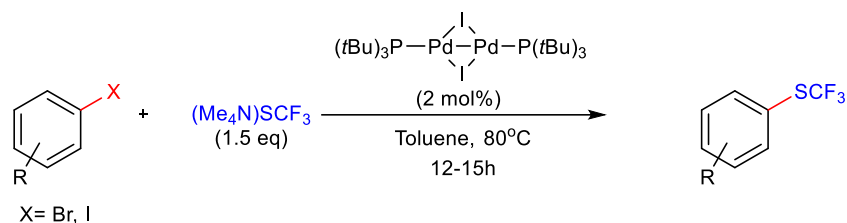


Proposed Mechanism:

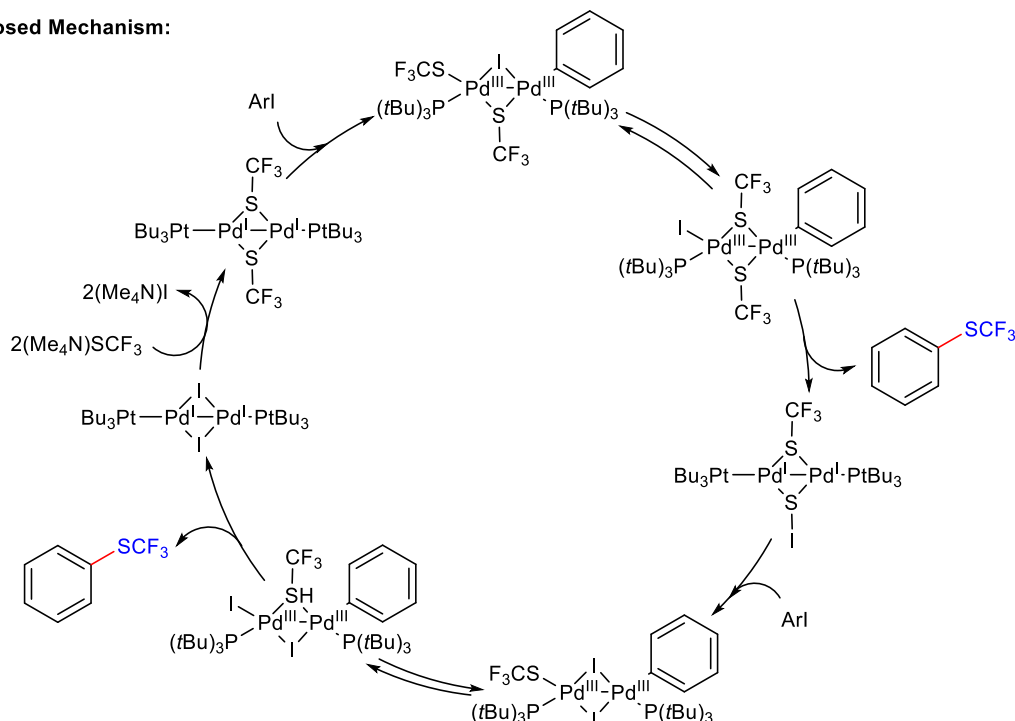


Scheme 1.4.4.4- A Cu-Mediated Trifluoromethylthiolation of Aryl Halides with Directing Groups, by Liu et al.

Recently, Schoenebeck *et al.* reported a di-nuclear Pd^{I} -mediated SCF_3 coupling of aryl iodides and aryl bromides (Scheme 1.4.4.5).⁹⁸ Distinct from previously published methods, this protocol presented an advantage such that it utilized an air-stable, recoverable Pd^{I} catalyst as opposed to Pd^0 . Substrate scope was broad using both aryl iodides and bromides, and both aryl halides were reactive with different substitutions on the aryl rings. Computational studies were compared with kinetic data and both support the catalytic cycle shown in Scheme 1.4.4.5.



Proposed Mechanism:



Scheme 1.4.4.5- A Dinuclear Pd^{II} -Catalyst Mediated Trifluoromethylthiolation by Schoenebeck et al.

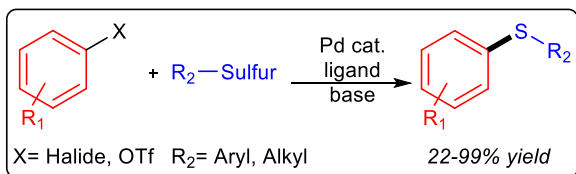
The requirement for syntheses of SCF_3 -containing compounds also rises with the increasing need for the development of novel biologically active compounds. Current methods all require the use of transition metal catalysis with aryl halides and/or directing groups. Thus, pre-functionalization of the starting material is required for the forging of these aryl- SCF_3 bonds. Current sources of the SCF_3 group have evolved from the initial toxic CF_3SSCF_3 reagent to now milder AgSCF_3 and organic $(\text{Me}_4\text{N})\text{SCF}_3$. Reaction temperatures still remain elevated ($80\text{-}140^\circ\text{C}$), and reaction times at around $8\text{-}24\text{h}$. This emphasizes the need for further development of alternative methods for the installation of SCF_3 groups if their use in novel bio-active compounds increases.

1.5 Summary

As demonstrated in this chapter, there are numerous S-arylation methods available, and it continues to be an area of constant development. A general summary of the approaches discussed in this chapter is presented in Scheme 1.5.1 and Scheme 1.5.2. Despite the copious number of methods available, the installation of aromatic C-S bonds continues to be challenging. They all suffer from the requirement of pre-functionalization of the starting material, require precious metal catalysis, and generate toxic by-products as waste. Although efficient, preference is turning away from transition metal catalysis in favour of more atom- and step-economic, environmentally friendly methods. The search for alternative sulfur sources also continues due to its odorous tendency in its free thiol form. These challenges persist also in the formation of aryl trifluoromethylthio groups, where the need for this functionality will only increase with the demand for novel drug derivatives. As a result of their fundamental importance, methods for the increased efficiency of S-arylation are required.

Transition Metal Catalysis:

Pd:



Pd Source: - Pd(OAc)₂
- Pd₂(dba)₃
- PdCl₂(dppf)

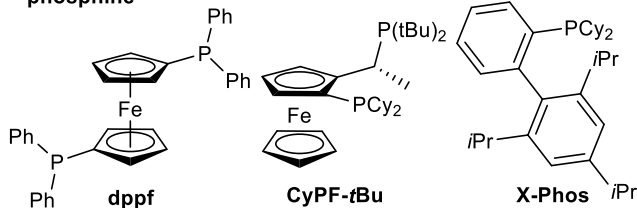
Sulfur Source: - Thiol (SH)
- Thiourea
- Disulfides (S-S)
- Na₂S₂O₃

Bases: - KOtBu
- CsCO₃, DMF, Dioxane, PTS/H₂O
- K₂CO₃
- K₃PO₄
- NaHMDS
- NEt₃

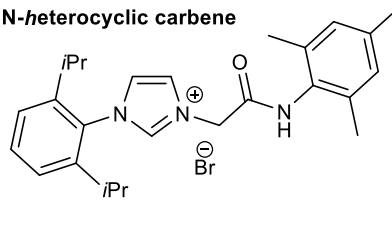
Conditions: - Toluene, DMSO, DME
- 40-100°C

Ligands:

- phosphine

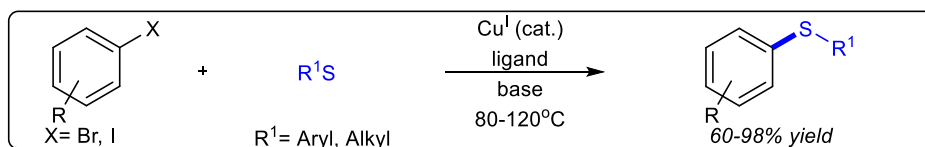


- N-heterocyclic carbene



Cu:

Cu (I):



Copper (I) Source: - CuBr
- CuI
- Cu₂O

Sulfur Source: - Thiol (SH)
- Na₂S 9H₂O
- Sulfonyl hydrazides

Bases: - phosphazene
- K₂CO₃, CsCO₃
- K₃PO₄
- KOH
- ionic bases

Ligands: - neocuproine
- ethylene glycol
- 1,10-phen
- bidentate oxygen/nitrogen
- tridentate oxygen/nitrogen

Conditions: - Dioxane, DMF, Toluene, DMSO, H₂O

Cu (II):



Sulfur Source: - Thiol (SH)
- Disulfides (RSSR)
- Electrophilic Sulfur (Thioimides)
- Sulfothioate salts

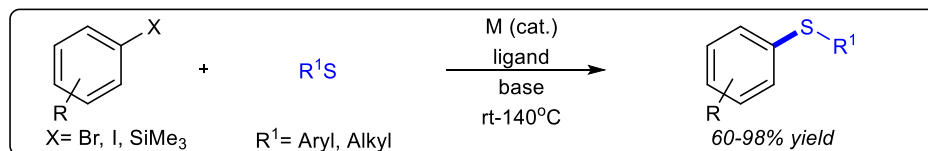
Copper (II) Source: - CuSO₄
- Cu(OAc)₂

Ligands: - bpy
- 1, 10-phen

Bases: - pyridine
- nBu₄NOH

Conditions: - rt - 140°C
- DMF, THF, EtOH, DMSO/H₂O
- N₂, O₂, Ar, air

Other Transition Metals:



Metals: - Ni
- Bi
- Rh
- In

Ligands: - BINOL
- Bidentate amine
- PPh₃
- POCOP

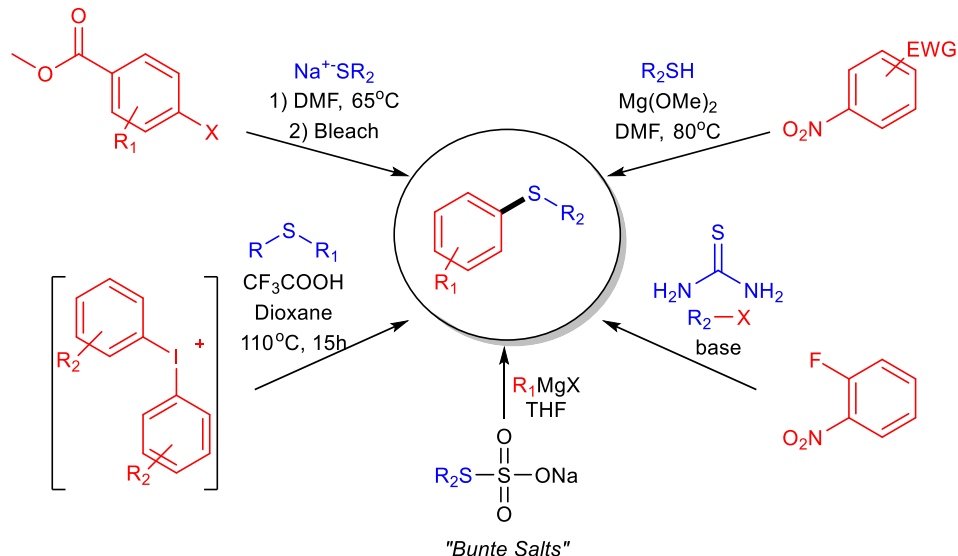
Sulfur Source: - Thiol (SH)
- Disulfides (RSSR)

Bases: - KOH
- NaOtBu

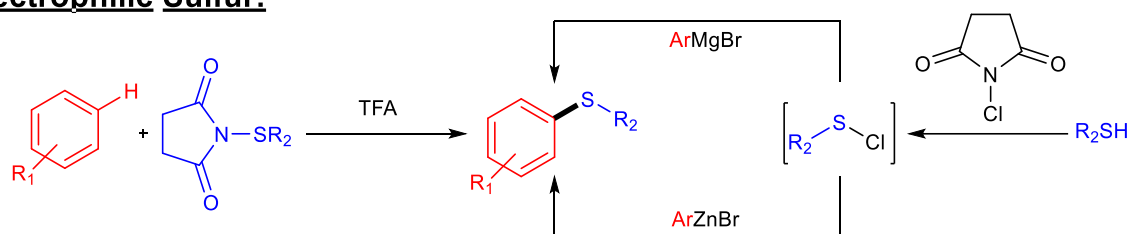
Conditions: - Toluene, DMSO, H₂O
- N₂, Ar, air

Scheme 1.5.1- General Summary of Transition Metal Catalyzed S-Arylation in Chapter 1

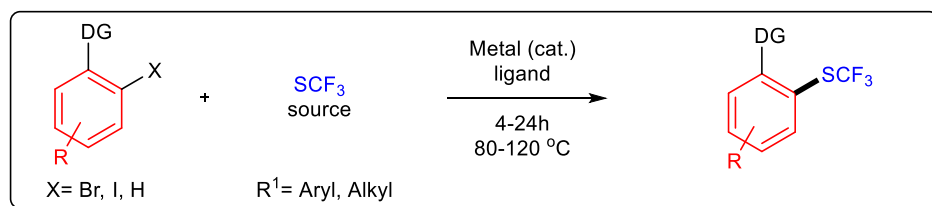
S_NAr:



Electrophilic Sulfur:



SCF₃:



Metals:
- Pd (I)
- Pd (II)
- Cu (I)
- Cu (II)

Directing Groups (DG):
- 8-aminoquinoline
- pyridyl
- amide
- imine oxime
- carboxyamide
- ester, ketone

SCF₃ Source:
- CF₃SSCF₃
- AgSCF₃
- Me₄NSCF₃

Ligands:
- Phen
- Selectfluor
- CH₃CN
- OTf

Solvents:
- DMSO, AcOH,
DME, DMF, Toluene,
MeCN

Scheme 1.5.2- General Summary of S_NAr, Electrophilic Sulfur, and Trifluoromethylthiolation S-Arylation Methods in Chapter 1

1.6 References

- 15 - Sulfur. In *Chemistry of the Elements (Second Edition)*, Greenwood, N. N.; Earnshaw, A., Eds. Butterworth-Heinemann: Oxford, 1997; pp 645-746.
- Eow, J. S. Recovery of sulfur from sour acid gas: A review of the technology. *Environ. Prog.* **2002**, 21 (3), 143-162.

3. A. W, H.; J. K, L. I. U.; D. W, D. Sulfur Recovery from Oil Sands. In *Sulfur: New Sources and Uses*, AMERICAN CHEMICAL SOCIETY: 1982; Vol. 183, pp 69-82.
4. (a) *CRC Handbook of Chemistry and Physics, 95th Edition*. 96 ed.; CRC Press: 2015; (b) Fontecave, M.; Ollagnier-de-Choudens, S.; Mulliez, E. Biological Radical Sulfur Insertion Reactions. *Chem. Rev.* **2003**, *103* (6), 2149-2166.
5. Oae, S.; Doi, J. *Organic sulfur chemistry*. CRC Press: 1991; Vol. 1.
6. OTTEN, H. Domagk and the development of the sulphonamides. *J. Antimicrob. Chemother.* **1986**, *17* (6), 689-690.
7. McGrath, N. A.; Brichacek, M.; Njardarson, J. T. A Graphical Journey of Innovative Organic Architectures That Have Improved Our Lives. *J. Chem. Educ.* **2010**, *87* (12), 1348-1349.
8. Dubois, L. H.; Nuzzo, R. G. Synthesis, structure, and properties of model organic surfaces. *Annu. Rev. Phys. Chem.* **1992**, *43* (1), 437-463.
9. Palomo, C.; Oiarbide, M.; López, R.; Gómez-Bengoa, E. Phosphazene bases for the preparation of biaryl thioethers from aryl iodides and arenethiols. *Tetrahedron Lett.* **2000**, *41* (8), 1283-1286.
10. Lindley, J. Tetrahedron report number 163 : Copper assisted nucleophilic substitution of aryl halogen. *Tetrahedron* **1984**, *40* (9), 1433-1456.
11. Weingarten, H. Mechanism of the Ullmann Condensation1. *J. Org. Chem.* **1964**, *29* (12), 3624-3626.
12. Paine, A. J. Mechanisms and models for copper mediated nucleophilic aromatic substitution. 2. Single catalytic species from three different oxidation states of copper in an Ullmann synthesis of triaryl amines. *J. Am. Chem. Soc.* **1987**, *109* (5), 1496-1502.
13. Mansour, M.; Giacomazzi, R.; Ouali, A.; Taillefer, M.; Jutand, A. Activation of aryl halides by Cu⁰/1,10-phenanthroline: Cu⁰ as precursor of CuI catalyst in cross-coupling reactions. *Chem. Commun.* **2008**, (45), 6051-6053.
14. Jiao, J.; Zhang, X.-R.; Chang, N.-H.; Wang, J.; Wei, J.-F.; Shi, X.-Y.; Chen, Z.-G. A Facile and Practical Copper Powder-Catalyzed, Organic Solvent- and Ligand-Free Ullmann Amination of Aryl Halides. *J. Org. Chem.* **2011**, *76* (4), 1180-1183.
15. Kürti, L.; Czákó, B. *Strategic Applications of Named Reactions in Organic Synthesis: Background and Detailed Mechanisms*. Elsevier Academic Press: 2005.
16. Beletskaya, I. P.; Cheprakov, A. V. Copper in cross-coupling reactions: The post-Ullmann chemistry. *Coord. Chem. Rev.* **2004**, *248* (21-24), 2337-2364.
17. Sambigao, C.; Marsden, S. P.; Blacker, A. J.; McGowan, P. C. Copper catalysed Ullmann type chemistry: from mechanistic aspects to modern development. *Chem. Soc. Rev.* **2014**, *43* (10), 3525-3550.
18. Font, M.; Parella, T.; Costas, M.; Ribas, X. Catalytic C-S, C-Se, and C-P Cross-Coupling Reactions Mediated by a CuI/CuIII Redox Cycle. *Organometallics* **2012**, *31* (22), 7976-7982.
19. Kiyomori, A.; Marcoux, J.-F.; Buchwald, S. L. An efficient copper-catalyzed coupling of aryl halides with imidazoles. *Tetrahedron Lett.* **1999**, *40* (14), 2657-2660.
20. Kelkar, A. A.; Patil, N. M.; Chaudhari, R. V. Copper-catalyzed amination of aryl halides: single-step synthesis of triaryl amines. *Tetrahedron Lett.* **2002**, *43* (40), 7143-7146.
21. Bates, C. G.; Gujadhur, R. K.; Venkataraman, D. A General Method for the Formation of Aryl-Sulfur Bonds Using Copper(I) Catalysts. *Org. Lett.* **2002**, *4* (16), 2803-2806.

22. Kwong, F. Y.; Buchwald, S. L. A General, Efficient, and Inexpensive Catalyst System for the Coupling of Aryl Iodides and Thiols. *Org. Lett.* **2002**, *4* (20), 3517-3520.
23. Ley, S. V.; Thomas, A. W. Modern Synthetic Methods for Copper-Mediated C(aryl)–O, C(aryl)–N, and C(aryl)–S Bond Formation. *Angew. Chem. Int. Ed.* **2003**, *42* (44), 5400-5449.
24. Kunz, K.; Scholz, U.; Ganzer, D. Renaissance of Ullmann and Goldberg Reactions - Progress in Copper Catalyzed C–N-, C–O- and C–S-Coupling. *Synlett* **2003**, *2003* (15), 2428-2439.
25. Eichman, C. C.; Stambuli, J. P. Transition Metal Catalyzed Synthesis of Aryl Sulfides. *Molecules* **2011**, *16* (1), 590.
26. Beletskaya, I. P.; Ananikov, V. P. Transition-Metal-Catalyzed C–S, C–Se, and C–Te Bond Formation via Cross-Coupling and Atom-Economic Addition Reactions. *Chem. Rev.* **2011**, *111* (3), 1596-1636.
27. Sujatha, A.; Thomas, A. M.; Thankachan, A. P.; Anilkumar, G. Recent advances in copper-catalyzed CS cross-coupling reactions. *ARKIVOC* **2015**, *1*, 1-28.
28. Herradura, P. S.; Pendola, K. A.; Guy, R. K. Copper-Mediated Cross-Coupling of Aryl Boronic Acids and Alkyl Thiols. *Org. Lett.* **2000**, *2* (14), 2019-2022.
29. Chan-Lam coupling reaction. In *Name Reactions*, Springer Berlin Heidelberg: 2006; pp 116-117.
30. Savarin, C.; Srogl, J.; Liebeskind, L. S. A Mild, Nonbasic Synthesis of Thioethers. The Copper-Catalyzed Coupling of Boronic Acids with N-Thio(alkyl, aryl, heteroaryl)imides. *Org. Lett.* **2002**, *4* (24), 4309-4312.
31. (a) Chan, D. M. T.; Lam, P. Y. S. Recent Advances in Copper-Promoted C–Heteroatom Bond Cross-Coupling Reactions with Boronic Acids and Derivatives. In *Boronic Acids*, Wiley-VCH Verlag GmbH & Co. KGaA: 2006; pp 205-240; (b) Qiao, J. X.; Lam, P. Y. S. Recent Advances in Chan–Lam Coupling Reaction: Copper-Promoted C–Heteroatom Bond Cross-Coupling Reactions with Boronic Acids and Derivatives. In *Boronic Acids*, Wiley-VCH Verlag GmbH & Co. KGaA: 2011; pp 315-361; (c) Thomas, A. W.; Ley, S. V. Copper-Catalyzed Arylations of Amines and Alcohols with Boron-Based Arylating Reagents. In *Modern Arylation Methods*, Wiley-VCH Verlag GmbH & Co. KGaA: 2009; pp 121-154.
32. (a) Taniguchi, N. Convenient Synthesis of Unsymmetrical Organochalcogenides Using Organoboronic Acids with Dichalcogenides via Cleavage of the S–S, Se–Se, or Te–Te Bond by a Copper Catalyst. *J. Org. Chem.* **2007**, *72* (4), 1241-1245; (b) Luo, P.-S.; Wang, F.; Li, J.-H.; Tang, R.-Y.; Zhong, P. Copper-Catalyzed Selective S-Arylation of 1,2-Bis(o-amino-1H-pyrazolyl) Disulfides with Arylboronic Acids. *Synthesis* **2009**, *2009* (06), 921-928; (c) Xu, H.-J.; Zhao, Y.-Q.; Feng, T.; Feng, Y.-S. Chan–Lam-Type S-Arylation of Thiols with Boronic Acids at Room Temperature. *J. Org. Chem.* **2012**, *77* (6), 2878-2884.
33. Migita, T.; Shimizu, T.; Asami, Y.; Shiobara, J.-i.; Kato, Y.; Kosugi, M. The Palladium Catalyzed Nucleophilic Substitution of Aryl Halides by Thiolate Anions. *Bull. Chem. Soc. Jpn.* **1980**, *53* (5), 1385-1389.
34. Murata, M.; Buchwald, S. L. A general and efficient method for the palladium-catalyzed cross-coupling of thiols and secondary phosphines. *Tetrahedron* **2004**, *60* (34), 7397-7403.
35. Fernández-Rodríguez, M. A.; Shen, Q.; Hartwig, J. F. A General and Long-Lived Catalyst for the Palladium-Catalyzed Coupling of Aryl Halides with Thiols. *J. Am. Chem. Soc.* **2006**, *128* (7), 2180-2181.

36. Shen, C.; Zhang, P.; Sun, Q.; Bai, S.; Hor, T. S. A.; Liu, X. Recent advances in C-S bond formation via C-H bond functionalization and decarboxylation. *Chem. Soc. Rev.* **2015**, *44* (1), 291-314.
37. Firouzbadi, H.; Iranpoor, N.; Gholinejad, M. One-Pot Thioetherification of Aryl Halides Using Thiourea and Alkyl Bromides Catalyzed by Copper(I) Iodide Free from Foul-Smelling Thiols in Wet Polyethylene Glycol (PEG 200). *Adv. Synth. Catal.* **2010**, *352* (1), 119-124.
38. Prasad, D. J. C.; Sekar, G. Cu-Catalyzed One-Pot Synthesis of Unsymmetrical Diaryl Thioethers by Coupling of Aryl Halides Using a Thiol Precursor. *Org. Lett.* **2011**, *13* (5), 1008-1011.
39. Ke, F.; Qu, Y.; Jiang, Z.; Li, Z.; Wu, D.; Zhou, X. An Efficient Copper-Catalyzed Carbon-Sulfur Bond Formation Protocol in Water. *Org. Lett.* **2011**, *13* (3), 454-457.
40. Wang, L.; Zhou, W.-Y.; Chen, S.-C.; He, M.-Y.; Chen, Q. A Highly Efficient Palladium-Catalyzed One-Pot Synthesis of Unsymmetrical Aryl Alkyl Thioethers under Mild Conditions in Water. *Adv. Synth. Catal.* **2012**, *354* (5), 839-845.
41. Qiao, Z.; Wei, J.; Jiang, X. Direct Cross-Coupling Access to Diverse Aromatic Sulfide: Palladium-Catalyzed Double C-S Bond Construction Using Na₂S₂O₃ as a Sulfurating Reagent. *Org. Lett.* **2014**, *16* (4), 1212-1215.
42. (a) Shi, Y.; Cai, Z.; Guan, P.; Pang, G. Carbon-Sulfur Coupling Reactions Catalyzed by Pd-NHC Complex. *Synlett* **2011**, *22* (14), 2090-2096; (b) Sayah, M.; Organ, M. G. Carbon-Sulfur Bond Formation of Challenging Substrates at Low Temperature by Using Pd-PEPPSI-IPent. *Chem.-Eur. J.* **2011**, *17* (42), 11719-11722.
43. Byeun, A.; Baek, K.; Han, M. S.; Lee, S. Palladium-catalyzed C-S bond formation by using N-amido imidazolium salts as ligands. *Tetrahedron Lett.* **2013**, *54* (49), 6712-6715.
44. Kumar, M. R.; Park, K.; Lee, S. Synthesis of Amido-N-imidazolium Salts and their Applications as Ligands in Suzuki-Miyaura Reactions: Coupling of Hetero- aromatic Halides and the Synthesis of Milrinone and Irbesartan. *Adv. Synth. Catal.* **2010**, *352* (18), 3255-3266.
45. Bastug, G.; Nolan, S. P. Carbon-Sulfur Bond Formation Catalyzed by [Pd(IPr*OMe)(cin)Cl] (cin = cinnamyl). *J. Org. Chem.* **2013**, *78* (18), 9303-9308.
46. Iwasaki, M.; Iyanaga, M.; Tsuchiya, Y.; Nishimura, Y.; Li, W.; Li, Z.; Nishihara, Y. Palladium-Catalyzed Direct Thiolation of Aryl C-H Bonds with Disulfides. *Chem.-Eur. J.* **2014**, *20* (9), 2459-2462.
47. (a) Dick, A. R.; Kampf, J. W.; Sanford, M. S. Unusually Stable Palladium(IV) Complexes: Detailed Mechanistic Investigation of C-O Bond-Forming Reductive Elimination. *J. Am. Chem. Soc.* **2005**, *127* (37), 12790-12791; (b) Whitfield, S. R.; Sanford, M. S. Reactivity of Pd(II) Complexes with Electrophilic Chlorinating Reagents: Isolation of Pd(IV) Products and Observation of C-Cl Bond-Forming Reductive Elimination. *J. Am. Chem. Soc.* **2007**, *129* (49), 15142-15143; (c) Racowski, J. M.; Dick, A. R.; Sanford, M. S. Detailed Study of C-O and C-C Bond-Forming Reductive Elimination from Stable C₂N₂O₂-Ligated Palladium(IV) Complexes. *J. Am. Chem. Soc.* **2009**, *131* (31), 10974-10983.
48. Canty, A. J.; Jin, H.; Skelton, B. W.; White, A. H. Oxidation of Complexes by (O₂CPh)₂ and (ER)₂ (E = S, Se), Including Structures of Pd(CH₂CH₂CH₂CH₂)(SePh)₂(bpy) (bpy = 2,2'-Bipyridine) and MMe₂(SePh)₂(L₂) (M = Pd, Pt; L₂ = bpy, 1,10-Phenanthroline) and C...O and C...E Bond Formation at Palladium(IV). *Inorg. Chem.* **1998**, *37* (16), 3975-3981.
49. Kao, H.-L.; Chen, C.-K.; Wang, Y.-J.; Lee, C.-F. An Efficient Copper-Catalyzed Cross-Coupling Reaction of Thiols with Aryl Iodides. *Eur. J. Org. Chem.* **2011**, *2011* (9), 1776-1781.

50. (a) Kumar, S.; Engman, L. Microwave-Assisted Copper-Catalyzed Preparation of Diaryl Chalcogenides. *J. Org. Chem.* **2006**, *71* (14), 5400-5403; (b) Zhang, S.; Qian, P.; Zhang, M.; Hu, M.; Cheng, J. Copper-Catalyzed Thiolation of the Di- or Trimethoxybenzene Arene C–H Bond with Disulfides. *J. Org. Chem.* **2010**, *75* (19), 6732-6735.
51. Chen, J.; Zhang, Y.; Liu, L.; Yuan, T.; Yi, F. Efficient Copper-Catalyzed Double S-Arylation of Aryl Halides with Sodium Sulfide in Peg-400. *Phosphorus, Sulfur Silicon Relat. Elem.* **2012**, *187* (11), 1284-1290.
52. Singh, N.; Singh, R.; Raghuvanshi, D. S.; Singh, K. N. Convenient MW-Assisted Synthesis of Unsymmetrical Sulfides Using Sulfonyl Hydrazides as Aryl Thiol Surrogate. *Org. Lett.* **2013**, *15* (22), 5874-5877.
53. Qiao, Z.; Ge, N.; Jiang, X. CO₂-promoted oxidative cross-coupling reaction for C-S bond formation via masked strategy in an odourless way. *Chem. Commun.* **2015**, *51* (51), 10295-10298.
54. Guo, Y.; Quan, Z.-J.; Da, Y.-X.; Zhang, Z.; Wang, X.-C. (2-Chlorobenzoyloxy)copper(i) catalyzed C-S cross-coupling of di(hetero)aryl disulfides with aryl boronic acids under base-free conditions. *RSC Adv.* **2015**, *5* (56), 45479-45483.
55. Yan, S.-Y.; Liu, Y.-J.; Liu, B.; Liu, Y.-H.; Shi, B.-F. Nickel-catalyzed thiolation of unactivated aryl C-H bonds: efficient access to diverse aryl sulfides. *Chem. Commun.* **2015**, *51* (19), 4069-4072.
56. (a) Yiannios, C. N.; Karabinos, J. V. Oxidation of Thiols by Dimethyl Sulfoxide. *J. Org. Chem.* **1963**, *28* (11), 3246-3248; (b) Wallace, T. J. Reactions of Thiols with Sulfoxides. I. Scope of the Reaction and Synthetic Applications. *J. Am. Chem. Soc.* **1964**, *86* (10), 2018-2021; (c) Fristad, W. E.; Peterson, J. R. Oxidative Coupling of Arylthiols to Diaryl Disulfides. *Synth. Commun.* **1985**, *15* (1), 1-5.
57. Rao, W.-H.; Shi, B.-F. Copper(II)-Catalyzed Direct Sulfonylation of C(sp²)–H Bonds with Sodium Sulfinates. *Org. Lett.* **2015**, *17* (11), 2784-2787.
58. Malik, P.; Chakraborty, D. Bi(III)-catalyzed C–S cross-coupling reaction. *Appl. Organomet. Chem.* **2012**, *26* (11), 557-561.
59. (a) Kwak, J.; Kim, M.; Chang, S. Rh(NHC)-Catalyzed Direct and Selective Arylation of Quinolines at the 8-Position. *J. Am. Chem. Soc.* **2011**, *133* (11), 3780-3783; (b) Kim, M.; Kwak, J.; Chang, S. Rhodium/N-Heterocyclic Carbene Catalyzed Direct Intermolecular Arylation of sp² and sp³ C–H Bonds with Chelation Assistance. *Angew. Chem. Int. Ed.* **2009**, *48* (47), 8935-8939.
60. Kim, M.; Chang, S. Rhodium(NHC)-Catalyzed Amination of Aryl Bromides. *Org. Lett.* **2010**, *12* (7), 1640-1643.
61. Kim, H. J.; Kim, M.; Chang, S. Rhodium(NHC)-Catalyzed O-Arylation of Aryl Bromides. *Org. Lett.* **2011**, *13* (9), 2368-2371.
62. (a) Arisawa, M.; Suzuki, T.; Ishikawa, T.; Yamaguchi, M. Rhodium-Catalyzed Substitution Reaction of Aryl Fluorides with Disulfides: p-Orientation in the Polyarylthiolation of Polyfluorobenzenes. *J. Am. Chem. Soc.* **2008**, *130* (37), 12214-12215; (b) Ajiki, K.; Hirano, M.; Tanaka, K. Rhodium-Catalyzed Reductive Coupling of Disulfides and Diselenides with Alkyl Halides, Using Hydrogen as a Reducing Agent. *Org. Lett.* **2005**, *7* (19), 4193-4195.
63. Lai, C.-S.; Kao, H.-L.; Wang, Y.-J.; Lee, C.-F. A general rhodium-catalyzed cross-coupling reaction of thiols with aryl iodides. *Tetrahedron Lett.* **2012**, *53* (33), 4365-4367.
64. Timpa, S. D.; Pell, C. J.; Ozerov, O. V. A Well-Defined (POCOP)Rh Catalyst for the Coupling of Aryl Halides with Thiols. *J. Am. Chem. Soc.* **2014**, *136* (42), 14772-14779.

65. Nishimoto, Y.; Okita, A.; Yasuda, M.; Baba, A. Synthesis of a Wide Range of Thioethers by Indium Triiodide Catalyzed Direct Coupling between Alkyl Acetates and Thiosilanes. *Org. Lett.* **2012**, *14* (7), 1846-1849.
66. (a) Kondoh, A.; Yorimitsu, H.; Oshima, K. Nucleophilic aromatic substitution reaction of nitroarenes with alkyl- or arylthio groups in dimethyl sulfoxide by means of cesium carbonate. *Tetrahedron* **2006**, *62* (10), 2357-2360; (b) Sreedhar, B.; Reddy, P. S.; Reddy, M. A. Catalyst-Free and Base-Free Water-Promoted S_NAr Reaction of Heteroaryl Halides with Thiols. *Synthesis* **2009**, *2009* (10), 1732-1738; (c) Duan, Z.; Ranjit, S.; Liu, X. One-Pot Synthesis of Amine-Substituted Aryl Sulfides and Benzo[b]thiophene Derivatives. *Org. Lett.* **2010**, *12* (10), 2430-2433; (d) Goriya, Y.; Ramana, C. V. The [Cu]-catalyzed S_NAr reactions: direct amination of electron deficient aryl halides with sodium azide and the synthesis of arylthioethers under Cu(II)-ascorbate redox system. *Tetrahedron* **2010**, *66* (38), 7642-7650; (e) Fier, P. S.; Hartwig, J. F. Synthesis and Late-Stage Functionalization of Complex Molecules through C-H Fluorination and Nucleophilic Aromatic Substitution. *J. Am. Chem. Soc.* **2014**, *136* (28), 10139-10147.
67. Frieman, B. A. An environmentally-friendly one-pot synthesis of 4-sulfonyl benzoic acids. *Tetrahedron Lett.* **2014**, *55* (22), 3295-3298.
68. Naeimi, H.; Moradian, M. Facile and Mild Displacement of Nitrite Ions in Electron-Deficient Nitroarenes by Alkyl or Aryl Thiols in the Presence of Magnesium Methoxide as a Solid Base Catalyst. *Synlett* **2012**, *23* (15), 2223-2226.
69. Beck, J. R.; Yahner, J. A. Synthesis of 2-cyano, 2-acyl, and 2-carboxamido derivatives of 3-aminobenzo[b]thiophene involving nitro displacement. *J. Org. Chem.* **1974**, *39* (23), 3440-3441.
70. Reeves, J. T.; Camara, K.; Han, Z. S.; Xu, Y.; Lee, H.; Busacca, C. A.; Senanayake, C. H. The Reaction of Grignard Reagents with Bunte Salts: A Thiol-Free Synthesis of Sulfides. *Org. Lett.* **2014**, *16* (4), 1196-1199.
71. Lu, G.-p.; Cai, C. An odorless, one-pot synthesis of nitroaryl thioethers via S_NAr reactions through the in situ generation of S-alkylisothiuronium salts. *RSC Adv.* **2014**, *4* (104), 59990-59996.
72. Imoto, M.; Matsui, Y.; Takeda, M.; Tamaki, A.; Taniguchi, H.; Mizuno, K.; Ikeda, H. A Probable Hydrogen-Bonded Meisenheimer Complex: An Unusually High S_NAr Reactivity of Nitroaniline Derivatives with Hydroxide Ion in Aqueous Media. *J. Org. Chem.* **2011**, *76* (15), 6356-6361.
73. Wagner, A. M.; Sanford, M. S. Transition-Metal-Free Acid-Mediated Synthesis of Aryl Sulfides from Thiols and Thioethers. *J. Org. Chem.* **2014**, *79* (5), 2263-2267.
74. Bielawski, M.; Aili, D.; Olofsson, B. Regiospecific One-Pot Synthesis of Diaryliodonium Tetrafluoroborates from Arylboronic Acids and Aryl Iodides. *J. Org. Chem.* **2008**, *73* (12), 4602-4607.
75. Hostier, T.; Ferey, V.; Ricci, G.; Gomez Pardo, D.; Cossy, J. Synthesis of Aryl Sulfides: Metal-Free C-H Sulfenylation of Electron-Rich Arenes. *Org. Lett.* **2015**, *17* (15), 3898-3901.
76. Li, H.-J.; Wu, Y.-C.; Dai, J.-H.; Song, Y.; Cheng, R.; Qiao, Y. Regioselective Electrophilic Aromatic Bromination: Theoretical Analysis and Experimental Verification. *Molecules* **2014**, *19* (3), 3401.
77. Holleman, A. F. Some Factors Influencing Substitution in the Benzene Ring. *Chem. Rev.* **1924**, *1* (2), 187-230.

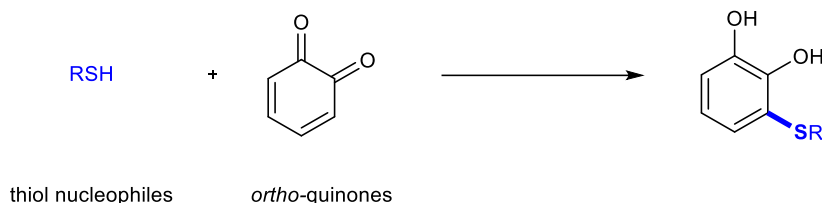
78. (a) Yadav, J. S.; Subba Reddy, B. V.; Jain, R.; Baishya, G. N-Chlorosuccinimide as a versatile reagent for the sulfenylation of ketones: a facile synthesis of α -ketothioethers. *Tetrahedron Lett.* **2008**, 49 (18), 3015-3018; (b) Schlosser, K. M.; Krasutsky, A. P.; Hamilton, H. W.; Reed, J. E.; Sexton, K. A Highly Efficient Procedure for 3-Sulfenylation of Indole-2-carboxylates. *Org. Lett.* **2004**, 6 (5), 819-821.
79. Cheng, J.-H.; Ramesh, C.; Kao, H.-L.; Wang, Y.-J.; Chan, C.-C.; Lee, C.-F. Synthesis of Aryl Thioethers through the N-Chlorosuccinimide-Promoted Cross-Coupling Reaction of Thiols with Grignard Reagents. *J. Org. Chem.* **2012**, 77 (22), 10369-10374.
80. Yonova, I. M.; Osborne, C. A.; Morrisette, N. S.; Jarvo, E. R. Diaryl and Heteroaryl Sulfides: Synthesis via Sulfenyl Chlorides and Evaluation as Selective Anti-Breast-Cancer Agents. *J. Org. Chem.* **2014**, 79 (5), 1947-1953.
81. Hansch, C.; Leo, A.; Taft, R. W. A survey of Hammett substituent constants and resonance and field parameters. *Chem. Rev.* **1991**, 91 (2), 165-195.
82. (a) Feiring, A. E. Chemistry in hydrogen fluoride. 7. A novel synthesis of aryl trifluoromethyl ethers. *J. Org. Chem.* **1979**, 44 (16), 2907-2910; (b) Nodiff, E. A.; Lipschutz, S.; Craig, P. N.; Gordon, M. Synthesis of Phenothiazines. III. Derivatives of Hydroxy- and Mercaptophenothiazines. *J. Org. Chem.* **1960**, 25 (1), 60-65.
83. (a) Billard, T.; Roques, N.; Langlois, B. R. Synthetic Uses of Thio- and Selenoesters of Trifluoromethylated Acids. 1. Preparation of Trifluoromethyl Sulfides and Selenides. *J. Org. Chem.* **1999**, 64 (11), 3813-3820; (b) Pooput, C.; Dolbier, W. R.; Médebielle, M. Nucleophilic Perfluoroalkylation of Aldehydes, Ketones, Imines, Disulfides, and Diselenides. *J. Org. Chem.* **2006**, 71 (9), 3564-3568; (c) Kieltsch, I.; Eisenberger, P.; Togni, A. Mild Electrophilic Trifluoromethylation of Carbon- and Sulfur-Centered Nucleophiles by a Hypervalent Iodine(III)-CF₃ Reagent. *Angew. Chem. Int. Ed.* **2007**, 46 (5), 754-757.
84. (a) Harris, J. F. The Free-radical Addition of Trifluoromethanesulfonyl Chloride to Haloolefins. *J. Am. Chem. Soc.* **1962**, 84 (16), 3148-3153; (b) Harris, J. F. Trifluoromethylthioalkanes, -olefins, and -acetylenes. *J. Org. Chem.* **1967**, 32 (7), 2063-2074; (c) Munavalli, S.; Rohrbaugh, D. K.; Rossman, D. I.; Wagner, W. G.; Durst, H. D. Trifluoromethylthiolation of Trimethylsilyl Enol Ethers. *Phosphorus, Sulfur Silicon Relat. Elem.* **2002**, 177 (4), 1021-1031.
85. (a) Boiko, V. N. Aromatic and heterocyclic perfluoroalkyl sulfides. Methods of preparation. *Beilstein Journal of Organic Chemistry* **2010**, 6, 880-921; (b) Andreades, S.; Harris, J. F.; Sheppard, W. A. Aryl Fluoroalkyl Sulfides. II. Preparation by Condensation of Trifluoromethanesulfonyl Chloride with Aromatic Systems. *J. Org. Chem.* **1964**, 29 (4), 898-900; (c) Haas, A.; Hellwig, V. Perhalogenmethylmercapto-heterocyclen, (VII) [1] konkurrenzreaktionen elektronenarmer, substituierter aromaten um die halogenmethylmercapto-BZW. Chlorgruppe von Cl₃-nFnCSCl in starken sauren. *Journal of Fluorine Chemistry* **1975**, 6 (6), 521-532; (d) Scribner, R. M. Some New Sulfonyl- and Trifluoromethylthio-p-benzoquinones. Their Reactions, Polarographic Reduction Potentials, and π Acid Strengths. *J. Org. Chem.* **1966**, 31 (11), 3671-3682.
86. (a) Man, E. H.; Coffman, D. D.; Muetterties, E. L. Synthesis and Properties of Bis-(trifluoromethylthio)-mercury. *J. Am. Chem. Soc.* **1959**, 81 (14), 3575-3577; (b) Adams, D. J.; Clark, J. H. Preparation of Trifluoromethyl Aryl Sulfides Using Silver(I) Trifluoromethanethiolate and an Inorganic Iodide. *J. Org. Chem.* **2000**, 65 (5), 1456-1460; (c) Clark, J. H.; Jones, C. W.; Kybett, A. P.; McClinton, M. A.; Miller, J. M.; Bishop, D.; Blade, R. J. The introduction of SCF₃ into aromatic substrates using CuSCF₃ and alumina-supported CuSCF₃. *Journal of Fluorine Chemistry* **1990**, 48 (2), 249-253; (d) Munavalli, S.; Wagner, G.

- W.; Bashir Hashemi, A.; Rohrbaugh, D. K.; Durst, H. D. Synthesis of (Trifluoromethylthio) Cubanes. *Synth. Commun.* **1997**, 27 (16), 2847-2851.
87. Toulgoat, F.; Alazet, S.; Billard, T. Direct Trifluoromethylthiolation Reactions: The “Renaissance” of an Old Concept. *Eur. J. Org. Chem.* **2014**, 2014 (12), 2415-2428.
88. Yang, X.; Wu, T.; Phipps, R. J.; Toste, F. D. Advances in Catalytic Enantioselective Fluorination, Mono-, Di-, and Trifluoromethylation, and Trifluoromethylthiolation Reactions. *Chem. Rev.* **2015**, 115 (2), 826-870.
89. (a) Teverovskiy, G.; Surry, D. S.; Buchwald, S. L. Pd-Catalyzed Synthesis of Ar-SCF₃ Compounds under Mild Conditions. *Angew. Chem. Int. Ed.* **2011**, 50 (32), 7312-7314; (b) Zhang, C.-P.; Vicić, D. A. Nickel-Catalyzed Synthesis of Aryl Trifluoromethyl Sulfides at Room Temperature. *J. Am. Chem. Soc.* **2012**, 134 (1), 183-185; (c) Kondratenko, N. V.; Kolomeytsev, A. A.; Popov, V. I.; Yagupolskii, L. M. Synthesis and Reactions of Trifluoromethylthio(seleno)- and Pentafluorophenylthio(seleno)-copper. *Synthesis* **1985**, 1985 (6/7), 667-669; (d) Yagupolskii, L. M.; Kondratenko, N. V.; Sambur, V. P. A New Method for the Syntheses of Aryl and Heteroaryl Trifluoromethyl Sulfides. *Synthesis* **1975**, 1975 (11), 721-723; (e) Adams, D. J.; Goddard, A.; Clark, J. H.; Macquarrie, D. J. Trifluoromethylthiodiazonation: a simple, efficient route to trifluoromethyl aryl sulfides. *Chem. Commun.* **2000**, (11), 987-988.
90. Tran, L. D.; Popov, I.; Daugulis, O. Copper-Promoted Sulfenylation of sp² C–H Bonds. *J. Am. Chem. Soc.* **2012**, 134 (44), 18237-18240.
91. Beurskens, P. T.; Cras, J. A.; Steggerda, J. J. Structure and properties of dibromo-N,N-dibutyldithiocarbamate complexes of copper(III) and gold(III). *Inorg. Chem.* **1968**, 7 (4), 810-813.
92. Willert-Porada, M. A.; Burton, D. J.; Baenziger, N. C. Synthesis and X-ray structure of bis(trifluoromethyl)(N,N-diethyldithiocarbamate)-copper; a remarkably stable perfluoroalkylcopper(III) complex. *Journal of the Chemical Society, Chemical Communications* **1989**, (21), 1633-1634.
93. Huffman, L. M.; Stahl, S. S. Carbon–Nitrogen Bond Formation Involving Well-Defined Aryl–Copper(III) Complexes. *J. Am. Chem. Soc.* **2008**, 130 (29), 9196-9197.
94. Xu, C.; Shen, Q. Palladium-Catalyzed Trifluoromethylthiolation of Aryl C–H Bonds. *Org. Lett.* **2014**, 16 (7), 2046-2049.
95. Yin, W.; Wang, Z.; Huang, Y. Highly ortho-Selective Trifluoromethylthiolation Reactions using a Ligand Exchange Strategy. *Adv. Synth. Catal.* **2014**, 356 (14-15), 2998-3006.
96. (a) Weng, Z.; He, W.; Chen, C.; Lee, R.; Tan, D.; Lai, Z.; Kong, D.; Yuan, Y.; Huang, K.-W. An Air-Stable Copper Reagent for Nucleophilic Trifluoromethylthiolation of Aryl Halides. *Angew. Chem. Int. Ed.* **2013**, 52 (5), 1548-1552; (b) Chen, Q.-Y.; Duan, J.-X. Direct trifluoromethylthiolation of aryl halides using methyl fluorosulfonyldifluoroacetate and sulfur. *Journal of the Chemical Society, Chemical Communications* **1993**, (11), 918-919.
97. Xu, J.; Mu, X.; Chen, P.; Ye, J.; Liu, G. Copper-Catalyzed Trifluoromethylthiolation of Aryl Halides with Diverse Directing Groups. *Org. Lett.* **2014**, 16 (15), 3942-3945.
98. Yin, G.; Kalvet, I.; Schoenebeck, F. Trifluoromethylthiolation of Aryl Iodides and Bromides Enabled by a Bench-Stable and Easy-To-Recover Dinuclear Palladium(I) Catalyst. *Angew. Chem. Int. Ed.* **2015**, 54 (23), 6809-6813.

2 Sulfur Addition to *ortho*-Quinones in Biological Contexts

2.1 Introduction

This chapter will discuss the ubiquity of sulfur in biology, focusing specifically on the transformation of sulfur addition to *ortho*-quinones. The addition of sulfur nucleophiles to *ortho*-quinones (Scheme 2.1.1) is a reaction that has been characterized in the past in the context of biology and biochemistry. It has been identified as the step that introduces sulfur into pheomelanin precursors¹, and has been postulated to be the step in which undesired carcinogenic estrogen quinones are sequestered and degraded². However, investigation of this transformation has been largely limited to the reaction of cysteine or glutathione as the thiol nucleophile, and naturally occurring *ortho*-quinones.

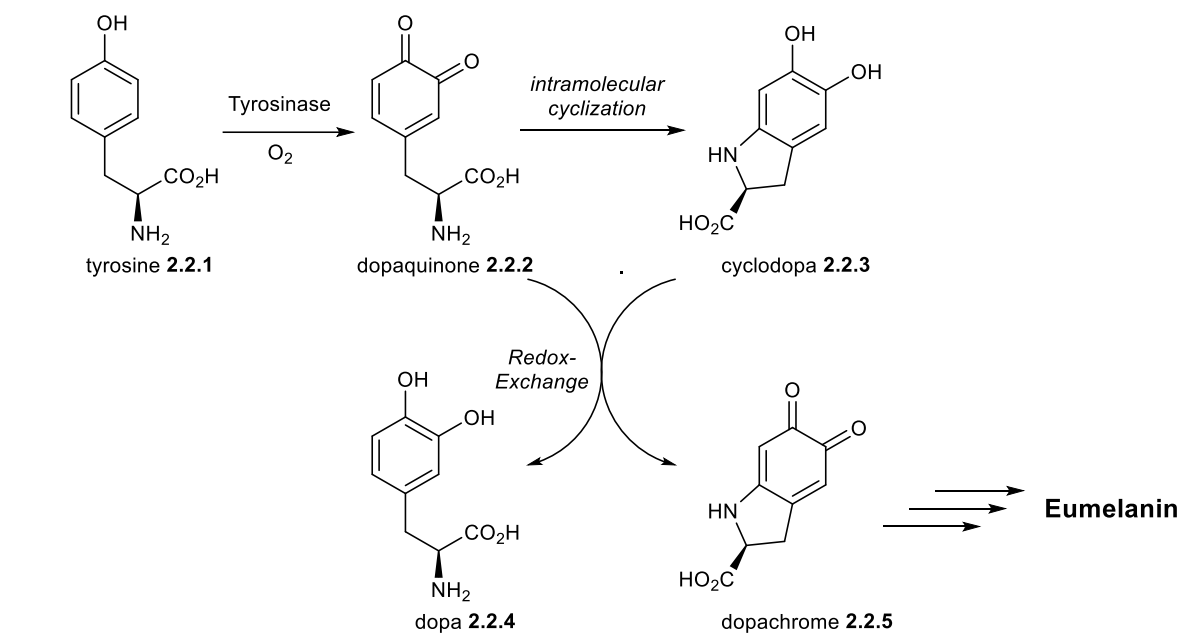


Scheme 2.1.1-General Scheme of Sulfur Addition to ortho-Quinones

As will be shown in 2.2, this transformation is central to the pigmentation process of melanogenesis, and in the production of the red pigment pheomelanin. This prevalence also extends to detoxification processes in biological systems, which will be discussed in 2.3. Specific studies on this transformation will be reviewed in 2.4, and proposed mechanisms in 2.5.

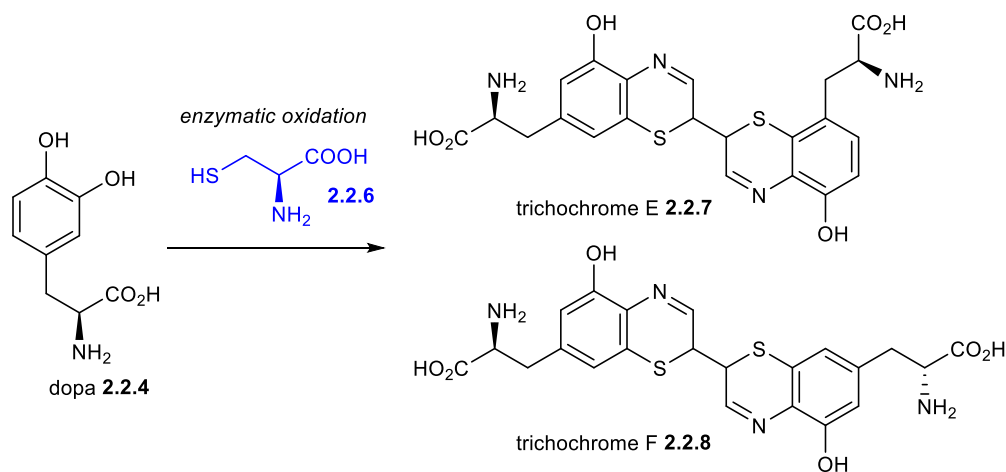
2.2 Melanogenesis

Melanogenesis is a pigmentation process that is ubiquitous in nature. Early studies of this process rapidly revealed that it results in the production of pigment polymers that can be classified as either: eumelanin (black), or pheomelanin (red). Extensive investigations have been conducted in order to characterize eumelanin intermediates from its starting building block tyrosine **2.2.1**, and what is known about its biosynthetic pathway, whose first steps are abbreviated in Scheme 2.2.1¹.

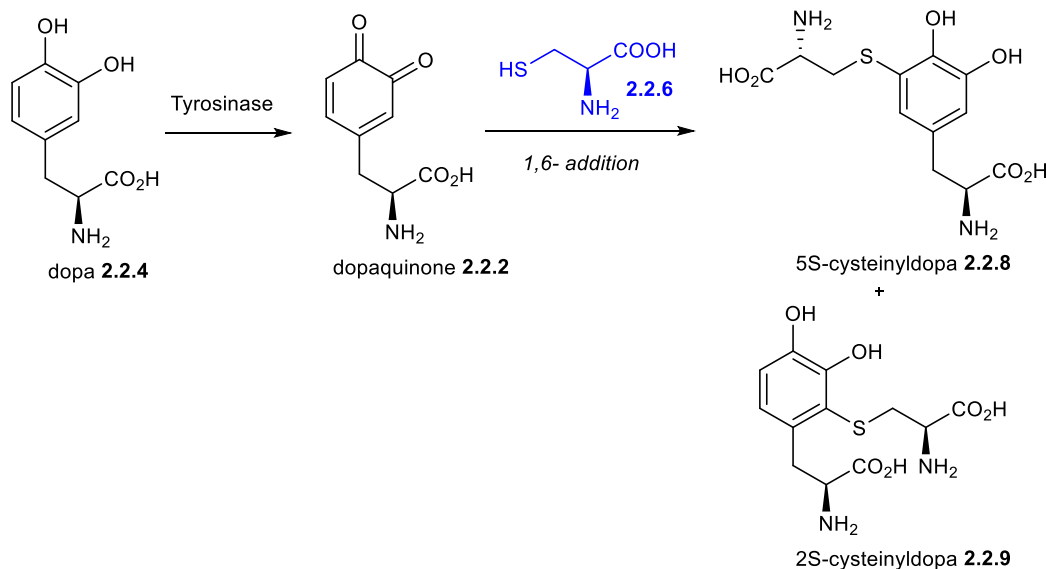


Scheme 2.2.1- The First Steps of the Biosynthetic Pathway of Eumelanin in Melanogenesis

The majority of investigations on melanogenesis have focused primarily on this eumelanin process. However, structurally speaking, little was known about its red counterpart pheomelanin until the late 1960s. In 1964, degradative studies confirmed the presence of nitrogen and sulfur atoms in pheomelanin structures. Subsequently, it was observed that the enzymatic oxidation of dopa **2.2.4** in the presence of cysteine **2.2.6** gave rise to the same pheomelanin trichochrome compounds **2.2.7** & **2.2.8** that were observed from isolation of feathers from New Hampshire hens (*gallus gallus*) (Scheme 2.2.2).³ It was later identified that regioisomers 5S- and 2S- cysteinyl-dopa were intermediates in the biosynthesis of these trichochrome products⁴. It was then hypothesized that these intermediates arose first from oxidation of dopa **2.2.4** to dopaquinone **2.2.2**, followed by 1,6-addition to cysteine **2.2.6** (Scheme 2.2.3).⁵ Interest in the synthesis of these cysteinyl-dopa compounds **2.2.8** & **2.2.9** increased further when it was identified that 5S-cysteinyl-dopa was present in high levels in the urine of individuals afflicted with melanoma⁶, while levels in healthy individuals are extremely low.

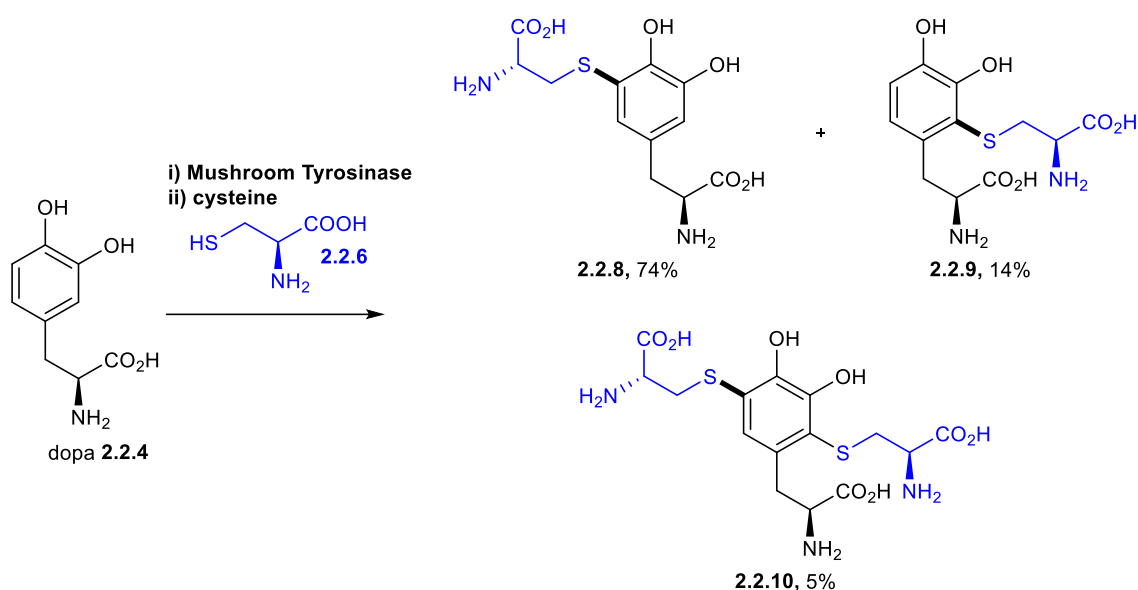


Scheme 2.2.2- Early Isolation of Trichochromes E 2.2.7 and F 2.2.8 from Enzymatic Oxidation of Dopa 2.2.4 in Presence of Cysteine



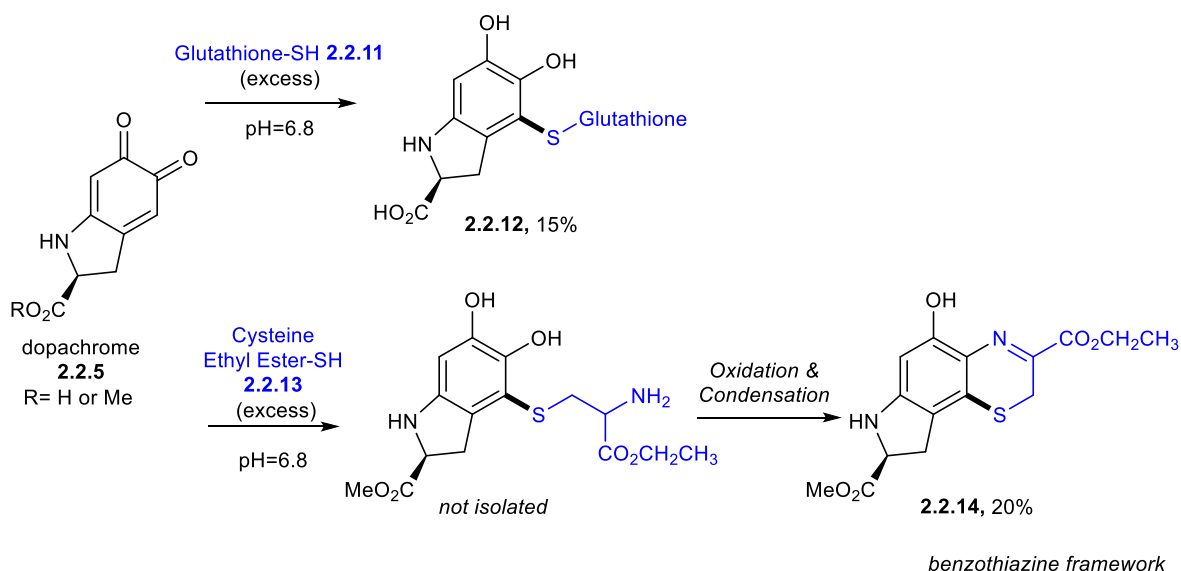
Scheme 2.2.3- Proposed Incorporation of Cysteine into Pheomelanin Pigments by Prota et al.

The direct synthesis of cysteinyldopas was then reported by Itoh and Prota.⁷ By mixing mushroom tyrosinase, dopa **2.2.4** and cysteine **2.2.6** in a pH 6.8 phosphate buffer, they reported the one step synthesis of the sulfur adduct 5-cysteinyldopa **2.2.8** in a 74% yield, along with its regioisomer, 2-cysteinyldopa **2.2.9** in 14% yield, and the di-thiol adduct **2.2.10** in 5% yield (Scheme 2.2.4). The formation of these products was observed through UV-Vis, and characterized by ¹H-NMR.



Scheme 2.2.4- Synthesis of Cysteinyl dopas with Mushroom Tyrosinase by Itoh et al.

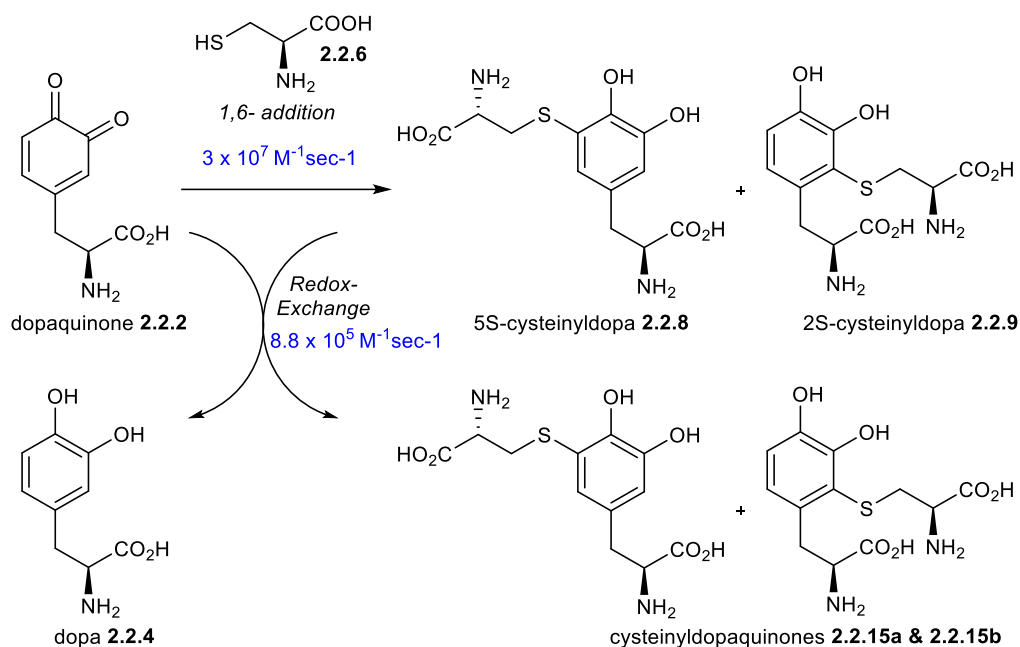
In 1987, it was known that dopachrome **2.2.5** arose from the oxidation of tyrosine during melanogenesis. Prota *et al.* demonstrated that glutathione **2.2.11**, a known thiol scavenger of reactive metabolites in the cell, reacted with dopachrome **2.2.5** to give the catechol-glutathione-adducts **2.2.12** in 15% yield, along with reduced catechol by-products that didn't contain sulfur in 70% yield (Scheme 2.2.5).⁸ The reaction was performed under biomimetic conditions, in pH 6.8 phosphate buffer. It was also shown that cysteine and its analogous ethyl ester **2.2.13** reacted with dopachrome through the same 1,6-addition, but underwent further oxidation and condensation to produce a benzothiazine heterocycle **2.2.14**. This further strengthened the hypothesis that the sulfur contained in melanin polymers arose from cysteine and glutathione, via their addition to quinone intermediates such as dopachrome.



Scheme 2.2.5- Reactions of Cysteine and Glutathione with Dopachrome 2.2.5, by Prota et al.

It was later reported by Land *et al.* that the rate constant for the thiol addition of cysteine **2.2.6** to dopaquinone **2.2.2** was $3 \times 10^7 \text{ M}^{-1}\text{sec}^{-1}$, quantifying this rapid transformation (Scheme 2.2.6).⁹ The same authors later reported another rate constant of $8.8 \times 10^5 \text{ M}^{-1}\text{sec}^{-1}$ for the redox exchange process between dopaquinone **2.2.2** and 5-S-cysteinyl-dopa **2.2.8**¹⁰, a rate constant thirty times less than the thiol addition. As discussed earlier, the biosynthetic pathway of the black pigment eumelanin involves the nitrogen cyclization of dopaquinone. The rate constant for this transformation of dopaquinone is 7.6 sec^{-1} . It was concluded that production of pheomelanin occurs only if there is a reasonably large concentration of cysteine present, i.e. if it is higher than $1 \mu\text{M}$. These results, calculated via pulse radiolysis, are consistent with the belief that the dictating factor of the pathway dopaquinone takes in melanogenesis, i.e. whether it undergoes cyclization

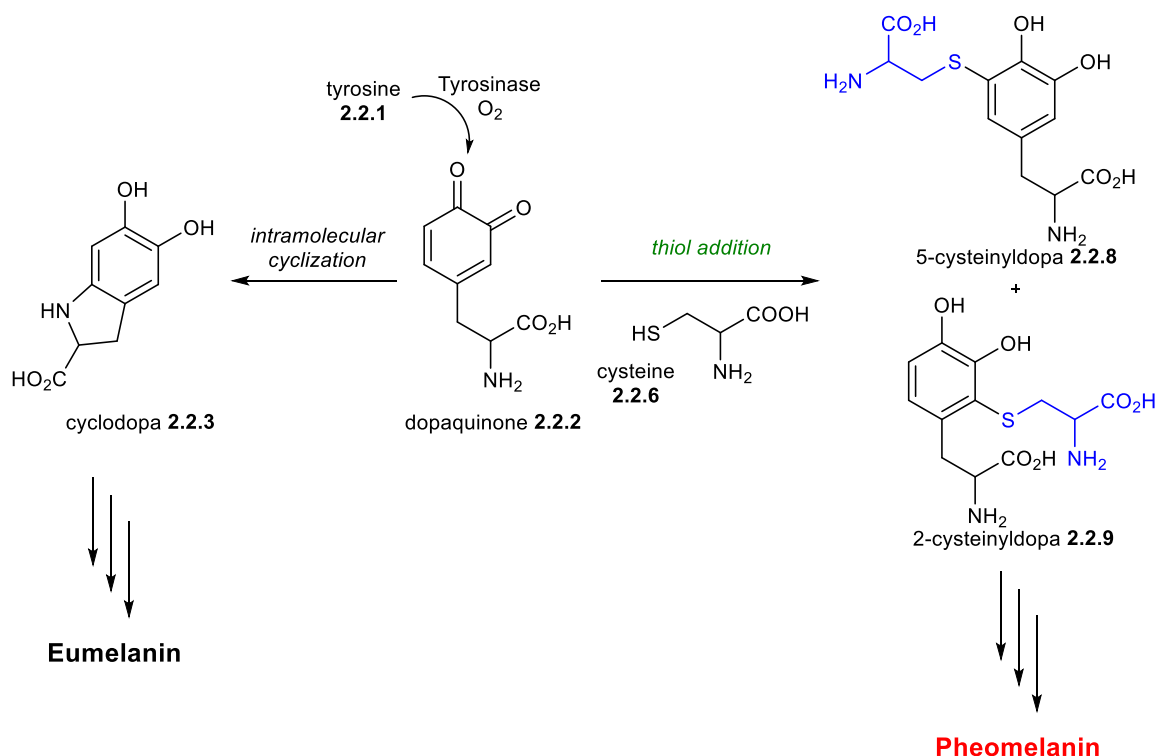
to form dopachrome, or whether it undergoes thiol addition to form cysteinyl-dopa compounds **2.15a** and **2.2.15b**, is the presence of cysteine in the melanosomal compartments of the cell.



Scheme 2.2.6- Calculated Rate Constants for the Thiol Addition of Cysteine to Dopaquinone, and for the Redox Exchange between dopaquinone and Cysteinyl-dopa Products

A review discussing important developments in melanogenesis was published in 2003.¹ It highlights the intrinsic reactivity of *ortho*-quinones with sulfur nucleophiles and briefly considers the two clear competitive reactions occurring in this transformation: 1) sulfur addition to *ortho*-quinones, and 2) redox exchange between the thiol-adduct catechol and the starting material *ortho*-quinone. At this time, elucidation of the first few steps in the biosynthetic pathway of pheomelanin from tyrosine are well-established. This includes the key step of the cysteine sulfur addition to the *ortho*-quinone dopaquinone. This step has been defined as the branch point in the pathways of the production of eumelanin (black pigment) and pheomelanin (red pigment), and is briefly summarized in Scheme 2.2.7. First, tyrosine **2.2.1** is oxidized by the enzyme tyrosinase to dopaquinone **2.2.2**. In the absence of cysteine, dopaquinone **2.2.2** undergoes an intramolecular cyclization to generate cyclodopa **2.2.3**, which, after subsequent oxidations and polymerizations, forms the black polymer eumelanin. If, however, cysteine **2.2.6** is present in high enough concentrations during the production of **2.2.2**, **2.2.2** is rapidly attacked by the thiol moiety of cysteine **2.2.6** to generate adducts 5-cysteinyl-dopa **2.2.8** and 2-cysteinyl-dopa **2.2.9**, which have been found to be precursors to pheomelanin.

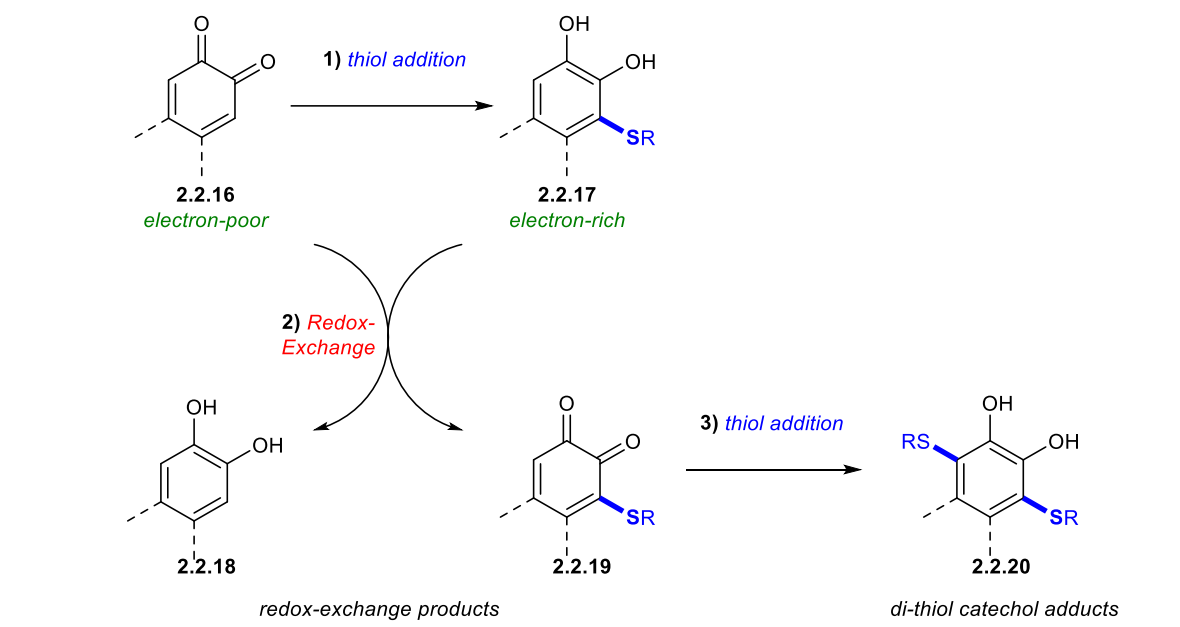
The exact mechanism by which cysteine concentrations are regulated is still unclear at this time, but it appears that it is regulated by the specific transcription of enzymes in the melanosome. It is known that the enzymes melanocyte stimulating hormone (MSH) and agouti signalling protein (ASP) play a large role.¹¹ When the receptor of MSH is stimulated, eumelanin production is elicited through an increase in tyrosinase production. However, if the MSH receptor is blocked or ASP overexpressed, pheomelanin production will override eumelanin production.¹² The expression of ASP results in a decrease in expression of all melanogenic genes.¹¹



Scheme 2.2.7- Thiol Addition: The Branch Point in Melanogenesis

An important transformation not yet discussed that occurs upon addition of sulfur to quinone is redox-exchange (Scheme 2.2.8). During melanogenesis, the products arising from thiol addition of cysteine to dopaquinone are electron rich. These electron-rich catechol products undergo redox exchange with the electron-poor dopaquinone to generate the analogous catechol and *ortho*-quinone products, which then continue forward along the melanogenic pathway. A similar transformation occurs between the catechol cyclodopa and dopaquinone, resulting in the generation of the analogous redox-exchange products which are precursors in eumelanin production. This process is instrumental when analyzing literature precedent for the addition of

sulfur nucleophiles to *ortho*-quinones, and provides an explanation for the frequent isolation of di-sulfur adducts. For example, redox exchange generates C3-sulfur-substituted *ortho*-quinone **2.2.19**, which can participate in an additional 1,6-addition with an additional sulfur nucleophile to generate a second C-S bond at C6 to form **2.2.20** (Scheme 2.2.8). While this process may be important to the pigmentation process, it complicates more general reactions between *ortho*-quinones and sulfur nucleophiles, which remains an underdeveloped transformation in synthesis. There are currently no strategies to suppress redox-exchange, and factors governing this process remain poorly understood.



Scheme 2.2.8- A General Scheme for the Process of Redox-Exchange

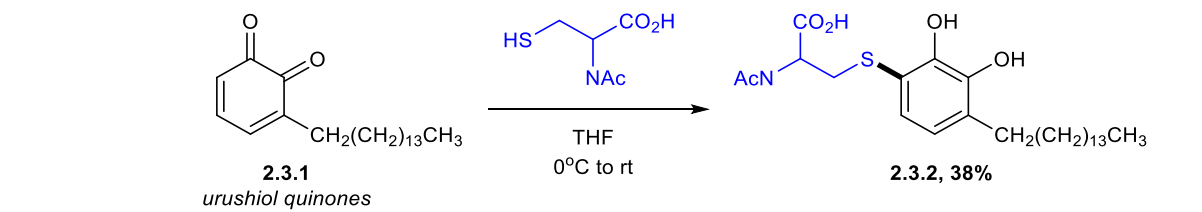
2.3 Addition to *ortho*-Quinones in Detoxification Pathways

Outside the field of melanogenesis, sulfur addition to *ortho*-quinones has also been explored within the context of detoxification pathways in biological systems. Central to these detoxification mechanisms is the thiol glutathione, which in many cells, accounts for over 90% of sulfur not found in proteins.¹³ As a protective mechanism, glutathione acts as an antioxidant by reacting with harmful electrophilic oxygen species, *e.g.* epoxides, through its thiol moiety to form conjugates, which are then excreted through the mercapturate pathway.¹³ Quinones are structures that are inherently electrophilic, oxidative, and widely pervasive in nature. Their significance has already been discussed in the context of melanogenesis. They can also be found as key components of the electron transport chain in cellular respiration and photosynthesis as ubiquinones, plastoquinones,

and menaquinones (vitamin K).¹⁴ As highly electrophilic species, they are sequestered by glutathione through nucleophilic addition as a means to mediate their toxicity in biological systems. This section will discuss the various transformations of glutathione and other biological thiols with *ortho*-quinones that have been identified.

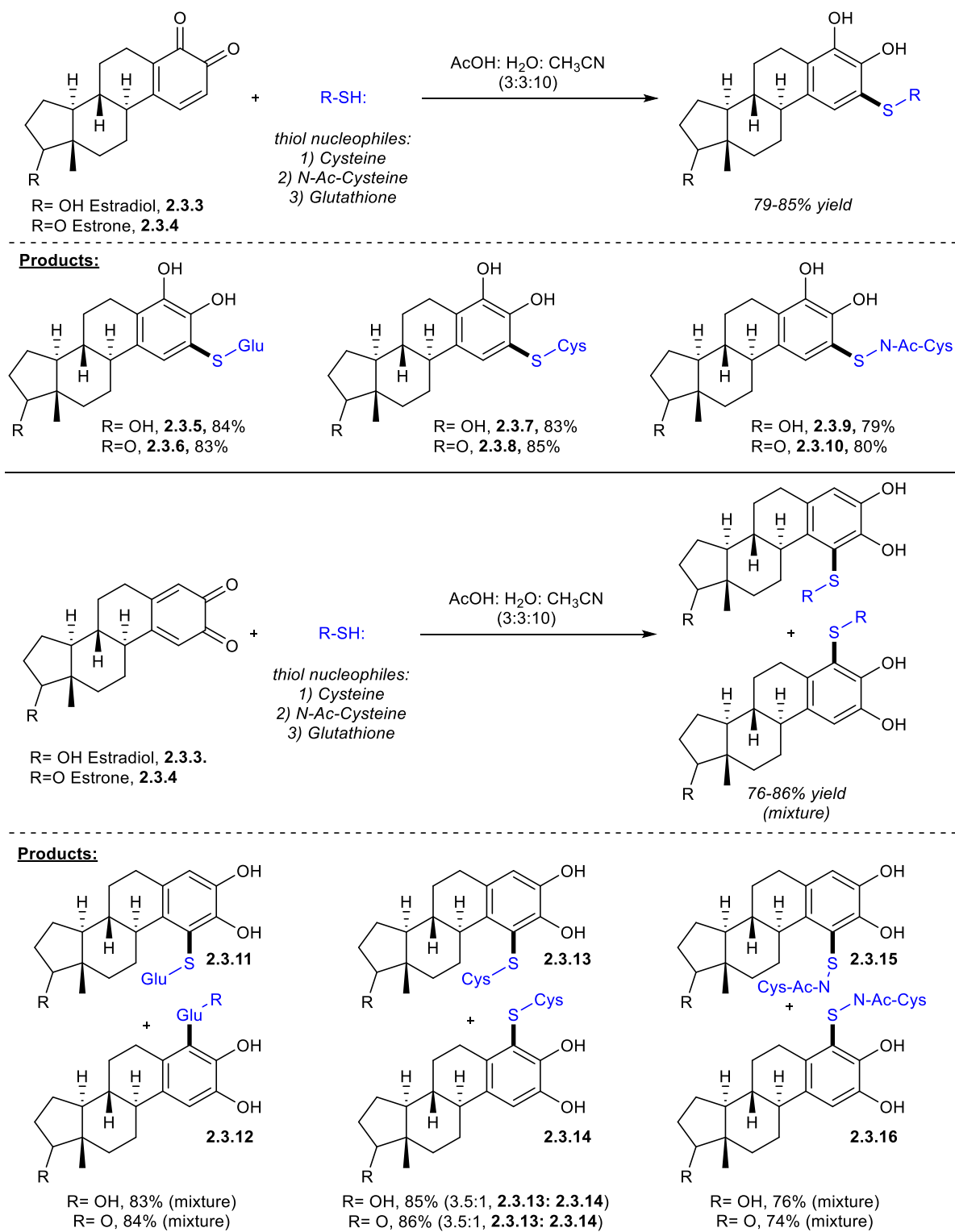
The intrinsic reactivity of *ortho*-quinones with sulfur nucleophiles was first discussed in 1975.¹⁵ It was thought that the products arising from oxidations of catecholamines in the brain were key factors in the development of mental illnesses such as schizophrenia, and highlighted the importance of investigating the fate of these reactive species. It was recognized that *ortho*-quinones undergo a variety of coupling reactions with nucleophiles in biological settings. Using cyclic voltometry, cysteine and glutathione was calculated to add to 4-methyl-*ortho*-quinone with a pseudo-first order rate constant of 361 and 122 sec⁻¹ respectively, with the *ortho*-quinone as the limiting reagent. By comparison, the nitrogen nucleophiles aniline and lysine were determined to have rate constants of 13.7 and 0.0065 sec⁻¹ respectively. However, these values are only approximate as they were collected under pseudo-first order conditions, using a five-fold excess of thiol at 0.5 mM.

The same research group then reported characterization of products arising from the regioselective addition of sulfur nucleophiles to urushiol *ortho*-quinones, which derive from catechols present in poison oak and poison ivy (*Anacardiaceae*) (Scheme 2.3.1).¹⁶ It was highlighted that N-acetylcysteine adds to the *ortho*-quinone **2.3.1** at C6 with quantitative conversion, but they report an isolated yield of **2.3.2** of only 38%. Concomitant reduction of the urushiol quinone to the corresponding catechol was also observed, indicating a competitive redox exchange. There were no further studies performed to determine the factors influencing regioselectivity of the reaction, but the authors noted that the reactivity was aligned with previous studies.¹⁷



Scheme 2.3.1- A Regiospecific Addition of N-Acetylcysteine to Urushiol Quinones, by Castagnoli et al

Catechol estrogen quinones have been identified as being carcinogenic metabolites in estrogen induced cancer.¹⁸ These quinones alter DNA through redox processes or result in DNA depurination through Michael addition.¹⁸⁻¹⁹ Cavalieri *et al.* demonstrated that glutathione added to these estrogen quinones and upon this, hypothesized that these adducts were sequestered in this fashion for catabolism via the mercapturic acid degradation pathway.² These authors subsequently synthesized a range of estrogen-catechol/glutathione conjugates via addition of the thiol to estrogen quinones in good yields, to be employed as standards for characterization for further studies (Scheme 2.3.2). However, in the case of the 2,3-*ortho*-quinones (Substrates **2.3.5-16**), the products could only be isolated as mixtures of regioisomers and were not isolable.

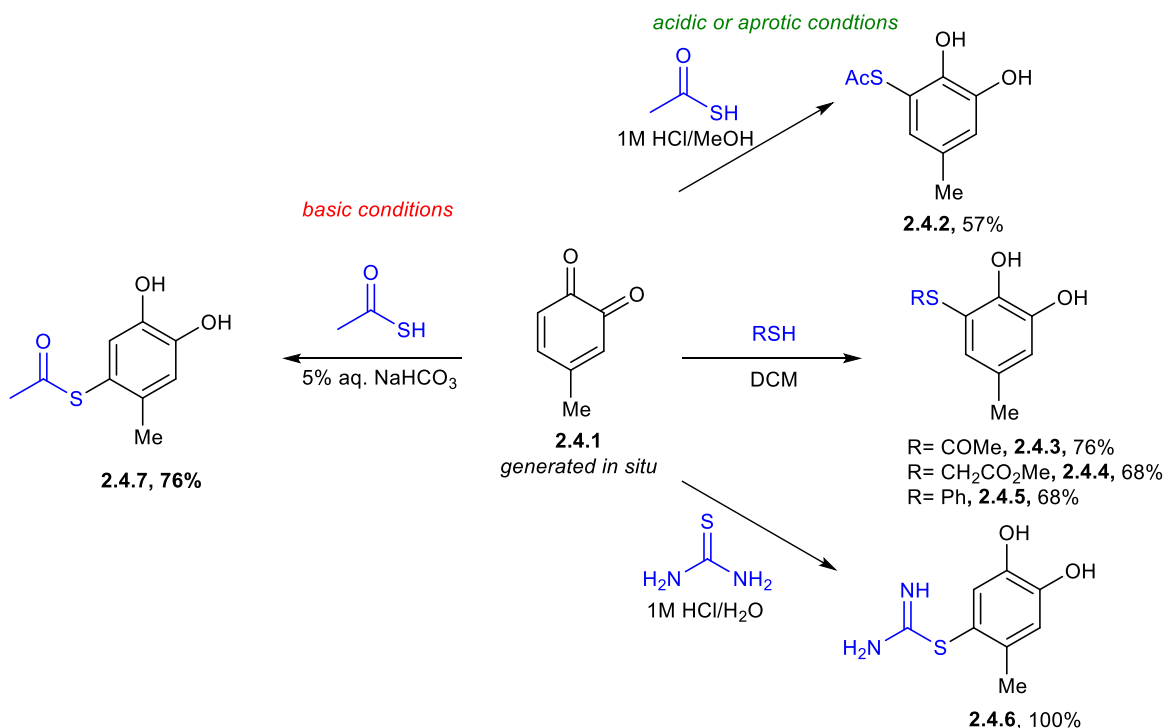


Scheme 2.3.2-Sulfur Addition to Catechol Estrogen Quinones by Cavalieri et al.

2.4 Studies on Thiol Addition to *ortho*-Quinones

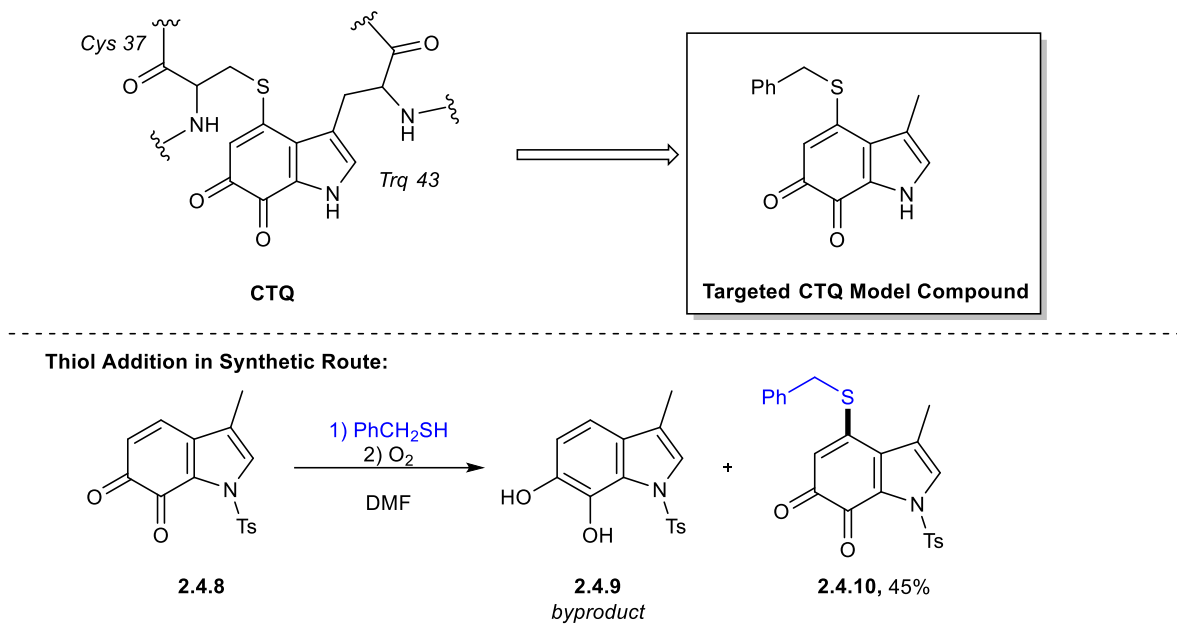
With the realized increasing presence of thiol addition to *ortho*-quinones, studies have begun to focus explicitly on this rapid transformation. Through a series of QSAR studies, the reactivity of thiols with 4-*mono*-substituted *ortho*-quinones was examined. It was shown that the rate constants of the thiol addition increased with the electron-withdrawing capacities of the substituent groups on the *ortho*-quinone. The second order rate constants ranged from 4×10^5 to 3×10^7 $\text{M}^{-1}\text{sec}^{-1}$, providing the first quantification of this rapid process. These calculated rate constants correlate reasonably well with the pseudo first order rate constants measured earlier by Adams *et al.*¹⁵

The regioselectivity of sulfur nucleophilic addition to *ortho*-quinones was examined briefly by Castagnoli *et al.* while targeting the synthesis of 6-mercaptodopamine, a compound associated with *in vivo* neuronal degeneration (Scheme 2.4.1).¹⁷ Four thiol nucleophiles were examined, with the specific aim of targeting 1,4-addition products. It was reported that under basic conditions, a 1,4-addition of thioacetic acid to 4-methyl-*ortho*-quinone **2.4.1** was achieved. Conversely, under neutral or acidic conditions, a 1,6-addition product was isolated (**2.4.2-6**). The change in regioselectivity was attributed to the thiol nucleophile. In basic conditions, a thiolate would be present as opposed to the thiol, and favour 1,4-addition to generate **2.4.7**. However, in neutral aprotic or acidic conditions, a less reactive neutral thiol is present, and thus would prefer the 1,6-addition due to the resulting anion possessing larger resonance stabilization. After further studies with thiourea in acidic conditions yielded the 1,4-product, a different regioisomer than otherwise predicted, it was noted that the inherent reactivity of thiol nucleophiles with *ortho*-quinones was just one of many unknown factors governing regioselectivity, which was not so readily predicted. From their observations, the authors decided upon a different route to their mercaptodopamine targets that did not involve addition to quinones.



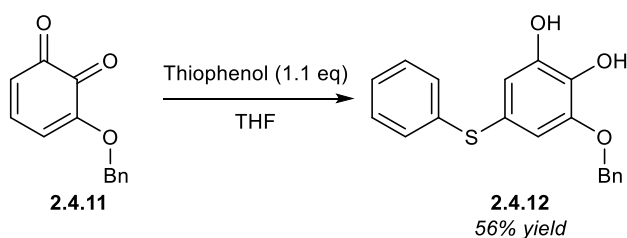
Scheme 2.4.1-Thiol-Additions to 4-Methyl-ortho-Quinone in Acidic, Aprotic, or Basic Media, by Castagnoli et al.

In 2004, Itoh *et al.* demonstrated the first example where thiol addition to *ortho*-quinone was synthetically useful.²⁰ Quinohemoprotein amine dehydrogenase (QH-AmDH) is a bacterial enzyme that contains an organic cofactor in its γ -subunit, CTQ.²¹ CTQ itself is a framework of tryptophan quinone bound to the thiol moiety of cysteine at the C-4 position (Scheme 2.4.2). Itoh *et al.* targeted a CTQ model compound in 7 steps, generating the desired aryl C-S bond through a 1,4-addition of benzylthiol to the tosylated-indolequinone **2.4.8**. The reaction was performed by mixing the quinone and thiol under an O_2 atmosphere in DMF, with a reported 45% isolated yield of the quinone-thiol adduct **2.4.10**. It was reported that along with isolating the desired product, the un-reacted catechol byproduct **2.4.9** was also obtained, a clear indication of redox exchange.



Scheme 2.4.2- A Synthesis of a Model Compound of the Organic Co-Factor in the γ -Subunit of QH-AmDH

In 2009, *ortho*-quinones were recognized by Pettus *et al.* as synthetically useful scaffolds with the ability to access a variety of functionalized molecules.²² Various transformations of *ortho*-quinone **2.4.11** were demonstrated with a variety of nucleophiles, including 1,2-addition, 1,4-addition, and etherification. More specifically, the 1,6-addition of thiophenol to quinone **2.4.11** was reported (Scheme 2.4.3). However, only one thiol addition was demonstrated, and **2.4.12** was isolated in a 56% yield.

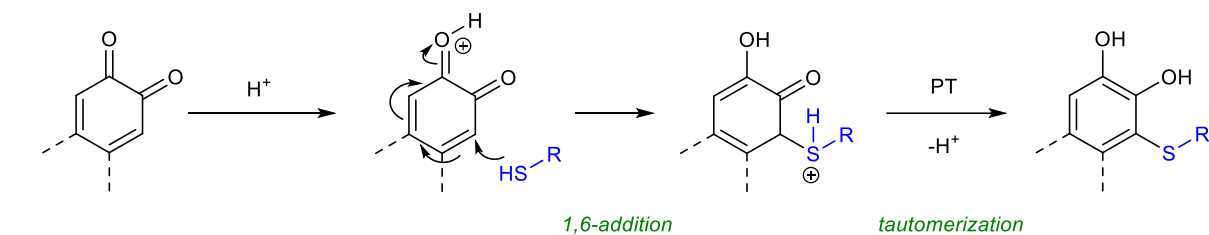


Scheme 2.4.3- Addition of thiophenol to 3-benzyl-ortho-quinone 2.4.11, by Pettus et al.

As such, quinones have now been recognized as a means to access a variety of functionalized molecules, including work on the synthesis of nitrogen containing heterocycles in our own group.²³ However, the addition of sulfur to quinones has not yet been exploited. These preliminary studies discussed above demonstrate precedent and the clear potential for the development of this transformation to an alternative S-arylation method.

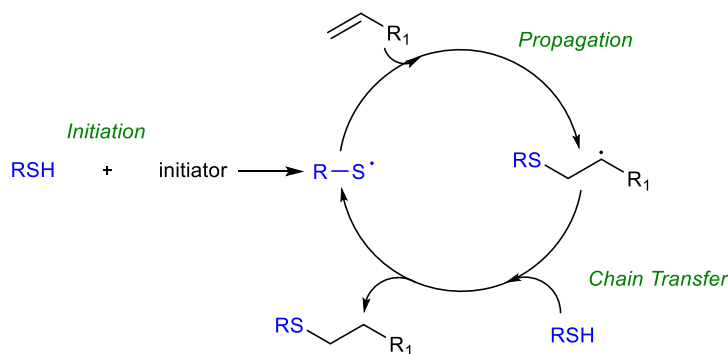
2.5 Plausible Mechanisms

This transformation has been shown to proceed under varying reaction conditions. In the biological studies discussed in Section 2.2, 2.3, and 2.4, the reaction is carried out in biomimetic conditions, i.e. in regulated pH \approx 6.8-7.0 buffer solutions. Given that the pK_a of the thiol moieties in cysteine and glutathione are 8.53 and 9.20 respectively²⁴, it is assumed that the thiol, and not the thiolate, is the active sulfur species in these reaction systems. Thus, one can envision the addition occurring through a 1,6-nucleophilic addition to quinone, as shown in (Scheme 2.5.1).



Scheme 2.5.1- A General Mechanism of 1,6-Addition to ortho-Quinone

Another possible mechanism that the addition occurs through is the thiol-ene reaction. The thiol-ene reaction is a transformation that has been known for a century, involving the addition of a thiol to an ene bond.²⁵ Historically, the term thio-ene has been used to denote reactions involving a radical mechanism, but some authors have also used the term to categorize all sulfur additions to ene bonds, including those mediated by base/nucleophilic processes. Within the context of this thesis, the term thio-ene will refer to the addition of thiol to an olefin via a radical mechanism, and the base/nucleophile mediated reactions will be referred to as conjugate additions. The thio-ene reaction cycle occurs via a radical pathway involving initiation, propagation, and termination steps, as shown in Scheme 2.5.2. Typically, the initiation step begins with reaction of thiol with a photoinitiator, forming a thiyl radical. Propagation involves the addition of the thiyl radical to the olefin to generate a carbon centered radical, with subsequent chain transfer to a second molecule of thiol to generate the final addition product.²⁵



Scheme 2.5.2- A General Mechanism of the Thiol-Ene Reaction

Due to the limited number of examples present and lack of attention afforded, currently no thorough investigations into the mechanism have been performed. Although it is clear that there are several disparate examples of this transformation in the literature, there has not yet been a comprehensive study on the synthetic utility of this transformation.

2.6 Summary

As discussed, the sulfur addition to *ortho*-quinones is: 1) a known process in literature²⁶, 2) a reaction shown to proceed rapidly, and 3) is accomplished without the requirement for external catalysis. This is exemplified by the ubiquity of this transformation in melanogenesis and in the detoxification of biological systems. However, the potential for this reaction to be an efficient S-arylation process has yet to be recognized. Albeit at first glance a simple transformation, it is evident that it is a reaction that comes not without its complexities and idiosyncrasies arising in regioselectivity and redox-exchange. In the next chapter, we will discuss the development and optimization of a facile method of C-S bond formation using sulfur addition to *ortho*-quinones.

2.7 References

1. Ito, S. A Chemist's View of Melanogenesis. *Pigment Cell Res.* **2003**, *16* (3), 230-236.
2. Cao, K.; Stack, D. E.; Ramanathan, R.; Gross, M. L.; Rogan, E. G.; Cavalieri, E. L. Synthesis and Structure Elucidation of Estrogen Quinones Conjugated with Cysteine, N-Acetylcysteine, and Glutathione. *Chem. Res. Toxicol.* **1998**, *11* (8), 909-916.
3. (a) Protá, G., Nicolaus, R. A. . *Gazzetta chimica Italiana* **1967**, *97*, 665; (b) Thomson, R. H. The Pigments of Reddish Hair and Feathers. *Angew. Chem. Int. Ed.* **1974**, *13* (5), 305-312.
4. Protá, G. S., G.; Petrillo, O.; Nicolaus, R. A. *Gazzetta chimica Italiana* **1969**, *99*, 1193.
5. Protá, G. S., G.; Nicolaus, R. A. *Gazzetta chimica Italiana* **1968**, *98*, 495.
6. Rorsman, H.; Rosengren, A. M.; Rosengren, E. Determination of 5-S-cysteinyl-dopa in melanomas with a fluorimetric method. *Yale J. Biol. Med.* **1973**, *46* (5), 516-522.
7. Ito, S.; Protá, G. A facile one-step synthesis of cysteinyl-dopas using mushroom tyrosinase. *Experientia* **1977**, *33* (8), 1118-9.
8. d'Ischia, M.; Napolitano, A.; Protá, G. Sulphydryl compounds in melanogenesis. *Tetrahedron* **1987**, *43* (22), 5357-5362.
9. Thompson, A.; Land, E. J.; Chedekel, M. R.; Subbarao, K. V.; Truscott, T. G. A pulse radiolysis investigation of the oxidation of the melanin precursors 3,4-dihydroxyphenylalanine (dopa) and the cysteinyl-dopas. *Biochim. Biophys. Acta* **1985**, *843* (1), 49-57.
10. Land, E. J.; Riley, P. A. Spontaneous Redox Reactions of Dopaquinone and the Balance between the Eumelanin and Pheomelanin Pathways. *Pigment Cell Res.* **2000**, *13* (4), 273-277.
11. Hearing, V. J. Biochemical control of melanogenesis and melanosomal organization. *J. Invest. Dermatol. Symp. Proc.* **1999**, 24-28.
12. Hida, T.; Wakamatsu, K.; Sviderskaya, E. V.; Donkin, A. J.; Montoliu, L.; Lynn Lamoreux, M.; Yu, B.; Millhauser, G. L.; Ito, S.; Barsh, G. S.; Jimbow, K.; Bennett, D. C. Agouti protein, mahogunin, and attractin in pheomelanogenesis and melanoblast-like alteration of melanocytes: a cAMP-independent pathway. *Pigment Cell Melanoma Res.* **2009**, *22* (5), 623-634.
13. Meister, A. Glutathione metabolism and its selective modification. *J. Biol. Chem.* **1988**, *263* (33), 17205-8.
14. Monks, T. J. J., D.C. The Metabolism and Toxicity of Quinones, Quinonimines, Quinone Methides, and Quinone-Thioethers. *Curr. Drug Metab.* **2002**, *3*, 425-438.

15. Tse, D. C. S.; McCreery, R. L.; Adams, R. N. Potential oxidative pathways of brain catecholamines. *J. Med. Chem.* **1976**, *19* (1), 37-40.
16. Liberato, D. J.; Byers, V. S.; Dennick, R. G.; Castagnoli, N. Regiospecific attack of nitrogen and sulfur nucleophiles on quinones derived from poison oak/ivy catechols (urushiols) and analogs as models for urushiol-protein conjugate formation. *J. Med. Chem.* **1981**, *24* (1), 28-33.
17. Chavdarian, C. G.; Castagnoli, N. Synthesis, redox characteristics, and in vitro norepinephrine uptake inhibiting properties of 2-(2-mercapto-4,5-dihydroxyphenyl)ethylamine (6-mercaptodopamine). *J. Med. Chem.* **1979**, *22* (11), 1317-1322.
18. Cavalieri, E.; Chakravarti, D.; Guttenplan, J.; Hart, E.; Ingle, J.; Jankowiak, R.; Muti, P.; Rogan, E.; Russo, J.; Santen, R.; Sutter, T. Catechol estrogen quinones as initiators of breast and other human cancers: Implications for biomarkers of susceptibility and cancer prevention. *Biochim. Biophys. Acta* **2006**, *1766* (1), 63-78.
19. Zhang, Q.; Tu, T.; d'Avignon, D. A.; Gross, M. L. Balance of Beneficial and Deleterious Health Effects of Quinones: A Case Study of the Chemical Properties of Genistein and Estrone Quinones. *J. Am. Chem. Soc.* **2009**, *131* (3), 1067-1076.
20. Murakami, Y.; Tachi, Y.; Itoh, S. A Model Compound of the Novel Organic Cofactor CTQ (Cysteine Tryptophylquinone) of Quinohemoprotein Amine Dehydrogenase. *Eur. J. Org. Chem.* **2004**, *2004* (14), 3074-3079.
21. McIntire, W.; Wemmer, D.; Chistoserdov, A.; Lidstrom, M. A new cofactor in a prokaryotic enzyme: tryptophan tryptophylquinone as the redox prosthetic group in methylamine dehydrogenase. *Science* **1991**, *252* (5007), 817-824.
22. Miller, L. A.; Marsini, M. A.; Pettus, T. R. R. Chemoselective Reactions of 3-Benzoyloxy-1,2-o-Quinone with Organometallic Reagents. *Org. Lett.* **2009**, *11* (9), 1955-1958.
23. Huang, Z.; Askari, M. S.; Esguerra, K. V. N.; Dai, T.-Y.; Kwon, O.; Ottenwaelder, X.; Lumb, J.-P. A bio-inspired synthesis of oxindoles by catalytic aerobic dual C-H functionalization of phenols. *Chem. Sci.* **2016**, *7* (1), 358-369.
24. Benesch, R. E.; Benesch, R. The Acid Strength of the -SH Group in Cysteine and Related Compounds. *J. Am. Chem. Soc.* **1955**, *77* (22), 5877-5881.
25. Lowe, A. B. Thiol-ene "click" reactions and recent applications in polymer and materials synthesis. *Polym. Chem.* **2010**, *1* (1), 17-36.

26. Greco, G.; Panzella, L.; Verotta, L.; d'Ischia, M.; Napolitano, A. Uncovering the Structure of Human Red Hair Pheomelanin: Benzothiazolylthiazinodihydroisoquinolines As Key Building Blocks. *J. Nat. Prod.* **2011**, *74* (4), 675-682.

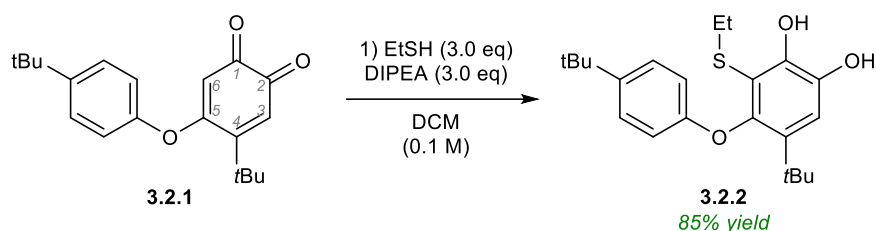
3 Experiments

3.1 Introduction

In Chapter 2, we discussed the addition of sulfur to *ortho*-quinones in biological contexts, covering the literature up to the present day for this specific transformation. Over the past two years we have examined this reaction for the development of a general method for S-arylation. Our initial experiments and thiol scope are detailed in sections 3.2 and 3.3, followed by optimization of our method in section 3.4. As will be shown in section 3.4, the regiochemistry of the addition becomes tunable by varying reaction conditions, and our regiochemical assignment from spectral data is described in section 3.5. Expansion of the reaction scope with respect to the *ortho*-quinone will be discussed in section 3.6. Section 3.7 includes a discussion on the Lewis acid magnesium bromide diethyl etherate ($\text{MgBr}_2 \cdot \text{Et}_2\text{O}$), as it will be shown in section 3.4 that it plays an important role as a beneficial additive in the reaction. Section 3.8 will include a discussion on the proposed mechanism of the transformation, and the factors governing regioselectivity. Finally, in 3.9, applications of the developed method to yield catechol ligands for iron-oxide nanoparticle conjugation will be discussed.

3.2 Initial Experiments

This work has origin in an initial experiment performed by Mr. Kenneth Esguerra (a Ph.D. candidate in the Lumb Group), who investigated the reaction of *ortho*-quinone **3.2.1** and ethanethiol using N,N-Diisopropylethylamine (DIPEA) as a Brønsted base (Scheme 3.2.1). Under these conditions, catechol **3.2.2** was isolated as a single regioisomer with C-S bond formation occurring exclusively at C6 in 85% isolated yield (See Section 3.4 for a detailed discussion on the assignment of regiochemistry). This result demonstrated aromatic C-S bond formation under remarkably mild reaction conditions, which motivated our work to develop this transformation into a more general methodology.

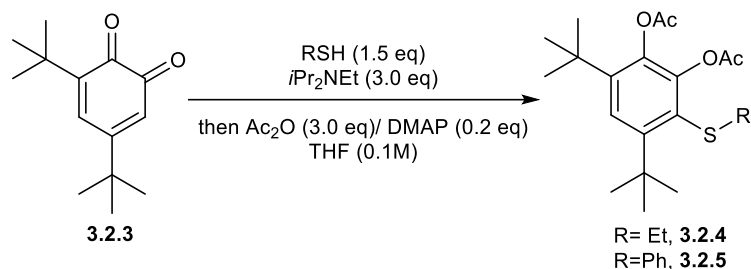


Scheme 3.2.1- Initial Experiment Investigating the Addition of Sulfur Nucleophiles to ortho-Quinones

As a point of departure, reaction conditions for C-S bond formation using 3,5-di-*tert*-butyl-*ortho*-quinone **3.2.3** as a model substrate were examined, due to its commercial availability and stability (Table 3.2.1). To simplify purification, crude reaction mixtures were treated with acetic anhydride (3.0 equiv) and catalytic amounts of 4-dimethylaminopyridine (DMAP). Under these conditions, the catechol is acetylated with high efficiency, and provides the corresponding bis-acetate, which is redox stable, and avoids complications of air-oxidation during isolation and purification.

In the early phases of the project, we compared the conditions developed by Mr. Esguerra with conditions reported previously in the literature (Table 3.2.1). All reactions proceeded to complete conversion. Under slightly modified conditions to those reported by Mr. Esguerra, namely using 1.5 equiv of ethanethiol and 3 equiv of DIPEA, the reaction provided **3.2.4** in 88% yield (Entry 1). Degassing the solvent by purging with N₂ immediately prior to use increased the reaction yield to 99% (Entry 2). Similar results were also obtained with thiophenol **3.2.5** (Entry 3 & 4). We hypothesize that removal of O₂ suppresses deleterious reactions that arise from reaction with the corresponding semi-quinone radical. Previously reported methods of thiol addition to quinones have involved a large range of acidic conditions with variable yields, ranging from mildly acidic (3:3:10 acetic acid : water : CH₃CN)¹ to strongly acidic²(2M sulfuric acid). Thus, we next examined the addition of ethanethiol to quinone **3.2.3** under acidic conditions, employing *para*-toluene sulfonic acid (p-TsOH) as a Brønsted acid (pK_a = -2.8 in H₂O³). Under these conditions, **3.2.3** is isolated in 63% yield. Finally, we wanted to examine if the reaction would proceed with greater efficiency under more strongly basic conditions, and as such, the use of a sodium thiolate was evaluated. This returned **3.2.3** in 79% yield. For all entries, despite the reaction proceeding to complete conversion, the only major product isolated was the desired thiol adduct. These preliminary reactions demonstrated that our conditions using

DIPEA as a mild Brønsted were the most efficient (Entries 2 and 4, Table 3.2.1), meriting further investigation.



Entry	Thiol	Conditions	Yield
1	Et	Basic (DIPEA)	88
2^a	Et	Basic (DIPEA)	99
3	Ph	Basic (DIPEA)	89
4^a	Ph	Basic (DIPEA)	92
5^b	Et	Strongly Basic (Sodium Thiolate)	79
6^c	Et	Acidic (pTsoH)	63

^aSolvent was degassed

^bSodium Thiolate used as nucleophile

^cpTsoH (1.0 eq), no DIPEA


Table 3.2.1-Initial Experiments with *ortho*-Quinone 3.2.3

3.3 Expansion of Thiol Substrate Scope

Given these promising initial experiments, we proceeded to expand the thiol scope with quinone **3.2.3**. Consistently good results were obtained between the reaction of **3.2.3** with primary, secondary and tertiary alkyl thiols, which provided products in yields > 80% (**3.2.4**, **3.2.6-8**, Table 3.3.1). Most importantly, sterically demanding *tert*-butyl-thiol (Substrate **3.2.8**) afforded the corresponding aryl C-S bond in 85%. Of the 30 recently reported methods discussed in Chapter 2, only two are able to couple the sterically hindered *tert*-butyl thiol.⁴ The first Chan-Lam conditions reported by Guy *et al.* give only a 2% yield for the tertiary alkyl thiol coupled product.⁵

Aryl thiols possessing electron-donating or electron-withdrawing groups at the *ortho*-, *meta*- and *para*-positions were also compatible with our standard reaction conditions (**3.2.11-17**, Table 3.3.1). 1- and 2-naphthalenethiols reacted well, providing substrates **3.2.8** and **3.2.9** in high yield. Of the aryl thiols evaluated, we were pleased to observe that yields were the same for 2-methylthiophenol and 4-methylthiophenol (Table 3.3.1), demonstrating the method's tolerance for *ortho*-substituents. Electron-withdrawing groups on the aryl ring were also tolerated, generating adducts **3.2.13-16** in high yields. It is important to note that of the recently reported


methods discussed in Chapter 1, few are able to couple secondary thiols, and even less in the case of tertiary thiol nucleophiles. Our method affords the tertiary *tert*-butyl thiol adduct **3.2.8** in a good yield of 85%. In addition, all transition metal catalyzed methods included the use of elevated temperatures, whereas our method has shown to proceed rapidly at room temperature. Our scope thus far demonstrates a broad electronic tolerance for substituent groups on the aromatic thiols evaluated. As such, this is a clear demonstration that our method is uniquely positioned to access both aryl-S-aryl and aryl-S-alkyl linkages, under mild reaction conditions that are transition-metal free.



3.2.3

R-SH (1.5 eq)
iPr₂NEt (3 eq)

then Ac₂O / DMAP
THF (0.1 M), rt



Substrate	R =	Yield (%)	Substrate	R =	Yield (%)
3.2.4	Et	99	3.2.11	2-MePh	95
3.2.5	Ph	99	3.2.12	4-MePh	95
3.2.6	Oct	85	3.2.13	3-OMePh	98
3.2.7	iPr	96	3.2.14	4-BrPh	90
3.2.8	tBu	85	3.2.15	4-ClPh	84
3.2.9	1-naph	95	3.2.16	4-F	88
3.2.10	2-naph	96	3.2.17	4-OMe	76

Table 3.3.1- Initial Thiol Substrate Scope with *ortho*-Quinone **3.2.3**

As a preliminary evaluation of quinone scope, we selected two electronically and sterically differentiated *ortho*-quinones in addition to quinone **3.2.1** (originally employed by Mr. Esguerra) (Figure 3.3.1), to evaluate the efficiency, chemo- and regioselectivity of our standard reaction conditions across a range of sterically and electronically distinct thiols.

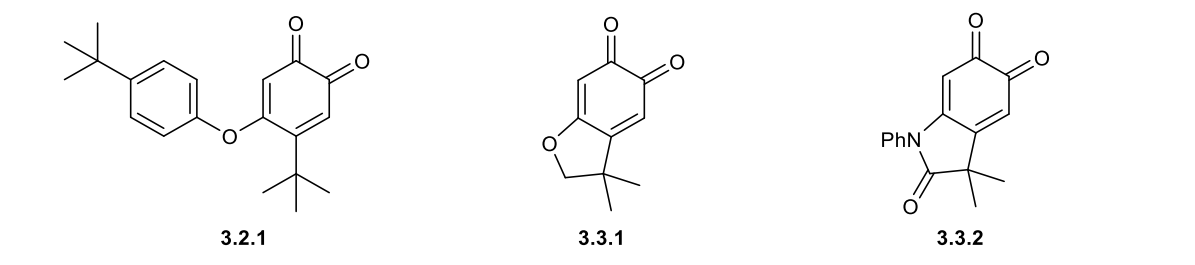


Figure 3.3.1-Quinones selected for Initial Substrate Scope

Beginning with **3.2.1**, high yields were obtained with alkyl thiols, furnishing the ethyl and octyl adduct **3.3.3** and **3.3.4** in 87 and 85% yield respectively (Table 3.3.2). A moderate yield was obtained with secondary alkyl thiol 2-propanethiol, with a 58% yield for **3.3.6**. For aromatic thiol scope, all yields were high, between 82-93%. Again, *ortho*-substituents were

tolerated, as demonstrated by substrate **3.3.8** in 90% yield. Electron-donating and –withdrawing substituents were also amenable to this quinone, with yields ranging from 82–91% (**3.3.9–12**).

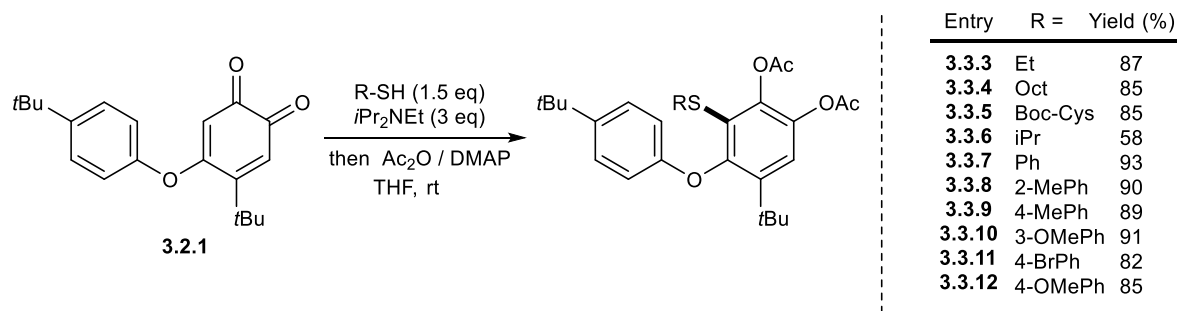


Table 3.3.2- Initial Thiol Substrate Scope with *ortho*-Quinone **3.2.1**

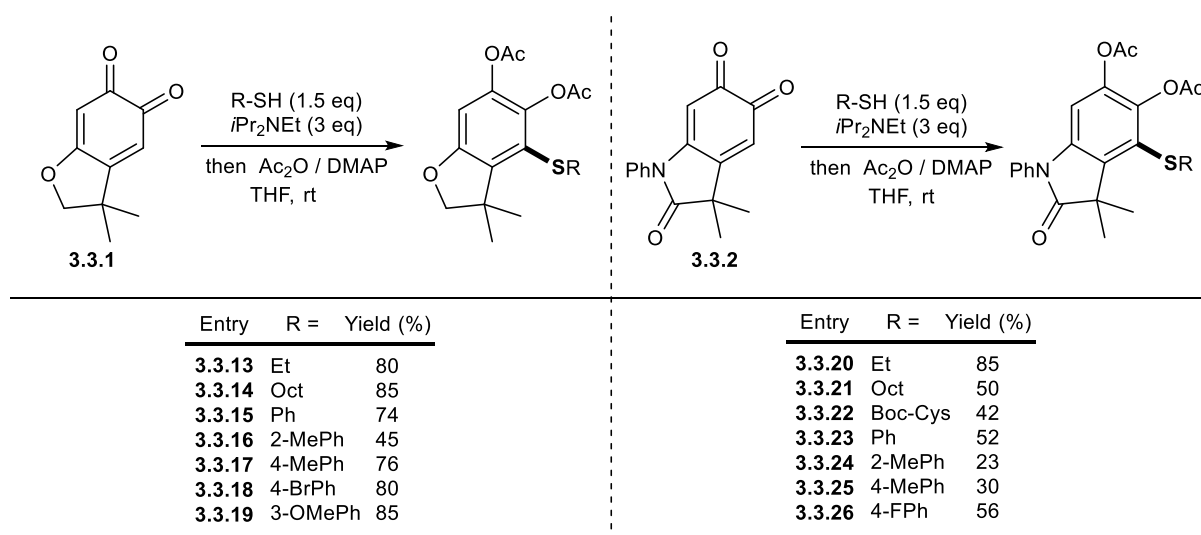
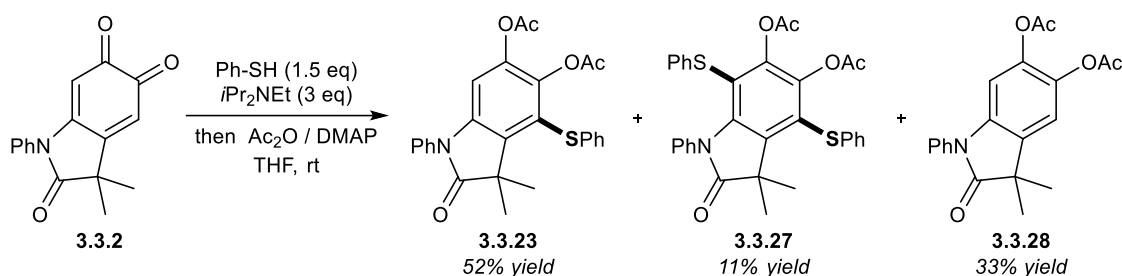


Table 3.3.3- Initial Thiol Substrate Scope with *ortho*-Quinones **3.3.1** and **3.3.2**

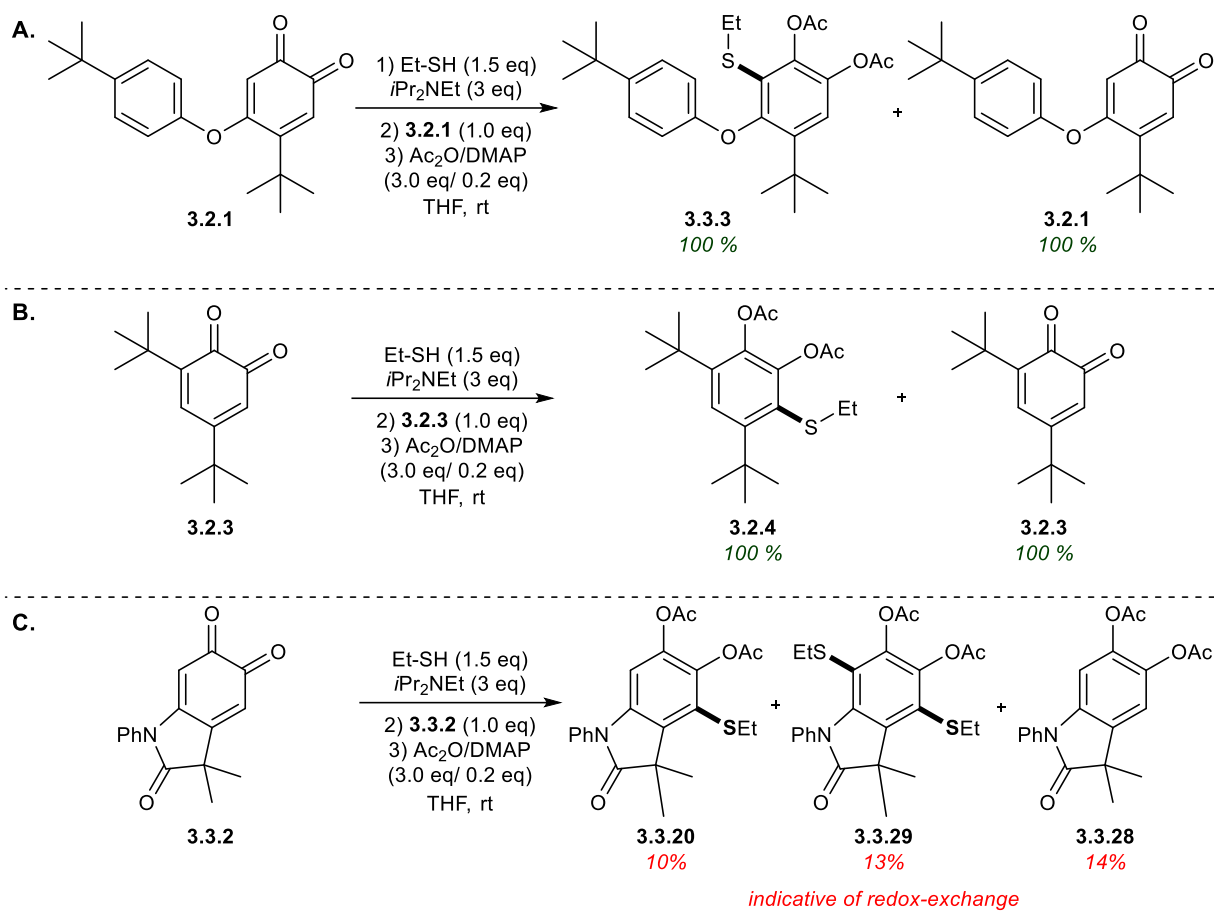
Expansion of the *ortho*-quinone scope to **3.3.1** showed similar reactivity trends similar to quinone **3.2.1**. Reasonable yields were obtained for alkyl thiols and most electron-withdrawing and –donating aromatic thiols (Entries **3.3.13–15**, **3.3.17–19**, Table 3.3.3), but a low yield of 45% was obtained with the reaction of 2-methylthiophenol (Entry **3.3.16**, Table 3.3.3). At first glance, one may attribute the decrease in yield to steric effects, however, given that the reaction of quinone **3.3.1** and 2-methylthiophenol gave product **3.3.9** in 90% yield, the reason may not be as straightforward. In addition, upon further expansion of the quinone scope to substrate **3.3.2**, it was found that with the exception of ethanethiol (Entry **3.3.21**, Table 3.3.3), all yields were obtained in diminished yields. A similar decrease in yield with **3.3.3** was also observed for the reaction with the sulfur nucleophile 2-methylthiophenol (Entry **3.3.25**, Table 3.3.3). Although all

thiol additions proceeded to complete conversion, it was noted that multiple products were obtained in the crude mixture isolated from reactions involving quinone **3.3.3**, and the mass balance of the reactions could not be accounted for. For the reaction of quinone **3.3.3** and thiophenol, (Entry **3.3.24**, Scheme 3.3.1), the di-thiol adduct **3.3.27** and bis-acetylated catechol **3.3.28** were isolated. The isolation of the di-thiol adduct **3.3.27** indicated that redox-exchange was occurring in the reaction, *i.e.* that the product **3.3.23** catechol was oxidizing to the quinone, and allowing for a second thiol addition to occur at C6. The bis-acetylated catechol **3.3.28** isolated is the product generated from the redox-exchange of starting material quinone **3.3.2**, and product **3.3.23**.



*Scheme 3.3.1- Isolation of Multiple Products from Reaction of ortho-quinone **3.3.2** and thiophenol*

As previously discussed in Chapter 2, redox-exchange is a process that is known to occur between electron-rich catechols and electron-poor quinones. In order to further substantiate whether redox-exchange was a process that was occurring with the *ortho*-quinones selected for thiol scope, the following experiments were performed. With *ortho*-quinones **3.2.1**, **3.2.3**, and **3.3.2**, the ethanethiol adducts (**3.2.4**, **3.3.3**, and **3.3.20**) were generated in solution (Scheme 3.3.2). At this point, instead of bis-acetylation of the product catechol, another equivalent of starting material quinone was added. This mixture was stirred for 1.5h, upon which acetic anhydride/DMAP was added.



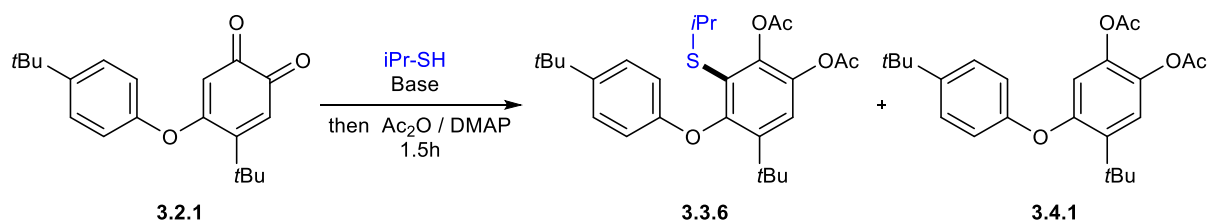
Scheme 3.3.2- Experiments Probing Redox-Exchange with A) 3.2.1, B) 3.2.3, C) 3.3.2

The experiment with quinone **3.2.1** yielded complete recovery of thiol-adduct products **3.1a** and un-consumed quinone **3.2.1**, indicative that redox-exchange was not occurring. A similar result was obtained for quinone **3.2.3**. However, the analogous experiment with quinone **3.3.2** gave complex mixtures, from which **3.3.20**, **3.3.29**, and **3.3.28**, were isolated. Mass balance also could not be accounted for. This result verified our hypothesis that redox-exchange was a deleterious process occurring during the thiol additions performed with quinone **3.3.2**. Although its effects observed in the thiol scope are not as pronounced as in the set of experiments in Scheme 3.3.1C, it provides an explanation for the diminished yields observed with the initial scope. Given these results, it was concluded that further optimization of the reaction was required. Although redox-exchange has been previously observed with the reaction of sulfur nucleophiles and *ortho*-quinones, there is no general approach to prevent this process from occurring. Upon examination of our current thiol scope, we selected a moderately yielding substrate, quinone **3.2.1** and 2-propanethiol (**3.3.6**, Table 3.3.2), to perform optimization studies.

Though redox-exchange active, quinone **3.3.2** was not employed for optimization after consideration of the feasibility and cost of generating **3.2.1** vs. **3.3.2**.

3.4 Optimization of Thiol Addition

We next proceeded with our optimization in the hopes that we would elucidate conditions in which the addition proceeded most efficiently and rapidly, and limit redox-exchange. First, it is important to note that throughout our optimization, all reactions proceeded to complete conversion. Second, for all entries, the mass balance is unaccounted for, and cannot be explained at this time. We began our optimization by evaluating different solvents (Table 3.4.1). The production of **3.4.1** was also monitored as an indicator of redox-exchange. Changing from tetrahydrofuran (THF) to the more polar protic solvent methanol (MeOH) returned a comparable yield of **3.3.6**, and suppressed the formation of **3.4.1**. The use of polar, aprotic dimethylformamide (DMF) ($\epsilon = 36.7$, $\mu = 1.88$)⁶ provided a similar yield of **3.3.6**, but also resulted in the formation of **3.4.1**. A similar result was obtained when ethyl acetate (EtOAc) ($\epsilon = 6.02$, $\mu = 1.88$)⁶ was used, observing little change in reactivity from DMF (Entries 1-5, Table 3.4.1). However, upon use of dioxane ($\epsilon = 2.25$, $\mu = 0.45$)⁶, product **3.3.6** was obtained in 69% yield, a 23% increase from the original yield observed with THF (Entry 5). Formation of **3.4.1** was also suppressed, compared to results in EtOAc or DMF. Thus, it appears the reactivity may be slightly increased through the use of a moderately polar aprotic solvent, with a lower dielectric constant and dipole moment.



Entry	Base	Temp	Solvent	Conc. (M)	Additive (0.25 eq)	Yield (%) [*]	
						3.3.6	3.4.1
1	DIPEA	rt	THF	0.1	-	56	11
2	DIPEA	rt	MeOH	0.1	-	60	-
3	DIPEA	rt	DMF	0.1	-	65	20
4	DIPEA	rt	EtOAc	0.1	-	60	24
5*	DIPEA	rt	Dioxane	0.1	-	68	14
6	DBU	rt	THF	0.1	-	-	-
7	pyridine	rt	THF	0.1	-	-	-
8	NEt ₃	rt	THF	0.1	-	32	18
9*	DIPEA	rt	THF	0.1	-	61	14
10	DIPEA	0	THF	0.1	-	60	14
11	DIPEA	-20	THF	0.1	-	62	14
12	DIPEA	rt	Dioxane	0.5	-	67	10
13*	DIPEA	rt	Dioxane	0.01	-	69	14
14	DIPEA	rt	Dioxane	0.05	-	74	8
15	DIPEA	rt	THF	0.05	-	72	10
16	DIPEA	rt	THF:Dioxane (1:1)	0.1	-	63	14
17	DIPEA	rt	THF:Dioxane (1:1)	0.05	-	67	16
18	DIPEA	rt	Dioxane	0.05	Ti(OiPr) ₄	56	22
19	DIPEA	rt	Dioxane	0.05	ZnCl ₂	64	10
20	DIPEA	rt	Dioxane	0.05	CuPF ₆	50	16
21*	DIPEA	rt	Dioxane	0.05	MgBr ₂ .Et ₂ O	90	3
22	DIPEA	rt	Dioxane	0.05	Zn(OTf) ₂	50	16
23	DIPEA	rt	Dioxane	0.05	MgBr ₂	97	2
24	DIPEA	rt	Dioxane	0.05	LiCl	63	16
25	DIPEA	rt	Dioxane	0.05	Mg(ClO) ₄	32	6
26	DIPEA	rt	Dioxane	0.05	LiBr	64	13
27	DIPEA	rt	Dioxane	0.05	MgCl ₂	94	<2
28	DIPEA	rt	Dioxane	0.1	MgBr ₂ .Et ₂ O	96	3
29	DIPEA	rt	THF	0.05	MgBr ₂ .Et ₂ O	73	10
30	DIPEA	rt	DCM	0.05	MgBr ₂ .Et ₂ O	72	6
31	DIPEA	rt	EtOAc	0.05	MgBr ₂ .Et ₂ O	82	9
32	DIPEA	rt	MeOH	0.05	MgBr ₂ .Et ₂ O	30	26
33	DIPEA	rt	DMF	0.05	MgBr ₂ .Et ₂ O	76	10
34	DIPEA	rt	Et ₂ O	0.05	MgBr ₂ .Et ₂ O	62	17
35	DIPEA	rt	Dioxane	0.05	MgBr ₂ .Et ₂ O (0.1 eq)	95	4
36	DIPEA	rt	Dioxane	0.05	MgBr ₂ .Et ₂ O (0.5 eq)	85	6
37	DIPEA	rt	Dioxane	0.05	MgBr ₂ .Et ₂ O (1.0 eq)	95	5

*Average of two yields

Table 3.4.1- Optimization of Thiol Addition with ortho-Quinone 3.2.1 & 2-propanethiol

We then wished to explore the role of base in the reaction. DIPEA, a tertiary amine base, has a pKa of roughly 11 (comparable to trimethylamine- pKa = 10.75 in H₂O⁷), and is often used in organic reactions due to its ability to be a hindered, non-nucleophilic base.⁸ Thus, alternative non- nucleophilic amine bases of varying pKas, including 1,8-diazabicycloundec-7-ene (DBU) (pKa=12 in DMSO), pyridine (pKa= 5.21), and triethylamine (NEt₃) (pKa= 10.75) were also examined.⁷ The transformation failed to take place when DBU and pyridine were used.

Triethylamine was found to generate **3.3.6**, in a lower yield of 32%, along with similar yields in the generation of **3.4.1** at 18% (Entries 6-8). It appears that the strength of the base, as well as its steric influence are governing factors in the reaction. Carbonate bases (K_2CO_3 , Na_2CO_3 , CsCO_3) had also previously been examined, in the reaction between quinone **3.2.1** and sulfur nucleophile N-(*tert*-Butoxycarbonyl)-L-cysteine methyl ester (Boc-Cysteine Methyl Ester), and were found to provide only small amounts of the desired product, with yields ranging from 17-30%. All bases were found to be less effective than DIPEA, confirming our selection of DIPEA as the optimal base for this transformation.

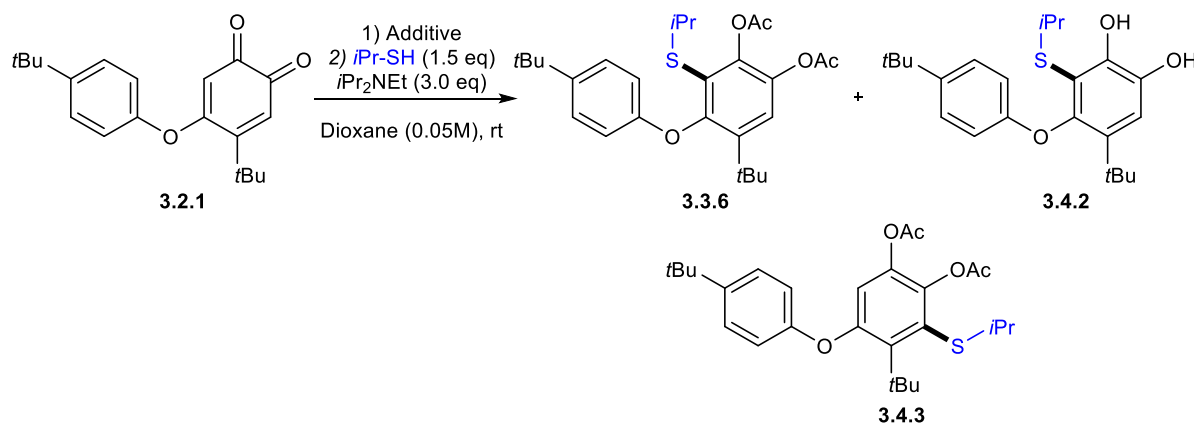
With dioxane and DIPEA as our optimized solvent and base respectively, we wanted to explore whether the reactivity could be tuned to favour the desired product at low temperatures of 0°C and -20°C (Entry 10-11). It was found that within the statistical error of the spectrometer there was no significant increase in yield of either **3.3.6** or **3.4.1** between the reaction at room temperature and ones performed at lower temperatures. The concentration of the reaction was also varied to explore whether redox-exchange could be influenced. An increase in concentration from 0.1 M to 0.5 M resulted in the same yield of **3.3.6** and similar generation of **3.4.1** (13 vs. 10 %, respectively) (Entries 12-13). A decrease in concentration to 0.05M resulted in a slight increase in **3.3.6** to 74%, and slight lowering of **3.4.1** to 8% (Entry 13). However, further decrease in concentration to 0.01M did not result in any statistically significant change in reactivity (Entry 23). In order to determine whether this observation was limited to dioxane, THF was re-evaluated as a solvent using a concentration of 0.05M (Entry 15). The yield of **3.3.6** was similar to that obtained in dioxane, but there was a slight increase in the production of the undesired **3.4.1**. A 1:1 mix of THF:Dioxane was also evaluated at 0.1 and 0.05 M concentrations, with no statistical difference in the production of either **3.3.6** or **3.4.1**. Thus, dioxane was chosen as a suitable solvent to proceed with the optimization.

In attempting to favour sulfur addition over redox-exchange, we evaluated a range of additives, with the goal of selectively increasing the rate of sulfur addition. To this end, hard and soft Lewis acids varying in valency were examined. Oxophilic, tetravalent titanium isopropoxide ($\text{Ti}(\text{O}i\text{Pr})_4$) resulted in a decreased yield of **3.3.6**, and an increase in the production of **3.4.1**. Divalent, hard ZnCl_2 gave a comparable yield, with little change observed in reactivity. Soft, redox-active Lewis acid CuPF_6 resulted in the lowest yield of **3.3.6**. Fortunately, it was

found that upon addition of $\text{MgBr}_2 \cdot \text{Et}_2\text{O}$, the yield of **3.3.6** increased to 86%, with a concomitant decrease in **3.4.1** to 5% (Entry 21). Having identified $\text{MgBr}_2 \cdot \text{Et}_2\text{O}$ as a beneficial additive, we further evaluated similarly hard alkali and alkaline earth metal Lewis acids LiCl , LiBr , MgBr_2 , MgCl_2 , and $\text{Mg}(\text{ClO})_4$. Upon examination of the results with the monovalent lithium containing Lewis acids (Entry 24 & 26), yields of **3.3.6** were found to be ineffective. It was observed that divalent magnesium Lewis acids MgCl_2 , and MgBr_2 had similarly beneficial effects on the reactivity (Entries 35, 39). Thus, $\text{MgBr}_2 \cdot \text{Et}_2\text{O}$ was chosen as the most optimal additive. Subsequent assessment of solvents was performed and it was confirmed that dioxane still yielded the greatest amount of **3.3.6** with suppressed production of **3.4.1**. (Entries 29-34). The inclusion of $\text{MgBr}_2 \cdot \text{Et}_2\text{O}$ in our reaction may have thus resulted in the promotion of reactivity of the thiol nucleophile with quinone, allowing for activated addition of the thiolate. However, varying the equivalencies of $\text{MgBr}_2 \cdot \text{Et}_2\text{O}$ did not affect the reactivity, generating products **3.3.6** in comparable yields with an average 90% while keeping production of **3.4.1** at a moderate 5% (Entries 35-37). To this end, it was believed that sufficient conditions had been elucidated to provide the thiol adduct with the greatest efficiency, while keeping redox-exchange at a minimum. (For a discussion on the role of $\text{MgBr}_2 \cdot \text{Et}_2\text{O}$ as additive, see Section 3.7)

During our investigation, it was hypothesized that it would be beneficial to have a product sequestering additive pre-mixed with the starting material such that upon addition, the catechol product would be immediately protected from further reactivity i.e. redox exchange. Following this rationale, the use of the *tert*-butyldimethylsilyl protecting group was examined, and compared to our usual method of bis-acetylation (Table 3.4.2). It was observed that *tert*-butyldimethylsilyl chloride (TBSCl) in sub-stoichiometric amounts resulted in an increased yield, generating the catechol, **3.4.2** in 89% yield (Entry 1, Table 3.4.2). There were no traces of bis-silylated catechol present in the crude mixture, and only the free, unprotected catechol could be detected in the crude NMR spectrum. Slightly lower yields were observed when reducing or increasing the equivalents of TBSCl (Entries 2 and 3). Since the silylated catechol was not detected, it is hypothesized that TBSCl may enhance reactivity by acting as a Lewis acid and promote the addition. Other catechol protecting methods were also investigated, using the reagents *tert*-butyldimethylsilyl trifluoromethanesulfonate (TBSOTf), and trifluoromethanesulfonic anhydride (Tf_2O), but these resulted in un-isolable complex mixtures. When Ac_2O was present at the beginning of the reaction, **3.3.6** was generated in a lowered 50%

yield, which can be attributed to the absence of DMAP, resulting in a lower rate of bis-acetylation (Entry 6). Surprisingly, upon inclusion of DMAP with Ac₂O at the beginning of the reaction, a different product was isolated from the reaction, the C3 regioisomer **3.4.3**, in 86% yield (Entry 7). The reaction was subsequently performed with solely DMAP, and **3.4.3** was once again observed, but at a lower yield of 60% (Entry 8). This was the first time the C3-adduct had been observed throughout our entire investigation with quinone **3.2.1**. (For a discussion on the assignment of regiochemistry of products **3.3.6** and **3.4.3**, see Section 3.5)

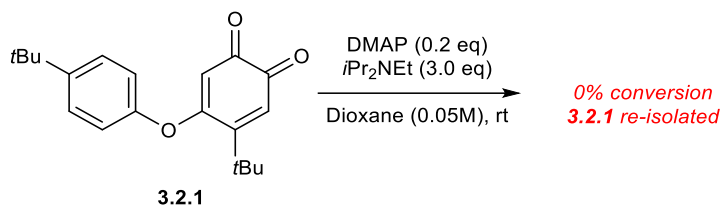


Entry	Additive	Additive (eq.)	NMR Yield (%)		
			3.3.6	3.4.2	3.4.3
1	TBSCl	0.5	-	89	-
2	TBSCl	0.1	-	76	-
3	TBSCl	1.0	-	72	-
4	TBSOTf	0.2	-	-	-
5	Tf ₂ O	2.25	-	-	-
6	Ac ₂ O	2.25	50	-	-
7	Ac ₂ O/DMAP	0.1	-	-	83
8	DMAP	1.0	-	-	60

Table 3.4.2- Investigation into Protecting Group Additives and Observation of Regioisomers with quinone **3.2.1**

From the result in Entry 8, Table 3.4.2, the effect of DMAP with quinone **3.2.1** was briefly investigated. DMAP was mixed with quinone **3.2.1** under the same reaction conditions, but in the absence of thiol (Scheme 3.4.1). Upon concentration of the crude mixture and NMR analysis, no new signals were observed in the spectrum. It was hypothesized that a DMAP-quinone adduct was transiently forming in the reaction, resulting in altering the site of addition of the thiol to quinone. However, this postulate could not be corroborated at this time, as no new NMR signals were observed. From these experiments, it appears that in cases where DMAP is present, the reactions generating the C6 and C3 adducts are competitive with one another. The

regioselectivity of the reaction deteriorates as the presence of DMAP prevents the addition of thiol to C6, resulting in addition at the only other site available for attack, C3. However, the mechanism of action of DMAP cannot be confirmed at this time, as well as a reasonable explanation of factors that govern the preferred regioselectivity observed with specific quinones.



Scheme 3.4.1- Investigation into effects of DMAP with quinone 3.2.1

3.5 Assignment of Regioisomers 3.3.6 and 3.4.3 from Spectral Data

As mentioned in Section 3D, the regioisomers **3.3.6** and **3.4.3** arising from the thiol addition of 2-propanethiol to quinone **3.2.1** were isolated and characterized on the basis of NMR spectral data. Full assignment of the ¹H-NMR spectrum of **3.3.6** and **3.4.3** is shown in Figure 3.5.1 and Figure 3.5.2. The change in regiochemistry of the addition was detected through a distinct change in the chemical shift of proton **A**, in Figure 3.5.1. As seen in the spectrum, proton **A** displays a chemical shift of $\delta = 7.23$ ppm, whereas in Figure 3.5.2, this singlet signal is observed at $\delta = 6.7$ ppm. In order to further confirm the regiochemistry of the sulfur adduct, NOESY, HSQC, HMBC, and 1-1 ADEQUATE NMR spectra were examined.

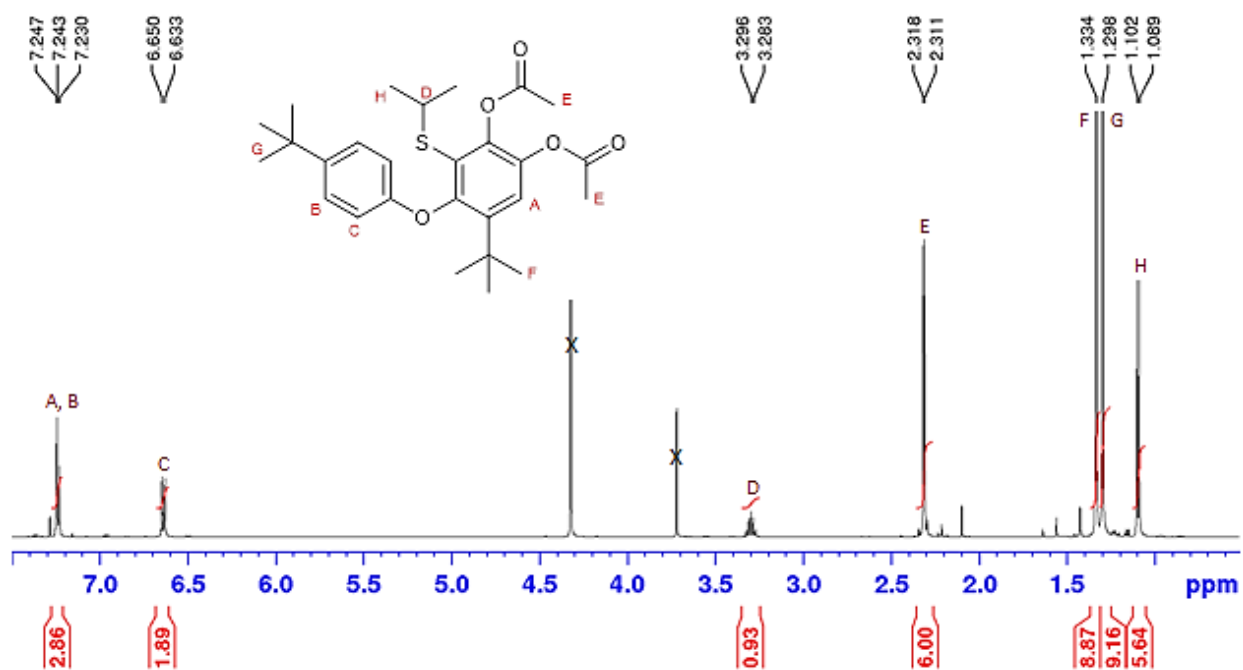


Figure 3.5.1- ^1H -NMR Spectrum of 3.3.6 in CDCl_3

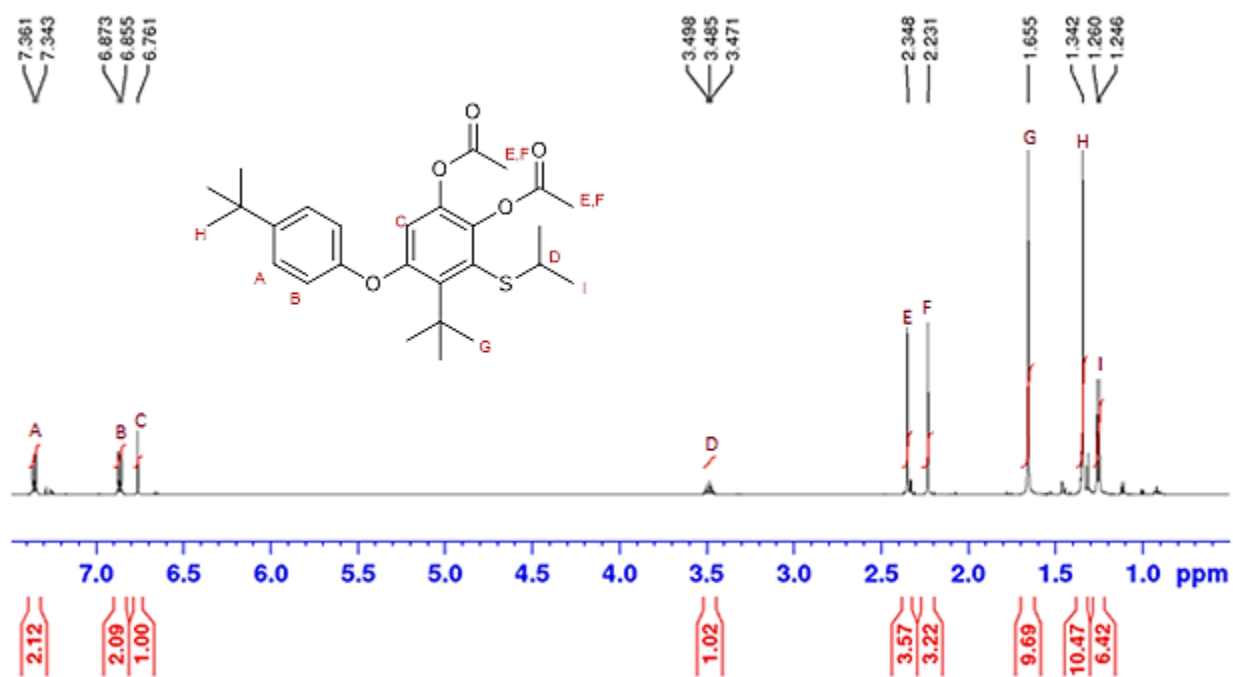


Figure 3.5.2- ^1H -NMR Spectrum of 3.4.3, in CDCl_3

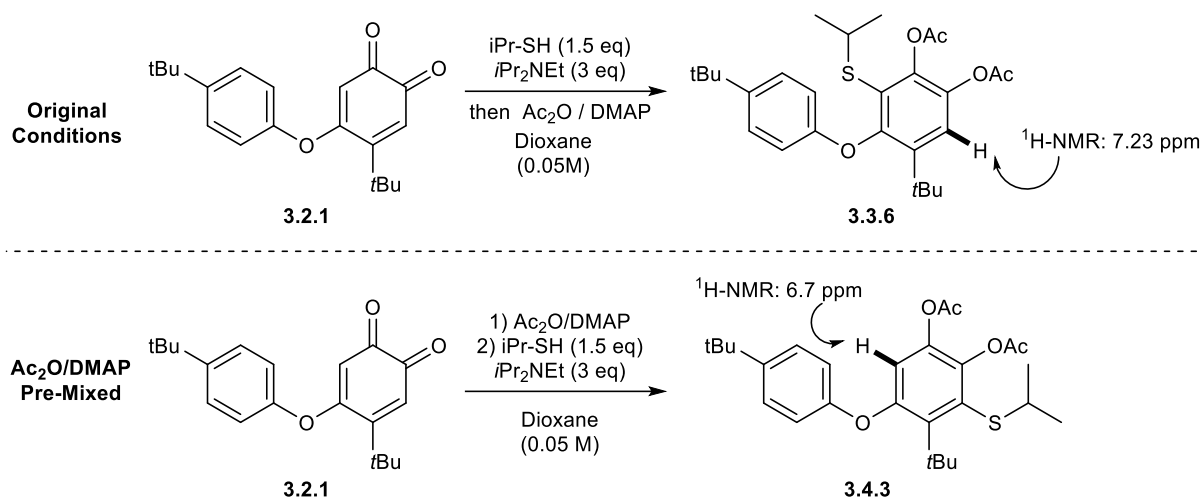


Figure 3.5.3- Detection of Regioisomers 3.3.6 and 3.4.3 through $^1\text{H-NMR}$ studies

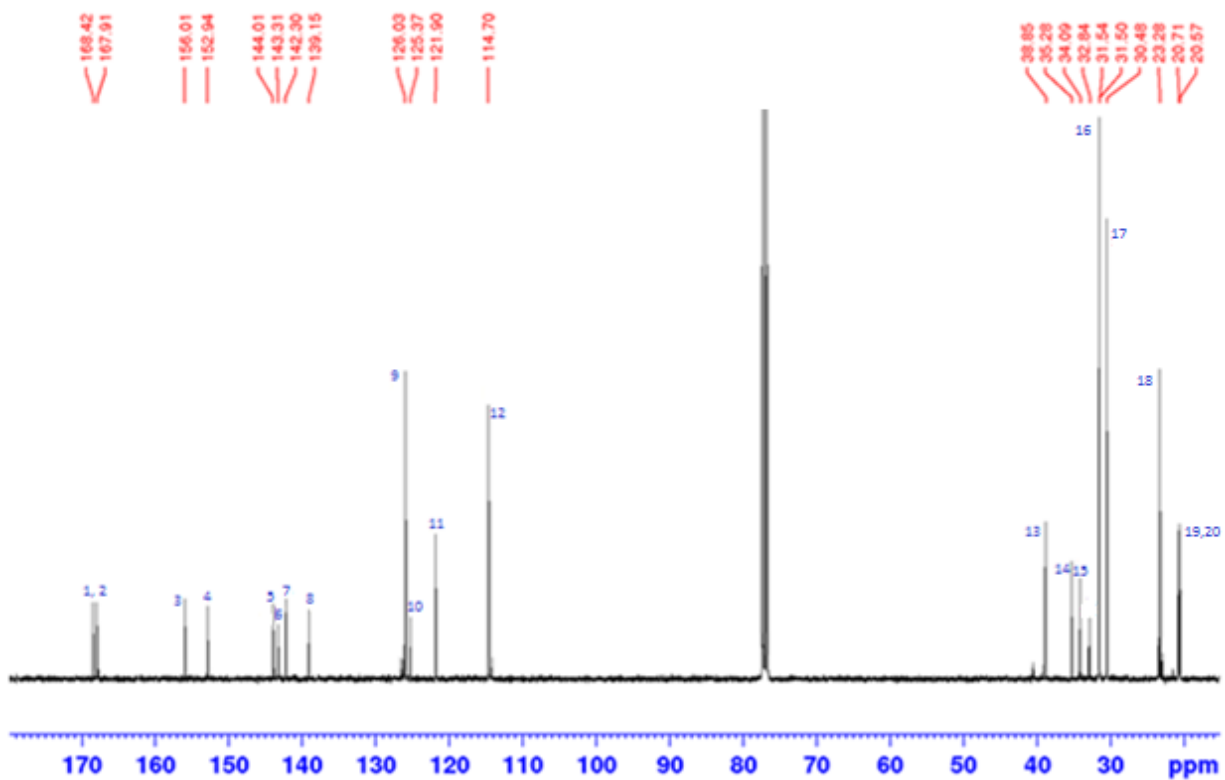


Figure 3.5.4- $^{13}\text{C-NMR}$ Spectrum of 3.3.6, in CDCl_3

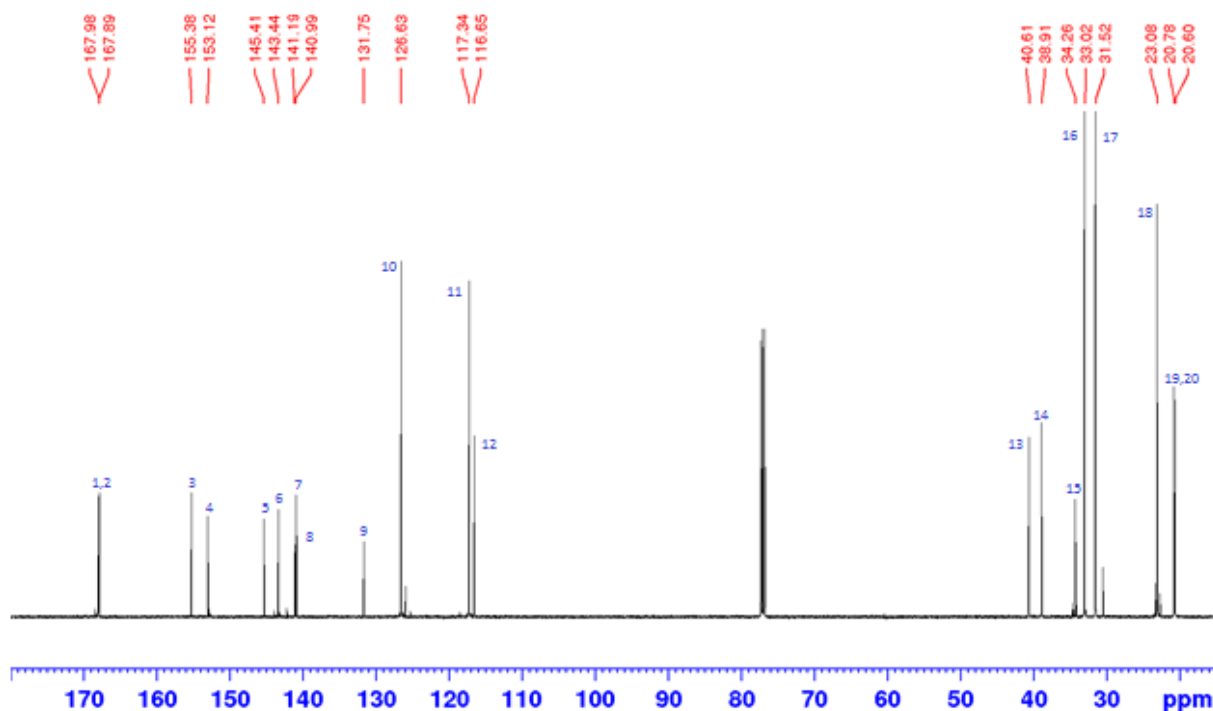


Figure 3.5.5- ^{13}C -NMR Spectrum of **3.4.3**, in CDCl_3

From the HSQC spectrum, all protons in the ^1H -NMR were assigned to their respective carbons in the ^{13}C spectrum, whose correlations can be seen in Figure 3.5.6. Further assignment of the quaternary carbons was performed with the HMBC spectrum, whose correlations are indicated in Figure 3.5.7. However, in the case of **3.3.6**, as both acetate peaks appear as one signal in the ^1H -NMR as protons **E**, we were unable to distinguish between them for carbons **20** and **21** at this time. Complete assignment of the ^{13}C -NMR spectrum was performed in conjunction with this data from the HSQC and HMBC, and the ^{13}C -chemical shift assignments are shown in Figure 3.5.8 below. (For full HSQC, HMBC, 1-1'ADEQUATE spectra of **3.3.6** and **3.4.3**, see Appendix B)

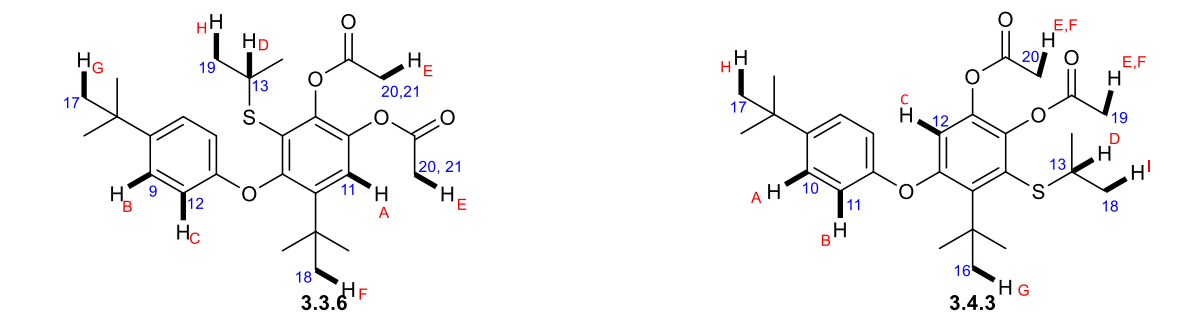


Figure 3.5.6- HSQC Correlations, leading to partial ^{13}C assignment of **3.3.6** and **3.4.3**

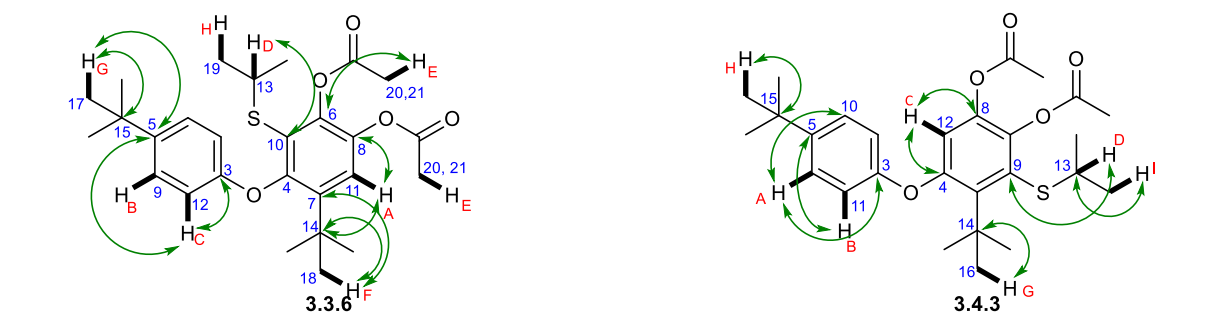


Figure 3.5.7- HMBC Correlations, as seen for **3.3.6** and **3.4.3**

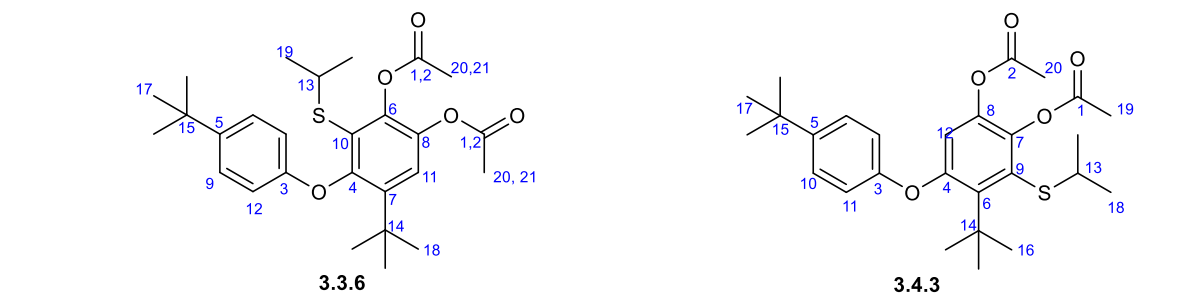


Figure 3.5.8- ^{13}C - NMR Spectrum Labels of **3.3.6** & **3.4.3**

Originally, it was thought that the NOESY, HSQC and HMBC experiments would be sufficient to confirm the regiochemistry of each compound. However, the NOESY spectra obtained did not provide any definitive correlations, and the HMBC spectrum displayed unexpected 4 bond coupling between protons and carbons, complicating the final assignment. Thus, the regiochemistry of sulfur addition was determined on the basis of a 1-1'-Adequate Sensitivity Double-Quantum Spectroscopy (ADEQUATE) experiment, which displays correlations for carbons and protons separated by two bonds. In the ADEQUATE spectrum acquired for **3.3.6** (Figure 3.5.9), proton **A** shows three correlations, to carbons **7**, **8**, and **11**. The signal from the spectrum that was integral in assigning the regiochemistry of **3.3.6** was the correlation between proton **A**, and carbon **7** (Figure 3.5.11). In some cases with the ADEQUATE experiment, one bond proton carbon correlations can be seen, which in this case is the signal seen between proton **A** and carbon **11**. These can be identified by overlaying the HSQC spectrum, or by further modulating the ADEQUATE $^1\text{J}_{\text{C-C}}$ delay from 60 Hz to 45 Hz, as was later confirmed with a test sample of ethylbenzene. For **3.4.3**, proton **C** also has three correlations, to carbons **4**, **8**, and **12**. In a similar fashion to the assignment of **3.3.6**, these correlations confirmed the regiochemistry assigned for this isomer.

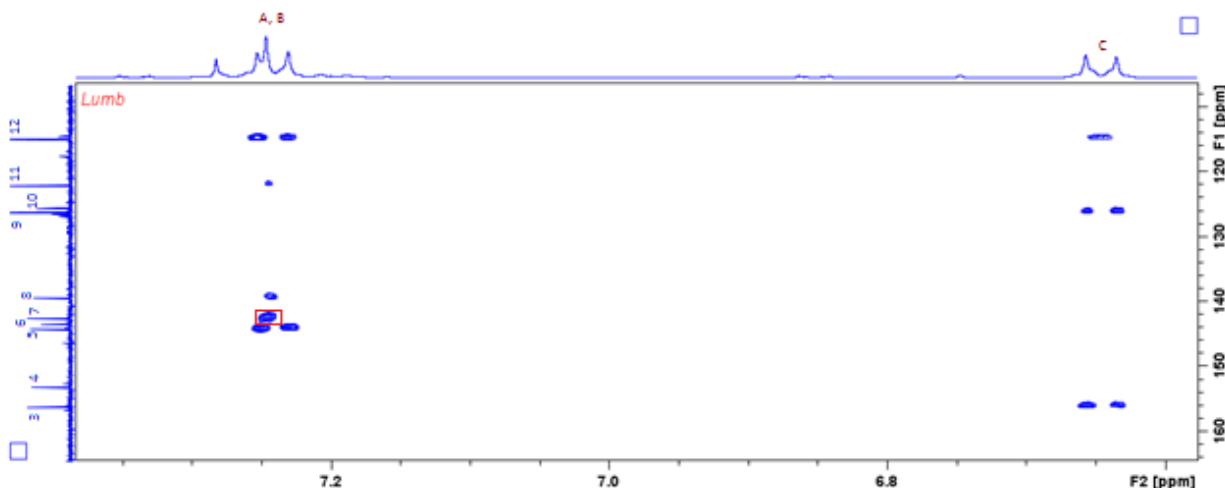


Figure 3.5.9- Key Correlation in 1,1'-ADEQUATE NMR Spectrum of **3.3.6**, in CDCl_3

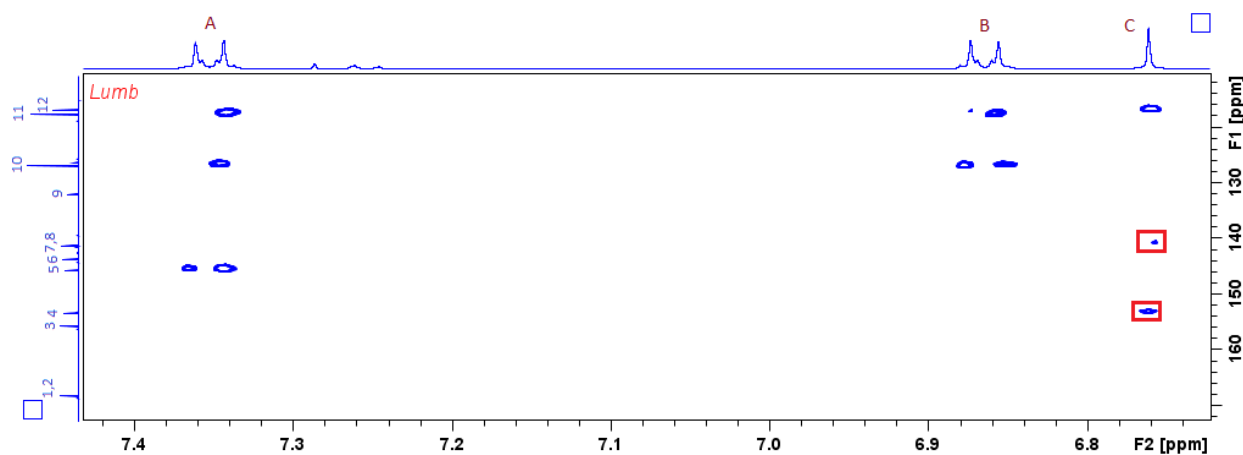


Figure 3.5.10- Key Correlations in 1,1'-ADEQUATE Spectra of **3.4.3**, in CDCl_3

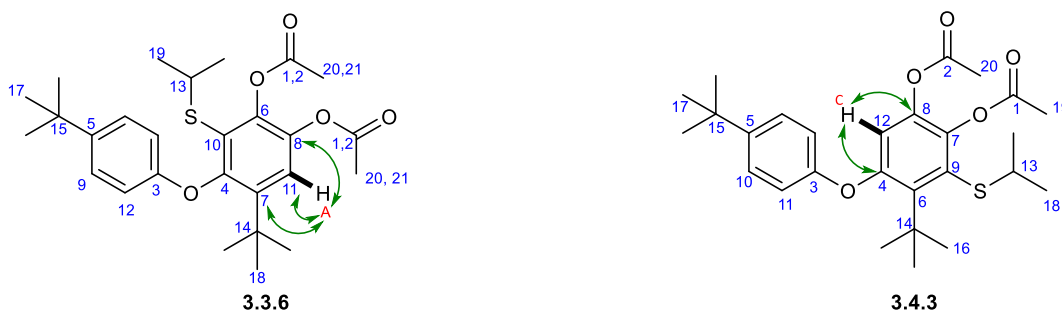


Figure 3.5.11- Correlations shown in the 1,1'-ADEQUATE Spectra for Proton A, **3.3.6**, and Proton C, **3.4.3**

From this spectral information, we deduce that for the observed C6-sulfur adducts, the resulting chemical shift of the proton signal at C3 is roughly $\delta = 7.2$ ppm. However, in cases where the C3-adduct is observed, the proton signal at C6 appears at $\delta = 6.7$ ppm. This can be

explained by electron donation of the *ortho*-aryloxy group, which results in the upfield shift in the ^1H -NMR frequency observed. This is also observed in the spectral data obtained for the C3-sulfur adducts of quinones **3.3.1** and **3.3.2**, where this proton signal appears on average at $\delta = 6.7$ ppm (Figure 3.5.12). (For characterization data of all sulfur adducts, see Appendix) For both quinones, the chemical shift can be explained by electron donation of the heteroatom (O or N) that is located in the *ortho*-position relative to the proton of interest.



Figure 3.5.12- Chemical Shift of the Proton Singlet Signal in Sulfur Adducts of Quinones **3.3.1** and **3.3.2**

3.6 Expansion of *ortho*-Quinone Scope and Observed Regioselectivity

At this point, further exploration of the scope of the quinone was desired. However, as previously discussed in Section 3.4, there were now four different sets of conditions that had shown promise in our reaction optimization (Table 3.6.1). These conditions were subsequently evaluated with quinone **3.6.1**. Similar to quinone **3.2.1**, **3.6.1** possesses a *tert*-butyl group at C4. However, at C5, it bears a methoxy- group as opposed to an aryloxy- group, which imparts more electron density to the quinone, thus making the resulting sulfur adduct catechol more prone to redox-exchange. We were interested in testing whether the effects that had been observed with quinone **3.2.1** with each of these sets of conditions could be applied to quinone **3.6.1** as well.

Conditions	Additive
1	-
2	TBSCl (0.25 eq)
3	MgBr ₂ ·Et ₂ O (0.25 eq)
4	Ac ₂ O/DMAP (3.0 eq)/(0.2 eq)

Table 3.6.1- Reaction Conditions Arising from Investigation of Thiol Addition

Beginning with ethanethiol (Entries 1-4, Table 3.6.2), Condition #1 produced the C6-adduct **3.6.2** in a 50% yield, and 26% of **3.6.4**, the redox-exchange product. Similar yields were

observed with TBSCl as additive, indicative of its inability to promote reactivity over redox-exchange in this instance. The use of Ac₂O/DMAP resulted in a decrease in the production of **3.6.2** at 14%, and 23% of the C3-adduct **3.6.3** was observed. The observed redox-exchange product **3.6.4** remained constant at 20% for this thiol nucleophile. When examining MgBr₂·Et₂O, the yield of **3.6.2** increased to 77%, with a concomitant decrease of **3.6.4** to 5%. As discussed earlier, quinone **3.6.1** is a more electron-rich quinone than **3.2.1**, and therefore more prone to redox-exchange. We speculate that MgBr₂·Et₂O increases the rate of addition of ethanethiol, making the C-S bond forming reaction faster than redox-exchange.

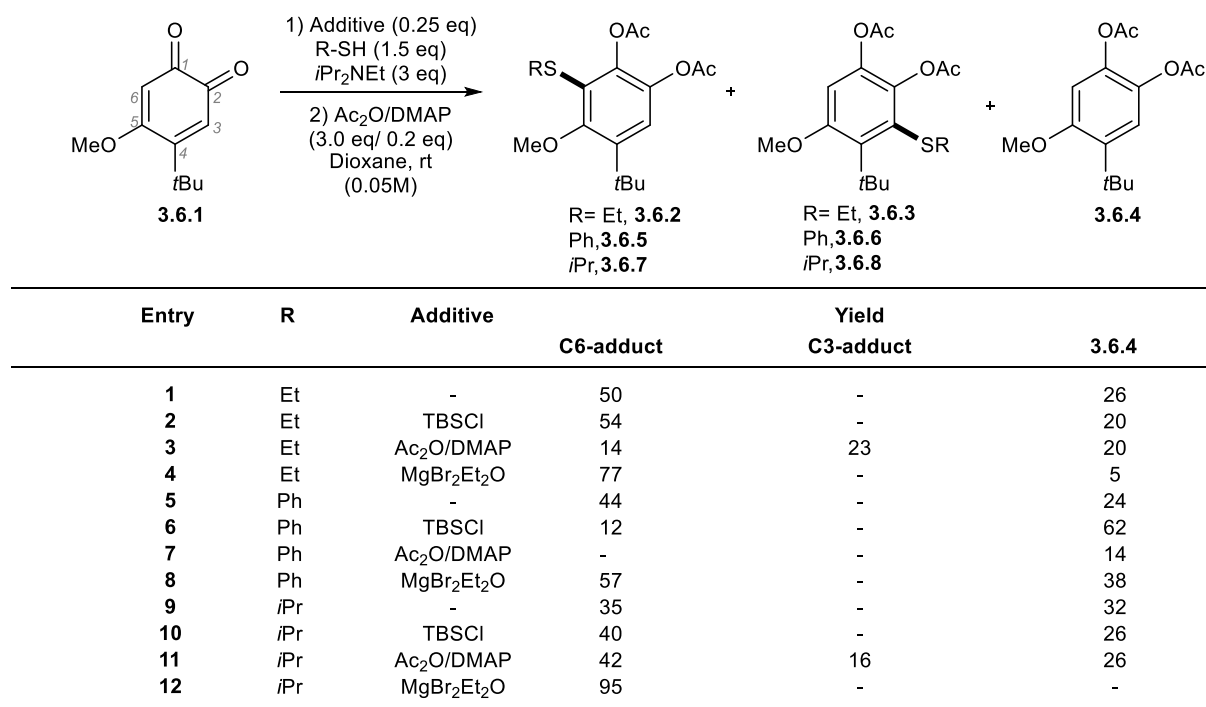


Table 3.6.2- Evaluating reaction conditions with mono-substituted quinone 3.6.1

With thiophenol, standard conditions yielded similar ratios of **3.6.5** : **3.6.4** (Entry 5-8, Table 3.6.2). However, in this instance, TBSCl decreased the yield of **3.6.5** to only 12%, and 62% of **3.6.4** was observed, indicative that redox-exchange was taking place at a rate faster than the thiol addition (Entry 6). Furthermore, as discussed previously, when Ac₂O/DMAP was employed, the reaction resulted in complex mixtures from which only 14% of **3.6.4** was identified. The use of MgBr₂·Et₂O resulted in an increase in yield from the standard reaction conditions to 57%, but an increase in redox-exchange product **3.6.4** was also observed, at 38%. The slightly lowered reactivity observed when comparing thiophenol to ethanethiol can be

attributed to the decreased nucleophilicity of the thiol nucleophile, where thiophenol is less reactive. However, with this substrate, a moderate yield thiol addition was still able to be attained.

Finally, with 2-propanethiol (Entries 9-12, Table 3.6.2), standard conditions yielded a roughly 1:1 ratio of **3.6.7** : **3.6.4**, at 35% and 32% respectively. A slight increase in **3.6.7** and decrease in **3.6.4** was observed with TBSCl, similar to ethanethiol. With Ac₂O/DMAP, there was a 10% increase in **3.6.7**, along with a similar production of **3.6.4** at 26%. The C3-regioisomer **3.6.8** was also observed in a 16% yield. The observation of regioisomers in cases with alkyl nucleophiles and their absence with aromatic nucleophiles suggest that the switch in regioselectivity observed in the Ac₂O/DMAP is applicable to only alkyl thiols. It is hypothesized that this effect is due to the transient formation of a DMAP-quinone adduct species, shown in Figure 3.6.1. Since the key difference between these alkyl and aromatic is their nucleophilicity, it is possible that if a DMAP-quinone species is transiently forming, the alkyl thiol is quick enough to add to C3 if the DMAP-quinone species is present (and to C6, when DMAP and quinone are separate), whereas thiophenol is not (Figure 3.6.1). After subsequent tautomerization and release of DMAP, this would yield the C3-regioisomer product, and explain this observed phenomenon in regioselectivity. However, there is no current explanation for the results in Entries 3, 7, and 11, which also seem to indicate that Ac₂O/DMAP may actually be detrimental to reactions involving quinone **3.6.1**. Finally, upon utilization of MgBr₂·Et₂O, the yield of **3.6.7** increased to 95%, and no other products were observed. In this instance, it appears that MgBr₂·Et₂O was able to promote the addition most sufficiently over redox-exchange, resulting in over a 60% increase from the standard conditions.

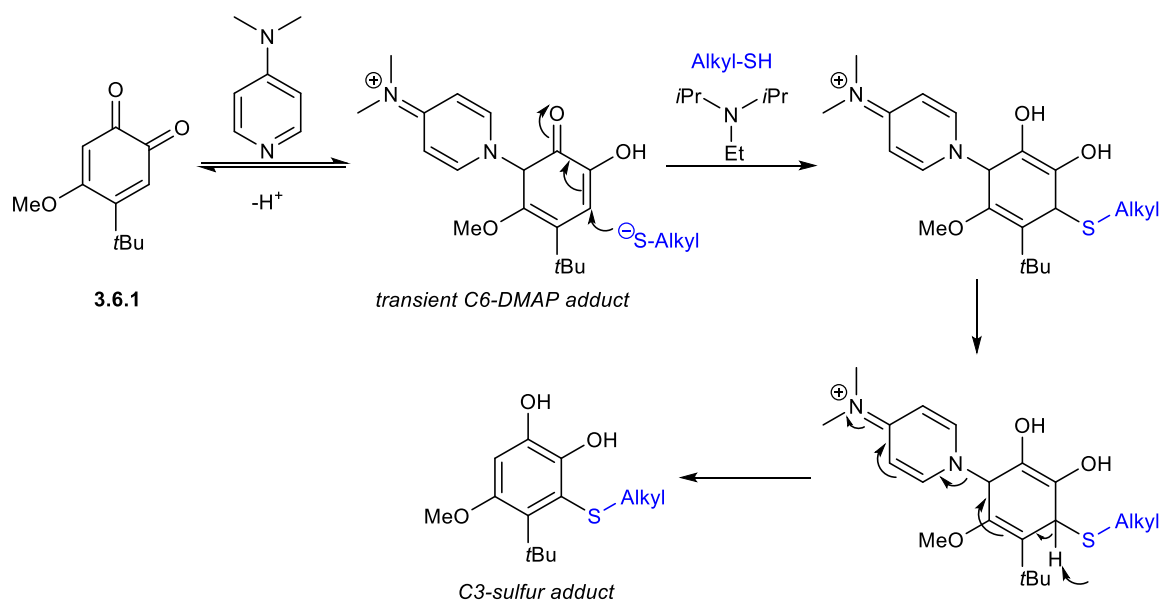
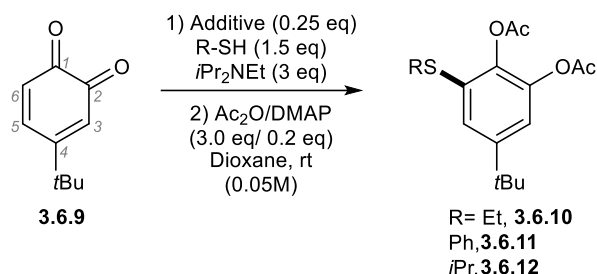


Figure 3.6.1- Hypothesized Mechanism of Action of DMAP on Regioselectivity

At this point, no *mono*-substituted quinones had been examined in our investigation. In order to evaluate each of these conditions, quinone **3.6.9** was utilized as a quinone with both C6 and C3 sites available for addition, thus allowing for further studies in regiochemistry. C5 was also available for addition, in order to explore whether a 1,4-thiol addition was possible.

We were pleased to observe that the reaction of quinone **3.6.9** and ethanethiol produced **3.6.10** in good to excellent yields for all sets of conditions, with the highest being no additive, at 93% (Entry 1, Table 3.6.3). Additives TBSCl and MgBr₂Et₂O appeared to have the same effect on the reactivity, at 88 and 89% yield respectively (Entries 2-3, Table 3.6.3). As these yields all differ within 5%, these are viewed as comparable and within experimental error. It appears that the addition already proceeds extremely efficiently under standard conditions, and the additives do little in this case to enhance the reactivity. The lowest yield was observed with Ac₂O/DMAP at 75%, and the same regioisomer, the C6 adduct **3.6.9**, was isolated in all cases. With thiophenol (Entries 5-8), all conditions produced yields of **3.6.11** also in good yields. Under standard reaction conditions, the reaction proceeded efficiently to give **3.6.11** at 88% yield (Entry 5). A slight increase to 92% was observed with TBSCl (Entry 6). MgBr₂Et₂O was not observed to increase reactivity, with a lowered yield observed at 78%. This was the first time a decreased yield was observed with this additive, in addition to examination of standard vs. additive conditions with an aromatic thiol nucleophile. Since these conditions were elucidated under

optimization with alkyl thiols, it suggests that $\text{MgBr}_2 \cdot \text{Et}_2\text{O}$ may not promote the addition in cases with aromatic thiols, due to their decreased nucleophilicity relative to alkyl thiols. A similar result of 76% was also observed with $\text{Ac}_2\text{O}/\text{DMAP}$. In the case of 2-propanethiol (Entries 9-12, Table 3.6.3), the standard conditions furnished **3.6.12** in 85% yield. The yield further increased to 95% when TBSCl was used. However, similarly to thiophenol, yields of 75% and 77% were observed when the $\text{Ac}_2\text{O}/\text{DMAP}$ and $\text{MgBr}_2 \cdot \text{Et}_2\text{O}$ conditions were employed respectively. It is unknown in each case why there is a consistent decrease of 10-15% in yield when $\text{Ac}_2\text{O}/\text{DMAP}$ is used.



Entry	R	Additive	Yield
1	Et	-	93
2	Et	TBSCl	88
3	Et	$\text{Ac}_2\text{O}/\text{DMAP}$	75
4	Et	$\text{MgBr}_2 \cdot \text{Et}_2\text{O}$	89
5	Ph	-	88
6	Ph	TBSCl	92
7	Ph	$\text{Ac}_2\text{O}/\text{DMAP}$	76
8	Ph	$\text{MgBr}_2 \cdot \text{Et}_2\text{O}$	78
9	<i>i</i> Pr	-	85
10	<i>i</i> Pr	TBSCl	95
11	<i>i</i> Pr	$\text{Ac}_2\text{O}/\text{DMAP}$	75
12	<i>i</i> Pr	$\text{MgBr}_2 \cdot \text{Et}_2\text{O}$	77

Table 3.6.3- Evaluating Reaction Conditions with mono-substituted quinone 3.6.9

The reaction was re-evaluated with quinone **3.3.2** in the presence of $\text{MgBr}_2 \cdot \text{Et}_2\text{O}$ with octanethiol (Entry 1, Table 3.6.4) and 2,6-dimethylthiophenol (Entry 2). Unfortunately, the addition of $\text{MgBr}_2 \cdot \text{Et}_2\text{O}$ did not appear to have a beneficial nor detrimental impact on the generation of the desired sulfur adduct. From these results, it appears that the beneficial effect that we have observed with $\text{MgBr}_2 \cdot \text{Et}_2\text{O}$ may be substrate specific and not applicable to all quinones and thiols.

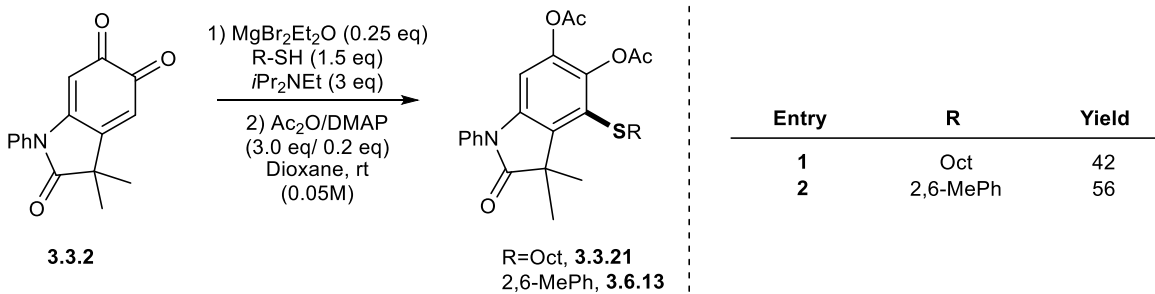


Table 3.6.4- Re-evaluation of sulfur addition to quinone **3.3.2** under Optimized Conditions

However, from these results, $\text{MgBr}_2 \cdot \text{Et}_2\text{O}$ was chosen as the most broadly effective additive to further expand the scope of the quinone, as it has shown promise, and in most cases that there was no demonstrated detrimental effect on reactivity. Conditions were evaluated with ethanethiol, thiophenol, and 2-propanethiol, thiols believed to be representative of the reactivity of the thiol scope.

A variety of 4,5-substituted quinones were evaluated. In the case of the comparably electron-poor *tri*-fluoroethanoxy- bearing quinone **3.6.14**, yields similar to those experienced with **3.6.1** were observed for ethanethiol (Entry **3.6.15**) and thiophenol (Entry **3.6.16**). An acceptable yield of 70% was observed in the case of *i*PrSH (Entry **3.6.17**). In each case, selective addition at C6 was observed. Similar yields and regioselectivity were also observed for the benzyloxy-containing quinone **3.6.18**. When changing the substituent at C4 on the quinone from *tert*-butyl to cyclohexyl, we begin to see erosion of regioselectivity at C6. In the case of *i*PrSH (Entry **3.6.22**), a yield of 23% was observed for the C6 adduct, while 32% of the C3 regioisomer was observed simultaneously.

In order to explore the regiochemistry of the reaction further, 4-*mono*-substituted quinones were then examined. As previously discussed, with 4-*tert*-butyl quinone **3.6.9**, all nucleophiles proceeded to react at the C6 position, generating moderate to good yields of 77-89%. In the case of 4-methyl quinone **3.6.23**, the same regioselectivity was observed, but with lower yields of around 70%. The lower yields observed may be attributed to the quinone stability in basic conditions. Control experiments performed by Zheng Huang (Ph.D. Candidate, Lumb Group, McGill University) observe that 4-Me-*ortho*-quinone undergoes complete decomposition upon introduction into basic media in 1 hour. This may be explained by the presence of

enolizable protons on the *ortho*-quinone, resulting in an equilibrium with an unstable *para*-quinone methide intermediate (Figure 3.6.3).

With the comparably more electron-rich 4-methoxy quinone **3.6.27**, a yield of 72% was observed for ethanethiol (Entry **3.6.28**). However, we see the yields diminish to 40% in the case of quinones **3.6.29** and **3.6.31**, both containing electron-withdrawing functionalities at C4. It is possible the quinone stability in solution is giving rise to the lower yields observed for these sulfur adducts. In the case of 1,2-naphthoquinone **3.6.33**, ethanethiol reacted selectively at C3, giving rise to the adduct with a 27% yield. This is the same regioselectivity observed by Cavalieri *et al.*⁹ with catechol estrogen quinones. (For additional information regarding these experiments, see Chapter 2C) In this case, the sulfur-adduct quinone was isolated. It is hypothesized that the resulting catechol product was too electron rich and participated in redox-exchange prior to the acetylation step. When examining quinone **3.6.35**, a quinone with no functionality, ethanethiol was found to react at C4, and 51% of **3.6.36** was isolated. This was the only case of 1,4-addition observed throughout our entire investigation, but is also our only example of a quinone bearing no functionality at C4. Upon examination of the substrate scope in Figure 3.6.2 as a whole, it appears that the reaction preferentially undergoes 1,6-addition, as demonstrated with the *mono*-substituted and 4,5-substituted quinones. This is the same regioselectivity that has been observed in literature precedent, as previously discussed in Chapter 2 (For a discussion on the assignment of regioselectivity, see Section 3.5, for further discussion on the factors governing regioselectivity, see Section 3.8).

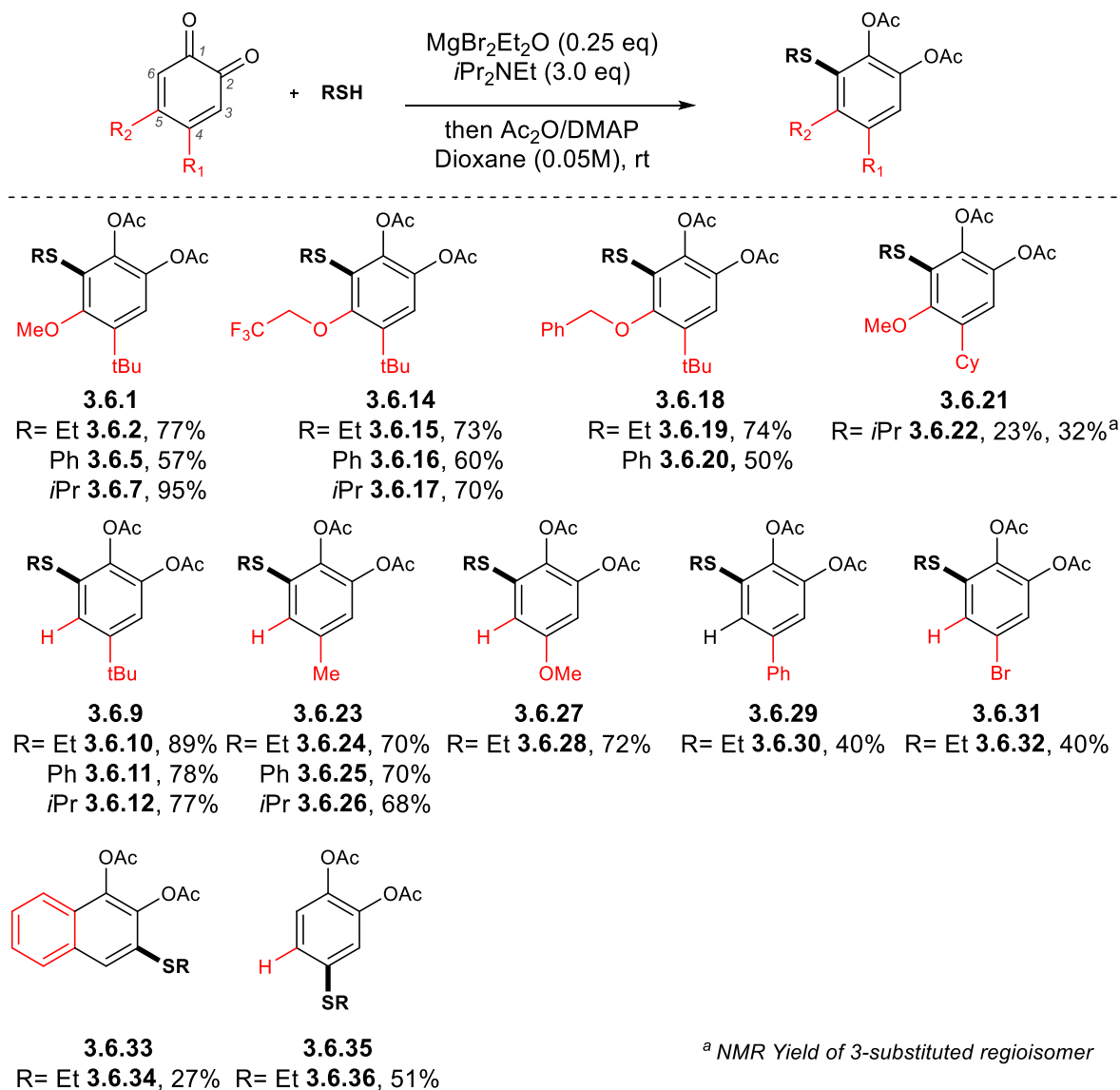


Figure 3.6.2- ortho-Quinone Substrate Scope

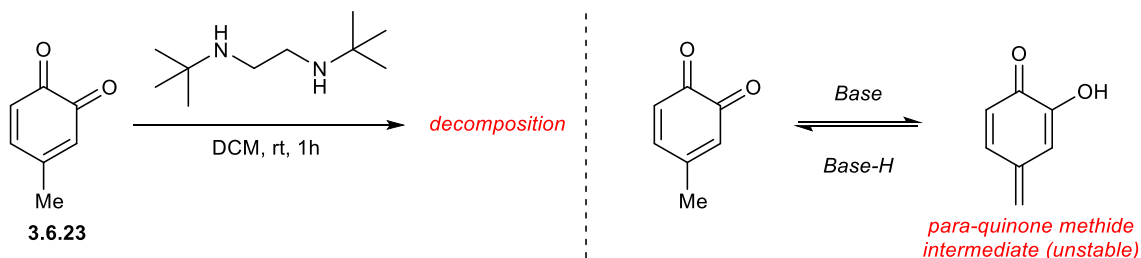
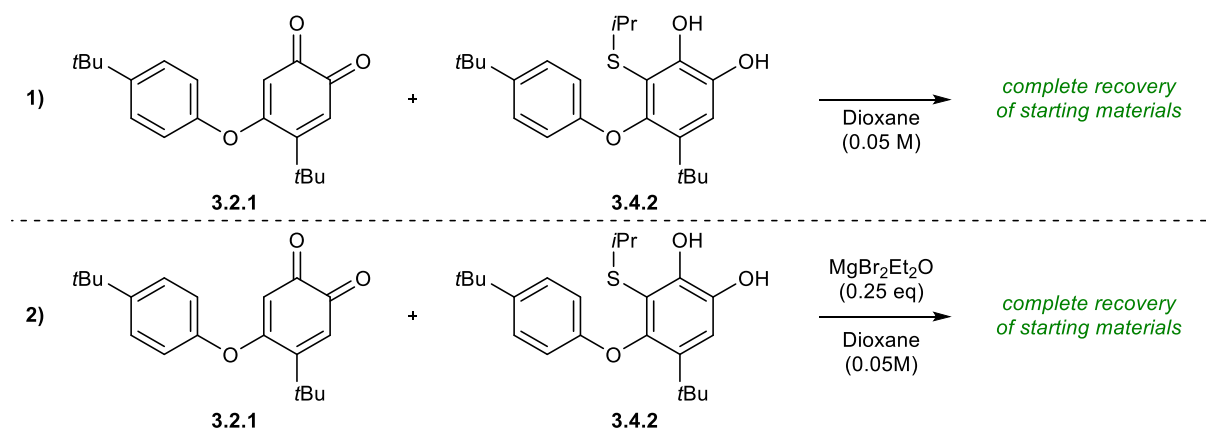


Figure 3.6.3- Control Experiment to Determine Stability of quinone **3.6.23** in Basic Media, performed by Zheng Huang

3.7 Investigations into the Role of $\text{MgBr}_2\cdot\text{Et}_2\text{O}$ as Additive

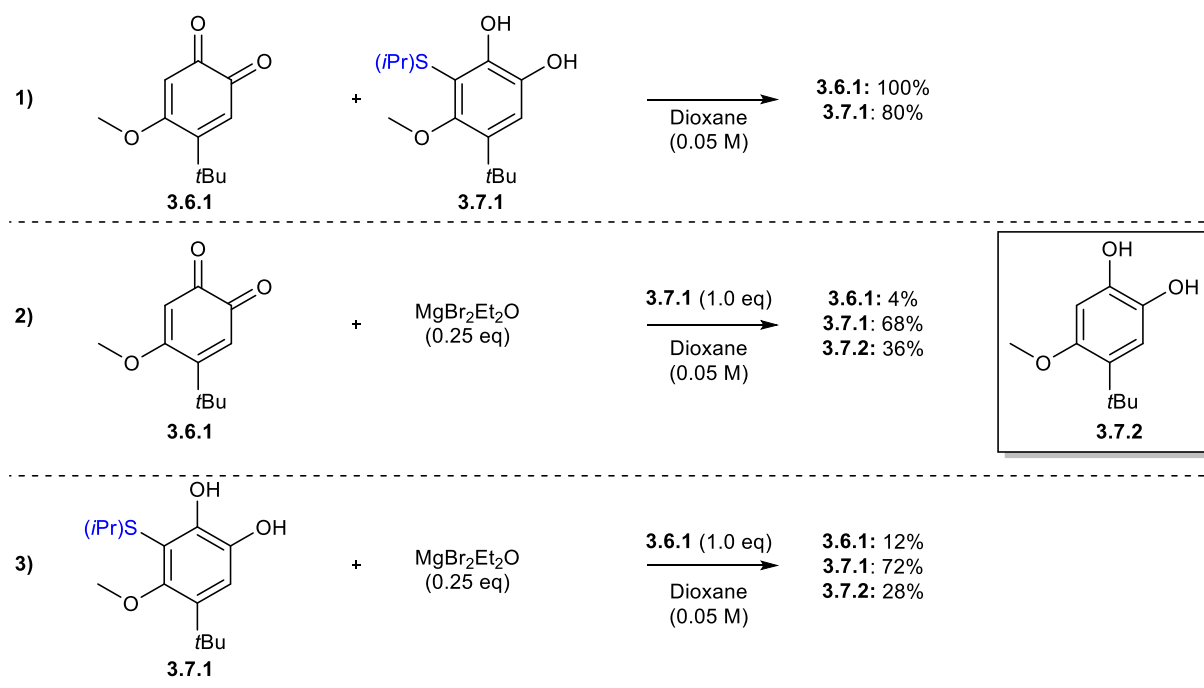
It was still unclear at this point the exact role that $\text{MgBr}_2\cdot\text{Et}_2\text{O}$ played in promoting the reaction. It was determined that some control experiments were necessary in order to explore this phenomenon further. To establish a baseline result for redox-exchange, quinone **3.2.1** and catechol **3.4.2** were mixed in dioxane for 1.5 hours (Scheme 3.7.1). Unexpectedly, upon concentration of the reaction mixture, both starting materials were recovered with no decomposition or new products observed (Entry 1). Both compounds were also recovered upon workup following reaction with $\text{MgBr}_2\cdot\text{Et}_2\text{O}$ (Entry 2). It was then concluded that redox-exchange was not occurring between **3.2.1** and **3.4.2**, and confirmed that $\text{MgBr}_2\cdot\text{Et}_2\text{O}$ did not promote nor inhibit this process from occurring.



*Scheme 3.7.1-Probing the effects of $\text{MgBr}_2\text{Et}_2\text{O}$ on Redox-Exchange between quinone **3.2.1** and product catechol **3.4.2***

Another baseline experiment was performed with *ortho*-quinone **3.6.1** and catechol **3.7.1** (Scheme 3.7.2). As stated previously, quinone **3.6.1**, unlike **3.2.1**, possesses a methoxy- group at C5 as opposed to an aryloxy- group. The change in these groups results in **3.6.1** being a more electron-rich quinone, and thus more prone to redox-exchange. Upon workup, 80% of the original catechol **3.7.1** was recovered, along with complete recovery of quinone **3.6.1**. No other products were observed in the crude mixture, and the cause of the loss of mass balance is not evident at this time. Upon reacting quinone **3.6.1** and $\text{MgBr}_2\cdot\text{Et}_2\text{O}$, and subsequent addition of catechol **3.7.1**, only 4% quinone **3.6.1**, 68% catechol **3.7.1**, and 36% of redox-exchange product **3.7.2** were recovered (Entry 2, Scheme 3.7.2). A similar result was obtained when quinone **3.6.1** was reacted with pre-mixed catechol **3.7.1** and $\text{MgBr}_2\cdot\text{Et}_2\text{O}$. These findings indicate that there

may be some redox-exchange occurring between **3.6.1** and **3.7.1**, and this may be the cause of the loss of mass balance that is unaccounted for. They also suggest that in the presence of $\text{MgBr}_2\cdot\text{Et}_2\text{O}$, the stability of both starting material quinone **3.6.1** and product **3.7.1**, may be called into question. It is well known that $\text{MgBr}_2\cdot\text{Et}_2\text{O}$ forms bidentate chelates with various species, and in many cases, activates nucleophilic addition reactions.¹⁰ One hypothesis is that $\text{MgBr}_2\cdot\text{Et}_2\text{O}$ may form a bidentate chelate with the quinone as shown in Figure 3.7.1, thus activating C3 or C6 for thiol addition. However, there are no current hypotheses on its effect on the stability of quinone **3.6.1**.



*Scheme 3.7.2- Investigation into $\text{MgBr}_2\cdot\text{Et}_2\text{O}$ as Additive with quinone **3.6.1** and catechol **3.7.1***

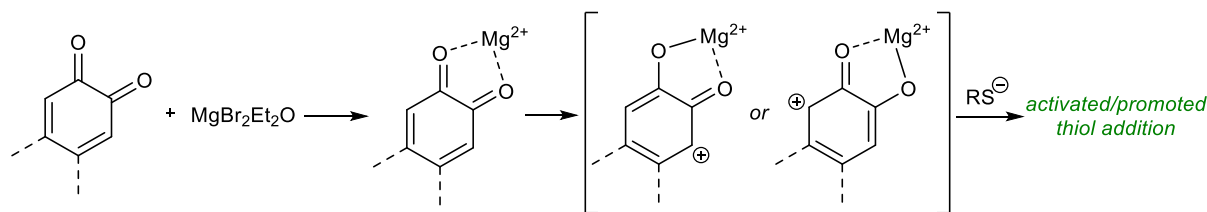


Figure 3.7.1- Hypothesized Role of $\text{MgBr}_2\cdot\text{Et}_2\text{O}$ as Additive

3.8 Mechanism of Addition and Factors Governing Regioselectivity

Through our initial experiments in Section 3.2, it has been observed that the addition proceeds most efficiently under basic conditions. As previously discussed in Chapter 2.4, there

are two plausible mechanisms by which this transformation could occur: 1) through a 1,6-addition, or 2) via a thio-ene reaction. However, it has not been corroborated as to which is more likely, i.e. whether it occurs as a two-electron process or through radical intermediates.

In order to further corroborate these hypotheses, the reaction was evaluated under the presence of radical scavengers (2,2,6,6-Tetramethylpiperidin-1-yl)oxyl (TEMPO) and 2,6-Bis(1,1-dimethylethyl)-4-methylphenol (BHT) with *ortho*-quinone **3.6.1**. (Entries 2 & 3, Table 3.8.1) The reactivity in the presence of these scavengers vs. standard reaction conditions without additive (Entry 1, Table 3.8.1) provided similar results. This appears to further indicate that the addition does not proceed via radical intermediates. Given these results, it is thought that the mechanism proceeds via the route involving a 1,6-addition of the sulfur nucleophile to the *ortho*-quinone, which yields the product catechol after subsequent tautomerization. This is shown with *ortho*-quinone **3.2.2** in Figure 3.8.1. As previously discussed in section 3.5, $\text{MgBr}_2 \cdot \text{Et}_2\text{O}$ has been known to improve the efficiency of nucleophilic addition reactions, and has been shown to be beneficial in most cases regarding this transformation. This further suggests that the 1,6-nucleophilic addition mechanism proposed is plausible.

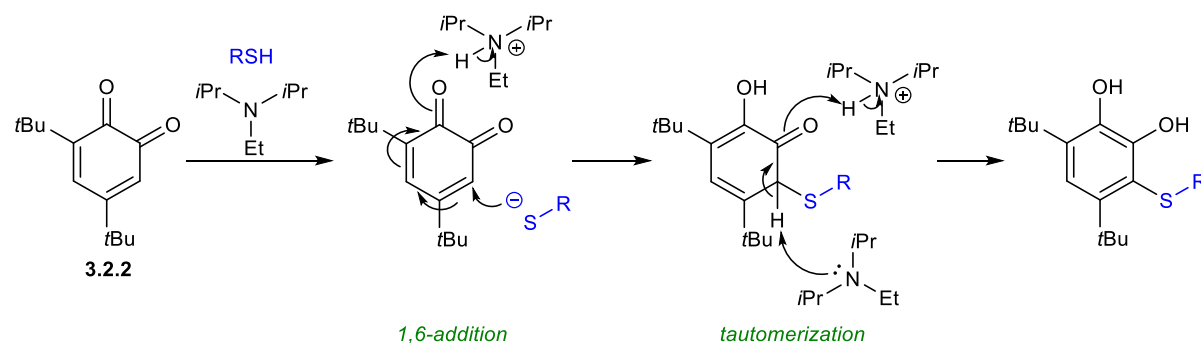


Figure 3.8.1- Proposed Mechanism of Thiol Addition for quinone **3.2.2**, 1,6-Addition

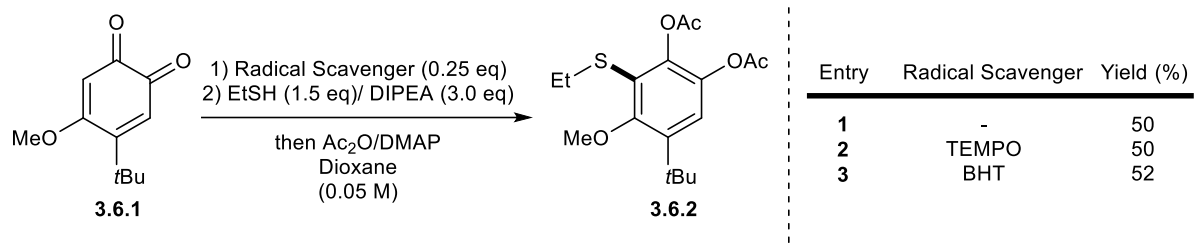


Table 3.8.1- Exploring Reactivity with Radical Scavengers with quinone 3.6.1

However, there still remains to be explained the observed C6 regioselectivity for *ortho*-quinone **3.2.1**, and the other 4-*tert*-butyl-5-alkoxy-quinone substrates explored in the *ortho*-quinone scope (Figure 3.8.2).

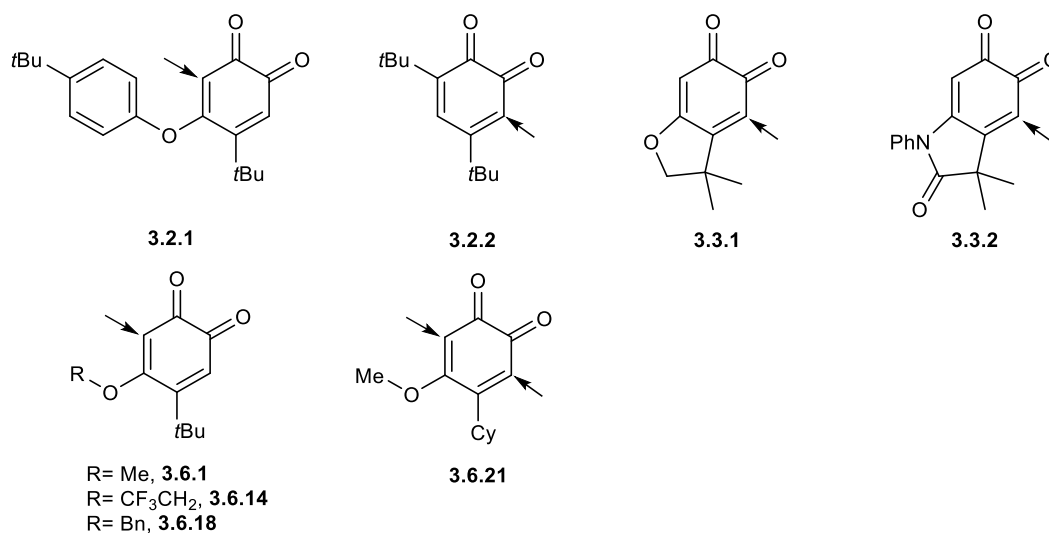


Figure 3.8.2- Summary of the regiochemistry observed for quinones

From an electronic perspective, electron donation by the aryloxy group at C5 results in decreased electrophilic character at C6, therefore allowing nucleophilic attack at C3 to be favoured. Preference for C3-adducts is the regiochemistry observed for quinones **3.3.1** and **3.3.2**, which have vinylogous ester and amide functionalities respectively. Conversely, from a steric perspective, it is conceivable that the addition preferentially occurs at C6 with quinones bearing a *tert*-butyl substituent at C4. The switch in regiochemistry from C6 to C3, observed for *ortho*-quinones **3.3.1** and **3.3.2** can be attributed to sterics, as these quinones possess a less encumbered geminal-dimethyl substituent bound in a five-membered ring at C4. With *ortho*-quinone **3.6.21**, which has a cyclohexyl substituent at C4, we begin to see both the C3 and C6 adducts using the optimized conditions (**3.6.22**, Figure 3.6.2), and subtle factors governing the selectivity begin to

emerge. As cyclohexyl substituents (Taft steric parameter(E_s)= 0.79¹¹) are sterically less encumbered than *tert*-butyl groups (E_s = 1.54¹¹), one can envision that while the addition is regioselective for C3, under sufficiently sterically demanding conditions (i.e. a *tert*-butyl substituent), the regioselectivity of the transformation may be altered. As the substituent at the C4 position increases in size, there is a switch in regioselectivity to C6, which overrides any electronic bias for the C3 position. It is also important to note that with our one example of quinone bearing no functionality at C4, the product isolated is the C4-adduct (**3.6.36**, Figure 3.6.2). As discussed in Chapter 2, Figure 14, Pettus *et al.* reported a 1,4-addition to C5 of 3-benzyl-*ortho*-quinone.¹² As it stands, it appears that the regioselectivity of the addition arises from the substituent pattern and functionality that the quinone bears, and is affected by the steric and electronic properties of the quinone. Due to the limited number of examples in the scope, it is challenging to come to definitive conclusions regarding the regioselectivity of the reaction at this time. However, we have empirically identified that certain additives, *e.g.* DMAP, can be capable of modulating the regioselectivity of the reaction for specific *ortho*-quinones **3.2.1** and **3.6.1**.

To summarize, thiol addition to quinones has been demonstrated as a mild, facile method of S-arylation. As our investigation has shown, there still remains some uncertainties regarding the regiochemistry of the addition and the degree by which this can be tunable through additives. However, it has been shown to be amenable to both aryl and alkyl thiols with moderate to high levels of efficiency for most quinones evaluated, demonstrating its potential to be a useful alternative to existing methods of C-S bond formation.

3.9 Application of Method to Access A Library of Catechols for IONP

Functionalization

It has been known for some time that catechols interact with inorganic materials such as metal ions or metal oxides to form bidentate coordination bonds.¹³ Related coordination chemistry is thought to allow blue mussels (*Mytilus edulis*) to adhere to surfaces, even in aqueous environments.^{13a, 14} In order to stick to surfaces in the ocean, they utilize appendages whose surface proteins produce large amounts of dopa.¹⁵ This biological adhesion mechanism has been exploited for the development of novel materials such as adhesives¹⁵⁻¹⁶, where most adhesive strength fails under wet conditions. Another case where this coordination has found

applications is in the development of aqueous stable superparamagnetic iron oxide nanoparticles (IONPs). IONPs are now essential components in various current technologies such as magnetic resonance imaging contrast agents¹⁷, magnetic separations¹⁸, drug targeting^{17b, 19}, and hybrid inorganic-organic nanomaterials²⁰. In order to have successful application of IONPs for the generation of useful materials, their properties such as nanoparticle size, stability, and dispersant identity must be rigorously identified and explored. Recently, the Blum group (McGill University) has demonstrated a method in exchanging oleic acid ligands on IONPs with catechol based ligands such as dopamine and tiron in aqueous environments.²¹ However, to explore the structure-activity relationship of catechols with IONPs, it is necessary to have a high-yielding and rapid synthesis of diverse catechols. As such, our optimized method of sulfur addition to *ortho*-quinones provides facile access to a library of functionalized catechols with tunable electronic (e.g. sulfur oxidation state) (Figure 3.9.1) and varying steric properties, presenting an excellent opportunity for development and collaboration (Figure 3.9.1).

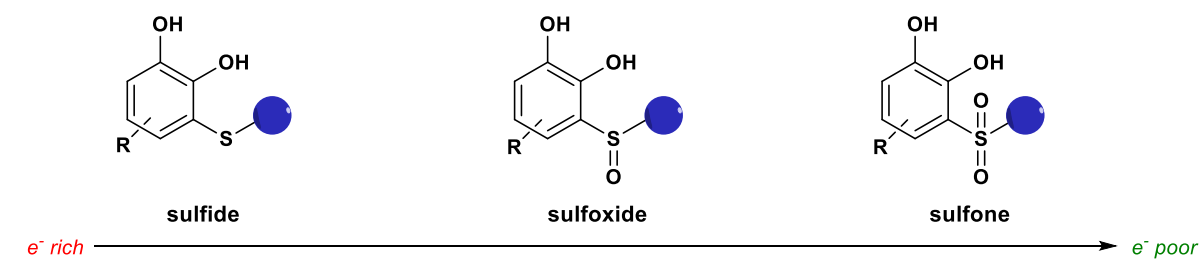
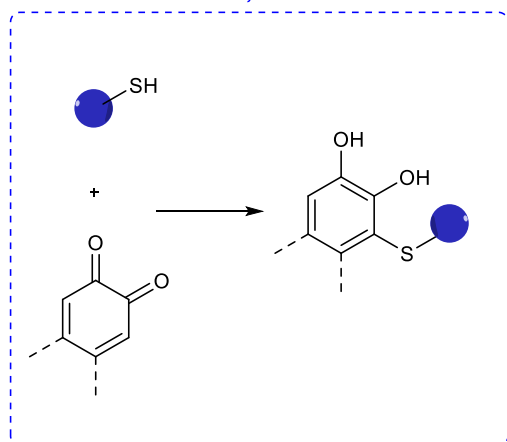


Figure 3.9.1- Lumb Group Thiol Addition Provides Access to Catechols Ranging in Electronic Properties

Lumb Group: Thiol Addition to Quinones for the Generation of Tunable, Functional Catechols



Blum Group: IONP Functionalization through Catechol Oleic Acid Ligand Exchange

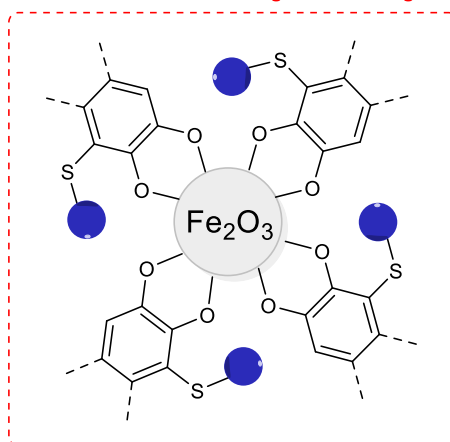


Figure 3.9.2- A General Graphic Depiction of the Lumb Group/Blum Group Collaboration for the Development of Functionalized Catechols for IONP Functionalization

A catechol with an alkyne functionality was targeted as a compound possessing a handle for late stage functionalization with click chemistry, and further studies of the surface chemistry properties of IONPs. In order to generate a catechol with an alkyne functionality, there were two possible ways in which the alkyne could be imparted to the molecule. The first, would be to have a terminal alkyne on the starting material quinone, which would then be converted to the catechol following subsequent thiol addition, providing the sulfur handle to access various oxidation states. The second, would be to have the terminal alkyne on an aliphatic thiol, and isolate the sulfur adduct catechol after thiol addition (Figure 3.9.3). After consideration of the efficiency and feasibility of both routes, it was decided that the use of an alkynyl thiol would be the quickest method in achieving our desired catechol. However, there are currently no commercially available free thiols possessing a terminal alkyne. Thus, it was thought that the most time- and cost- efficient route to this thiol was to begin from the commercially available 4-pentyn-1-ol **3.9.1** (\$42/10 g, Oakwood Chemical)²², and convert the free alcohol to a thiol (Figure 3.9.3).

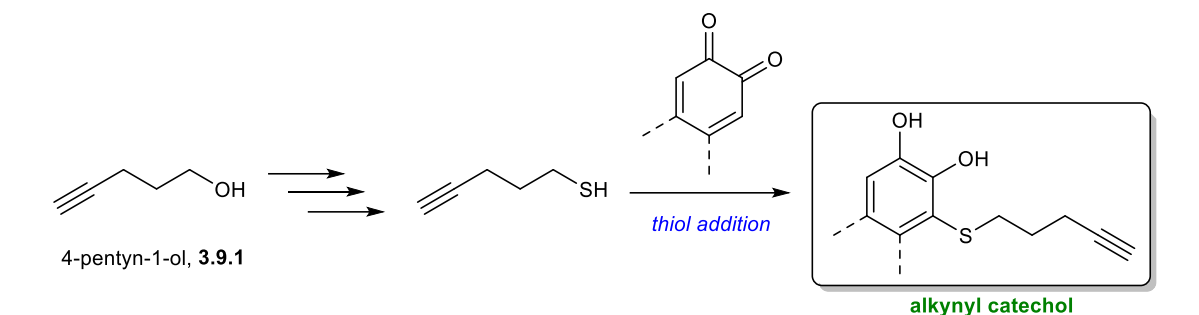
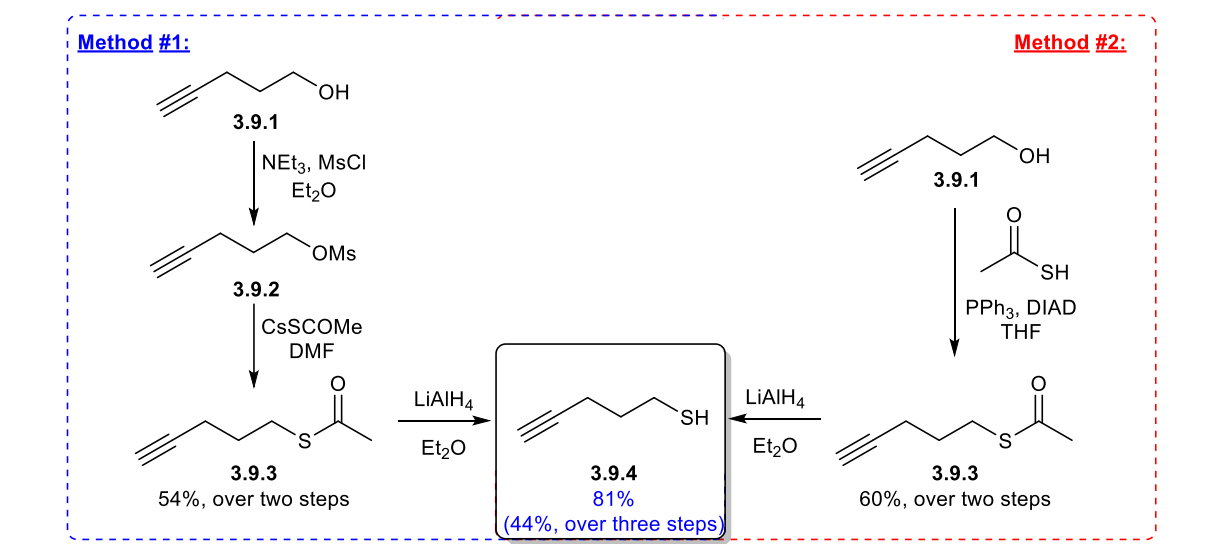


Figure 3.9.3- Proposed Synthesis of Alkynyl Catechols

We chose two possible routes to generate the desired thiol, due to their seeming simplicity and feasibility to scale-up after familiarization. These two methods are shown in Scheme 3.9.1. Method #1 involves mesylation of the alcohol **3.9.1**, followed by a S_N2 displacement of the mesylate **3.9.2** to generate the alkynyl thioacetate **3.9.3**.²³ Reduction of **3.9.3** then generates the corresponding thiol **3.9.4**. Method #2 involves a Mitsunobu reaction with thioacetic acid to generate **3.9.3**²⁴, followed by $LiAlH_4$ reduction to provide the **3.9.4**.

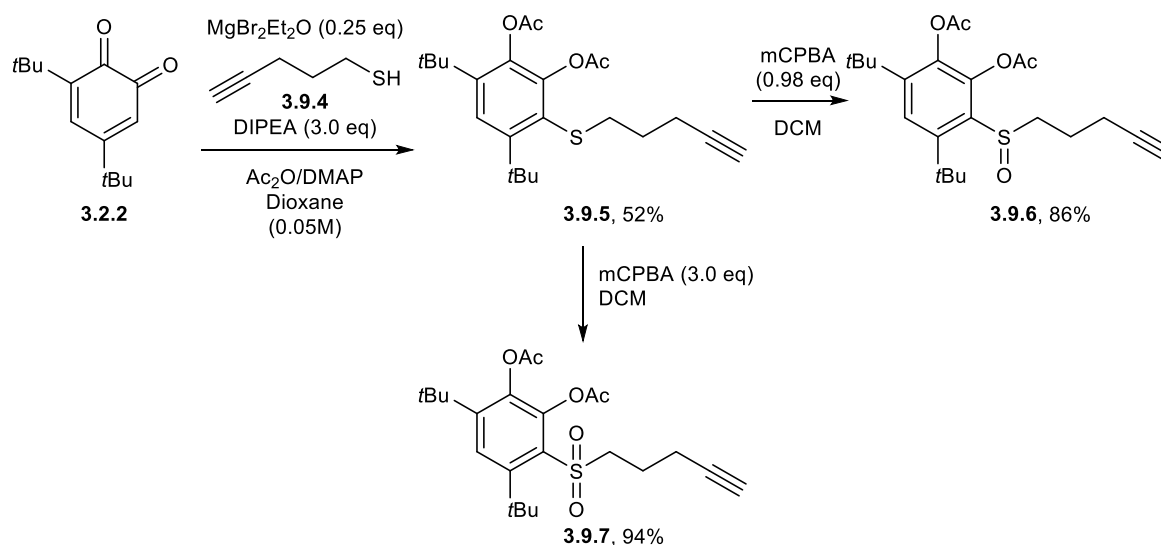


Scheme 3.9.1- Synthetic Routes examined for the Synthesis of 4-pentyn-1-thiol **3.9.4**

Both methods were subsequently evaluated on a 10 and 20 mmol scale, with the specific aim of readily generating the thiol on large scale. It was found that although generation of mesylate **3.9.2** occurred readily, the limiting factor was the sluggish moderately yielding displacement reaction to generate **3.9.3** (54% over two steps). Subsequent lithium aluminum hydride ($LiAlH_4$) reduction furnished the alkynyl thiol **3.9.4** in 81% yield (44% over three steps). An alternative route was also considered. Method #2 was one step shorter to generate **3.9.4**, and

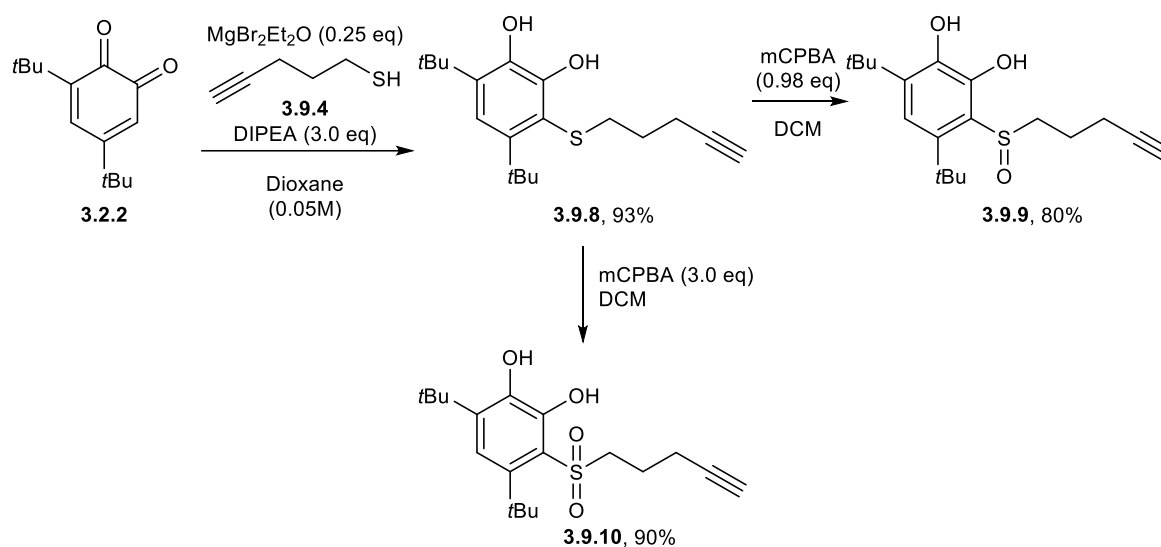
appeared to be more efficient than Method #1. However, on large scale, upon workup of the reaction we encountered extreme difficulty purifying excess triphenylphosphine from the desired product. After numerous titrations and purifications, the highest yields and purity obtained for thioacetate **3.9.3** from Method #2 was 60% on 10 mmol scale, a comparable yield to Method #1 (54%). After consideration of the difficulty and feasibility of both methods, Method #1 was selected for its operational simplicity.

4-pentyn-1-thiol **3.9.4** was then reacted with quinone **3.2.2** under our optimized thiol addition conditions to furnish **3.9.5** (Scheme 3.9.2). On 2 mmol scale, **3.9.5** was isolated in 52% yield, with some material sacrificed in favor of purity during purification (**3.9.5** and the bis-acetate of quinone **3.2.2** are co-polar in the purification solvent, despite multiple attempts at finding alternatives. This is hypothesized to be due to π -stacking, as the presence of toluene in the chromatographic solvent remained our best purification technique). Subsequent *meta*-chloroperoxybenzoic acid (mCPBA) oxidation of **3.9.5** yielded the desired sulfoxide **3.9.6** after 20 minutes, in 86% yield. Further mCPBA oxidation of **3.9.5** to the sulfone was more delayed, but provided **3.9.7** after three days in 94% yield. Oxone was also evaluated as a potential oxidant as an attempt to furnish **3.9.7** in less time. However, this could only provide the sulfoxide **3.9.6** in 86% yield from the sulfide **3.9.5** after three days. Thus, the mCPBA oxidation was selected as a general, mild, and effective method to furnish both sulfoxide and sulfone.



Scheme 3.9.2- Synthesis of Alkynyl Bis-Acetates **3.9.5**, **3.9.6**, and **3.9.7**

Originally, it was envisioned that bis-acetylation of the catechol was required prior to the oxidation of the sulfide to the corresponding sulfoxide and sulfone, for reasons involving catechol stability. However, subsequent investigation revealed that the oxidation of the free catechol sulfide **3.9.8**, followed by reductive workup, was also just as effective in generating the sulfoxide **3.9.9** (80% yield) (Scheme 3.9.3). This then removed the requirement for a subsequent de-acetylation step after the generation of bis-acetates **3.9.5**, **3.9.6**, and **3.9.7**. It is presumed that the *ortho*-quinone is generated in the oxidation, but is subsequently reduced upon the reductive workup. **3.9.8** was then oxidized to the sulfoxide **3.9.9** and sulfone **3.9.10** (90% yield) using the same mCPBA oxidation step involving the aforementioned bis-acetates.



Scheme 3.9.3- Synthesis of Catechols 3.9.8, Sulfoxide 3.9.9, and Sulfone 3.9.10

The sulfide **3.9.8**, sulfoxide **3.9.9**, and sulfone **3.9.10** catechols were then evaluated by Shoronia Cross (Ph.D. Candidate, Blum Group, McGill University) for attachment to the IONPs. However, initial attempts at isolating the catechol-conjugated IONPs were not successful due to altered solubility of the resulting nanoparticles. In order to probe whether there was a successful conjugation, a click reaction with a fluorescent probe, Cy5, was performed on any isolated IONPs. Unfortunately, no fluorescence was detected from any isolated IONP material from reaction with **3.9.8**, **3.9.9**, and **3.9.10**.

In the process of determining the reason behind the failed IONP conjugation attempt, we realized an important difference between the previous successful catechols and our newly

prepared catechols. In their previous work, the Blum group used the catechols tiron **3.9.11** and dopamine **3.9.12** for conjugation (Figure 3.9.4).

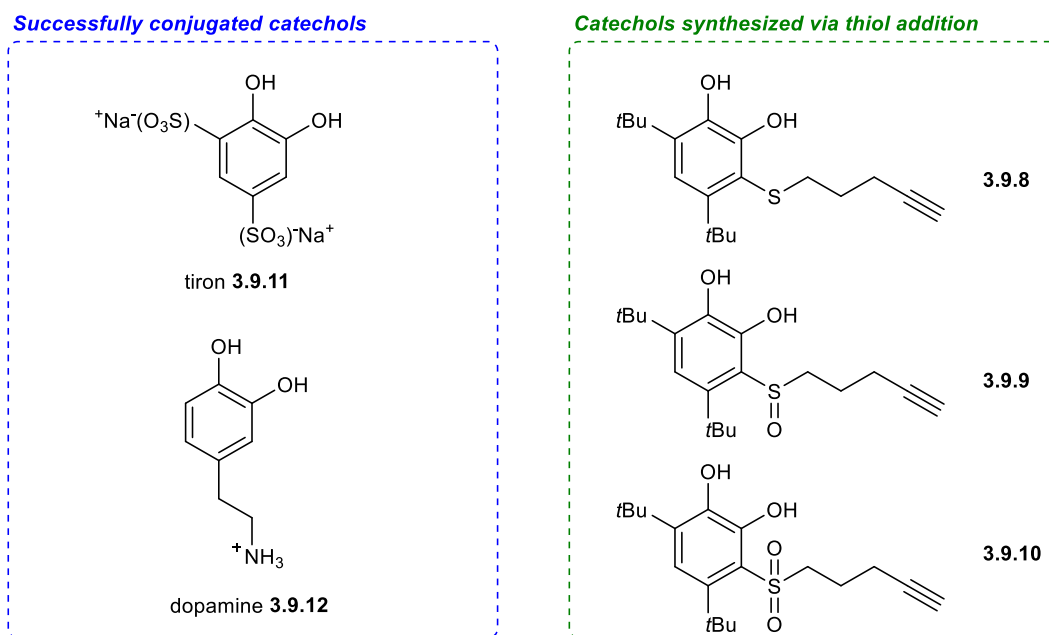
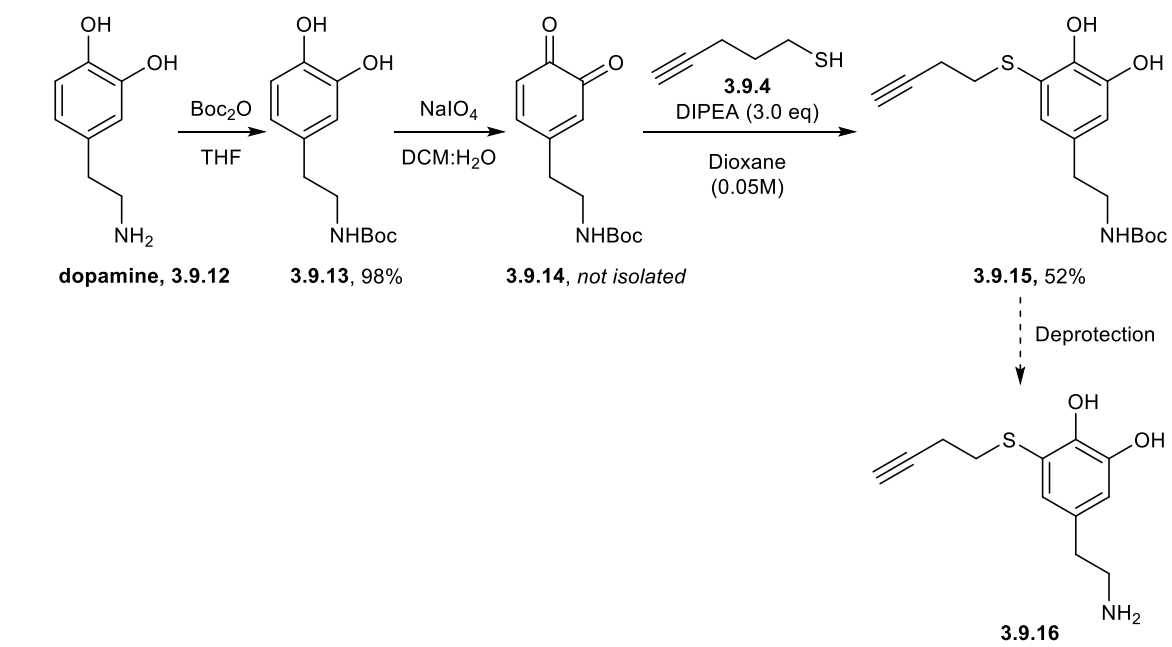


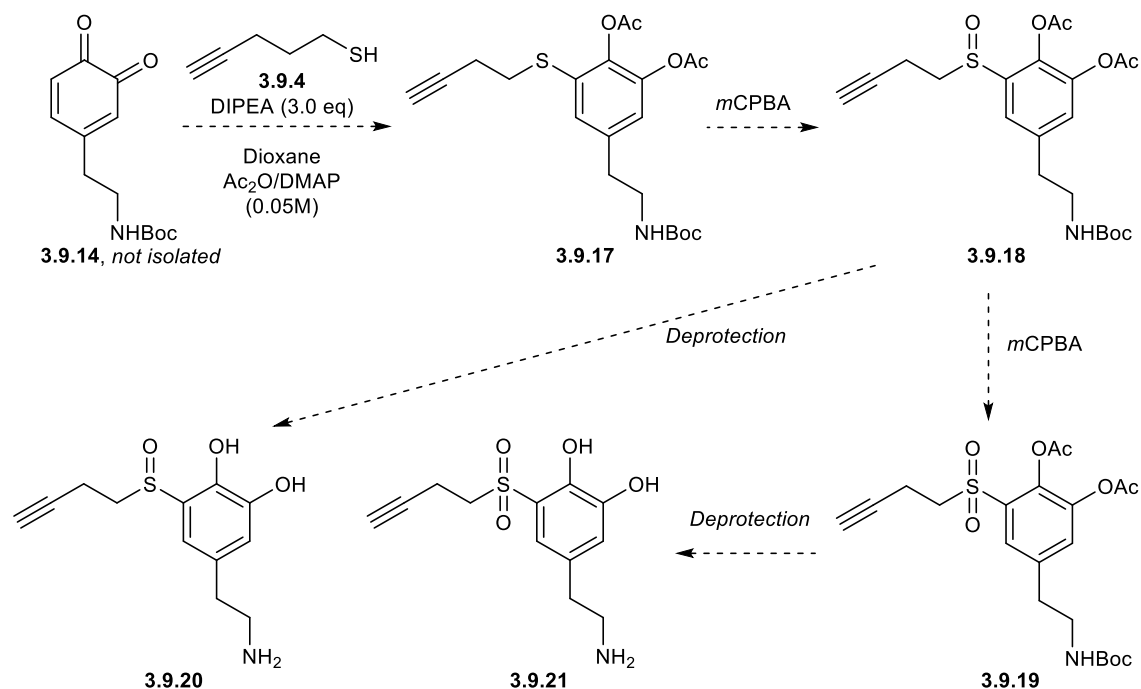
Figure 3.9.4- Catechols conjugated to IONPs by the Blum Group vs. Our alkynyl catechols

Upon comparison of tiron **3.9.11** and dopamine **3.9.12** to our synthesized sulfur-containing catechols, it is clear that one of the main differences between these groups of molecules is the presence of localized charge. The Blum group has taken advantage of this charge to tune their workup procedure for isolation. After performing their ligand exchange with the IONPs, their procedure involves using a neodymium magnet to retrieve any nanoparticles from the DCM/HCl solution, and subsequent washing with hexanes and methanol to remove any unconjugated catechol. This has proven successful in cases with tiron and dopamine, where its charge prevents the IONPs from washing away in non-polar solvents such as hexanes. However, in the case with our sulfur-containing catechols, our molecules have increased steric bulk and are substantially more lipophilic than **3.9.11** or **3.9.12**. Little is known about the solubility differences imparted to the IONP once the catechol is conjugated, but it is possible that any **3.9.8- 3.9.9-** and **3.9.10-** conjugated nanoparticles may have been discarded during the hexanes wash. Another hypothesis was that the catechols did not participate in the ligand exchange entirely, and were subsequently washed away resulting in no Cy5-conjugated dye and no detection of novel conjugated IONP ligands.

Given these results, another catechol was targeted (**3.9.16**, Scheme 3.9.4), one that was more similar to dopamine and possessed a free amine in order to confer charge onto the overall molecule. To generate **3.9.16**, we started with the boc-protection of dopamine to yield **3.9.13** in 98% yield. Subsequent oxidation with sodium *meta*-periodate generated quinone **3.9.14**, which was immediately reacted with 4-pentyn-1-thiol to furnish product **3.9.15** in 52% yield. The lesser yield in the case of this thiol addition may again be attributed to the stability of the quinone in basic media due to enolizable protons. Future directions include the final step in the synthesis of catechol **3.9.16** after Boc-deprotection, as well as subsequent steps to yield the analogous sulfoxide **3.9.20** and sulfone **3.9.21** (Scheme 3.9.5). This will be investigated by Matt Halloran, (M.Sc. candidate, Lumb Group). Subsequent re-evaluation of the charged catechols with the IONPs will then provide further trends as to the types of catechols amenable for use with IONPs, as well as provide direction to the development of a general method for IONP-catechol ligand exchange.



Scheme 3.9.4- Alternative Targeted Catechol 3.9.16 for IONP functionalization



Scheme 3.9.5- Future Synthetic Route to Sulfoxide and Sulfone- Dopamine Derivative Catechols 3.9.20, 3.9.21

3.10 Summary

Upon demonstration of successful thiol additions to o-quinones by Kenneth Esguerra, the reaction's scope was expanded and found amenable to a variety of thiol nucleophiles. With quinones that do not participate in redox-exchange, both aliphatic and aromatic thiols provided high yields of the expected products. Primary, secondary, and tertiary thiols were all discovered to be productive nucleophiles. The range of aromatic thiols proved to be equally diverse with good yields observed *ortho*, *meta*, and *para* substituted thiophenol with electronically-donating nor –withdrawing substituents affecting the reaction's performance. Upon identifying the large variety of tolerated thiols, the reaction was further investigated to determine conditions that were suitable to all quinones. Four modifications to the conditions were identified from the optimization, namely 1) Dioxane as the solvent, 2) MgBr₂·Et₂O as a catalytic Lewis acid, 3) Pre-mixing of acetic anhydride and DMAP and 4) DMAP as an additive. Depending on slight variations to the conditions, it was possible to selectively obtain either regioisomer with quinone **3.2.1**, highlighting the versatility of the technique. Following the elucidation of these conditions, expansion of the *ortho*-quinone scope was performed, allowing for variability of steric and electronic properties, providing variable yields. All optimized conditions proceed with greater

efficiency in cases where the *ortho*-quinone is less susceptible to redox-exchange and decomposition under basic conditions. Unbeknownst at the onset of the study, the substitution pattern on the *ortho*-quinone influences the regioselectivity observed, and thus further study of the quinone scope is required in order to fully determine the active trends in reactivity. Therefore, prediction of the regioselectivity of the reaction remains challenging. Although the addition of MgBr₂·Et₂O and/or DMAP was identified to promote the reaction or generate specific regioisomers, subsequent experiments appear to indicate their effectiveness remains substrate-specific. Further investigation of the influence quinone structure exerts on the reaction may assist in determining conditions that furnish higher yields and afford complete regiochemical control.

Thiol addition to *ortho*-quinones is: 1) a known process in literature, 2) a reaction shown to proceed rapidly, and 3) can be accomplished without external catalysis. Future developments of interest include studies to probe and influence regioselectivity patterns and, and expansion of productive thiols to include amino thiols for application in the synthesis of benzothiazines. These experiments are to be conducted by Matt Halloran. Although still in development, this method was applied successfully towards a synthesis of catechols with tunable electronic properties for the purpose of functionalizing IONPs. This demonstrates that this method is synthetically useful, most notably for the facile synthesis and derivatization of catechols for use in material chemistry. Through our investigations, the functionalization of IONPs with catechols shows promise yet still merits further investigation. Subsequent studies in developing these catechols for use with IONP will be carried out by Shoronia Cross and Matt Halloran.

3.11 References

1. Cao, K.; Stack, D. E.; Ramanathan, R.; Gross, M. L.; Rogan, E. G.; Cavalieri, E. L. Synthesis and Structure Elucidation of Estrogen Quinones Conjugated with Cysteine, N-Acetylcysteine, and Glutathione. *Chem. Res. Toxicol.* **1998**, *11* (8), 909-916.
2. Chioccare, F.; Novellino, E. A Convenient One Step Synthesis of 5-Cystein-S-tyldopa Using Ceric Ammonium Nitrate. *Synth. Commun.* **1986**, *16* (8), 967-971.
3. Guthrie, J. P. Hydrolysis of esters of oxy acids: pK_a values for strong acids; Brønsted relationship for attack of water at methyl; free energies of hydrolysis of esters of oxy acids; and a linear relationship between free energy of hydrolysis and pK_a holding over a range of 20 pK units. *Can. J. Chem.* **1978**, *56* (17), 2342-2354.
4. (a) Bastug, G.; Nolan, S. P. Carbon–Sulfur Bond Formation Catalyzed by [Pd(IPr*OMe)(cin)Cl] (cin = cinnamyl). *J. Org. Chem.* **2013**, *78* (18), 9303-9308; (b) Reeves, J. T.; Camara, K.; Han, Z. S.; Xu, Y.; Lee, H.; Busacca, C. A.; Senanayake, C. H. The Reaction of Grignard Reagents with Bunte Salts: A Thiol-Free Synthesis of Sulfides. *Org. Lett.* **2014**, *16* (4), 1196-1199.

5. Herradura, P. S.; Pendola, K. A.; Guy, R. K. Copper-Mediated Cross-Coupling of Aryl Boronic Acids and Alkyl Thiols. *Org. Lett.* **2000**, 2 (14), 2019-2022.
6. Dalton Research Group, U. o. W. Dielectric Constants of Common Solvents. **2007**.
7. Ripin, D. H. E., D.A. pKa's of Nitrogen Acids. **2005**.
8. Sorgi, K. L. Diisopropylethylamine. In *e-EROS*, John Wiley & Sons, Ltd: 2001.
9. Cavalieri, E.; Chakravarti, D.; Guttenplan, J.; Hart, E.; Ingle, J.; Jankowiak, R.; Muti, P.; Rogan, E.; Russo, J.; Santen, R.; Sutter, T. Catechol estrogen quinones as initiators of breast and other human cancers: Implications for biomarkers of susceptibility and cancer prevention. *Biochim. Biophys. Acta* **2006**, 1766 (1), 63-78.
10. (a) Keck, G. E.; Castellino, S. On the origins of stereoselectivity in chelation controlled nucleophilic additions to .beta.-alkoxy aldehydes: solution structures of Lewis acid complexes via NMR spectroscopy. *J. Am. Chem. Soc.* **1986**, 108 (13), 3847-3849; (b) Black, T. H.; Fader, L. Magnesium Bromide. In *e-EROS*, John Wiley & Sons, Ltd: 2001; (c) Evans, D. A.; Downey, C. W.; Shaw, J. T.; Tedrow, J. S. Magnesium Halide-Catalyzed Anti-Aldol Reactions of Chiral N-Acylthiazolidinethiones. *Org. Lett.* **2002**, 4 (7), 1127-1130; (d) Evans, D. A.; Tedrow, J. S.; Shaw, J. T.; Downey, C. W. Diastereoselective Magnesium Halide-Catalyzed anti-Aldol Reactions of Chiral N-Acyloxazolidinones. *J. Am. Chem. Soc.* **2002**, 124 (3), 392-393.
11. Sigman, M. S.; Miller, J. J. Examination of the Role of Taft-Type Steric Parameters in Asymmetric Catalysis. *J. Org. Chem.* **2009**, 74 (20), 7633-7643.
12. Miller, L. A.; Marsini, M. A.; Pettus, T. R. R. Chemoselective Reactions of 3-Benzyloxy-1,2-o-Quinone with Organometallic Reagents. *Org. Lett.* **2009**, 11 (9), 1955-1958.
13. (a) Lee, H.; Scherer, N. F.; Messersmith, P. B. Single-molecule mechanics of mussel adhesion. *Proc. Natl. Acad. Sci.* **2006**, 103 (35), 12999-13003; (b) McBride, M. B.; Wesselink, L. G. Chemisorption of catechol on gibbsite, boehmite, and noncrystalline alumina surfaces. *Environ. Sci. Technol.* **1988**, 22 (6), 703-708.
14. (a) Waite, J. H. ADHESION IN BYSSALLY ATTACHED BIVALVES. *Biol. Rev.* **1983**, 58 (2), 209-231; (b) Waite, J. H. Nature's underwater adhesive specialist. *Int. J. Adhes. Adhes.* **1987**, 7 (1), 9-14.
15. Lee, B. P.; Messersmith, P. B.; Israelachvili, J. N.; Waite, J. H. Mussel-Inspired Adhesives and Coatings. *Annu. Rev. Mater. Res.* **2011**, 41 (1), 99-132.
16. (a) Faure, E.; Falentin-Daudré, C.; Jérôme, C.; Lyskawa, J.; Fournier, D.; Woisel, P.; Detrembleur, C. Catechols as versatile platforms in polymer chemistry. *Prog. Polym. Sci.* **2013**, 38 (1), 236-270; (b) Sedó, J.; Saiz-Poseu, J.; Busqué, F.; Ruiz-Molina, D. Catechol-Based Biomimetic Functional Materials. *Adv. Mater.* **2013**, 25 (5), 653-701.
17. (a) Lee, C.-M.; Jeong, H.-J.; Kim, E.-M.; Kim, D. W.; Lim, S. T.; Kim, H. T.; Park, I.-K.; Jeong, Y. Y.; Kim, J. W.; Sohn, M.-H. Superparamagnetic iron oxide nanoparticles as a dual imaging probe for targeting hepatocytes in vivo. *Magn. Reson. Med.* **2009**, 62 (6), 1440-1446; (b) Zhang, J. L.; Srivastava, R. S.; Misra, R. D. K. Core-Shell Magnetite Nanoparticles Surface Encapsulated with Smart Stimuli-Responsive Polymer: Synthesis, Characterization, and LCST of Viable Drug-Targeting Delivery System. *Langmuir* **2007**, 23 (11), 6342-6351.
18. Xu, C.; Xu, K.; Gu, H.; Zheng, R.; Liu, H.; Zhang, X.; Guo, Z.; Xu, B. Dopamine as A Robust Anchor to Immobilize Functional Molecules on the Iron Oxide Shell of Magnetic Nanoparticles. *J. Am. Chem. Soc.* **2004**, 126 (32), 9938-9939.
19. Dandamudi, S.; Campbell, R. B. The drug loading, cytotoxicity and tumor vascular targeting characteristics of magnetite in magnetic drug targeting. *Biomaterials* **2007**, 28 (31), 4673-4683.

20. Sanchez, C.; Soler-Illia, G. J. d. A. A.; Ribot, F.; Lalot, T.; Mayer, C. R.; Cabuil, V. Designed Hybrid Organic–Inorganic Nanocomposites from Functional Nanobuilding Blocks. *Chem. Mater.* **2001**, *13* (10), 3061-3083.
21. Korpany, K. V.; Habib, F.; Murugesu, M.; Blum, A. S. Stable water-soluble iron oxide nanoparticles using Tiron. *Mater. Chem. Phys.* **2013**, *138* (1), 29-37.
22. Chemical, O. 4-Pentyn-1-ol.
<http://www.oakwoodchemical.com/ProductsList.aspx?CategoryID=-2&txtSearch=80866>
(accessed January 29, 2016).
23. Journet, M.; Rouillard, A.; Cai, D.; Larsen, R. D. Double Radical Cyclization/ β -Fragmentation of Acyclic ω -Yne Vinyl Sulfides. Synthesis of 3-Vinyldihydrothiophene and Dihydrothiopyran Derivatives. A New Example of a 5-endo-trig Radical Cyclization. *J. Org. Chem.* **1997**, *62* (25), 8630-8631.
24. Yaqub, M.; Walsh, J. J.; Keyes, T. E.; Proust, A.; Rinfray, C.; Izzet, G.; McCormac, T.; Forster, R. J. Electron Transfer to Covalently Immobilized Keggin Polyoxotungstates on Gold. *Langmuir* **2014**, *30* (15), 4509-4516.

Appendix

A1: Experimental Procedures and Data

Table of Contents

1.	General Experimental	125
2.	General Procedures for Thiol Additions	125
a)	General Procedure A, <i>Standard Pre-Optimized Conditions</i>	125
b)	General Procedure B, <i>Standard Optimized Conditions</i>	125
c)	General Procedure C, <i>MgBr₂Et₂O Optimized Conditions</i>	126
d)	General Procedure D, <i>TBSCl Conditions</i>	126
e)	General Procedure E, <i>Pre-Mixed Ac₂O/DMAP Conditions</i>	126
f)	General Procedure F, <i>Bis-Acetylation Conditions</i>	126
3.	Experimental Procedures	126
a)	Procedure for 3.3, Scheme 3.3.2	126
b)	General Procedure for Optimization, 3.4, Table 3.4.1	127
c)	Procedures for 3.4, Table 3.4.2	127
d)	Procedure for 3.4, Scheme 4	127
e)	Procedures for 3.7, Scheme 3.7.1	128
f)	Procedures for 3.7, Scheme 3.7.2	128
g)	Procedure for 3.8, Table 3.8.1	128
4.	Procedures for the Synthesis of Starting Materials	128
a)	General Procedure for the Generation of quinone 3.2.1	128
b)	General Procedure for the Generation of <i>mono</i> -substituted <i>ortho</i> -quinone coupling partners	128
c)	General Procedure for the Generation of 4,5-substituted <i>ortho</i> -quinone coupling partners	129
d)	General Procedure for the Generation of Sulfur Adduct Catechols	129
5.	Experimental Amounts and Reagents	130
a)	3.2, Table 3.2.1:	130
b)	3.3, Table 3.3.1, 3.3.2, 3.3.3:	130
c)	3.3, Scheme 3.3.2:	131
d)	3.4, Table 3.4.1	133
e)	3.4, Table 3.4.2	136
f)	3.4, Scheme 3.4.1:	137
g)	3.6, Table 3.6.2:	137
h)	3.6, Table 3.6.3:	139
i)	3.7, Scheme 3.7.1:	141
j)	3.7, Scheme 3.7.2:	141

k)	3.8, Table 3.8.1:	141
6.	Synthesis and Characterization of Compounds.....	142
a)	Substrates in Table 3.3.1:	142
b)	Substrates in Table 3.3.2:	147
c)	Substrates in Table 3.3.3:	152
d)	Substrates in Table 3.6.2:	157
e)	3.9, Blum Group Collaboration Substrates	164
i)	4-pentyn-1-thiol, 3.9.4	164
ii)	Synthesis of Catechol Ligands for IONP Functionalization	165
7.	References:.....	168

1. General Experimental

All chemicals and solvents were purchased from Sigma Aldrich, Alfa Aesar, TCI, or Oakwood Chemicals. All solvents were dried and purified using an MBraun MB SPS 800 or Innovative Technology PureSolv MD 7. Unless otherwise stated, reactions were performed in flame-dried glassware under a nitrogen or argon atmosphere. Column chromatography was conducted using 200-400 mesh silica gel from Silicycle. ¹H-NMR spectra were acquired using Bruker Ascend 500 MHz, Bruker Ascend 400 MHz, and Varian Inova 400 MHz spectrometers. Chemical shifts (δ) are reported in parts per million (ppm) and are calibrated to the residual solvent peak. Coupling constants (J) are reported in Hz. Multiplicities are reported using the following abbreviations: s = singlet; d = doublet; t = triplet; q = quartet; m = multiplet (range of multiplet is given). ¹³C-NMR spectra were acquired using Bruker Ascend 125 MHz, Bruker Ascend 100 MHz, and Varian Inova 100 MHz spectrometers. Chemical shifts (δ) are reported in parts per million (ppm) and are calibrated to the residual solvent peak. High resolution mass spectrometry was performed by Dr. Nadim Saade and Dr. Alexander Wahba in the Mass Spectrometry Facility at McGill University. High resolution mass spectra (HRMS) were recorded using a Bruker maXis Impact TOF mass spectrometer by electrospray ionization time of flight reflectron experiments. Low resolution mass spectra were recorded in the Lumb Group laboratory using an Agilent 5975C TAD Series GC/MSD EI-quadrupole mass spectrometer. All infrared spectra were recorded in the Integrated Laboratory Facility (Rm. 121) on a Bruker ALPHA FT-IR spectrometer. Analytical thin-layer chromatography was performed on pre-coated 250 mm layer thickness silica gel 60 F254 plates (EMD Chemicals Inc.).

All experimental procedures and their results are presented in order of appearance in Chapter 3. Unless otherwise stated, all reactions proceeded to complete conversion. All NMR Yields were calculated from crude reaction mixture NMRs acquired with 30 μ L of nitromethane as an internal standard.

2. General Procedures for Thiol Additions

a) General Procedure A, *Standard Pre-Optimized Conditions*

A flame-dried 10 mL microwave vial equipped with a Teflon coated stir-bar and a rubber septum was charged with *ortho*-quinone (0.5 mmol, 1 eq), and dry, degassed THF (2.5 mL). In a separate, flame dried 10 mL microwave vial, thiol (0.75 mmol, 1.5 eq) and N,N-diisopropylethylamine (DIPEA) (1.5 mmol, 3 eq) were dissolved in dry, degassed THF (2.5 mL). Using a syringe, the resulting solution was rapidly added to the test tube containing the quinone, and the reaction mixture was stirred at rt for 1.5 hours, upon which the reaction was worked up with General Procedure F, which was then purified by silica column chromatography to yield the final product.

b) General Procedure B, *Standard Optimized Conditions*

A flame-dried 10 mL microwave vial equipped with a Teflon coated stir-bar and a rubber septum was charged with *ortho*-quinone (0.5 mmol, 1 eq) and dry, degassed dioxane (5 mL). In a separate, flame dried 10 mL microwave vial, thiol (0.75 mmol, 1.5 eq) and DIPEA (1.5 mmol, 3 eq) were dissolved in dry, degassed dioxane (5 mL). Using a syringe, the resulting solution was rapidly added to the test tube containing the quinone, and the reaction mixture was stirred at rt for 1.5 hours, upon which the reaction was worked up with General Procedure F, which was then purified by silica column chromatography to yield the final product.

c) General Procedure C, *MgBr₂Et₂O* Optimized Conditions

A flame-dried 10 mL microwave vial equipped with a Teflon coated stir-bar and a rubber septum was charged with *ortho*-quinone (0.5 mmol, 1 eq), magnesium bromide ethyl etherate ($\text{MgBr}_2 \cdot \text{Et}_2\text{O}$) (0.125 mmol, 0.25 eq), and dry, degassed dioxane (5 mL). In a separate, flame dried 10 mL microwave vial, thiol (0.75 mmol, 1.5 eq) and DIPEA (1.5 mmol, 3 eq) were dissolved in dry, degassed dioxane (5 mL). Using a syringe, the resulting solution was rapidly added to the test tube containing the quinone, and the reaction mixture was stirred at rt for 1.5 hours, upon which the reaction was worked up with General Procedure F, which was then purified by silica column chromatography to yield the final product.

d) General Procedure D, *TBSCl* Conditions

A flame-dried 10 mL microwave vial equipped with a Teflon coated stir-bar and a rubber septum was charged with *ortho*-quinone (0.5 mmol, 1 eq), *tert*-butyldimethylsilyl chloride (TBSCl) (0.125 mmol, 0.25 eq), and dry, degassed dioxane (5 mL). In a separate, flame dried 10 mL microwave vial, thiol (0.75 mmol, 1.5 eq) and DIPEA (1.5 mmol, 3 eq) were dissolved in dry, degassed dioxane (5 mL). Using a syringe, the resulting solution was rapidly added to the test tube containing the quinone, and the reaction mixture was stirred at rt for 1.5 hours. , upon which the reaction was worked up with General Procedure F, which was then purified by silica column chromatography to yield the final product.

e) General Procedure E, *Pre-Mixed Ac₂O/DMAP* Conditions

A flame-dried 10 mL microwave vial equipped with a Teflon coated stir-bar and a rubber septum was charged with *ortho*-quinone (0.5 mmol, 1 eq), Ac_2O (1.5 mmol, 3.0 eq), DMAP (0.1 mmol, 0.2 eq), and dry, degassed dioxane (5 mL). In a separate, flame dried 10 mL microwave vial, thiol (0.75 mmol, 1.5 eq) and DIPEA (1.5 mmol, 3 eq) were dissolved in dry, degassed dioxane (5 mL). Using a syringe, the resulting solution was rapidly added to the test tube containing the quinone, and the reaction mixture was stirred at rt for 1.5 hours. The reaction mixture was then extracted with EtOAc (3 x 10 mL), washed with 2M HCl, dried over MgSO_4 to yield the crude product, which was then analyzed by crude mixture NMR.

f) General Procedure F, *Bis-Acetylation* Conditions

Ac_2O (3 eq) and DMAP (12.217 mg, 0.10 mmol, 0.20 eq) were then added, and the reaction mixture was stirred for another 2 hours at rt. The reaction mixture was then extracted with EtOAc (3 x 10 mL), washed with 2M HCl, dried over MgSO_4 to yield a crude mixture.

3. Experimental Procedures

a) Procedure for 3.3, Scheme 3.3.2

In a flame-dried 10mL test tube equipped with a Teflon coated stir-bar and rubber septum, quinone (0.5 mmol, 1.0 eq) was dissolved in THF (5 mL, 0.1 M). In a separate test tube, ethanethiol (0.054 mL, 0.75 mmol, 1.5 eq) and DIPEA (0.261 mL, 1.5 mmol, 3.0 eq) were dissolved in THF. The resulting solution was then rapidly added to the solution containing the quinone, and stirred for 1.5h. Another equivalent of quinone (0.5 mmol, 1.0 eq) was then added, and the reaction was stirred for another 1.5h, upon which the reaction was worked up with General Procedure F.

b) General Procedure for Optimization, 3.4, Table 3.4.1

- i) A flame-dried 10 mL microwave vial equipped with a Teflon coated stir-bar and a rubber septum was charged with *ortho*-quinone (0.5 mmol, 1 eq), and dry, degassed solvent (2.5 mL). In a separate, flame dried 10 mL microwave vial, thiol (0.75 mmol, 1.5 eq) and base (1.5 mmol, 3 eq) were dissolved in dry, degassed solvent. Using a syringe, the resulting solution was rapidly added to the test tube containing the quinone, and the reaction mixture was stirred at rt for 1.5 hours, upon which the reaction was worked up with General Procedure F, which was then analyzed by crude mixture NMR.
- ii) A flame-dried 10 mL microwave vial equipped with a Teflon coated stir-bar and a rubber septum was charged with *ortho*-quinone (0.5 mmol, 1 eq), Lewis acid (0.125 mmol, 0.25 eq), and dry, degassed solvent. In a separate, flame dried 10 mL microwave vial, thiol (0.75 mmol, 1.5 eq) and base (1.5 mmol, 3 eq) were dissolved in dry, degassed solvent. Using a syringe, the resulting solution was rapidly added to the test tube containing the quinone, and the reaction mixture was stirred at rt for 1.5 hours, upon which the reaction was worked up with General Procedure F, which was then analyzed by crude mixture NMR.

c) Procedures for 3.4, Table 3.4.2

- i) A flame-dried 10 mL microwave vial equipped with a Teflon coated stir-bar and a rubber septum was charged with *ortho*-quinone (0.5 mmol, 1 eq), TBSCl (0.25, 0.05, or 0.5 mmol) and dry, degassed dioxane (5 mL). In a separate, flame dried 10 mL microwave vial, thiol (0.75 mmol, 1.5 eq) and DIPEA (1.5 mmol, 3 eq) were dissolved in dry, degassed dioxane (5 mL). Using a syringe, the resulting solution was rapidly added to the test tube containing the quinone, and the reaction mixture was stirred at rt for 1.5 hours, upon which the reaction was worked up with General Procedure F, which was then analyzed by crude mixture NMR.
- ii) A flame-dried 10 mL microwave vial equipped with a Teflon coated stir-bar and a rubber septum was charged with *ortho*-quinone (0.5 mmol, 1 eq), protecting group (TBSOTf, Tf₂O, or Ac₂O) (1.125 mmol, 2.25 eq), and dry, degassed dioxane (5 mL). In a separate, flame dried 10 mL microwave vial, thiol (0.75 mmol, 1.5 eq) and DIPEA (1.5 mmol, 3 eq) were dissolved in dry, degassed dioxane (5 mL). Using a syringe, the resulting solution was rapidly added to the test tube containing the quinone, and the reaction mixture was stirred at rt for 1.5 hours, upon which the reaction was worked up with General Procedure F, which was then analyzed by crude mixture NMR.
- iii) A flame-dried 10 mL microwave vial equipped with a Teflon coated stir-bar and a rubber septum was charged with *ortho*-quinone (0.5 mmol, 1 eq), DMAP (12.217 mg, 0.1 mmol, 0.2 eq), and dry, degassed dioxane (5 mL). In a separate, flame dried 10 mL microwave vial, thiol (0.75 mmol, 1.5 eq) and DIPEA (1.5 mmol, 3 eq) were dissolved in dry, degassed dioxane (5 mL). Using a syringe, the resulting solution was rapidly added to the test tube containing the quinone, and the reaction mixture was stirred at rt for 1.5 hours, upon which the reaction was worked up with General Procedure F, which was then analyzed by crude mixture NMR.

d) Procedure for 3.4, Scheme 4

In a flame-dried, 10 mL test tube equipped with a Teflon stir-bar and rubber septum, quinone **3.1** and DMAP (12.217 mg, 0.1 mmol, 0.2 eq) were dissolved in dry, degassed dioxane (10 mL). DIPEA (0.261 mL, 1.5 mmol, 3.0 eq) was then added, and the reaction was stirred for 1.5h, upon which the reaction was concentrated *in vacuo* and analyzed by NMR in CDCl₃.

e) Procedures for 3.7, Scheme 3.7.1

Entry 1: In a flame-dried test tube equipped with a rubber septum and Teflon coated stir-bar quinone **3.2.1** (156 mg, 0.5 mmol, 1 eq) and catechol **3.4.2** (194.28 mg, 0.5 mmol, 1 eq) were mixed in dioxane (10 mL), and stirred for 1.5h. The reaction mixture was then concentrated *in vacuo* to yield complete recovery of starting materials.

Entry 2: In a flame-dried test tube equipped with a rubber septum and Teflon coated stir-bar quinone **3.2.1** (156 mg, 0.5 mmol, 1eq), $\text{MgBr}_2 \cdot \text{Et}_2\text{O}$ (32.278 mg, 0.125 mmol, 0.25 eq) and catechol **3.4.2** (194.28 mg, 0.5 mmol, 1eq) were mixed in dioxane (10 mL), and stirred for 1.5h. The reaction mixture was then extracted with EtOAc (3 x 10 mL), washed with H_2O , dried with MgSO_4 , and concentrated *in vacuo* to yield complete recovery of starting materials.

f) Procedures for 3.7, Scheme 3.7.2

Entry 1: In a flame-dried test tube equipped with a Teflon coated stir-bar, quinone **3.6.1** (97.115 mg, 0.5 mmol, 1.0 eq) was dissolved in dioxane (10 mL). Catechol **3.7.1** (119.165 mg, 0.5 mmol, 1.0 eq) was then added, and the reaction was stirred for 1.5 h, upon which the crude mixture was concentrated *in vacuo*.

Entry 2: In a flame-dried test tube equipped with a Teflon coated stir-bar, quinone **3.6.1** (97.115 mg, 0.5 mmol, 1.0 eq) and $\text{MgBr}_2 \cdot \text{Et}_2\text{O}$ (32.278 mg, 0.125 mmol, 0.25 eq) were dissolved in dioxane (10 mL). Catechol **3.7.1** (119.165 mg, 0.5 mmol, 1.0 eq) was then added, and then reaction was stirred for 1.5h, upon which the crude mixture was concentrated *in vacuo*.

Entry 3: In a flame-dried test tube equipped with a Teflon coated stir-bar, catechol **3.7.1** (119.165 mg, 0.5 mmol, 1.0 eq) and $\text{MgBr}_2 \cdot \text{Et}_2\text{O}$ (32.278 mg, 0.125 mmol, 0.25 eq) were dissolved in dioxane (10 mL). Quinone **3.6.1** (97.115 mg, 0.5 mmol, 1.0 eq) was then added, and then reaction was stirred for 1.5h, upon which the crude mixture was concentrated *in vacuo*.

g) Procedure for 3.8, Table 3.8.1

A flame-dried 10 mL microwave vial equipped with a Teflon coated stir-bar and a rubber septum was charged with *ortho*-quinone (0.5 mmol, 1 eq), radical scavenger (0.125 mmol, 0.25 eq), and dry, degassed dioxane (5 mL). In a separate, flame dried 10 mL microwave vial, thiol (0.75 mmol, 1.5 eq) and DIPEA (1.5 mmol, 3 eq) were dissolved in dry, degassed dioxane (5 mL). Using a syringe, the resulting solution was rapidly added to the test tube containing the quinone, and the reaction mixture was stirred at rt for 1.5 hours, upon which the reaction was worked up with General Procedure F, which was then analyzed by crude mixture NMR.

4. Procedures for the Synthesis of Starting Materials

a) General Procedure for the Generation of quinone 3.2.1

Quinone **3.2.1** was generated according to a procedure previously reported by our group.¹

b) General Procedure for the Generation of *mono*-substituted *ortho*-quinone coupling partners

A 25 mL round bottom flask was charged with a Teflon coated stir-bar, catechol (0.5 mmol, 1 eq), and sodium *meta*-periodate (0.55 mmol, 1.1 eq). Dichloromethane (DCM) (10 mL) was then added to dissolve the flask contents, upon dissolution, deionized water (5 mL) was added, upon which the clear mixture turned dark orange. The flask was then equipped with a rubber septum and stirred for 45 minutes. The reaction mixture was then diluted with DCM and H_2O , and extracted with DCM

(3 x 25 mL). The mixture was then concentrated *in vacuo* and then used immediately in the next reaction.

c) General Procedure for the Generation of 4,5-substituted *ortho*-quinone coupling partners

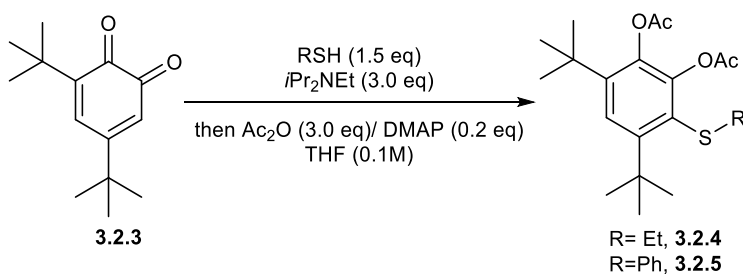
All 4,5-substituted *ortho*-quinones were synthesized according to a procedure previously reported by our group.²

d) General Procedure for the Generation of Sulfur Adduct Catechols

A flame-dried 10 mL microwave vial equipped with a Teflon coated stir-bar and a rubber septum was charged with *ortho*-quinone (0.5 mmol, 1 eq), MgBr₂·Et₂O (0.125 mmol, 0.25 eq), and dry, degassed dioxane (5 mL). In a separate, flame dried 10 mL microwave vial, thiol (0.75 mmol, 1.5 eq) and DIPEA (1.5 mmol, 3 eq) were dissolved in dry, degassed dioxane (5 mL). Using a syringe, the resulting solution was rapidly added to the test tube containing the quinone, and the reaction mixture was stirred at rt for 1.5 hours. The reaction mixture was then extracted with EtOAc (3 x 10 mL), washed with 2M HCl, dried over MgSO₄ to yield the crude product catechol, which was purified by silica column chromatography to yield the final product.

5. Experimental Amounts and Reagents

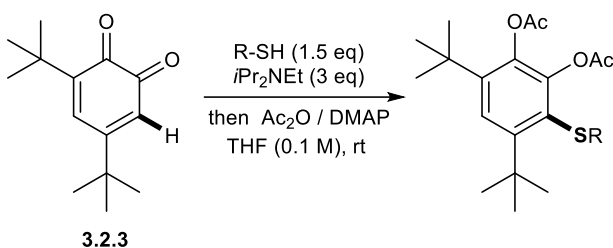
a) 3.2, Table 3.2.1:



Entry	R	Yield
1	Et	88
2	Et	99 ^a
3	Ph	89
4	Ph	92 ^a
5 ^b	Et	79
6 ^c	Et	63

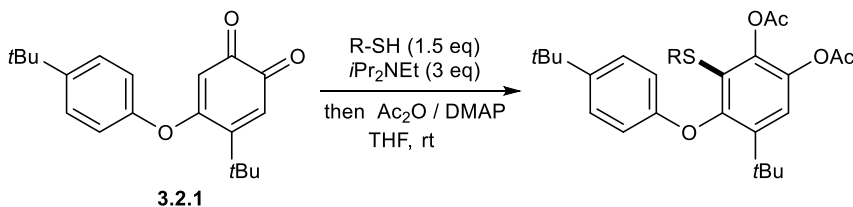
[a] Reactions performed on a 0.5 mmol scale of quinone. [b] Entries 1-4, performed according to General Procedure A. [c] Entries 1 and 3 performed with dry, un-degassed THF. [d] Entry 5, sodium ethanethiolate used. [e] Entry 6, with *para*-toluenesulfonic acid (pTsOH) (95.11 mg, 0.5 mmol, 1.0 eq) as additive, DIPEA was excluded.

b) 3.3, Table 3.3.1, 3.3.2, 3.3.3:



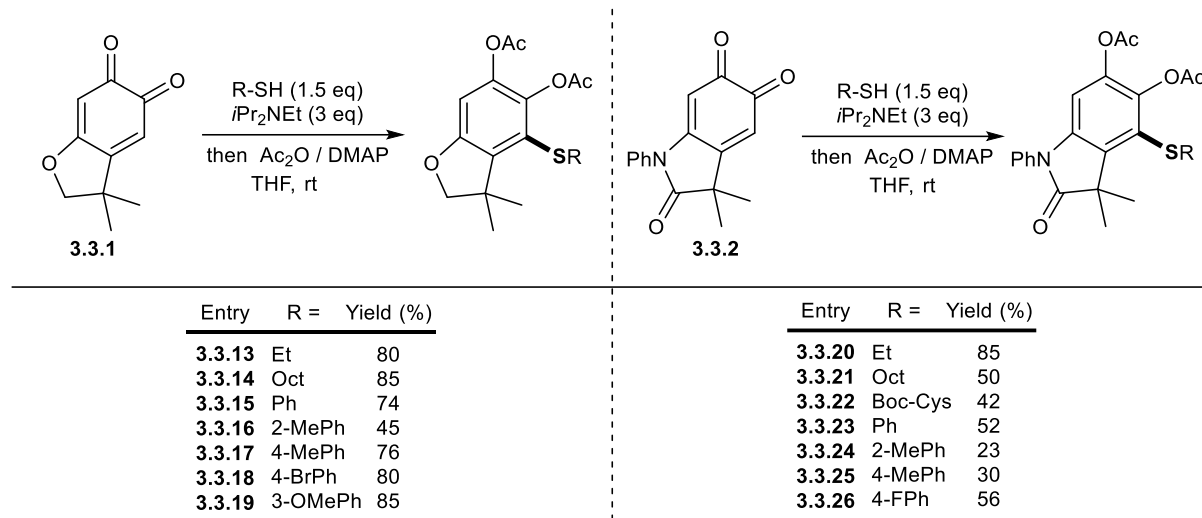
Entry	R =	Yield (%)	Entry	R =	Yield (%)
3.2.4	Et	99	3.2.11	2-MePh	95
3.2.5	Ph	99	3.2.12	4-MePh	95
3.2.6	Oct	85	3.2.13	3-OMePh	98
3.2.7	<i>i</i> Pr	96	3.2.14	4-BrPh	90
3.2.8	<i>t</i> Bu	85	3.2.15	4-ClPh	84
3.2.9	1-naph	95	3.2.16	4-F	88
3.2.10	2-naph	96	3.2.17	4-OMe	76

[a] Reactions performed on 0.5 mmol scale of quinone, according to General Procedure A



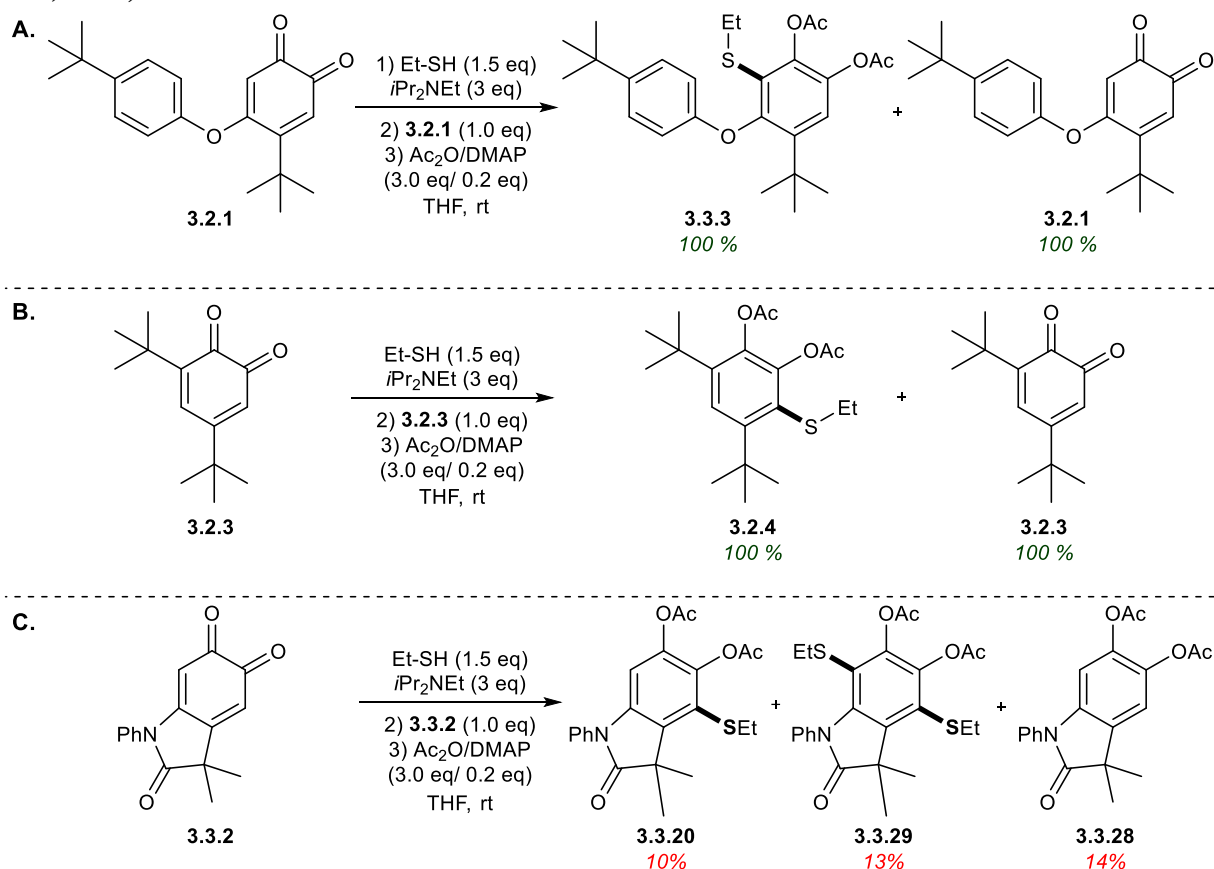
Entry	R =	Yield (%)
3.3.3	Et	87
3.3.4	Oct	85
3.3.5	Boc-Cys	85
3.3.6	<i>i</i> Pr	58
3.3.7	Ph	93
3.3.8	2-MePh	90
3.3.9	4-MePh	89
3.3.10	3-OMePh	91
3.3.11	4-BrPh	82
3.3.12	4-OMePh	85

[a] Reactions performed on 0.5 mmol scale of quinone, according to General Procedure A



[a] Reactions performed on 0.5 mmol scale of quinone, according to General Procedure A

c) 3.3, Scheme 3.3.2:

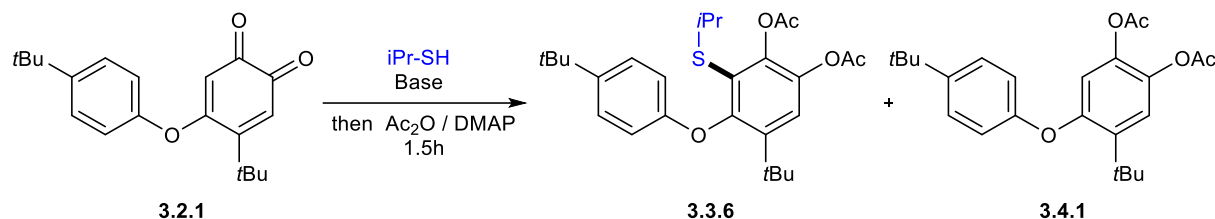


[a] Reactions performed on 0.5 mmol scale of quinone, according to procedures outlined in 3a.

Amounts and Reagents used for Scheme 3.3.2:

Entry	Quinone	Thiol	Base	Acetylation	Yield
1	3.2.1 (220.32 mg, 1.0 mmol, 2.0 eq)	EtSH (0.054 mL, 0.75 mmol, 1.5 eq)	DIPEA (0.261 mL, 1.5 mmol, 3.0 eq)	Ac ₂ O (0.141 mL, 1.5 mmol, 3.0 eq)/ DMAP (12.217 mg, 0.1 mmol, 0.2 eq)	100%
2	3.2.3 (312.42 mg, 1.0 mmol, 2.0 eq)	EtSH (0.054 mL, 0.75 mmol, 1.5 eq)	DIPEA (0.261 mL, 1.5 mmol, 3.0 eq)	Ac ₂ O (0.141 mL, 1.5 mmol, 3.0 eq)/ DMAP (12.217 mg, 0.1 mmol, 0.2 eq)	100%
3	3.3.2 (133.64 mg, 0.5 mmol, 2.0 eq)	EtSH (0.027 mL, 0.375 mmol, 1.5 eq)	DIPEA (0.131 mL, 1.5 mmol, 3.0 eq)	Ac ₂ O (0.071 mL, 0.75 mmol, 3.0 eq)/ DMAP (6.11 mg, 0.05 mmol, 0.2 eq)	3.3.20: 10% 3.3.29: 13% 3.3.28: 14%

d) 3.4, Table 3.4.1



Amounts and Reagents used for Optimization (3.4, Table 3.4.1):

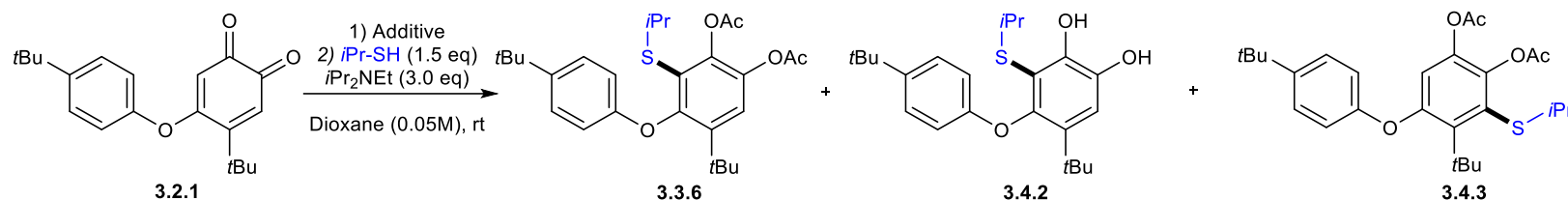
Entry	Base	Solvent	Conc. (M)	Temp. (°C)	Additive	Yield	
						3.3.6	3.4.1
1 ^a	DIPEA (0.261 mL, 1.5 mmol, 3.0 eq)	THF (5 mL)	0.1	rt	-	56	11
2 ^a	DIPEA (0.261 mL, 1.5 mmol, 3.0 eq)	MeOH (5 mL)	0.1	rt	-	60	-
3 ^a	DIPEA (0.261 mL, 1.5 mmol, 3.0 eq)	DMF (5 mL)	0.1	rt	-	65	20
4 ^a	DIPEA (0.261 mL, 1.5 mmol, 3.0 eq)	EtOAc (5 mL)	0.1	rt	-	60	24
5 ^a	DIPEA (0.261 mL, 1.5 mmol, 3.0 eq)	Dioxane (5 mL)	0.1	rt	-	68	14
6 ^a	DBU (0.224 mL, 1.5 mmol, 3.0 eq)	THF (5 mL)	0.1	rt	-	-	-
7 ^a	Pyridine (0.121 mL, 1.5 mmol, 3.0 eq)	THF (5 mL)	0.1	rt	-	-	-
8 ^a	NEt ₃ (0.209 mL, 1.5 mmol, 3.0 eq)	THF (5 mL)	0.1	rt	-	32	18
9 ^a	DIPEA (0.261 mL, 1.5 mmol, 3.0 eq)	THF (5 mL)	0.1	rt	-	61	14
10 ^{ac}	DIPEA (0.261 mL, 1.5 mmol, 3.0 eq)	THF (5 mL)	0.1	0	-	60	14
11 ^{ad}	DIPEA (0.261 mL, 1.5 mmol, 3.0 eq)	THF (5 mL)	0.1	-20	-	62	14
12 ^a	DIPEA (0.261 mL, 1.5 mmol, 3.0 eq)	Dioxane (1 mL)	0.5	rt	-	67	10

13^a	DIPEA (0.261 mL, 1.5 mmol, 3.0 eq)	Dioxane (50 mL)	0.01	rt	-	69	14
14^a	DIPEA (0.261 mL, 1.5 mmol, 3.0 eq)	Dioxane (10 mL)	0.05	rt	-	74	8
15^a	DIPEA (0.261 mL, 1.5 mmol, 3.0 eq)	THF (10 mL)	0.05	rt	-	72	10
16^a	DIPEA (0.261 mL, 1.5 mmol, 3.0 eq)	THF:Dioxane (1:1) (10 mL)	0.1	rt	-	63	14
17^a	DIPEA (0.261 mL, 1.5 mmol, 3.0 eq)	THF:Dioxane (1:1) (10 mL)	0.05	rt	-	67	16
18^b	DIPEA (0.261 mL, 1.5 mmol, 3.0 eq)	Dioxane (10 mL)	0.05	rt	Ti(OiPr) ₄ (35.527 mg, 0.125 mmol, 0.25 eq)	56	22
19^b	DIPEA (0.261 mL, 1.5 mmol, 3.0 eq)	Dioxane (10 mL)	0.05	rt	ZnCl ₂ (17.037 mg, 0.125 mmol, 0.25 eq)	64	10
20^b	DIPEA (0.261 mL, 1.5 mmol, 3.0 eq)	Dioxane (10 mL)	0.05	rt	CuPF ₆ (46.59 mg, 0.125 mmol, 0.25 eq)	50	16
21^b	DIPEA (0.261 mL, 1.5 mmol, 3.0 eq)	Dioxane (10 mL)	0.05	rt	MgBr ₂ ·Et ₂ O (32.278 mg, 0.125 mmol, 0.25 eq)	86	5
22^b	DIPEA (0.261 mL, 1.5 mmol, 3.0 eq)	Dioxane (10 mL)	0.05	rt	Zn(OTf) ₂ (45.44 mg, 0.125 mmol, 0.25 eq)	50	16
23^b	DIPEA (0.261 mL, 1.5 mmol, 3.0 eq)	Dioxane (10 mL)	0.05	rt	MgBr ₂ (23.013 mg, 0.125 mmol, 0.25 eq)	97	2
24^b	DIPEA (0.261 mL, 1.5 mmol, 3.0 eq)	Dioxane (10 mL)	0.05	rt	LiCl (5.298 mg, 0.125 mmol, 0.25 eq)	63	16
25^b	DIPEA (0.261 mL, 1.5 mmol, 3.0 eq)	Dioxane (10 mL)	0.05	rt	Mg(ClO) ₄ (27.90 mg, 0.125 mmol, 0.25 eq)	32	6
26^b	DIPEA (0.261 mL, 1.5 mmol, 3.0 eq)	Dioxane (10 mL)	0.05	rt	LiBr (10.85 mg, 0.125 mmol, 0.25 eq)	64	13
27^b	DIPEA (0.261 mL, 1.5 mmol, 3.0 eq)	Dioxane (10 mL)	0.05	rt	MgCl ₂ (11.90 mg, 0.125 mmol, 0.25 eq)	94	2
28^b	DIPEA (0.261 mL, 1.5 mmol, 3.0 eq)	Dioxane (5 mL)	0.1	rt	MgBr ₂ ·Et ₂ O (32.278 mg, 0.125 mmol, 0.25 eq)	96	3
29^b	DIPEA (0.261 mL, 1.5 mmol, 3.0 eq)	THF (10 mL)	0.05	rt	MgBr ₂ ·Et ₂ O (32.278 mg, 0.125 mmol, 0.25 eq)	73	10
30^b	DIPEA (0.261 mL, 1.5 mmol, 3.0 eq)	DCM (10 mL)	0.05	rt	MgBr ₂ ·Et ₂ O (32.278 mg, 0.125 mmol, 0.25 eq)	72	6

31^{bi}	DIPEA (0.261 mL, 1.5 mmol, 3.0 eq)	EtOAc (10 mL)	0.05	rt	MgBr ₂ ·Et ₂ O (32.278 mg, 0.125 mmol, 0.25 eq)	82	9
32^b	DIPEA (0.261 mL, 1.5 mmol, 3.0 eq)	MeOH (10 mL)	0.05	rt	MgBr ₂ ·Et ₂ O (32.278 mg, 0.125 mmol, 0.25 eq)	30	26
33^b	DIPEA (0.261 mL, 1.5 mmol, 3.0 eq)	DMF (10 mL)	0.05	rt	MgBr ₂ ·Et ₂ O (32.278 mg, 0.125 mmol, 0.25 eq)	76	10
34^b	DIPEA (0.261 mL, 1.5 mmol, 3.0 eq)	Et ₂ O (10 mL)	0.05	rt	MgBr ₂ ·Et ₂ O (32.278 mg, 0.125 mmol, 0.25 eq)	62	17
35^b	DIPEA (0.261 mL, 1.5 mmol, 3.0 eq)	Dioxane (10 mL)	0.05	rt	MgBr ₂ ·Et ₂ O (12.911 mg, 0.05 mmol, 0.1 eq)	95	4
36^b	DIPEA (0.261 mL, 1.5 mmol, 3.0 eq)	Dioxane (10 mL)	0.05	rt	MgBr ₂ ·Et ₂ O (64.558 mg, 0.25 mmol, 0.5 eq)	85	6
37^[bi]	DIPEA (0.261 mL, 1.5 mmol, 3.0 eq)	Dioxane (10 mL)	0.05	rt	MgBr ₂ ·Et ₂ O (129.115 mg, 0.5 mmol, 1.0 eq)	95	5

[a] Reactions performed according to procedure listed in 3bi [b] Reactions performed according to procedure listed in 3bii [c] Reaction temperature at 0°C [d] Reaction temperature at -20°C

e) 3.4, Table 3.4.2

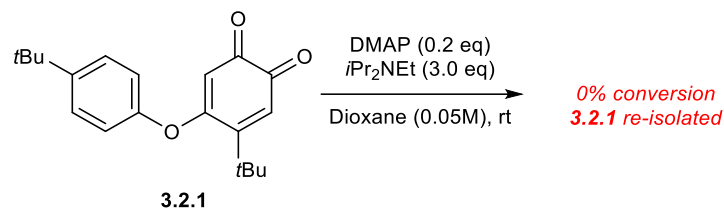


Amounts and Reagents used for Table 3.4.2:

Entry	Base	Solvent	Conc. (M)	Additive	Yield		
					3.3.6	3.4.2	3.4.3
1 ^[a]	DIPEA (0.261 mL, 1.5 mmol, 3.0 eq)	Dioxane (10 mL)	0.05	TBSCl (37.68 mg, 0.25 mmol, 0.5 eq)	-	89	-
2 ^[a]	DIPEA (0.261 mL, 1.5 mmol, 3.0 eq)	Dioxane (10 mL)	0.05	TBSCl (7.536 mg, 0.05 mmol, 0.1 eq)	-	76	-
3 ^[a]	DIPEA (0.261 mL, 1.5 mmol, 3.0 eq)	Dioxane (10 mL)	0.05	TBSCl (75.36 mg, 0.5 mmol, 1.0 eq)	-	72	-
4 ^[b]	DIPEA (0.261 mL, 1.5 mmol, 3.0 eq)	Dioxane (10 mL)	0.05	TBSOTf (0.203 mL, 1.125 mmol, 2.25 eq)	-	-	-
5 ^[b]	DIPEA (0.261 mL, 1.5 mmol, 3.0 eq)	Dioxane (10 mL)	0.05	Tf ₂ O (0.189 mL, 1.125 mmol, 2.25 eq)	-	-	-
6 ^[b]	DIPEA (0.261 mL, 1.5 mmol, 3.0 eq)	Dioxane (10 mL)	0.05	Ac ₂ O (0.105 mL, 1.125 mmol, 2.25 eq)	50	-	-
7 ^[c]	DIPEA (0.261 mL, 1.5 mmol, 3.0 eq)	Dioxane (10 mL)	0.05	Ac ₂ O (0.105 mL, 2.25 eq, 2.25 eq) DMAP (12.217 mg, 0.1 mmol, 0.2 eq)	-	-	83
8 ^[d]	DIPEA (0.261 mL, 1.5 mmol, 3.0 eq)	Dioxane (10 mL)	0.05	DMAP (12.217 mg, 0.1 mmol, 0.2 eq)	-	-	60

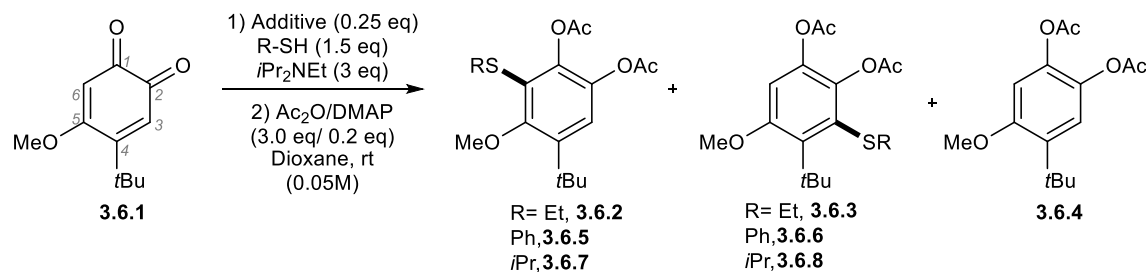
[a] Reactions performed according to procedure outlined in 3ci [b] Performed according to procedures in 3cii. [c] Performed according to General Procedure E. [d] Performed according to procedure in 3ciii.

f) 3.4, Scheme 3.4.1:



[a] Performed on a 0.5 mmol scale with respect to quinone **3.2.1**.

g) 3.6, Table 3.6.2:



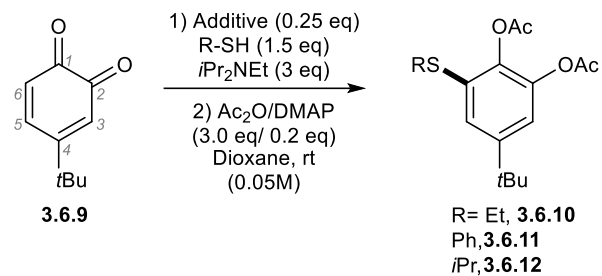
Entry	R	Additive	Yield		
			C6-adduct	C3-adduct	3.6.4
1	Et	-	50	-	26
2	Et	TBSCl	54	-	20
3	Et	Ac ₂ O/DMAP	14	23	20
4	Et	MgBr ₂ Et ₂ O	77	-	5
5	Ph	-	44	-	24
6	Ph	TBSCl	12	-	62
7	Ph	Ac ₂ O/DMAP	-	-	14
8	Ph	MgBr ₂ Et ₂ O	57	-	38
9	iPr	-	35	-	32
10	iPr	TBSCl	40	-	26
11	iPr	Ac ₂ O/DMAP	42	16	26
12	iPr	MgBr ₂ Et ₂ O	95	-	-

[a] Performed on a 0.5 mmol scale with quinone **3.6.1** [b] Entries 1, 5, 9 performed according to General Procedure B [b] Entries 2, 6, 10 performed according to General Procedure D. [c] Entries 4, 8, 12 performed according to General Procedure C. [d] Entries 3, 7, and 11 performed according to General Procedure E.

Amounts and Reagents used in Table 3.6.2:

Entry	Base	Solvent	Thiol	Additive	Yield		
					C6-adduct	C3-adduct	3.6.4
1	DIPEA (0.261 mL, 1.5 mmol, 3.0 eq)	Dioxane (10 mL)	EtSH (0.054 mL, 0.75 mmol, 1.5 eq)	-	50	-	26
2	DIPEA (0.261 mL, 1.5 mmol, 3.0 eq)	Dioxane (10 mL)	EtSH (0.054 mL, 0.75 mmol, 1.5 eq)	TBSCl (18.84 mg, 0.125 mmol, 0.25 eq)	54	-	20
3	DIPEA (0.261 mL, 1.5 mmol, 3.0 eq)	Dioxane (10 mL)	EtSH (0.054 mL, 0.75 mmol, 1.5 eq)	Ac ₂ O (0.141 mL, 1.5 mmol, 3.0 eq) DMAP (12.217 mg, 0.1 mmol, 0.2 eq)	14	23	20
4	DIPEA (0.261 mL, 1.5 mmol, 3.0 eq)	Dioxane (10 mL)	EtSH (0.054 mL, 0.75 mmol, 1.5 eq)	MgBr ₂ ·Et ₂ O (32.378 mg, 0.125 mmol, 0.25 eq)	77	-	5
5	DIPEA (0.261 mL, 1.5 mmol, 3.0 eq)	Dioxane (10 mL)	PhSH (0.076 mL, 0.75 mmol, 1.5 eq)	-	44	-	24
6	DIPEA (0.261 mL, 1.5 mmol, 3.0 eq)	Dioxane (10 mL)	PhSH (0.076 mL, 0.75 mmol, 1.5 eq)	TBSCl (18.84 mg, 0.125 mmol, 0.25 eq)	12	-	62
7	DIPEA (0.261 mL, 1.5 mmol, 3.0 eq)	Dioxane (10 mL)	PhSH (0.076 mL, 0.75 mmol, 1.5 eq)	Ac ₂ O (0.141 mL, 1.5 mmol, 3.0 eq) DMAP (12.217 mg, 0.1 mmol, 0.2 eq)	-	-	14
8	DIPEA (0.261 mL, 1.5 mmol, 3.0 eq)	Dioxane (10 mL)	PhSH (0.076 mL, 0.75 mmol, 1.5 eq)	MgBr ₂ ·Et ₂ O (32.378 mg, 0.125 mmol, 0.25 eq)	57	-	38
9	DIPEA (0.261 mL, 1.5 mmol, 3.0 eq)	Dioxane (10 mL)	<i>i</i> PrSH (0.070 mL, 0.75 mmol, 1.5 eq)	-	35	-	32
10	DIPEA (0.261 mL, 1.5 mmol, 3.0 eq)	Dioxane (10 mL)	<i>i</i> PrSH (0.070 mL, 0.75 mmol, 1.5 eq)	TBSCl (18.84 mg, 0.125 mmol, 0.25 eq)	40	-	26
11	DIPEA (0.261 mL, 1.5 mmol, 3.0 eq)	Dioxane (10 mL)	<i>i</i> PrSH (0.070 mL, 0.75 mmol, 1.5 eq)	Ac ₂ O (0.141 mL, 1.5 mmol, 3.0 eq) DMAP (12.217 mg, 0.1 mmol, 0.2 eq)	32	16	26
12	DIPEA (0.261 mL, 1.5 mmol, 3.0 eq)	Dioxane (10 mL)	<i>i</i> PrSH (0.070 mL, 0.75 mmol, 1.5 eq)	MgBr ₂ ·Et ₂ O (32.378 mg, 0.125 mmol, 0.25 eq)	95	-	-

h) 3.6, Table 3.6.3:



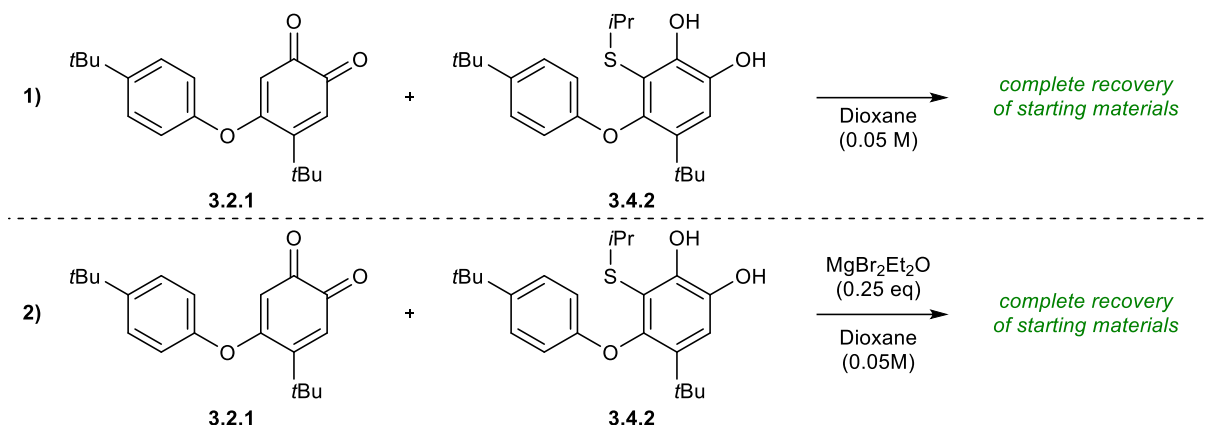
Entry	R	Additive	Yield
1	Et	-	93
2	Et	TBSCl	88
3	Et	Ac ₂ O/DMAP	75
4	Et	MgBr ₂ Et ₂ O	89
5	Ph	-	88
6	Ph	TBSCl	92
7	Ph	Ac ₂ O/DMAP	76
8	Ph	MgBr ₂ Et ₂ O	78
9	<i>i</i> Pr	-	85
10	<i>i</i> Pr	TBSCl	95
11	<i>i</i> Pr	Ac ₂ O/DMAP	75
12	<i>i</i> Pr	MgBr ₂ Et ₂ O	77

[a] Performed on a 0.5 mmol scale with quinone **3.6.9**. [b] Entries 1, 5, 9 performed according to General Procedure B [b]Entries 2, 6, 10 performed according to General Procedure D. [c] Entries 4, 8, 12 performed according to General Procedure C [d] Entries 3, 7, and 11 performed according to General Procedure E.

Amounts and Reagents Used in Table 3.6.3:

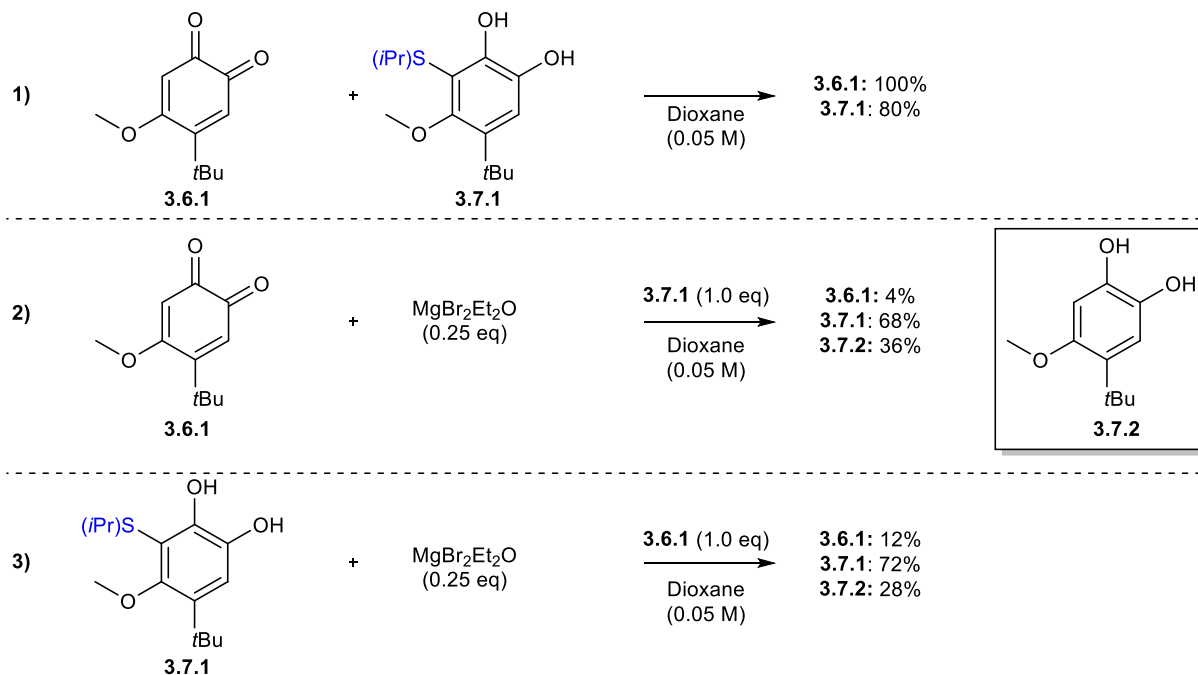
Entry	Base	Solvent	Thiol	Additive	Yield
1	DIPEA (0.261 mL, 1.5 mmol, 3.0 eq)	Dioxane (10 mL)	EtSH (0.054 mL, 0.75 mmol, 1.5 eq)	-	93
2	DIPEA (0.261 mL, 1.5 mmol, 3.0 eq)	Dioxane (10 mL)	EtSH (0.054 mL, 0.75 mmol, 1.5 eq)	TBSCl (18.84 mg, 0.125 mmol, 0.25 eq)	88
3	DIPEA (0.261 mL, 1.5 mmol, 3.0 eq)	Dioxane (10 mL)	EtSH (0.054 mL, 0.75 mmol, 1.5 eq)	Ac ₂ O (0.141 mL, 1.5 mmol, 3.0 eq) DMAP (12.217 mg, 0.1 mmol, 0.2 eq)	75
4	DIPEA (0.261 mL, 1.5 mmol, 3.0 eq)	Dioxane (10 mL)	EtSH (0.054 mL, 0.75 mmol, 1.5 eq)	MgBr ₂ ·Et ₂ O (32.378 mg, 0.125 mmol, 0.25 eq)	89
5	DIPEA (0.261 mL, 1.5 mmol, 3.0 eq)	Dioxane (10 mL)	PhSH (0.076 mL, 0.75 mmol, 1.5 eq)	-	88
6	DIPEA (0.261 mL, 1.5 mmol, 3.0 eq)	Dioxane (10 mL)	PhSH (0.076 mL, 0.75 mmol, 1.5 eq)	TBSCl (18.84 mg, 0.125 mmol, 0.25 eq)	92
7	DIPEA (0.261 mL, 1.5 mmol, 3.0 eq)	Dioxane (10 mL)	PhSH (0.076 mL, 0.75 mmol, 1.5 eq)	Ac ₂ O (0.141 mL, 1.5 mmol, 3.0 eq) DMAP (12.217 mg, 0.1 mmol, 0.2 eq)	76
8	DIPEA (0.261 mL, 1.5 mmol, 3.0 eq)	Dioxane (10 mL)	PhSH (0.076 mL, 0.75 mmol, 1.5 eq)	MgBr ₂ ·Et ₂ O (32.378 mg, 0.125 mmol, 0.25 eq)	78
9	DIPEA (0.261 mL, 1.5 mmol, 3.0 eq)	Dioxane (10 mL)	<i>i</i> PrSH (0.070 mL, 0.75 mmol, 1.5 eq)	-	85
10	DIPEA (0.261 mL, 1.5 mmol, 3.0 eq)	Dioxane (10 mL)	<i>i</i> PrSH (0.070 mL, 0.75 mmol, 1.5 eq)	TBSCl (18.84 mg, 0.125 mmol, 0.25 eq)	95
11	DIPEA (0.261 mL, 1.5 mmol, 3.0 eq)	Dioxane (10 mL)	<i>i</i> PrSH (0.070 mL, 0.75 mmol, 1.5 eq)	Ac ₂ O (0.141 mL, 1.5 mmol, 3.0 eq) DMAP (12.217 mg, 0.1 mmol, 0.2 eq)	75
12	DIPEA (0.261 mL, 1.5 mmol, 3.0 eq)	Dioxane (10 mL)	<i>i</i> PrSH (0.070 mL, 0.75 mmol, 1.5 eq)	MgBr ₂ ·Et ₂ O (32.378 mg, 0.125 mmol, 0.25 eq)	77

i) 3.7, Scheme 3.7.1:



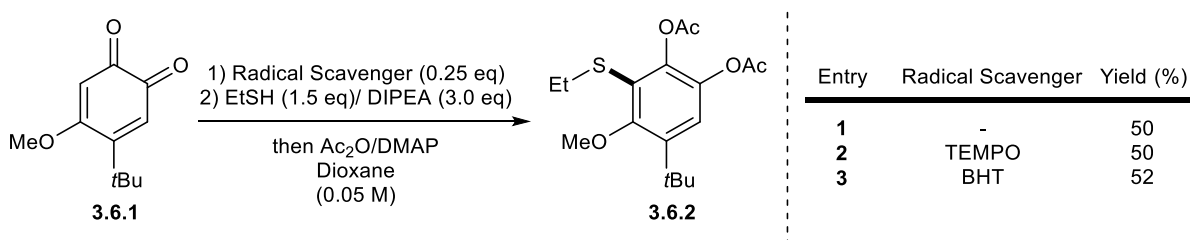
[a] Performed on a 0.5 mmol scale with quinone **3.2.1**.

j) 3.7, Scheme 3.7.2:



[a] Performed on a 0.5 mmol scale with quinone **3.6.1**.

k) 3.8, Table 3.8.1:



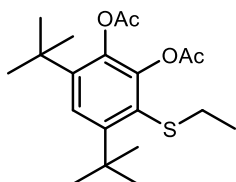
[a] Performed on a 0.5 mmol scale with quinone **3.6.1**. [b] Entry 1 performed according to General Procedure B [c] Entries 2 & 3 performed according to procedure outlined in 3f.

Amounts and Reagents used in Table 3.8.1:

Entry	Base	Solvent	Thiol	Radical Scavenger	Yield
1	DIPEA (0.261 mL, 1.5 mmol, 3.0 eq)	Dioxane (10 mL)	EtSH (0.054 mL, 0.75 mmol, 1.5 eq)	-	50
2	DIPEA (0.261 mL, 1.5 mmol, 3.0 eq)	Dioxane (10 mL)	EtSH (0.054 mL, 0.75 mmol, 1.5 eq)	TEMPO (19.531 mg, 0.125 mmol, 0.25 eq)	50
3	DIPEA (0.261 mL, 1.5 mmol, 3.0 eq)	Dioxane (10 mL)	EtSH (0.054 mL, 0.75 mmol, 1.5 eq)	BHT (27.543 mg, 0.125 mmol, 0.25 eq)	52

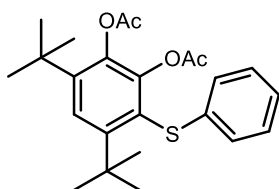
6. Synthesis and Characterization of Compounds

a) Substrates in Table 3.3.1:



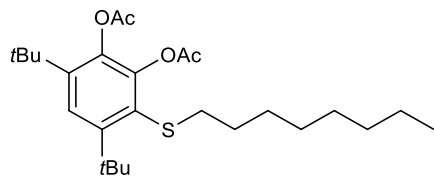
3.2.4: Synthesized according to general procedure A. Purified with silica column chromatography (5:1 Hexanes: EtOAc), 99% yield.

Rf: 0.3 (5:1 Hexanes: EtOAc). **¹H-NMR:** (400 MHz, CDCl₃): 7.39 (s, 1H), 2.83 (q, *J*= 7.4 Hz, 2H), 2.31 (s, 6H), 1.54 (s, 9H), 1.35 (s, 9H), 1.25 (t, *J*= 7.4 Hz, 3H). **¹³C-NMR:** (125 MHz, CDCl₃): 168.4, 167.9, 150.6, 146.7, 141.6, 127.0, 122.7, 37.6, 35.2, 31.1, 30.2, 20.78, 14.20. **IR:** (neat) ν = 2961.9, 1777.8, 1440.1, 1393.7, 1367.1, 1230.1, 1197.3, 1142.9, 1011.4, 968.3 cm⁻¹. **HRMS (m/z):** Calc for C₂₀H₃₀NaO₄S: [M+Na]⁺: 389.18, found 389.1759.



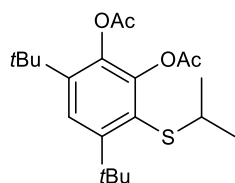
3.2.5: Synthesized according to general procedure A, 99% yield.

Rf: 0.5 (5:1 Hexanes: EtOAc). **¹H-NMR:** (400 MHz, CDCl₃): 7.51 (s, 1H), 7.20 (t, *J*=7.6 Hz, 2H), 7.08 (t, *J*=7.3 Hz, 1H), 6.99 (d, *J*=7.3 Hz, 2H), 2.24 (s, 3H), 1.99 (s, 3H), 1.51 (s, 9H), 1.38 (s, 9H). **¹³C-NMR:** (125 MHz): 168.2, 167.9, 151.6, 146.9, 143.3, 140.8, 138.0, 129.1, 128.8, 127.2, 125.6, 125.0, 123.1, 122.9, 37.6, 31.1, 30.23, 20.90, 20.24. **HRMS (m/z):** Calc for C₂₄H₃₀NaO₄S, [M+Na]⁺: 438.18, found 437.1770.



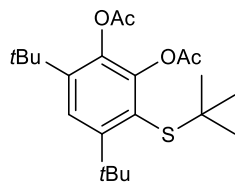
3.2.6: Synthesized according to general procedure A. Purified with silica column chromatography (5:1 Hexanes: EtOAc), 85% yield.

R_f: 0.5 (5:1 Hexanes: EtOAc). **¹H-NMR:** (500 MHz, CDCl₃): 7.39 (s, 1H), 2.81 (broad t, 2H), 2.31 (s, 6H), 1.63 (m, 2H), 1.54 (s, 9H), 1.42-1.29 (m, 10H), 1.35 (s, 9H), 0.90 (t, J=7.2 Hz, 3H). **¹³C-NMR:** (125 MHz, CDCl₃): 168.3, 167.8, 150.5, 146.7, 141.6, 140.2, 127.7, 122.6, 37.6, 37.1, 35.2, 31.8, 31.1, 30.2, 29.3, 29.2, 29.1, 29.1, 22.6, 21.0, 20.7, 14.1. **IR:** (neat) ν= 2956.2, 2925.0, 2855.0, 1777.4, 1392.5, 1198.6, 1142.2 cm⁻¹. **HRMS (m/z):** Calc for C₂₆H₄₂NaO₄S: [M+Na]⁺: 473.27 found 473.2707.



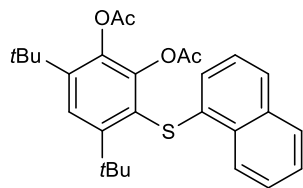
3.2.7: Synthesized according to general procedure A. Purified with silica column chromatography (5:1 Hexanes: EtOAc), 96% yield.

R_f: 0.4 (5:1 Hexanes: EtOAc). **¹H-NMR:** (400 MHz, CDCl₃): 7.37 (s, 1H), 3.51 (sep, J = 6.5 Hz, 1H), 2.29 (s, 3H), 2.27 (s, 3H), 1.51 (s, 9H), 1.33 (s, 9H), 1.22 (d, J = 6.4 Hz 3H). **¹³C-NMR:** (125 MHz, CDCl₃): 168.4, 167.6, 150.7, 146.3, 141.3, 140.0, 126.5, 122.6, 39.7, 37.6, 35.2, 31.4, 30.2, 23.2, 21.0, 20.8. **IR:** (neat) ν= 2961.3, 1766.4, 1364.6, 1189.2, 1144.3 cm⁻¹. **HRMS (m/z):** Calc. for C₂₁H₃₂NaO₄S: [M+Na]⁺: 403.1914, found 403.1915.



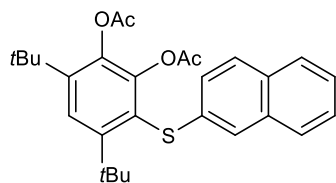
3.2.8: Synthesized according to general procedure A. Purified with silica column chromatography (5:1 Hexanes: EtOAc), 85% yield.

R_f: 0.4 (5:1 Hexanes: EtOAc). **¹H-NMR:** (400 MHz, CDCl₃): 7.38 (s, 1H), 2.29 (s, 3H), 2.26 (s, 3H), 1.52 (s, 9H), 1.33 (s, 9H), 1.33 (s, 9H). **¹³C-NMR:** (125 MHz, CDCl₃): 168.3, 167.6, 151.8, 147.0, 141.9, 139.8, 126.1, 122.7, 49.6, 37.8, 32.3, 31.9, 30.2, 21.2, 21.0. **IR:** (neat) ν= 2958.8, 1775.7, 1365.0, 1194.4, 1139.2 cm⁻¹. **LRMS (EI-QMS) (m/z):** Calc for C₂₂H₃₄O₄S: 394.22, found 394.2



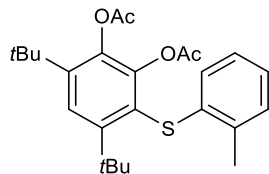
3.2.9: Synthesized according to general procedure A. Purified with silica column chromatography (5:1 Hexanes: EtOAc), 95% yield.

Rf: 0.5 (5:1 Hexanes: EtOAc). **¹H-NMR:** (500 MHz, CDCl₃): 8.40 (d, *J*=8.5 Hz, 1H), 7.87 (d, *J*=8.5 Hz, 1H), 7.64-7.51 (m, 5H), 7.60 (s, 1H), 2.24 (s, 3H), 1.59 (s, 9H), 1.44 (s, 9H). **¹³C-NMR** (125 MHz, CDCl₃): 168.1, 167.9, 152.0, 146.8, 143.5, 141.0, 135.0, 133.6, 131.0, 130.5, 128.7, 127.3, 126.5, 126.2, 126.0, 125.7, 125.3, 123.8, 123.3, 37.7, 35.5, 31.2, 30.3, 20.9, 20.2. **IR:** (neat) ν = 3054.1, 2961.0, 2870.3, 1777.5, 1761.2, 1368.0, 1195.7, 1186.3, 1143.3, 791.1, 770.8 cm⁻¹. **LRMS (EI-QMS) m/z:** Calc for C₂₈H₃₂O₄S 464.20, found 422.3.



3.2.10: Synthesized according to general procedure A. Purified with silica column chromatography (5:1 Hexanes: EtOAc), 96% yield.

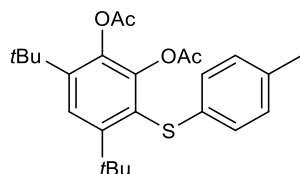
Rf: 0.5 (5:1 Hexanes: EtOAc). **¹H-NMR:** (500 MHz, CDCl₃): 7.78 (d, *J*=7.9 Hz, 1H), 7.74 (d, *J*=8.5 Hz, 1H), 7.72 (d, *J*=7.5 Hz, 1H), 7.60 (s, 1H), 7.43 (ddd, *J*=6.9,6.9,1.3 Hz, 1H), 7.39 (ddd, *J*=6.8,6.6,1.3 Hz, 1H), 7.35 (d, *J*=1.7 Hz, 1H), 7.17 (dd, *J*=8.6,1.9 Hz, 1H), 2.27 (s, 3H), 1.99 (s, 3H), 1.58 (s, 9H), 1.46 (s, 9H). **¹³C-NMR** (125 MHz, CDCl₃): 168.1, 168.0, 151.6, 147.1, 143.5, 140.8, 135.5, 133.9, 131.3, 128.3, 127.7, 127.2, 126.4, 125.1, 124.2, 123.3, 123.0, 122.6, 37.6, 35.5, 31.1, 30.3, 20.9, 20.4. **IR:** (neat) ν = 3058.5, 2968.4, 2871.5, 1774.1, 1765.4, 1741.1, 1366.2, 1190.5, 1143.7 cm⁻¹. **HRMS m/z:** Calc for C₂₈H₃₂O₄S: [M+Na]⁺: 487.19, found 487.1914.



3.2.11: Synthesized according to general procedure A. Purified with silica column chromatography (9:1 Hexanes: EtOAc), 95% yield.

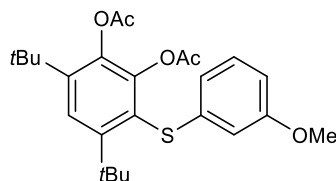
Rf: 0.3 (9:1 Hexanes: EtOAc). **¹H-NMR:** (500 MHz, CDCl₃): 7.56 (s, 1H), 7.13 (d, *J*=7.2 Hz, 1H), 7.06 (dd, *J*=7.9,6.3 Hz, 1H), 7.03 (dd, *J*=7.8,7.0 Hz, 1H), 6.60 (d, *J*=7.5 Hz, 1H), 2.45 (s, 3H), 2.27 (s, 3H), 1.99 (s, 3H), 1.55 (s, 9H), 1.43 (s, 9H). **¹³C-NMR:** (125 MHz): 168.1, 167.8,

151.8, 146.8, 143.3, 140.8, 137.1, 133.6, 129.5, 126.7, 125.4, 124.7, 123.2, 122.9, 37.6, 35.4, 31.1, 30.3, 20.9, 20.2, 20.1. **IR:** (neat) ν = 2960.9, 1767.8, 1366.6, 1187.3, 1140.7, 1012.4, 743.3 cm^{-1} **HRMS (m/z):** Calc for $\text{C}_{25}\text{H}_{32}\text{NaO}_4\text{S}$ $[\text{M}+\text{Na}]^+$: 451.19, found 451.1935



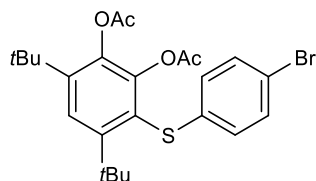
3.2.12: Synthesized according to general procedure A. Purified with silica column chromatography (9:1 Hexanes: EtOAc), 95% yield.

R_f: 0.3 (9:1 Hexanes: EtOAc). **¹H-NMR:** (500 MHz, CDCl_3): 7.52 (s, 1H), 7.04 (d, J =8.1 Hz, 2H), 6.91 (d, J =8.1 Hz, 2H), 2.29 (s, 3H), 2.27 (s, 3H), 2.03 (s, 3H), 1.54 (s, 9H), 1.41 (s, 9H). **¹³C-NMR:** (125 MHz): 168.1, 167.9, 151.5, 146.9, 143.1, 140.7, 134.6, 134.5, 129.6, 125.6, 123.3, 123.0, 37.6, 35.4, 31.1, 30.3, 21.0, 20.3. **IR:** (neat) ν = 2969.1, 1771.8, 1752.3, 1737.2, 1363.8, 1199.6, 1145.5, 803.8 cm^{-1} **HRMS (m/z):** Calc. for $\text{C}_{25}\text{H}_{32}\text{NaO}_4\text{S}$: $[\text{M}+\text{Na}]^+$: 451.1914, found 451.1911.



3.2.13: Synthesized according to general procedure A. Purified with silica column chromatography (9:1 Hexanes: EtOAc), 98% yield.

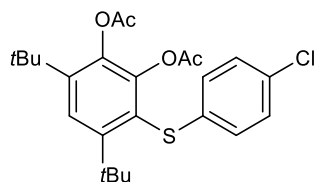
R_f: 0.3 (9:1 Hexanes: EtOAc). **¹H-NMR:** (500 MHz, CDCl_3): 7.53 (s, 1H), 7.14 (dd, J =8.1, 8.1 Hz, 1H), 6.66 (d, J =8.4 Hz, 1H), 6.64 (d, J =8.5 Hz, 1H), 6.51 (s, 1H), 3.73 (s, 3H), 2.27 (s, 3H), 2.05 (s, 3H), 1.54 (s, 9H), 1.41 (s, 9H). **¹³C-NMR:** (125 MHz): 168.0, 159.9, 151.6, 146.9, 143.4, 140.7, 139.4, 129.5, 123.0, 122.7, 118.0, 111.2, 110.6, 55.1, 37.6, 35.4, 31.1, 30.2, 20.9, 20.3. **IR:** (neat) ν = 2967.6, 1763.7, 1430.2, 1368.0, 1230.1, 1198.9, 1143.2, 1047.1, 1012.6, 873.5, 772.7 cm^{-1} **LRMS (EI-QMS) m/z:** Calc for $\text{C}_{25}\text{H}_{32}\text{O}_5\text{S}$: 444.20, found 444.3.



3.2.14: Synthesized according to general procedure A. Purified with silica column chromatography (9:1 Hexanes: EtOAc), 90% yield.

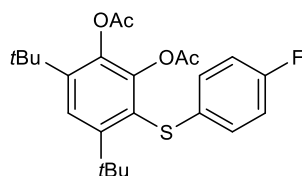
R_f: 0.5 (9:1 Hexanes: EtOAc). **¹H-NMR:** (500 MHz, CDCl_3): 7.53 (s, 1H), 7.34 (d, J =8.5 Hz, 2H), 6.86 (d, J =8.5 Hz, 2H), 2.28 (s, 1H), 2.05 (s, 1H), 1.51 (s, 9H), 1.40 (s, 9H). **¹³C-NMR:** (125

MHz): 168.1, 167.8, 151.6, 146.8, 143.8, 140.8, 137.4, 131.8, 126.9, 123.3, 122.1, 118.5, 37.5, 35.4, 31.1, 30.2, 20.9, 20.3. **IR:** (neat) ν = 2962.4, 2871.3, 1775.7, 1366.6, 1198.4, 1144.6, 731.3 cm^{-1} . **LRMS (EI-QMS) (m/z):** Calc for $\text{C}_{24}\text{H}_{29}\text{BrO}_4\text{S}$: 492.10, found 492.3.



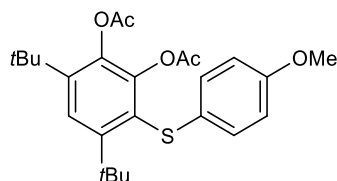
3.2.15: Synthesized according to general procedure A. Purified with silica column chromatography (9:1 Hexanes: EtOAc), 84% yield.

R_f: 0.5 (9:1 Hexanes: EtOAc). **¹H-NMR:** (500 MHz, CDCl_3): 7.53 (s, 1H), 7.20 (d, J =8.8 Hz, 2H), 6.92 (d, J =8.7 Hz, 2H), 2.28 (s, 3H), 2.05 (s, 3H), 1.52 (s, 9H), 1.40 (s, 9H). **¹³C-NMR:** (125 MHz): 168.1, 167.8, 151.6, 146.8, 143.7, 136.7, 130.6, 128.9, 126.6, 123.3, 122.3, 121.4, 118.4, 37.5, 35.4, 31.2, 20.9, 20.3. **IR:** (neat) ν = 2967.0, 1776.3, 1765.2, 1365.6, 1195.3, 1144.3, 1009.5, 731.0 cm^{-1} . **HRMS (ESI-MS) (m/z):** Calc. for $\text{C}_{24}\text{H}_{29}\text{ClNaO}_4\text{S}$: 471.1367, found 471.1374.



3.2.16: Synthesized according to general procedure A. Purified with silica column chromatography (9:1 Hexanes: EtOAc), 88% yield.

R_f: 0.5 (9:1 Hexanes: EtOAc). **¹H-NMR:** (500 MHz, CDCl_3): 7.53 (s, 1H), 6.97 (d, J =6.9 Hz, 2H), 6.96 (d, J =9.8 Hz, 2H), 2.28 (s, 3H), 2.05 (s, 3H), 1.54 (s, 9H), 1.41 (s, 9H). **¹³C-NMR:** (125 MHz): 168.1, 167.7, 161.8, 159.8, 151.5, 146.8, 143.5, 140.8, 133.1, 127.2, 127.1, 123.2, 123.1, 116.0, 115.8, 37.5, 35.4, 31.1, 30.2, 20.9, 20.3. **IR:** (neat) ν = 2974.0, 1774.7, 1489.3, 1366.7, 1189.2, 1142.8, 1011.7, 908.1, 821.63, 729.2 cm^{-1} . **LRMS (EI-QMS) m/z:** Calc for $\text{C}_{24}\text{H}_{29}\text{FO}_4\text{S}$: 432.18, found 432.3.

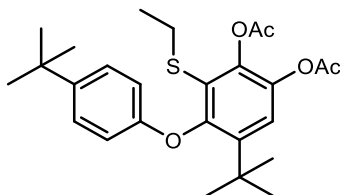


3.2.17: Synthesized according to general procedure A. Purified with silica column chromatography (9:1 Hexanes: EtOAc), 76% yield.

R_f: 0.2 (9:1 Hexanes: EtOAc). **¹H-NMR:** (500 MHz, CDCl_3): 7.51 (s, 1H), 6.96 (d, J =9.0 Hz, 2H), 6.80 (d, J =8.9 Hz, 2H), 3.76 (s, 3H), 2.26 (s, 3H), 2.04 (s, 3H), 1.54 (s, 9H), 1.39 (s,

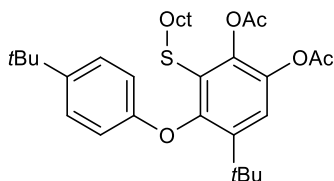
9H). **¹³C-NMR**: (125 MHz): 168.1, 167.8, 157.5, 151.3, 146.8, 143.0, 140.7, 128.9, 127.2, 123.9, 123.0, 114.6, 60.4, 55.2, 37.6, 35.3, 31.1, 30.2, 20.9, 20.3, 14.2. **IR**: (neat) ν = 2959.7, 1772.8, 1493.8, 1364.3, 1199.5, 1146.1, 872.1, 821.0 cm^{-1} **LRMS (EI-QMS) (m/z)**: Calc. for $\text{C}_{25}\text{H}_{32}\text{O}_5\text{S}$: 444.20, found 444.4

b) Substrates in Table 3.3.2:



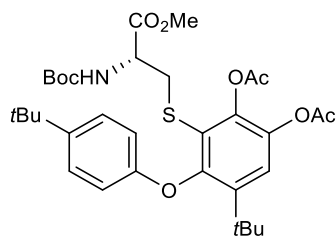
3.3.3: Synthesized according to general procedure A. Purified with silica column chromatography (5:1 Hexanes: EtOAc), 87% yield.

Rf: 0.5 (5:1 Hexanes: EtOAc). **¹H-NMR**: (500 MHz, CDCl_3): 7.25 (s, 1H), 7.23 (d, J = 9.1 Hz, 2H), 6.66 (d, J = 9.1 Hz, 2H), 2.68 (q, J = 7.4 Hz, 2H), 2.31 (s, 6H), 1.33 (s, 9H), 1.29 (s, 9H), 1.03 (t, J = 7.4 Hz, 3 H) **¹³C-NMR**: (125 MHz, CDCl_3): 168.4, 167.9, 156.0, 152.7, 144.1, 143.1, 142.4, 139.2, 126.1, 125.5, 121.8, 114.7, 35.3, 34.1, 31.5, 30.5, 28.9, 20.7, 20.5, 14.6. **IR**: (neat) ν =2961.5, 2869.8, 1774.1, 1507.8, 1367.4, 1198.6, 1159.6 cm^{-1} **HRMS (m/z)**: Calc for $\text{C}_{26}\text{H}_{34}\text{NaO}_5\text{S}$ $[\text{M}+\text{Na}]^+$: 481.2019, found 481.2027.



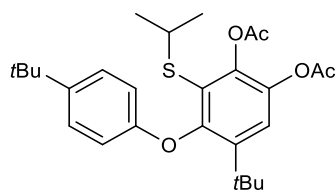
3.3.4: Synthesized according to general procedure A. Purified with silica column chromatography (5:1 Hexanes: EtOAc), 85% yield.

Rf: 0.5 (5:1 Hexanes: EtOAc). **¹H-NMR**: (500 MHz, CDCl_3): 7.26 (d, J =8.9 Hz, 2H), 7.24 (s, 1H), 6.67 (d, J =8.9 Hz, 2H), 2.65 (t, J =7.2 Hz, 2H), 2.33 (s, 3H), 2.32 (s, 3H), 1.34 (s, 9H), 1.31 (s, 9H), 1.28-1.24 (m, 12H), 0.90 (t, J =6.9 Hz, 3H). **¹³C-NMR**: (125 MHz): 168.4, 167.9, 156.0, 152.8, 144.1, 143.1, 142.3, 139.1, 126.0, 125.8, 121.7, 114.7, 35.3, 34.9, 34.1, 31.8, 31.6, 30.5, 29.4, 29.2, 29.1, 28.6, 22.7, 20.7, 20.6, 14.1. **IR**: (neat) ν = 2957.6, 2927.0, 1773.7, 1507.8, 1439.8, 1366.7, 1195.6, 1158.6, 1011.7, 941.2, 890.4, 827.4, cm^{-1} . **HRMS (m/z)**: Calc for $\text{C}_{32}\text{H}_{46}\text{KO}_5\text{S}$: $[\text{M}+\text{K}]^+$: 581.2698, found 581.2718



3.3.5: Synthesized according to general procedure A. Purified with silica column chromatography (5:1 Hexanes: EtOAc), 85% yield.

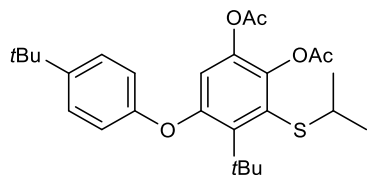
¹H-NMR: (500 MHz, CDCl₃): 7.28 (s, 1H), 7.25 (d, *J*=8.9 Hz, 2H), 6.67 (d, *J*= 8.4 Hz, 2H), 5.43 (d, *J*=8.0 Hz, 1H), 4.39 (ddd, *J*=7.9, 4.7, 4.5, Hz, 1H), 3.36 (s, 3H), 3.22 (dd, *J*=13.5, 4.8 Hz, 1H), 3.10 (dd, *J*=13.5, 4.6 Hz, 1H), 2.35 (s, 3H), 2.32 (s, 3H), 1.45 (s, 9H), 1.34 (s, 9H), 1.30 (s, 9H). **¹³C-NMR:** (125 MHz): 170.7, 168.2, 167.9, 159.1, 155.1, 144.4, 143.2, 142.7, 139.4, 126.3, 124.3, 122.9, 114.6, 79.9, 53.2, 52.4, 36.8, 35.4, 34.1, 31.5, 30.5, 28.3, 20.7, 20.5. **IR:** (neat) ν = 2962.2, 1773.4, 1774.2, 1506.8, 1366.0, 1195.8, 1157.1, 1011.4, 828.1, 730.2 cm⁻¹. **HRMS (m/z):** Calc. for C₃₃H₄₅NNaO₉S: [M+Na]⁺: 654.2707, found 654.2725.



3.3.6: Synthesized according to general procedure A. Purified with silica column chromatography (5:1 Hexanes: EtOAc), 58% yield.

Also synthesized according to general procedure C, 90% yield.

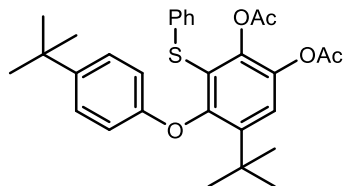
¹H-NMR: (500 MHz, CDCl₃): 7.26 (d, *J*= 9.1 Hz, 2H), 7.24 (s, 1H), 6.65 (d, *J*= 9.1 Hz, 2H), 3.31 (sep, *J*= 6.7 Hz, 1H), 2.32 (s, 6H), 1.34 (s, 9H), 1.31 (s, 9H), 1.11 (d, *J*= 6.7 Hz, 6H). **¹³C-NMR:** (125 MHz): 168.4, 167.9, 156.0, 153.0, 144.0, 143.3, 142.3, 139.2, 126.7, 126.1, 121.9, 118.6, 114.7, 38.9, 35.3, 34.8, 34.1, 33.0, 31.6, 31.5, 30.5, 29.9. **IR:** (neat) ν = 2961.5, 1769.8, 1366.0, 1197.7, 1159.2, 730.6 cm⁻¹. **HRMS (m/z):** Calc. for C₂₇H₃₆NaO₅S: [M+Na]⁺: 495.2176, found 495.2179.



3.4.3: Synthesized according to General Procedure E. Purified with silica column chromatography, (5% DCM in Toluene), 83% yield

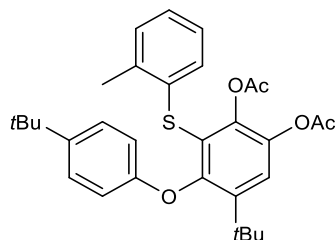
¹H-NMR: (500 MHz, CDCl₃): 7.35 (d, *J*= 8.8 Hz, 2H), 6.86 (d, *J*=8.8 Hz, 2H), 6.76 (s, 1H), 3.48 (hep, *J*= 6.7 Hz, 1H), 2.34 (s, 3H), 2.23 (s, 3H), 1.65 (s, 9H), 1.34 (s, 9H), 1.25 (d, *J*=6.7

Hz, 6H). **¹³C-NMR**: (125 MHz): 168.0, 167.9, 155.4, 153.1, 145.4, 143.4, 141.2, 141.0, 131.7, 126.6, 117.3, 116.6, 40.6, 38.9, 34.3, 33.0, 31.5, 23.1, 20.8, 20.6.



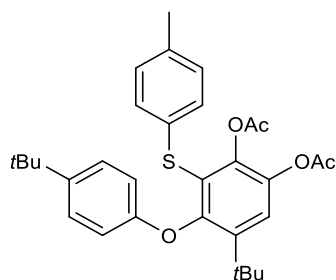
3.3.7: Synthesized according to general procedure A. Purified with silica column chromatography (5:1 Hexanes: EtOAc), 93% yield.

R_f: 0.52 (5:1 Hexanes: EtOAc). **¹H-NMR**: (500 MHz, CDCl₃): 7.36 (s, 1H), 7.21-7.11 (m, 5H), 7.01 (d, 2H), 6.58 (d, 2H), 2.30 (s, 3H), 2.12 (s, 3H), 1.35 (s, 9H), 1.30 (s, 9H). **¹³C-NMR**: (125 MHz, CDCl₃): 168.3, 167.7, 156.2, 152.6, 144.2, 143.1, 142.8, 139.4, 135.9, 128.6, 128.0, 126.0, 125.9, 123.8, 122.8, 115.0, 35.4, 34.1, 31.5, 30.5, 20.7, 20.2. **IR** (neat) ν = 2960.9, 1772.2, 1507.3, 1366.3, 1194.2, 1158.4, 1011.6, 941.3, 828.1, 735.8 cm⁻¹. **HRMS (m/z)**: Calc. for C₃₀H₃₄NaO₅S [M+Na]⁺: 529.2019, found 529.2031.



3.3.8: Synthesized according to general procedure A. Purified with silica column chromatography (9:1 Hexanes: EtOAc), 90% yield.

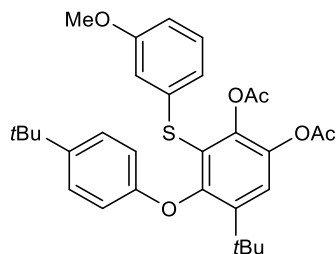
R_f: 0.3 (9:1 Hexanes: EtOAc). **¹H-NMR**: (500 MHz, CDCl₃): 7.34 (s, 1H), 7.16 (d, *J*=8.7 Hz, 2H), 7.05-7.01 (m, 3H), 6.88 (d, *J*=7.5 Hz, 1H), 6.48 (d, *J*=8.9 Hz, 2H), 2.32 (s, 3H), 2.15 (s, 3H), 1.98 (s, 3H), 1.35 (s, 9H), 1.29 (s, 9H). **¹³C-NMR**: (125 MHz): 168.3, 167.7, 155.5, 152.2, 144.2, 143.0, 142.8, 139.3, 136.3, 134.5, 129.9, 127.9, 126.1, 125.8, 123.2, 122.4, 115.1, 35.4, 34.1, 31.5, 30.4, 20.7, 20.2, 19.9. **IR**: (neat) ν = 2966.9, 1763.5, 1440.0, 1368.5, 1228.6, 1198.6, 1160.2, 1060.1, 1012.3, 948.4, 905.2, 882.0, 826.9, 746.6 cm⁻¹. **HRMS (m/z)**: Calc for C₃₁H₃₆NaO₅S: [M+Na]⁺: 543.22, found 543.2197.



3.3.9: Synthesized according to general procedure A. Purified with silica column chromatography (9:1 Hexanes: EtOAc), 89% yield.

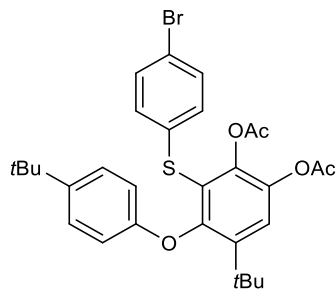
R_f: 0.2 (9:1 Hexanes: EtOAc). **¹H-NMR:** (500 MHz, CDCl₃): 7.35 (s, 1H), 7.22 (d, *J*=8.9 Hz, 2H), 6.99 (d, *J*=8.2 Hz, 2H), 6.93 (d, *J*=8.2 Hz, 2H), 6.59 (d, *J*=8.9 Hz, 2H), 2.32 (s, 6H), 2.15 (s, 3H), 1.36 (s, 9H), 1.31 (s, 9H). **¹³C-NMR:** (125 MHz): 168.3, 167.7, 156.3, 152.5, 144.2, 142.7, 139.5, 135.8, 132.2, 129.4, 128.4, 126.0, 124.4, 122.6, 115.0, 35.4, 34.1, 31.5, 30.5, 21.0, 20.3. **IR:** (neat) ν = 2960.9, 1772.9, 1507.4, 1441.1, 1366.6, 1194.2, 1157.5, 1012.0, 941.2, 828.1, 736.0, 551.6 cm⁻¹

HRMS: Calc for C₃₁H₃₆NaO₅S: [M+Na]⁺: 543.2176, found 543.2183.



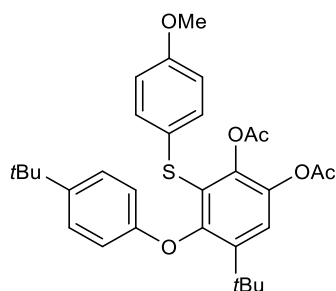
3.3.10: Synthesized according to general procedure A. Purified with silica column chromatography (9:1 Hexanes: EtOAc), 91% yield.

R_f: 0.2 (9:1 Hexanes: EtOAc). **¹H-NMR:** (500 MHz, CDCl₃): 7.35 (s, 1H), 7.20 (d, *J*=8.9 Hz, 2H), 7.07 (dd, *J*=8.1, 7.8 Hz, 1H), 6.67 (dd, *J*=8.2, 2.0 Hz, 1H), 6.59 (m, 3H), 6.53 (d, *J*=2.1 Hz, 1H), 3.71 (s, 3H), 2.32 (s, 3H), 2.14 (s, 3H), 1.35 (s, 9H), 1.29 (s, 9H). **¹³C-NMR:** (125 MHz): 168.3, 167.7, 159.6, 156.2, 152.7, 144.2, 143.2, 142.8, 139.5, 137.1, 129.3, 126.0, 123.6, 122.9, 120.3, 115.0, 112.8, 112.3, 55.1, 35.5, 34.1, 31.5, 30.5, 20.7, 20.2. **IR:** (neat) ν = 2960.8, 1767.1, 1589.5, 1439.9, 1365.5, 1245.5, 1228.6, 1194.8, 1156.8, 1060.4, 1039.1, 1011.5, 941.8, 857.1, 827.2, 774.2 cm⁻¹. **HRMS (m/z):** Calc for C₃₁H₃₆NaO₆S: [M+Na]⁺: 559.2125, found 559.2152.



3.3.11: Synthesized according to general procedure A. Purified with silica column chromatography (5:1 Hexanes: EtOAc), 82% yield.

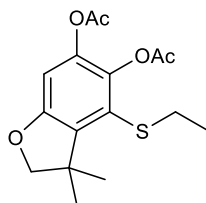
R_f: 0.3 (5:1 Hexanes: EtOAc). **¹H-NMR:** (500 MHz, CDCl₃): 7.36 (s, 1H), 7.27 (d, *J*=8.5 Hz, 2H), 7.17 (d, *J*=9.0 Hz, 2H), 6.83 (d, *J*=8.5 Hz, 2H), 6.53 (d, *J*=8.87 Hz, 2H), 2.33 (s, 3H), 2.17 (s, 3H), 1.33 (s, 9H), 1.29 (s, 9H). **¹³C-NMR:** (125 MHz): 168.3, 167.7, 156.0, 152.7, 144.4, 143.2, 143.1, 139.5, 135.1, 131.5, 129.3, 126.0, 123.2, 123.0, 119.5, 115.0, 35.5, 34.1, 31.5, 30.4, 20.7, 20.3. **IR:** (neat) ν = 2961.2, 1770.2, 1507.1, 1472.3, 1440.9, 1366.1, 1194.5, 1157.6, 1059.7, 1007.1, 940.6, 894.2, 827.5, 810.5, 735.9 cm⁻¹. **HRMS (m/z):** Calc for C₃₀H₃₃BrNaO₅S: [M+Na]⁺: 607.1124, found 607.1120.



3.3.12: Synthesized according to general procedure A. Purified with silica column chromatography (9:1 Hexanes: EtOAc), 85% yield.

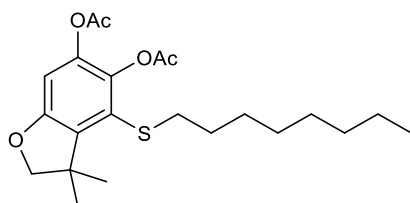
R_f: 0.2 (9:1 Hexanes: EtOAc). **¹H-NMR:** (500 MHz, CDCl₃): 7.30 (s, 1H), 7.23 (d, *J*=8.9 Hz, 2H), 7.02 (d, *J*=8.9 Hz, 2H), 6.74 (d, *J*=8.9 Hz, 2H), 6.59 (d, *J*=8.9 Hz, 2H), 3.77 (s, 3H), 2.31 (s, 3H), 2.18 (s, 3H), 1.33 (s, 9H), 1.31 (s, 9H). **¹³C-NMR:** (125 MHz): 168.3, 167.7, 158.5, 156.2, 152.2, 144.1, 142.8, 142.7, 139.4, 130.9, 126.3, 126.0, 125.3, 122.4, 114.9, 114.3, 55.3, 35.4, 34.7, 34.1, 31.6, 30.9, 30.5, 20.7, 20.3. **IR:** (neat) ν = 2958.0, 1767.6, 1492.7, 1365.7, 1195.4, 1155.2, 1010.4, 823.7 cm⁻¹. **HRMS:** Calc. for C₃₁H₃₆NaO₆S: [M+Na]⁺: 559.2125, found 559.2129.

c) Substrates in Table 3.3.3:



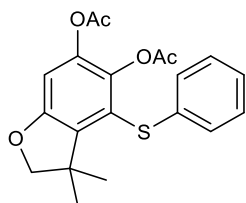
3.3.13: Synthesized according to general procedure A. Purified with silica column chromatography (9:1 Hexanes: EtOAc), 80% yield.

R_f: 0.35 (9:1 Hexanes: EtOAc). **¹H-NMR:** (500 MHz, CDCl₃): 6.63 (s, 1H), 4.25 (s, 2H), 2.87 (q, *J*=7.5 Hz, 2H), 2.34 (s, 3H), 2.28 (s, 3H), 1.54 (s, 6H), 1.27 (t, *J*=7.5 Hz, 3H). **¹³C-NMR:** (125 MHz): 168.3, 168.2, 157.1, 142.5, 138.1, 136.6, 125.6, 105.3, 85.5, 44.4, 30.1, 26.9, 20.7, 20.5, 14.8. **IR:** (neat) ν = 2959.2, 2877.9, 1760.6, 1605.8, 1414.0, 1367.0, 1200.3, 1169.4, 1134.7, 1061.2, 1007.4, 991.3, 925.8, 911.8, 881.4 cm⁻¹. **HRMS (m/z):** Calc for C₁₆H₂₀NaO₅S: [M+Na]⁺: 347.0924, found 347.0924.



3.3.14: Synthesized according to general procedure A. Purified with silica column chromatography (9:1 Hexanes: EtOAc), 85% yield.

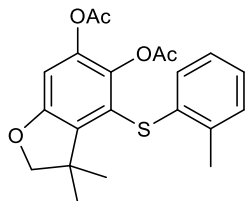
R_f: 0.55 (9:1 Hexanes: EtOAc). **¹H-NMR:** (500 MHz, CDCl₃): 6.62 (s, 1H), 4.24 (s, 2H), 2.83 (t, *J*=7.3 Hz, 2H), 2.33 (s, 6H), 2.27 (s, 6H), 1.62 (tt, *J*=7.5, 7.2 Hz, 2H), 1.53 (s, 6H), 1.28 (m, 10H), 0.90 (t, *J*=7.2 Hz, 3H). **¹³C-NMR:** (125 MHz): 168.4, 168.2, 157.1, 142.5, 138.0, 136.4, 126.2, 105.3, 85.4, 44.4, 36.4, 31.8, 29.8, 29.2, 29.0, 26.8, 22.6, 20.7, 20.5, 14.1. **IR:** (neat) ν = 2926.6, 1773.7, 1588.9, 1367.2, 1197.7, 1166.8, 1136.2, 1062.8, 1009.6, 918.9, 879.0 cm⁻¹. **HRMS (m/z):** Calc for C₂₂H₃₂KO₅S: [M+K]⁺: 447.1602, found 447.1620.



3.3.15: Synthesized according to general procedure A. Purified with silica column chromatography (5:1 Hexanes: EtOAc), 74% yield.

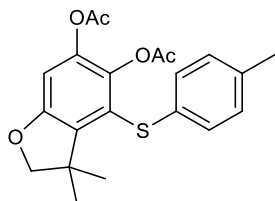
R_f: 0.5 (5:1 Hexanes: EtOAc). **¹H-NMR:** (400 MHz, CDCl₃): 7.25 (dd, *J*=7.8, 7.5 Hz, 2H), 7.15 (t, *J*=7.5, 7.3 Hz, 1H), 7.11 (d, *J*=7.3 Hz, 3H), 6.75 (s, 1H), 4.28 (s, 2H), 2.24 (s, 3H), 2.01 (s,

3H), 1.49 (s, 6H). **¹³C-NMR**: (125 MHz): 168.1, 157.5, 143.1, 137.8, 137.1, 136.7, 129.0, 127.0, 125.7, 122.8, 106.5, 85.6, 85.3, 44.5, 42.1, 27.4, 26.7, 20.7, 20.0. **IR**: (neat) ν = 2968.6, 2925.7, 1777.8, 1763.7, 1201.7, 1164.5, 1132.1, 880.1, 745.6, 690.4 cm^{-1} . **LRMS (EI-QMS) (m/z)**: Calc for $\text{C}_{20}\text{H}_{20}\text{O}_5\text{S}$: 372.10, found 372.2.



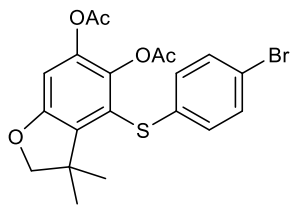
3.3.16: Synthesized according to general procedure A. Purified with silica column chromatography (9:1 Hexanes: EtOAc), 45% yield.

Rf: 0.25 (9:1 Hexanes: EtOAc). **¹H-NMR**: (400 MHz, CDCl_3): 7.16 (d, J =7.4 Hz, 1H), 7.06 (m, 2H), 6.78 (d, J =7.0 Hz, 1H), 6.75 (s, 1H), 4.28 (s, 2H), 2.44 (s, 3H), 2.24 (s, 3H), 1.96 (s, 3H), 1.48 (s, 6H). **¹³C-NMR**: (125 MHz): 168.1, 168.0, 157.5, 143.0, 137.0, 134.9, 129.9, 126.9, 126.8, 125.5, 106.4, 85.6, 44.5, 29.7, 26.6, 20.7, 20.2, 19.8. **IR**: (neat) ν = 2962.0, 1775.7, 1366.3, 1199.3, 1168.5, 1063.1, 1009.9, 919.9, 879.1 cm^{-1} . **LRMS (EI-QMS) m/z**: Calc for $\text{C}_{21}\text{H}_{22}\text{O}_5\text{S}$: 386.12, found 386.3



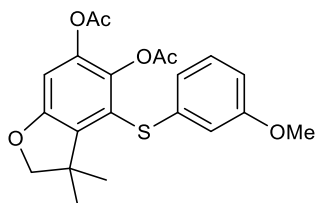
3.3.17: Synthesized according to general procedure A. Purified with silica column chromatography (9:1 Hexanes: EtOAc), 76% yield.

Rf: 0.15 (9:1 Hexanes: EtOAc). **¹H-NMR**: (500 MHz, CDCl_3): 7.06 (d, J =8.2 Hz, 4H), 7.03 (d, J =8.5 Hz, 2H), 6.74 (s, 1H), 4.28 (s, 2H), 2.31 (s, 3H), 2.23 (s, 3H), 2.02 (s, 3H), 1.50 (s, 6H). **¹³C-NMR**: (125 MHz): 168.1, 168.1, 157.4, 143.0, 137.8, 137.0, 135.6, 133.1, 129.7, 127.2, 123.3, 106.3, 85.6, 44.5, 26.7, 21.0, 20.7, 20.0. **IR**: (neat) ν = 2969.9, 1742.5, 1366.8, 1204.0 cm^{-1} . **LRMS (EI-QMS) (m/z)**: Calc for $\text{C}_{21}\text{H}_{22}\text{O}_5\text{S}$: 386.12, found 386.1.



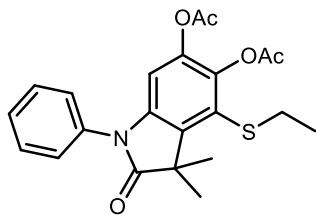
3.3.18: Synthesized according to general procedure A. Purified with silica column chromatography (9:1 Hexanes: EtOAc), 80% yield.

Rf: 0.2 (9:1 Hexanes: EtOAc). **¹H-NMR:** (400 MHz, CDCl₃): 7.35 (d, *J*=8.5 Hz, 2H), 6.96 (d, *J*=8.5 Hz, 2H), 6.76 (s, 1H), 4.27 (s, 2H), 2.24 (s, 3H), 2.05 (s, 3H), 1.46 (s, 6H). **¹³C-NMR:** (125 MHz): 168.0, 157.6, 143.2, 137.8, 137.3, 136.2, 132.2, 132.0, 129.4, 128.1, 121.9, 119.3, 107.0, 85.5, 44.5, 26.7, 20.7, 20.0. **IR:** (neat) ν = 2957.9, 1768.0, 1741.1, 1460.2, 1366.2, 1205.3, 1011.0, 772.3 cm⁻¹. **LRMS (EI-QMS) m/z:** Calc for C₂₀H₁₉BrO₅S: 450.01, found 450.2.



3.3.19: Synthesized according to general procedure A. Purified with silica column chromatography (9:1 Hexanes: EtOAc), 85% yield.

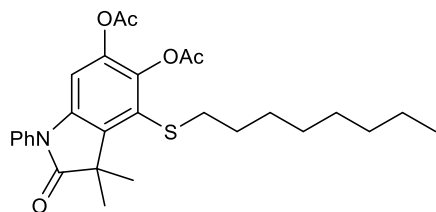
Rf: 0.3 (9:1 Hexanes: EtOAc). **¹H-NMR:** (500 MHz, CDCl₃): 7.15 (t, *J*= 7.9 Hz, 1H), 6.75 (s, 1H), 6.71 (m, 2H), 6.63 (t, 1H), 4.28 (s, 2H), 3.74 (s, 3H), 2.24 (s, 3H), 2.04 (s, 3H), 1.49 (s, 6H). **¹³C-NMR:** (125 MHz): 168.2, 168.0, 160.0, 157.5, 143.1, 138.1, 137.9, 137.2, 129.8, 122.6, 119.2, 112.1, 111.7, 106.6, 85.6, 55.2, 44.5, 26.7, 20.7, 20.0. **IR:** (neat) ν = 2962.0, 1769.5, 1711.9, 1588.5, 1363.8, 1196.7, 1167.1, 1136.7, 1063.0, 1010.5, 771.9 cm⁻¹. **LRMS (EI-QMS) (m/z):** Calc for C₂₁H₂₂O₆S: 402.11, found 402.3.



3.3.20: Synthesized according to general procedure A. Purified with silica column chromatography (5:1 Hexanes: EtOAc), 85% yield.

Rf: 0.34 (5:1 Hexanes: EtOAc). **¹H-NMR:** (400 MHz, CDCl₃): 7.50 (t, 2H), 7.41-7.36 (m, 3H), 6.64 (s, 1H), 2.91 (q, *J*= 7.4 Hz, 2H), 2.35 (s, 3H), 2.22 (s, 3H), 1.69 (s, 6H), 1.29 (t, *J*= 7.4 Hz, 3H). **¹³C-NMR:** (125 MHz): 180.4, 169.2, 168.1, 142.4, 141.1, 140.0, 135.6, 134.0, 129.8, 129.7, 128.4, 127.0, 126.4, 126.7, 118.1, 105.1, 46.7, 30.2, 23.4, 20.9, 20.5, 14.9. **IR:** (neat) ν = 2969.4,

2930.5, 2869.8, 1773.4, 1725.7, 1606.3, 1496.8, 1417.9, 1368.3, 1195.5, 1151.9, 1010.2, 944.3 cm^{-1} . **HRMS (m/z):** Calc for $\text{C}_{22}\text{H}_{23}\text{NaO}_5\text{S}$: $[\text{M}+\text{Na}]^+$: 436.1189, found 436.1196.

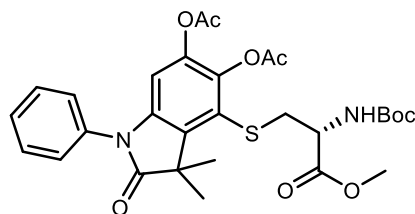


3.3.21: Synthesized according to general procedure A. Purified with silica column chromatography (5:1 Hexanes: EtOAc), 50% yield.

Rf: 0.2 (5:1 Hexanes: EtOAc). **$^1\text{H-NMR}$:** (500 MHz, CDCl_3): 7.52 (t, 2H), 7.41-7.36 (m, 3H), 6.63 (s, 1H), 2.88 (t, 2H), 2.36 (s, 3H), 2.24 (s, 3H), 1.69-1.64 (m, 8H), 1.42-1.28 (m, 10H), 0.89 (t, 3H)

$^{13}\text{C-NMR}$: (125 MHz): 180.5, 168.2, 142.4, 141.1, 139.9, 135.5, 134.0, 129.8, 128.4, 127.6, 126.7, 105.0, 46.7, 36.4, 31.8, 29.8, 29.1, 28.9, 23.3, 22.6, 20.6, 20.5, 14.1. **IR:** (neat) ν = 2969.5, 2928.3, 2851.6, 1766.5, 1735.8, 1416.6, 1369.5, 1184.9, 1151.5, 1013.7, 927.50, 761.5 cm^{-1} .

HRMS (m/z): Calc. for $\text{C}_{28}\text{H}_{35}\text{NNaO}_5\text{S}$: 520.2128, found 520.2129.

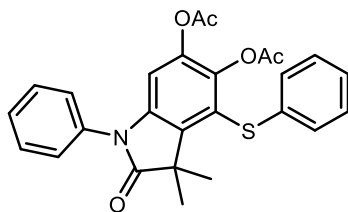


3.3.22: Synthesized according to general procedure A. Purified with silica column chromatography (5:1 Hexanes: EtOAc), 42% yield.

Rf: 0.20 (5:1 Hexanes: EtOAc). **$^1\text{H-NMR}$:** (400 MHz, CDCl_3): 7.51 (t, 2H), 7.41 (t, 1H), 7.34(d, 2H), 6.66 (s, 1H), 3.76 (s, 1H), 3.36 (m, 2H), 2.38 (s, 3H), 2.23(s, 3H), 1.66 (s, 6H), 1.45 (s, 9H).

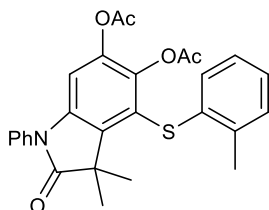
$^{13}\text{C-NMR}$: (125 MHz): 180.2, 170.8, 168.1, 168.0, 155.0, 142.6, 141.3, 139.7, 135.6, 133.9, 129.8, 128.5, 126.7, 126.0, 105.7, 80.4, 53.3, 52.8, 46.7, 38.5, 28.3, 24.9, 23.4, 23.2 20.6, 20.4.

IR: (neat) ν = 2970.1, 2927.3, 1776.2, 1713.2, 1607.9, 1499.3, 1419.3, 1368.0, 1320.1, 1197.4, 1154.1, 1049.7 1011.8, 921.1, 876.3 cm^{-1} . **HRMS (m/z):** Calc for $\text{C}_{29}\text{H}_{34}\text{N}_2\text{NaO}_9\text{S}$: $[\text{M}+\text{Na}]^+$: 609.1877, found 609.1888.



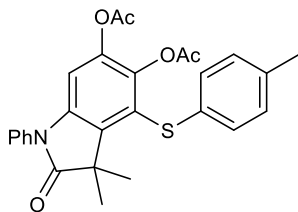
3.3.23: Synthesized according to general procedure A. Purified with silica column chromatography (5:1 Hexanes: EtOAc), 52% yield.

R_f: 0.16 (5:1 Hexanes: EtOAc). **¹H-NMR:** (400 MHz, CDCl₃): 7.57-7.53 (2H, m), 7.46-7.41 (3H, m), 7.30-7.36 (2H, m), 7.21-7.16 (3H, m), 6.77 (1H s), 2.21 (3H, s), 2.01 (3H, s), 1.68 (6H, s). **¹³C-NMR:** (125 MHz): 180.3, 168.1, 167.8, 142.9, 141.5, 139.6, 136.1, 133.9, 129.9, 129.1, 128.5, 127.3, 126.7, 126.2, 124.5, 106.1, 46.7, 23.9, 20.7, 20.0. **IR:** (neat) ν = 2975.7, 2930.5, 2870.0, 1773.7, 1726.6, 1606.0, 1496.8, 1418.1, 1367.3, 1194.3, 1151.6, 1092.0, 1071.8, 1010.1, 943.9 cm⁻¹. **HRMS (m/z):** Calc for C₂₆H₂₃NNaO₅S: [M+Na]⁺: 484.1189, found 484.1200.



3.3.24: Synthesized according to general procedure A. Purified with silica column chromatography (9:1 Hexanes: EtOAc), 23% yield.

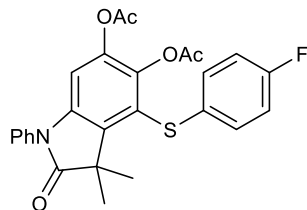
R_f: 0.1 (9:1 Hexanes: EtOAc). **¹H-NMR:** (500 MHz, CDCl₃): 7.55 (m, 2H), 7.44 (m, 3H), 7.19 (dd, 1H), 7.12-7.07 (m, 2H), 6.82 (dd, 1H), 6.77 (s, 1H), 2.49 (s, 3H), 2.20 (s, 3H), 1.95 (s, 3H), 1.67 (s, 6H). **¹³C-NMR:** (125 MHz): 180.3, 168.1, 167.7, 142.9, 141.5, 139.4, 136.0, 135.3, 135.2, 134.0, 130.1, 129.8, 128.5, 127.3, 126.9, 126.8, 126.0, 124.7, 105.9, 46.7, 23.2, 20.7, 20.4, 19.8. **IR:** (neat) ν = 2969.8, 1766.1, 1726.9, 1418.1, 1367.0, 1196.9, 1132.2, 1009.1, 747.9 cm⁻¹. **HRMS (m/z):** Calc for C₂₇H₂₅NNaO₅S: 498.1346, found 498.1353.



3.3.25: Synthesized according to general procedure A. Purified with silica column chromatography (5:1 Hexanes: EtOAc), 30% yield.

R_f: 0.2 (5:1 Hexanes: EtOAc). **¹H-NMR:** (500 MHz, CDCl₃): 7.55 (t, *J*=8.1 Hz, 2H), 7.44 (t, *J*=9.0 Hz, 2H), 7.09 (m, 4H), 6.76 (s, 1H), 2.32 (s, 3H), 2.20 (s, 3H), 2.02 (s, 3H), 1.69 (s, 6H).

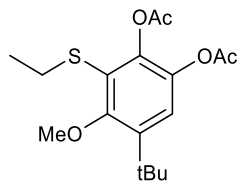
¹³C-NMR: (125 MHz): 180.3, 168.1, 167.9, 142.9, 141.4, 139.5, 136.1, 136.0, 134.0, 132.4, 129.9, 129.8, 128.5, 127.5, 126.7, 125.0, 105.9, 46.7, 23.3, 21.0, 20.7, 20.0. **IR:** (neat) ν = 2970.3, 1766.4, 1727.8, 1565.5, 1199.5, 1180.1, 1150.3, 1007.1, 797.8 cm^{-1} . **HRMS (m/z):** Calc. for $\text{C}_{27}\text{H}_{25}\text{NNaO}_5\text{S}$: 498.1346, found 498.1354.



3.3.26: Synthesized according to general procedure A. Purified with silica column chromatography (5:1 Hexanes: EtOAc), 56% yield.

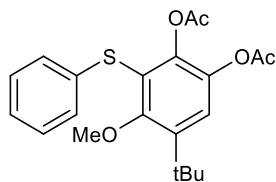
Rf: 0.2 (5:1 Hexanes:EtOAc). **¹H-NMR:** (500 MHz, CDCl_3): 7.55 (t, J =7.8 Hz, 2H), 7.42 (m, 3H), 7.16 (m, 1.98), 6.99 (t, J =8.5 Hz, 2H), 6.76 (s, 1H), 2.21 (s, 3H), 2.05 (s, 3H), 1.68 (s, 6H). **¹³C-NMR:** (125 MHz): 180.2, 168.0, 167.7, 162.5, 160.5, 143.0, 141.5, 139.5, 136.0, 133.9, 131.1, 129.9, 129.3, 128.5, 126.7, 124.6, 116.4, 116.2, 106.2, 46.7, 23.3, 20.6, 20.0. **IR:** (neat) ν = 2970.4, 2931.5, 1773.7, 1726.5, 1606.6, 1590.7, 1489.0, 1367.7, 1193.9, 1151.7, 1134.7, 1010.0, 915.9, 826.7, 730.2, 693.2, 629.1 cm^{-1} . **HRMS (m/z):** Calc. for $\text{C}_{26}\text{H}_{22}\text{FNNaO}_5\text{S}$: 502.1095, found 502.1105.

d) Substrates in Table 3.6.2:



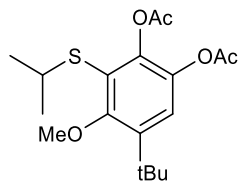
3.6.2: Synthesized according to general procedure C. Purified with silica column chromatography (5:1 Hexanes: EtOAc), 77% yield.

Rf: 0.5 (5:1 Hexanes: EtOAc). **¹H-NMR:** (500 MHz, CDCl_3): 7.07 (s, 1H), 4.00 (s, 3H), 2.84 (q, J =7.5 Hz, 2H), 2.34 (s, 3H), 2.28 (s, 3H), 1.38 (s, 9H), 1.14 (t, J =7.4 Hz, 3H). **¹³C-NMR:** (125 MHz): 168.6, 168.0, 159.2, 142.6, 141.8, 137.8, 123.8, 121.2, 60.9, 35.2, 33.0, 30.6, 28.4, 20.6, 20.5, 14.6. **IR:** (neat) ν = 2962.4, 2870.4, 1770.0, 1367.5, 1194.7, 1155.6, 1066.2, 1011.0, 931.3, 891.2 cm^{-1} . **LRMS (EI-QMS) m/z:** Calc for $\text{C}_{17}\text{H}_{24}\text{O}_5\text{S}$: 340.13, found 340.2.



3.6.5: Synthesized according to general procedure C. Purified with silica column chromatography (5:1 Hexanes: EtOAc), 57% yield.

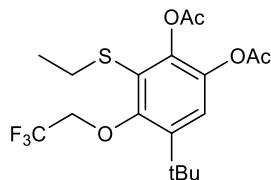
R_f: 0.5 (5:1 Hexanes: EtOAc). **¹H-NMR:** (500 MHz, CDCl₃): 7.24-7.20 (m, 3H), 7.15-7.12 (m, 3H), 3.95 (s, 3H), 2.28 (s, 3H), 2.14 (s, 3H), 1.39 (s, 9H). **¹³C-NMR:** (125 MHz): 168.5, 167.8, 159.5, 142.8, 142.5, 138.3, 136.3, 128.8, 127.0, 125.7, 122.7, 121.7, 61.7, 35.3, 30.5, 20.7, 20.2. **IR:** (neat) ν = 2961.7, 1769.9, 1465.0, 1429.0, 1367.6, 1194.8, 1155.5, 1066.1, 1011.6, 931.5, 892.8, 741.0 cm⁻¹. **LRMS (EI-QMS) m/z:** Calc for C₂₁H₂₄O₅S: 388.13, found 388.3.



3.6.7: Synthesized according to general procedure C. Purified with silica column chromatography (5:1 Hexanes: EtOAc), 95% yield.

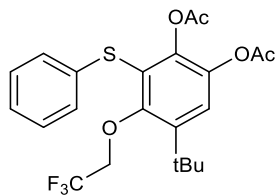
R_f: 0.5

¹H-NMR: (500 MHz, CDCl₃): 7.07 (s, 1H), 4.00 (s, 3H), 3.47 (hep, *J*= 6.7 Hz, 1H), 2.33 (s, 3H), 2.29 (s, 3H), 1.38 (s, 9H), 1.17 (d, *J*= 6.7 Hz, 6H). **¹³C-NMR:** (125 MHz): 168.6, 168.0, 159.4, 142.8, 141.8, 137.8, 123.8, 121.3, 60.9, 38.0, 35.2, 30.5, 23.2, 20.7, 20.6. **IR:** (neat) ν = 2962.6, 1770.3, 1449.0, 1428.0, 1367.2, 1195.7, 1156.1, 1065.1, 1011.1, 984.9, 931.1, 891.5 cm⁻¹. **¹LRMS (EI-QMS) (m/z):** Calc for C₁₈H₂₆O₅S: 354.15, found 354.3.



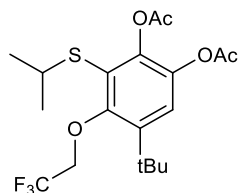
3.6.15: Synthesized according to general procedure C. Purified with silica column chromatography (5:1 Hexanes: EtOAc), 73% yield.

R_f: 0.4 (5:1 Hexanes: EtOAc). **¹H-NMR:** (500 MHz, CDCl₃): 7.15 (s, 1H), 4.75 (q, *J*=8.4 Hz, 2H), 2.86 (q, *J*=7.4 Hz, 2H), 2.35 (s, 3H), 2.30 (s, 3H), 1.40 (s, 9H), 1.13 (t, *J*=7.4 Hz, 3H). **¹³C-NMR:** (125 MHz): 168.4, 168.0, 154.8, 143.1, 142.5, 139.0, 124.3, 122.2, 68.2, 67.9, 67.6, 67.3, 35.4, 30.4, 28.9, 20.6, 20.5, 14.4. **IR:** (neat) ν =2966.4, 1775.1, 1444.3, 1369.7, 1275.2, 1200.7, 1158.6, 1080.0, 1037.7, 1013.5, 961.3, 938.7, 893.2 cm⁻¹. **LRMS (EI-QMS) m/z:** Calc for C₁₈H₂₃F₃O₅S: 408.12, found 408.3.



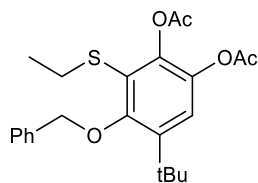
3.6.16: Synthesized according to general procedure C. Purified with silica column chromatography (4% DCM in Toluene), 60% yield.

Rf: 0.3 (4% DCM in Toluene). **¹H-NMR:** (500 MHz, CDCl₃): 7.27 (s, 1H), 7.24-7.10 (m, 5H), 4.65 (q, *J*=8.27 Hz, 2H), 2.29 (s, 3H), 2.17 (s, 3H), 1.39 (s, 9H). **¹³C-NMR:** (125 MHz): 168.3, 167.7, 154.9, 143.2, 143.0, 139.4, 135.2, 129.0, 128.2, 127.2, 126.2, 123.4, 122.2, 121.8, 68.9, 68.6, 68.3, 68.0, 35.5, 30.4, 20.6, 20.2. **IR:** (neat) ν = 2964.0, 1772.5, 1440.3, 1386.5, 1193.1, 1152.5, 1080.3, 938.9, 873.5, 740.8, 687.2, cm⁻¹. **LRMS (EI-QMS) m/z:** Calc for C₂₂H₂₃F₃O₅S: 456.12, found 456.3.



3.6.17: Synthesized according to general procedure C. Purified with silica column chromatography (5% DCM in Toluene), 70% yield.

Rf: 0.3 (5% DCM in Toluene). **¹H-NMR:** (500 MHz, CDCl₃): 7.16 (s, 1H), 4.75 (q, *J*= 8.56 Hz, 2H), 3.50 (hep, *J*=6.78 Hz, 1H), 2.34 (s, 3H), 2.30 (s, 3H), 1.40 (s, 9H), 1.15 (d, *J*=6.78 Hz, 6H). **¹³C-NMR:** (125 MHz): 168.4, 168.0, 155.0, 143.3, 142.4, 139.0, 124.5, 124.2, 122.3, 122.2, 68.3, 68.1, 67.8, 67.5, 38.9, 35.3, 30.4, 23.0, 20.6, 20.5. **IR:** (neat) ν =2963.6, 1774.5, 1442.7, 1368.3, 1197.8, 1158.0, 1079.3, 1037.4, 939.0 cm⁻¹. **LRMS (EI-QMS) m/z:** Calc for C₁₉H₂₅F₃O₅S: 422.14, found 422.3.

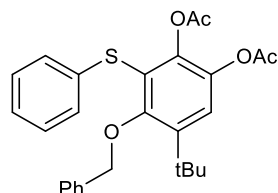


3.6.19: Synthesized according to general procedure C. Purified with silica column chromatography (5% EtOAc in Toluene), 74% yield.

Rf: 0.4 (5% EtOAc in Toluene). **¹H-NMR:** (500 MHz, CDCl₃): 7.55 (d, *J*= 7.7 Hz, 2H), 7.44-7.33 (m, 3H), 7.14 (s, 1H), 5.32 (s, 2H), 2.83 (q, *J*=7.4 Hz, 2H), 2.36 (s, 3H), 2.31 (s, 3H), 1.42 (s, 9H), 1.09 (t, *J*=7.4 Hz, 3H). **¹³C-NMR:** (125 MHz): 168.6, 168.1, 157.5, 142.9, 142.3, 138.1, 137.8, 128.4, 127.6, 127.2, 124.5, 121.6, 74.0, 35.4, 30.7, 28.9, 20.7, 20.6, 14.5. **IR:** (neat)

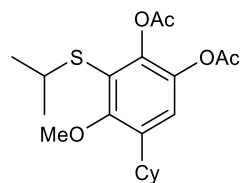
$\nu=2962.2, 1769.6, 1438.4, 1366.0, 1193.3, 1155.3, 1064.3, 1011.0, 937.2, 891.8, 734.7 \text{ cm}^{-1}$

¹LRMS (EI-QMS) m/z: Calc for C₂₃H₂₈O₅S: 416.17, found 416.3.



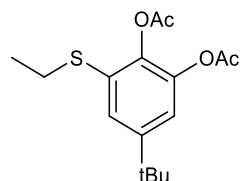
3.6.20: Synthesized according to general procedure C. Purified with silica column chromatography (5% EtOAc in Toluene), 50% yield.

R_f: 0.5 (5% EtOAc in Toluene). **¹H-NMR:** (500 MHz, CDCl₃): 7.33-7.28 (m, 5H), 7.26 (s, 1H), 7.21-7.09 (m, 5H), 5.25 (s, 2H), 2.30 (s, 3H), 2.16 (s, 3H), 1.39 (s, 9H). **¹³C-NMR:** (125 MHz): 168.5, 167.8, 157.5, 142.9, 142.9, 138.6, 137.4, 136.1, 128.8, 128.6, 128.3, 128.2, 127.5, 127.2, 127.0, 125.8, 122.9, 122.3, 74.6, 66.3, 35.5, 30.6, 20.7, 20.2. **IR:** (neat) $\nu=2961.7, 1770.6, 1478.5, 1366.5, 1195.3, 1156.0, 1065.4, 1011.3, 984.7, 935.9, 892.8, 876.0, 738.2, 696.5 \text{ cm}^{-1}$. **HRMS (m/z):** Calc. for C₂₇H₂₈NaO₅S: [M+Na]⁺: 487.1550, found 487.1551.



3.6.22: Synthesized according to general procedure C. Purified with silica column chromatography (5:1 Hexanes: EtOAc), 50% yield.

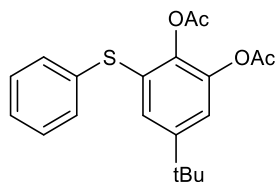
R_f: 0.4 (5:1 Hexanes:EtOAc). **¹H-NMR:** (500 MHz, CDCl₃): 7.01 (s, 1H), 3.88 (s, 3H), 3.51 (hep, $J=6.7 \text{ Hz}$, 1H), 2.94 (1H), 2.33 (s, 3H), 2.28 (s, 3H), 1.87-1.76 (m, 5H), 1.49-1.17 (m, 5H), 1.21 (d, $J=6.7 \text{ Hz}$, 6H). **¹³C-NMR:** (125 MHz): 168.5, 168.1, 157.0, 142.2, 139.7, 139.2, 123.5, 121.5, 61.5, 38.4, 37.4, 34.1, 31.4, 30.9, 27.4, 26.9, 26.1, 23.5, 23.3, 20.7, 20.6. **IR:** 2927.4, 2852.0, 1772.7, 1459.3, 1367.4, 1201.9, 1167.3, 1097.8, 1020.7, 931.9, 886.5 cm^{-1} . **LRMS (EI-QMS) (m/z):** Calc for C₂₀H₂₈O₅S: 380.17, found 380.3.



3.6.10: Synthesized according to general procedure C. Purified with silica column chromatography (5:1 Hexanes: EtOAc), 89% yield.

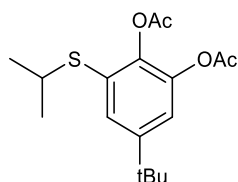
R_f: 0.5 (5:1 Hexanes: EtOAc). **¹H-NMR:** (500 MHz, CDCl₃): 7.29 (d, $J=2.3 \text{ Hz}$, 1H), 7.04 (d, $J=2.2 \text{ Hz}$, 1H), 2.92 (q, $J=7.4 \text{ Hz}$, 2H), 2.34 (s, 3H), 2.29 (s, 3H), 1.33 (s, 9H), 1.31 (t, $J=7.4 \text{ Hz}$, 3H). **¹³C-NMR:** (125 MHz): 168.3, 168.0, 149.9, 142.4, 139.0, 130.5, 125.2, 118.7, 34.8,

31.2, 27.8, 20.7, 20.4, 14.3. **IR:** 2964.0, 1770.4, 1367.5, 1196.6, 1159.4, 1012.1, 966.1, 886.5 cm^{-1} . **LRMS (EI-QMS) m/z:** Calc for $\text{C}_{16}\text{H}_{22}\text{O}_4\text{S}$: 310.12, found 310.2.



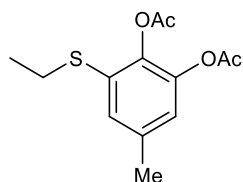
3.6.11: Synthesized according to general procedure C. Purified with silica column chromatography (5:1:1 Hexanes:Toluene:EtOAc), 78% yield.

R_f: 0.45 (5:1:1 Hexanes:Toluene:EtOAc) **¹H-NMR:** (500 MHz, CDCl_3): 7.36-7.25 (m, 5H), 7.18 (d, $J=2.2$ Hz, 1H), 7.11 (d, $J=2.2$ Hz, 1H), 2.30 (s, 3H), 2.23 (s, 3H), 1.24 (s, 9H). **¹³C-NMR:** (125 MHz): 168.3, 167.9, 150.2, 142.7, 139.3, 134.5, 131.0, 129.7, 129.2, 127.3, 127.3, 120.0, 34.8, 31.1, 20.7, 20.2. **IR:** (neat) $\nu=2964.3, 1773.4, 1477.7, 1368.5, 1202.2, 1160.4, 1013.4, 887.2$ cm^{-1} . **LRMS (EI-QMS) m/z:** Calc for $\text{C}_{20}\text{H}_{22}\text{O}_4\text{S}$: 358.12, found 358.2.



3.6.12: Synthesized according to general procedure C. Purified with silica column chromatography (5:1:1 Hexanes:EtOAc:Toluene), 77% yield.

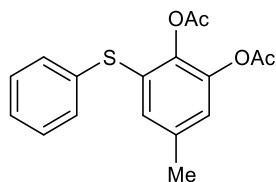
R_f: 0.3 (5:1:1 Hexanes:EtOAc:Toluene). **¹H-NMR:** (500 MHz, CDCl_3): 7.37 (d, 1H), 7.08 (d, 1H), 3.35 (hep, 1H), 2.33 (s, 3H), 2.28 (s, 3H), 1.32 (s, 9H), 1.28 (d, 6H). **¹³C-NMR:** (125 MHz): 168.3, 168.1, 149.7, 142.5, 140.3, 129.5, 128.2, 119.7, 38.4, 34.8, 31.3, 31.2, 23.2, 20.7. **IR** (neat) $\nu=2962.7, 1771.3, 1366.3, 1197.0, 1159.0, 1011.2, 730.5$ cm^{-1} . **HRMS:** Calc. for $\text{C}_{17}\text{H}_{24}\text{NaO}_4\text{S}$: $[\text{M}+\text{Na}]^+$: 347.1288, found 347.1295.



3.6.24: Synthesized according to general procedure C. Purified with silica column chromatography (7% DCM in Toluene), 70% yield.

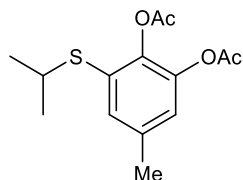
R_f: 0.1 (7% DCM in Toluene). **¹H-NMR:** (500 MHz, CDCl_3): 7.06 (d, $J=2.0$ Hz, 1H), 6.87 (d, $J=2.0$ Hz, 1H), 2.91 (q, $J=7.4$ Hz, 2H), 2.35 (s, 3H), 2.34 (s, 3H), 2.28 (s, 3H), 1.31 (t, $J=7.4$ Hz, 3H). **¹³C-NMR:** (125 MHz): 168.4, 168.0, 142.5, 138.7, 136.7, 131.4, 127.7, 121.7, 27.3, 21.1, 20.7, 20.3, 14.2. **IR:** 2968.8, 2928.6, 1767.9, 1467.7, 1368.4, 1199.5, 1176.9, 1118.5,

1020.5, 888.3, 637.2 cm^{-1} . **LRMS (EI-QMS) m/z:** Calc for $\text{C}_{13}\text{H}_{16}\text{O}_4\text{S}$: 268.08, found 268.1 m/z.



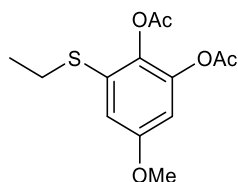
3.6.25: Synthesized according to general procedure C. Purified with silica column chromatography (5:1:1 Hexanes: EtOAc: Toluene), 70%

Rf: 0.3 (5:1:1 Hexanes:EtOAc:Toluene). **$^1\text{H-NMR}$:** (500 MHz, CDCl_3): 7.38-7.28 (m, 5H), 6.93 (s, 2H), 2.29 (s, 3H), 2.27 (s, 3H), 2.25 (s, 3H). **$^{13}\text{C-NMR}$:** (125 MHz, CDCl_3): 168.3, 168.0, 142.8, 139.1, 137.0, 134.0, 131.6, 130.6, 130.1, 129.3, 127.6, 127.2, 123.9, 123.1, 21.0, 20.7, 20.2. **IR** (neat) ν = 2958.2, 1768.4, 1468.8, 1367.6, 1198.5, 1175.5, 1019.9, 886.7, 744.4, 690.6 cm^{-1} . **HRMS (m/z):** Calc for $\text{C}_{17}\text{H}_{16}\text{NaO}_4\text{S}$ $[\text{M}+\text{Na}]^+$: 339.0662, found 339.0667.



3.6.26: Synthesized according to general procedure C. Purified with silica column chromatography (5% DCM in Toluene), 68% yield.

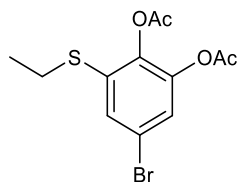
Rf: 0.1 (5% DCM in Toluene). **$^1\text{H-NMR}$:** (500 MHz, CDCl_3): 7.16 (d, J = 1.5 Hz, 1H), 6.91 (d, J = 1.5 Hz, 1H), 3.37 (hep, J = 6.7 Hz, 1H), 2.36 (s, 3H), 2.33 (s, 3H), 1.30 (s, J = 6.7 Hz, 3H). **$^{13}\text{C-NMR}$:** (125 MHz): 168.3, 168.1, 142.6, 140.1, 136.5, 130.8, 130.3, 122.7, 38.1, 23.2, 21.0, 20.7, 20.4. **IR:** (neat) ν =2964.9, 2926.3, 1769.1, 1466.7, 1367.9, 1200.6, 1177.9, 1118.4, 1020.5, 886.6 cm^{-1} . **LRMS (EI-QMS) m/z:** Calc for $\text{C}_{14}\text{H}_{18}\text{O}_4\text{S}$: 282.09, found 282.1.



3.6.28: The starting material *ortho*-quinone was synthesized according to general procedure C, and then used immediately in general procedure C. Purified with silica column chromatography (5:1:1 Hexanes: EtOAc: Toluene), 72% yield.

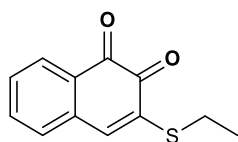
Rf: 0.2 (5:1:1 Hexanes: EtOAc: Toluene). **$^1\text{H-NMR}$:** (500 MHz, CDCl_3): 6.77 (d, J = 2.9 Hz, 1H), 6.59 (d, J = 2.9 Hz, 1H), 3.80 (s, 3H), 2.92 (q, J = 7.4 Hz, 2H), 2.33 (s, 3H), 2.29 (s, 3H), 1.33 (t, J = 7.4 Hz, 3H). **$^{13}\text{C-NMR}$:** (125 MHz): 168.2, 168.1, 157.5, 143.3, 134.4, 132.6, 112.5, 106.2, 55.8, 27.1, 20.7, 20.3, 14.1. **IR:** (neat) ν =2969.0, 2932.4, 1771.5, 1600.8, 1587.6, 1471.6,

1438.6, 1369.6, 1199.1, 1172.7, 1043.4, 1013.9, 885.1 cm^{-1} . **LRMS (EI-QMS) m/z:** Calc for $\text{C}_{13}\text{H}_{16}\text{O}_5\text{S}$: 284.07, found 284.1.



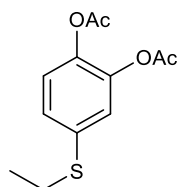
3.6.32: Synthesized according to general procedure C. Purified with silica column chromatography (5: 0.25 Toluene: EtOAc), 40% yield.

Rf: 0.5 (5: 0.25 Toluene: EtOAc). **$^1\text{H-NMR}$:** (500 MHz, CDCl_3): 7.31 (d, $J=2.1$ Hz, 1H), 7.21 (d, $J=2.1$ Hz, 1H), 2.93 (q, $J=7.3$ Hz, 2H), 2.34 (s, 3H), 2.29 (s, 3H), 1.34 (t, $J=7.3$ Hz, 3H). **$^{13}\text{C-NMR}$:** (125 MHz, CDCl_3): 167.7, 167.4, 143.3, 139.7, 134.5, 128.4, 123.8, 118.9, 29.7, 27.0, 20.6, 20.2, 13.9. **IR:** 2919.4, 1772.5, 1198.4, 1156.9, 1067.8, 948.5, 786.2 cm^{-1} . **LRMS (EI-QMS) m/z:** Calc for $\text{C}_{12}\text{H}_{13}\text{BrO}_4\text{S}$: 331.97, found 332.0 m/z.



3.6.34: Synthesized according to general procedure C. Purified with silica column chromatography (5% DCM in Toluene), 27% yield.

Rf: 0.4 (5% DCM in Toluene). **$^1\text{H-NMR}$:** (500 MHz, CDCl_3): 8.20 (dd, $J=7.6, 1.4$ Hz, 1H), 7.86 (dd, $J=8.0, 1.0$ Hz, 1H), 7.70 (dt, $J=7.6, 1.5$ Hz, 1H), 7.59 (dt, $J=7.6, 1.1$ Hz, 1H), 6.44 (s, 1H), 3.10 (q, $J=7.4$ Hz, 2H), 1.52 (t, $J=7.4$ Hz, 3H). **$^{13}\text{C-NMR}$:** (125 MHz, CDCl_3): 179.6, 176.3, 135.0, 133.8, 131.1, 130.5, 129.3, 125.2, 119.7, 26.0, 12.7. **IR:** (neat) $\nu=2961.9, 1773.8, 1507.5, 1367.6, 1199.9, 1160.2, 1012.4$ cm^{-1} . **HRMS (m/z):** Calc. for $\text{C}_{12}\text{H}_{10}\text{NaO}_5\text{S}$: $[\text{M}+\text{Na}]^+$: 241.0924, found 241.0292.



3.6.36: Synthesized according to general procedure C. Purified with silica column chromatography (5% EtOAc in Toluene), 51% yield.

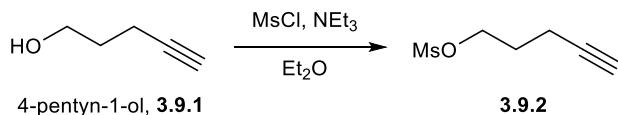
Rf: 0.25 (5% EtOAc in Toluene). **$^1\text{H-NMR}$:** (500 MHz, CDCl_3): 7.25 (d, $J=2.5$ Hz, 1H), 7.24 (d, $J=7.2$ Hz, 1H), 7.06 (dd, $J=7.2, 2.5$ Hz, 1H), 2.93 (q, $J=7.5$ Hz, 2H), 2.36 (s, 3H), 2.30 (s, 3H), 1.32 (t, $J=7.5$ Hz). **$^{13}\text{C-NMR}$:** (125 MHz): 168.2, 167.8, 143.0, 140.9, 132.2, 126.8, 126.5, 120.9,

27.2, 20.7, 20.3, 14.2. **IR:** (neat) ν =2965.3, 2931.2, 1771.2, 1581.8, 1450.6, 1368.6, 1198.0, 1160.9, 1011.2, 936.9 cm^{-1} . **LRMS (EI-QMS) m/z:** Calc for $\text{C}_{12}\text{H}_{14}\text{O}_4\text{S}$: 254.06, found 254.1.

e) 3.9, Blum Group Collaboration Substrates

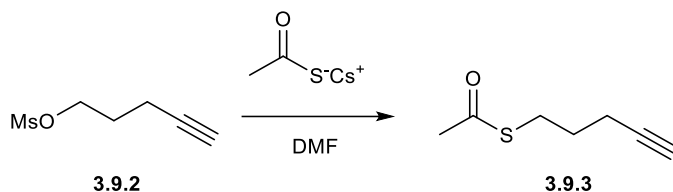
i) 4-pentyn-1-thiol, 3.9.4

Method #1:



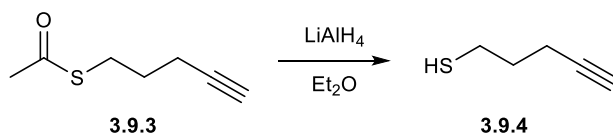
To a flame-dried round bottom flask, 4-pentyn-1-ol (0.93 mL, 10 mmol, 1.0 eq) was dissolved in Et_2O (80 mL), NEt_3 (4.18 mL, 30 mmol, 3.0 eq) was added, and cooled to -20°C . MsCl (1.55 mL, 20 mmol, 2.0 eq) in Et_2O (20 mL) was then added dropwise over 30 min, and the resulting mixture was stirred for 30 min. The reaction was then warmed to rt, and acidified with 2M HCl , extracted with Et_2O and washed with water, brine, dried over MgSO_4 , and concentrated *in vacuo* to yield the final product in quantitative yield. **3.9.2** was then used in the next step without further purification. Characterization data is in accordance with previous literature precedent³.

3.9.2: $^1\text{H-NMR}$ (500 MHz, CDCl_3): 4.37 (t, $J=6.0$ Hz, 2H), 3.05 (s, 3H), 2.39 (dt, $J=6.6$, 2.7 Hz, 2H), 2.03 (t, $J=2.7$ Hz, 1H), 1.98 (pen, $J=6.6$ Hz, 2H)



In a flame-dried, round bottom flask, cesium thioacetate (10 mmol, 1.1 eq) was suspended in DMF (50 mL), and mesylate (9.09 mmol, 1 eq) in DMF (5 mL) was added. The reaction mixture was stirred for 20h, and then extracted with Et_2O , washed with water, brine, and dried with MgSO_4 , concentrated *in vacuo* to yield the final alkynyl thioacetate product **3.9.3** in 54% yield. Characterization data is in accordance with previous literature precedent³.

3.9.3: $^1\text{H-NMR}$ (500 MHz, CDCl_3): 2.99 (t, $J=7.1$ Hz, 2H), 2.35 (s, 3H), 2.29 (dt, $J=7.1$, 2.7 Hz, 2H), 1.99 (t, $J=2.7$ Hz, 1H), 1.82 (pen, $J=7.1$ Hz, 2H)

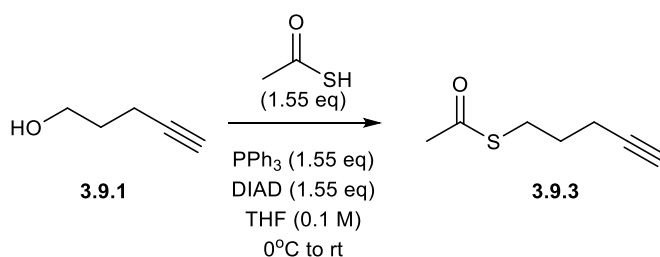


In a flame dried, round bottom flask, the alkynyl thioacetate was dissolved in Et_2O and cooled to 0°C . LiAlH_4 was then added portionwise at 0°C , and the reaction was stirred for 3h at rt. The

reaction was then cooled to 0°C, and quenched by adding 2M HCl dropwise, extracted with DCM, dried with MgSO₄, and concentrated *in vacuo* to yield the final product. The resulting product was not isolated but used immediately. Characterization data is in accordance with previous literature precedent³.

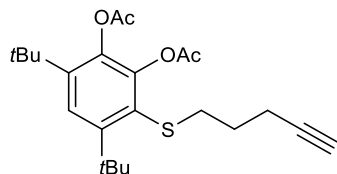
3.9.4: ¹H-NMR (500 MHz, CDCl₃): 2.62 (dt, *J*=7.0 Hz, 2H), 2.31 (dt, *J*=6.9, 2.6 Hz, 2H), 1.94 (t, *J*=2.6 Hz, 1H), 1.78 (pen, *J*= 6.9 Hz, 2H), 1.34 (t, *J*=7.0 Hz, 1H)

Method #2



In a flame dried, round bottom flask, PPh₃ (4.065g, 15.5 mmol, 1.55 eq) was dissolved in THF (90 mL, 0.1M) and cooled to 0°C. DIAD (3.05 mL, 15.5 mmol, 1.55 eq) was then added, and stirred for 30 min. 4-pentyn-1-ol (0.93 mL, 10 mmol, 1.0 eq) and thioacetic acid (1.092 mL, 15.5 mmol, 1.55 eq) in THF (10 mL) were added dropwise. The reaction was then warmed to rt, and stirred for 16h. The reaction was then quenched with sat. NH₄Cl solution, extracted with EtOAc, dried with MgSO₄ and concentrated in vacuo. The resulting crude was then titrated with hexanes to remove triphenylphosphine oxide, and was purified by flash column chromatography (10% EtOAc in Hexanes) to yield **3.9.3** in 60% yield. Characterization data is in accordance with previous literature precedent⁴, as well as the spectral data acquired by an alternate procedure as described above³.

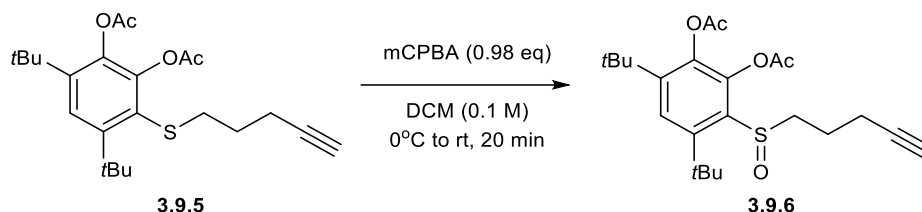
ii) Synthesis of Catechol Ligands for IONP Functionalization



3.9.5: Synthesized according to general procedure C. Purified with silica column chromatography (0.5% then 2% EtOAc in Toluene), 93% yield.

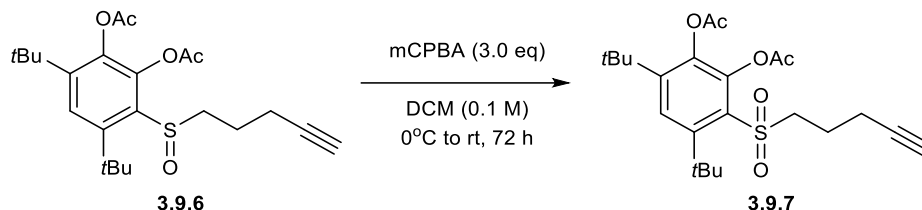
Rf: 0.5 (2% EtOAc in Toluene). **¹H-NMR:** (400 MHz, CDCl₃): 7.40 (s, 1H), 2.93 (t, *J*=7.2 Hz, 2H), 2.34 (s, 3H), 2.33 (s, 3H), 2.33 (tt, *J*=7.2;2.6 Hz, 2H) 1.98 (t, *J*=2.6 Hz, 1H), 1.87 (tt, *J*=7.2;7.2 Hz, 2H), 1.54 (s, 9H), 1.35 (s, 9H). **¹³C-NMR:** (125 MHz, CDCl₃): 168.4, 167.8, 150.7, 146.6, 141.9, 140.2, 126.7, 122.8, 83.3, 69.0, 37.6, 35.7, 35.2, 31.1, 30.2, 28.3, 21.0, 20.8, 17.9.

IR (neat): ν= 2961.04, 1776.81, 1367.61, 1199.28, 1143.14, 1011.96 cm⁻¹. **HRMS (ESI-MS) (m/z):** Calc. for C₂₃H₃₂O₄S: 405.20941, found 405.20890.



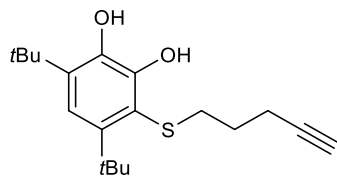
3.9.6: In a flame-dried 25 mL round-bottom flask equipped with a teflon stir-bar and rubber septum, **3.9.5** (0.5 mmol, 1.0 eq) was dissolved in DCM (5 mL, 0.1M), and cooled to 0°C. mCPBA (105.69 mg, 0.49 mmol, 0.98 eq) was added portion-wise and the reaction was stirred for 20 min. The reaction was then diluted with DCM, and treated with saturated aqueous Na₂S₂O₃ solution, sat. NaHCO₃ solution, brine, dried with MgSO₄, and concentrated *in vacuo*. The crude mixture was then purified with silica column chromatography (25% Acetone in Hexanes, then 30% Acetone in Hexanes), to give **3.9.6** in 86% yield.

Rf: 0.4 (30% Acetone in Hexanes). **¹H-NMR:** (400 MHz, CDCl₃): 7.41 (s, 1H), 3.86 (ddd, 1H), 3.00 (ddd, 1H), 2.52-2.39 (m, 2H), 2.33 (s, 3H), 2.30 (s, 3H), 2.20-2.04 (m, 2H), 1.99 (t, *J* = 2.6 Hz, 1H), 1.49 (s, 9H), 1.37 (s, 9H). **¹³C-NMR:** (125 MHz, CDCl₃): 168.4, 167.7, 147.2, 145.4, 144.6, 141.9, 132.5, 122.8, 82.6, 69.7, 49.6, 37.1, 35.5, 32.4, 30.1, 23.6, 20.9, 20.8, 17.5. **IR** (neat): ν = 2962.77, 1784.06, 1367.01, 1195.98, 1144.33, 1012.55, 894.21 cm⁻¹. **HRMS (ESI-MS) (m/z):** Calc. for C₂₃H₃₃O₅S: 421.20432, found 421.20404.



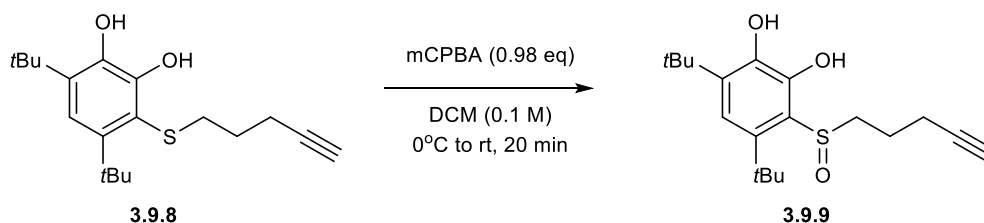
3.9.7: In a flame-dried 25 mL round-bottom flask equipped with a teflon stir-bar and rubber septum, **3.9.6** was dissolved in DCM, and cooled to 0°C. mCPBA (3.0 eq) was added portion-wise and the reaction warmed to rt and stirred for 3 days. The reaction was then diluted with DCM, and treated with saturated aqueous Na₂S₂O₃ solution, sat. NaHCO₃ solution, brine, dried with MgSO₄, and concentrated *in vacuo*. The crude mixture was then purified with silica column chromatography (15% Acetone in Hexanes), to give **3.22** in 95% yield.

Rf: 0.5 (15% Acetone in Hexanes). **¹H-NMR:** (400 MHz, CDCl₃): 7.64 (s, 1H), 3.55 (t, *J* = 7.6 Hz, 2H), 2.40 (dt, *J* = 6.9, 2.8 Hz, 2H), 2.34 (s, 3H), 2.33 (s, 3H), 2.02 (t, *J* = 2.6 Hz, 1H), 1.60 (s, 9H), 1.38 (s, 9H). **¹³C-NMR:** (125 MHz, CDCl₃): 168.1, 167.0, 149.6, 146.9, 143.9, 141.3, 131.8, 125.2, 82.2, 70.0, 56.3, 37.9, 35.7, 32.7, 29.9, 21.3, 20.9, 20.8, 17.5. **IR:** (neat) ν = 2961.1, 1787.7, 1366.3, 1192.2, 1150.9, 1010.9, 862.1, 633.0 cm⁻¹. **HRMS (ESI-MS) (m/z):** Calc. for C₂₃H₃₂O₆NaS: 459.18118, found 459.18081.



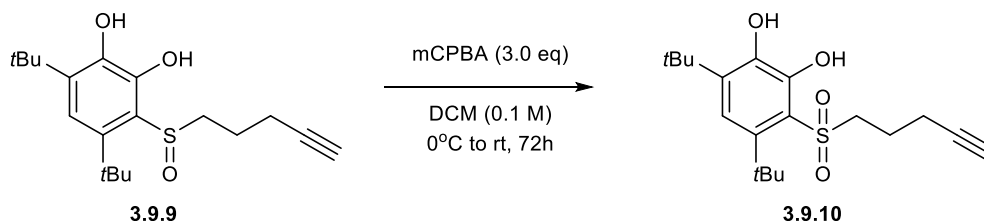
3.9.8: Synthesized according to general procedure C, with modifications: No Ac₂O/DMAP. Purified with silica column chromatography (4:2 Hexanes:Toluene), 93% yield.

R_f: 0.4. **¹H-NMR:** (400 MHz, CDCl₃): 6.93 (s, 1H), 2.81 (t, *J*=7.4 Hz, 2H), 2.38 (dt, *J*= 6.9, 2.6 Hz, 2H), 2.02 (t, *J*=2.6 Hz, 1H), 1.91 (tt, *J*= 7.4, 6.9 Hz, 2H), 1.51 (s, 9H), 1.43 (s, 9H). **¹³C-NMR:** (125 MHz, CDCl₃): 145.3, 143.2, 140.6, 136.0, 116.0, 115.2, 82.8, 69.5, 50.9, 36.8, 36.2, 35.1, 31.5, 29.3, 27.8, 17.8. **IR:** ν = 3545.2, 3306.1, 2954.5, 2867.9, 1606.5, 1563.9, 1483.6, 1394.3, 1361.5, 1288.6, 1235.1, 961.0, 865.9, 846.4, 634.4 cm⁻¹. **HRMS (m/z):** Calc. for C₁₉H₂₇O₂S: 319.1737, found 319.1737.



3.9.9: In a flame-dried 25 mL round-bottom flask equipped with a teflon stir-bar and rubber septum, catechol **3.9.8** was dissolved in DCM, and cooled to 0°C. mCPBA (0.98 eq) was added portion-wise and the reaction was stirred for 20 min. The reaction was then diluted with DCM, and treated with saturated aqueous Na₂S₂O₃ solution, sat. NaHCO₃ solution, brine, dried with MgSO₄, and concentrated *in vacuo*. The crude mixture was then purified with silica column chromatography (25% Acetone in Hexanes, then 30% Acetone in Hexanes), to give **3.9.9** in 80% yield.

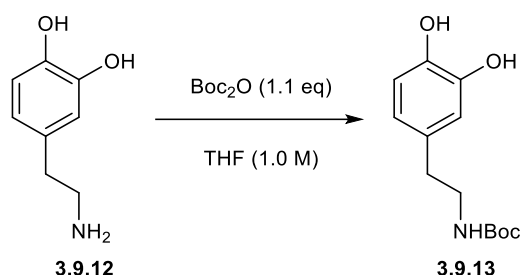
R_f: 0.4. **¹H-NMR:** (500 MHz, CDCl₃): 6.88 (s, 1H), 6.15 (s, 1H), 3.69 (ddd, *J*= 13.7, 8.2, 5.3 Hz, 1H), 3.14 (ddd, *J*= 13.7, 8.1, 8.1 Hz, 1H), 2.54-2.41 (m, 2H), 2.23-2.11 (m, 2H), 2.01 (t, *J*= 2.7 Hz, 1H), 1.42 (s, 9H), 1.41 (s, 9H). **¹³C-NMR:** (125 MHz, CDCl₃): 148.4, 143.3, 138.0, 137.9, 119.1, 115.5, 82.2, 70.0, 50.7, 36.2, 35.2, 32.5, 29.1, 23.1, 17.4. **IR (neat):** **HRMS (m/z):** Calc. for C₁₉H₂₇O₃S: 335.1686, found 335.1678.



3.9.10: In a flame-dried 25 mL round-bottom flask equipped with a teflon stir-bar and rubber septum, **3.9.9** (0.4 mmol, 1.0 eq) was dissolved in DCM (4 mL, 1.0 eq), and cooled to 0°C. mCPBA (207.084 mg, 1.2 mmol, 3.0 eq) was added portion-wise and the reaction warmed to rt

and stirred for 3 days. The reaction was then diluted with DCM, and treated with saturated aqueous Na₂S₂O₃ solution, sat. NaHCO₃ solution, brine, dried with MgSO₄, and concentrated *in vacuo*. The crude mixture was then purified with silica column chromatography (15% Acetone in Hexanes), to give **3.9.10** in 90% yield.

R_f: 0.5 (15% Acetone in Hexanes). **¹H-NMR**: (400 MHz, CDCl₃): 6.57 (s, 1H), 3.57 (t, *J*=7.6 Hz, 2H), 2.46 (dt, *J*= 6.7, 2.7 Hz, 2H), 2.18 (tt, *J*= 7.6, 6.7 Hz), 2.05 (t, *J*= 2.7 Hz, 1H), 1.45 (s, 9H), 1.28 (s, 9H). **¹³C-NMR**: (125 MHz, CDCl₃): 160.7, 159.7, 158.7, 149.3, 135.2, 126.5, 81.7, 70.4, 55.5, 38.3, 37.0, 30.7, 28.7, 20.3, 17.4. **IR (neat)**: ν= 2961.24, 1759.2, 1366.8, 1320.4, 1152.6, 1128.3, 976.9, 645.0 cm⁻¹.



3.9.13: In a flame-dried 100 mL round bottom flask equipped with a Teflon stir-bar and rubber septum, dopamine hydrochloride (500 mg, 2.636 mmol, 1 eq) was dissolved in THF (2 mL). 4.0 mL of saturated aqueous NaHCO₃ solution was then added to the reaction mixture with a syringe. Di-tert-butyl-dicarbonate (0.67 mL, 2.90 mmol, 1.1 eq) was then added with a syringe, and the reaction was stirred for 2h. The reaction mixture was then extracted with EtOAc (3 x 20 mL), washed with brine, and dried with MgSO₄ to yield the product in 98% yield. Product **3.9.13** was used without further purification. Characterization data obtained is in accordance with previously published literature spectra⁵.

¹H-NMR (500 MHz, CDCl₃): 6.81 (d, *J*=7.9 Hz, 1H), 6.72 (d, *J*=1.8 Hz, 1H), 6.60 (d, *J*=7.9 Hz, 1H), 5.89 (brs, 2H), 4.63 (brs, 1H), 3.34 (dd, *J*=7.9, 5.4 Hz, 2H), 2.68 (t, *J*=7.9 Hz, 2H), 1.46 (s, 9H)

7. References:

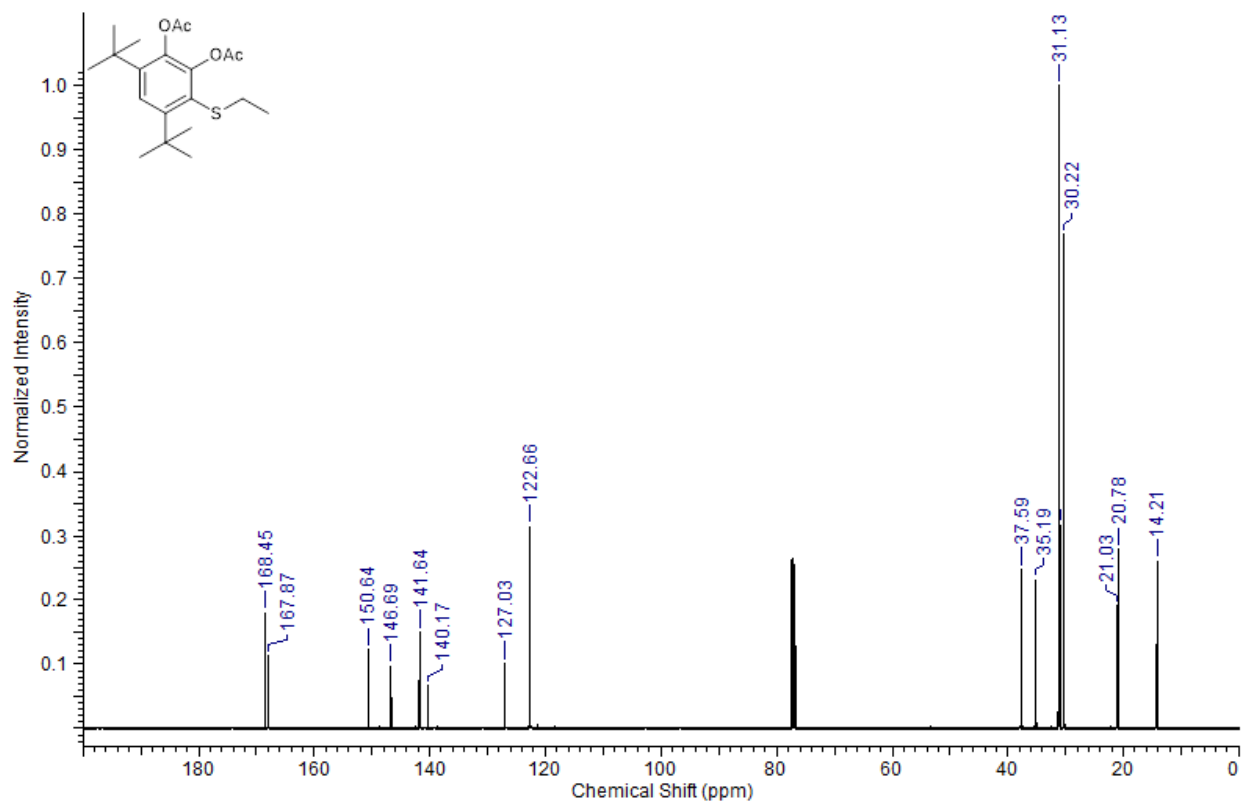
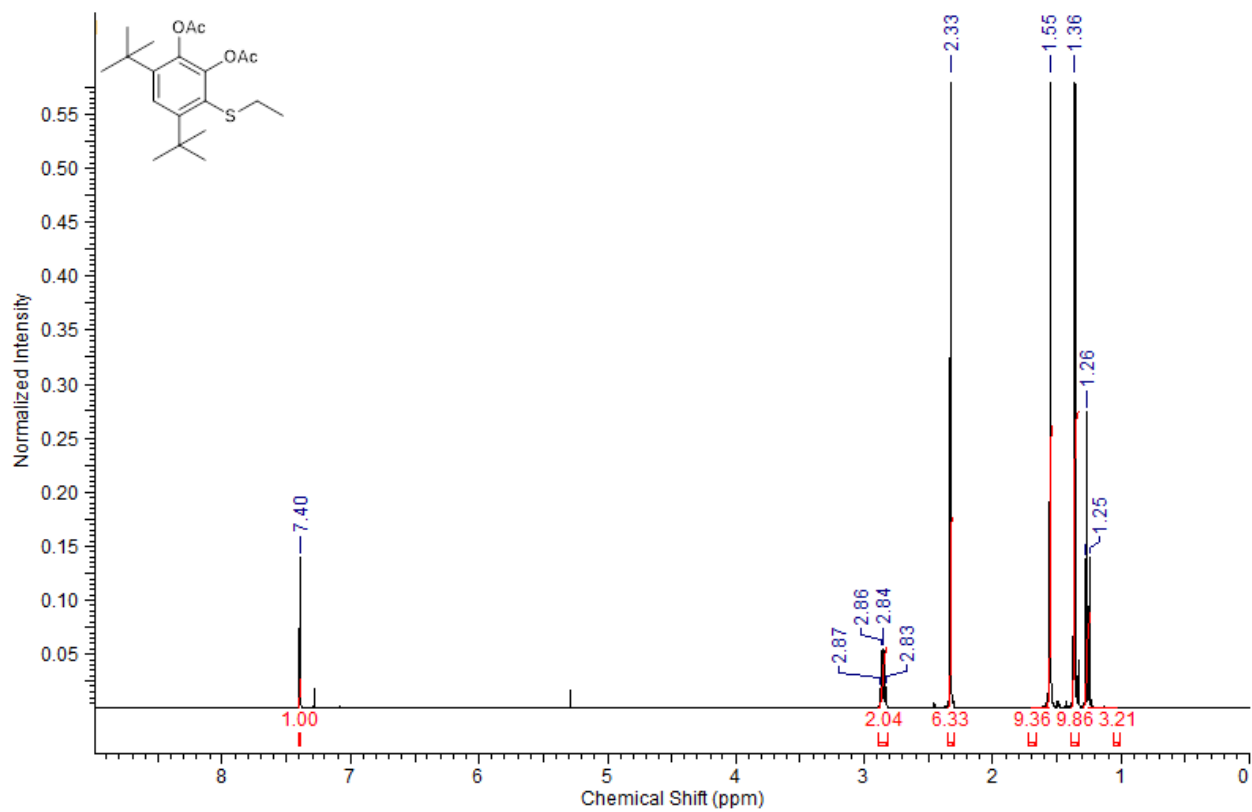
1. Esguerra, K. V. N.; Fall, Y.; Lumb, J.-P. A Biomimetic Catalytic Aerobic Functionalization of Phenols. *Angew. Chem.* **2014**, *126* (23), 5987-5991.
2. Huang, Z.; Kwon, O.; Esguerra, K. V. N.; Lumb, J.-P. A divergent and selective synthesis of ortho- and para-quinones from phenols. *Tetrahedron* **2015**, *71* (35), 5871-5885.
3. Journet, M.; Rouillard, A.; Cai, D.; Larsen, R. D. Double Radical Cyclization/ β -Fragmentation of Acyclic ω -Yne Vinyl Sulfides. Synthesis of 3-Vinyldihydrothiophene and Dihydrothiopyran Derivatives. A New Example of a 5-endo-trig Radical Cyclization. *J. Org. Chem.* **1997**, *62* (25), 8630-8631.
4. Yaqub, M.; Walsh, J. J.; Keyes, T. E.; Proust, A.; Rinfray, C.; Izzet, G.; McCormac, T.; Forster, R. J. Electron Transfer to Covalently Immobilized Keggin Polyoxotungstates on Gold. *Langmuir* **2014**, *30* (15), 4509-4516.

5. Nemoto, H.; Nishiyama, T.; Akai, S. Nucleophilic Deoxyfluorination of Catechols. *Org. Lett.* **2011**, *13* (10), 2714-2717.

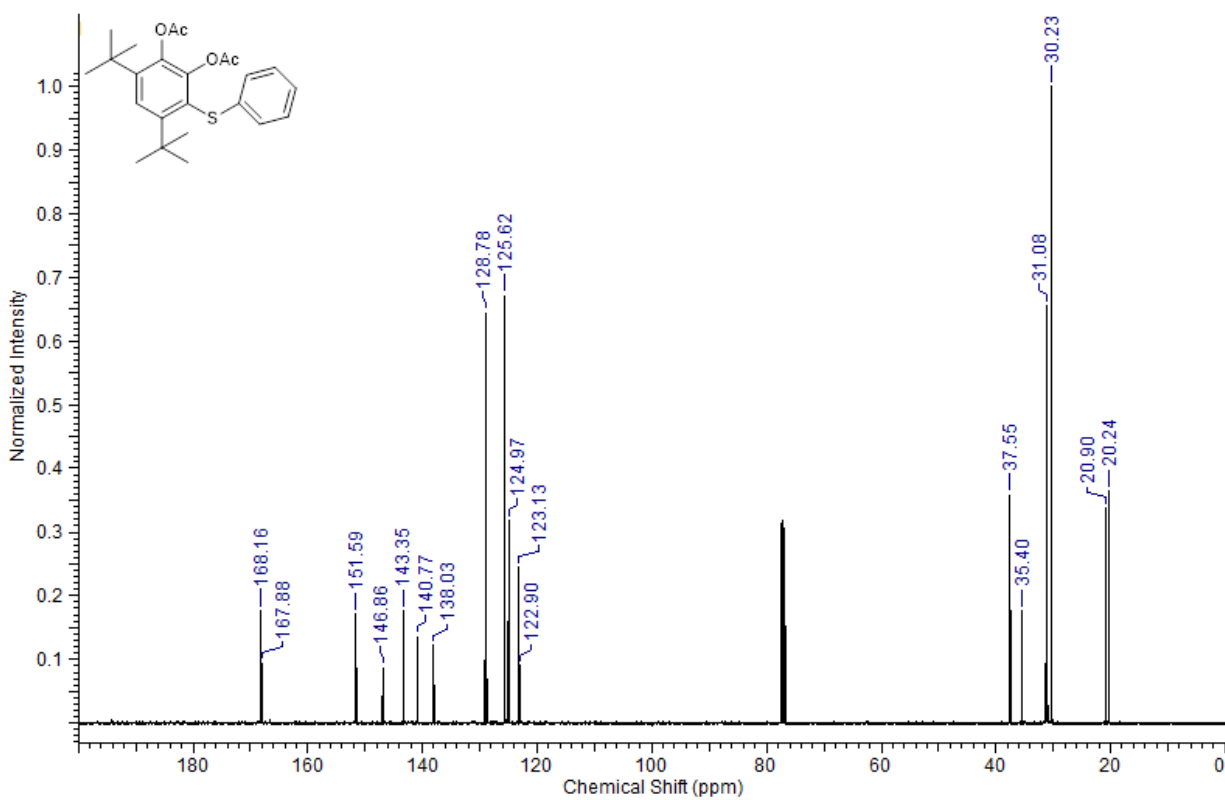
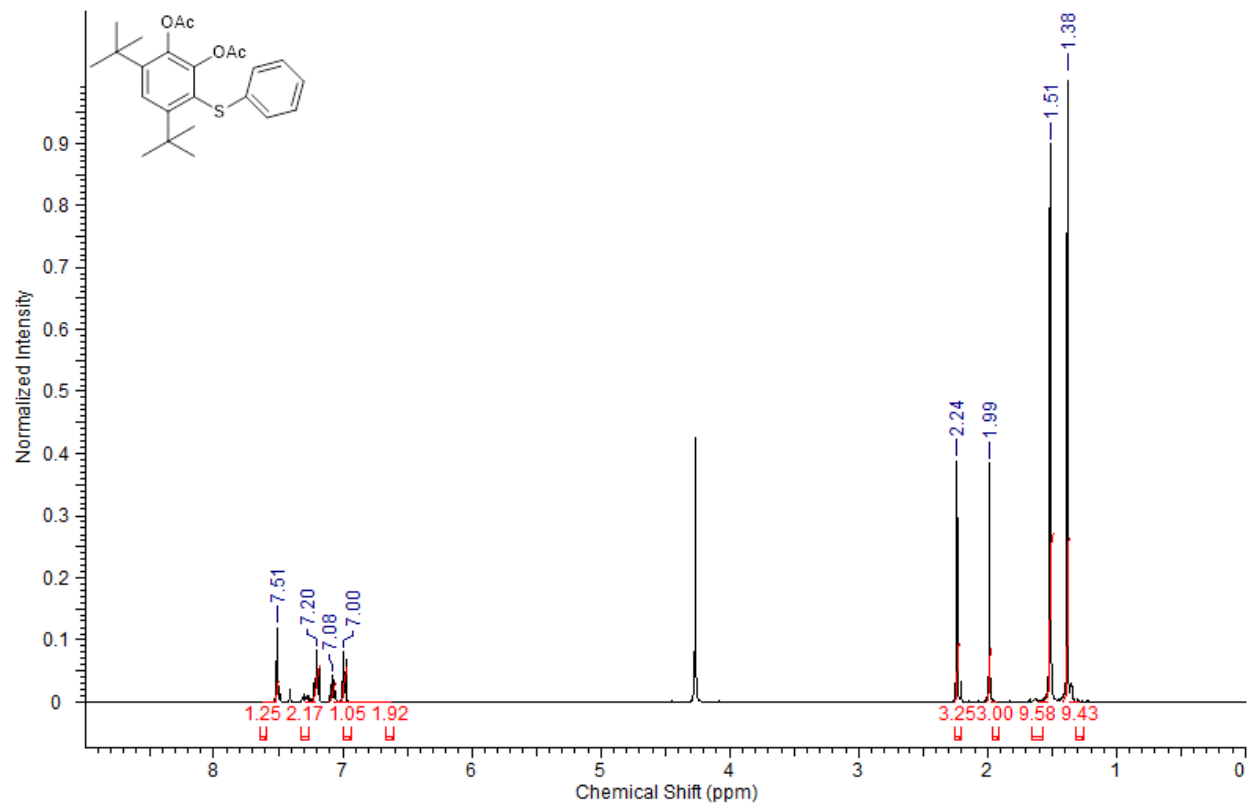
A2: Spectral Data

a) Substrates in Table 3.3.1:

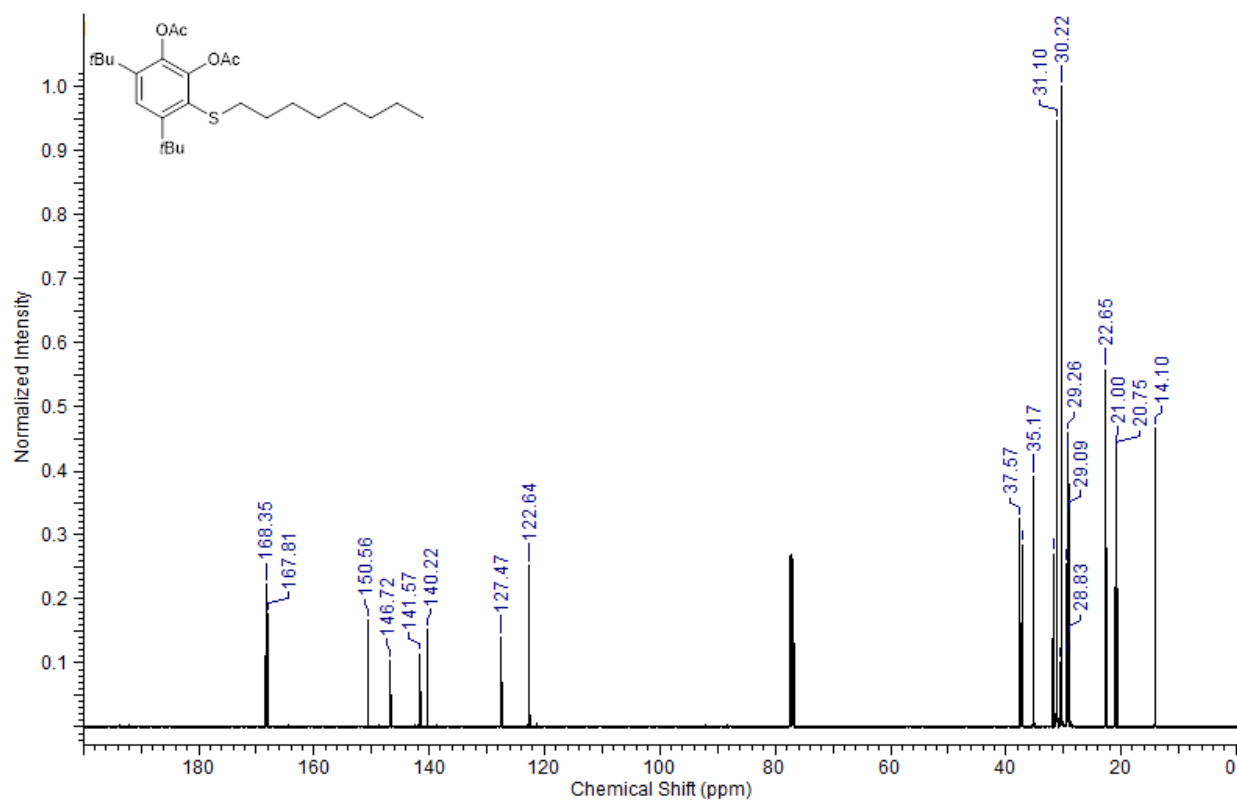
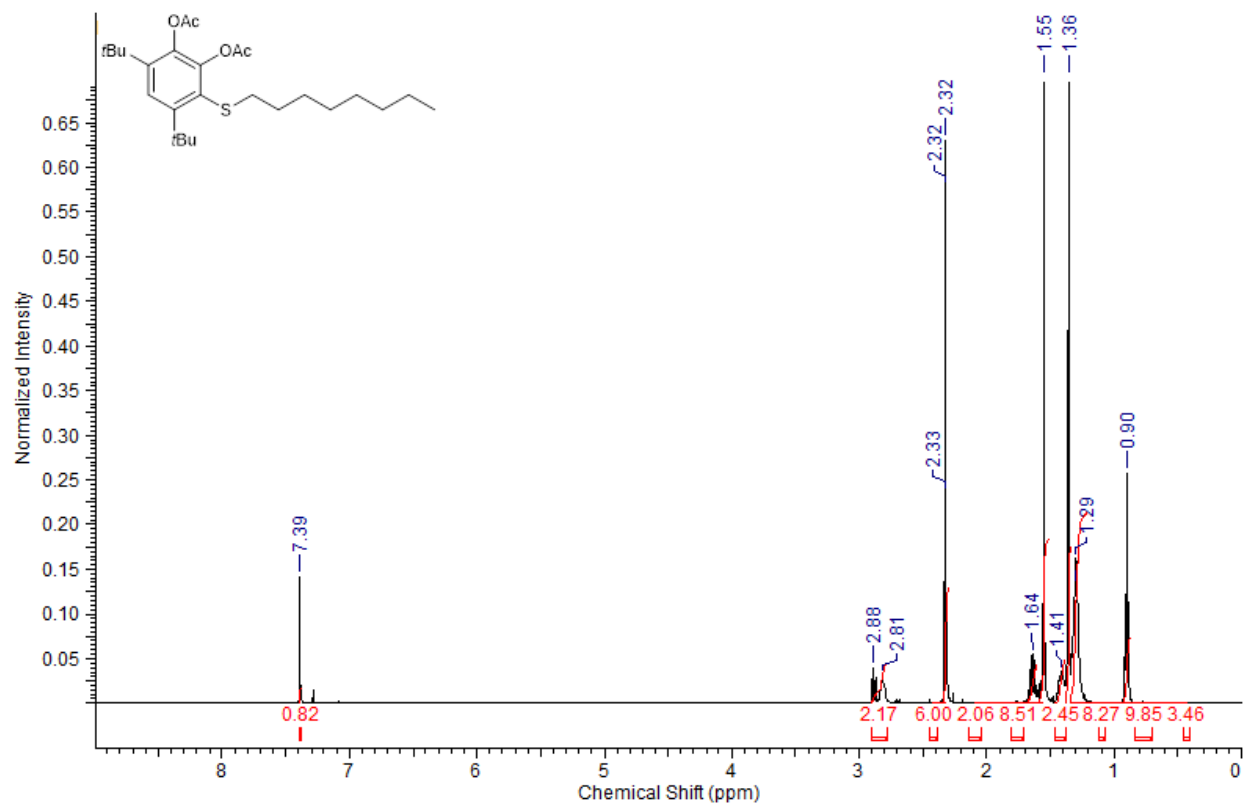
3.2.4:



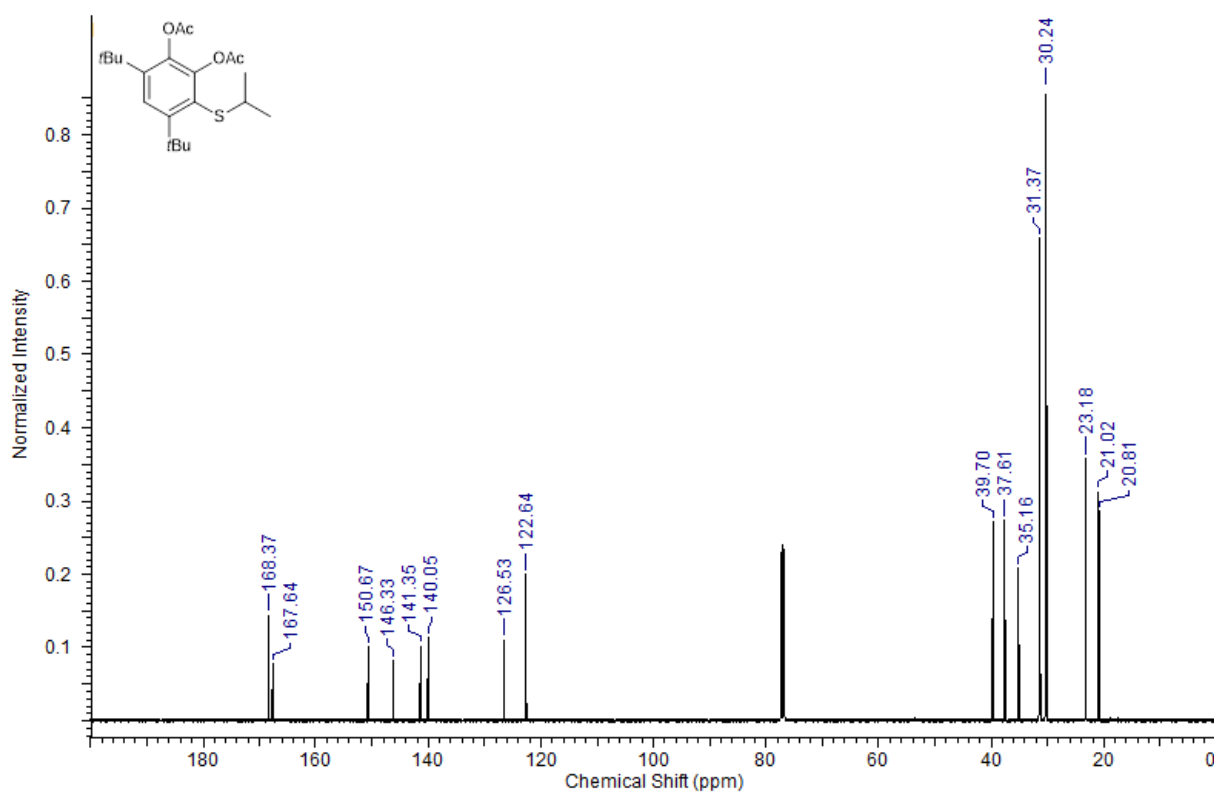
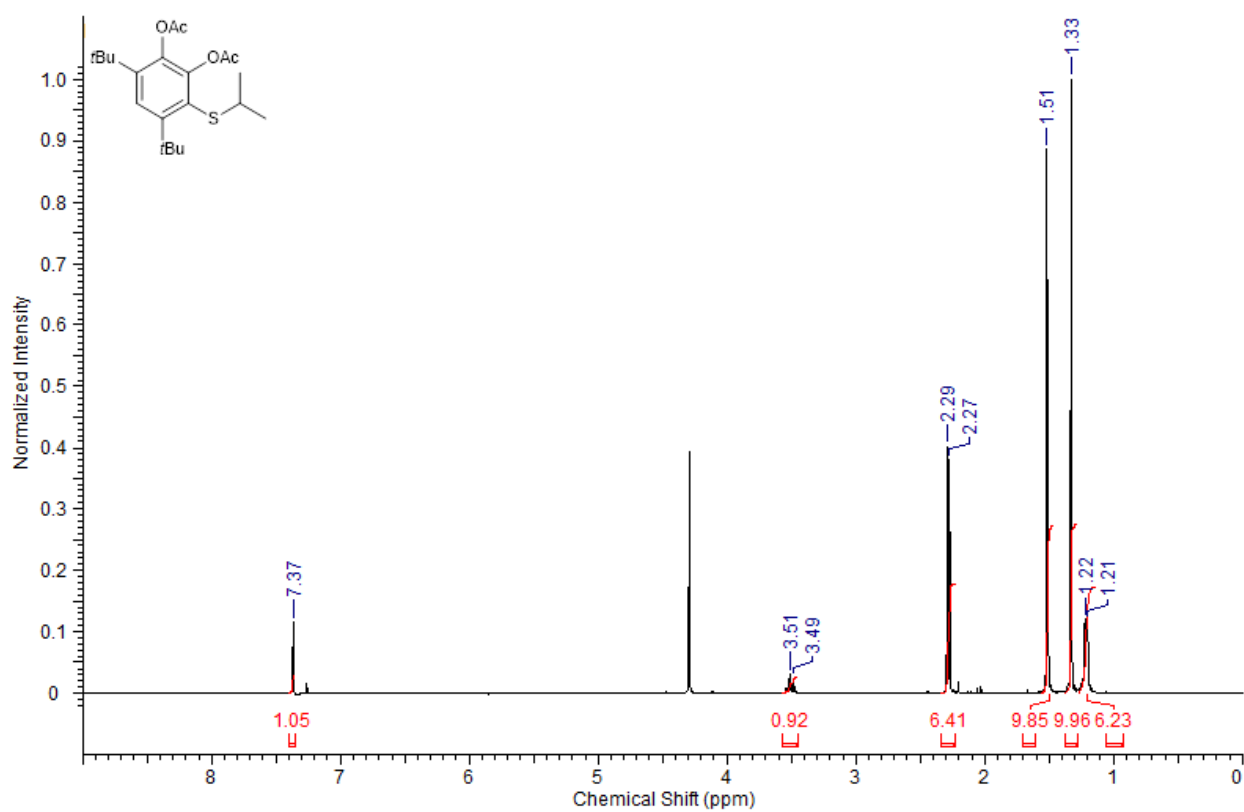
3.2.5:



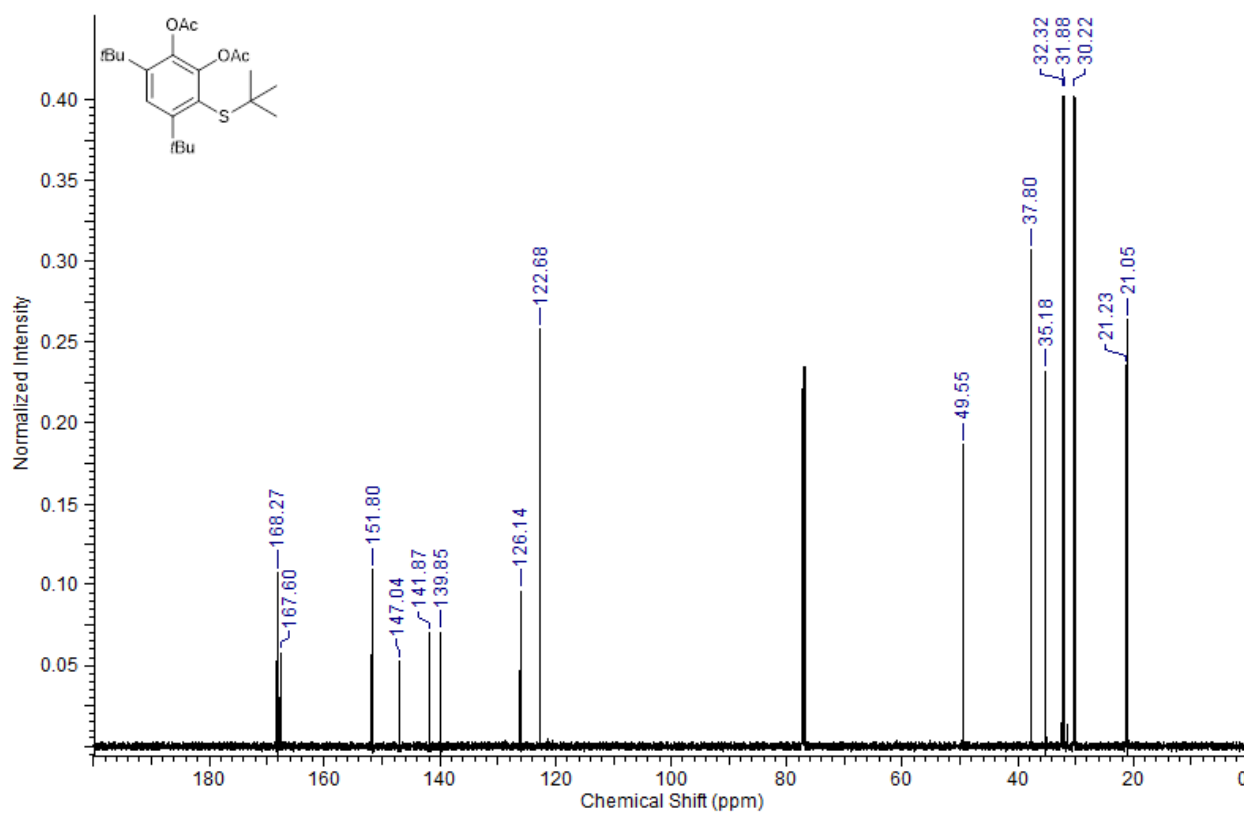
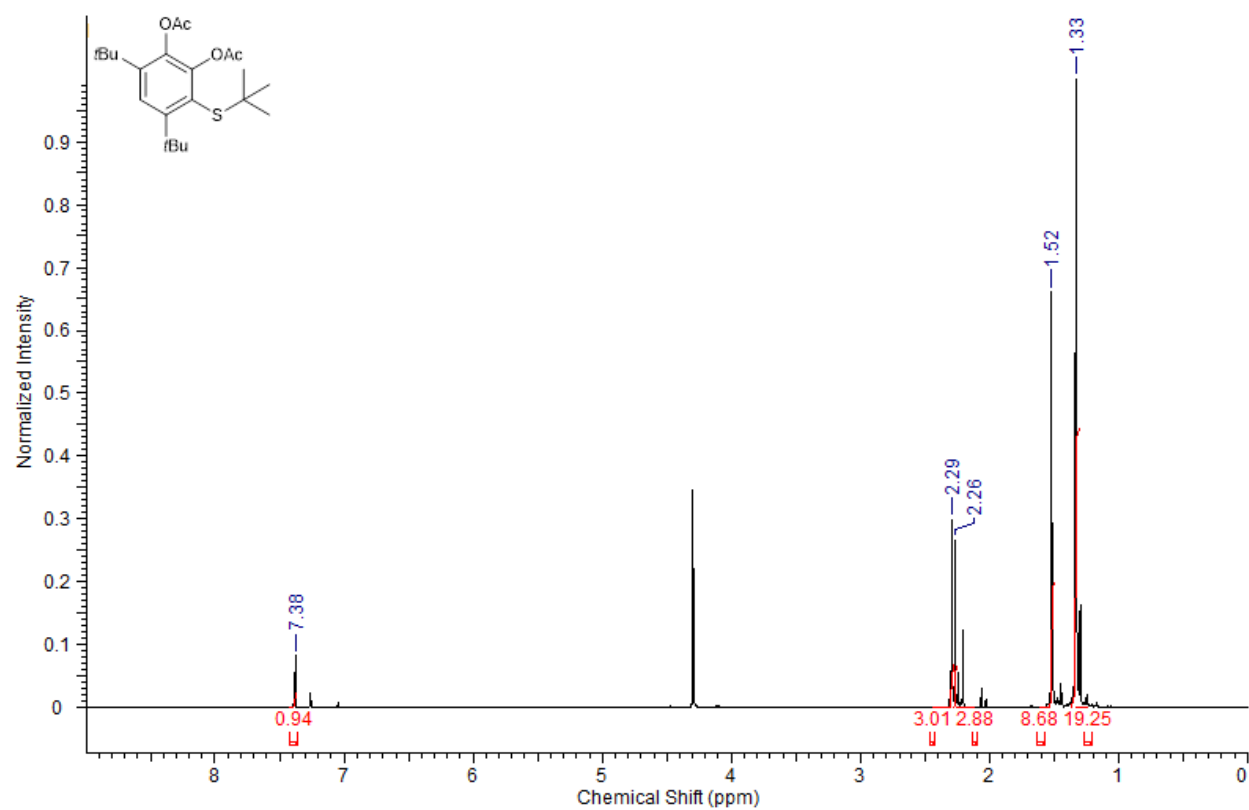
3.2.6:



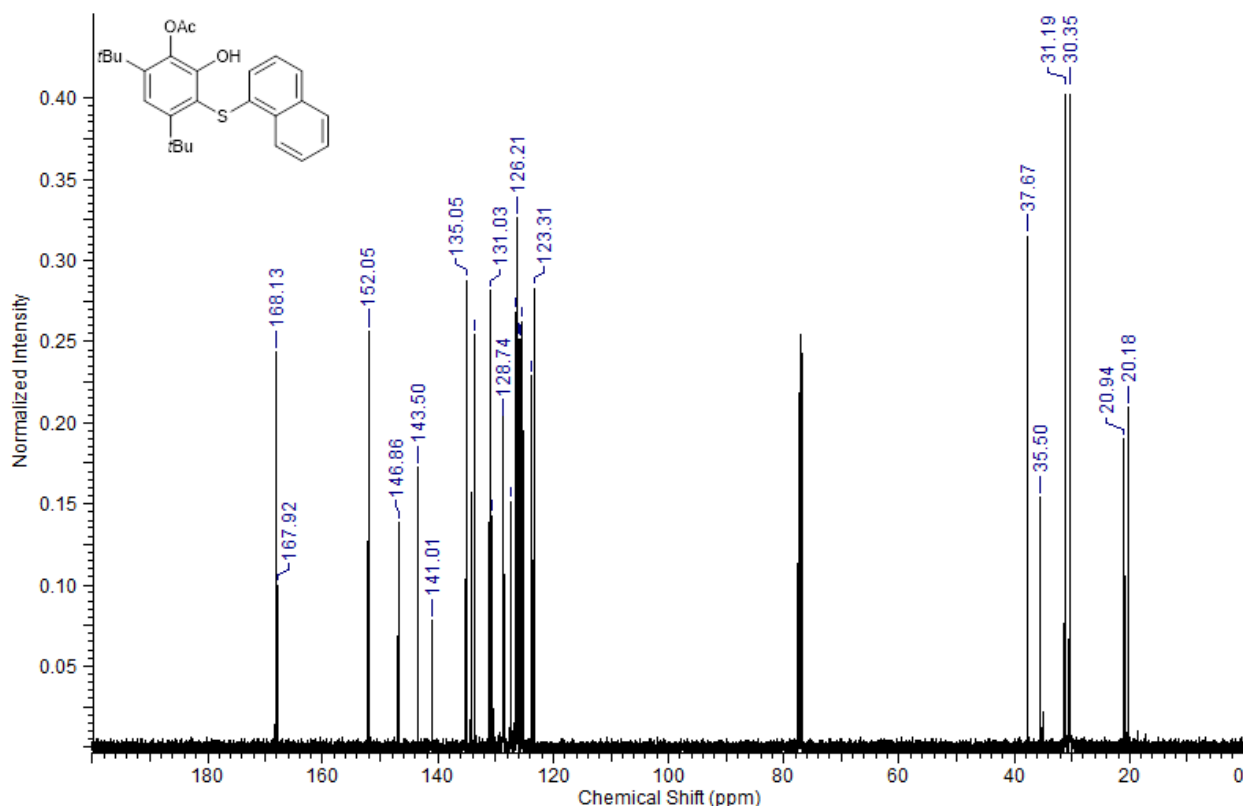
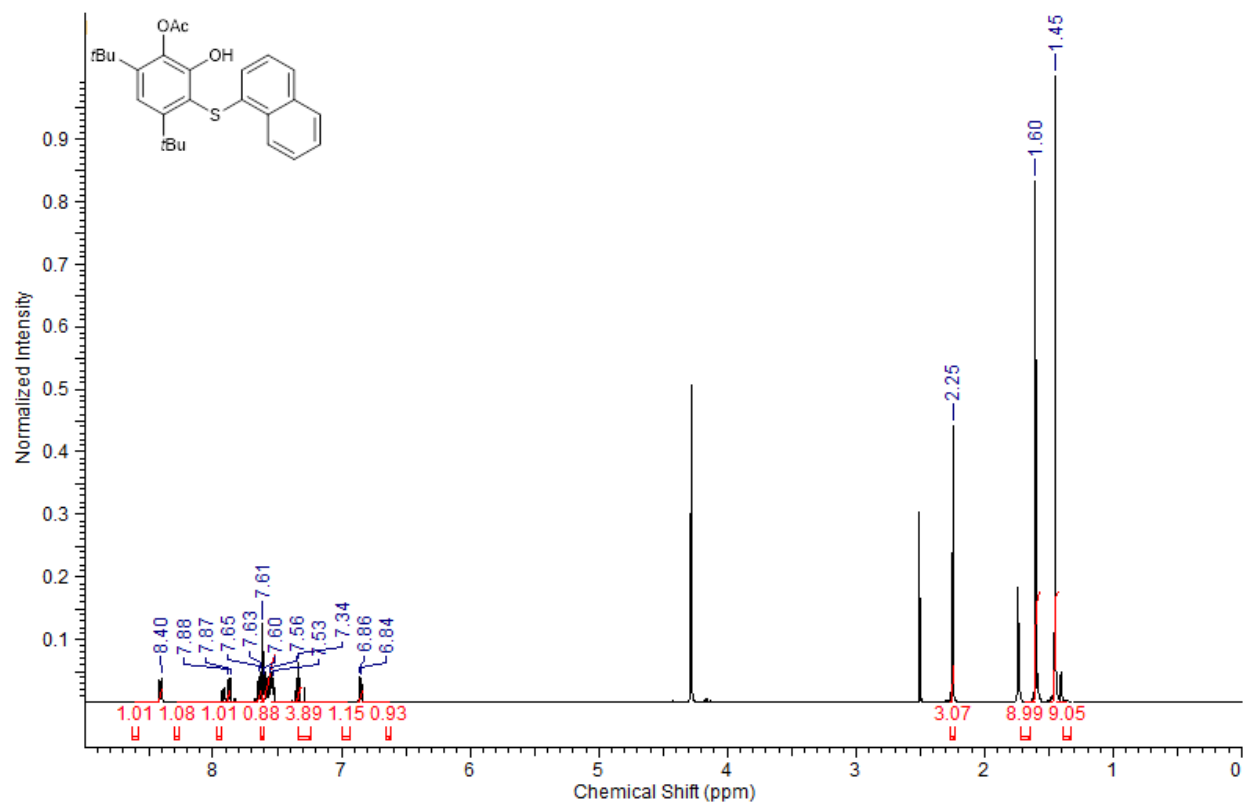
3.2.7:



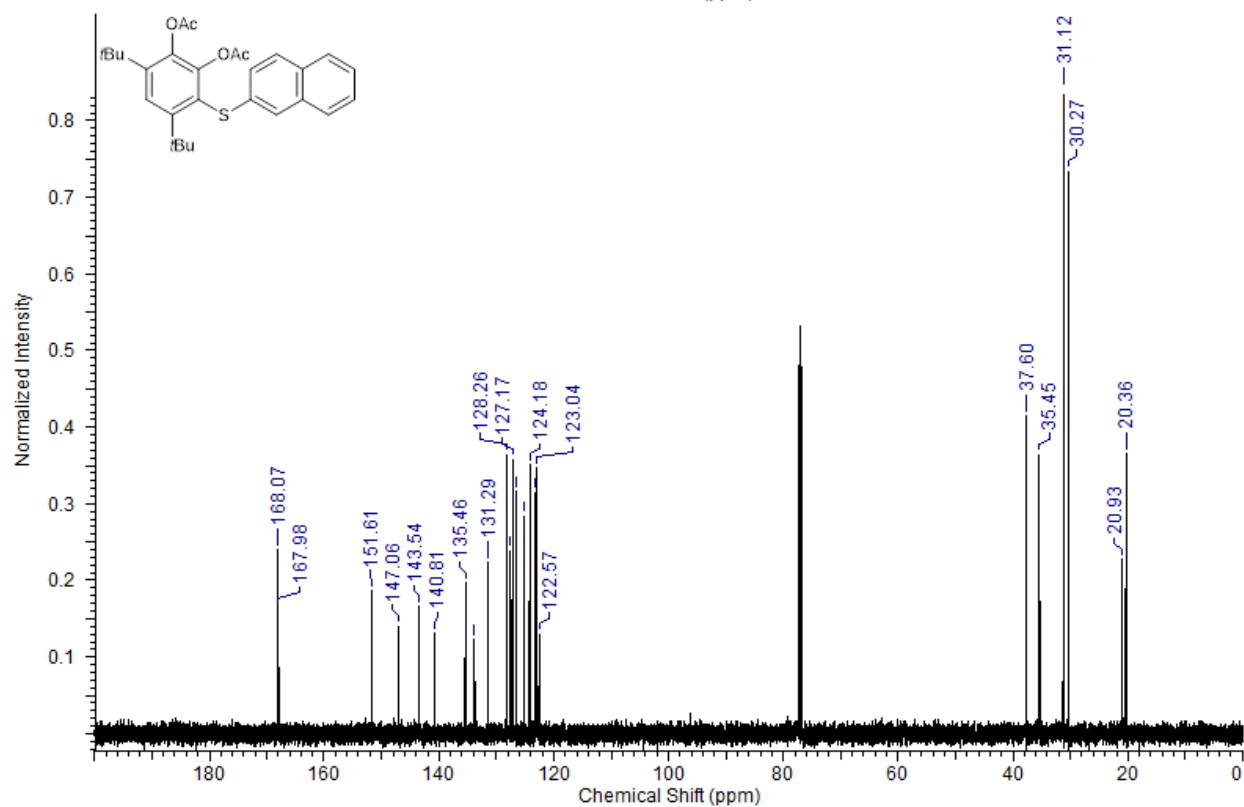
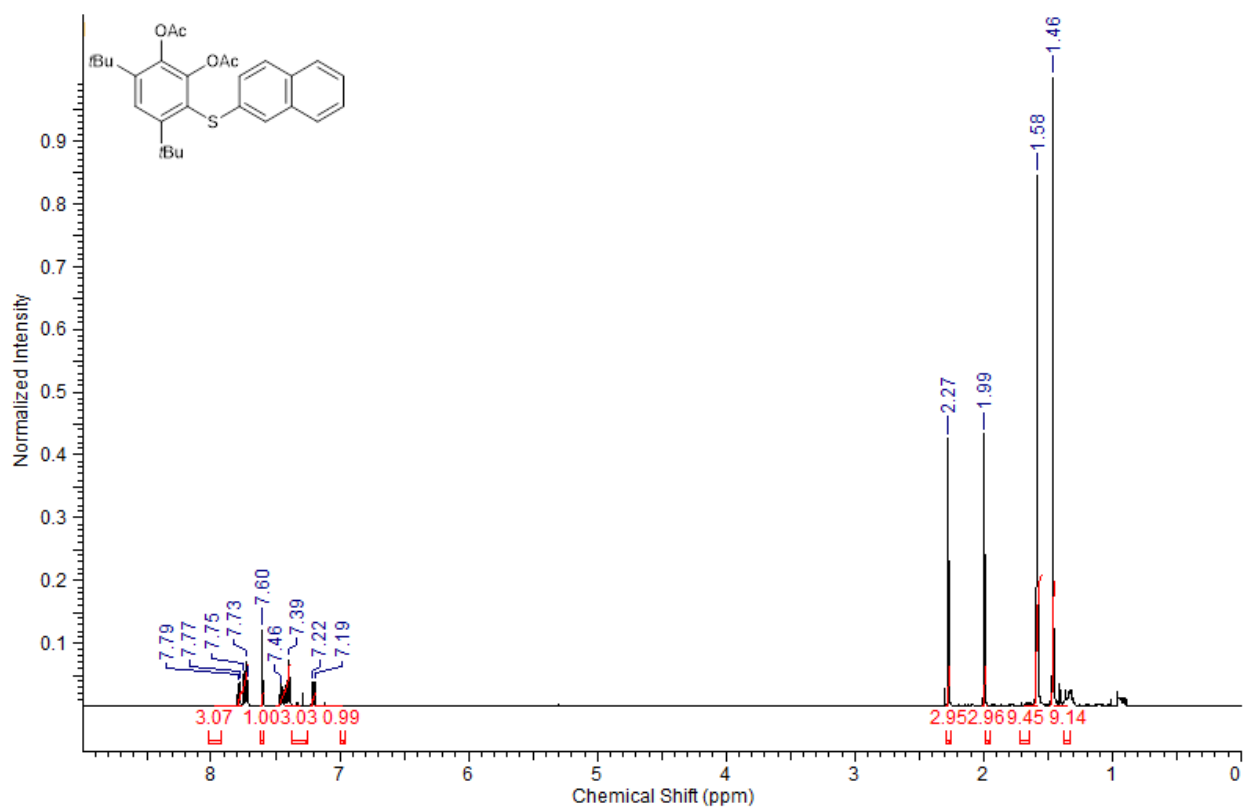
3.2.8:



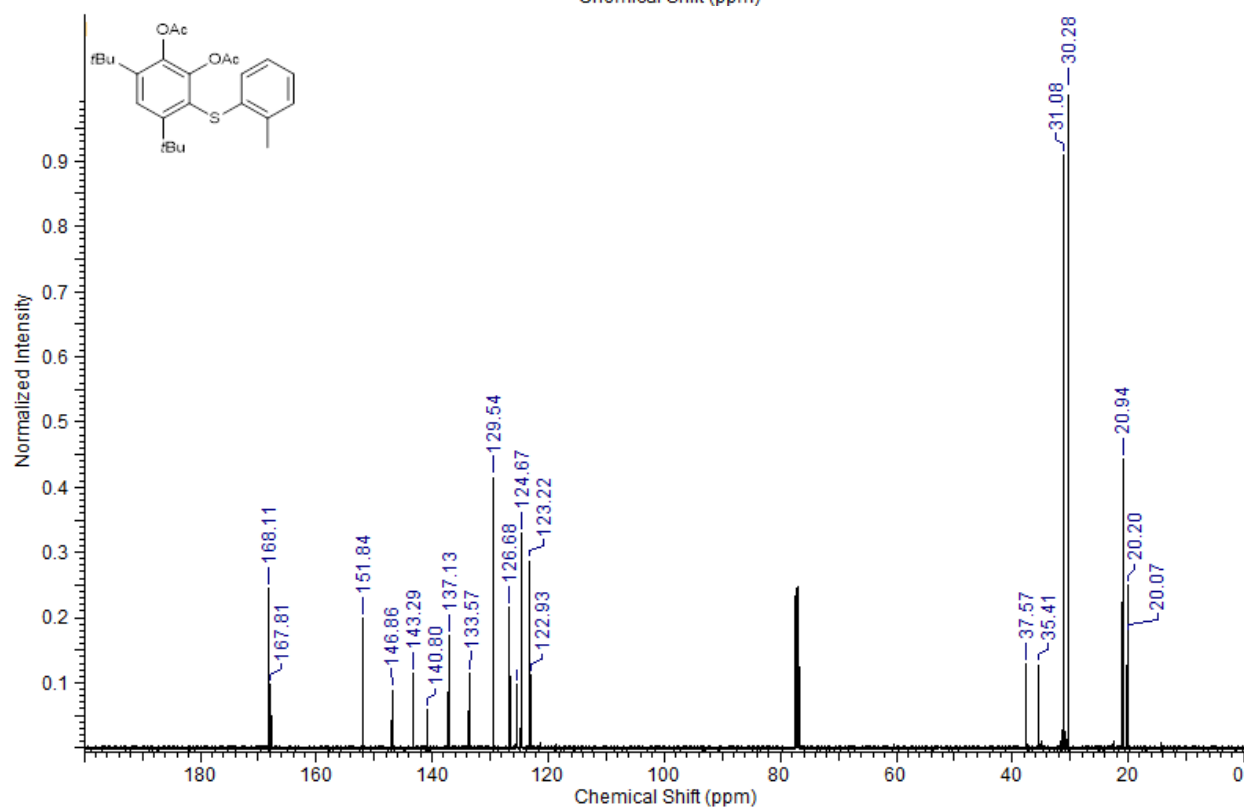
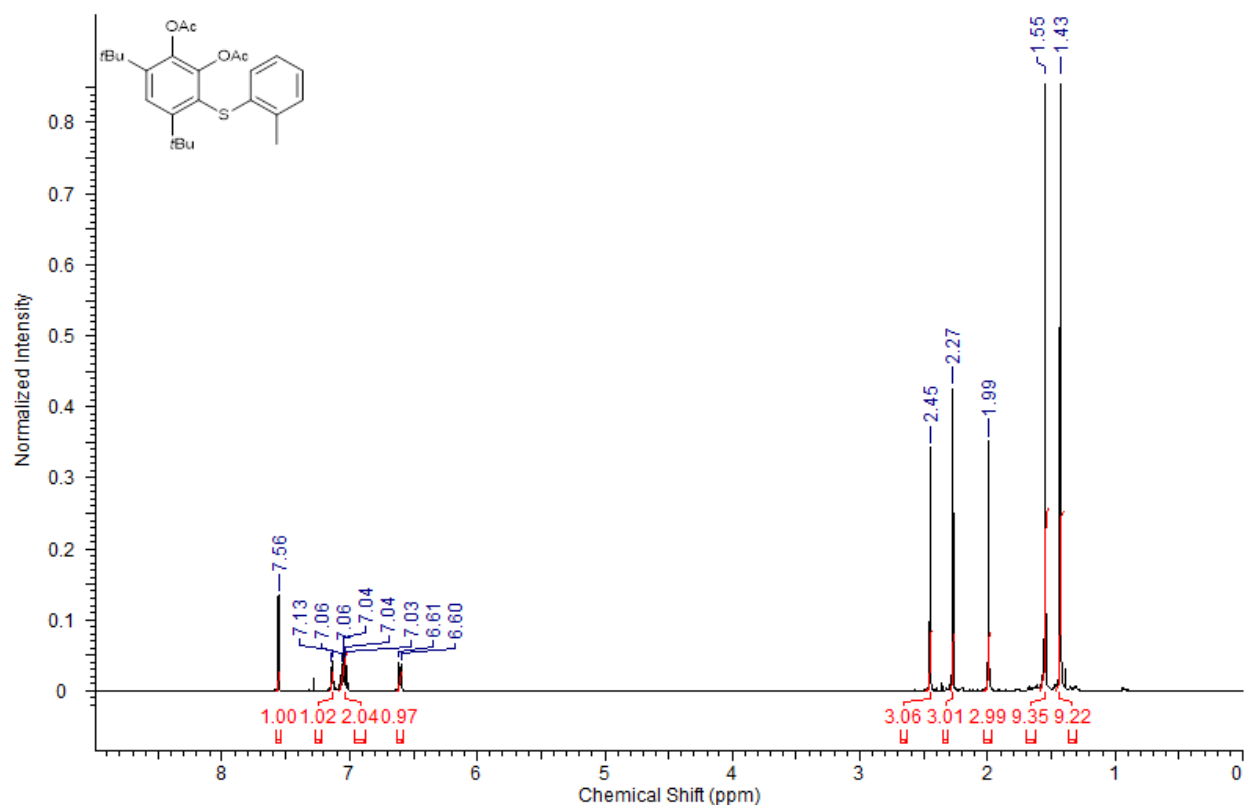
3.2.9:



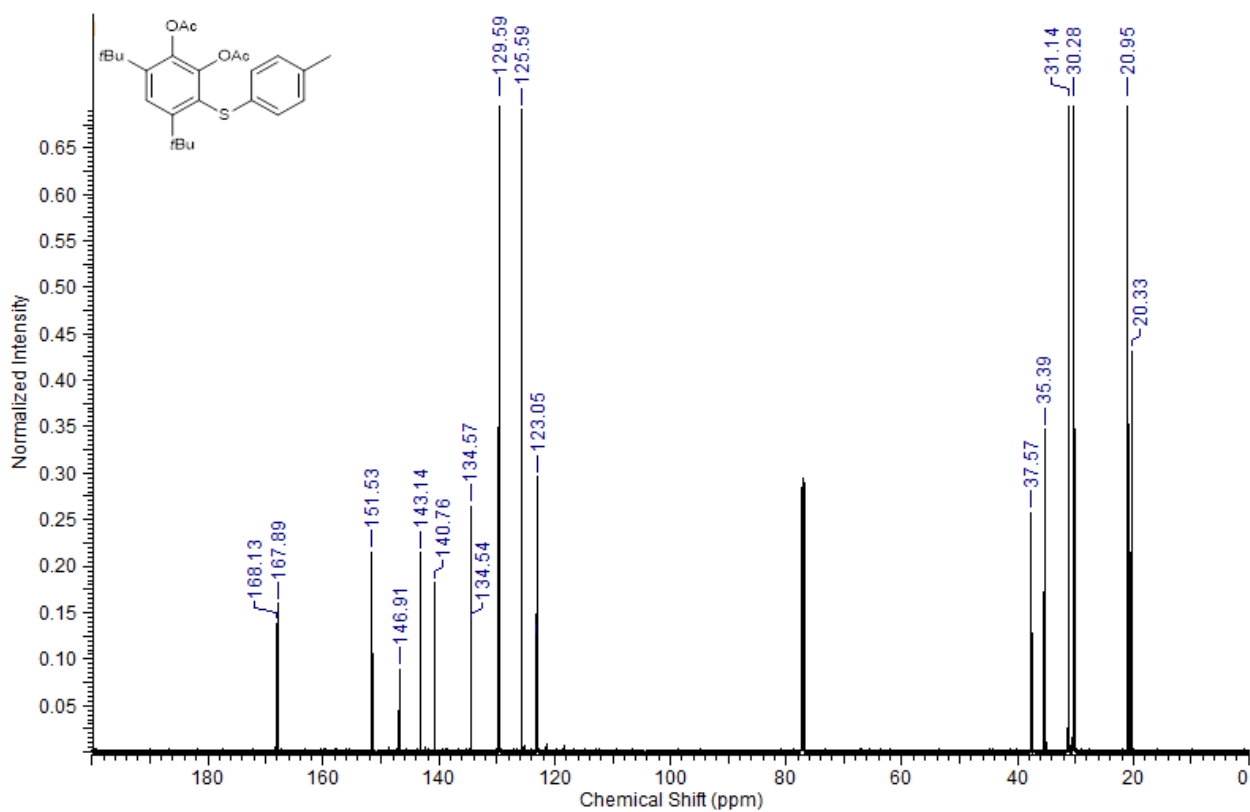
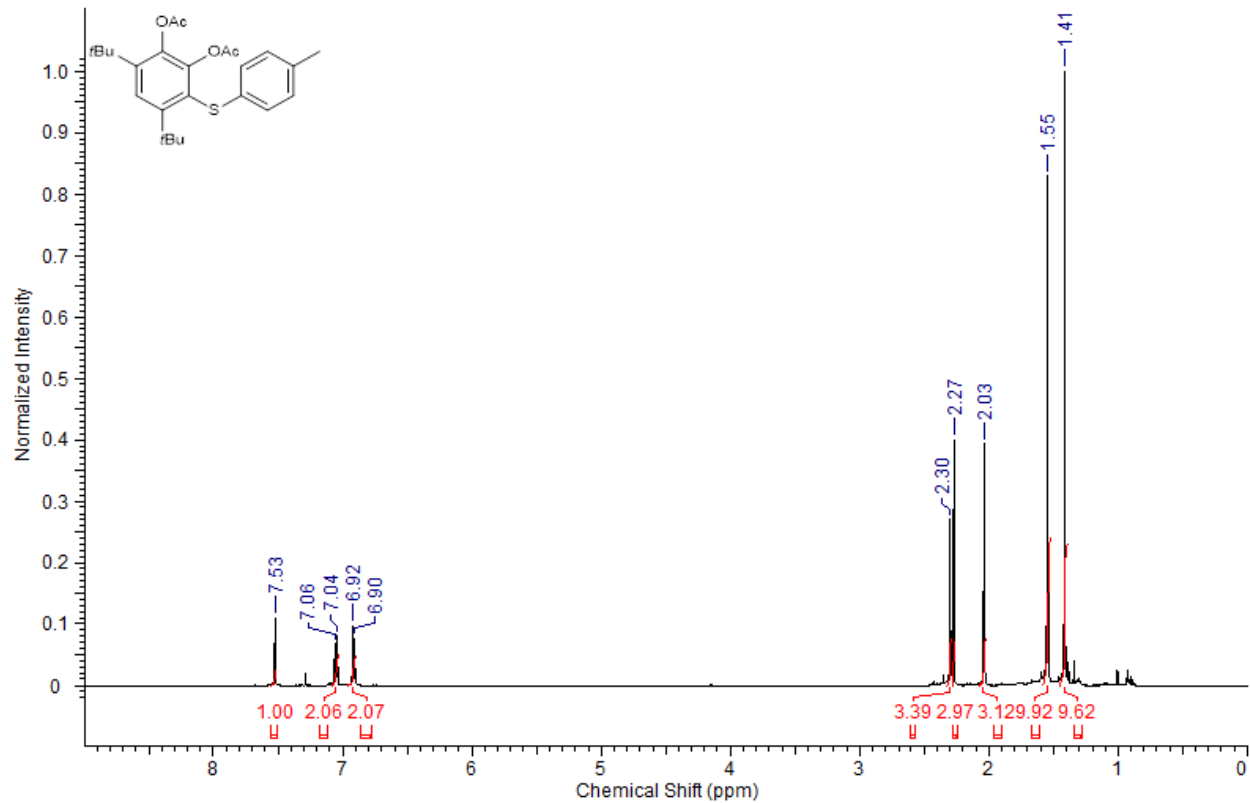
3.2.10:



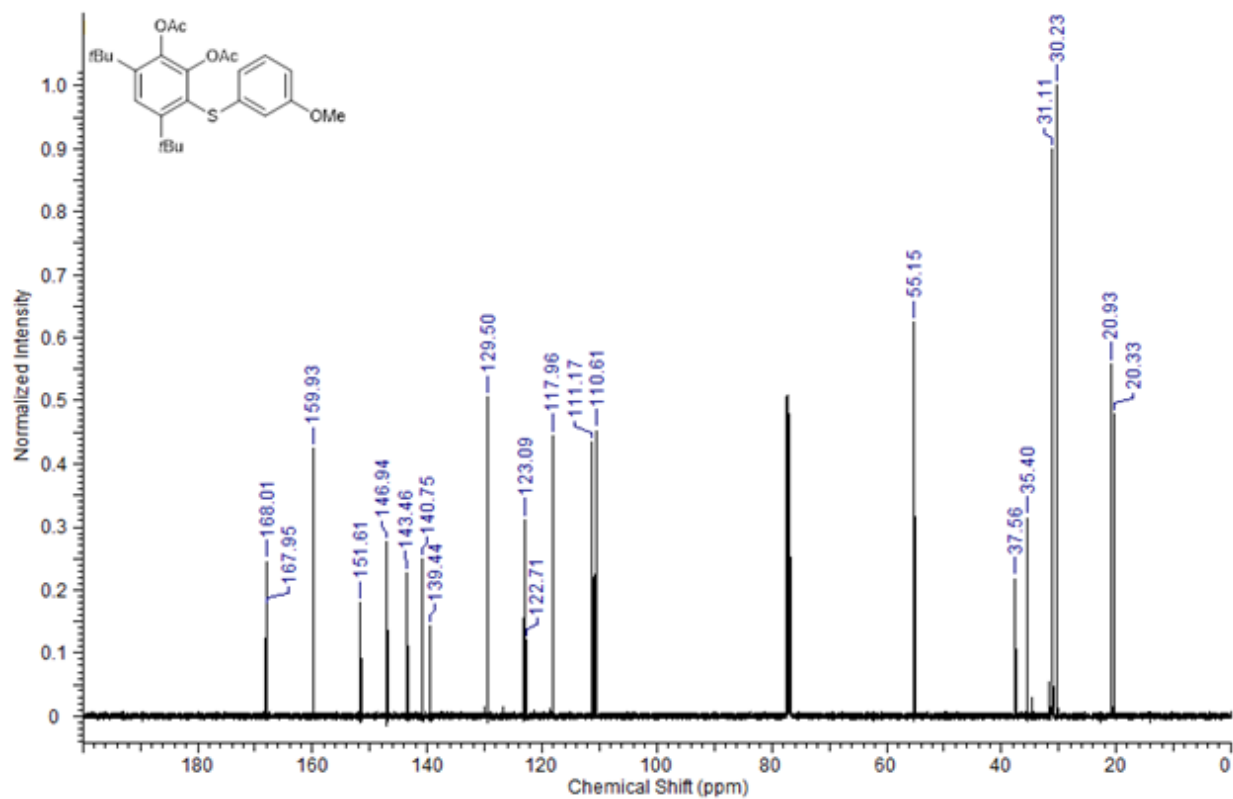
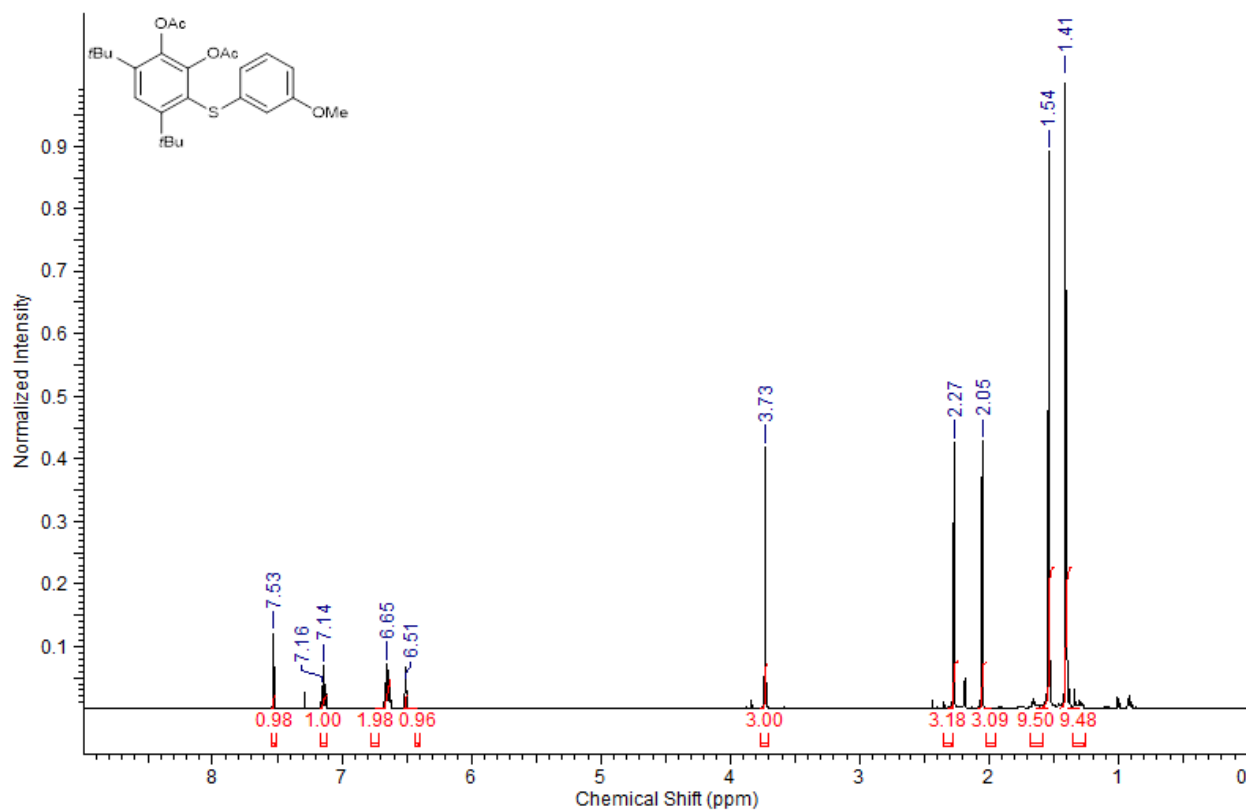
3.2.11:



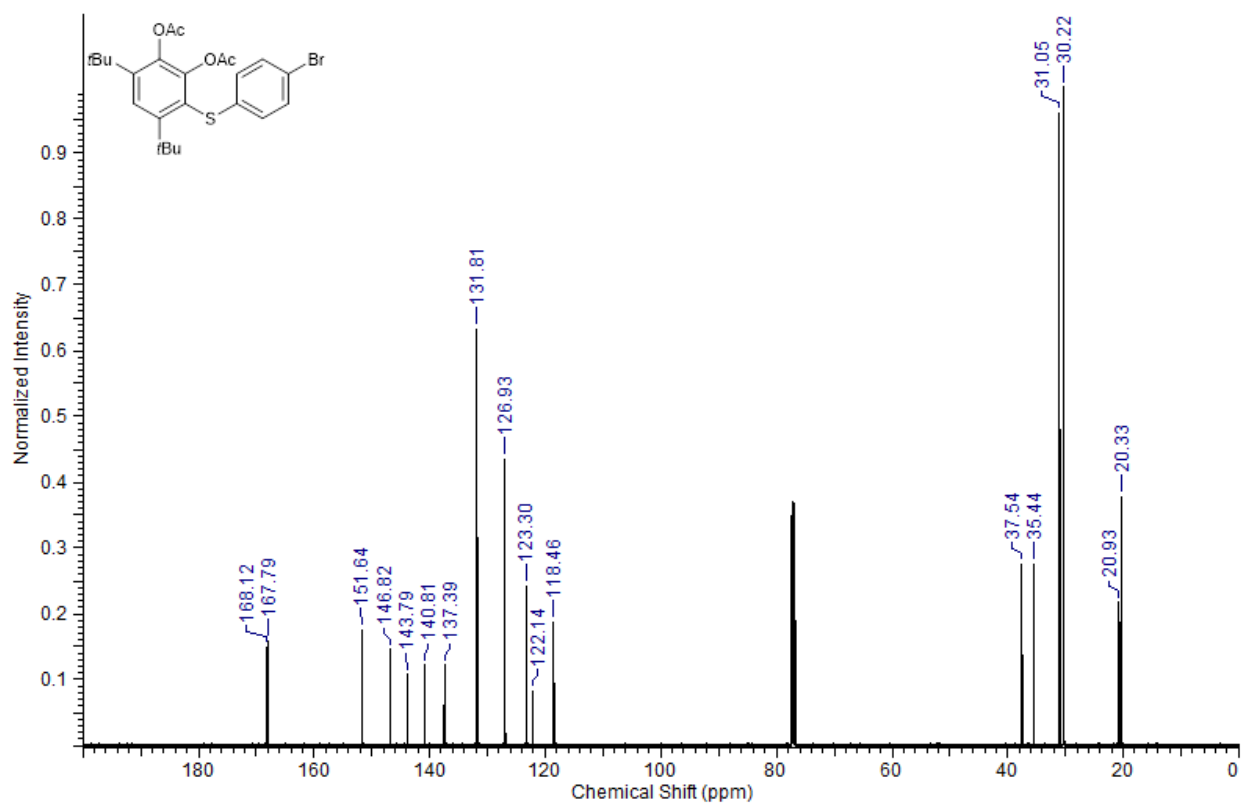
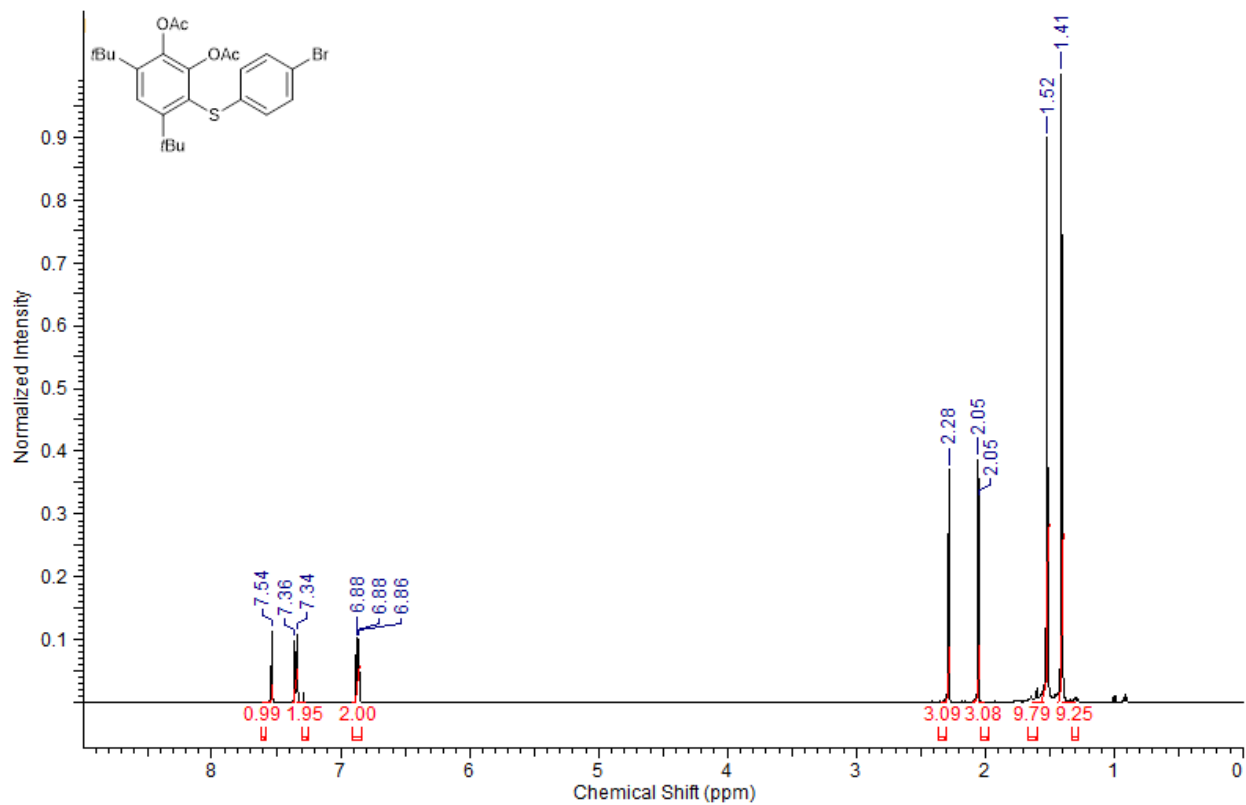
3.2.12:



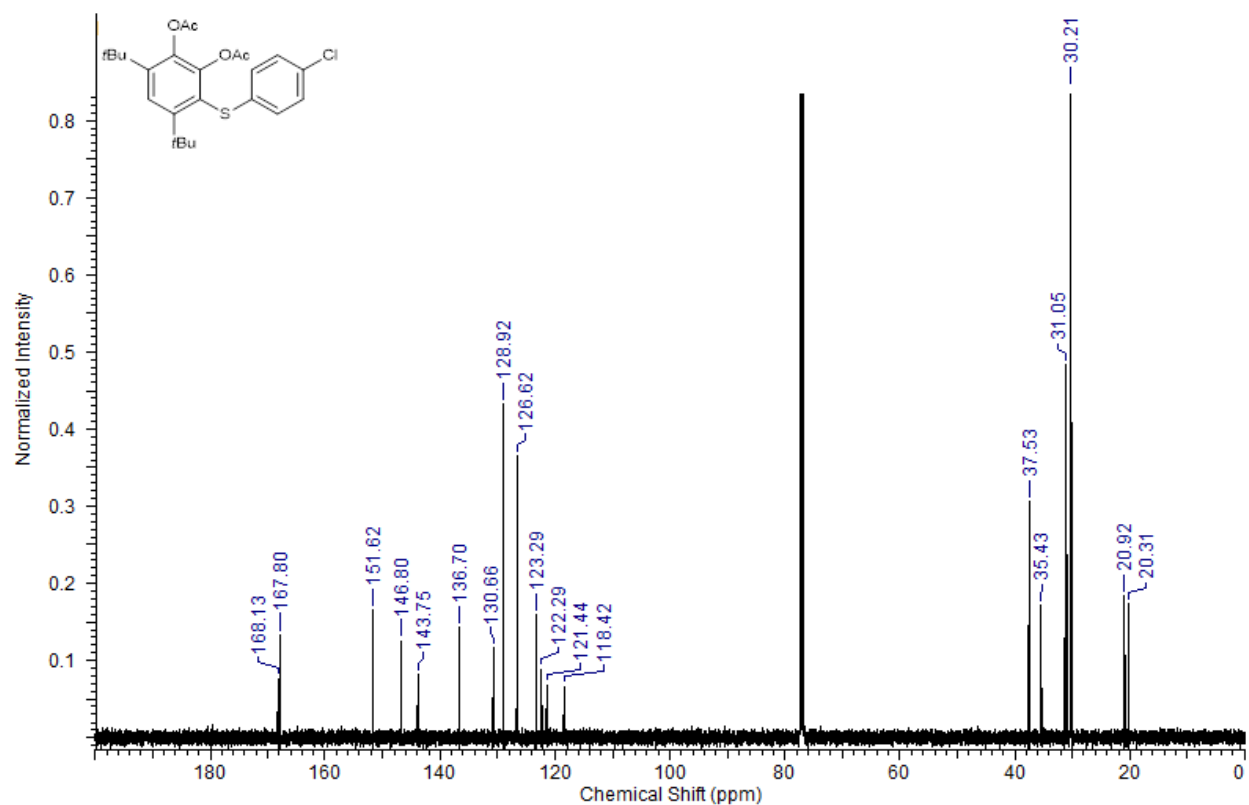
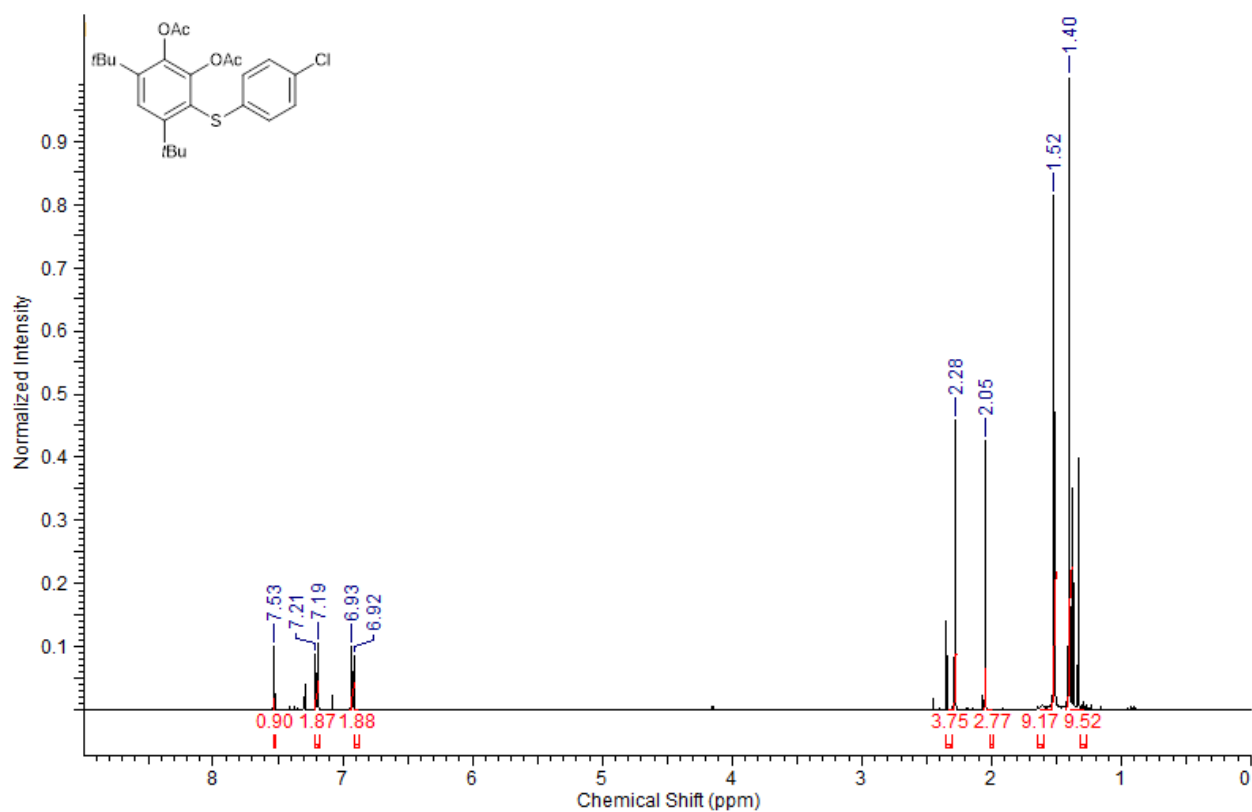
3.2.13:



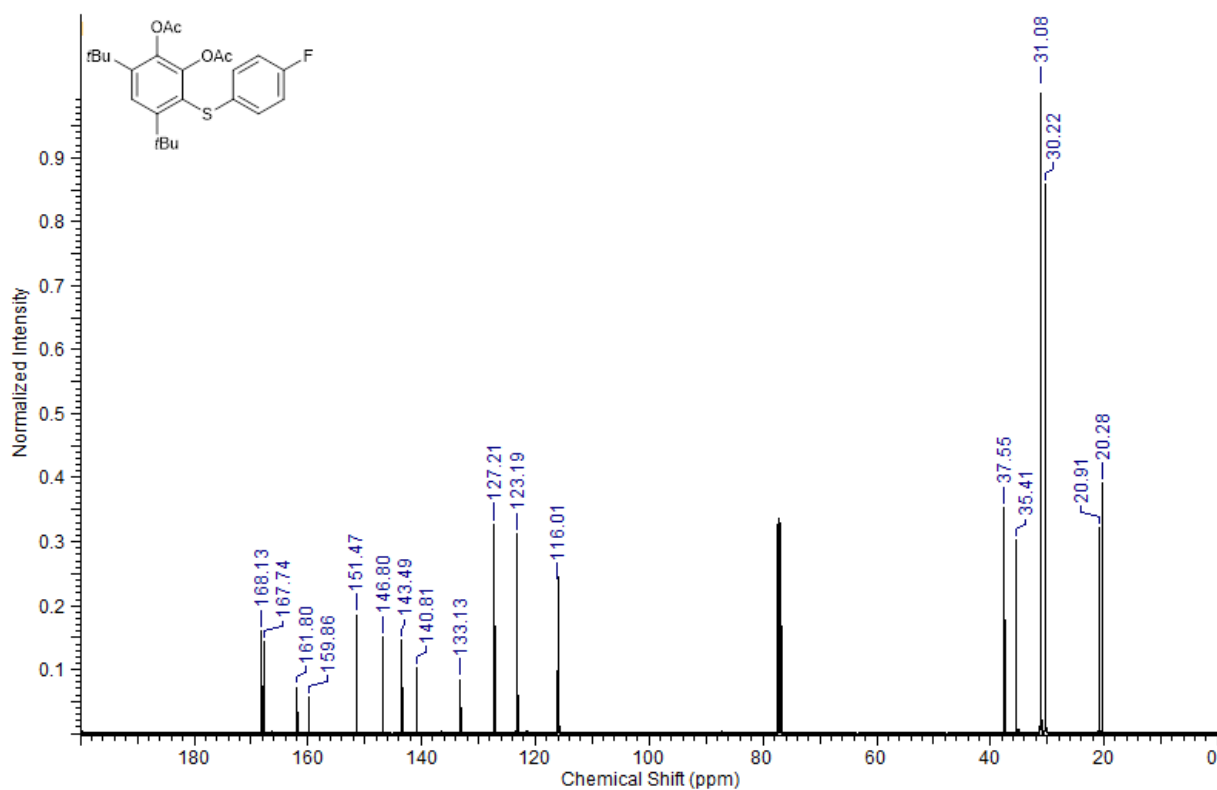
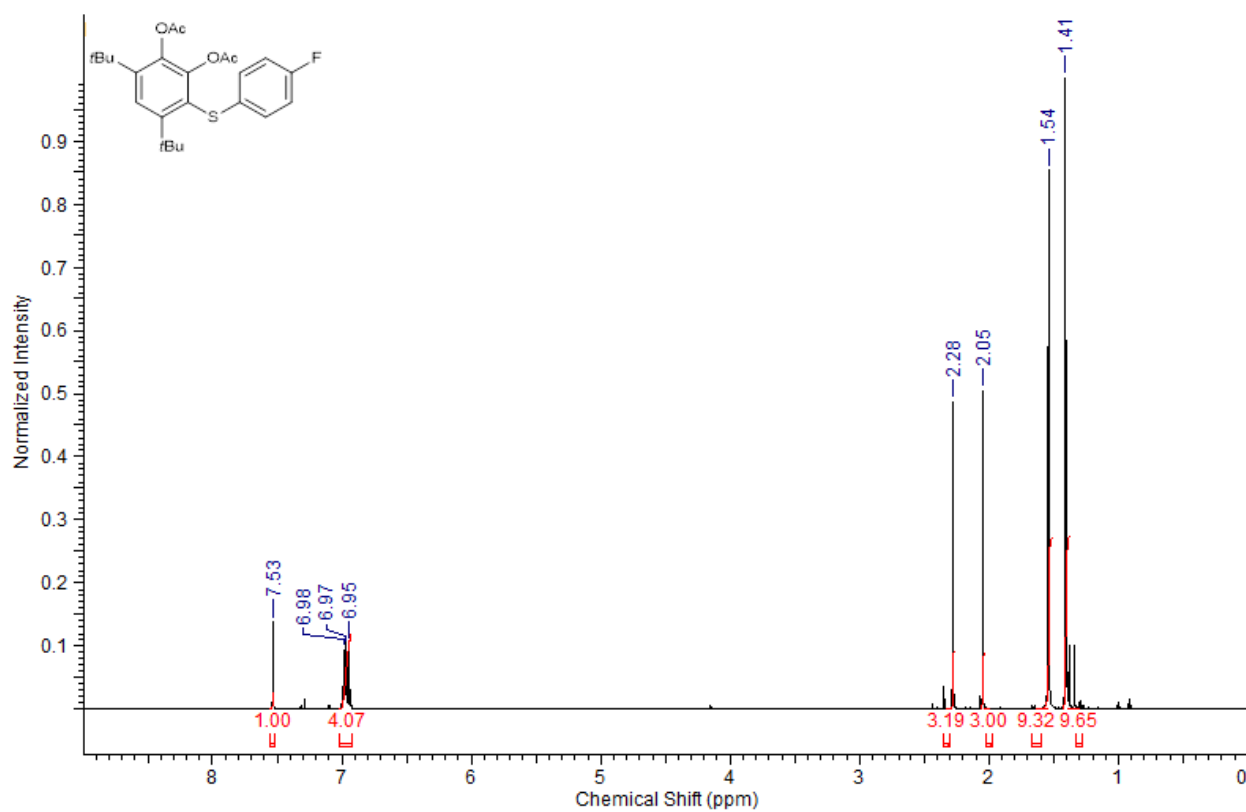
3.2.14:



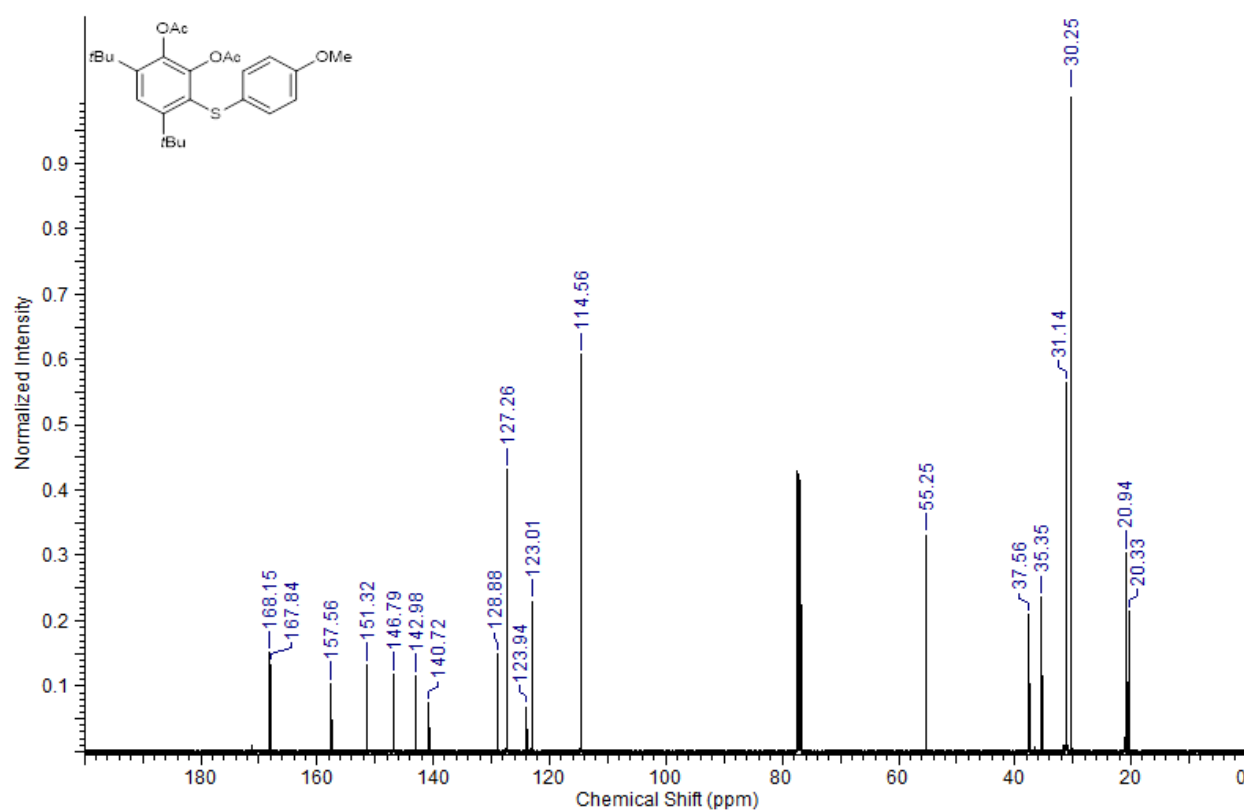
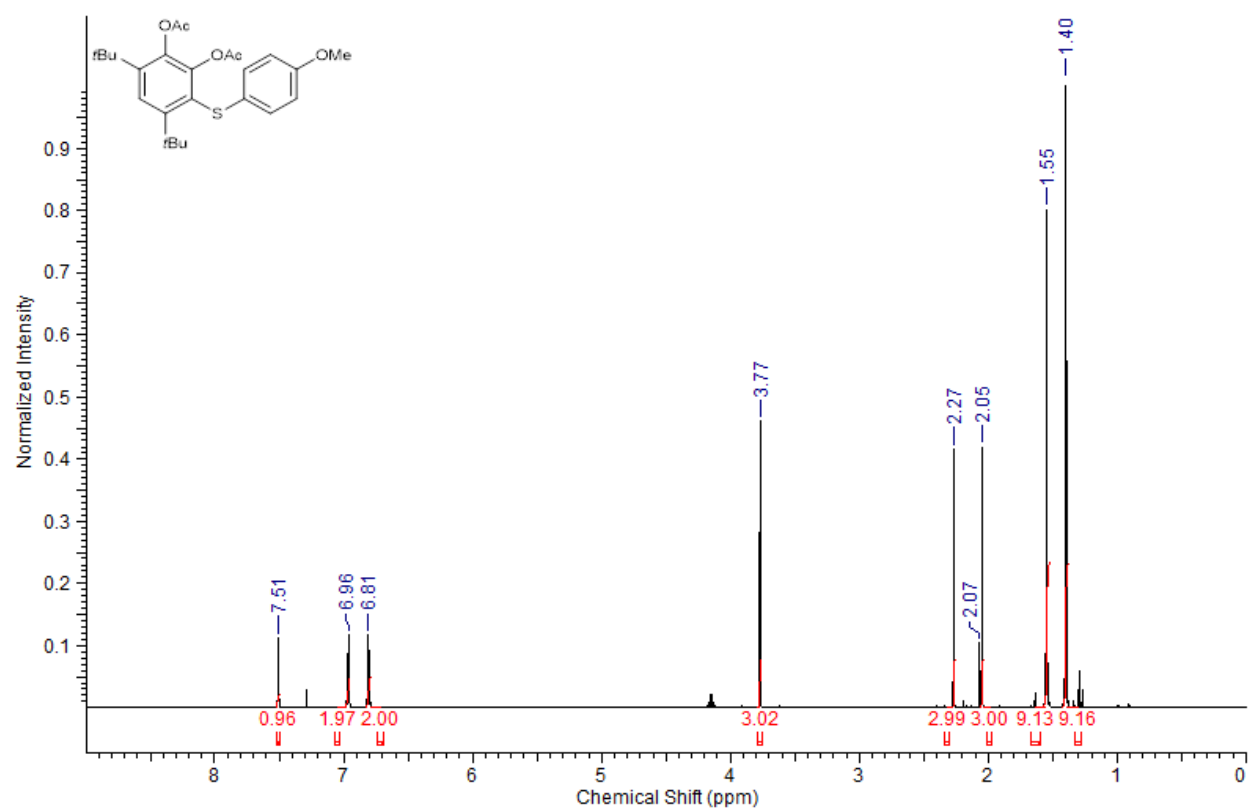
3.2.15:



3.2.16:

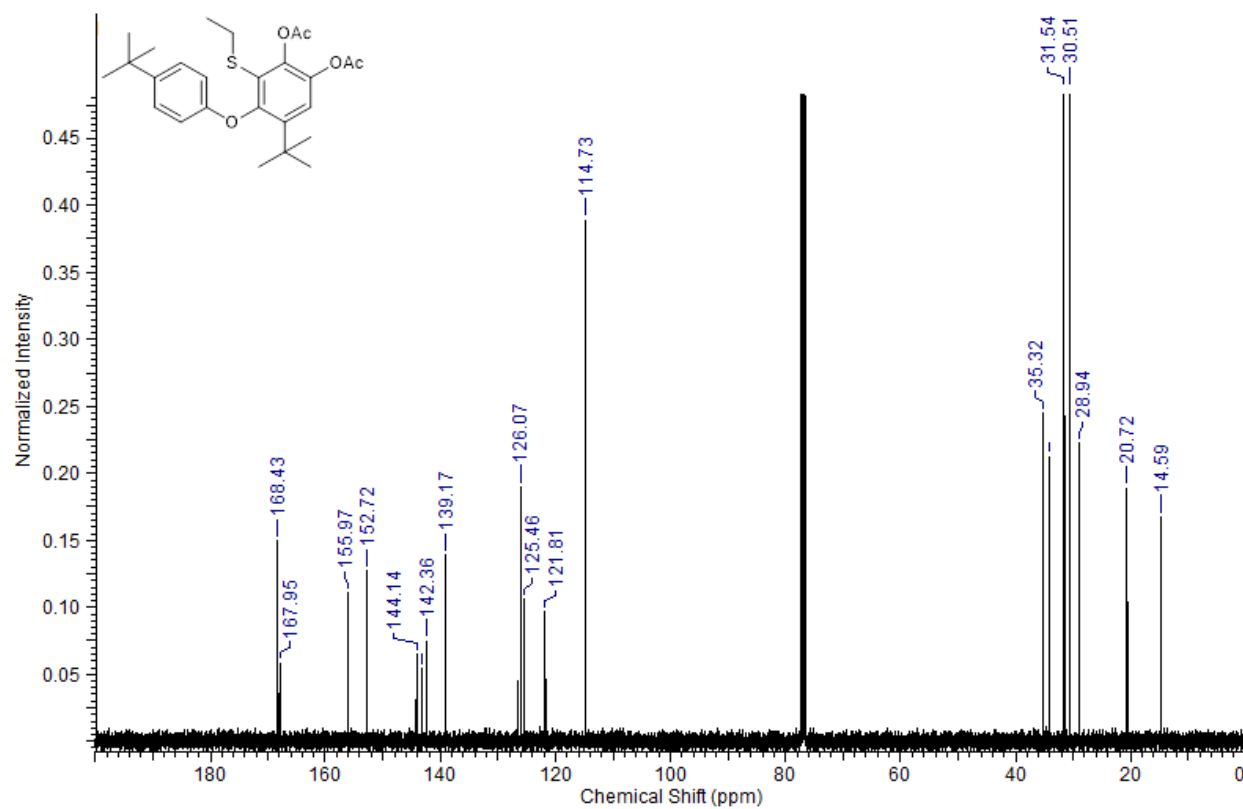
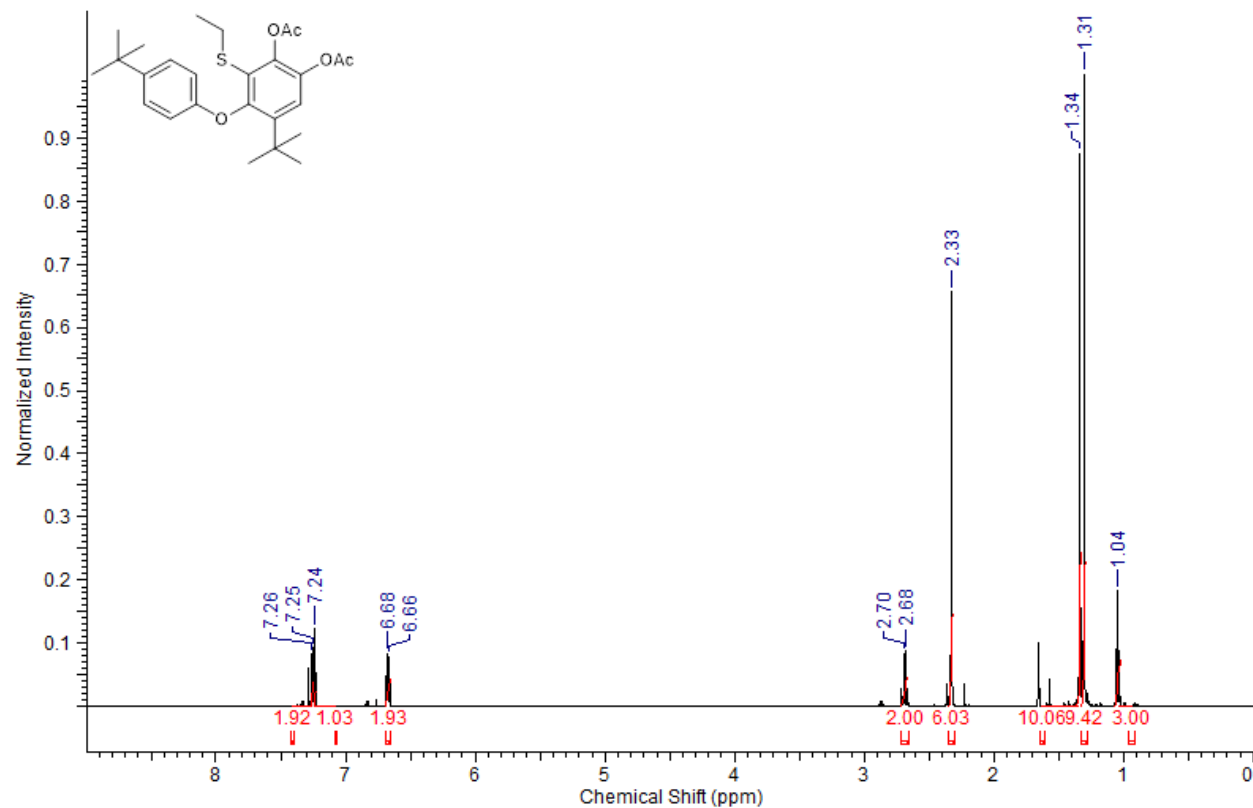


3.2.17:

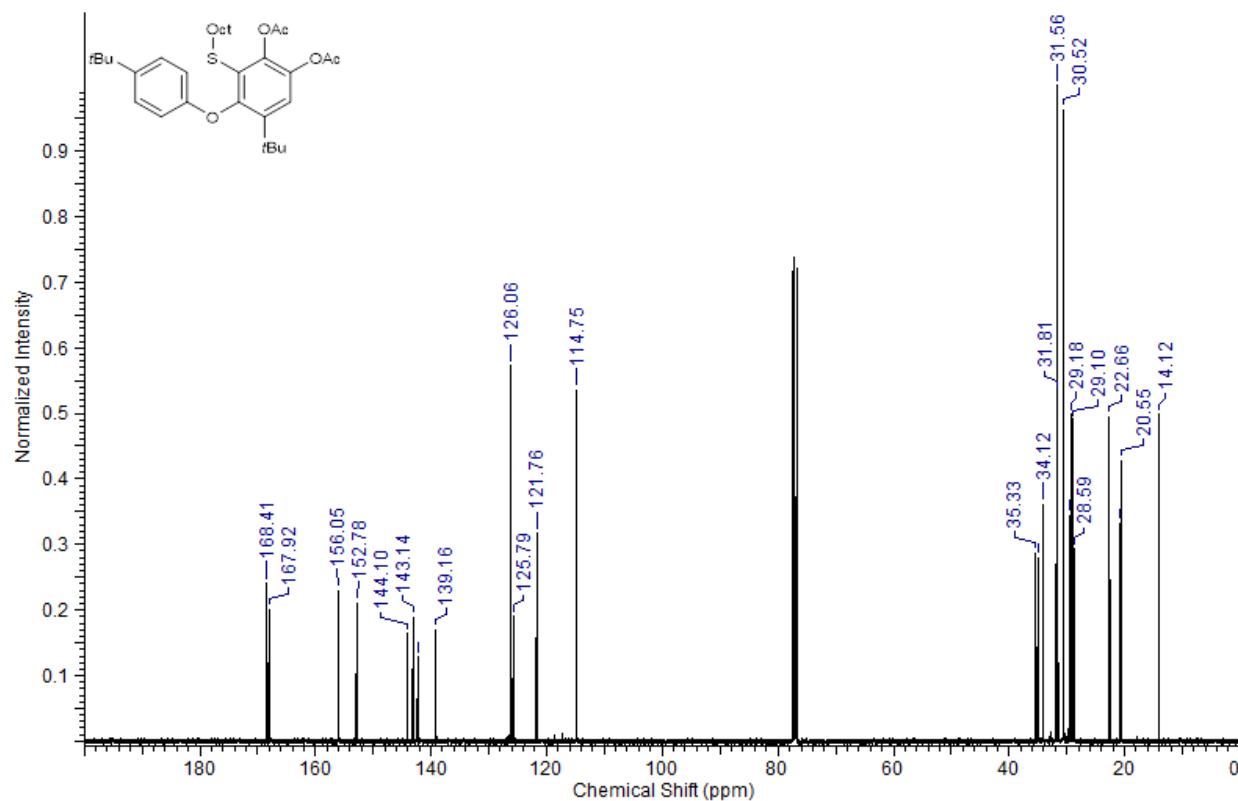
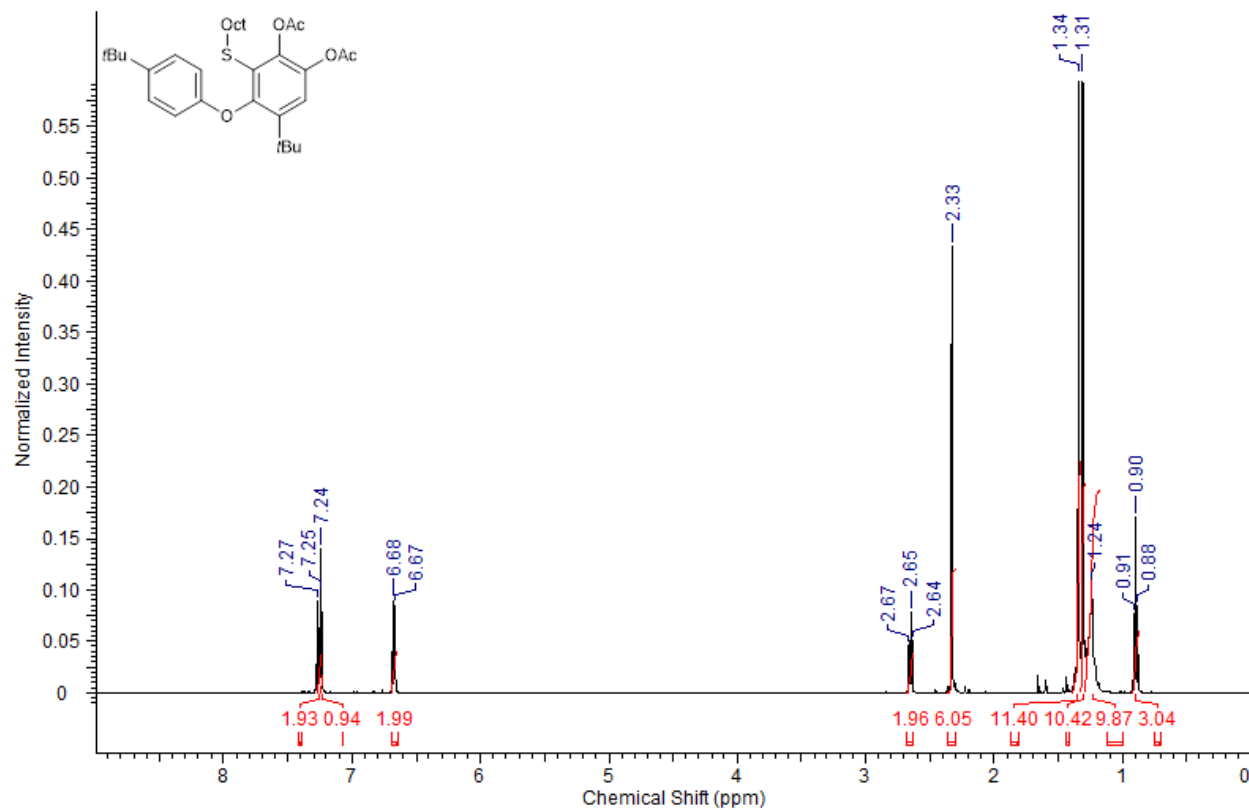


b) Substrates in Table 3.3.2:

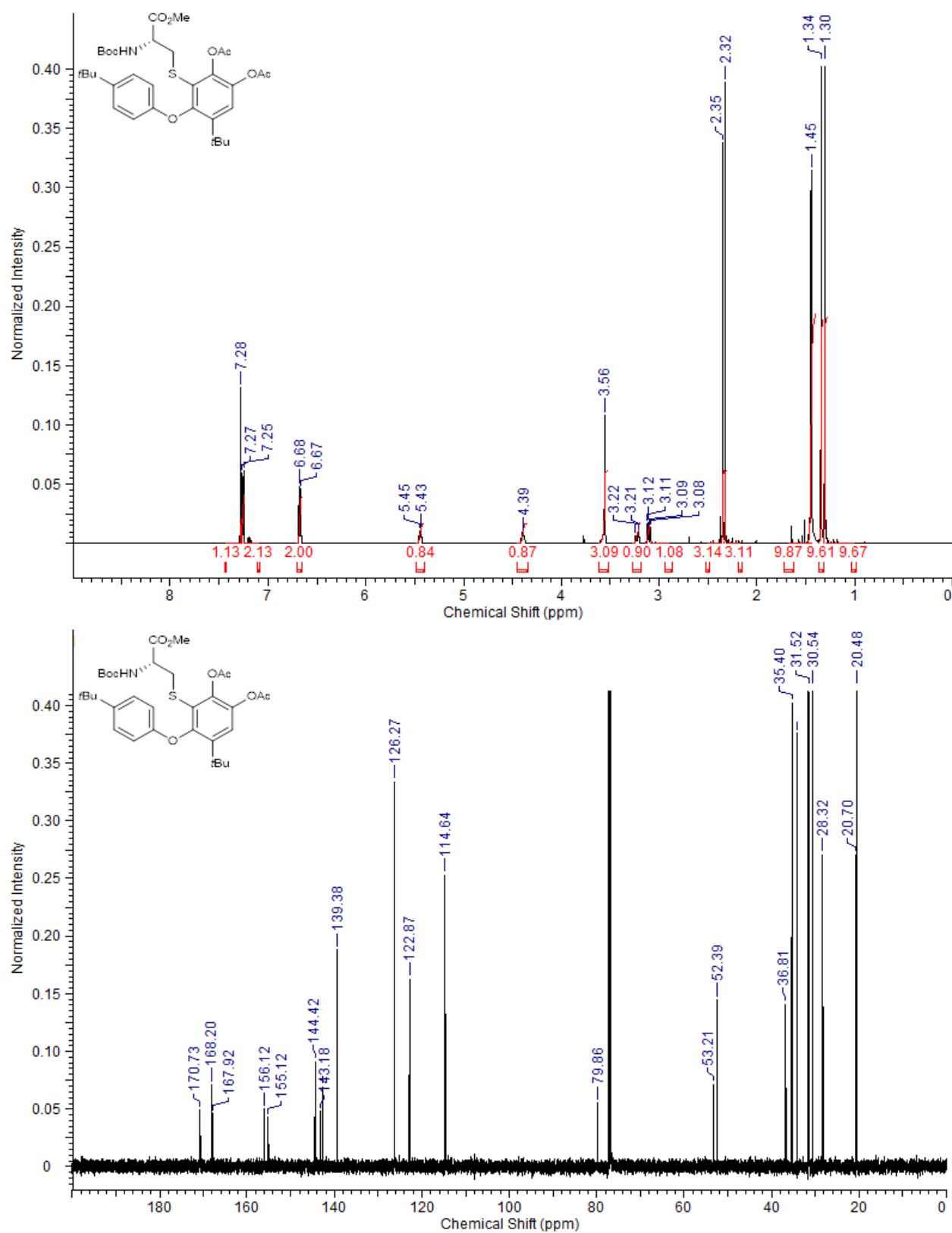
3.3.3:



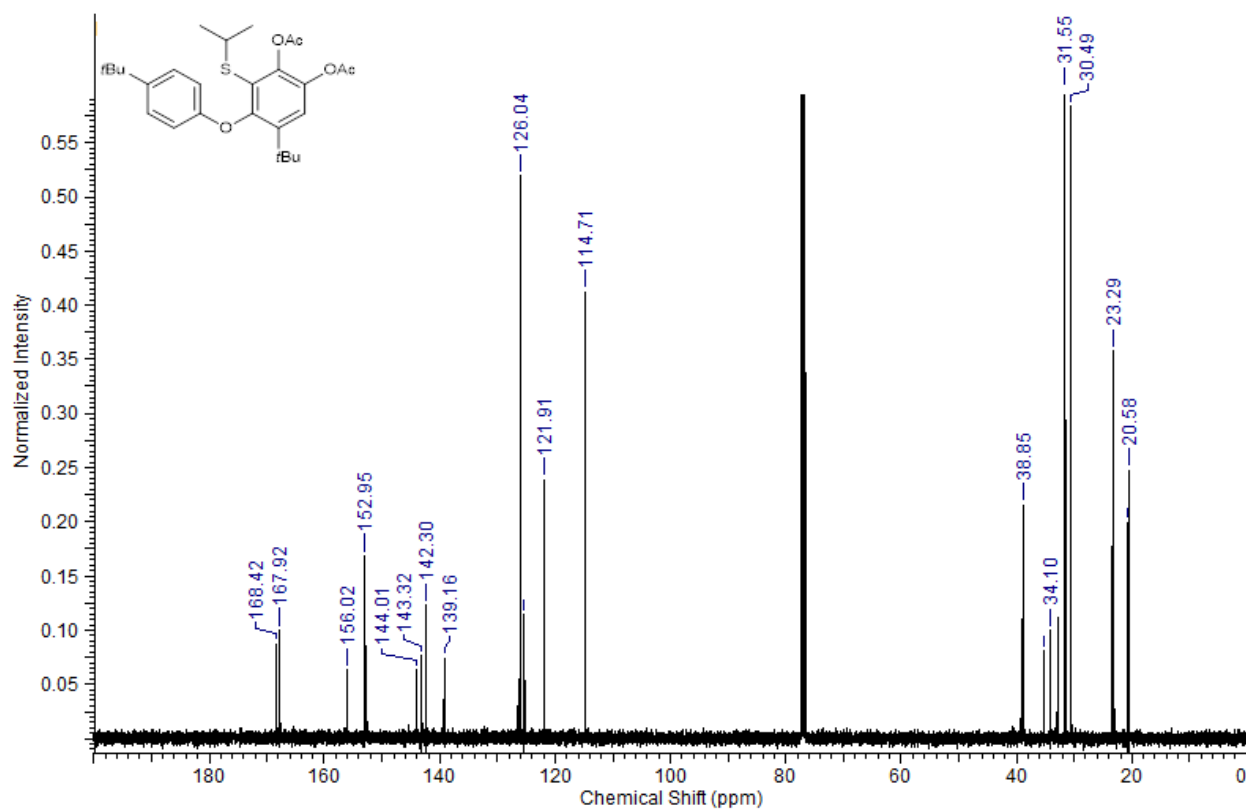
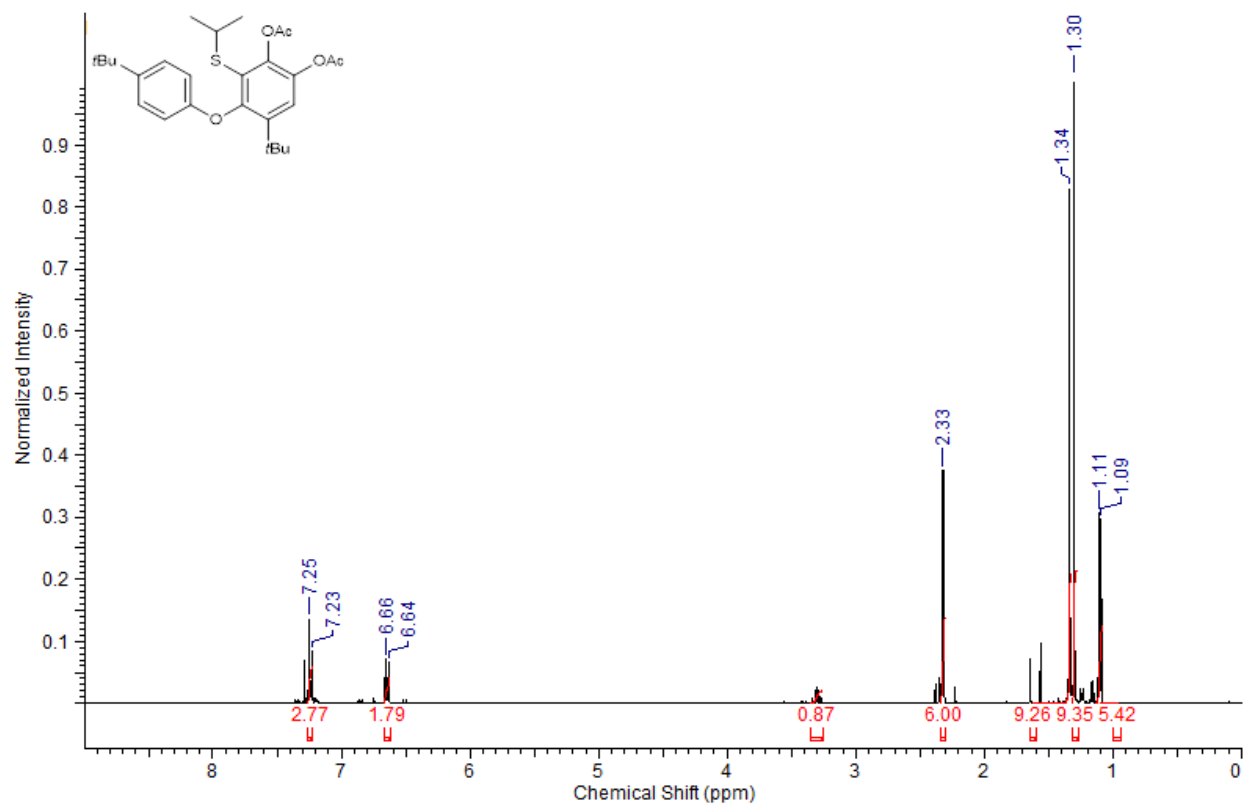
3.3.4:



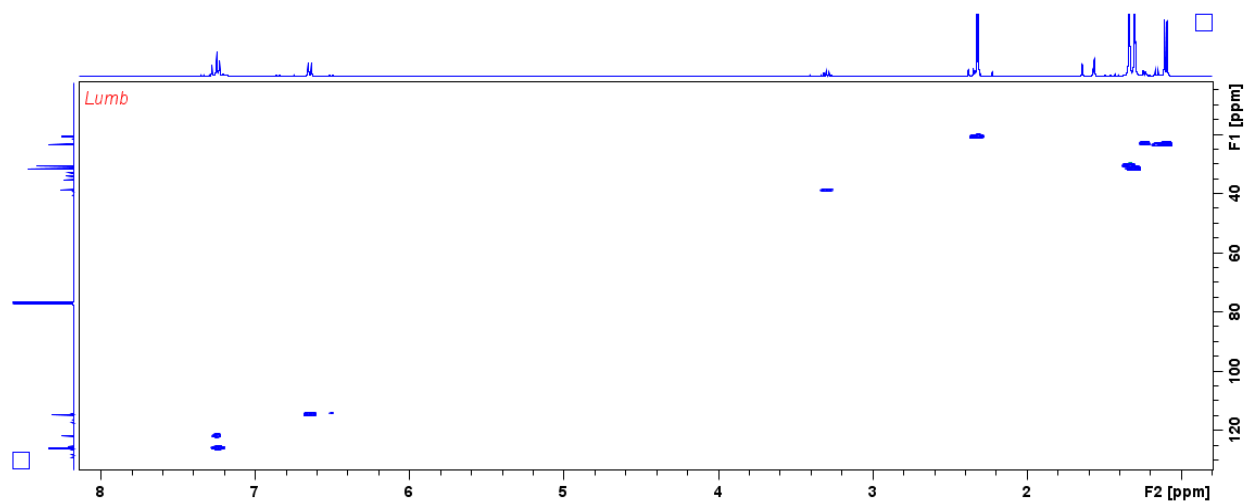
3.3.5:



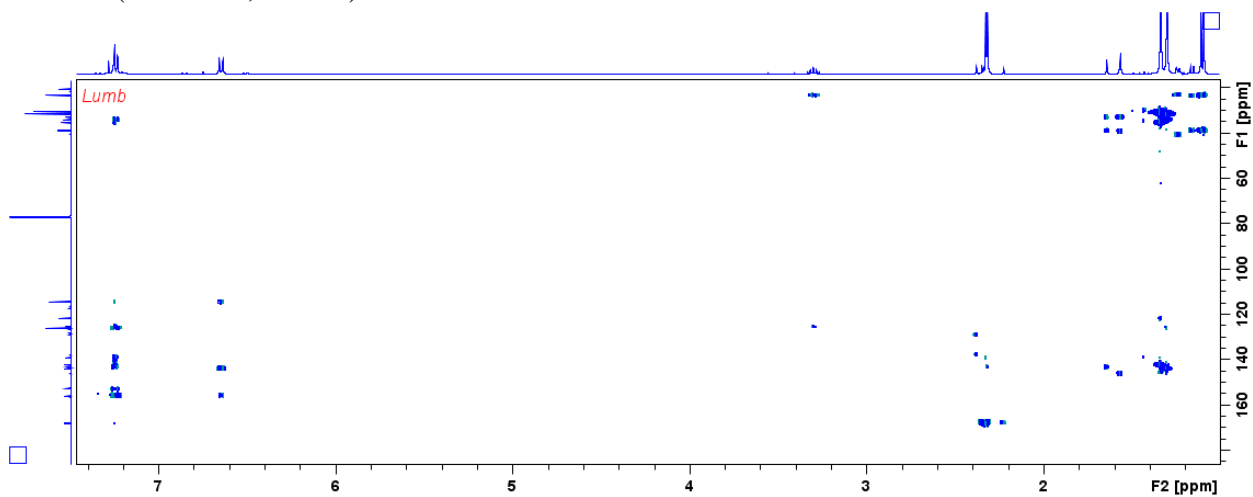
3.3.6:



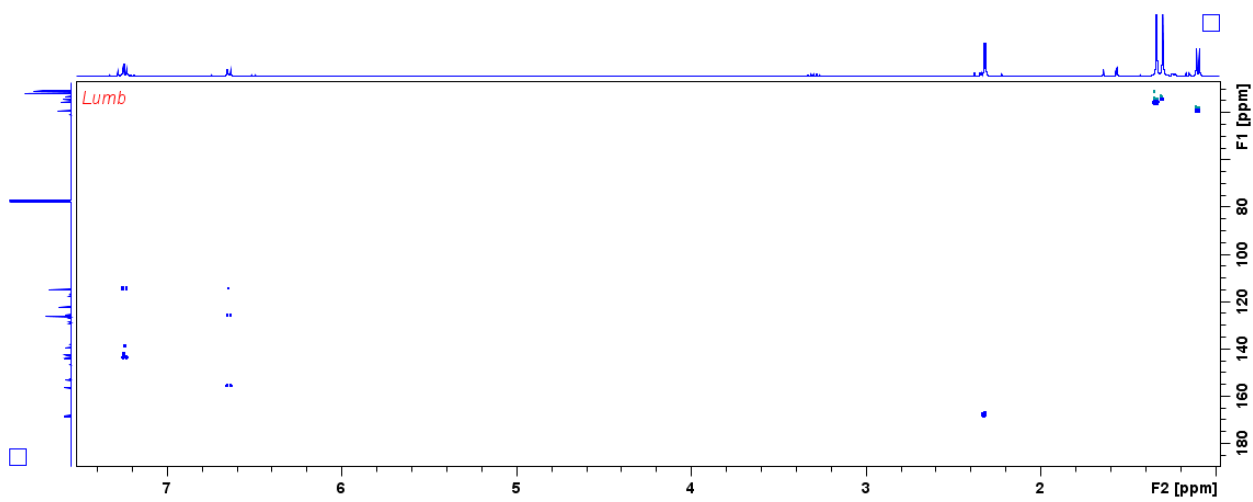
HSQC (500 MHz, CDCl₃):



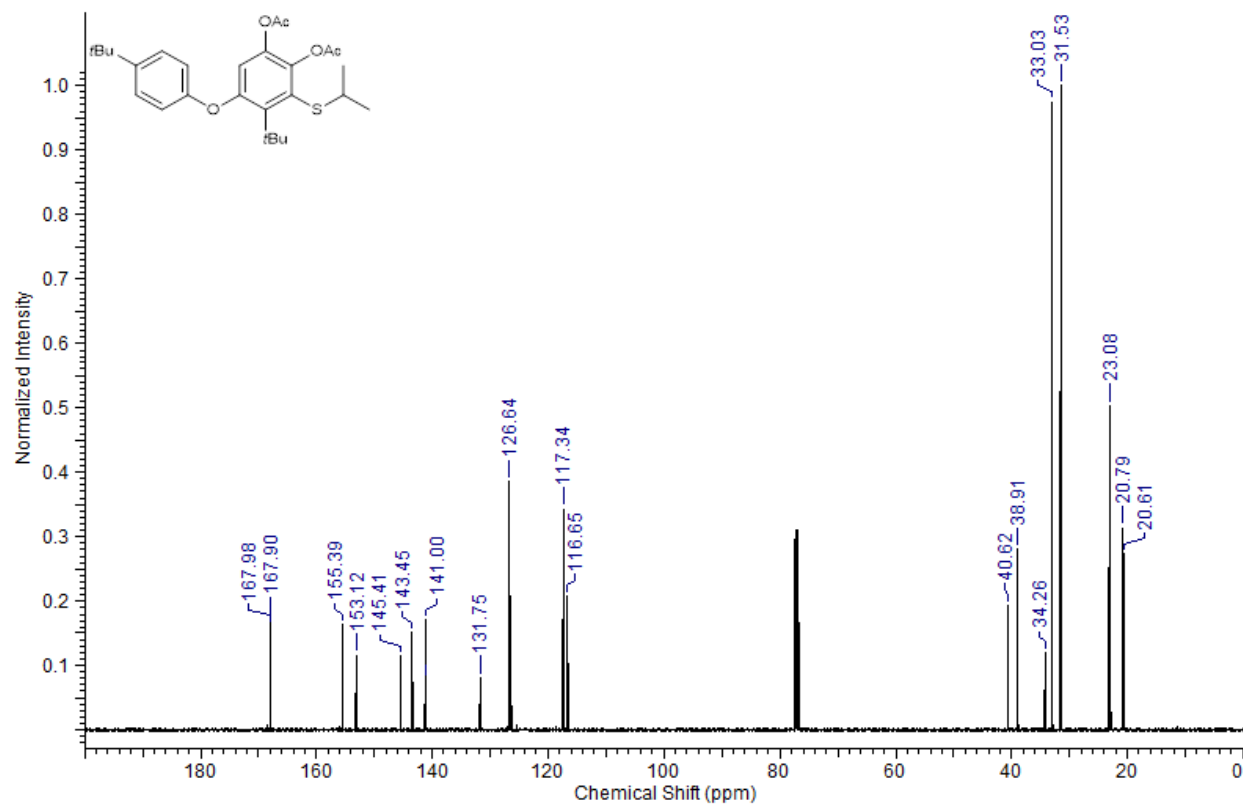
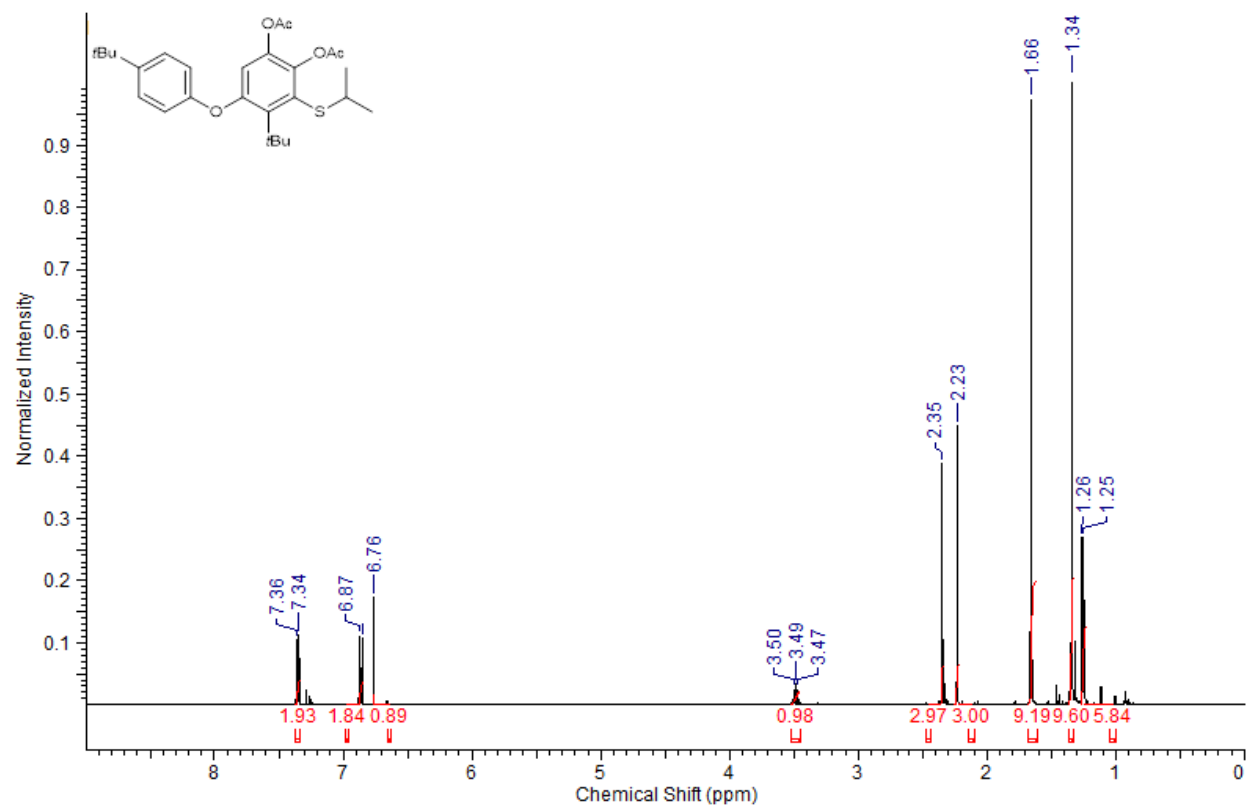
HMBC (500 MHz, CDCl₃):



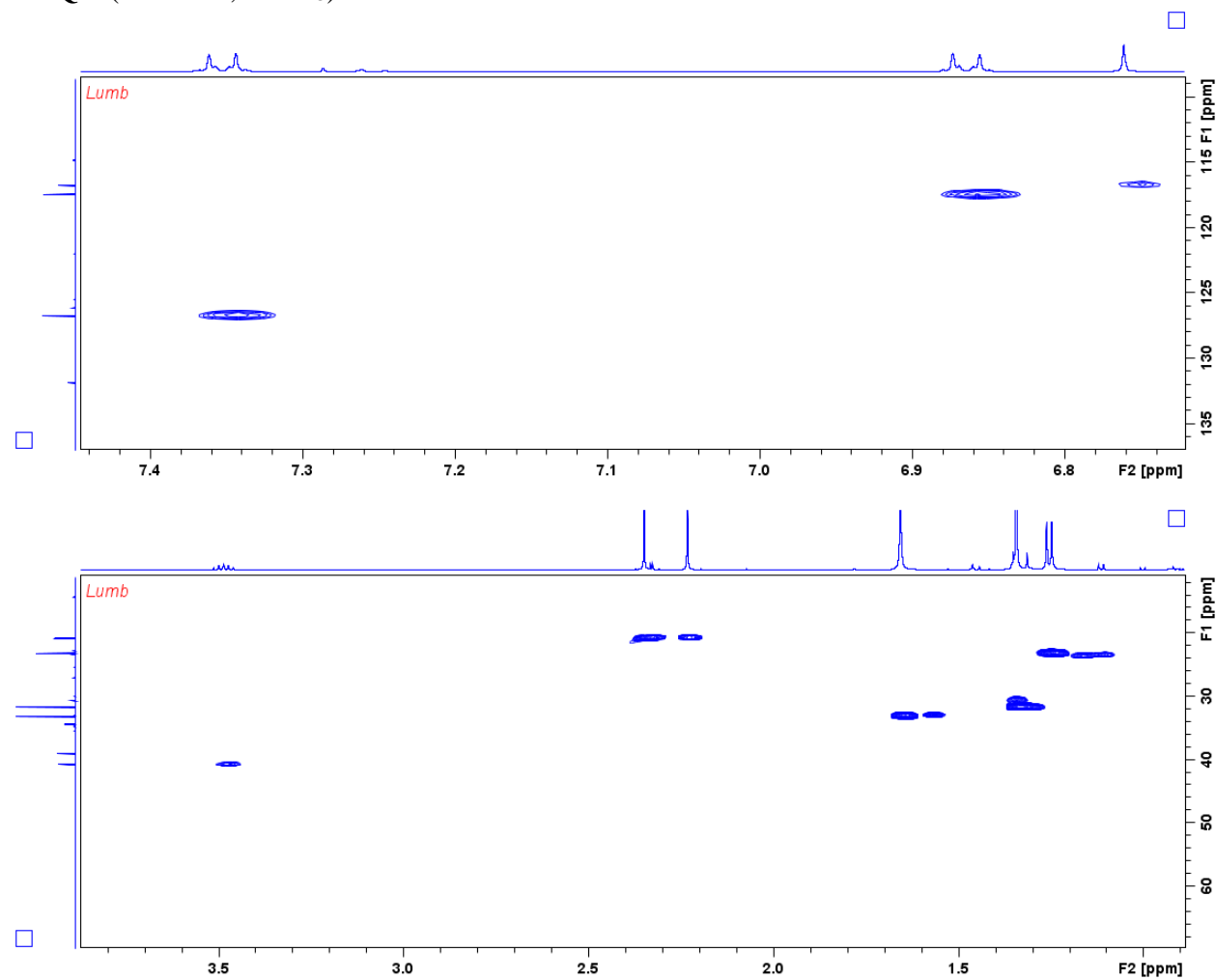
1-1'-ADEQUATE (500 MHz, CDCl₃):



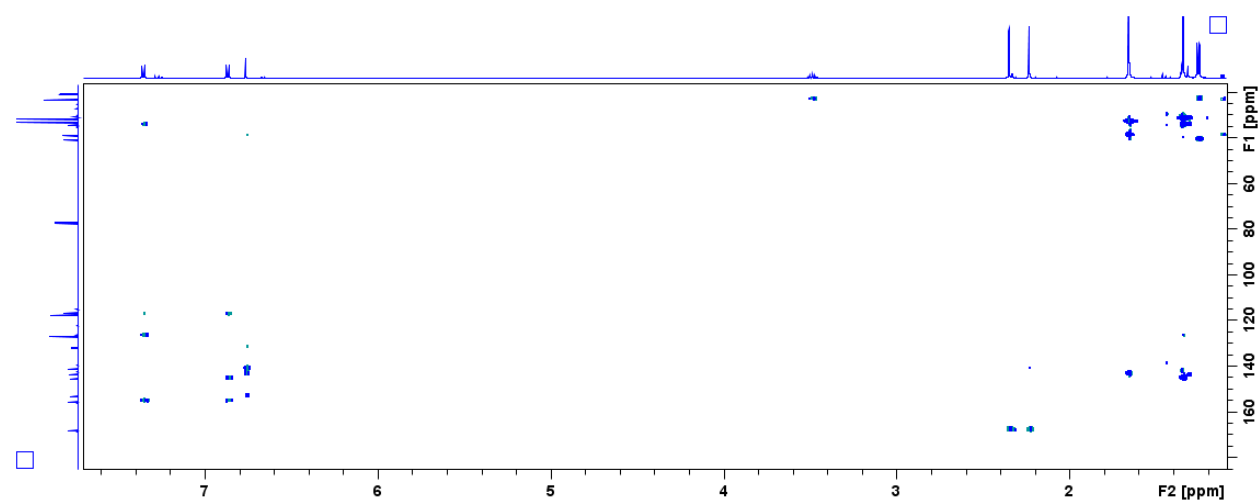
3.4.3:



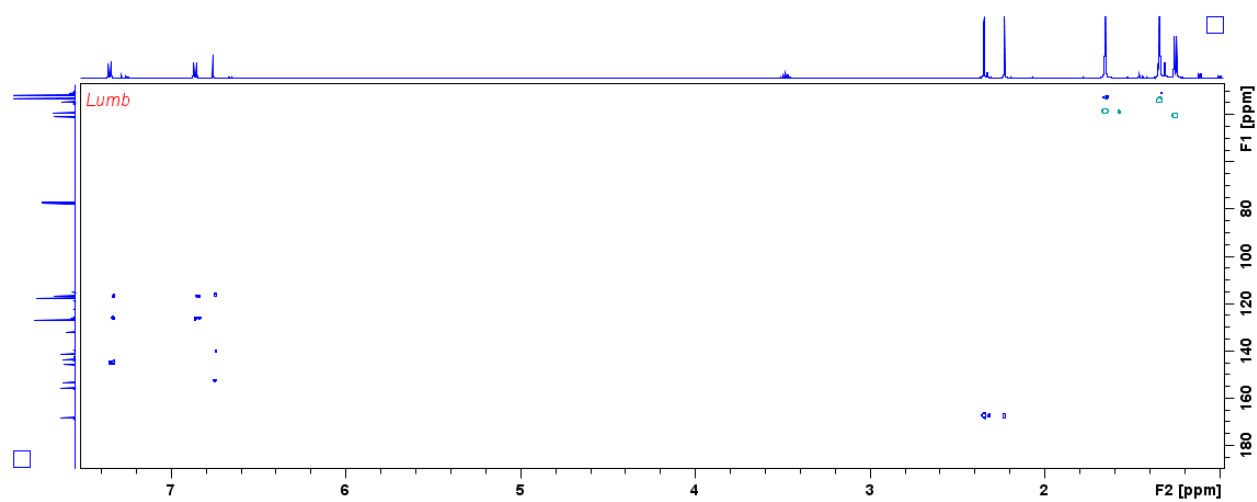
HSQC (500MHz, CDCl₃):



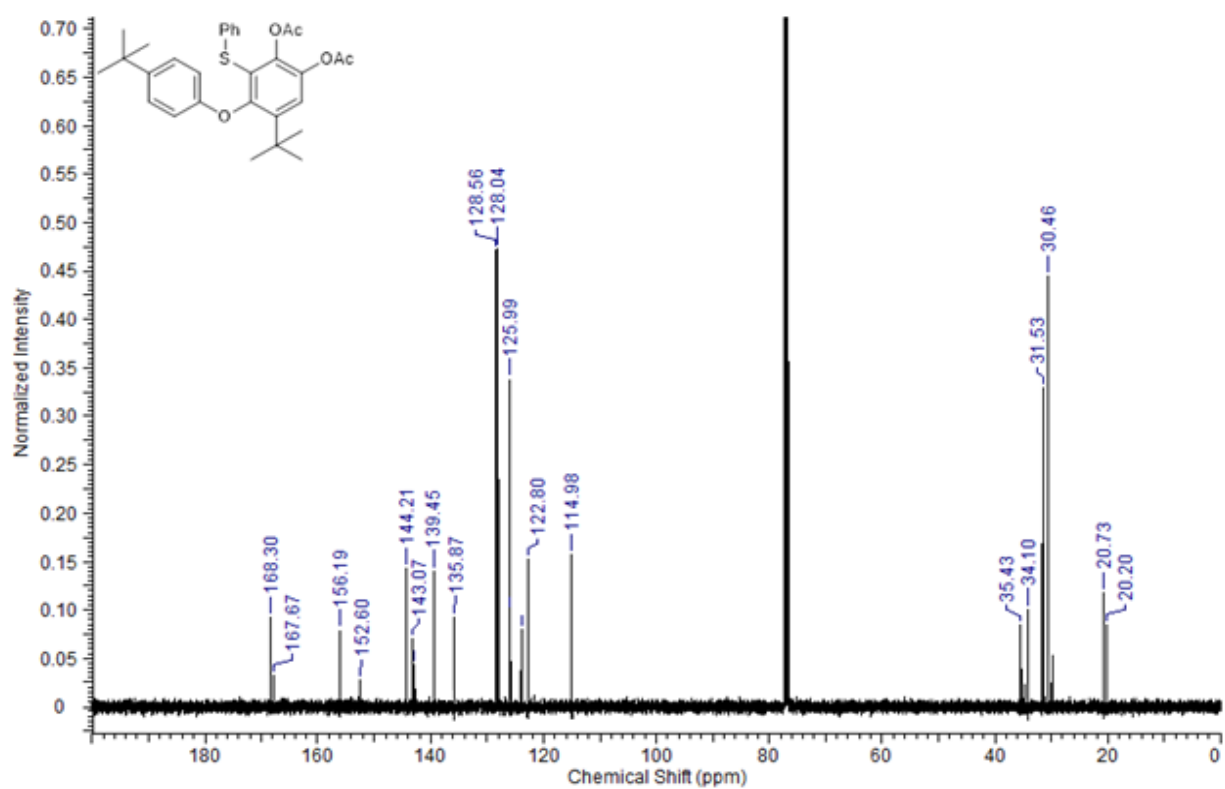
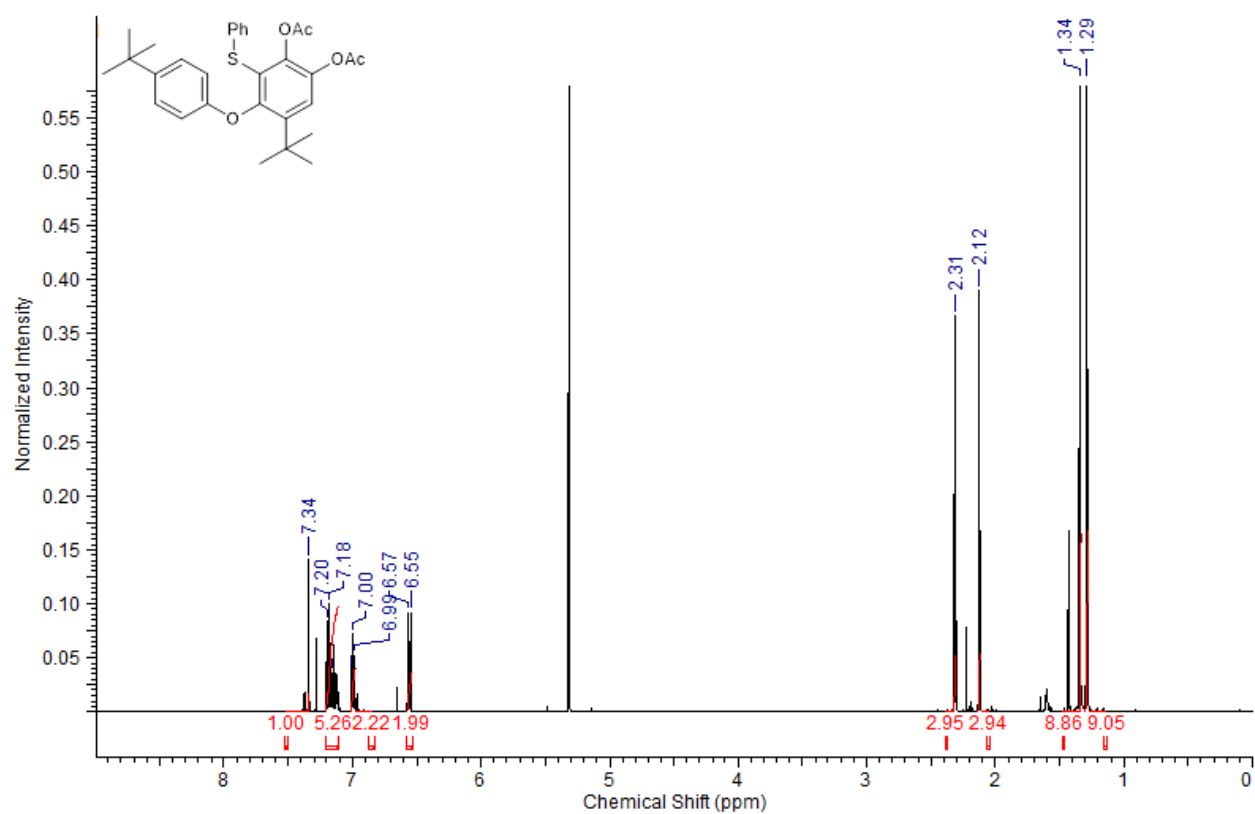
HMBC (500 MHz, CDCl₃):



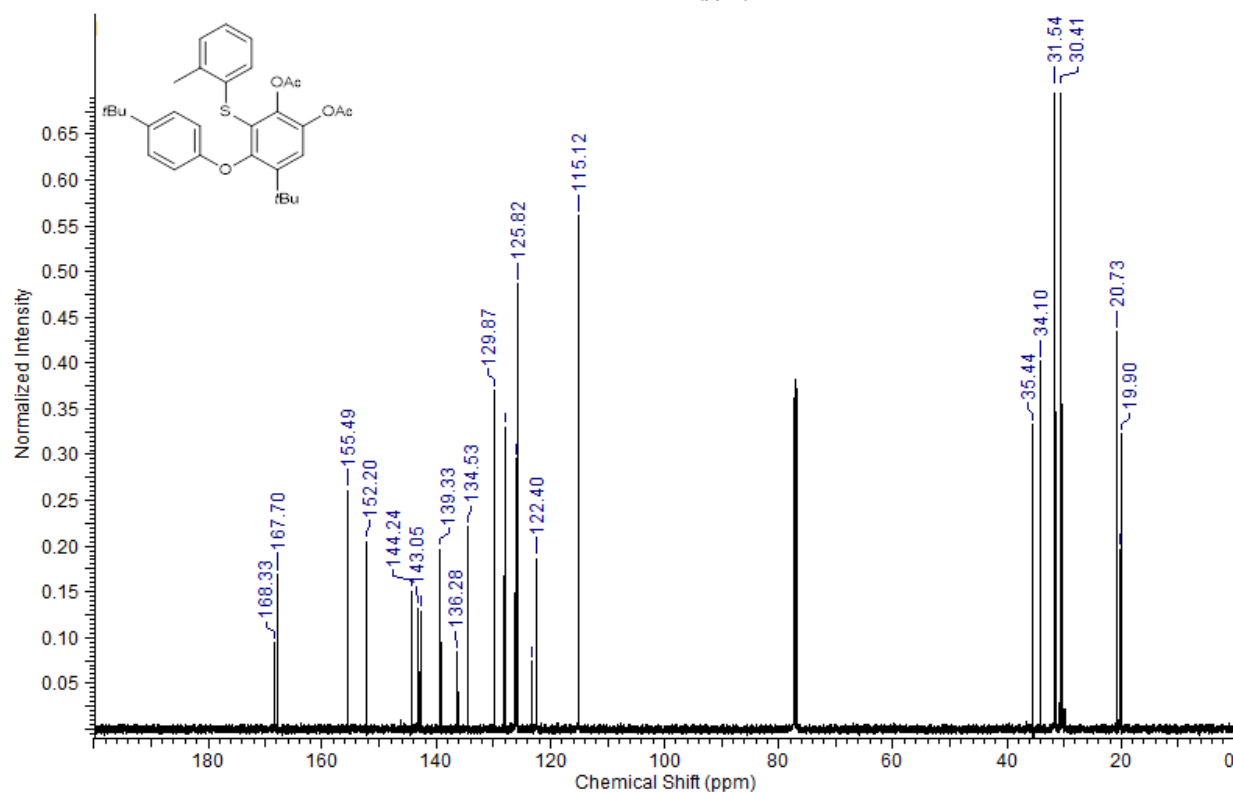
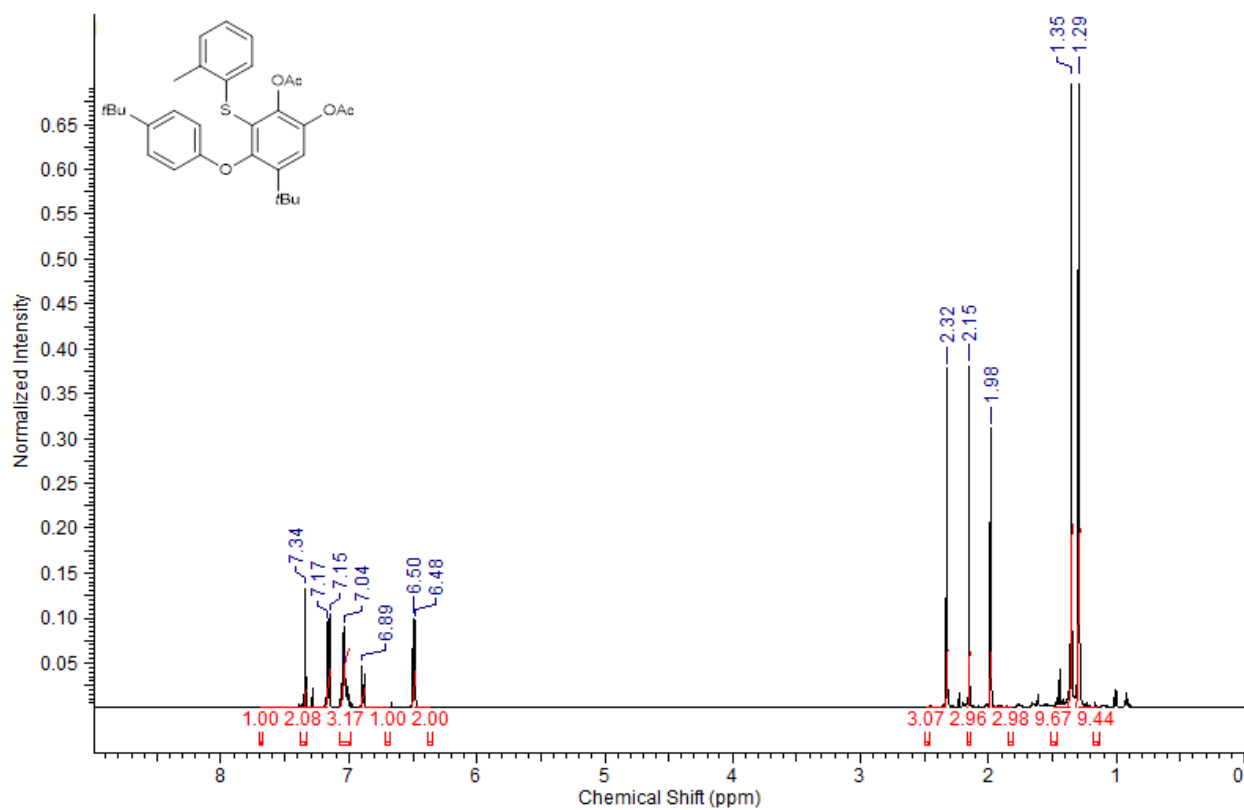
1-1'-ADEQUATE (500 MHz, CDCl₃):



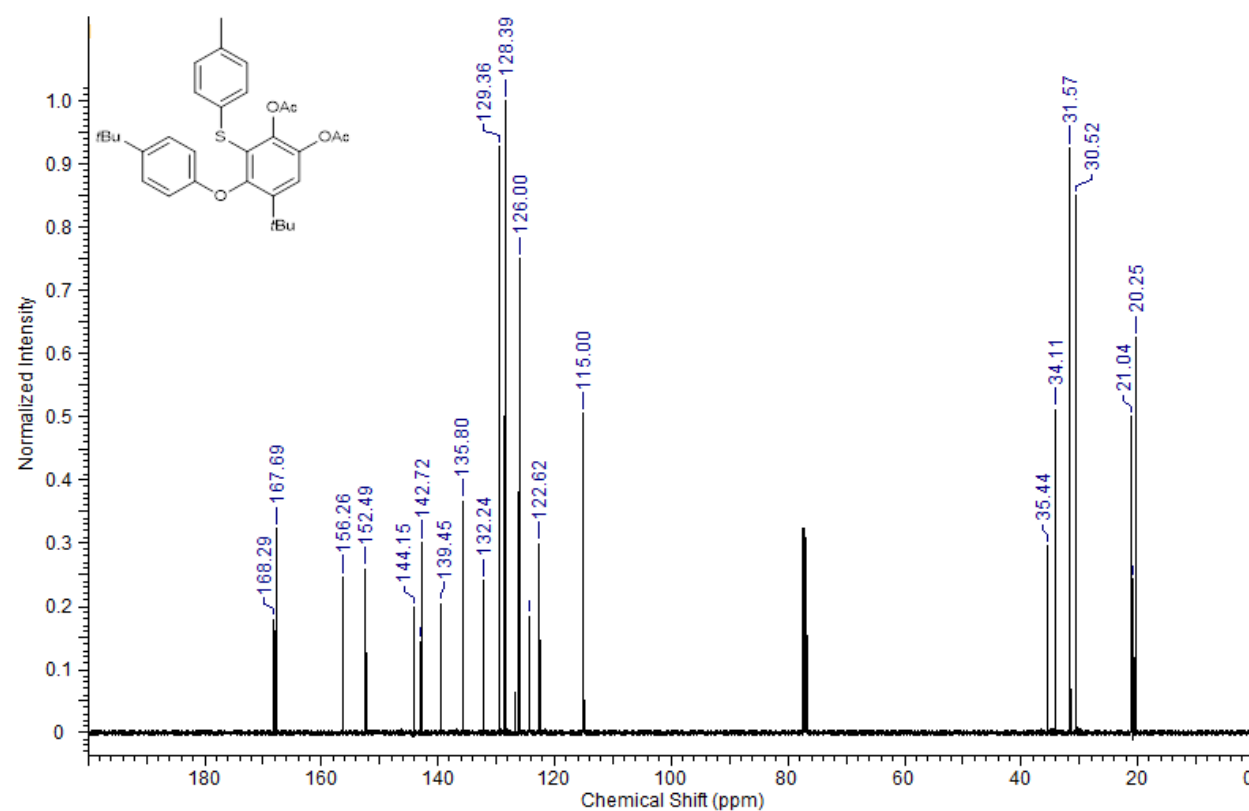
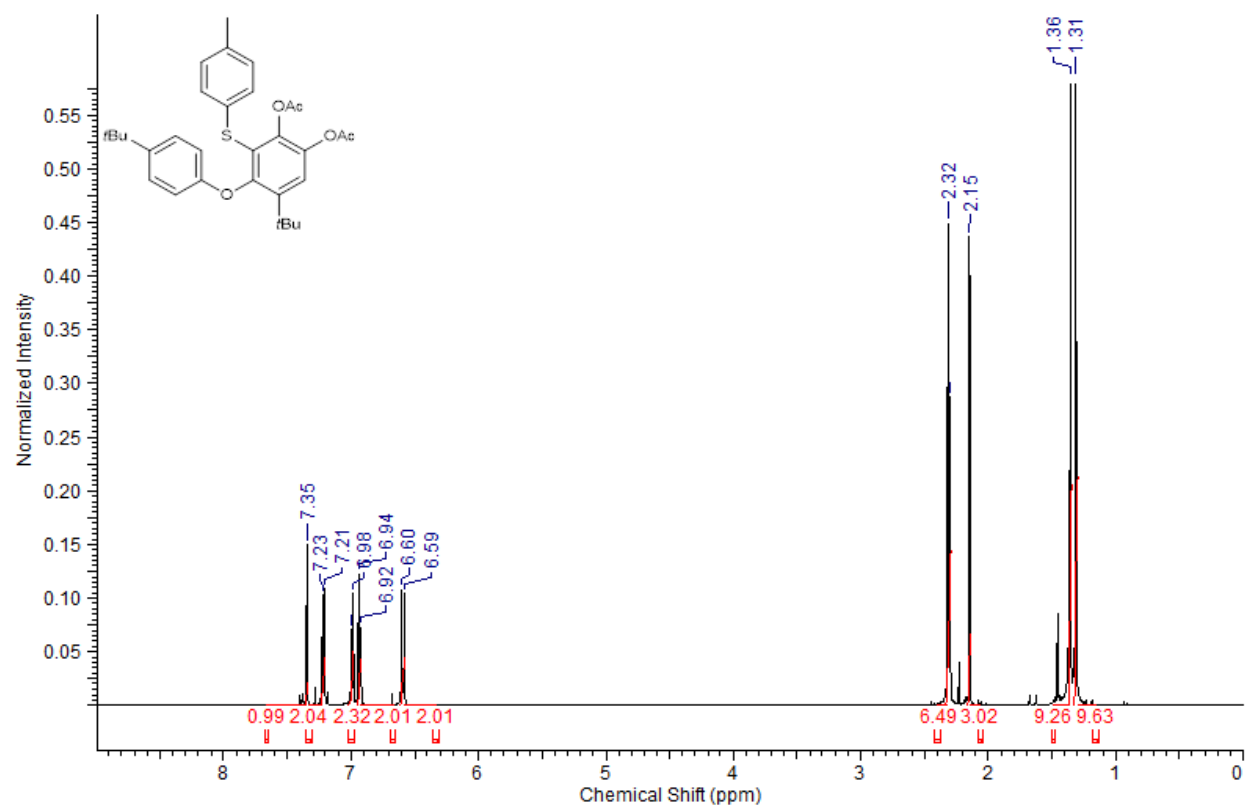
3.3.7:



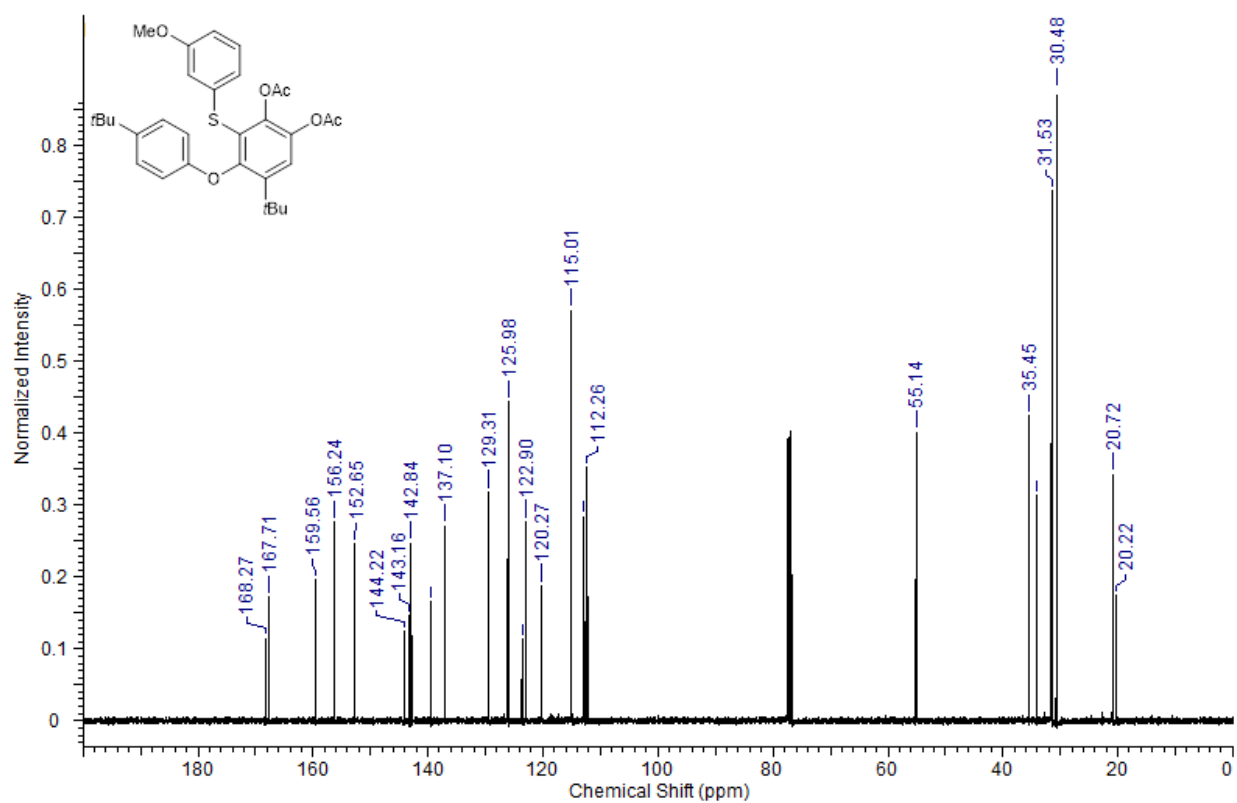
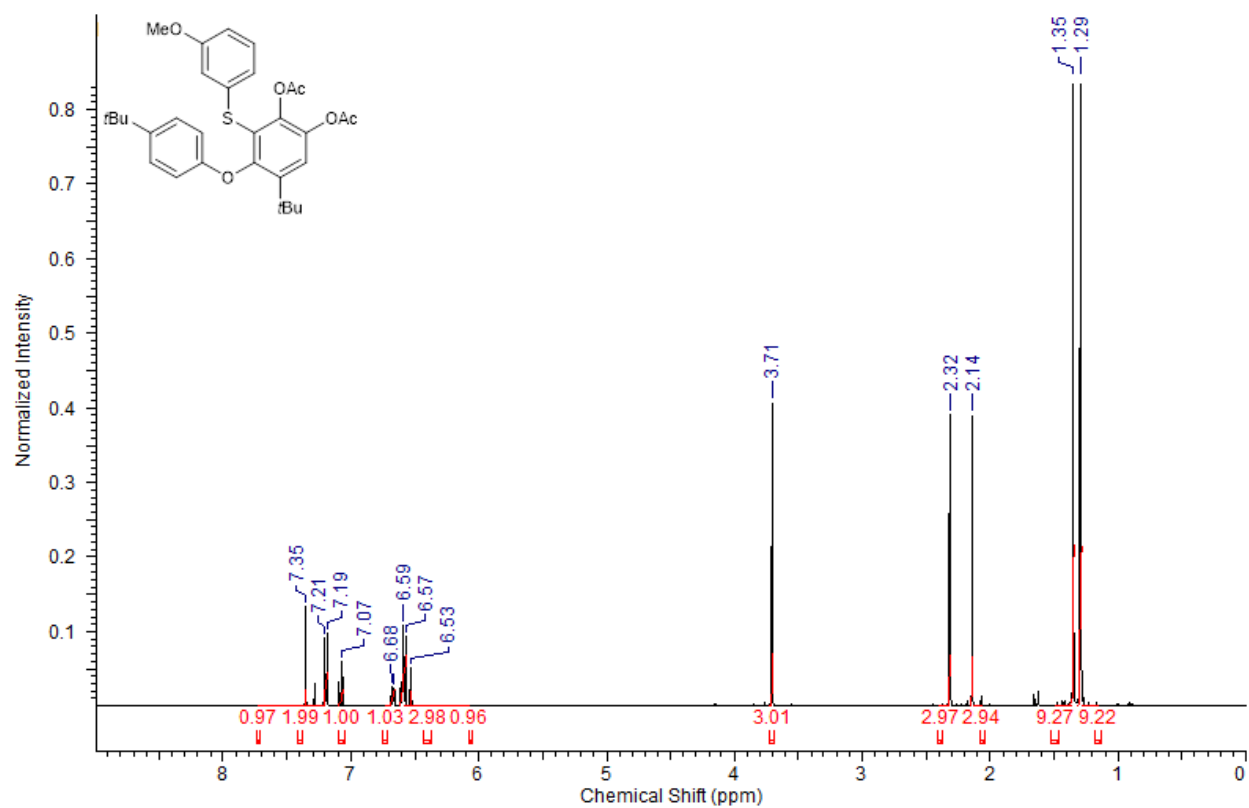
3.3.8:



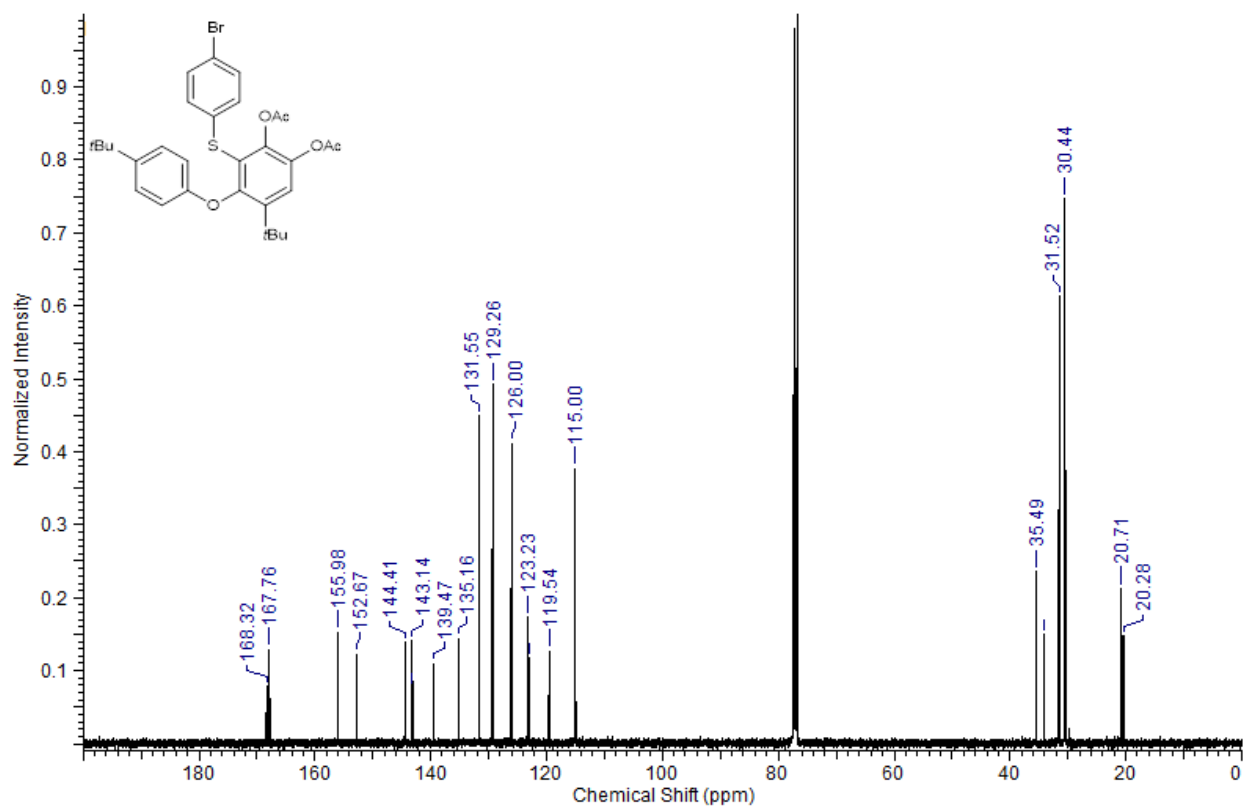
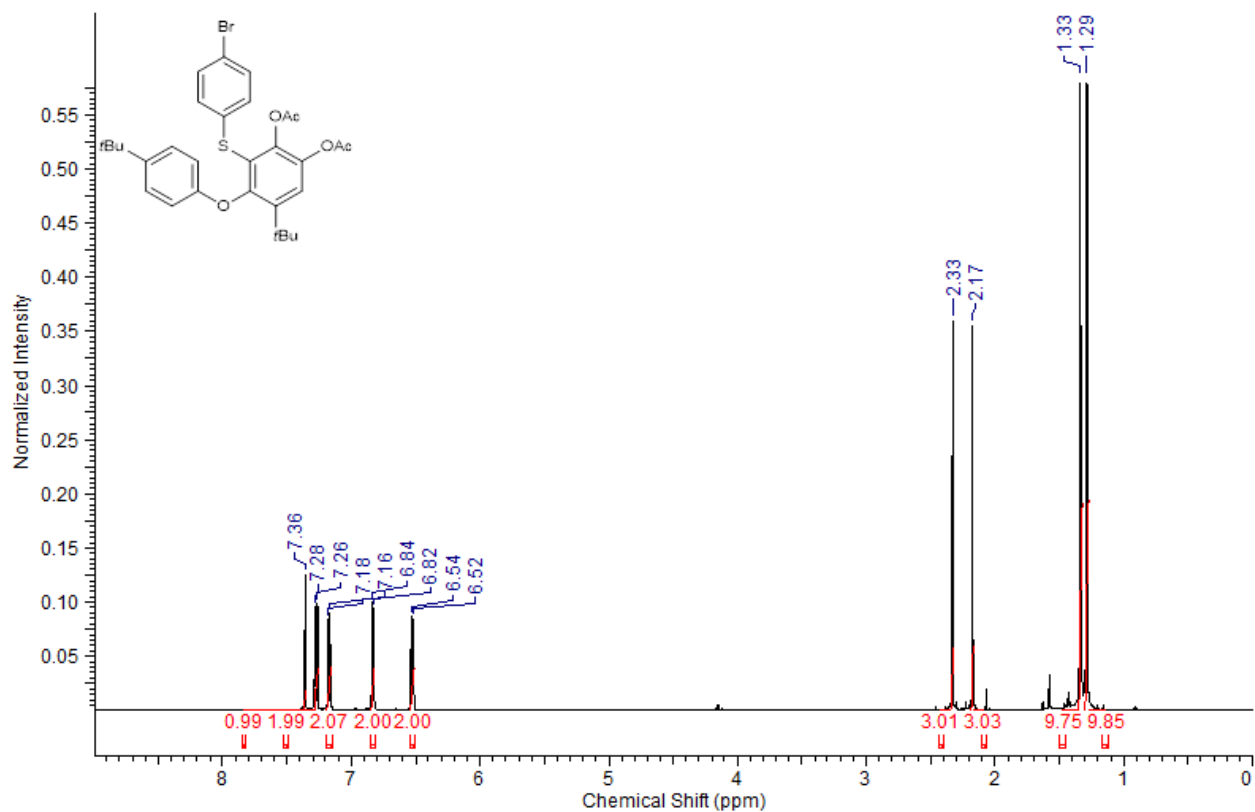
3.3.9:



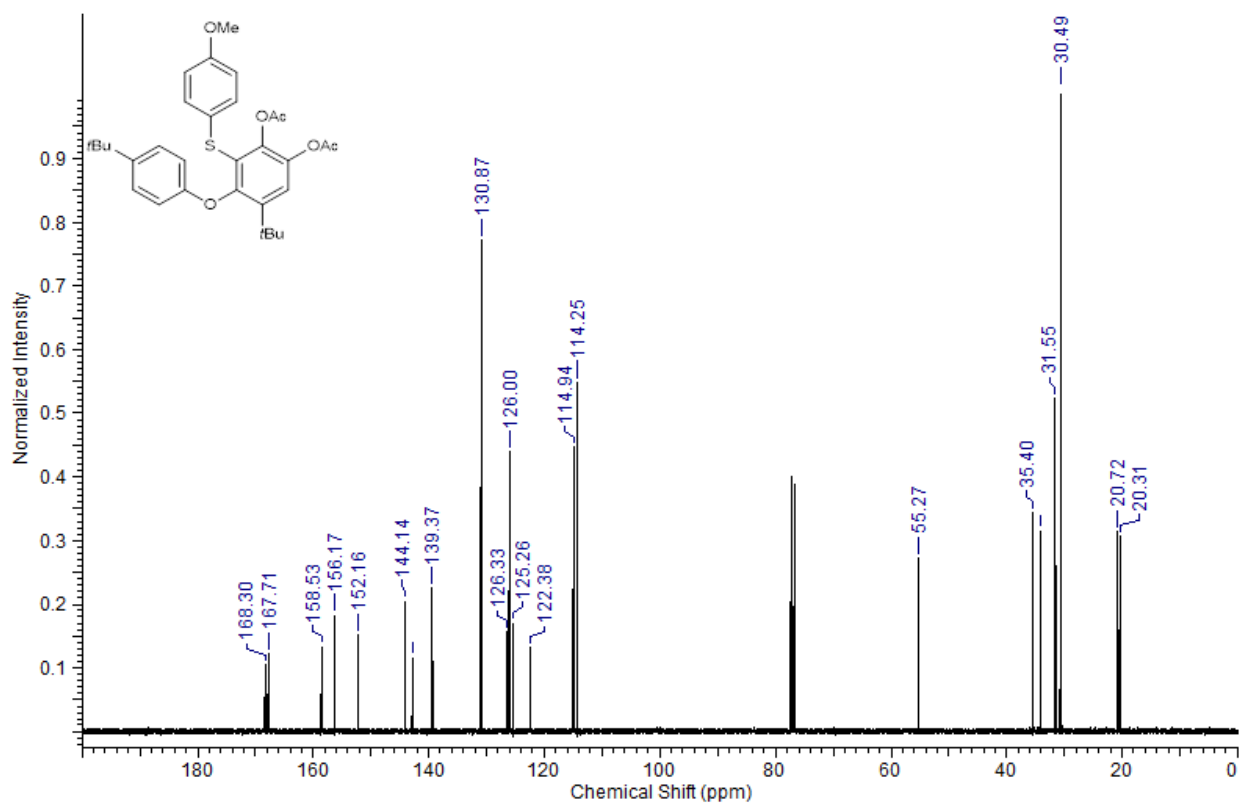
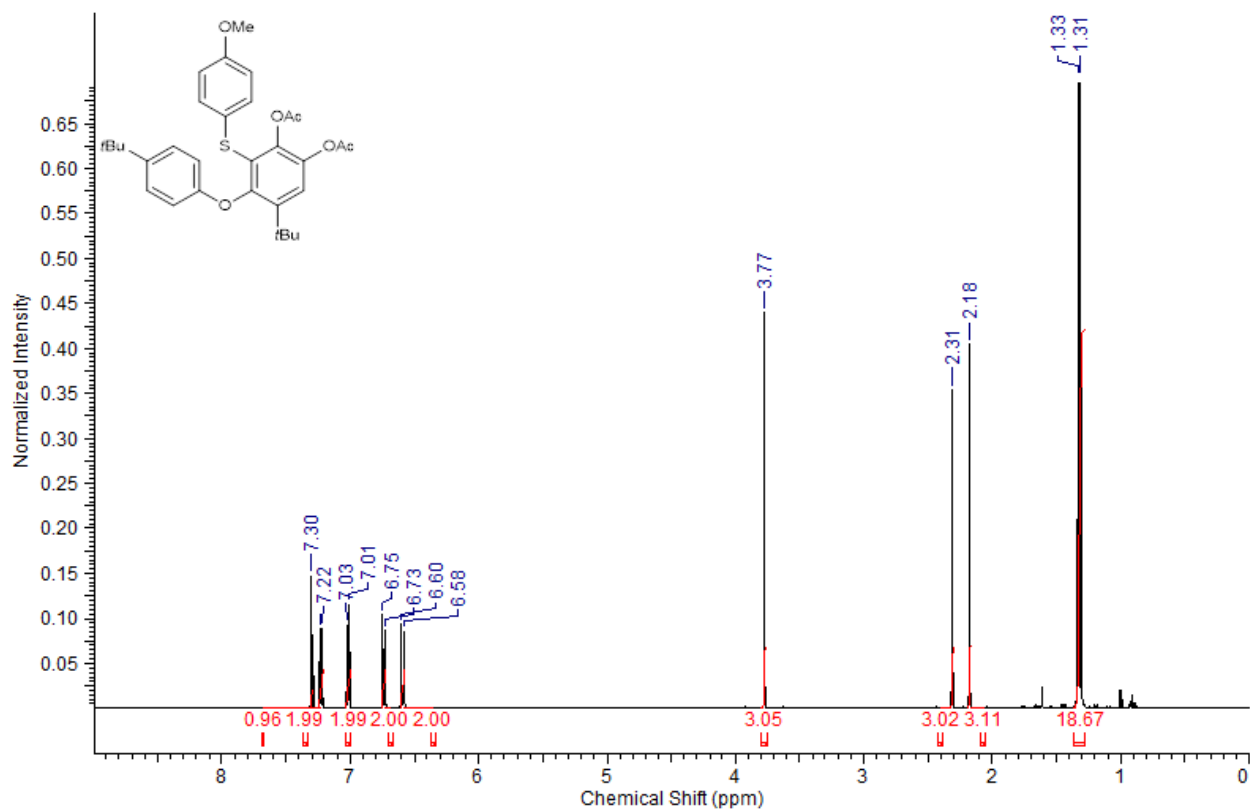
3.3.10:



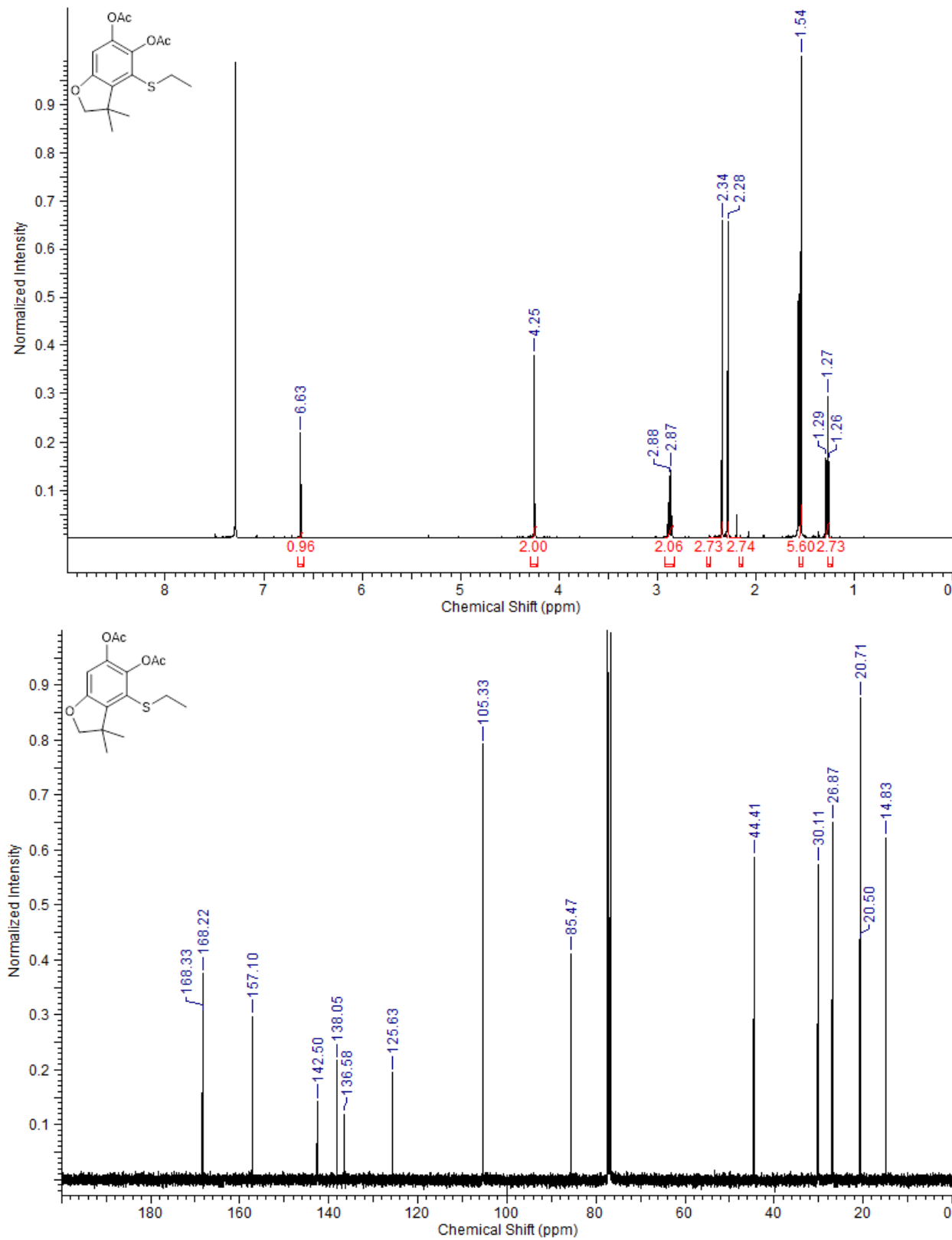
3.3.11:



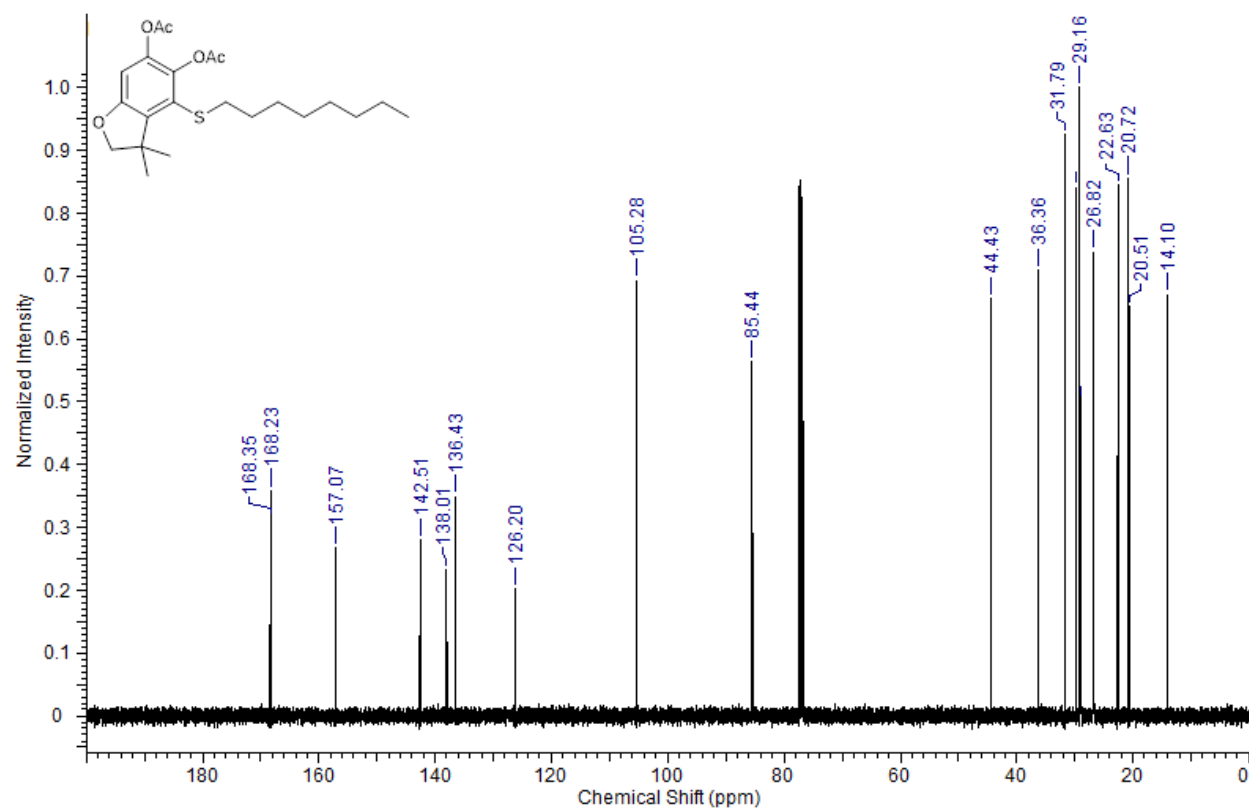
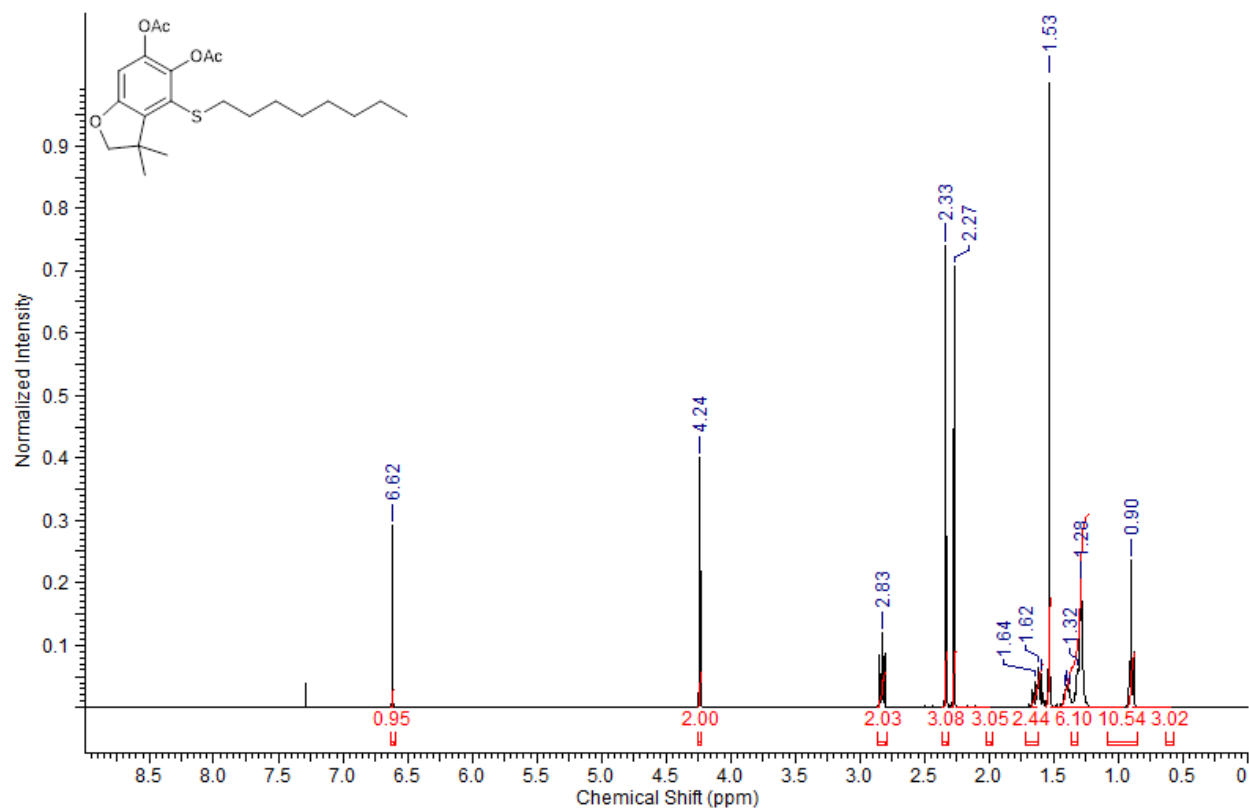
3.3.12:



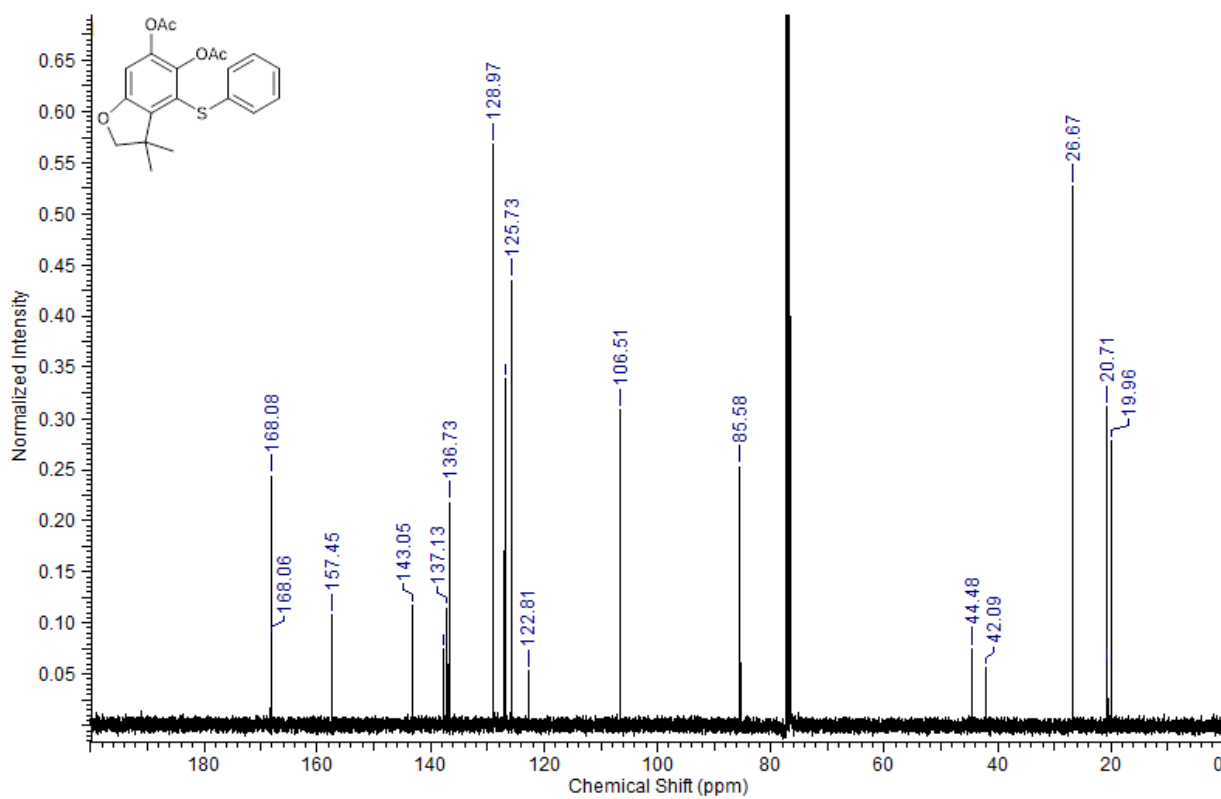
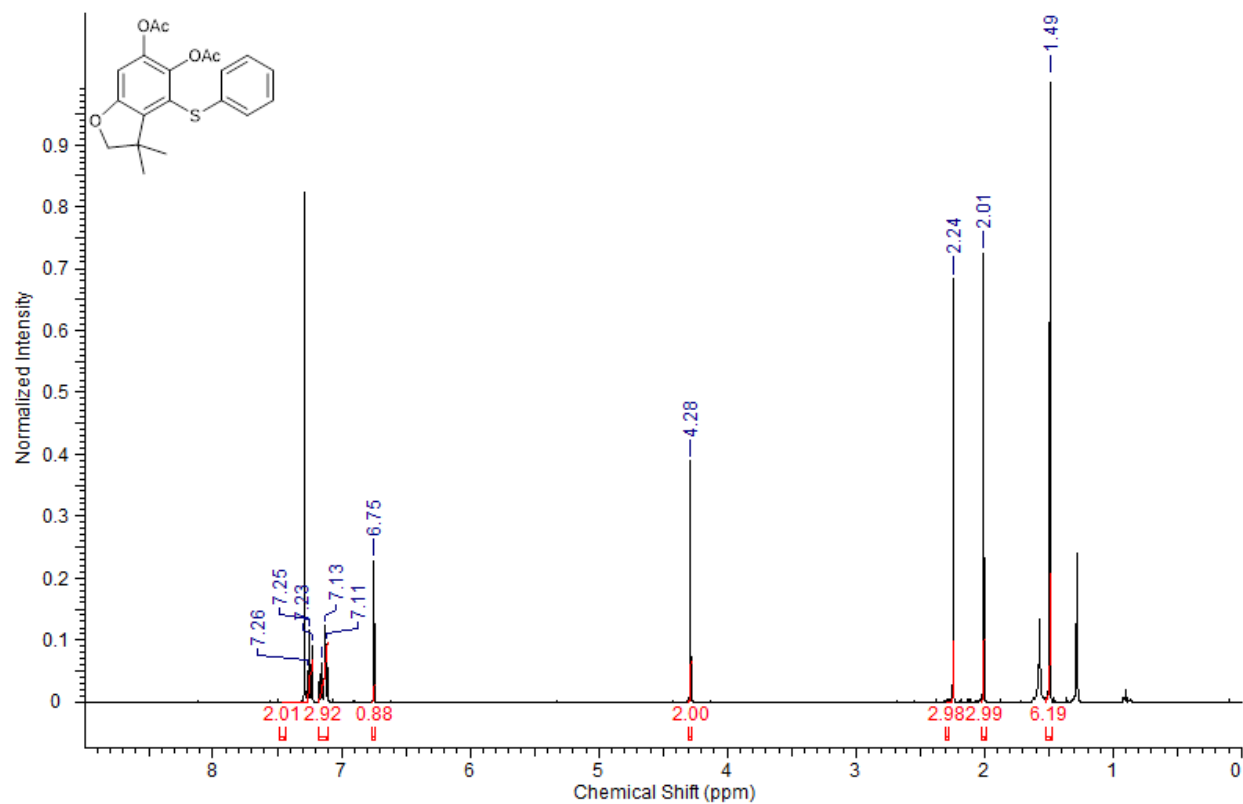
c) Substrates in Table 3.3.3:
3.3.13:



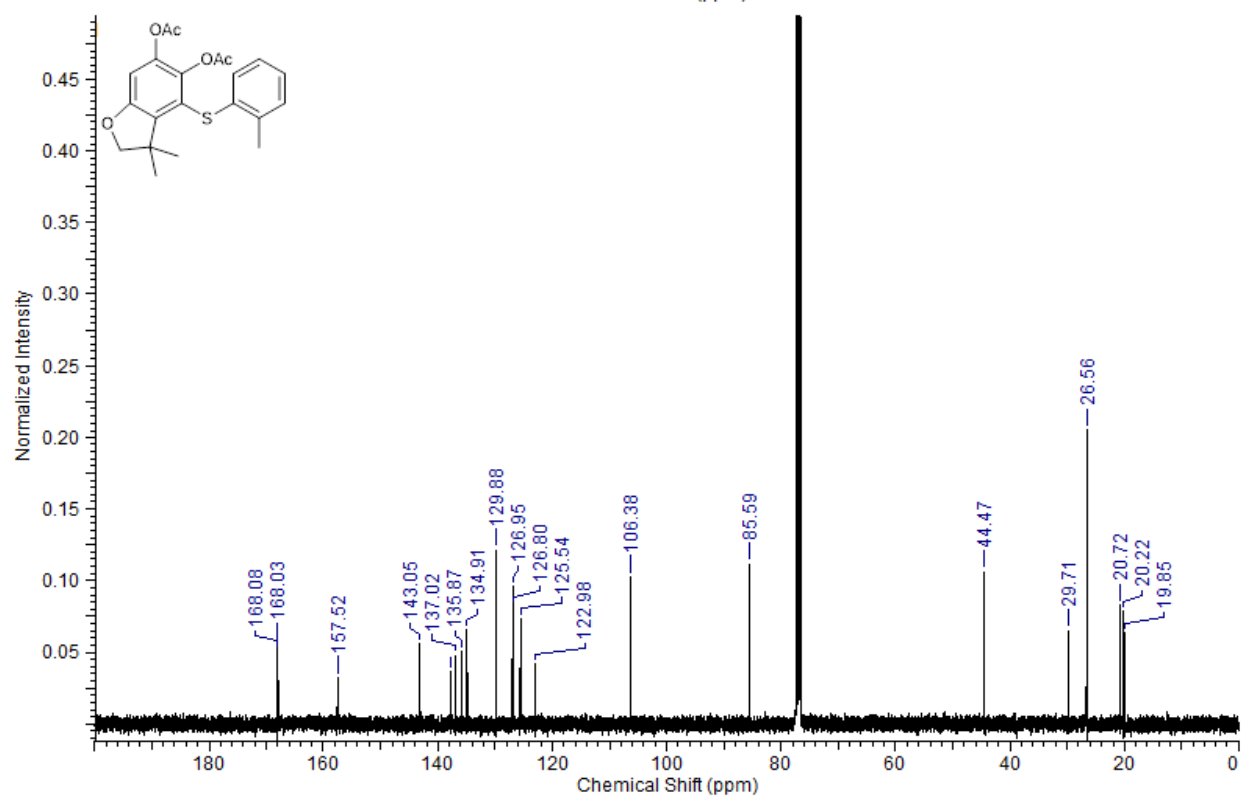
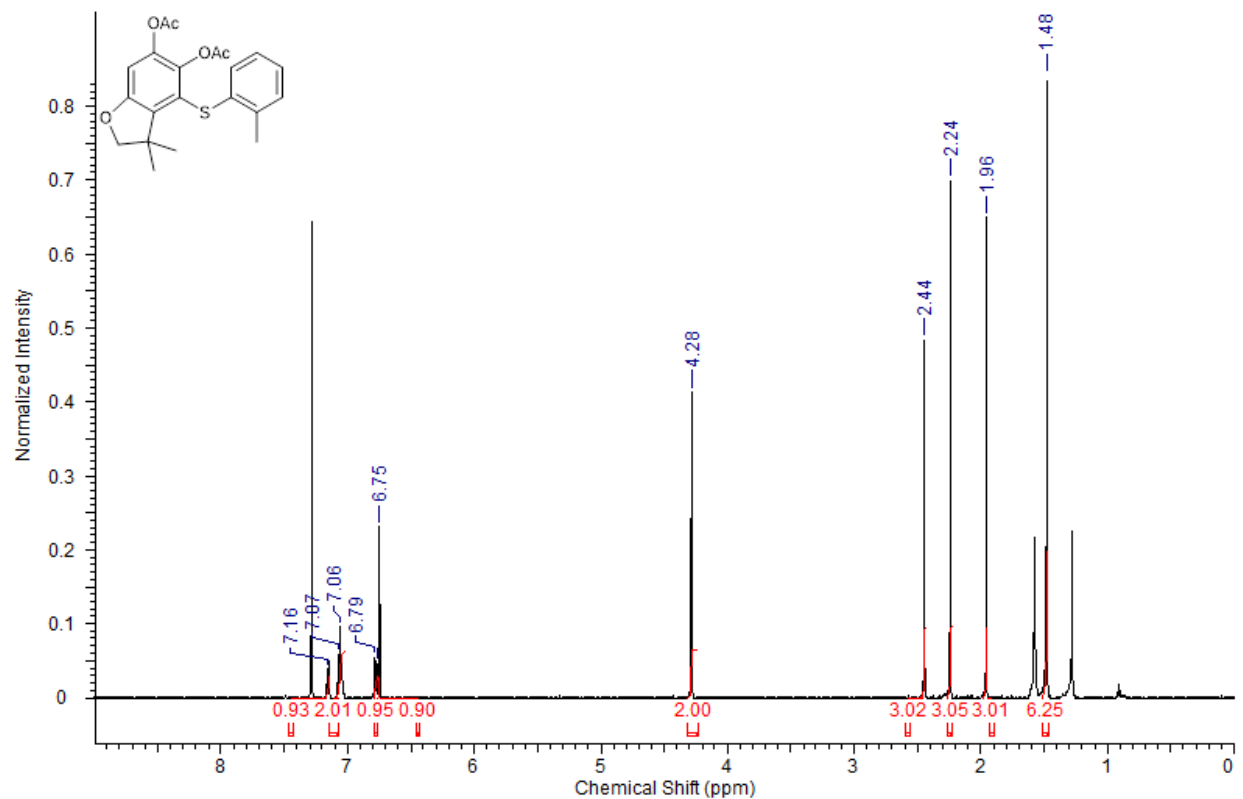
3.3.14:



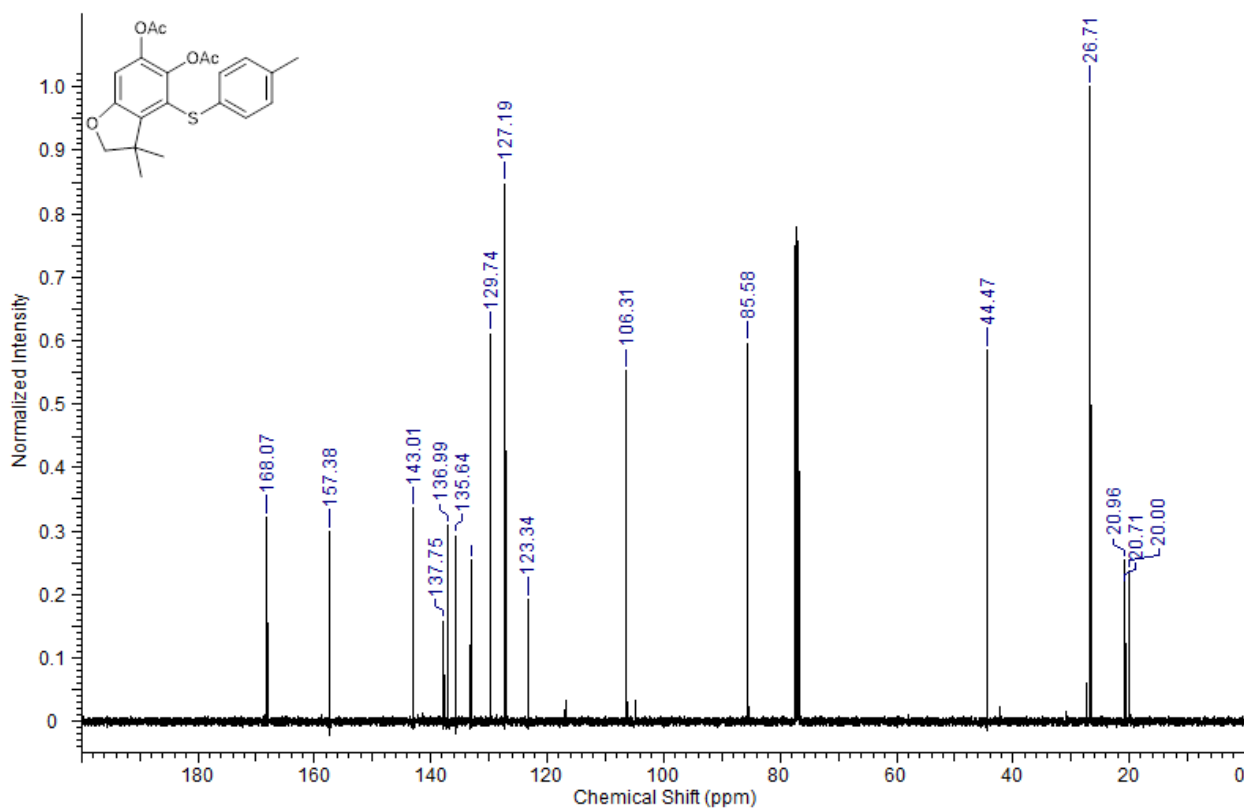
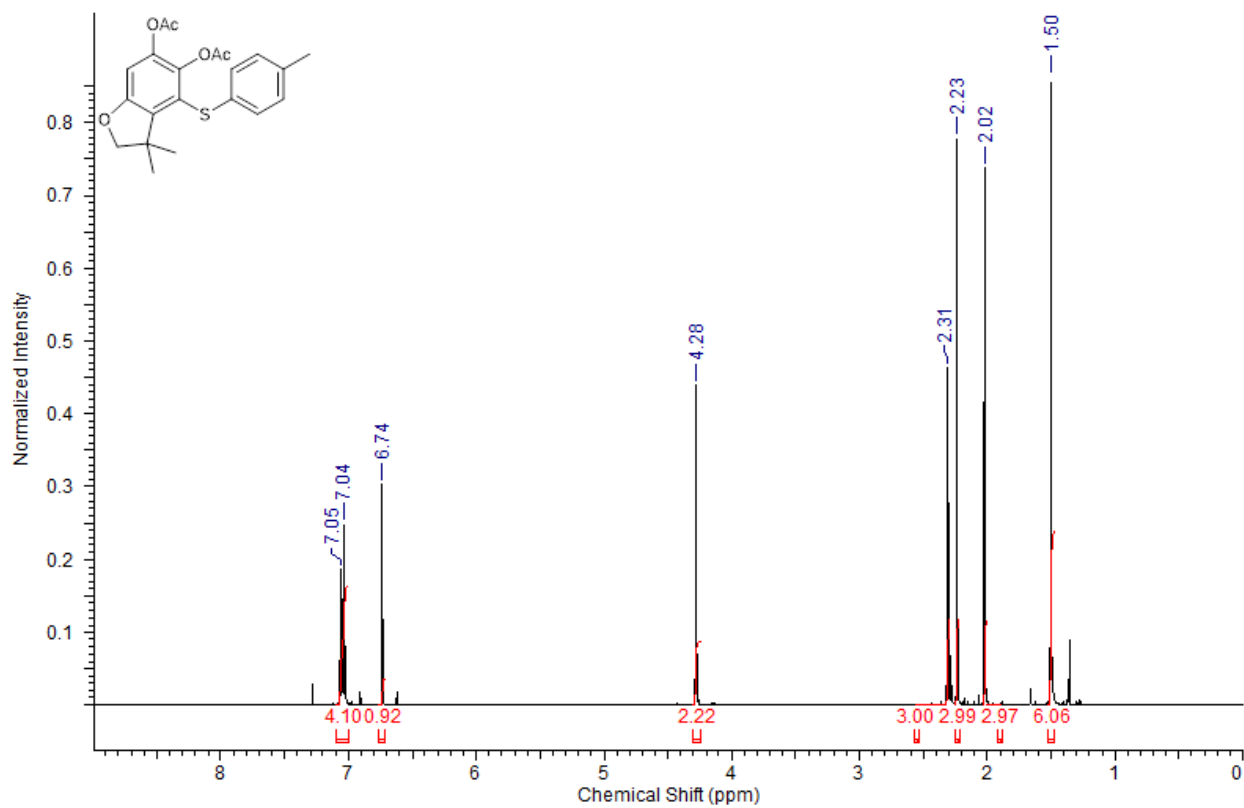
3.3.15:



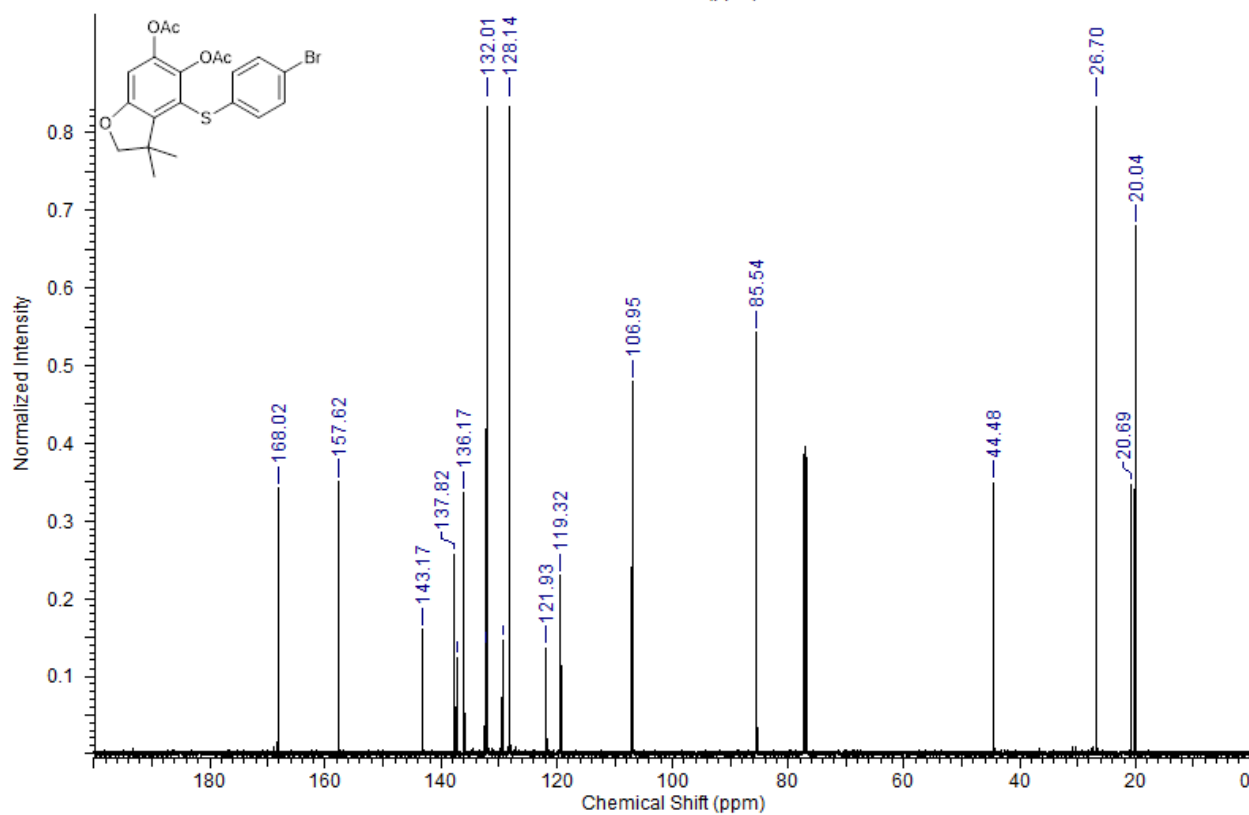
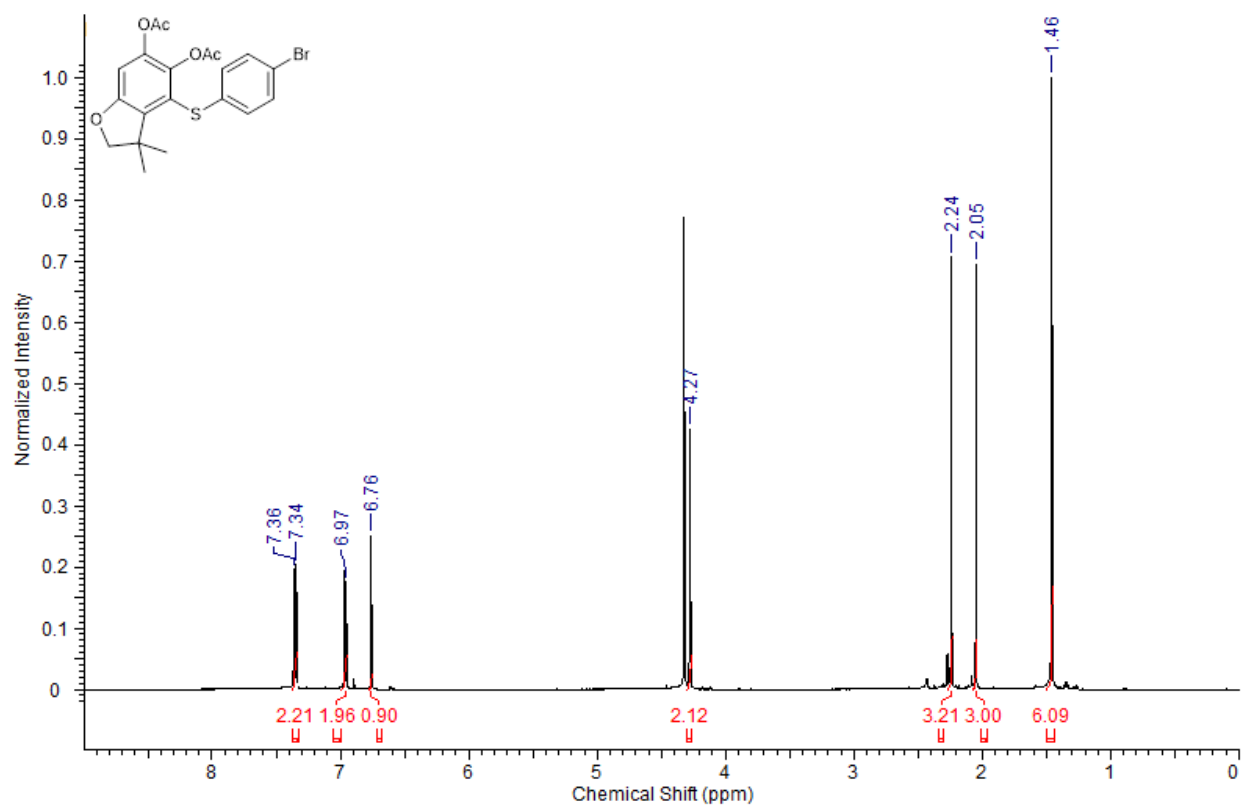
3.3.16:



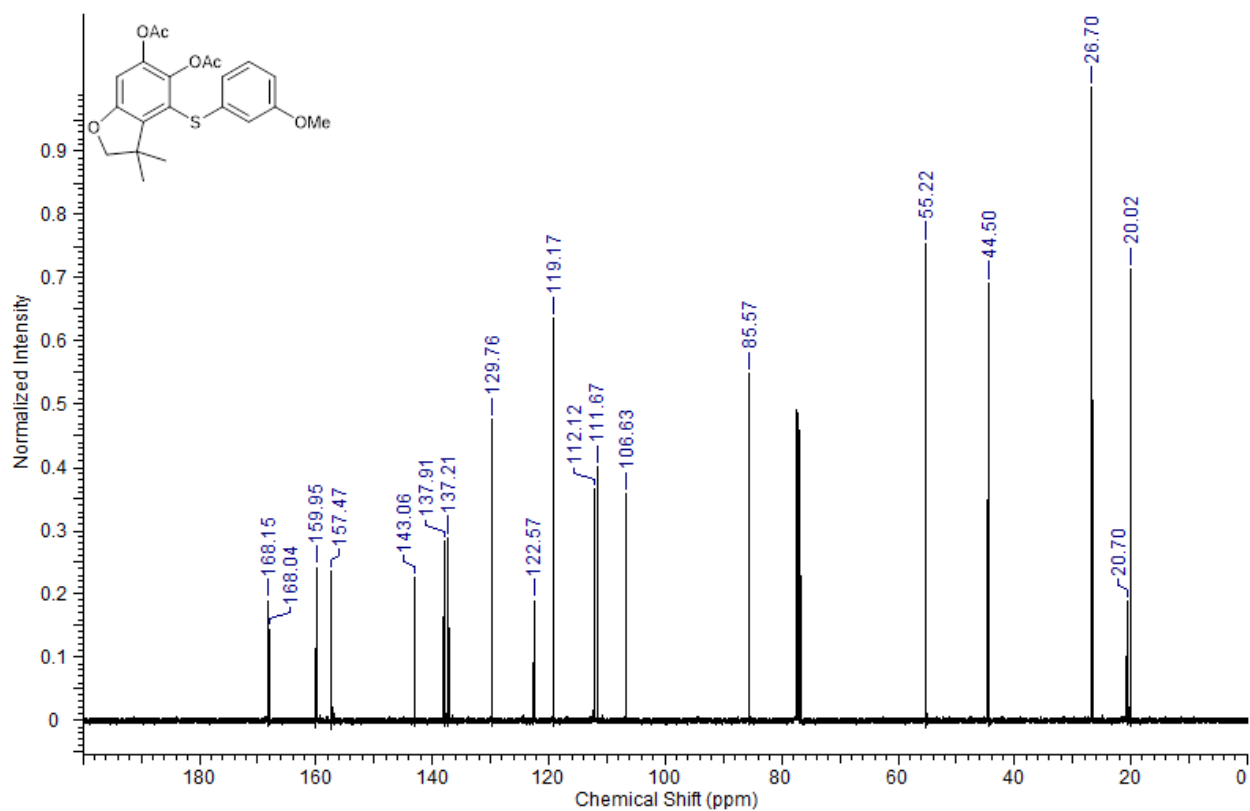
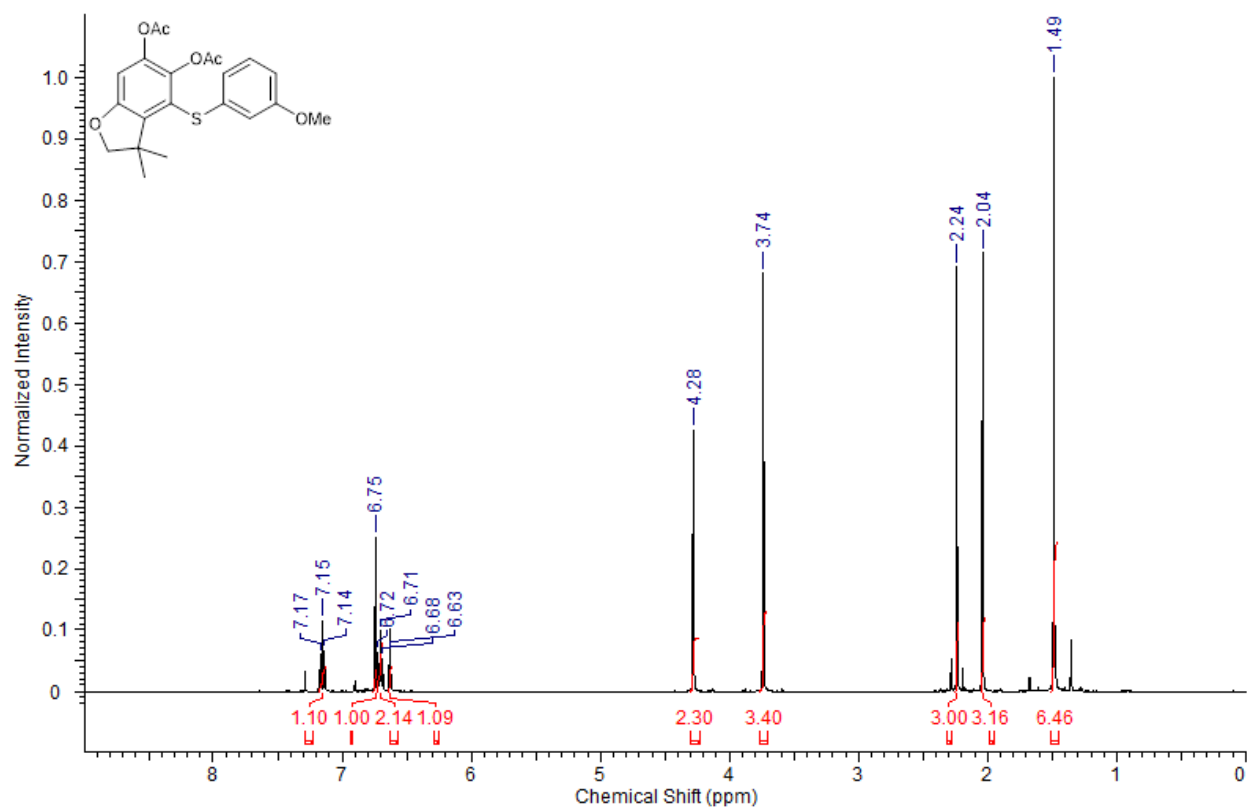
3.3.17:



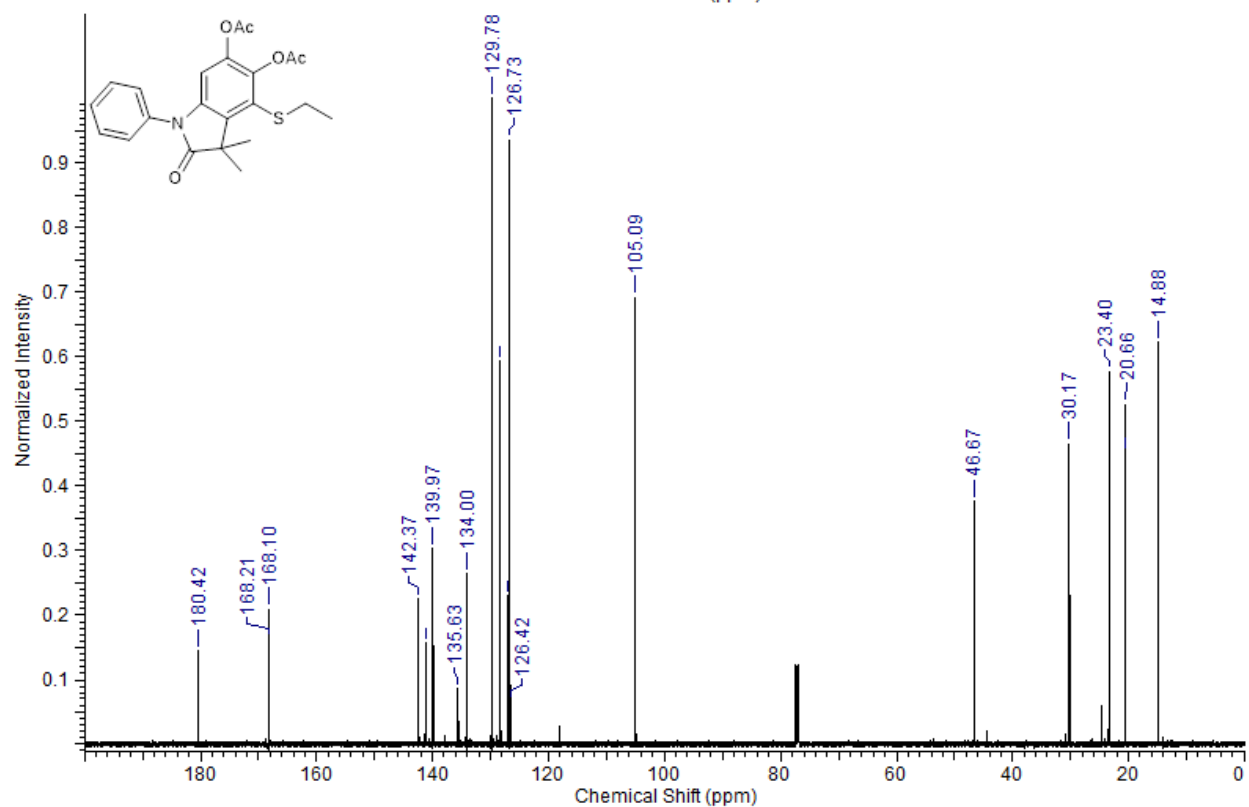
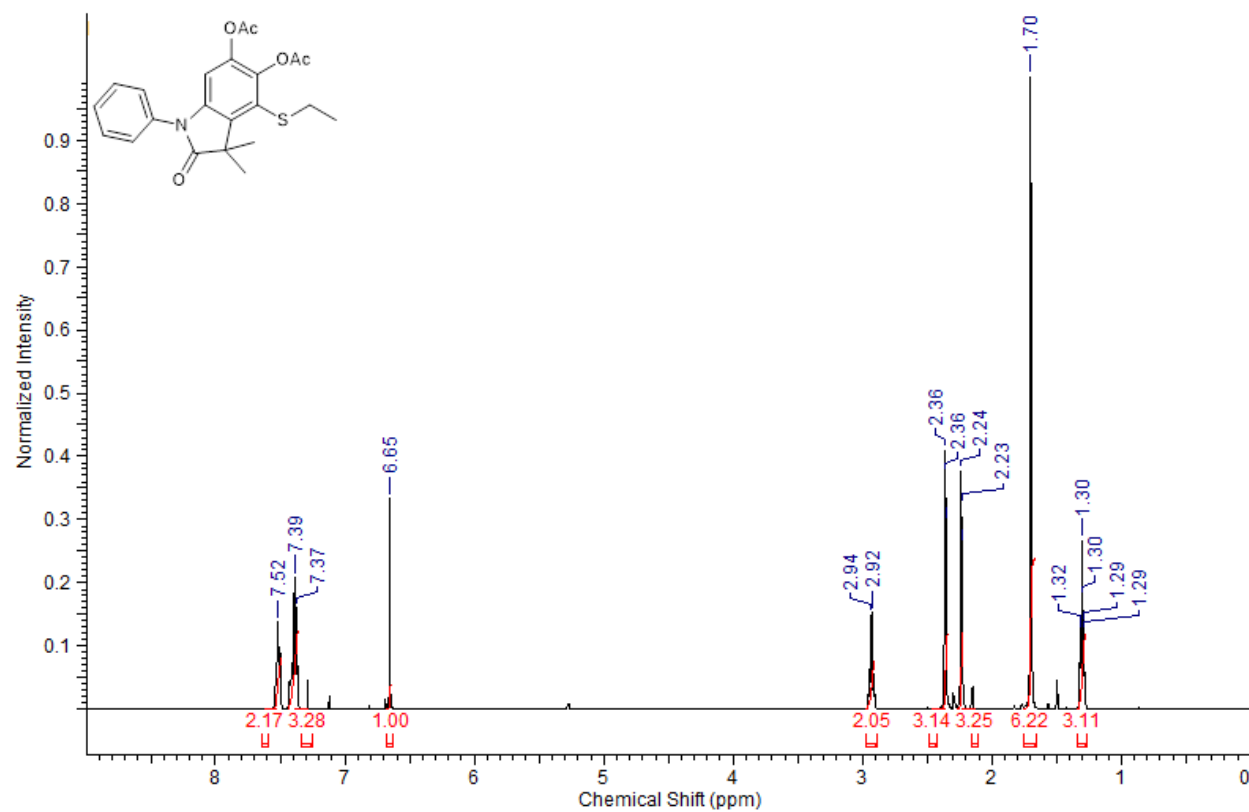
3.3.18:



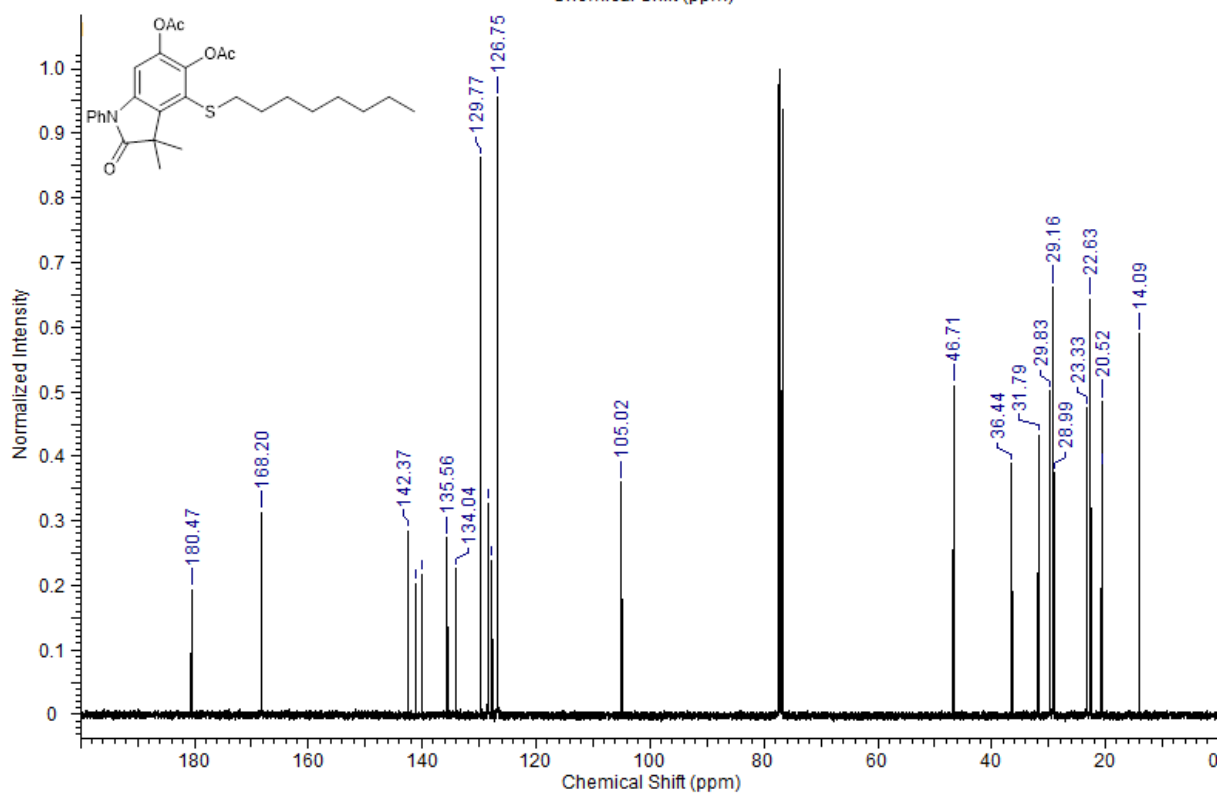
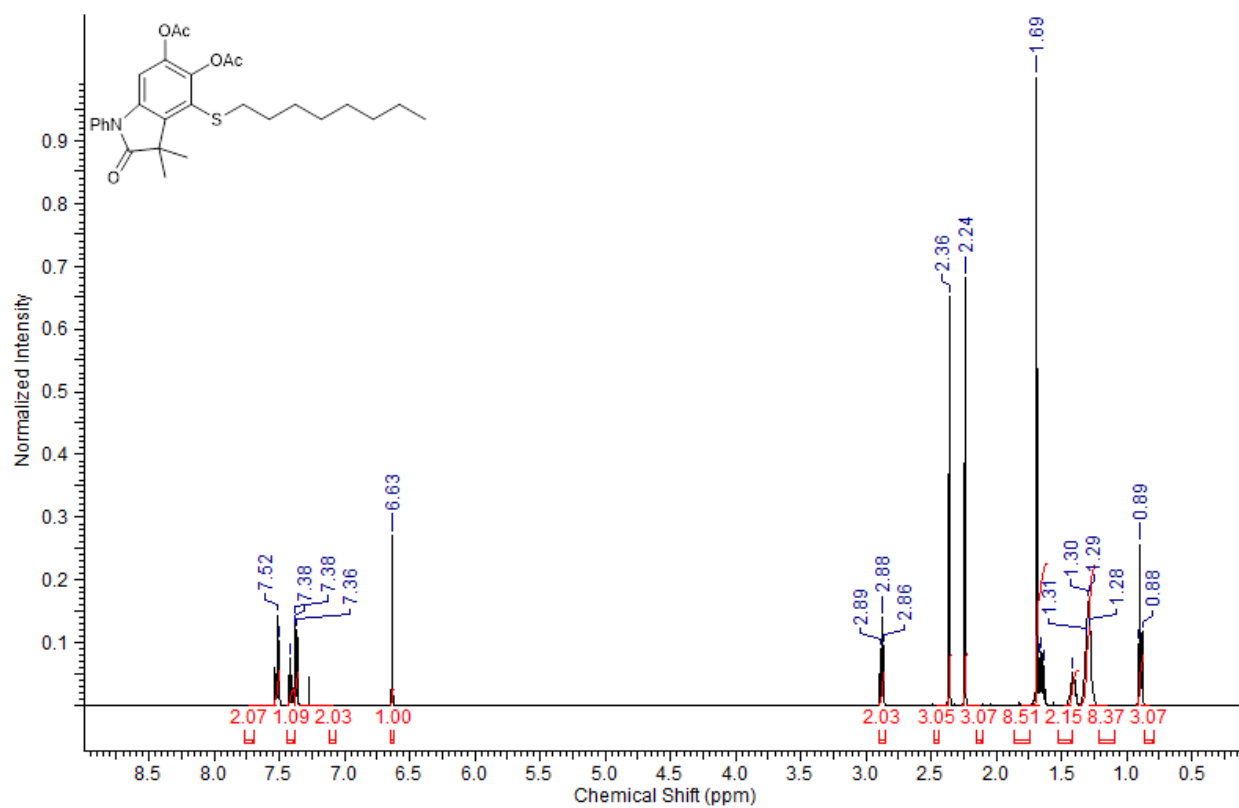
3.3.19:



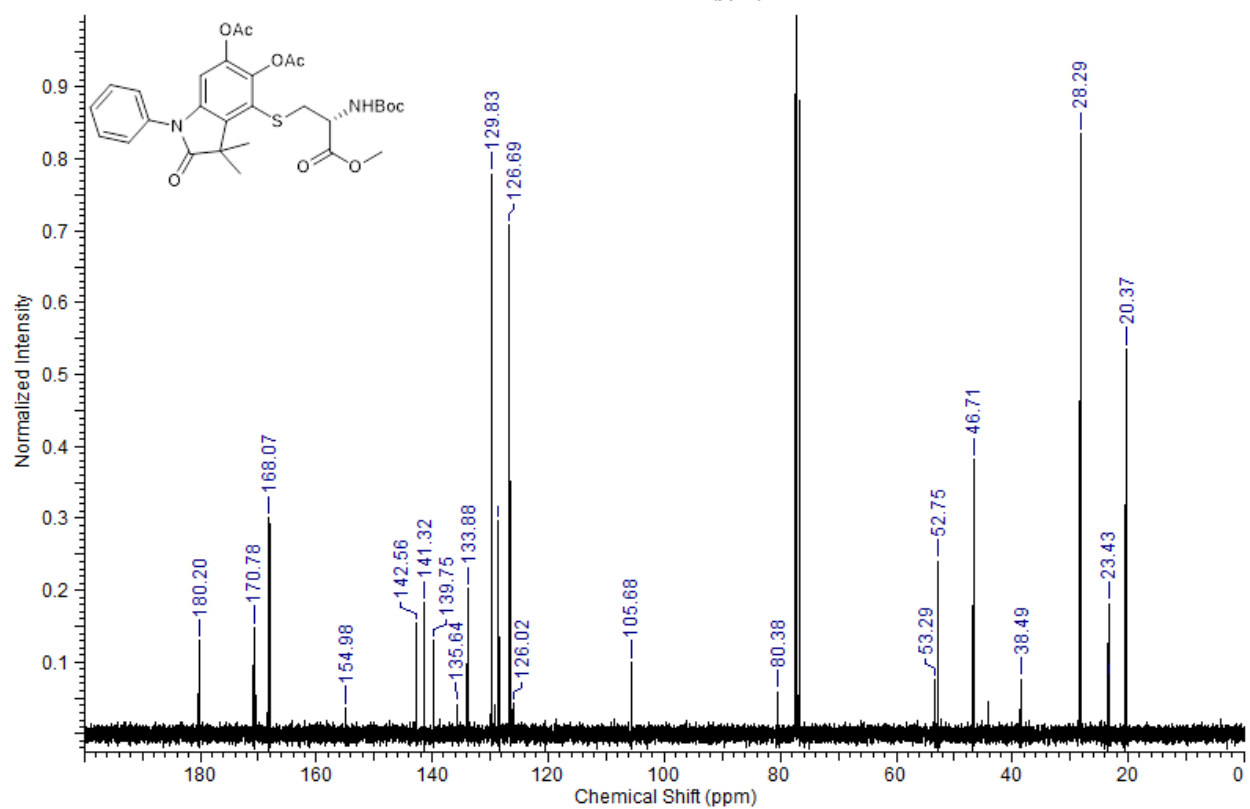
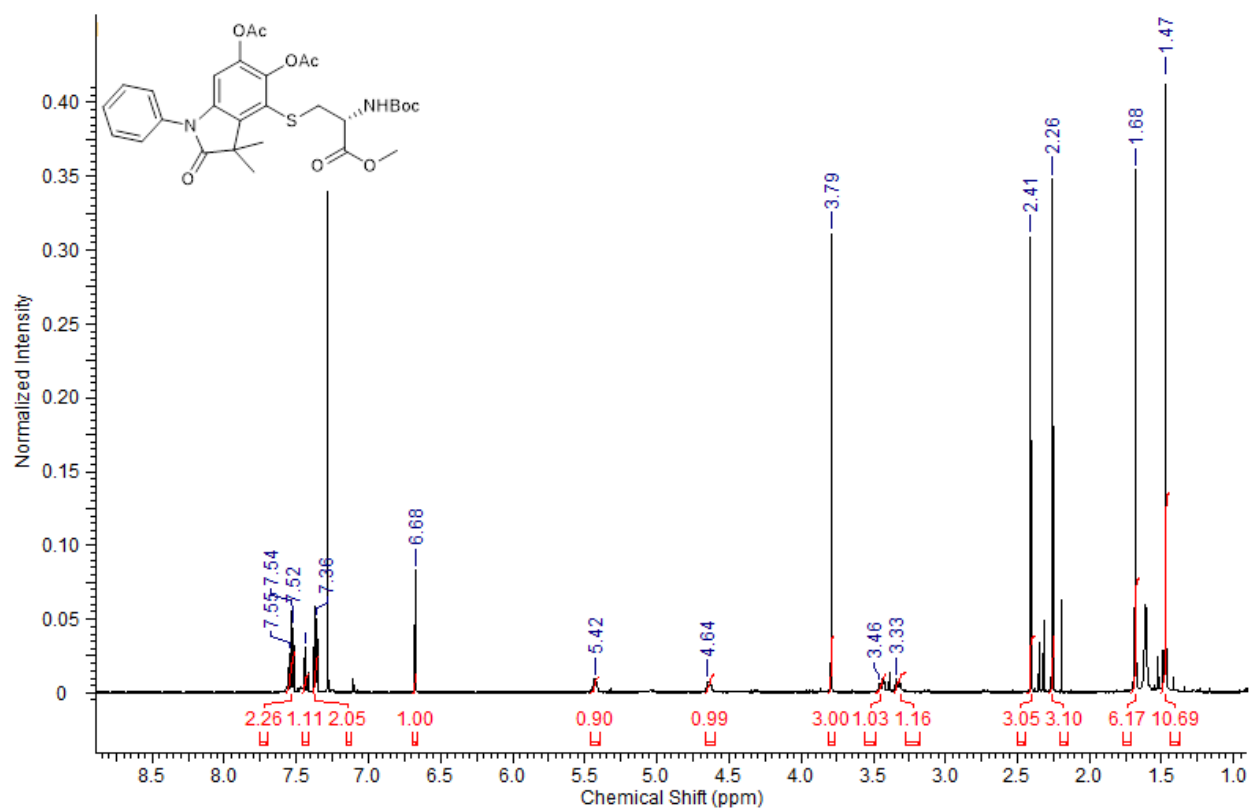
3.3.20:



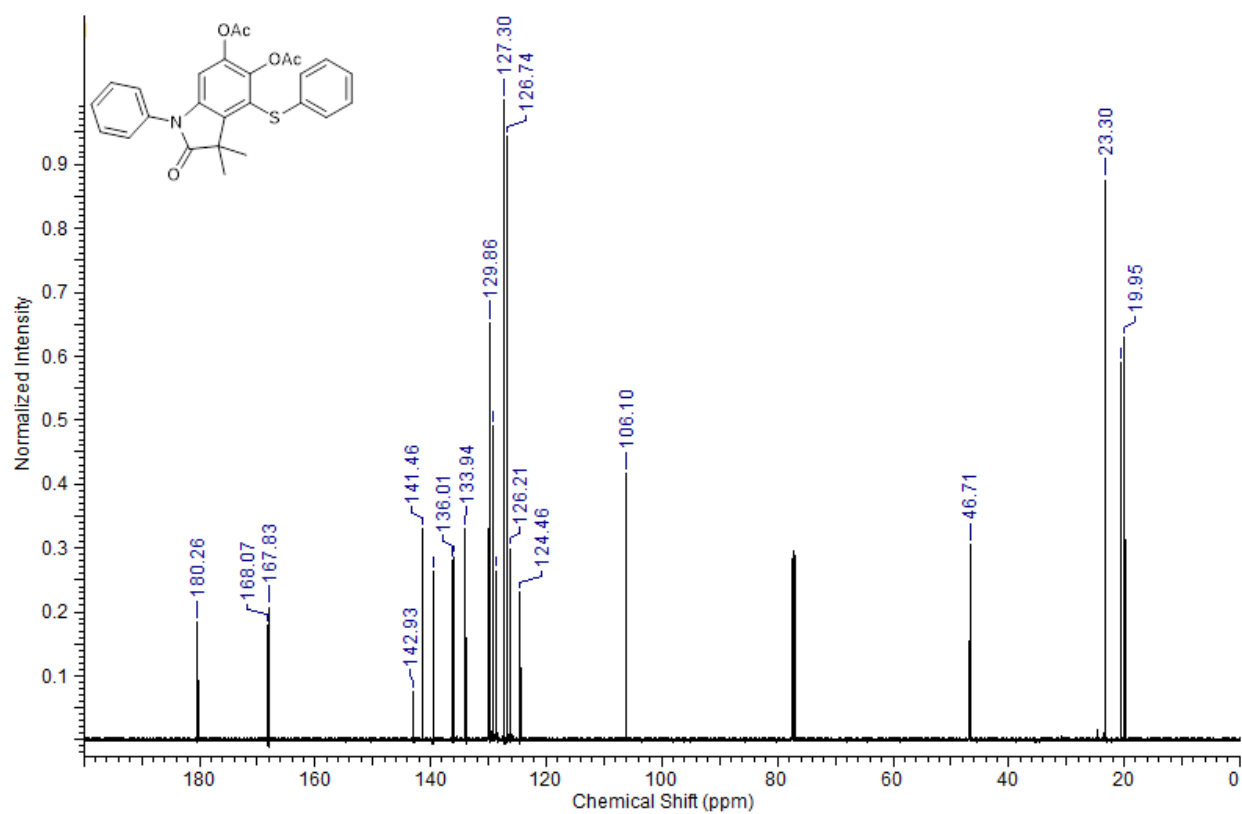
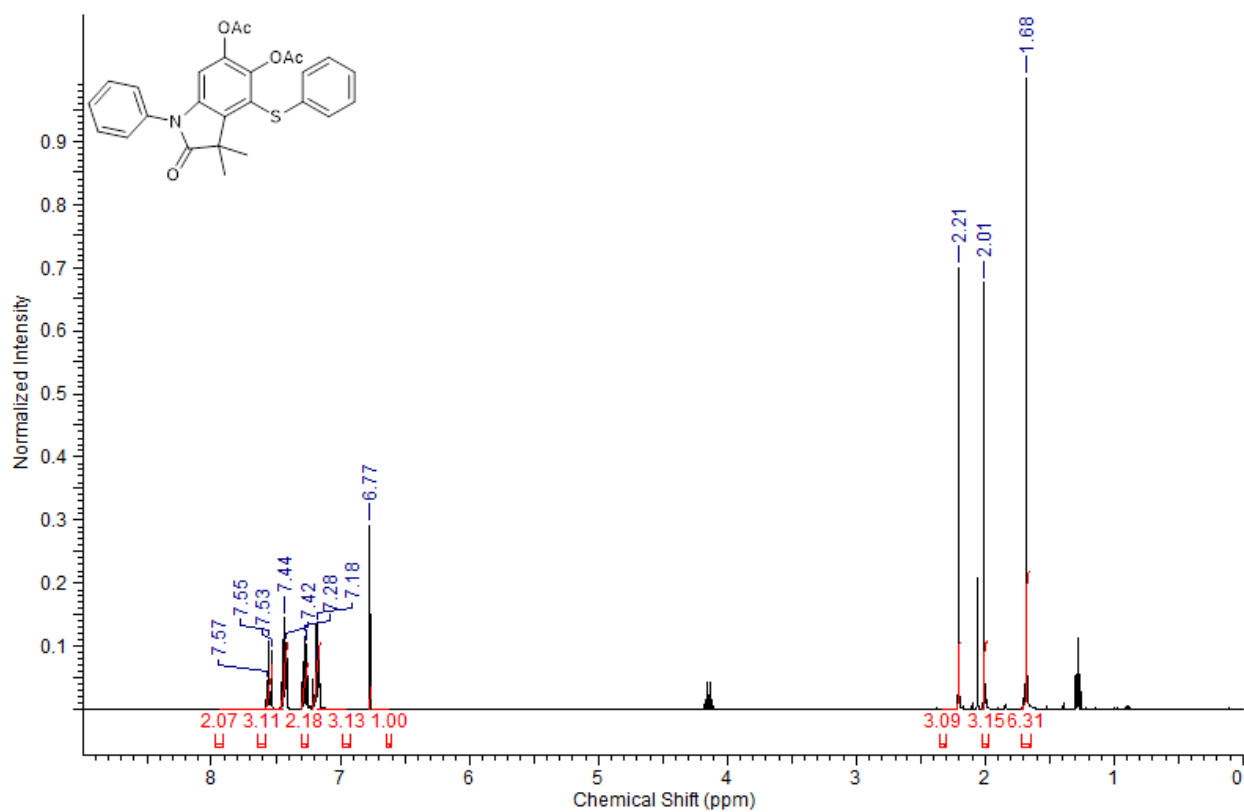
3.3.21:



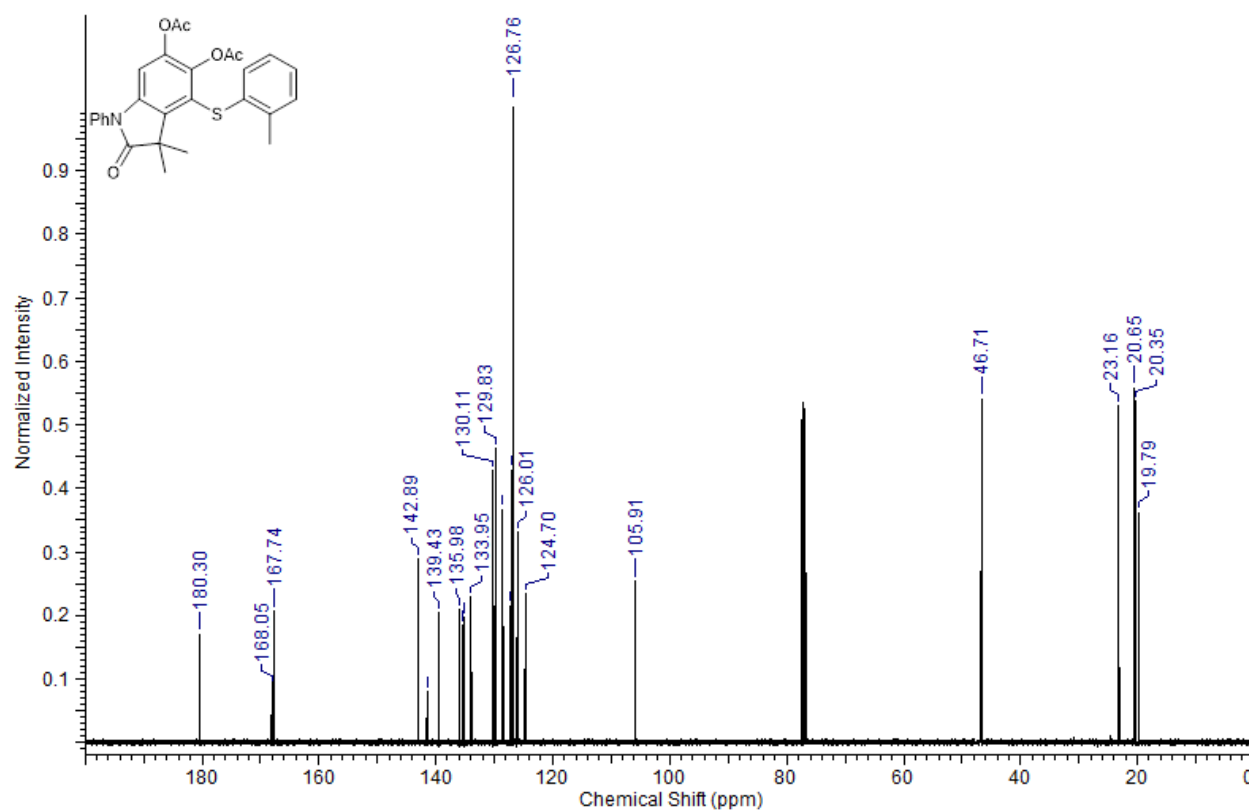
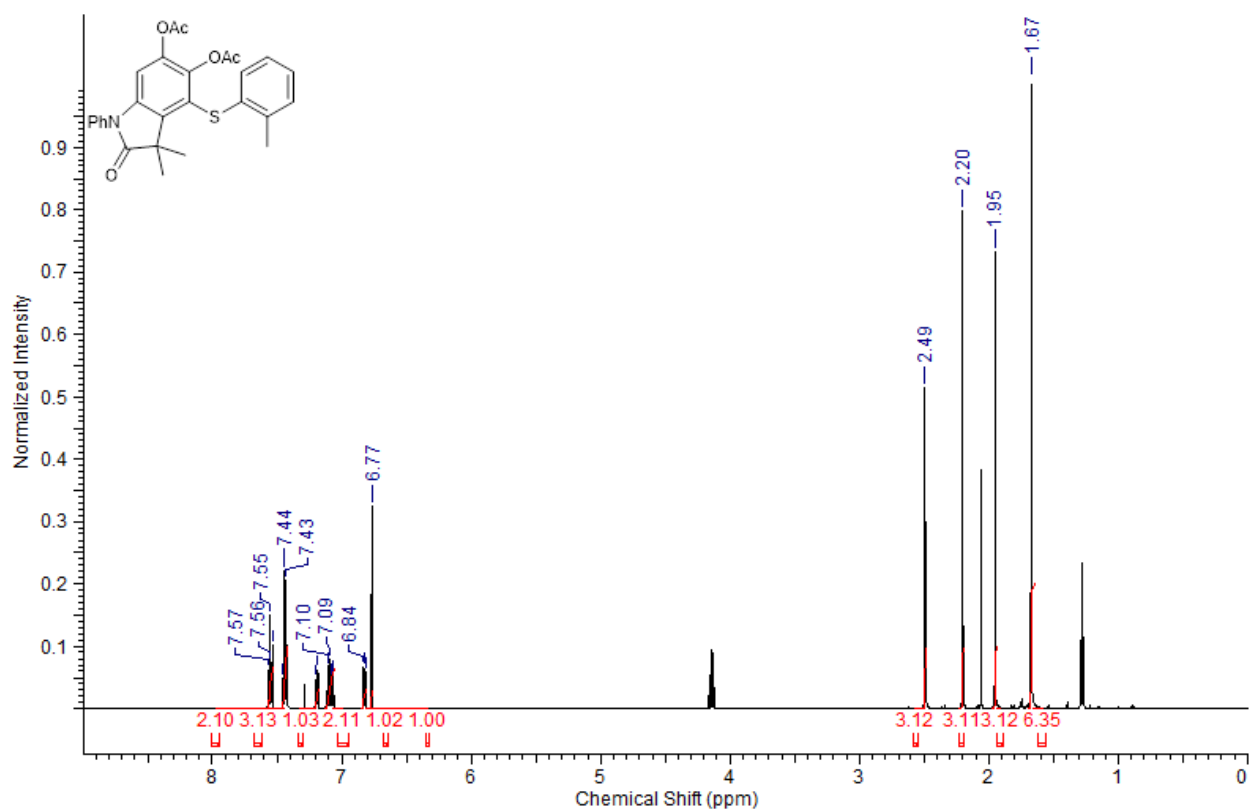
3.3.22:



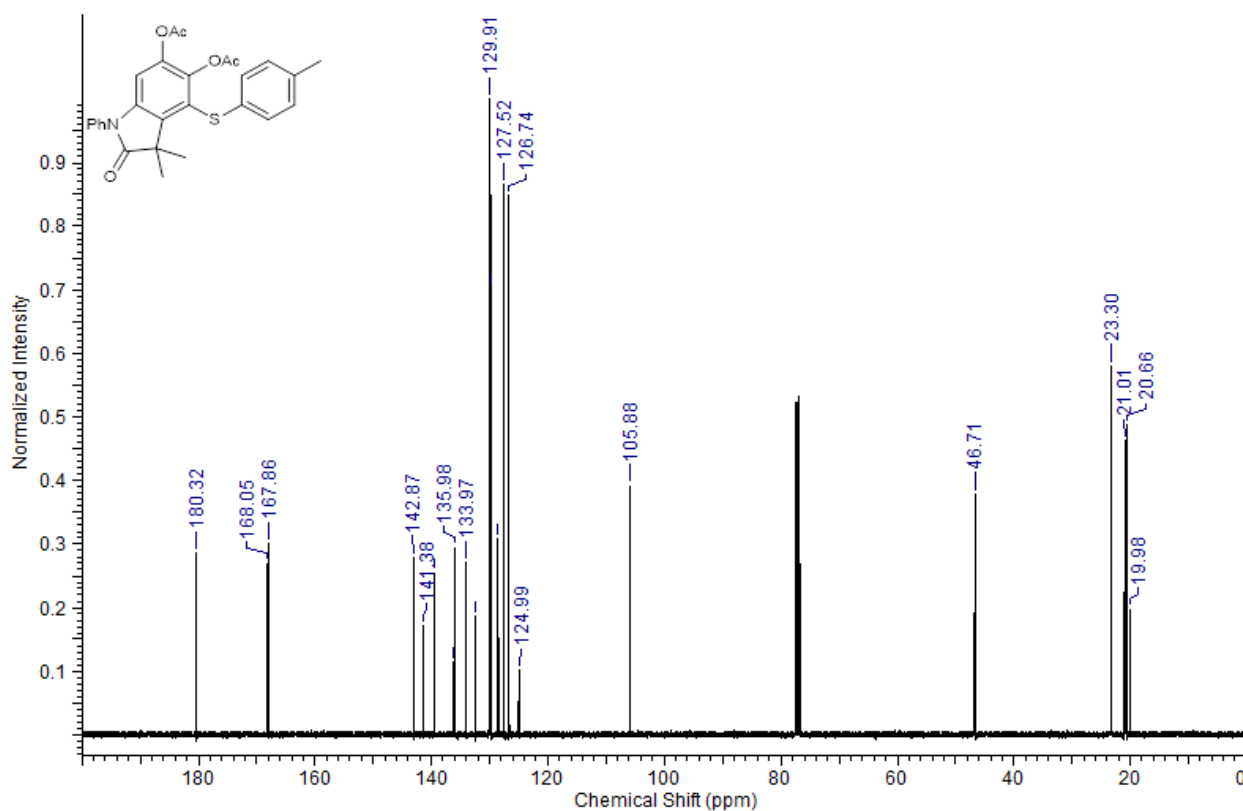
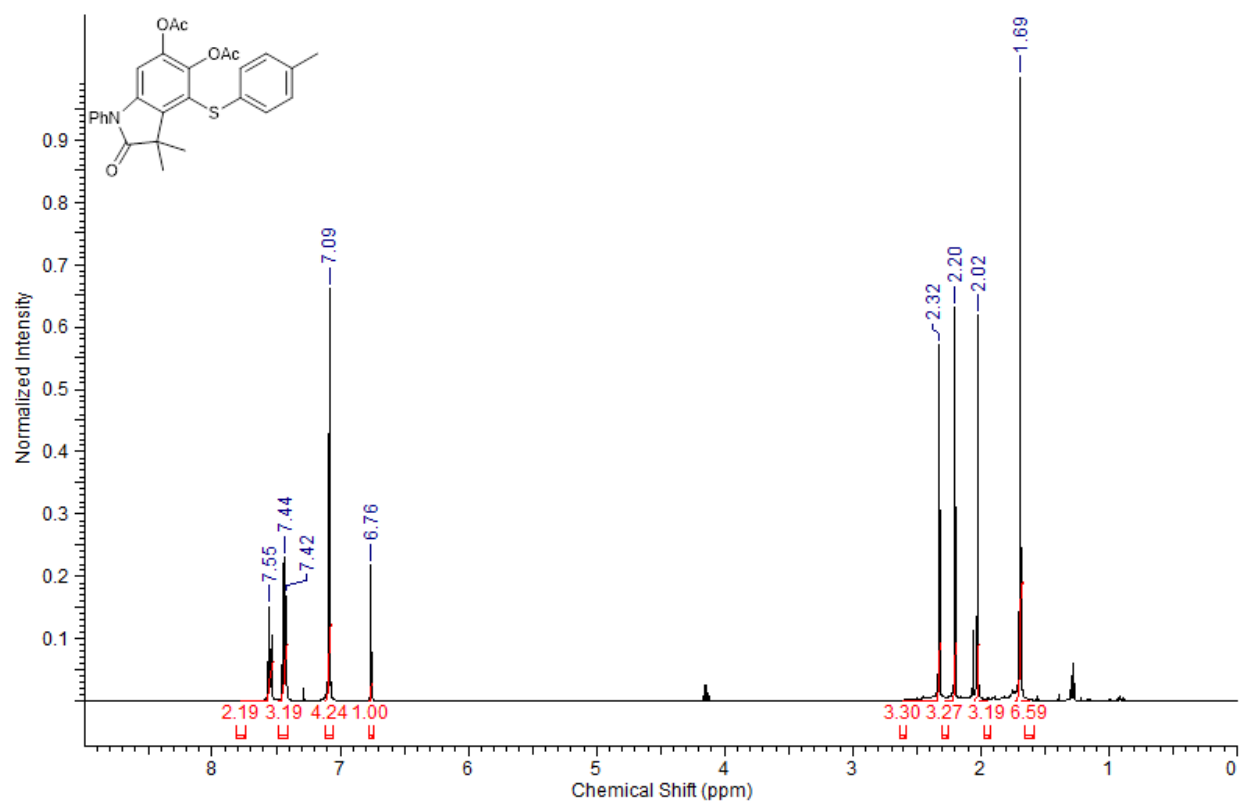
3.3.23:



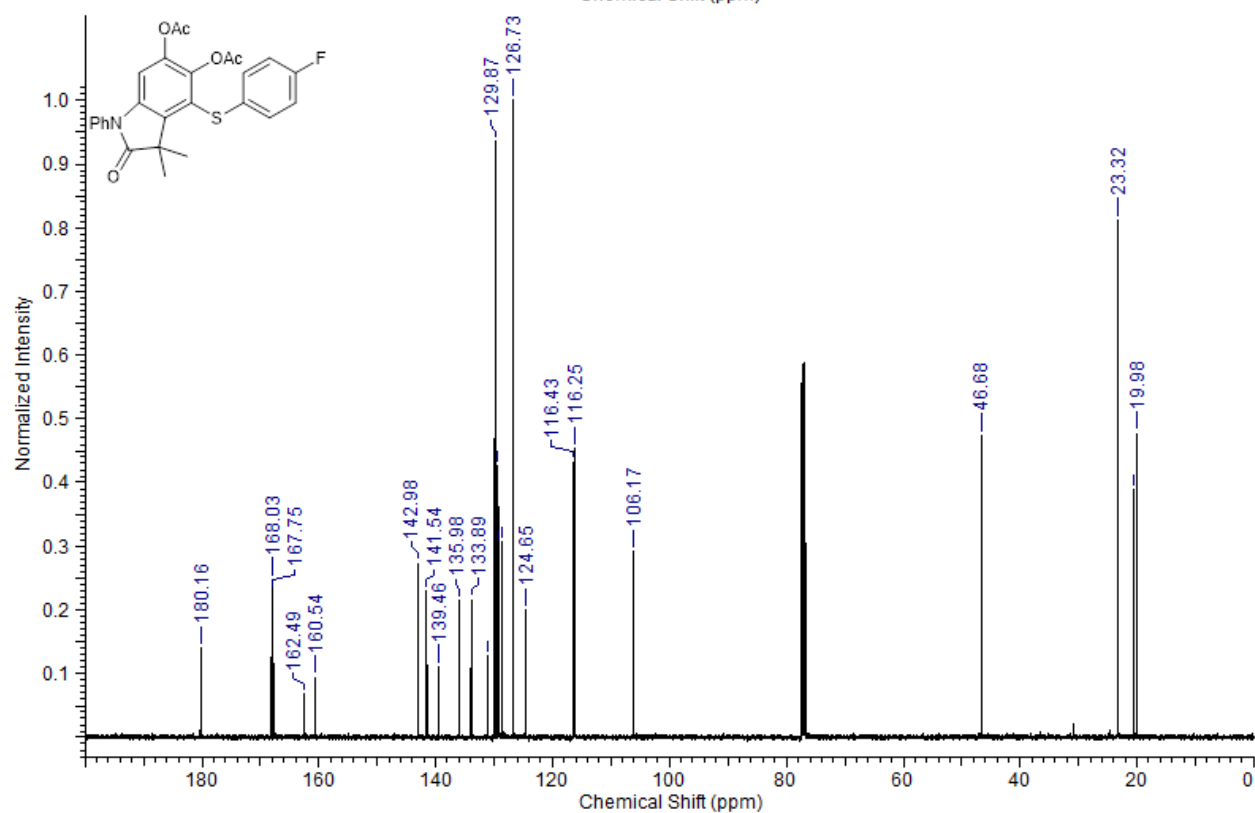
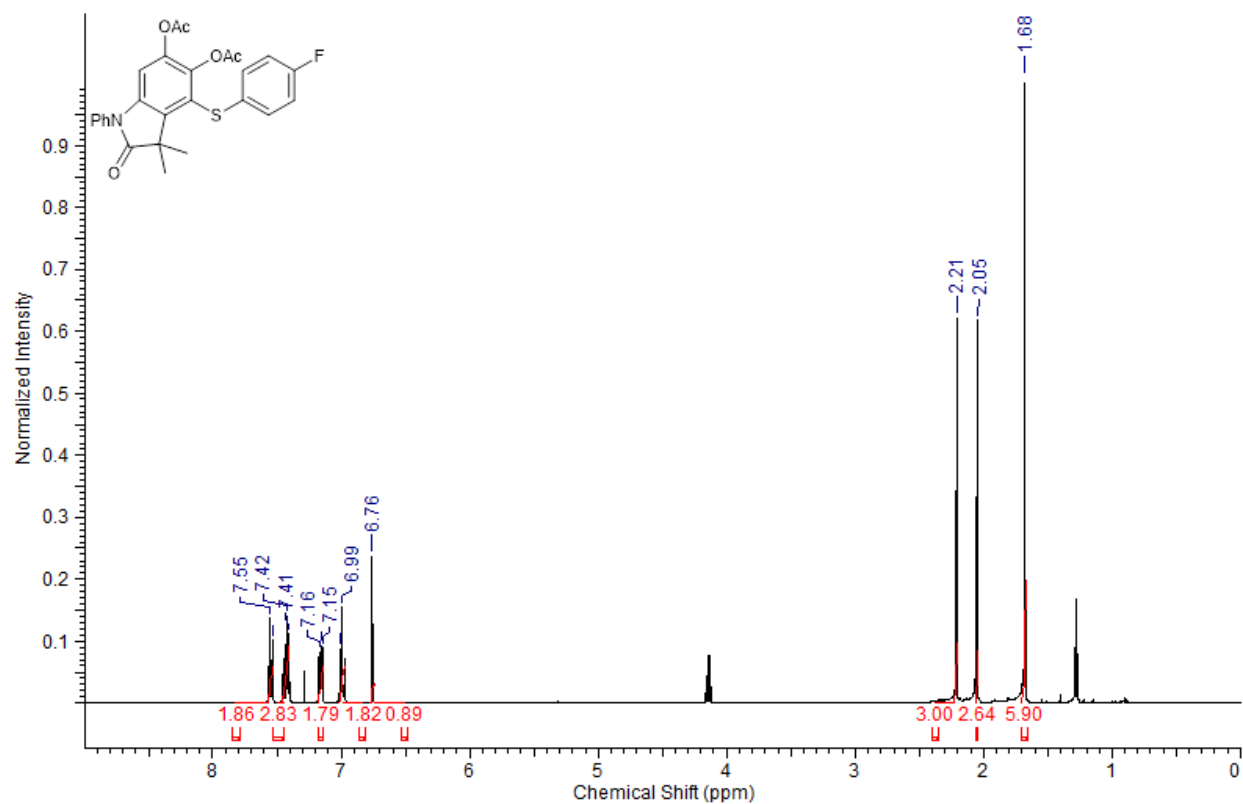
3.3.24:



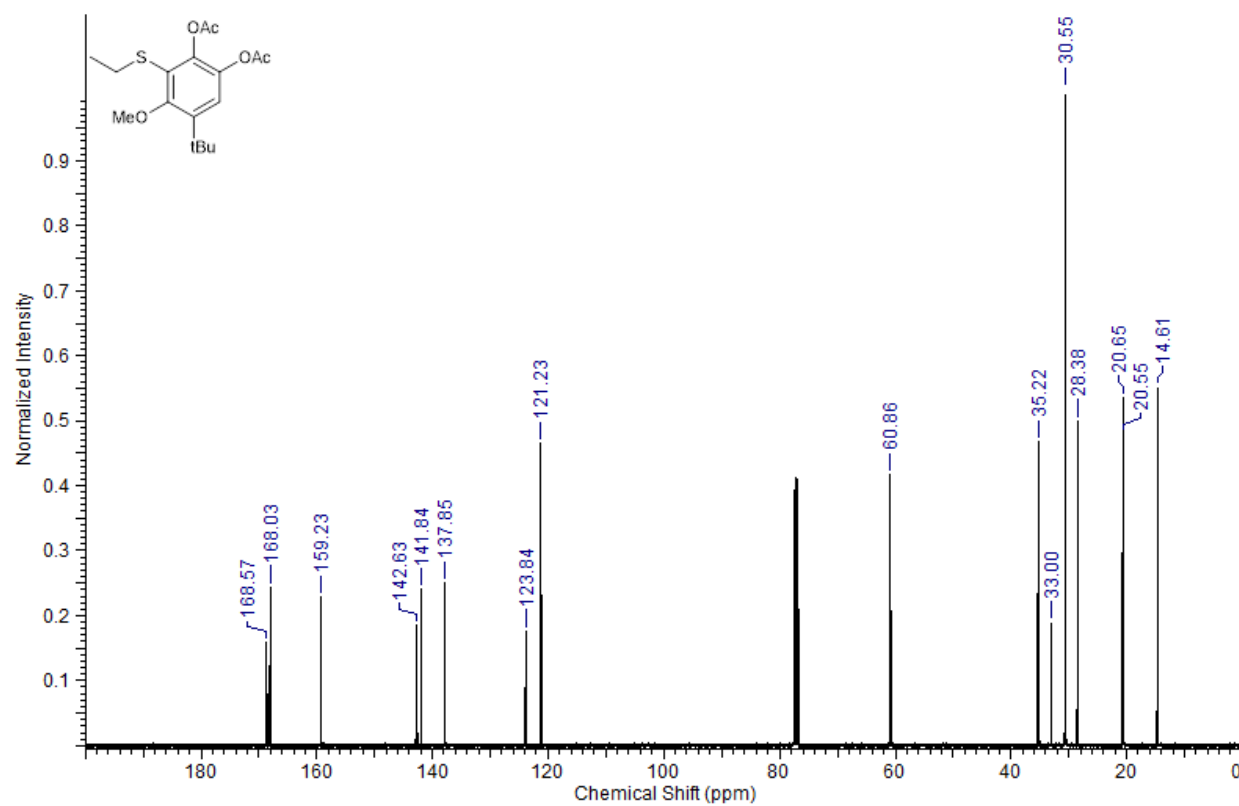
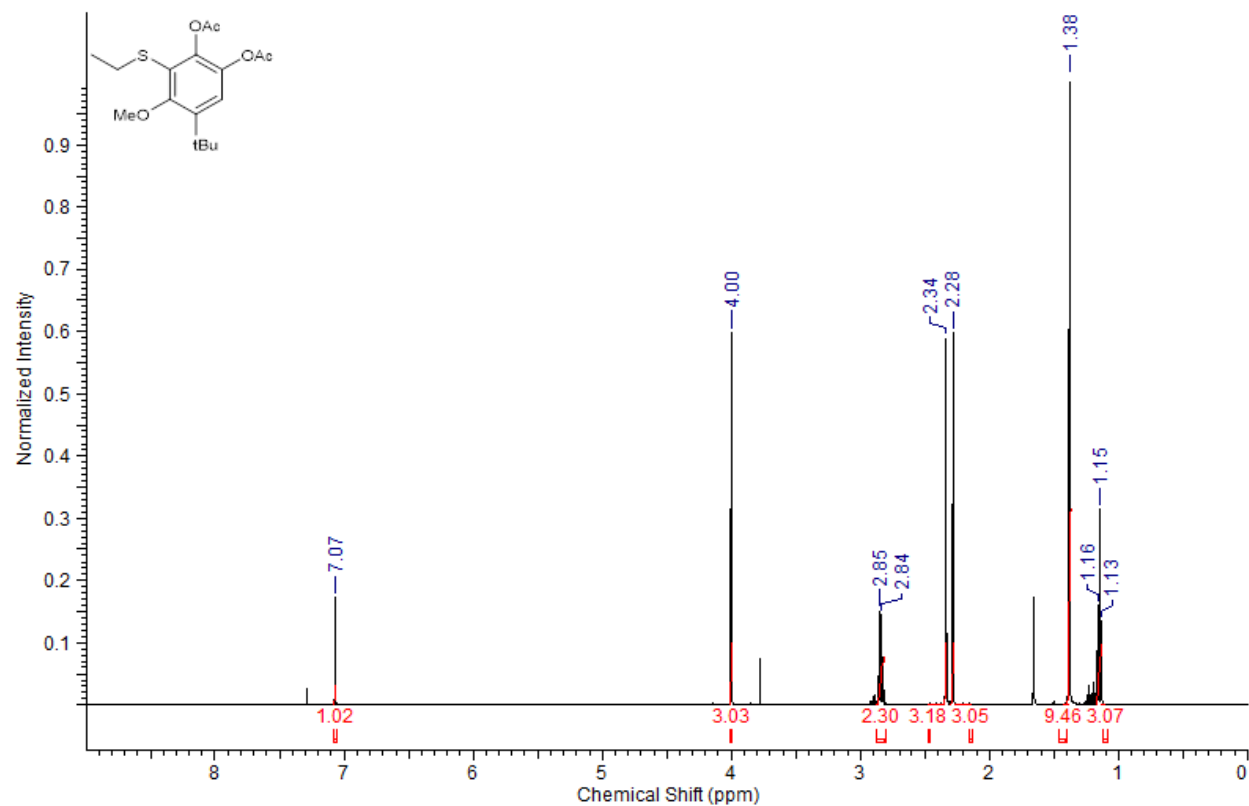
3.3.25:



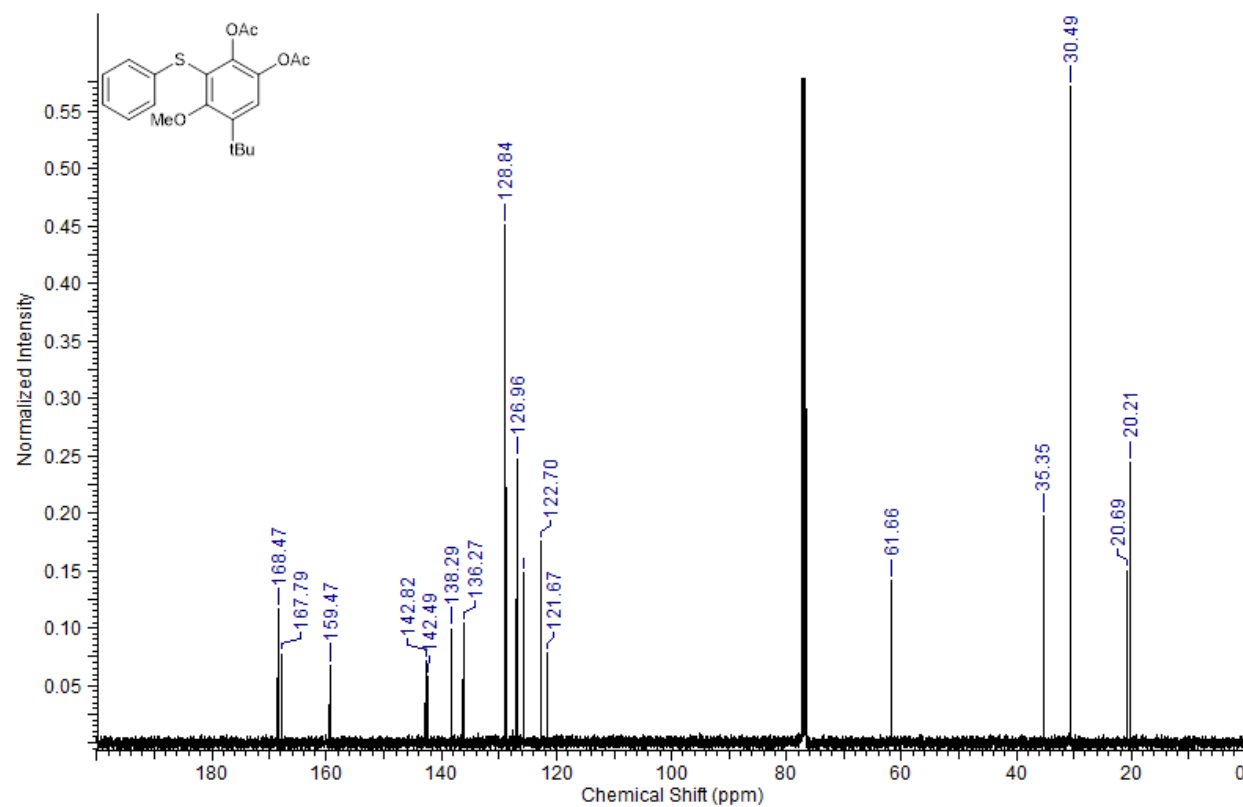
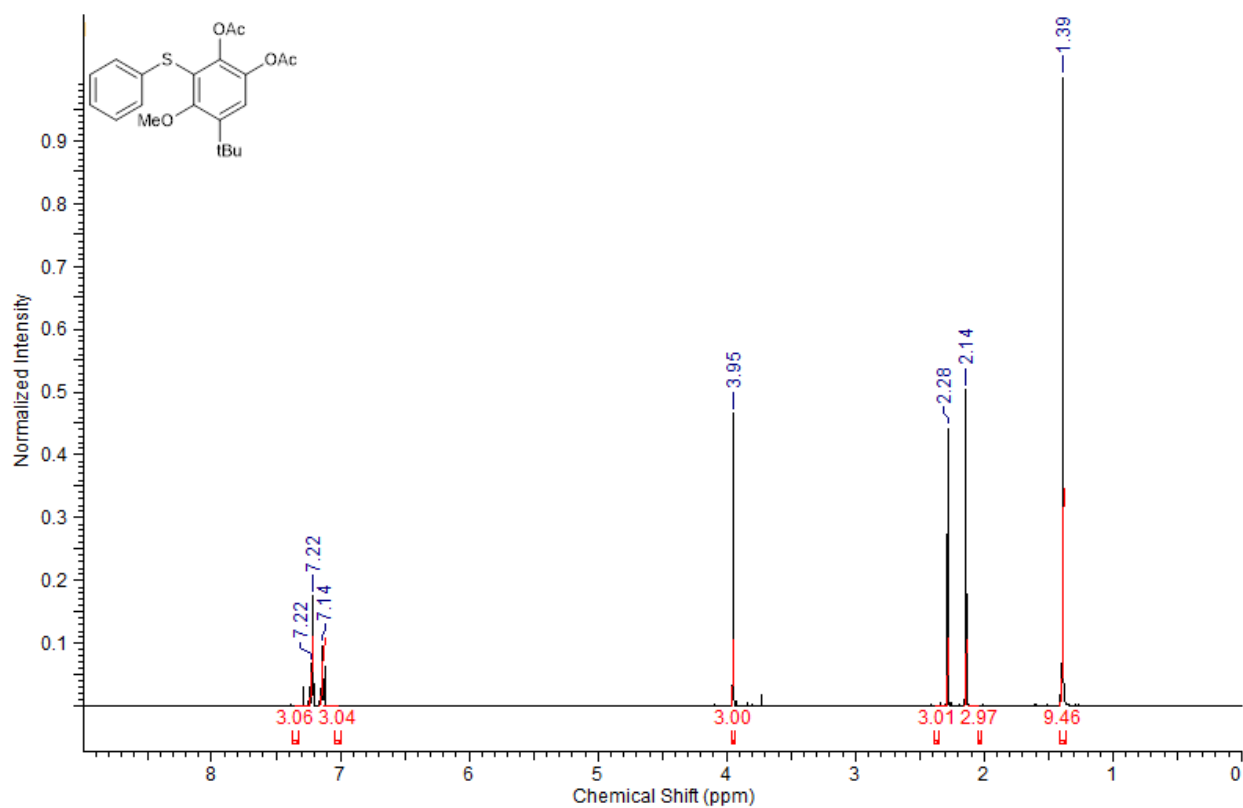
3.3.26:



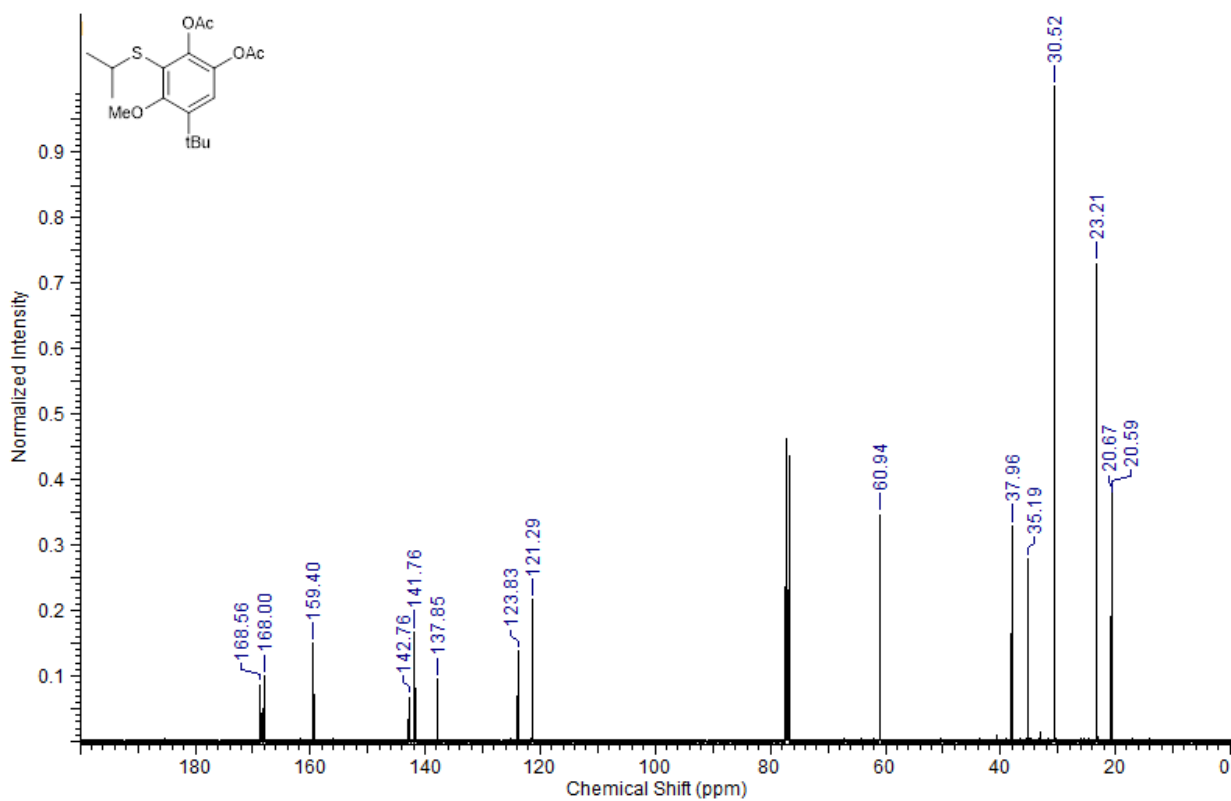
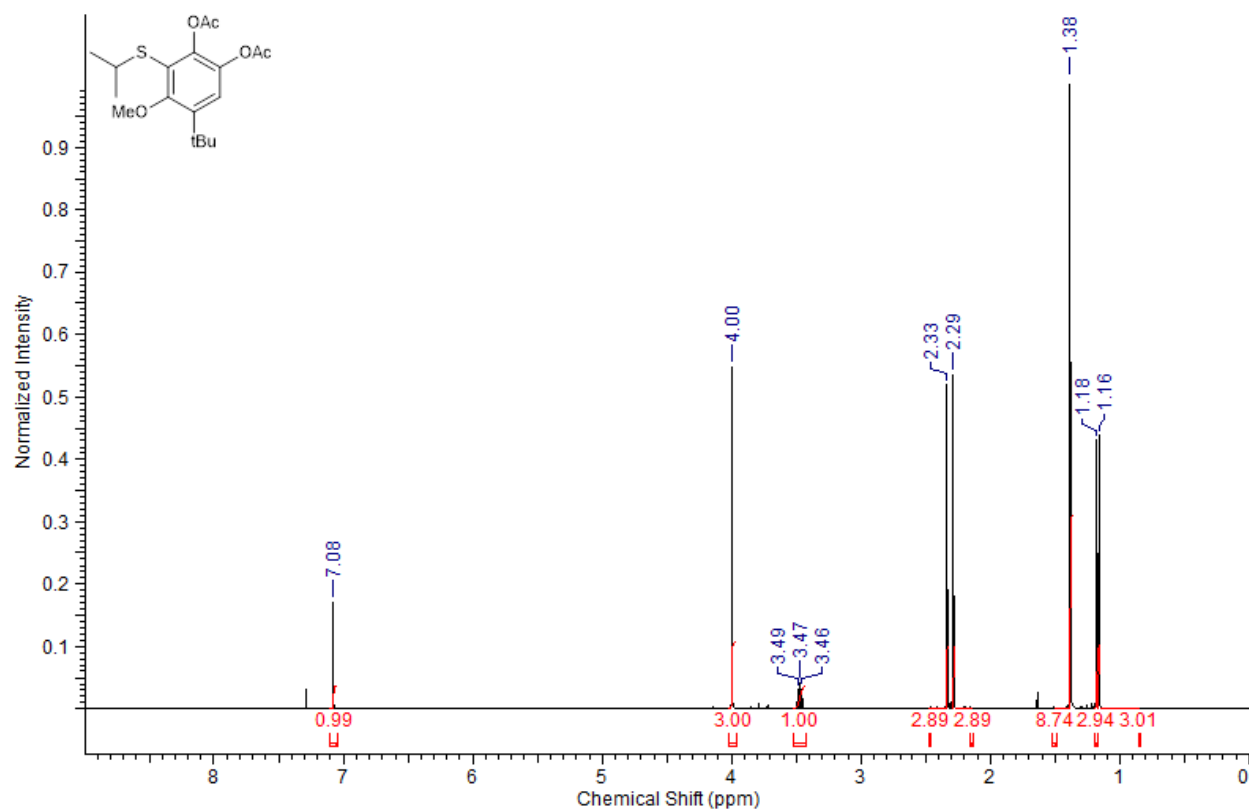
d) Substrates in Table 3.6.2:
3.6.2:



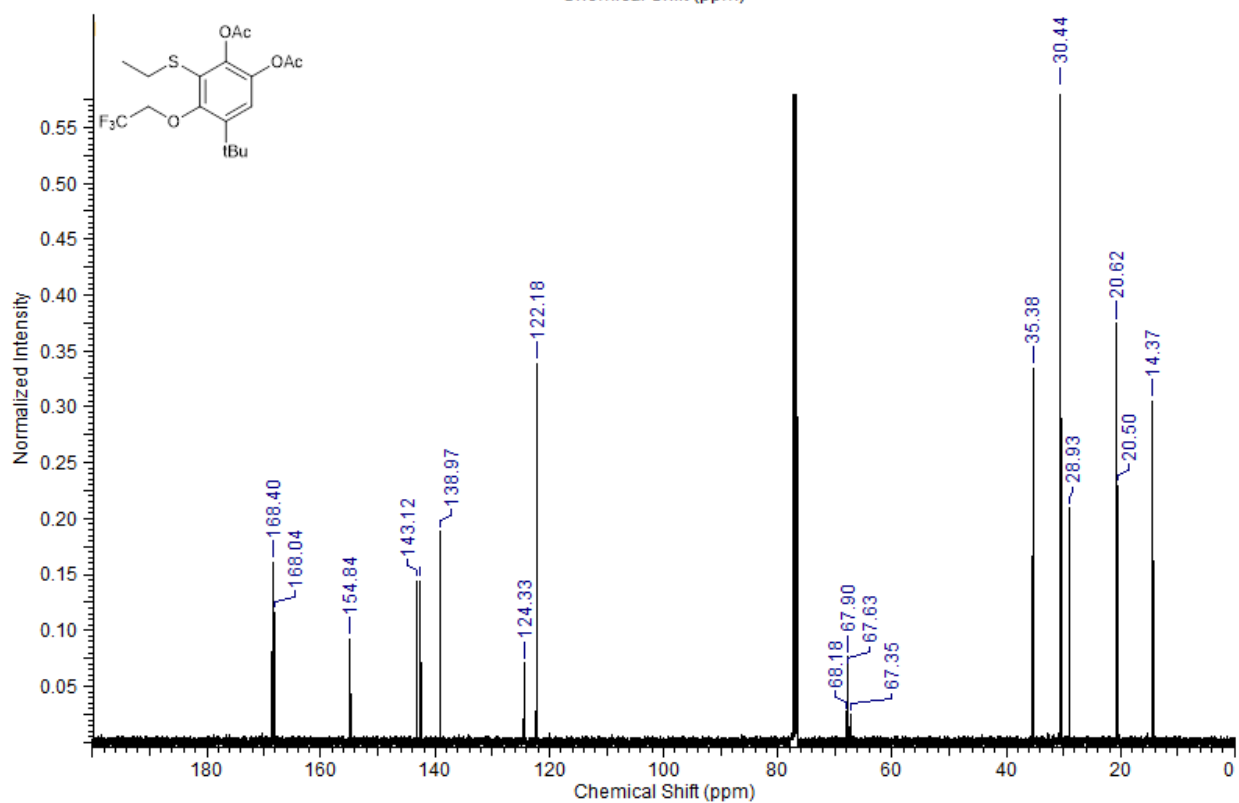
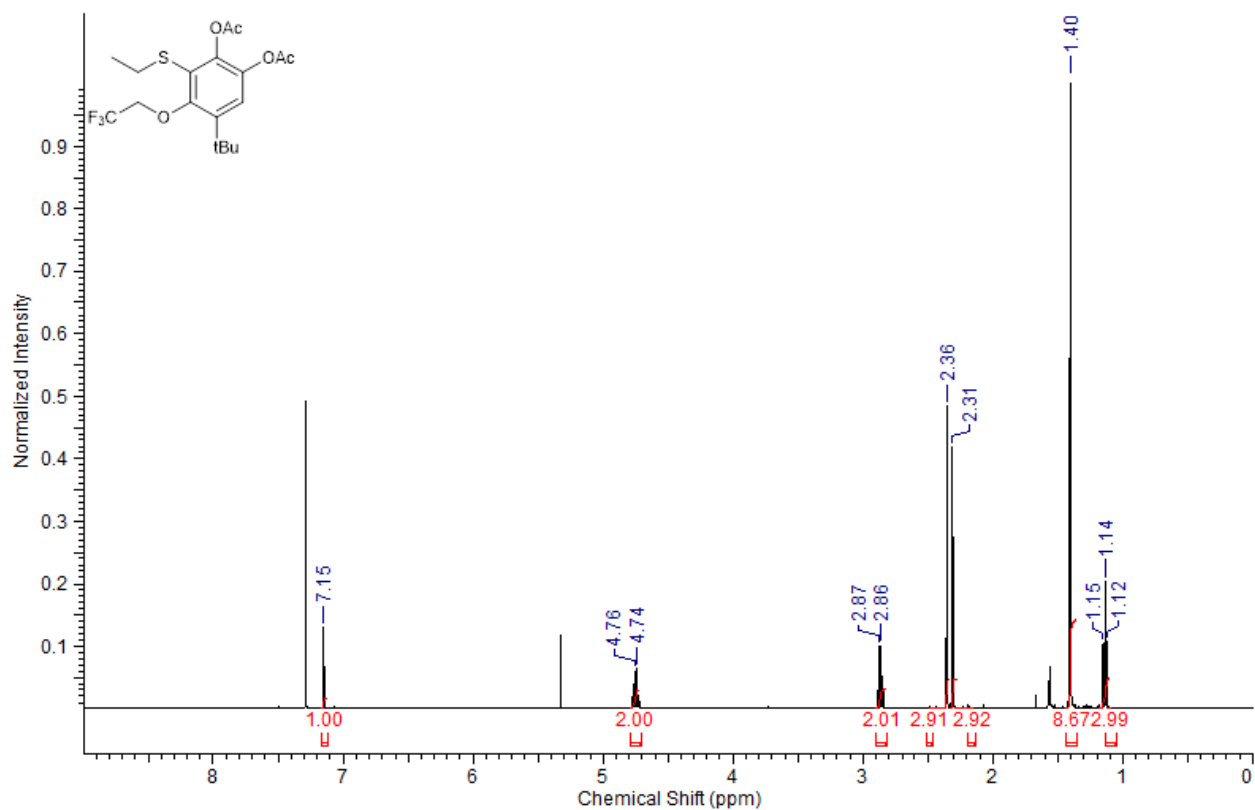
3.6.5:



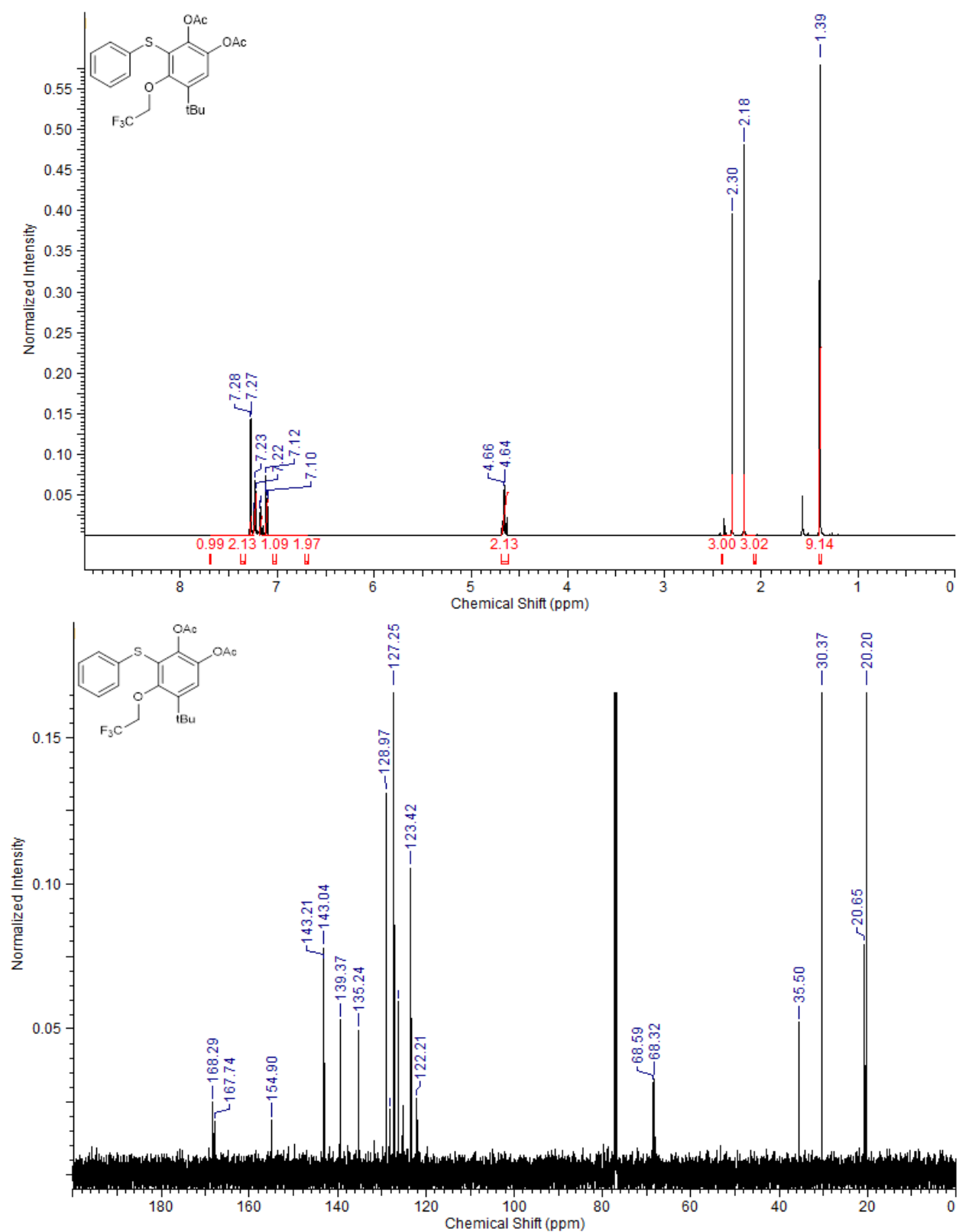
3.6.7:



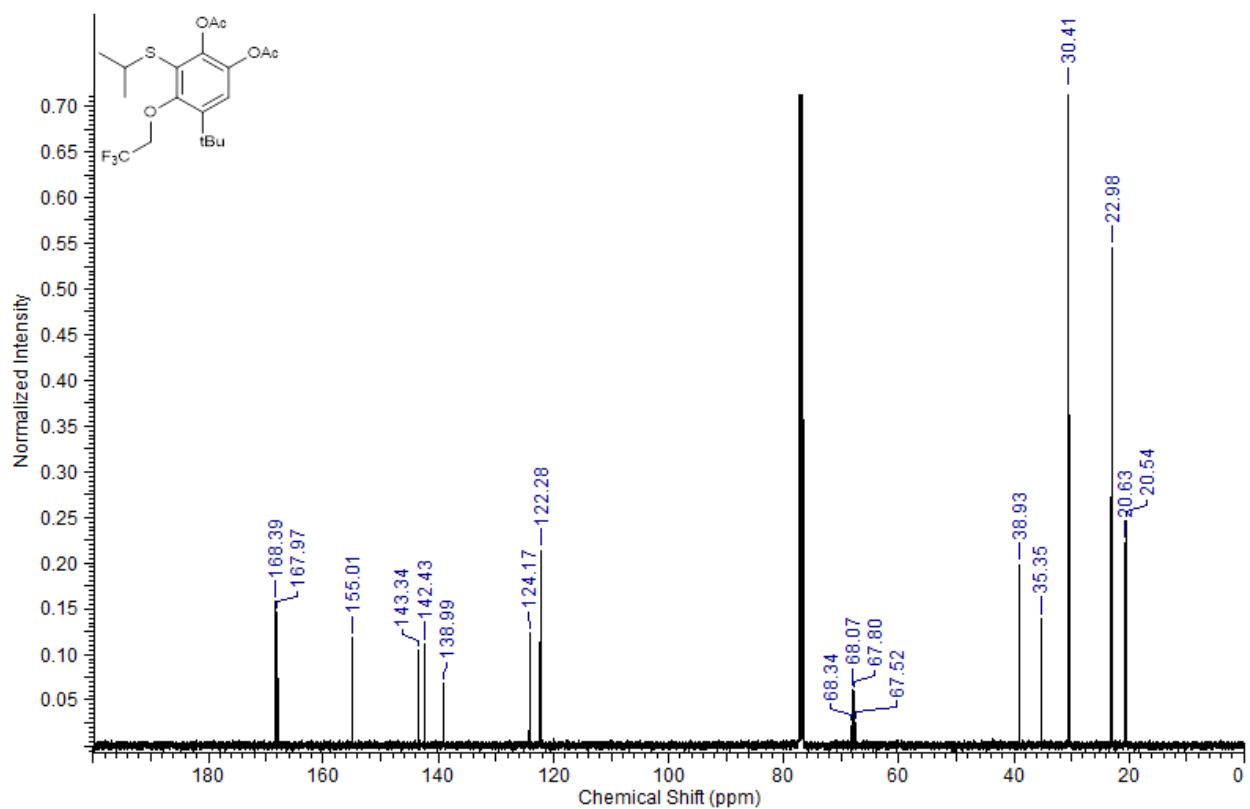
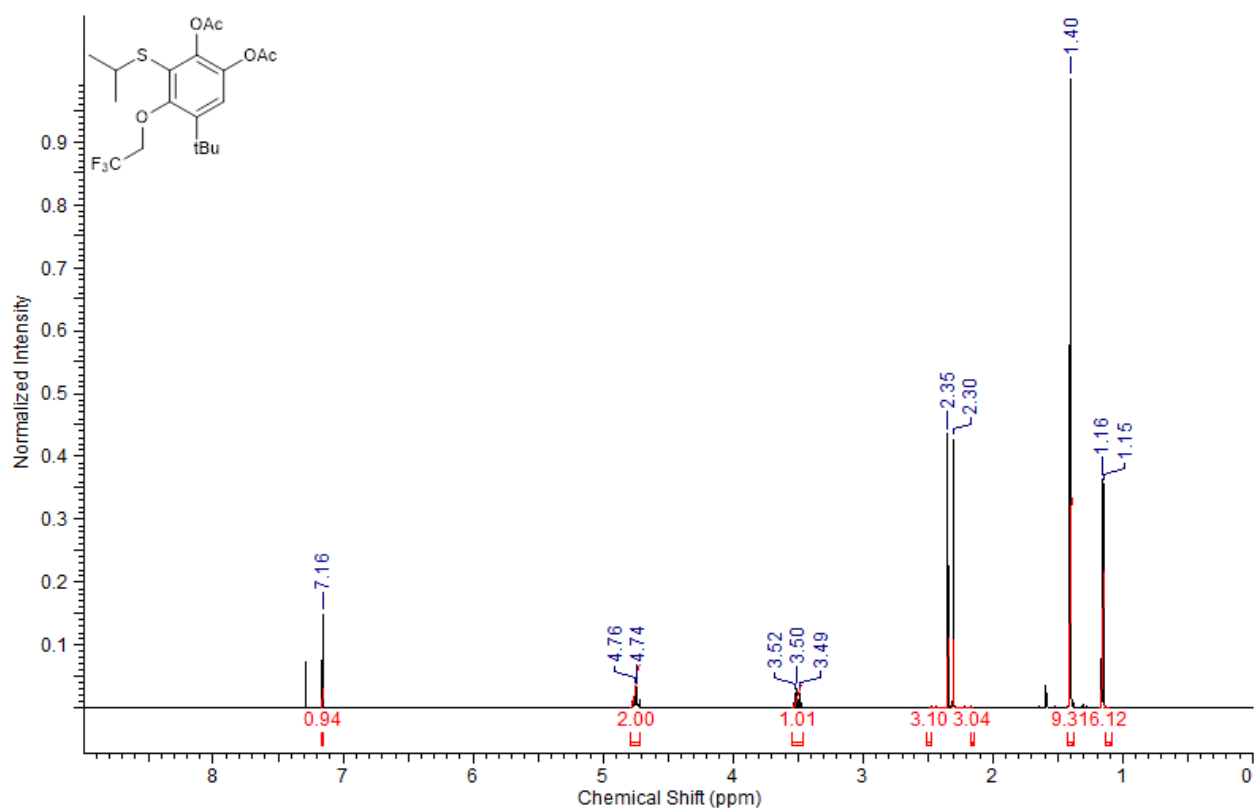
3.6.15:



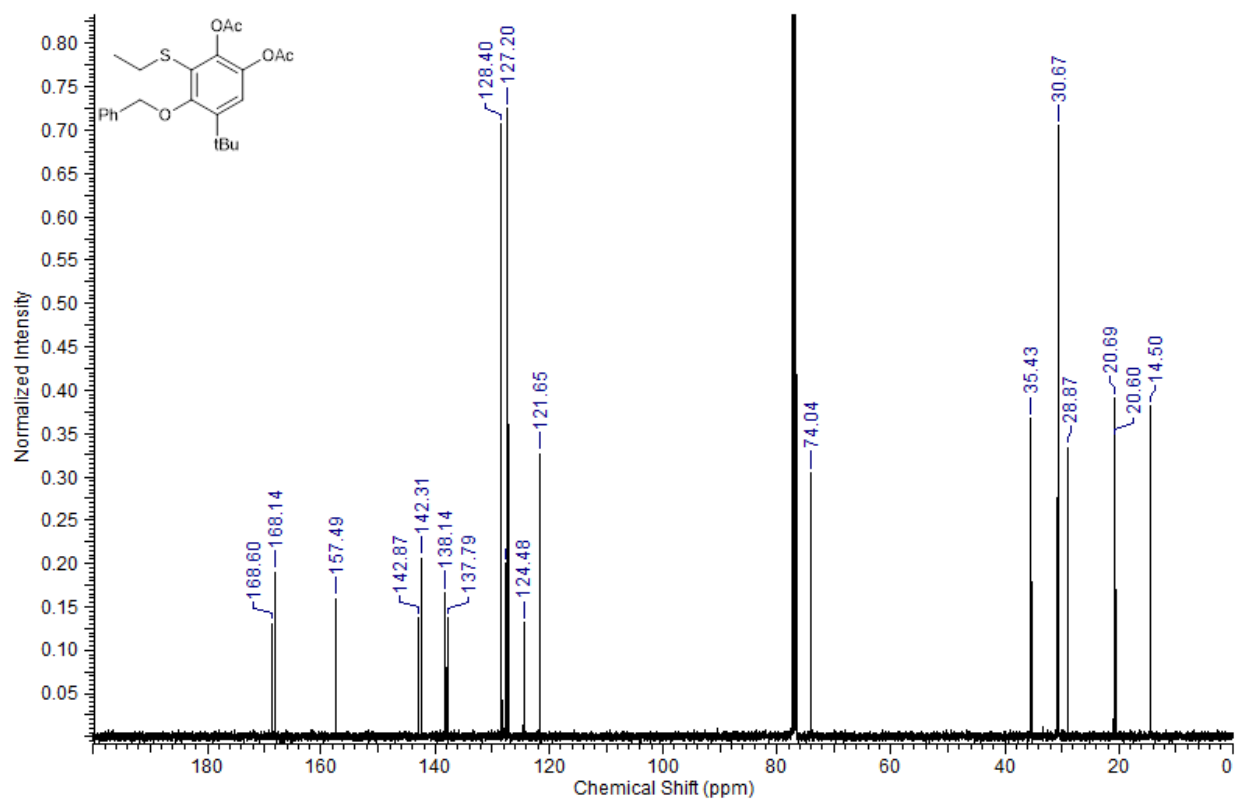
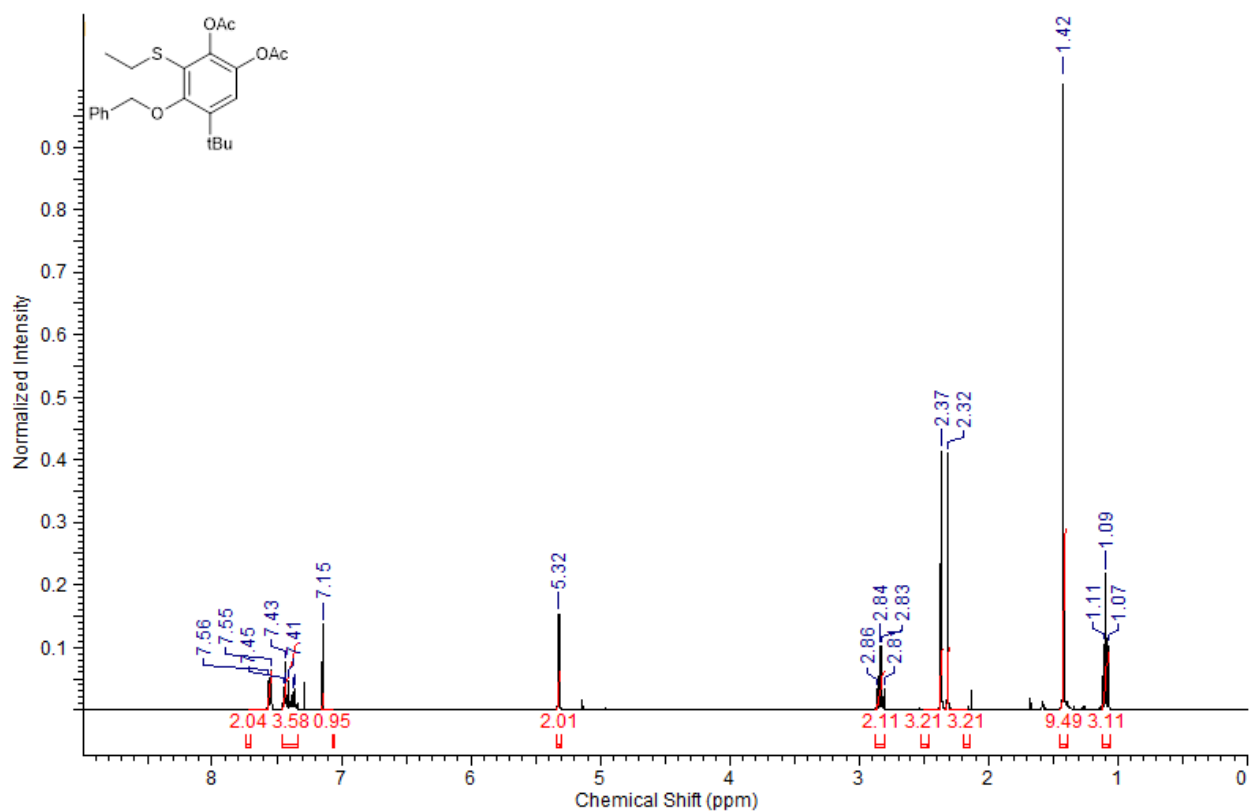
3.6.16:



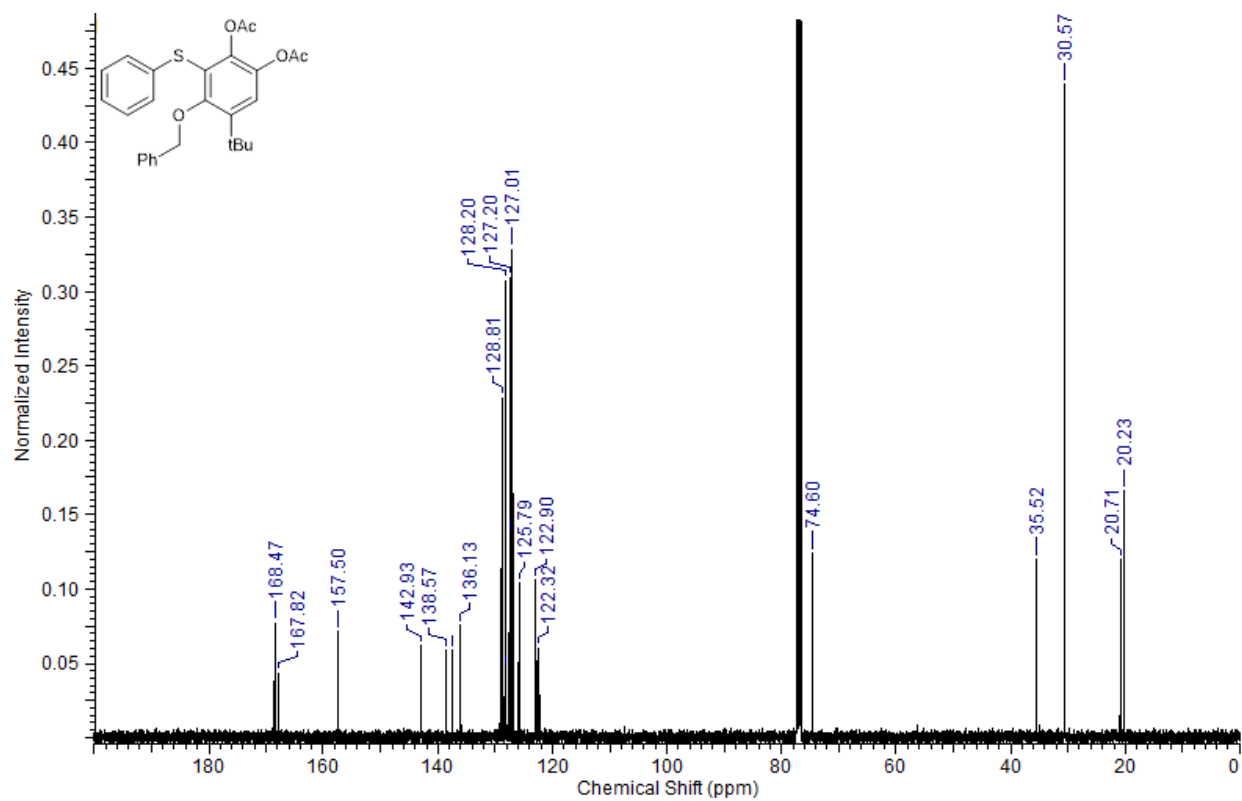
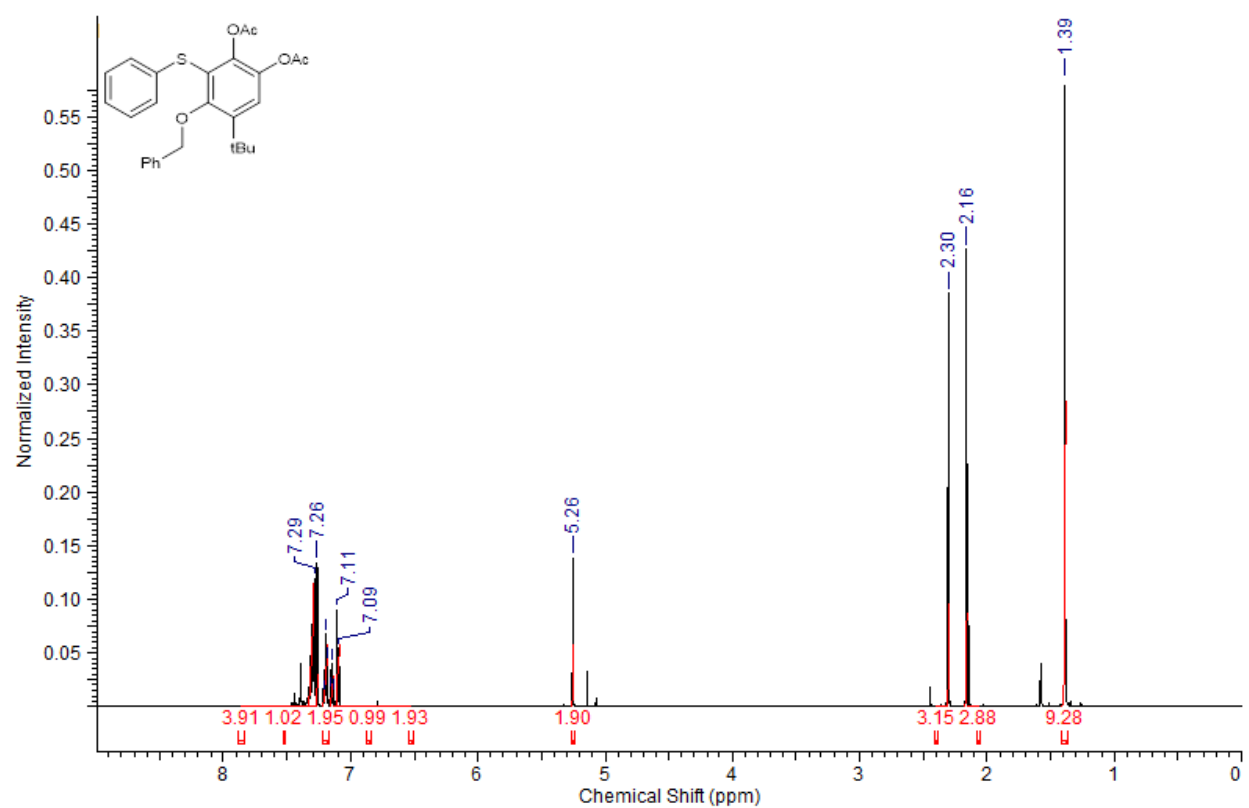
3.6.17:



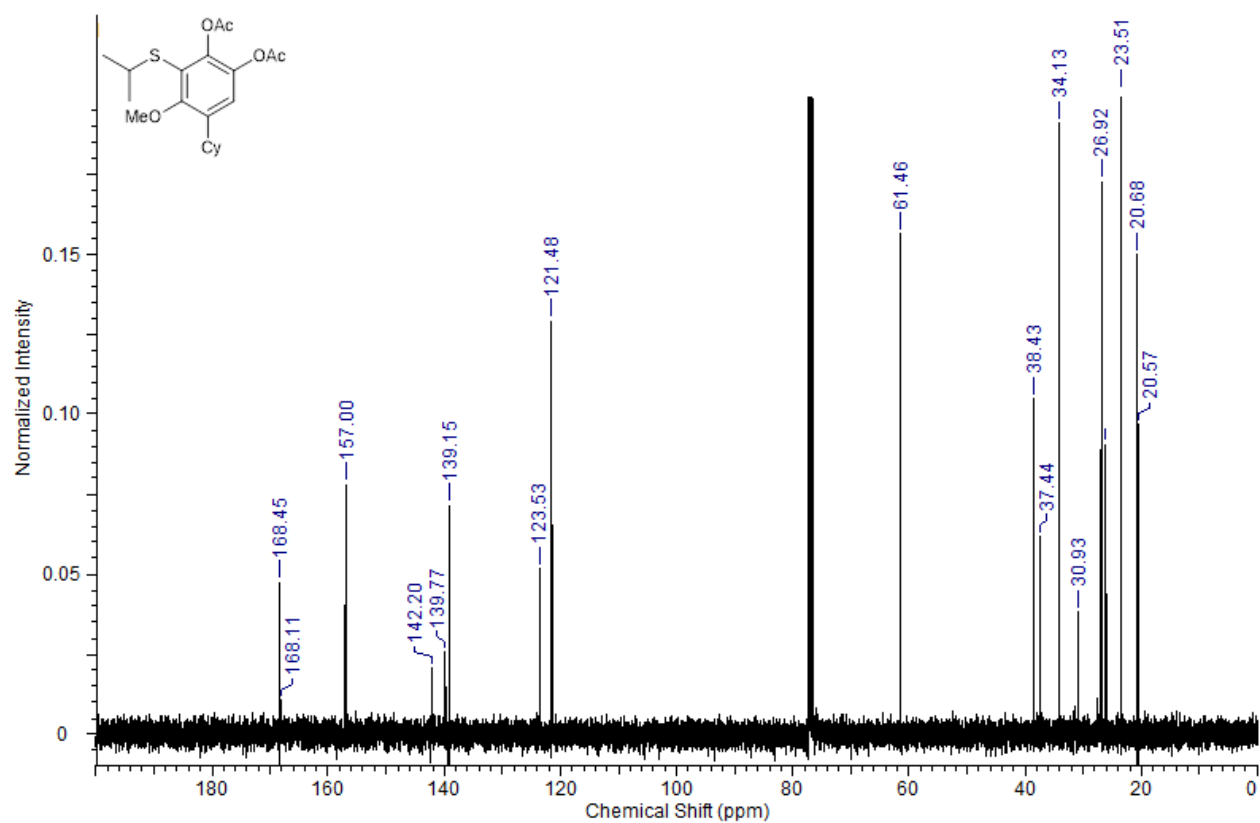
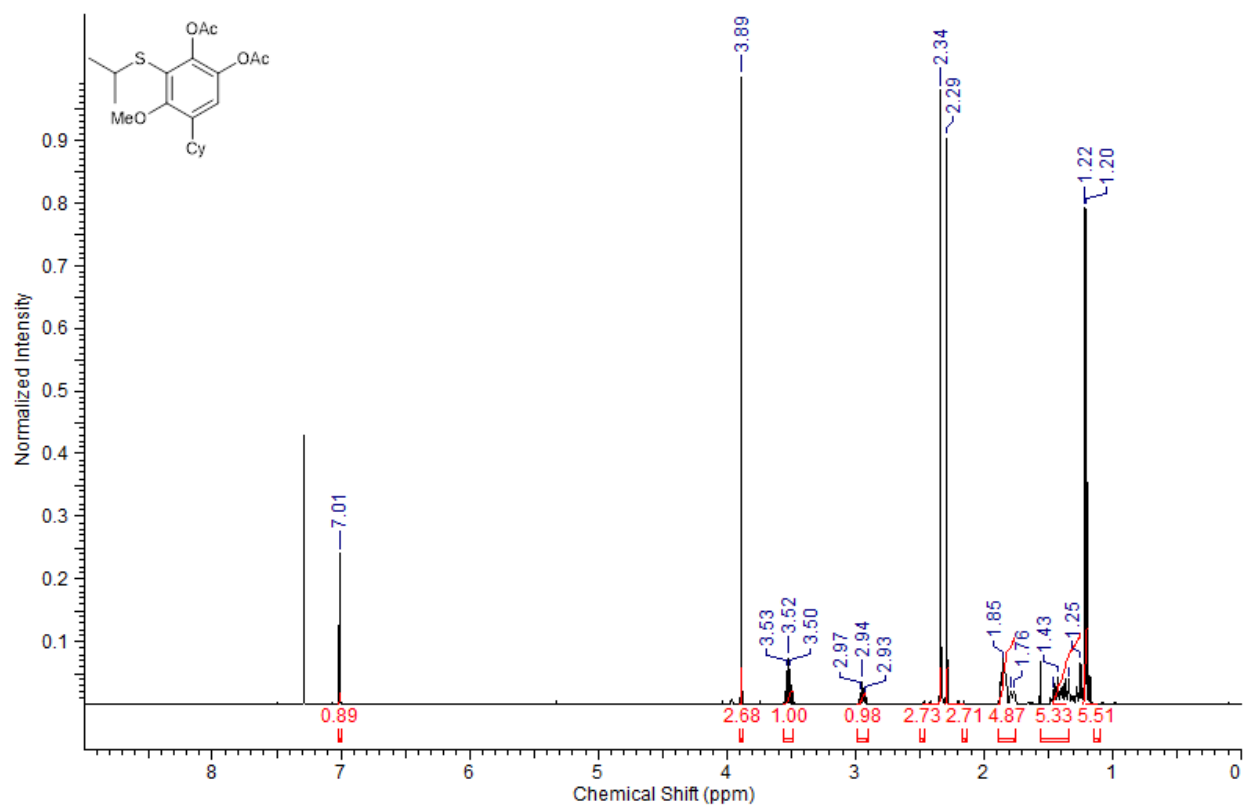
3.6.19:



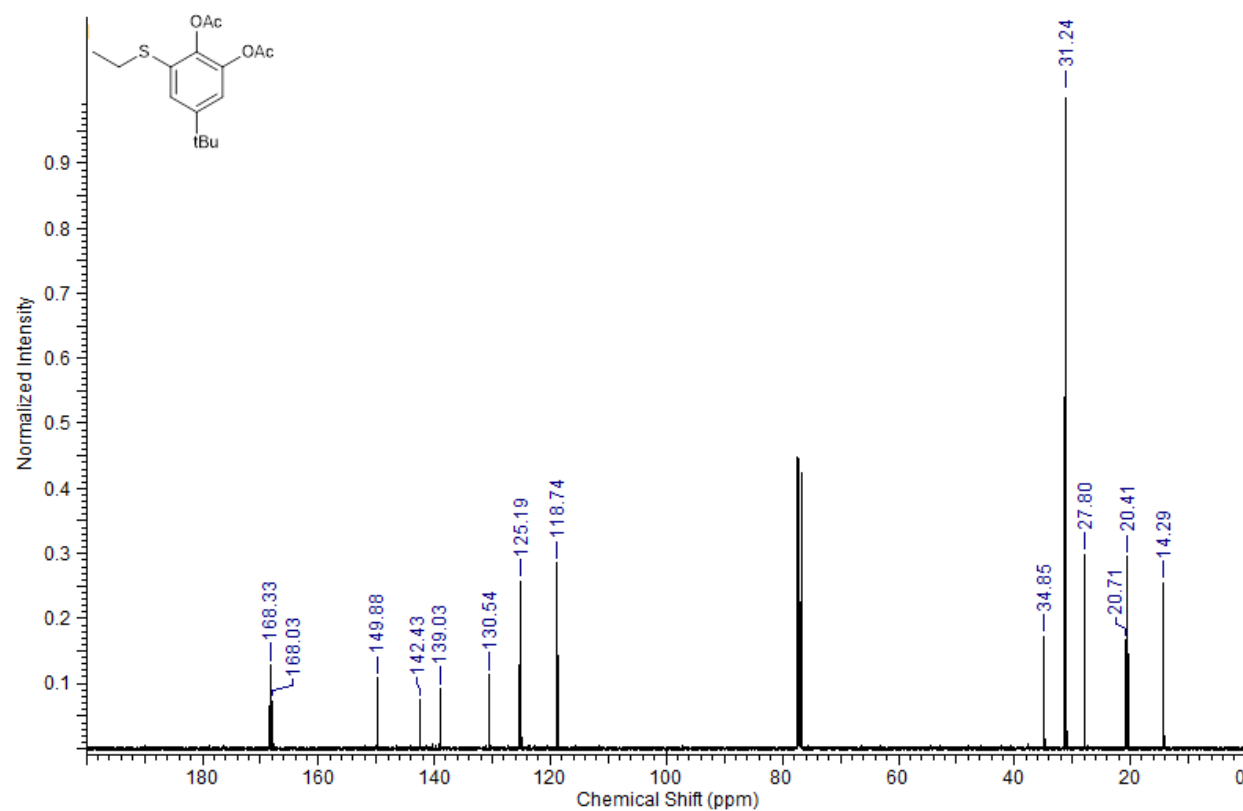
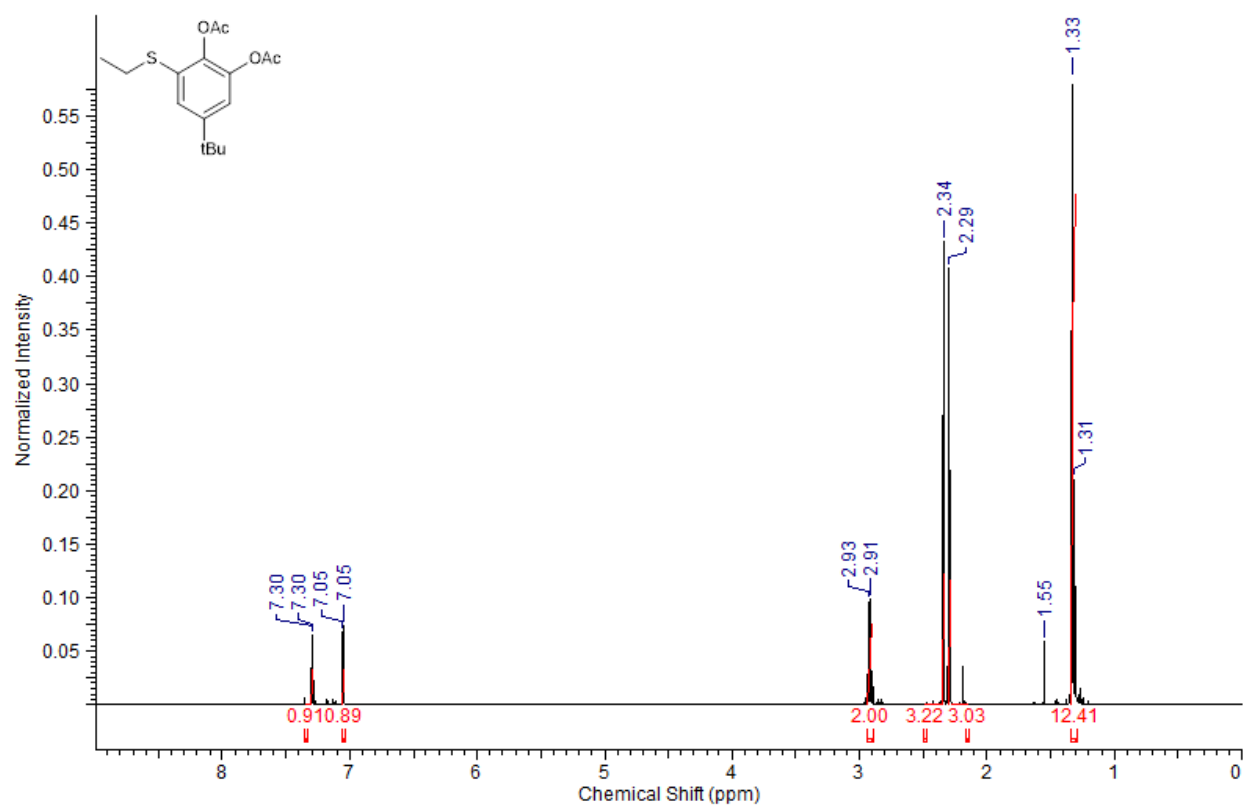
3.6.20:



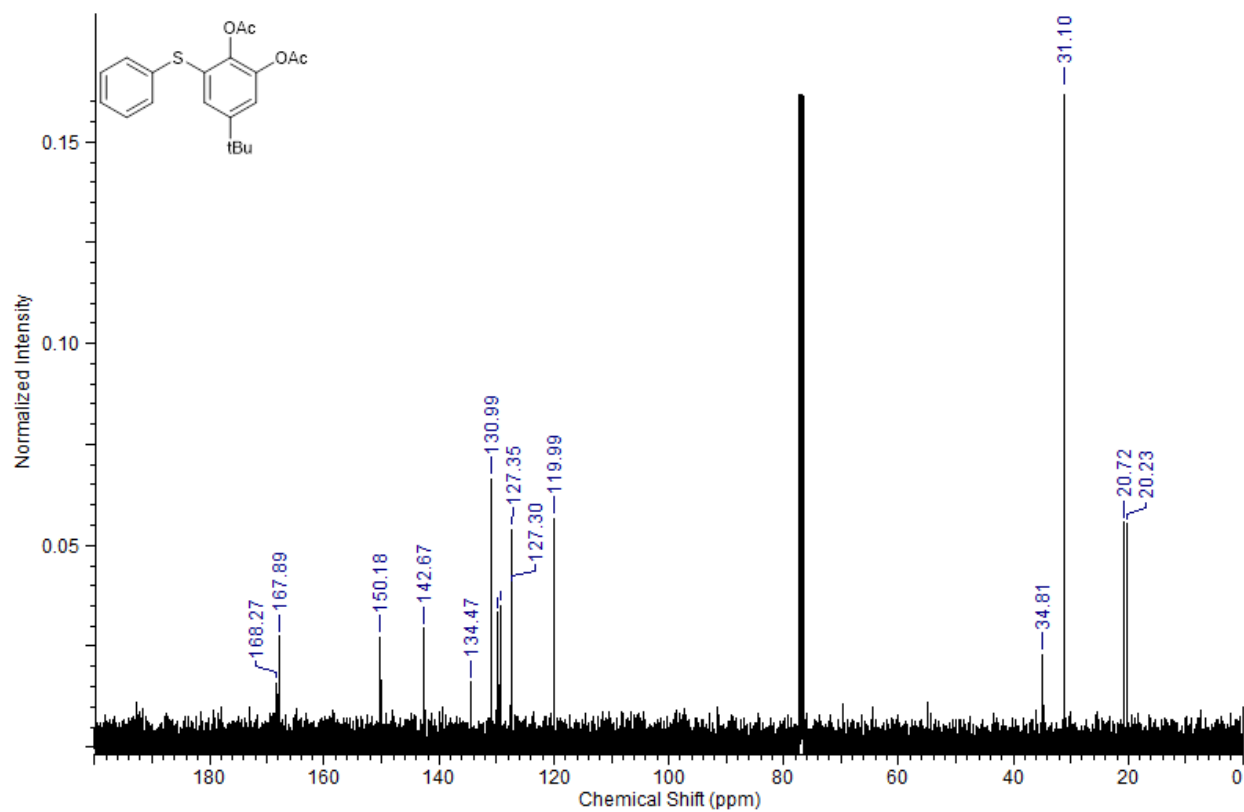
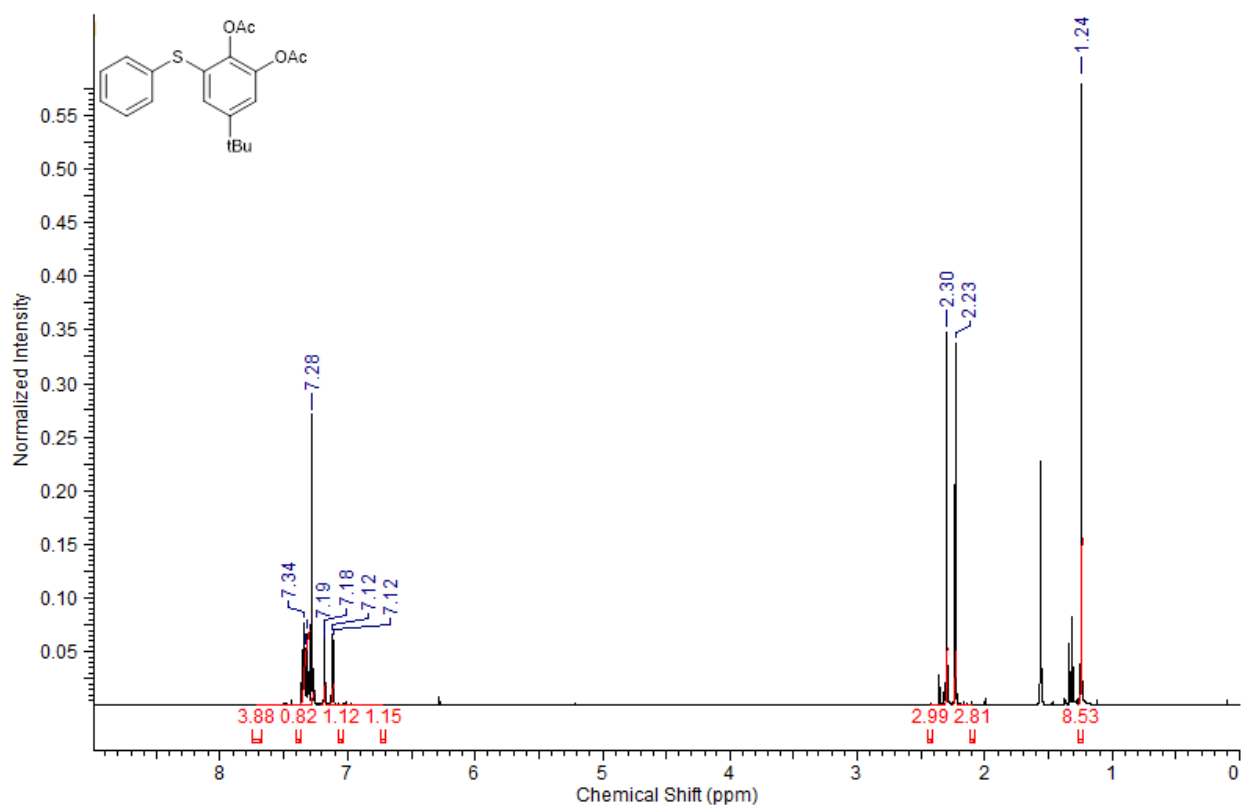
3.6.22:



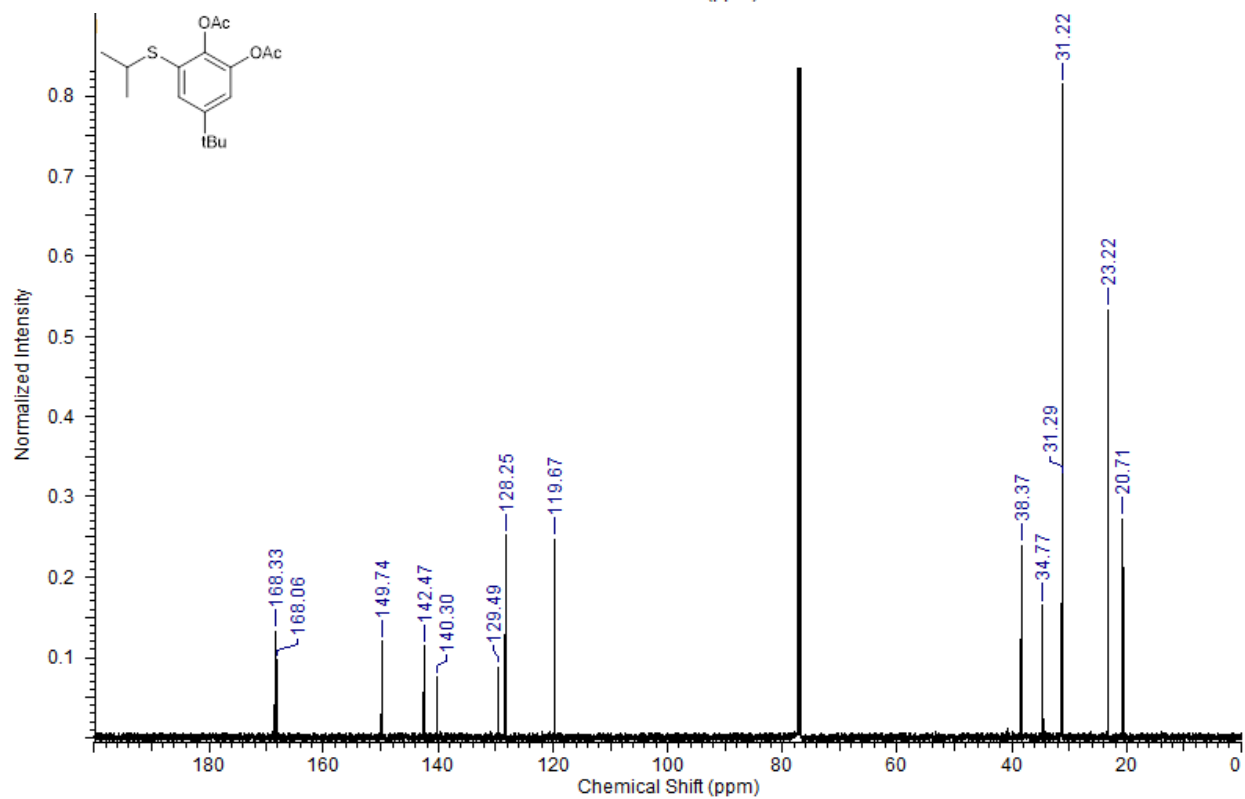
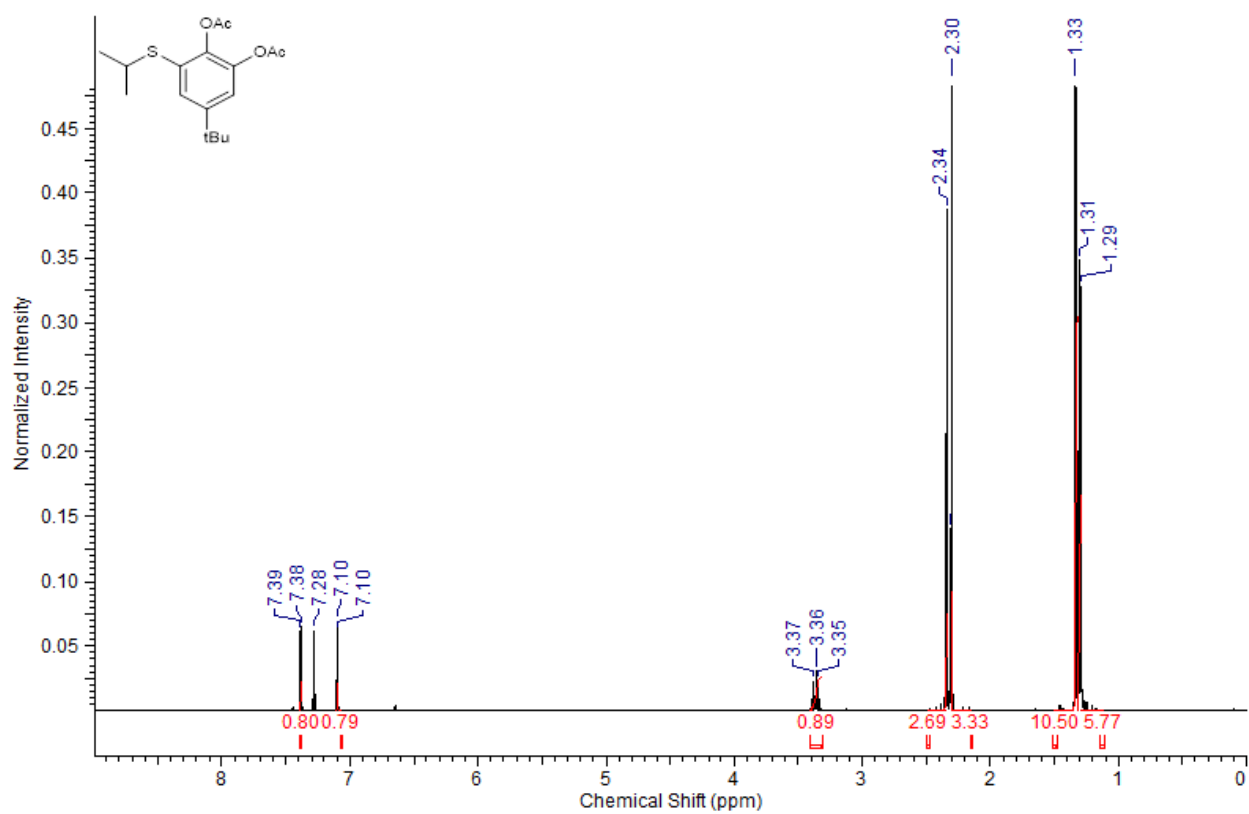
3.6.10:



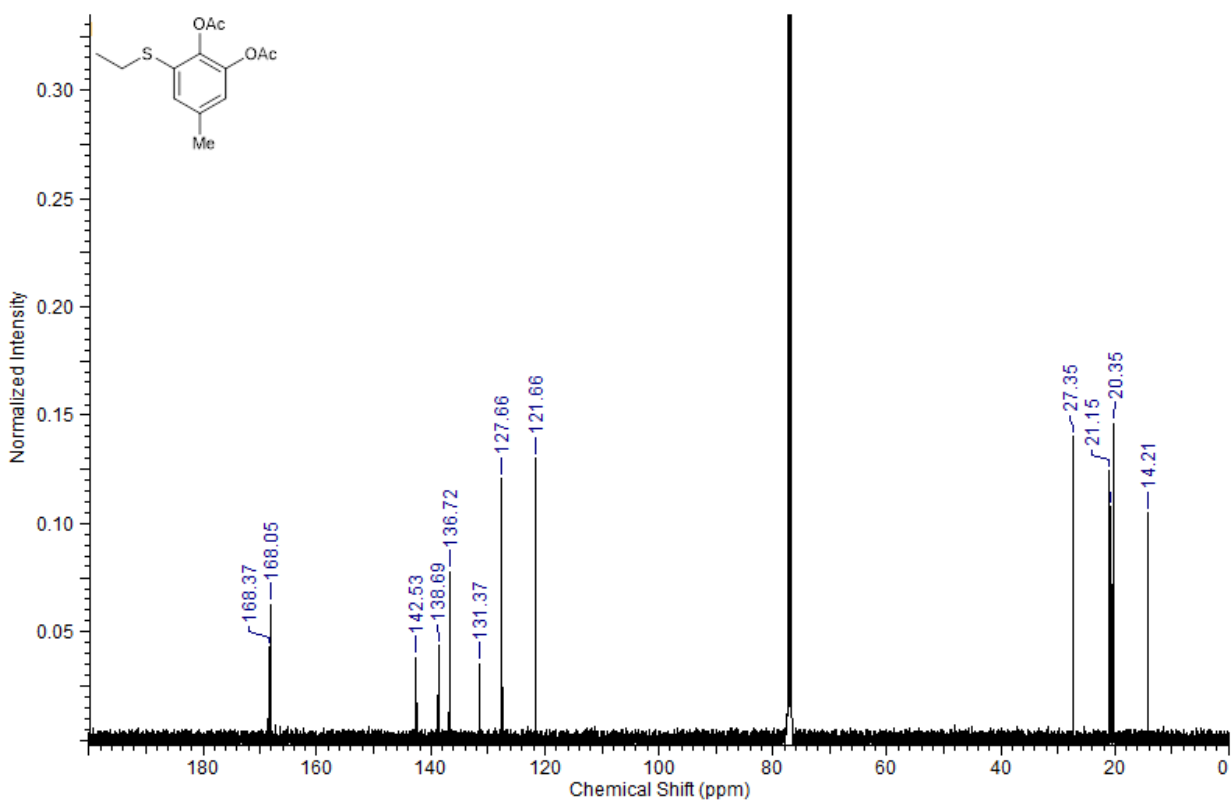
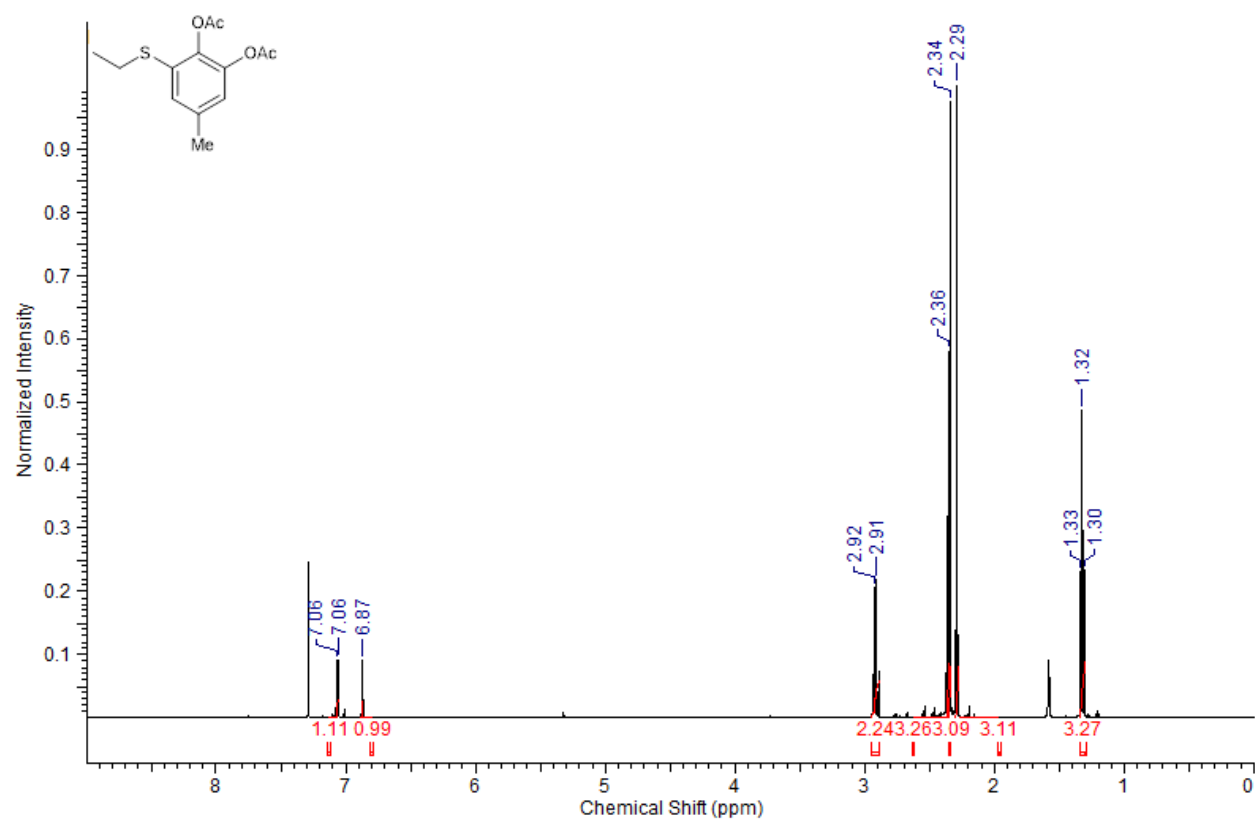
3.6.11:



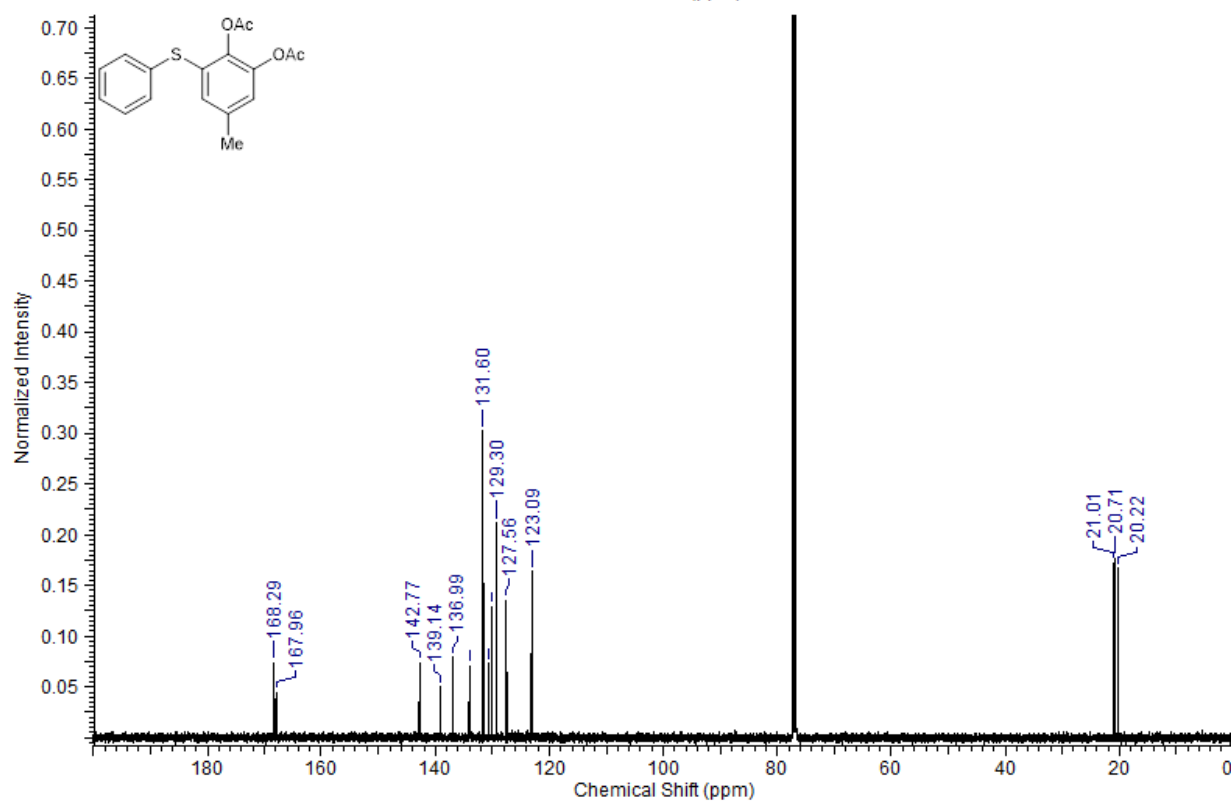
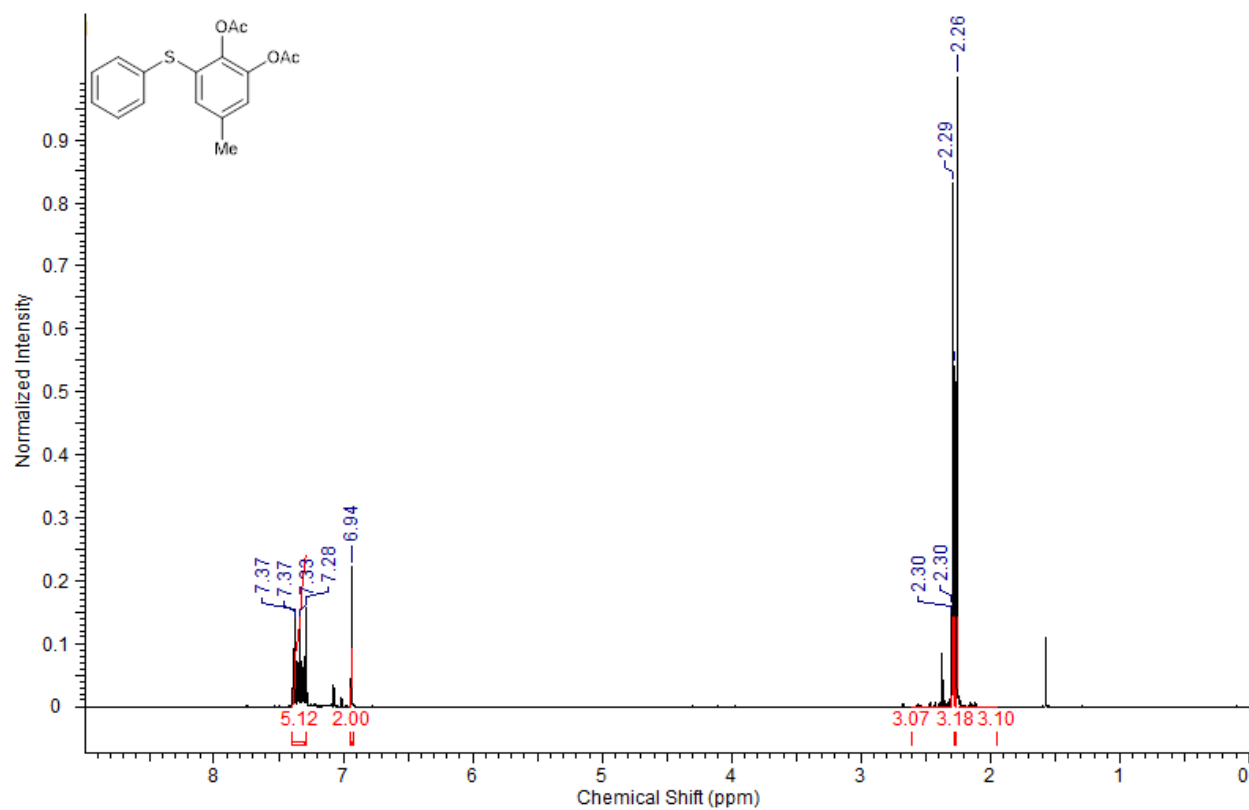
3.6.12:



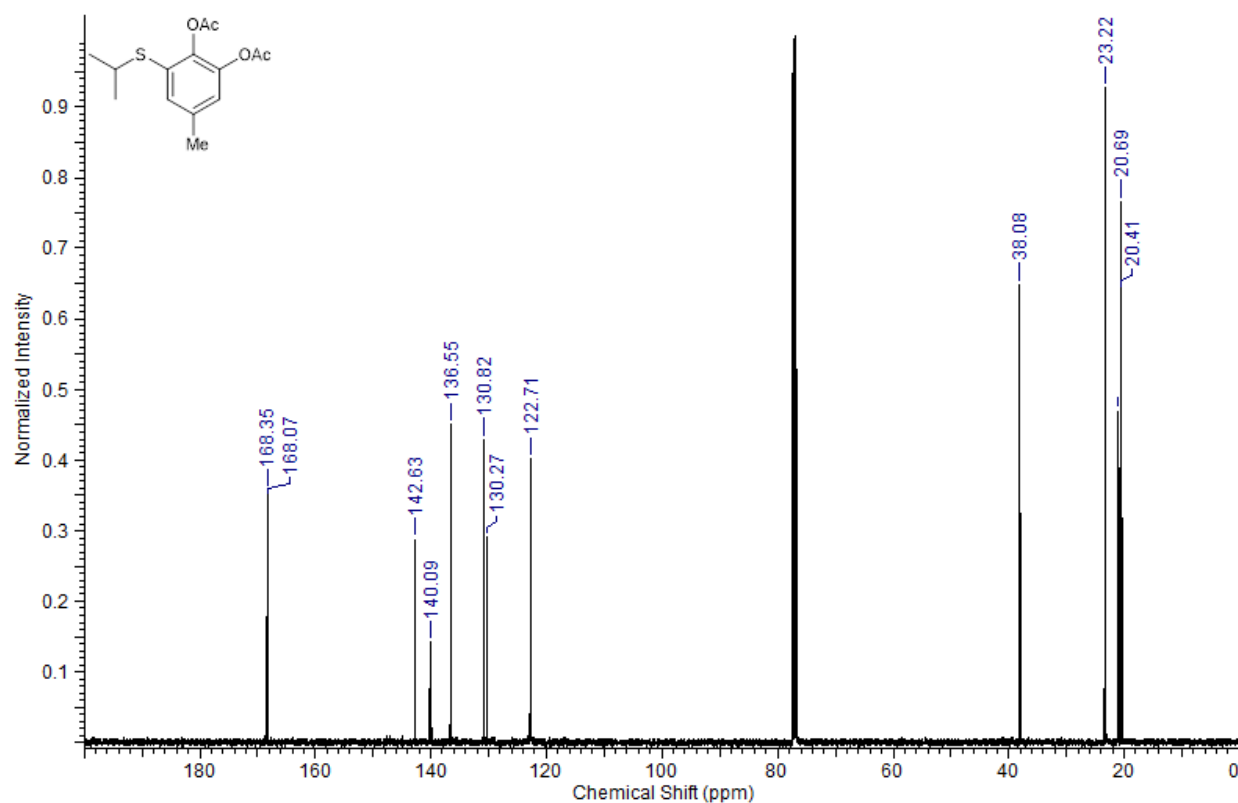
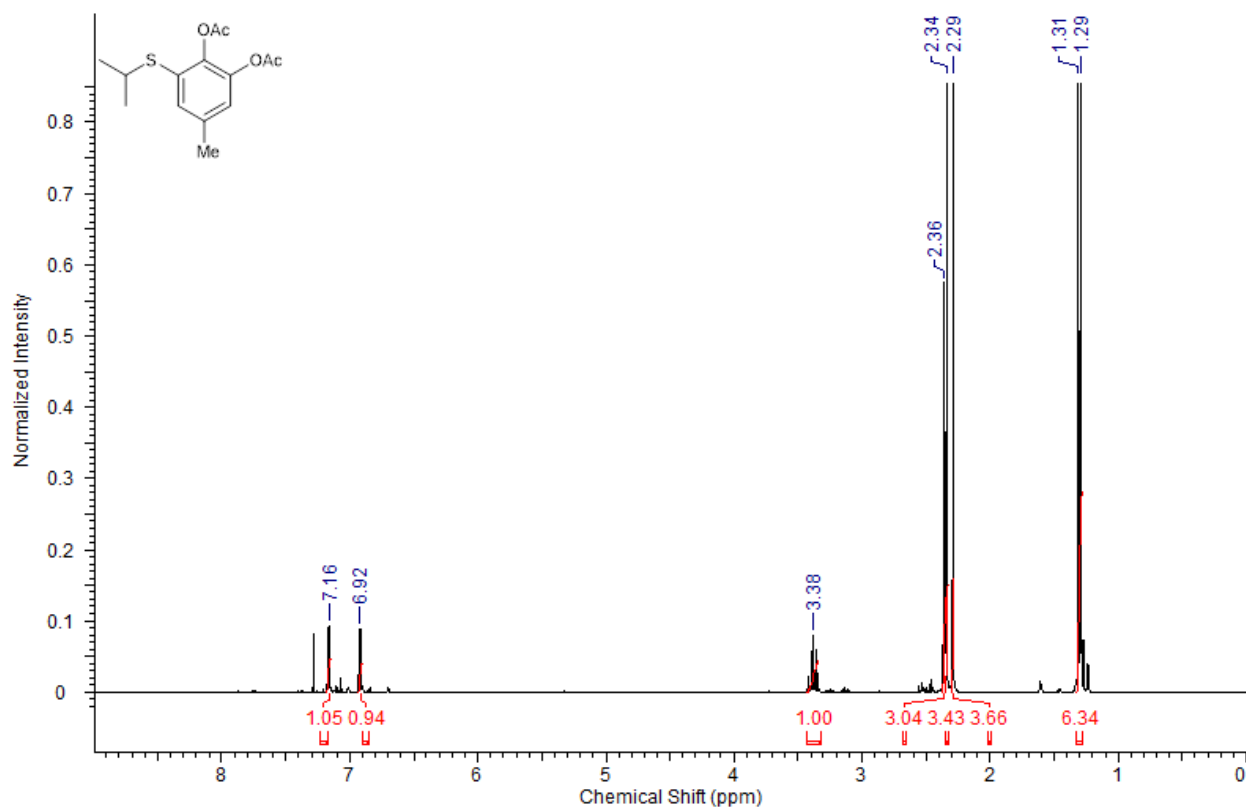
3.6.24:



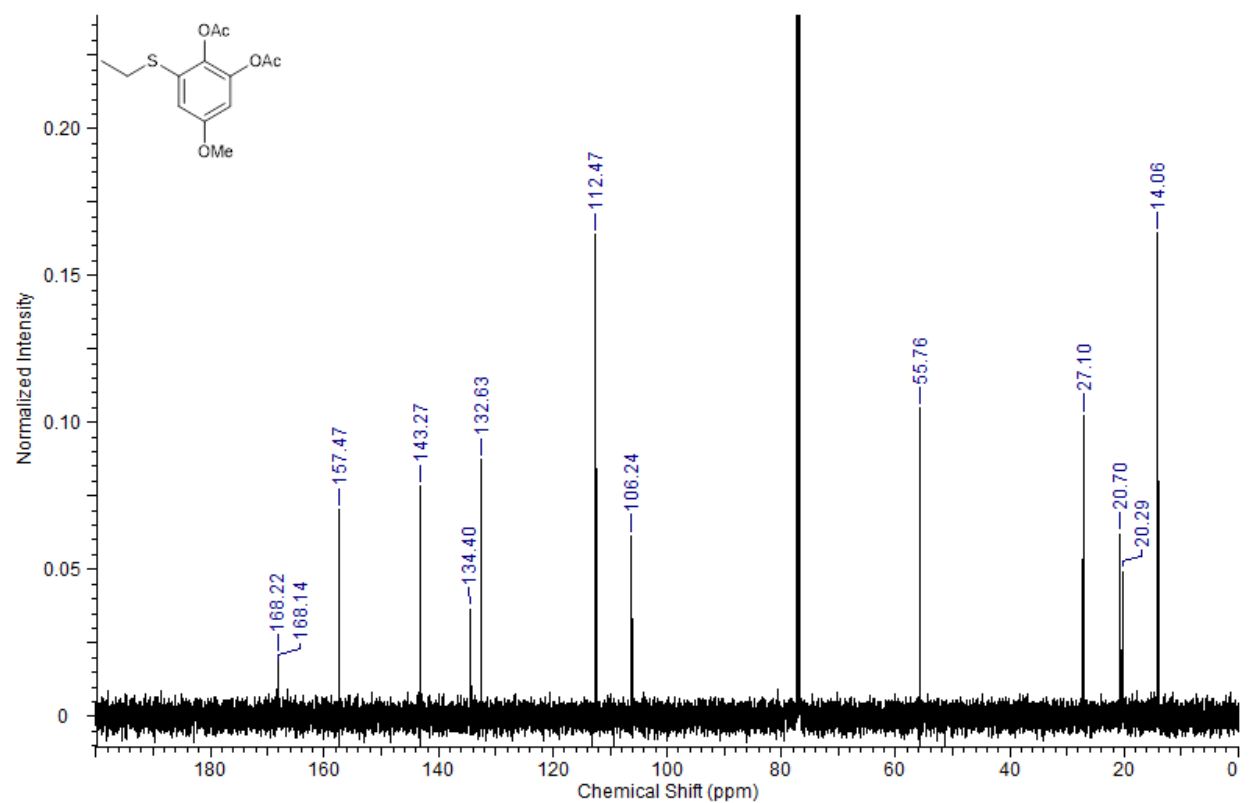
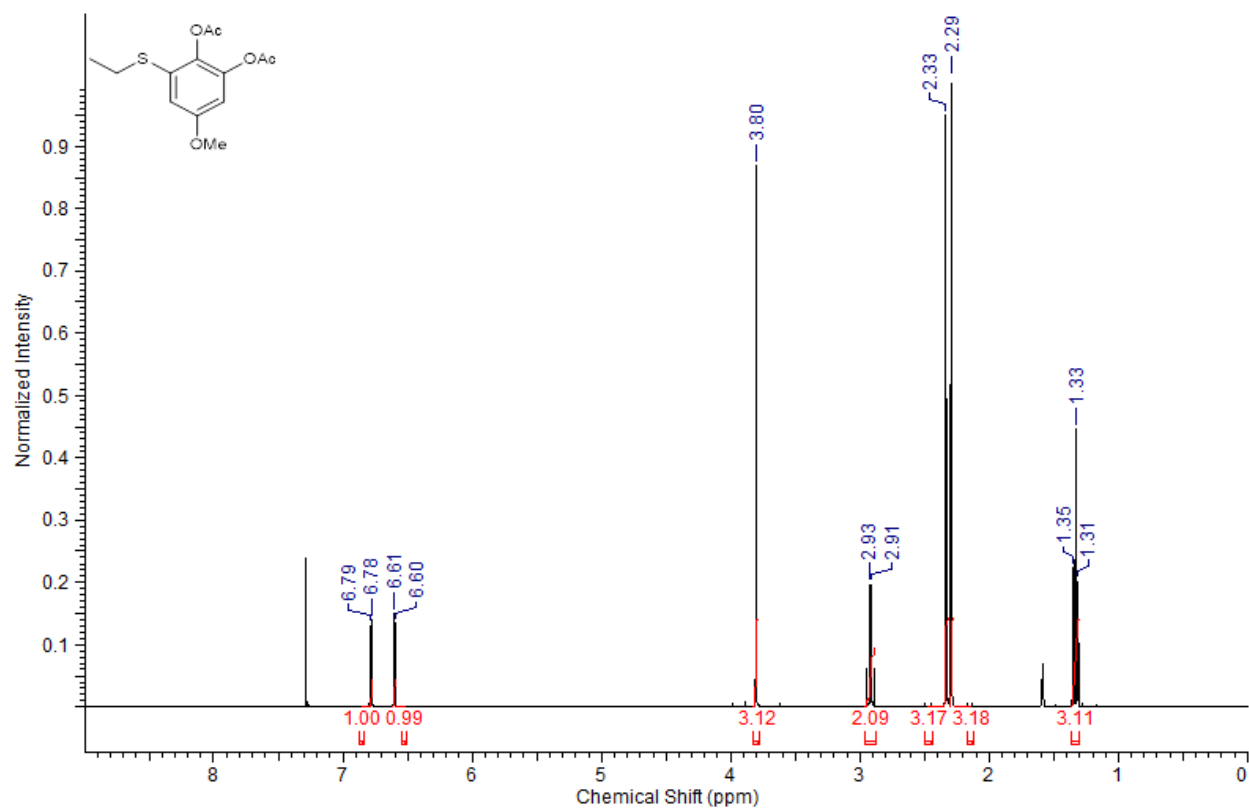
3.6.25:



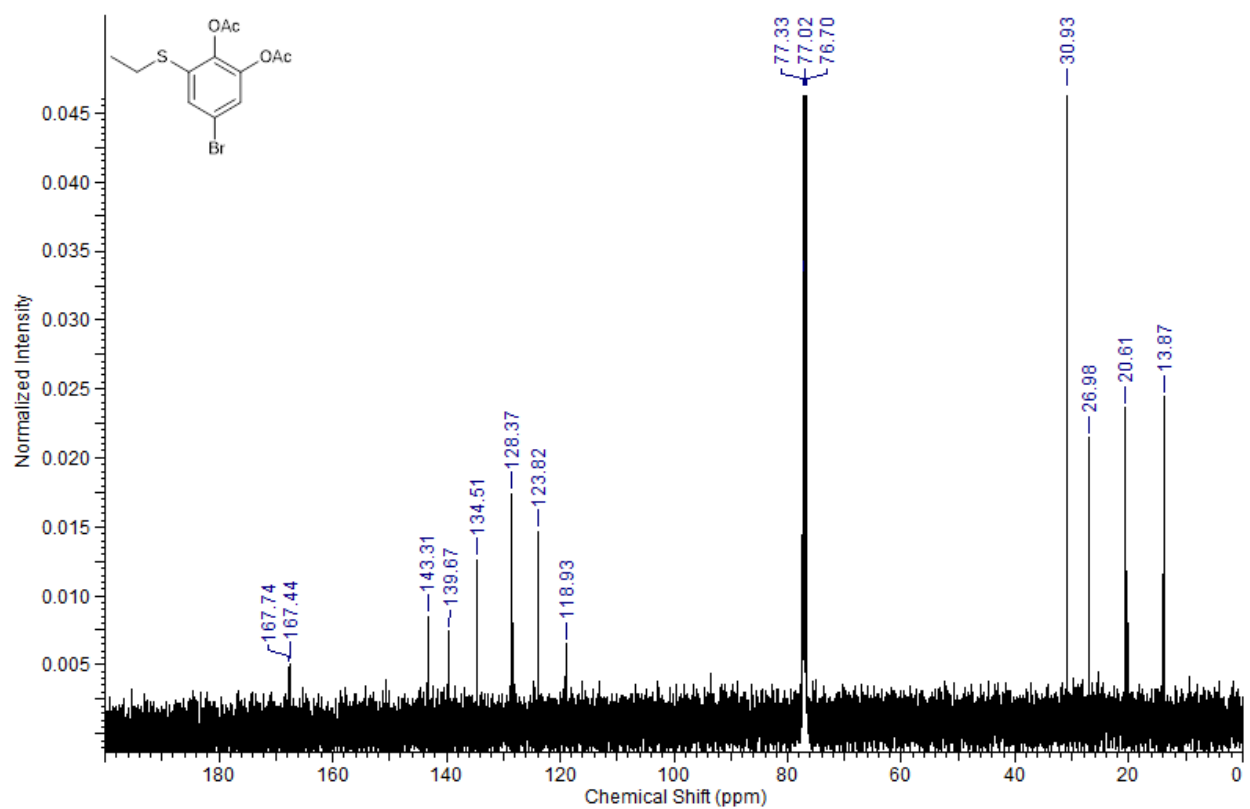
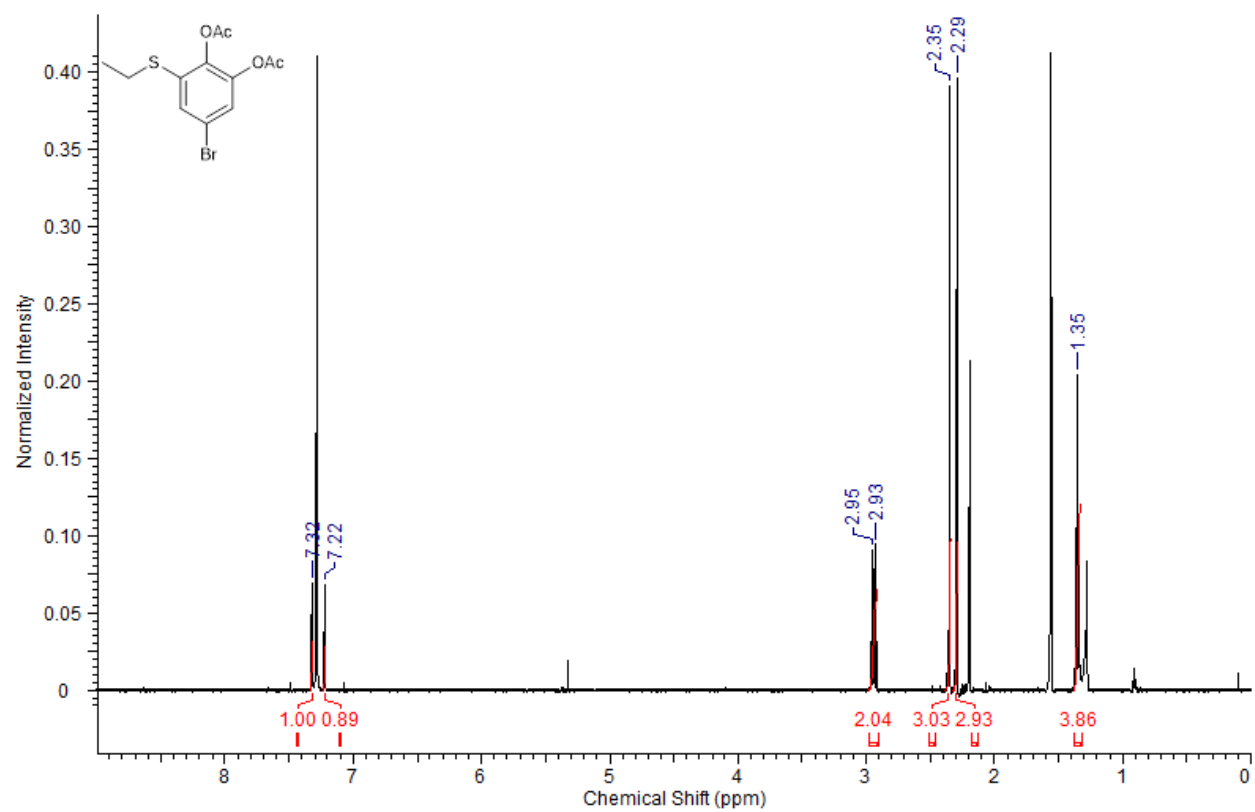
3.6.26:



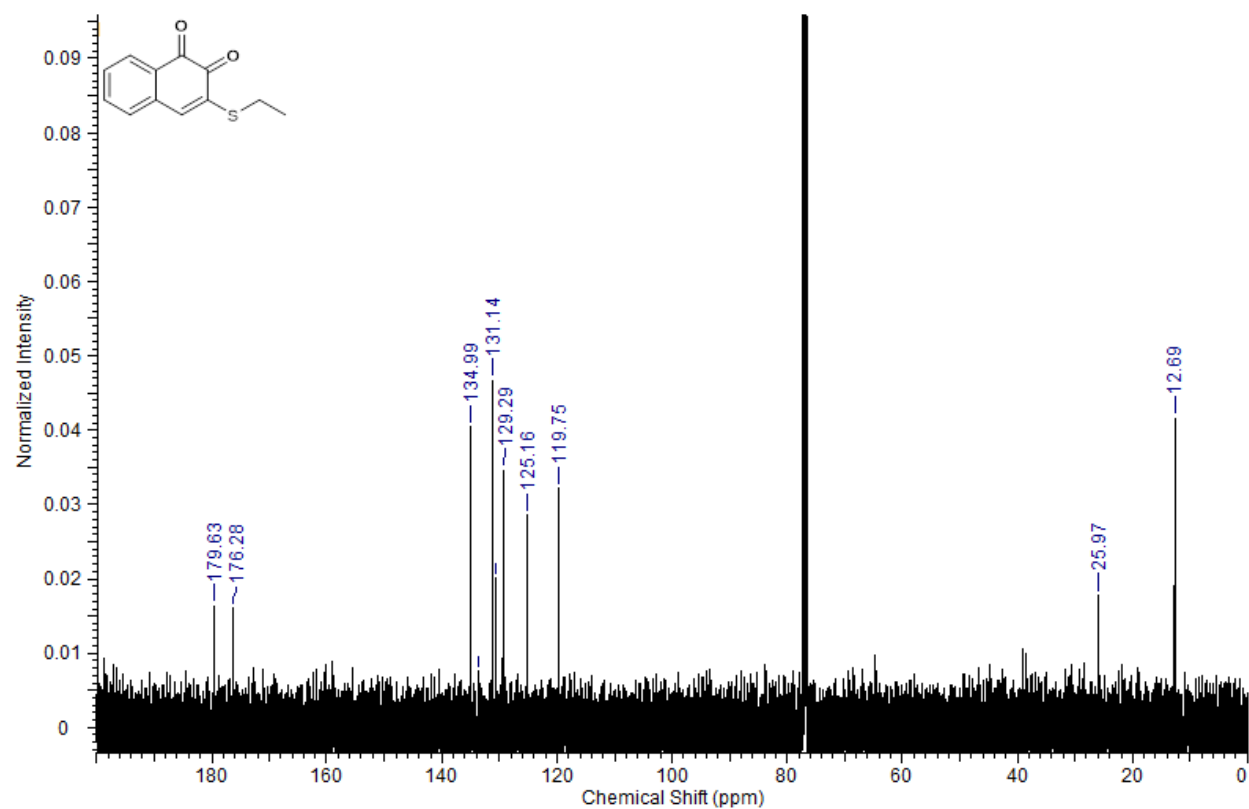
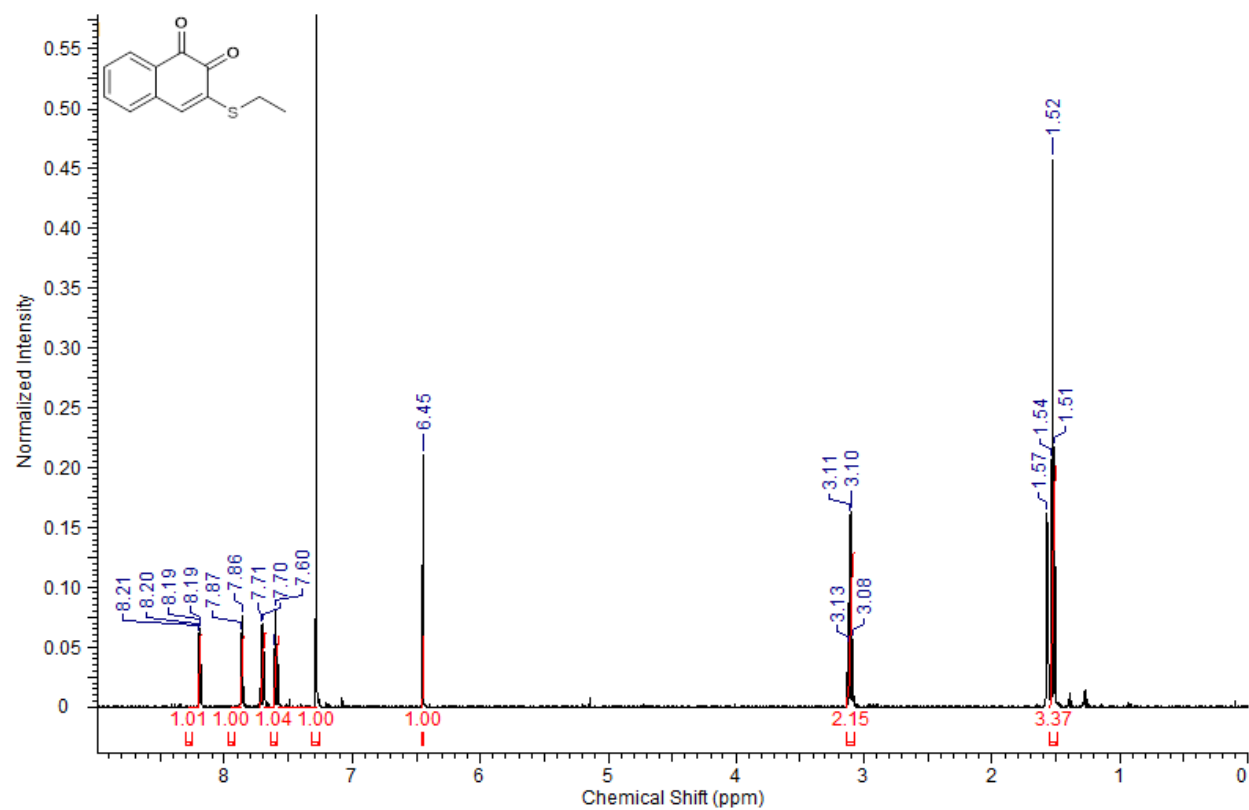
3.6.28:



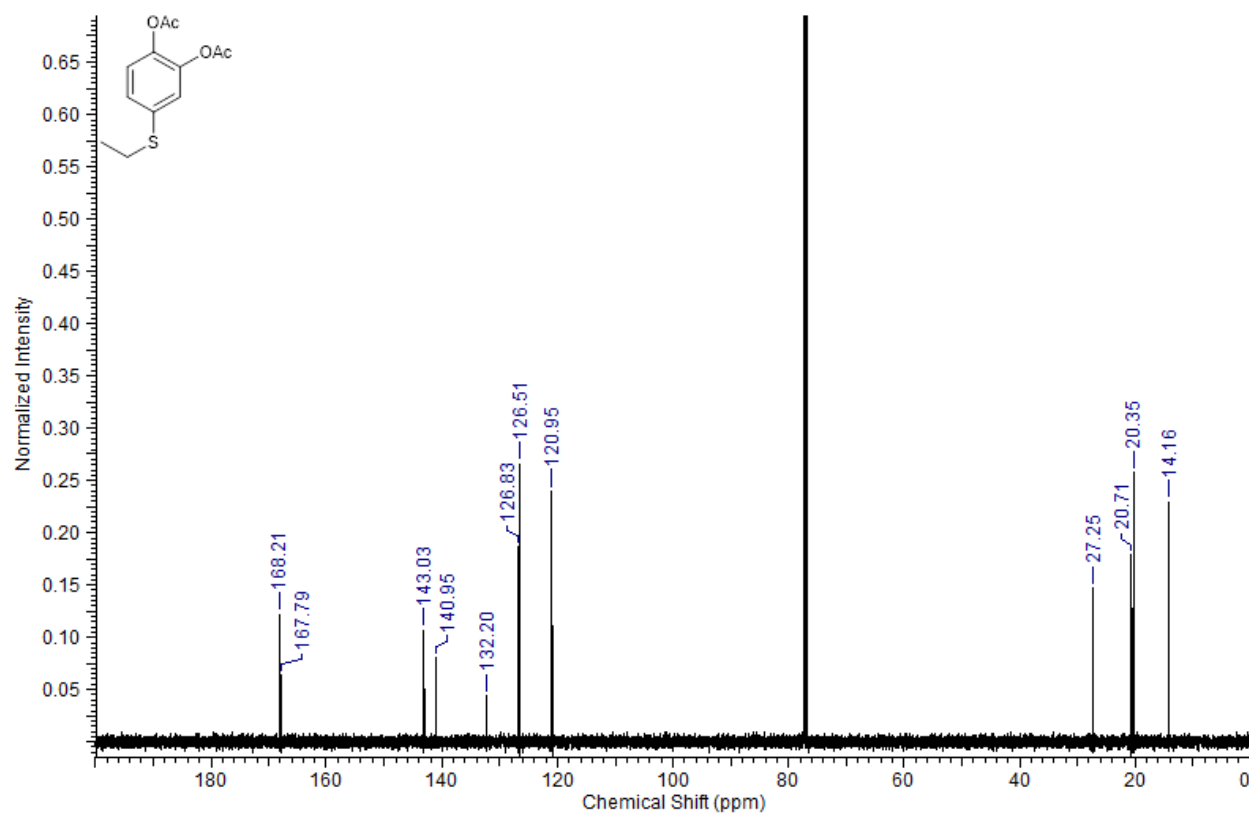
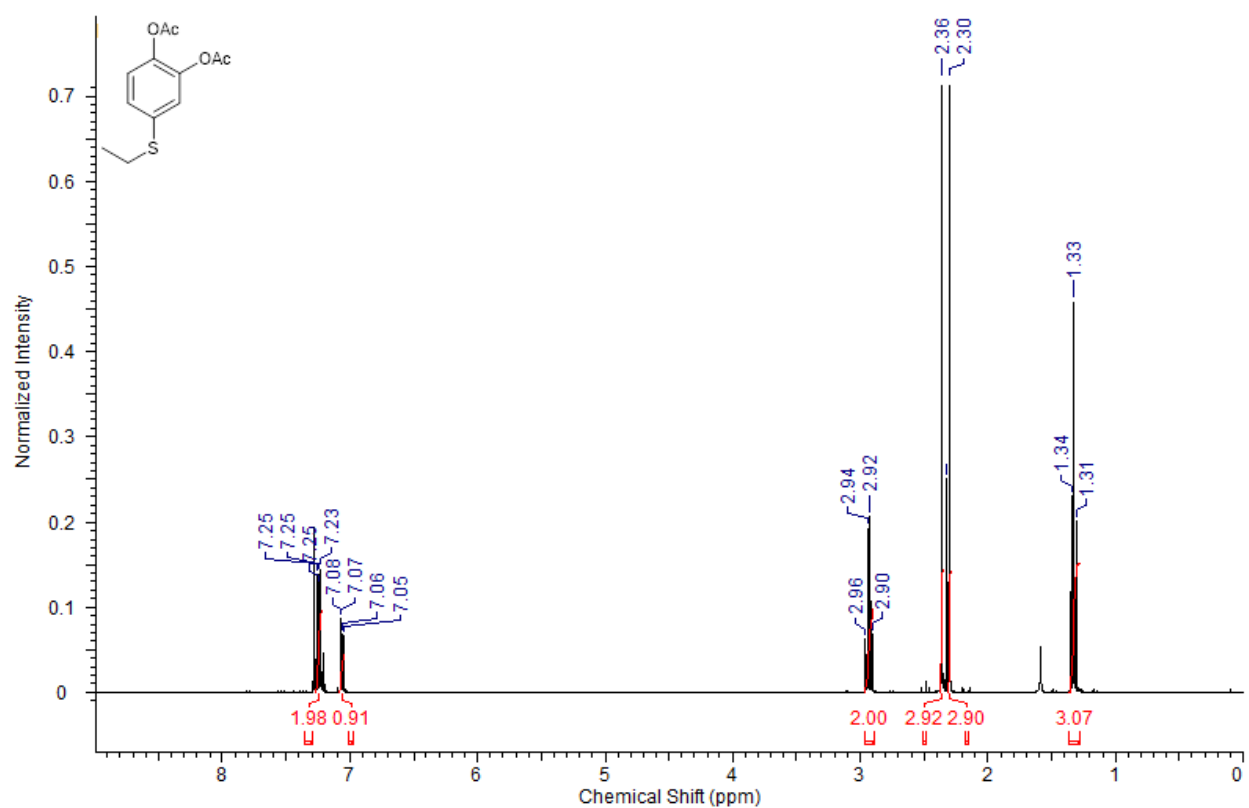
3.6.32:



3.6.34:

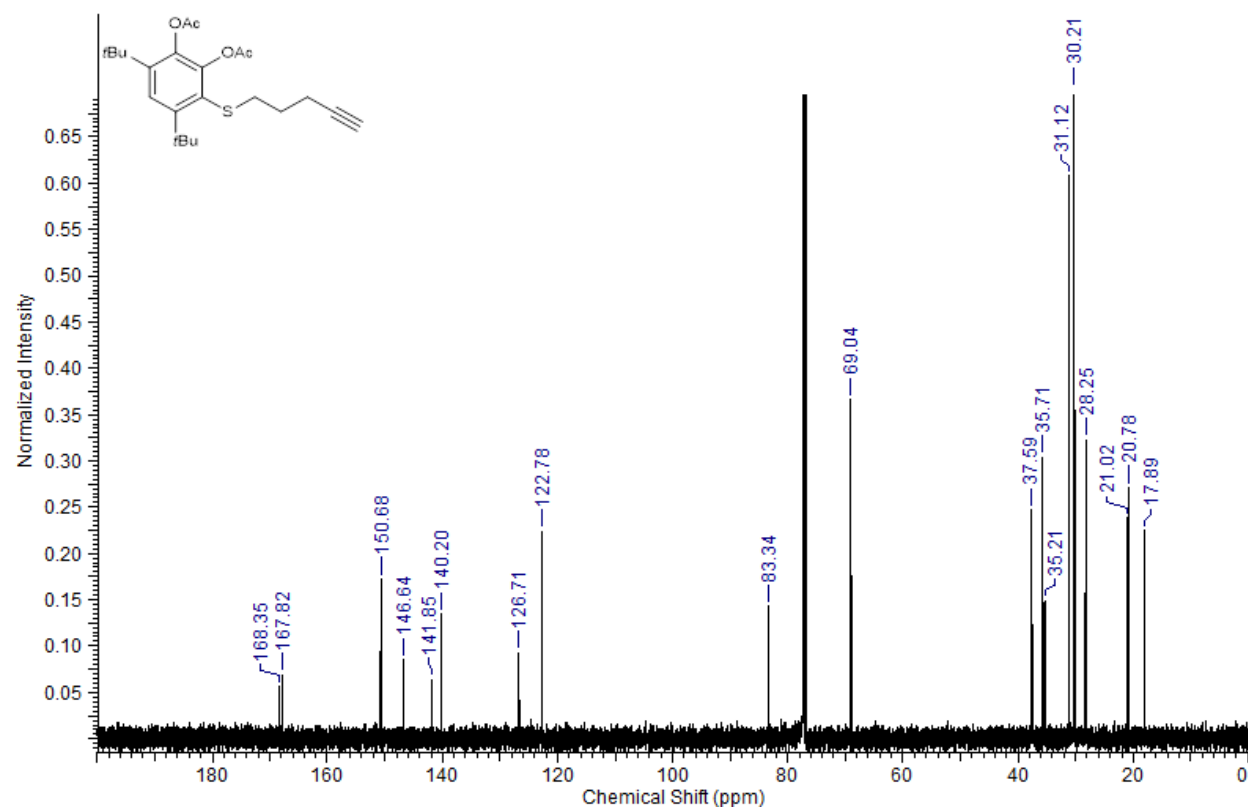
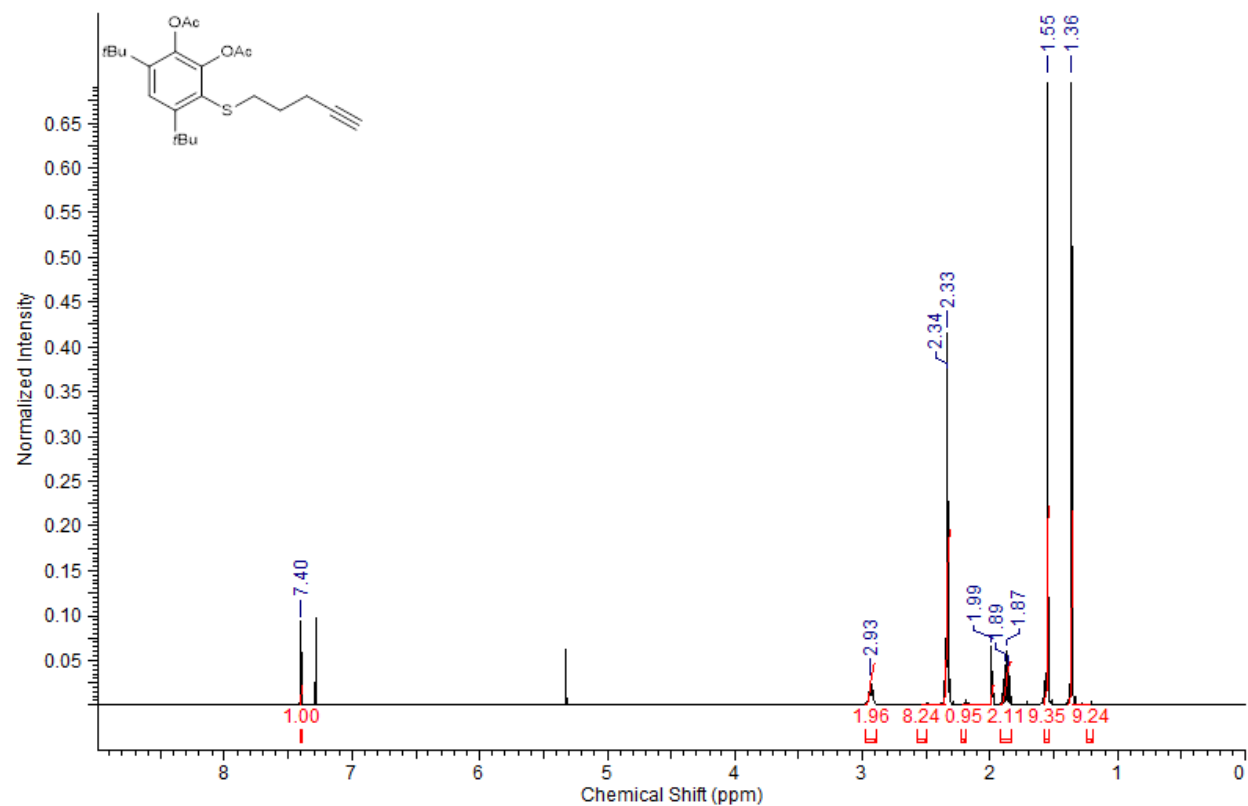


3.6.36:

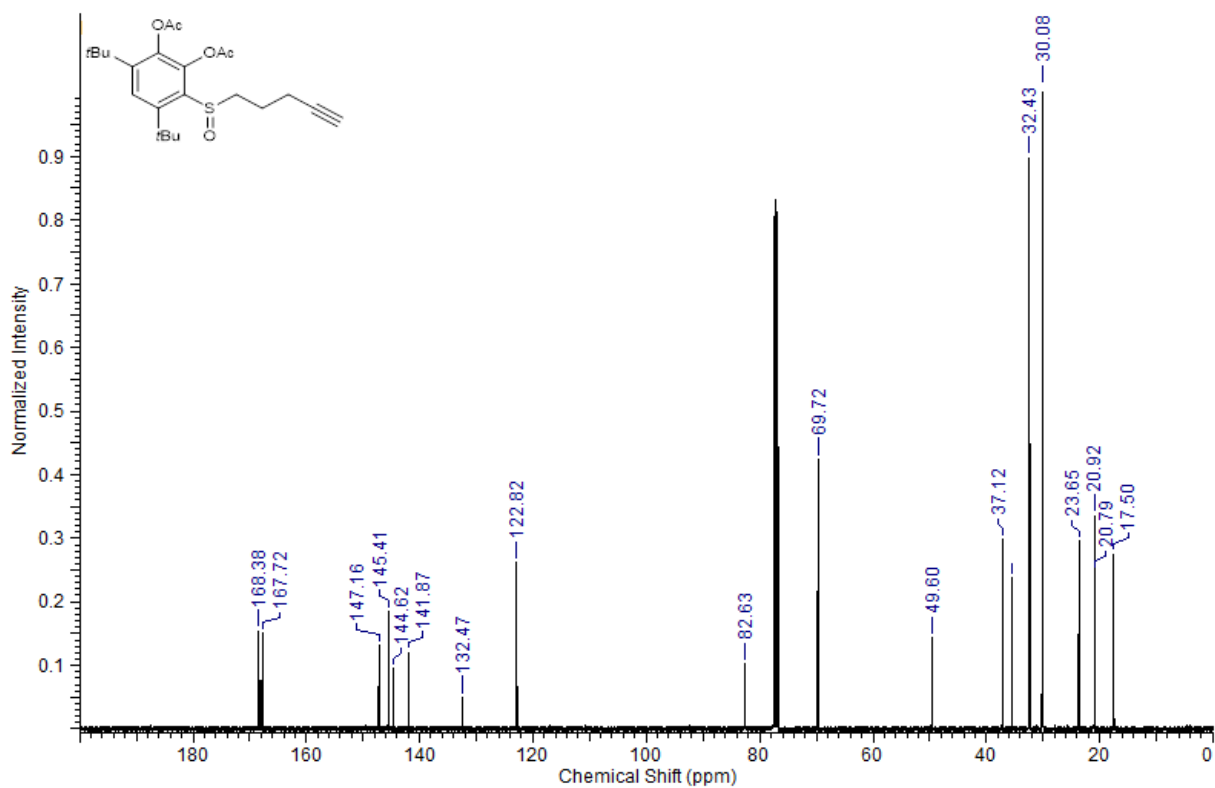
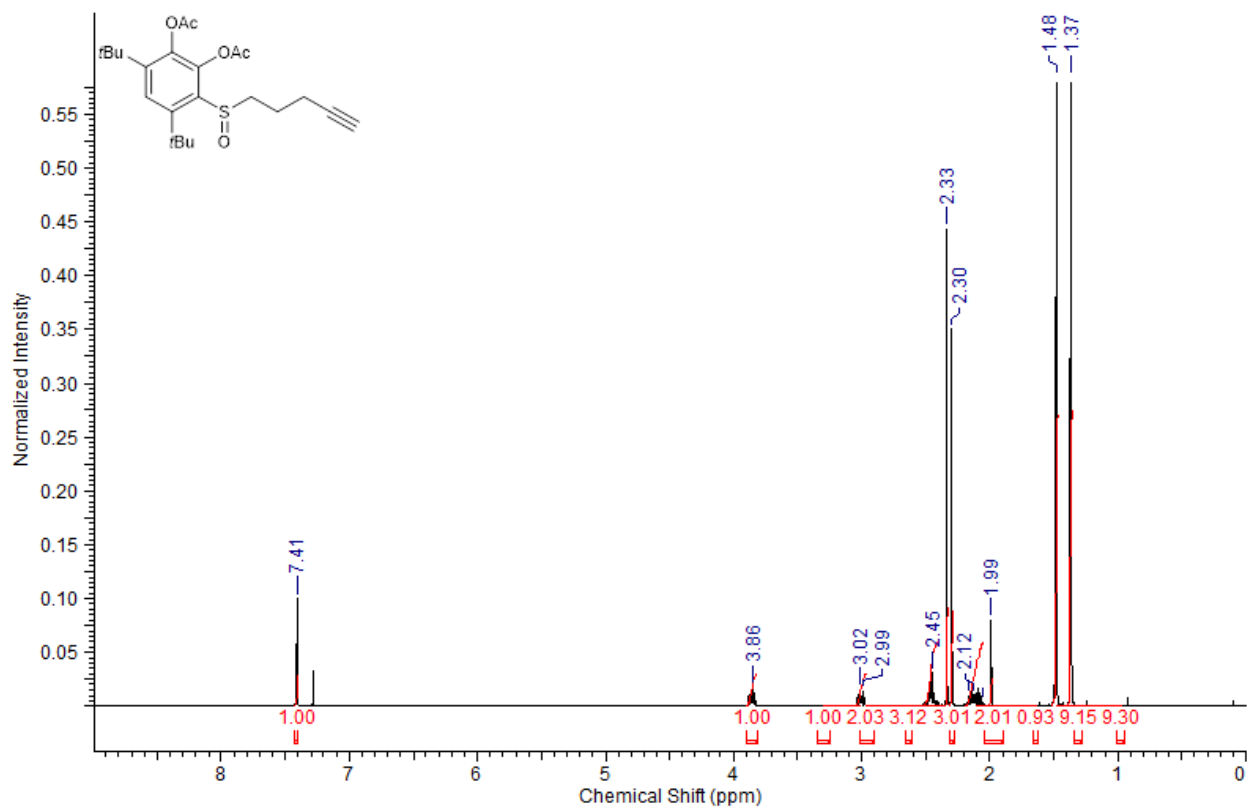


e) 3.9, Blum Group Collaboration Substrates

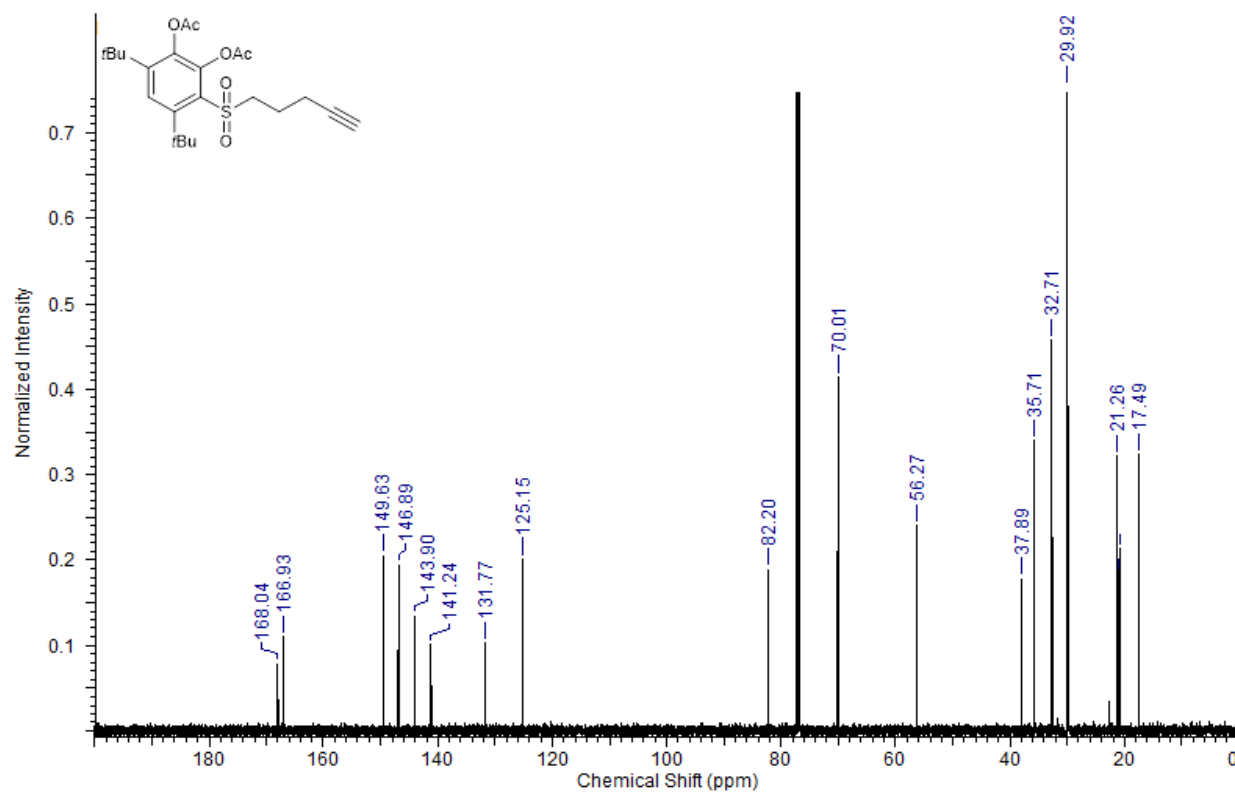
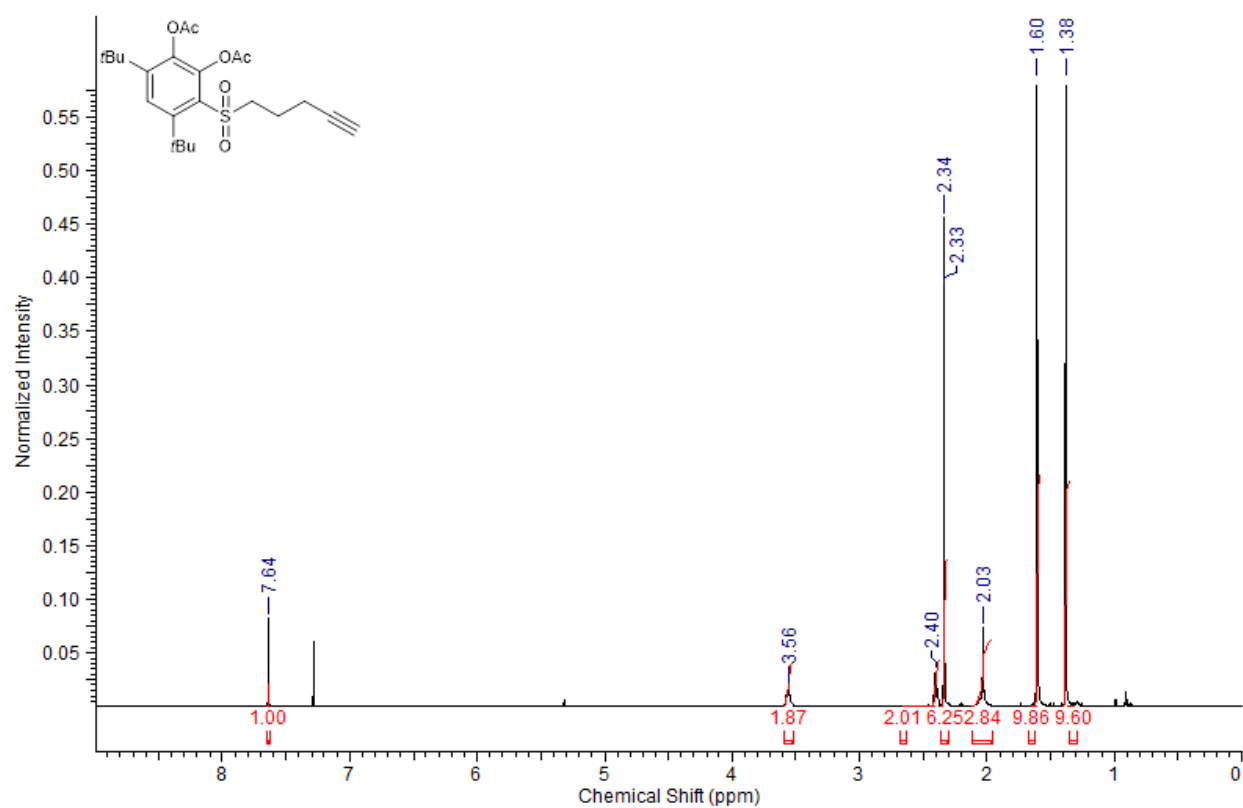
3.9.5:



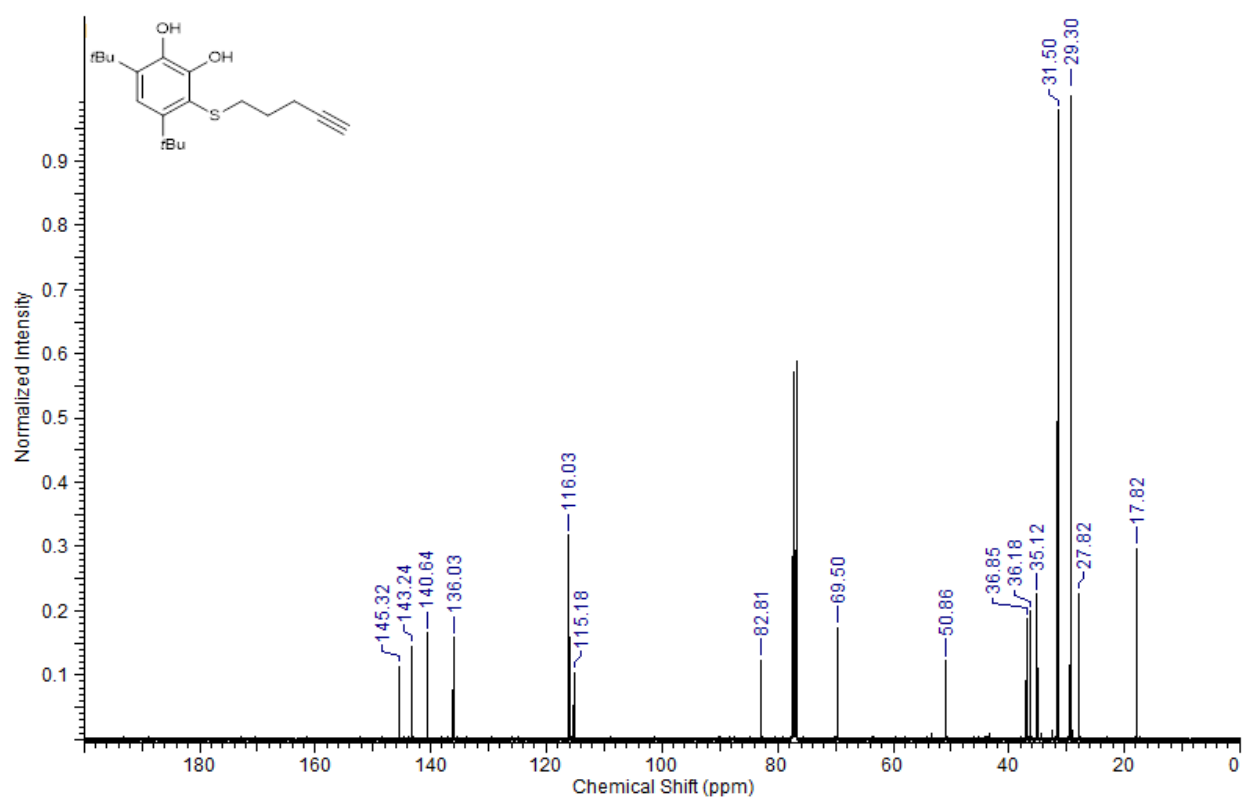
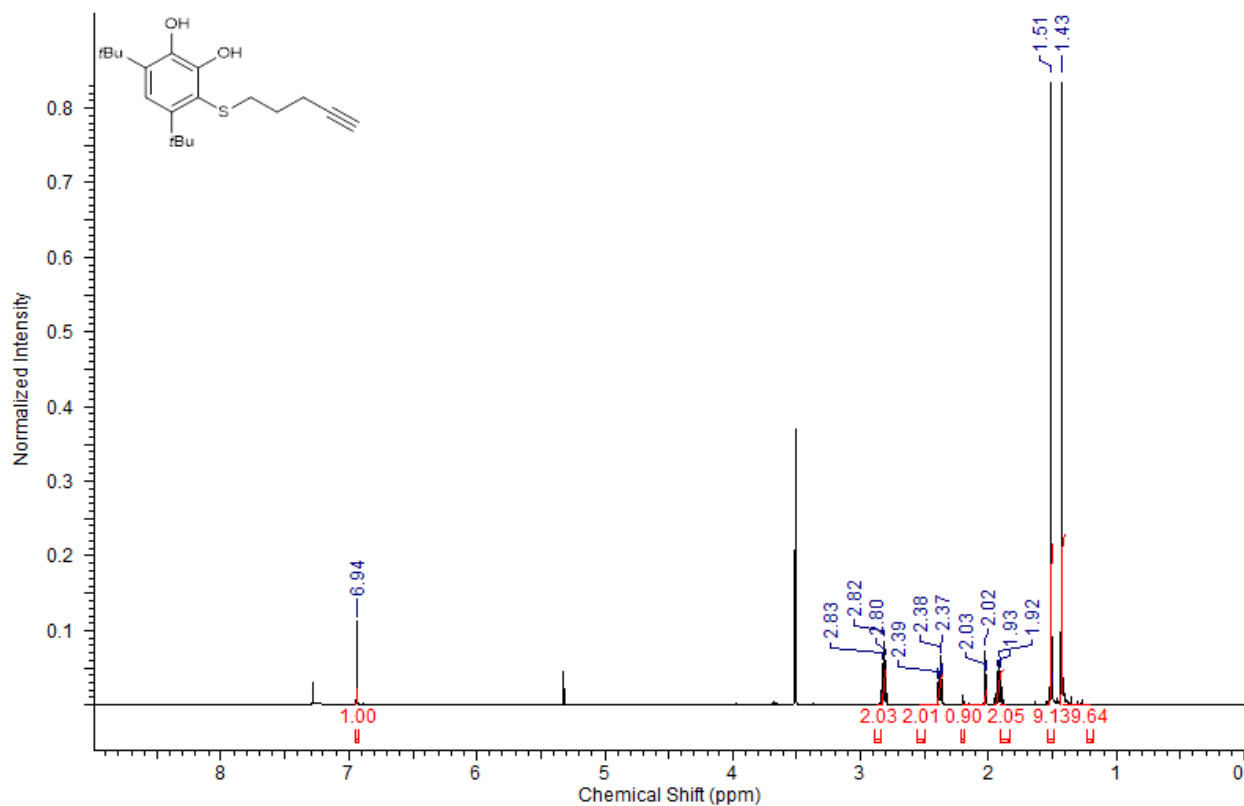
3.9.6:



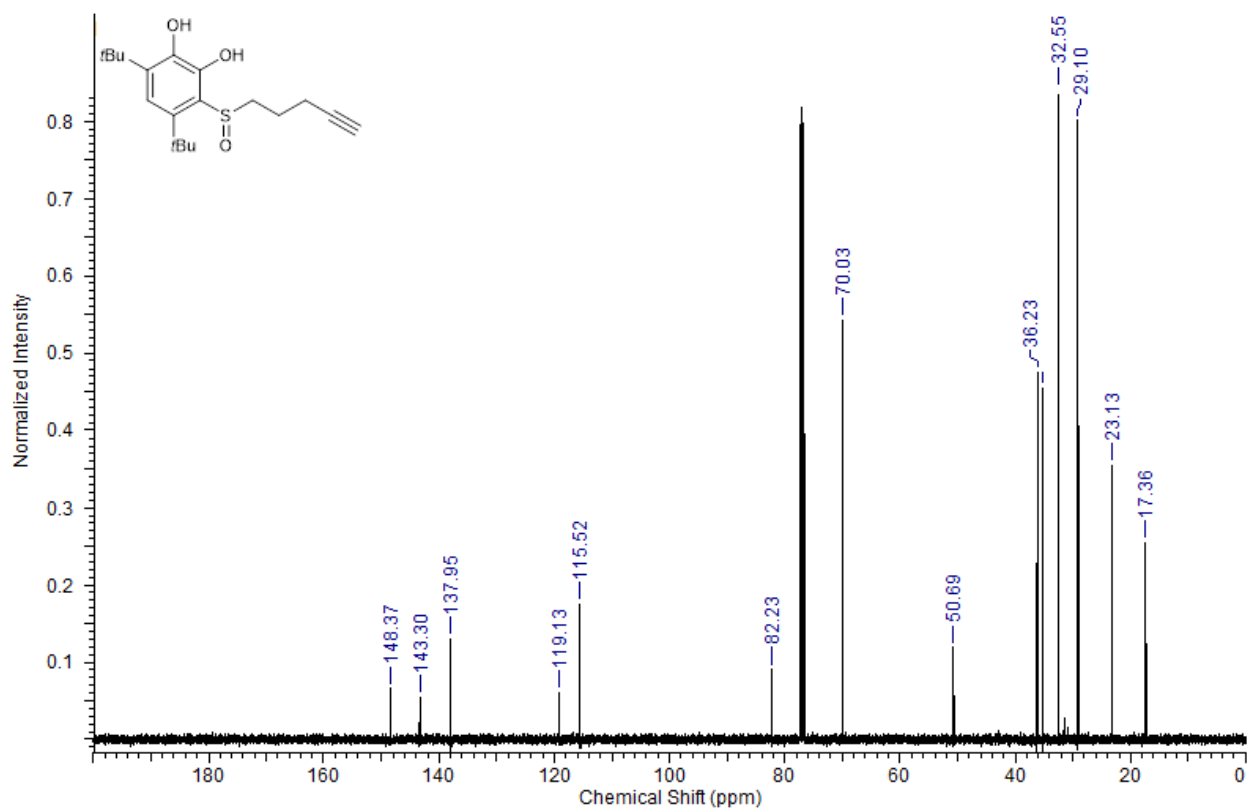
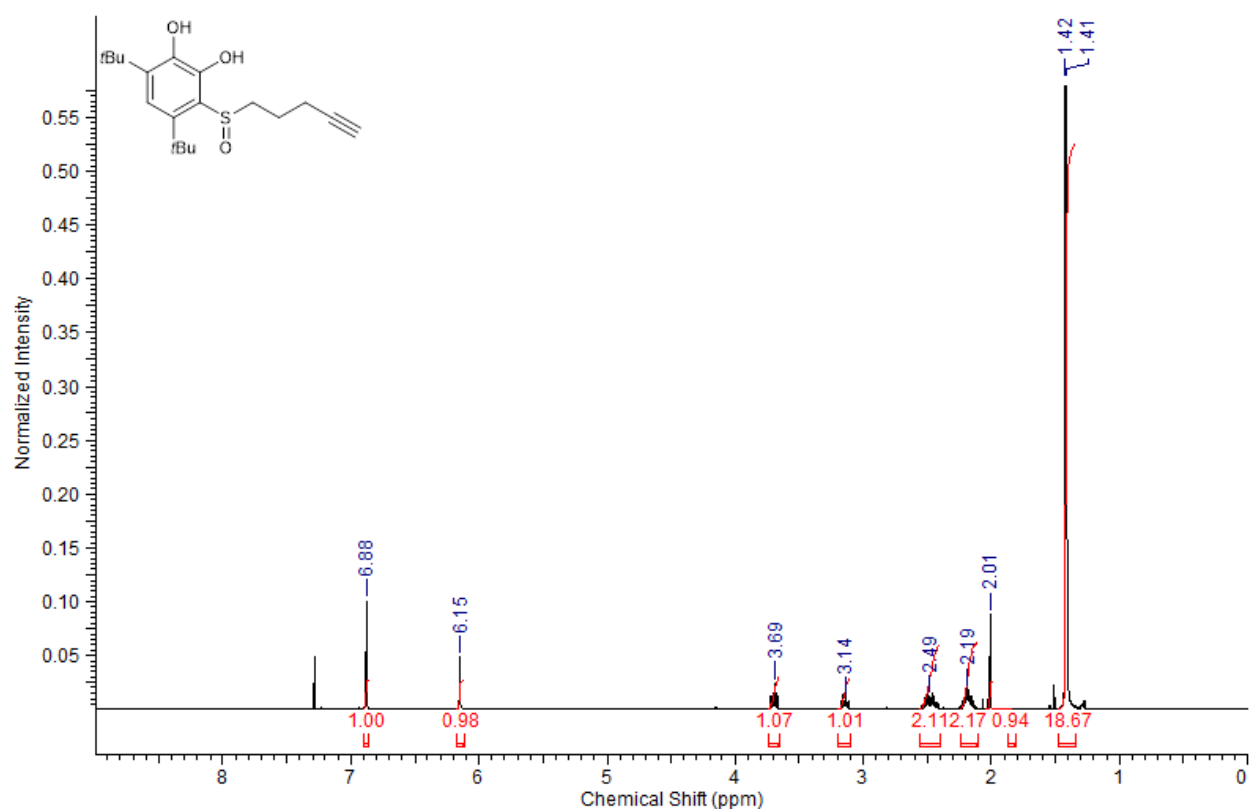
3.9.7:



3.9.8:



3.9.9:



3.9.10:

